Springer Theses
Recognizing Outstanding Ph.D. Research

Mark Greenhalgh

Iron-Catalysed Hydrofunctionalisation of Alkenes and Alkynes

Springer

Springer Theses

Recognizing Outstanding Ph.D. Research

Aims and Scope

The series "Springer Theses" brings together a selection of the very best Ph.D. theses from around the world and across the physical sciences. Nominated and endorsed by two recognized specialists, each published volume has been selected for its scientific excellence and the high impact of its contents for the pertinent field of research. For greater accessibility to non-specialists, the published versions include an extended introduction, as well as a foreword by the student's supervisor explaining the special relevance of the work for the field. As a whole, the series will provide a valuable resource both for newcomers to the research fields described, and for other scientists seeking detailed background information on special questions. Finally, it provides an accredited documentation of the valuable contributions made by today's younger generation of scientists.

Theses are accepted into the series by invited nomination only and must fulfill all of the following criteria

- They must be written in good English.
- The topic should fall within the confines of Chemistry, Physics, Earth Sciences, Engineering and related interdisciplinary fields such as Materials, Nanoscience, Chemical Engineering, Complex Systems and Biophysics.
- The work reported in the thesis must represent a significant scientific advance.
- If the thesis includes previously published material, permission to reproduce this must be gained from the respective copyright holder.
- They must have been examined and passed during the 12 months prior to nomination.
- Each thesis should include a foreword by the supervisor outlining the significance of its content.
- The theses should have a clearly defined structure including an introduction accessible to scientists not expert in that particular field.

More information about this series at http://www.springer.com/series/8790

Mark Greenhalgh

Iron-Catalysed Hydrofunctionalisation of Alkenes and Alkynes

Doctoral Thesis accepted by
the University of Edinburgh, UK

Springer

Author
Dr. Mark Greenhalgh
School of Chemistry
University of St. Andrews
Fife
UK

Supervisor
Dr. Stephen Thomas
School of Chemistry
University of Edinburgh
Edinburgh
UK

ISSN 2190-5053 ISSN 2190-5061 (electronic)
Springer Theses
ISBN 978-3-319-33662-6 ISBN 978-3-319-33663-3 (eBook)
DOI 10.1007/978-3-319-33663-3

Library of Congress Control Number: 2016937387

Printed on acid-free paper

This Springer imprint is published by Springer Nature
The registered company is Springer International Publishing AG Switzerland

Parts of this thesis have been published in the following journal articles:

1. *Iron-Catalyzed, Highly Regioselective Synthesis of α-Aryl Carboxylic Acids from Styrene Derivatives and CO_2.*
Greenhalgh, M. D.; Thomas, S. P. *J. Am. Chem. Soc*. **2012**, *134*, 11900–11903—Highlighted in *Synform*, 2012/12: DOI: 10.1055/s-0032-1317501.

2. *Chemo-, Regio-, and Stereoselective Iron-Catalysed Hydroboration of Alkenes and Alkynes.*
Greenhalgh, M. D.; Thomas, S. P. *Chem. Commun.* **2013**, *49*, 11230–11232.

3. *Iron-Catalysed Chemo-, Regio-, and Stereoselective Hydrosilylation of Alkenes and Alkynes Using a Bench-Stable Iron(II) Pre-Catalyst.*
Greenhalgh, **M. D.;** Frank D. J.; Thomas, S. P. *Adv. Synth. Catal.* **2014**, *356*, 584–590.

4. *Iron-Catalysed Hydromagnesiation: Synthesis and Characterisation of Benzylic Grignard Reagent Intermediate and Application in the Synthesis of Ibuprofen.*
Greenhalgh, **M. D.;** Kolodziej, A.; Sinclair F.; Thomas, S. P. *Organometallics* **2014**, *33*, 5811–5819.

5. *Broad Scope Hydrofunctionalization of Styrene Derivatives Using Iron-Catalyzed Hydromagnesiation.*
Jones, A. S.; Paliga, J. F.; **Greenhalgh, M. D.;** Quibell, J. M.; Steven, A. Thomas, S. P. *Org. Lett.* **2014**, *16*, 5964–5967—Highlighted in *Synfacts* **2015**, *11*, 186.

Supervisor's Foreword

It is a great pleasure to be able to introduce the Ph.D. work of Dr. Mark Greenhalgh, the quality of which has been recognised by its inclusion in the Springer Thesis Series. Mark was an exceptional Ph.D. student who completed an unparalleled body of work during his Ph.D at Edinburgh. The work in Mark's thesis has been published at the highest level, and his results and ideas have led to three industry-funded Ph.D. studentships and grant income in excess of £1 million.

Mark's thesis deals with the development and application of sustainable homogenous iron catalysts in chemical synthesis. With an ever-growing global demand for sustainability, the development of catalytic processes for fine and bulk chemical synthesis is of paramount importance to satisfy the continued worldwide reliance on the chemical industry for manufactured commodity products. Many of the processes used to make these products however are heavily reliant on precious metal catalysts, such as rhodium, platinum and palladium. These metals are scarce and expensive, with their prices highly sensitive to supply restrictions. The increasing pressure on the supply and demand of these resources has been recognised by the EU, with a sustainable basis for the life-cycle of minerals identified as a primary objective over the coming years. Research into the use of inexpensive and earth abundant alternatives is therefore required to meet these international goals. Iron is the fourth most abundant element in the earth's crust, non-toxic, environmentally benign and inexpensive. These attractive attributes have been recognised with a recent effort by internationally leading research groups to investigate the use of iron-based catalysts in chemical synthesis.

This thesis details research efforts into the development of iron-catalysed hydrosilylation, hydroboration and hydromagnesiation reactions with excellent referencing and scientific argument. The work has focussed on providing methodologies that use only commercially available materials and non-specialised techniques, with the intention that the developed science could be widely adopted by the chemical community. To this end, the in situ reduction of iron-pre-catalysts has been developed and used to enable air- and moisture-stable methodologies. It provides not only an in-depth review of the area, but offers a level of insight well

beyond that expected from a Ph.D. student. In short, Mark was one of the unique students whom does not work for you, but works with you. As should be apparent from the quality of the thesis presented here, I fully believe Mark to be a rising star and future research leader.

Edinburgh, UK
March 2016

Dr. Stephen Thomas

Abstract

The iron-catalysed hydrofunctionalisation of alkenes and alkynes has been developed to give a range of functionalised products with control of regio-, chemo- and stereochemistry. Using a bench-stable iron(II) pre-catalyst, the hydrosilylation, hydroboration, hydrogermylation and hydromagnesiation of alkenes and alkynes has been achieved.

Iron-catalysed hydrosilylation, hydroboration and hydrogermylation of terminal, 1,1- and 1,2-disubstituted alkyl and aryl alkenes and alkynes was developed, in which the active iron catalyst was generated in situ (Scheme 1). Alkyl and vinyl silanes and pinacol boronic esters were synthesised in good to excellent yield in the presence of a range of functional groups. Catalyst loadings as low as 0.07 mol% were demonstrated, along with catalyst turnover frequencies of up to 60,000 mol h^{-1}.

The iron-catalysed formal hydrocarboxylation of a range of styrene derivatives has been developed for the synthesis of α-aryl carboxylic acids using carbon dioxide and ethylmagnesium bromide as the stoichiometric hydride source

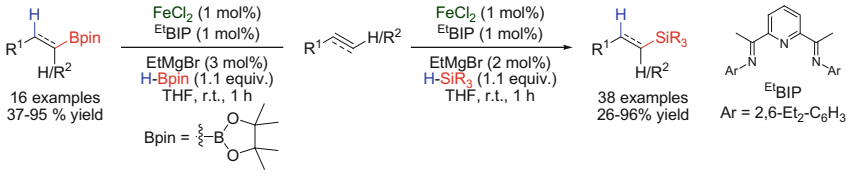

Scheme 1 Iron-catalysed hydrosilylation and hydroboration of alkenes and alkynes

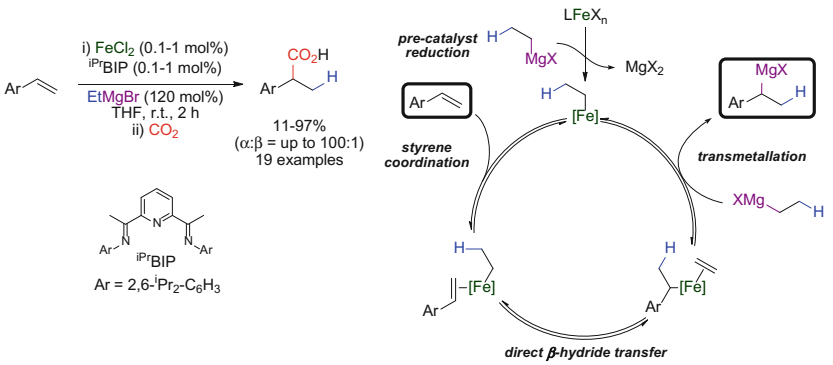

Scheme 2 Iron-catalysed hydromagnesiation of styrene derivatives

(Scheme 2). Detailed mechanistic studies have shown this reaction proceeds by iron-catalysed hydromagnesiation to give an intermediate benzylic organomagnesium reagent. The nature of the active catalyst and reaction mechanism have been proposed.

Preface

The ability to synthesise molecules in a controlled manner is essential for the development of products used in everyday life, such as plastics, fabrics, fertilisers and pharmaceuticals. With ever-growing global chemical demand and energy consumption, the development of efficient, energy-saving synthetic processes is of paramount importance. Catalysis offers the single most powerful method that can be used to improve the yield and efficiency of molecular synthesis whilst also reducing waste and energy consumption. Iron is one of the most abundant elements on earth and therefore is the ideal choice as a catalyst for future applications.

This work developed novel reactions catalysed by an inexpensive, non-toxic and environmentally benign iron catalyst. The controlled and efficient synthesis of a range of molecular structures was achieved. Experiments have provided insight into how these reactions work, which should not only provide a greater understanding of the science involved, but also direct future developments towards highly efficient catalysts and catalytic processes.

Contents

Abbreviations

18-crown-6	1,4,7,10,13,16-Hexaoxacyclooctadecane
Ac	Acetyl
acac	Acetylacetonate
Ar	Aryl
atm.	Atmospheres
BAr_4^F	Tetrakis[3,5-bis(trifluoromethyl)phenyl]borate
BDPP	2,4-Bis(diphenylphosphino)pentane
BIP	Bis(imino)pyridine
bMepi	1,3-Bis(6′-methyl-2′-pyridylimino)isoindolate
Bn	Benzyl
BOX	Bis(oxazoline)
Bpin	4,4,5,5-Tetramethyl-1,3,2-dioxaborolane
Bu	Butyl
COD	1,5-Cyclooctadiene
COE	Cyclooctene
COSY	Correlation spectroscopy
Cp	Cyclopentadienyl
Cy	Cyclohexyl
DACH	1,2-Diaminocyclohexane
DBU	1,8-Diazabicyclo[5.4.0]undec-7-ene
DCT	Dibenzo[*a*,*e*]cyclooctatetraene
DMAP	4-Dimethylaminopyridine
DMF	*N*,*N*-Dimethylformamide
DMSO	Dimethyl sulfoxide
dppe	1,2-Bis(diphenylphosphino)ethane
dppp	1,2-Bis(diphenylphosphino)propane
dr	Diastereomeric ratio
E	Element
ee	Enantiomeric excess
EI	Electron impact

equiv.	Equivalents
ESI	Electrospray ionisation
Et	Ethyl
EWG	Electron-withdrawing group
GCMS	Gas chromatography mass spectrometry
HMBC	Heteronuclear multiple bond correlation
HMDS	Bis(trimethylsilyl)amide
HPLC	High-performance liquid chromatography
HRMAS	High-resolution magic angle spinning
HRMS	High-resolution mass spectrometry
HSQC	Heteronuclear single quantum coherence
IMes	1,3-Bis(2,4,6-trimethylphenyl)imidazol-2-ylidene
IR	Infrared
J	Coupling constant in Hz
L	Ligand
m.p.	Melting point
M	Metal
Me	Methyl
Mes	Mesityl
NBS	*N*-Bromosuccinimide
NMP	*N*-Methylpyrrolidine
NMR	Nuclear magnetic resonance
nOe	Nuclear Overhauser effect
ox	Oxalate
Ph	Phenyl
PHOX	Phosphinooxazoline
Pr	Propyl
py	Pyridine
Rf	Retention factor
r.t.	Room temperature
TBAF	Tetrabutylammonium fluoride
Terpy	Terpyridine
Tf	Trifluoromethanesulfonyl
THF	Tetrahydrofuran
TMEDA	*N*,*N*,*N*′,*N*′-Tetramethylethylenediamine
TOF	Turnover frequency
TON	Turnover number
Tr	Triphenylmethyl
Ts	*para*-Toluenesulfonyl
UV	Ultraviolet

Chapter 1
Introduction

Abstract The development of efficient and sustainable catalytic methodologies for the construction of complex molecular frameworks is essential for the advancement of synthetic chemistry. The hydrofunctionalisation of alkenes and alkynes can be used for the construction of carbon-carbon and carbon-heteroatom bonds, and represent a potentially 100 % atom-economic process. Transition-metal-catalysed hydrofunctionalisation reactions have therefore found numerous applications in industrial and fine chemical synthesis for the introduction of new functionality in a controlled manner. This chapter introduces the state-of-the-art in this field of chemistry, with a particular focus on methods using inexpensive first row transition-metal catalysts.

The development of efficient and sustainable methodologies for the construction of complex molecular frameworks is essential for the advance of synthetic chemistry. Catalysis can be used to improve the yield and efficiency of these processes whilst also reducing waste and energy consumption, and can give products in high and tuneable chemo- regio- and stereoselectivity.

Transition-metal-catalysed cross-coupling reactions are one of the most versatile methods for the controlled construction of carbon–carbon and carbon–heteroatom bonds (Scheme 1.1) [1]. Cross-coupling reactions are highly applicable to fine chemical synthesis due to the wide range of coupling partners available and considerable literature precedent for these reactions. The hydrofunctionalisation of alkenes and alkynes is an alternative approach to the construction of carbon–carbon and carbon–heteroatom bonds, and represents a potentially 100 % atom-economic process (Scheme 1.1) [2]. Alkenes and alkynes are readily available, diversely-functionalised, bench-stable reagents, which are not intrinsically hazardous [3]. The introduction of new functionality in a controlled manner results in an increase in molecular complexity and presents an opportunity for further synthetic manipulations. Transition-metal-catalysed hydrofunctionalisation reactions have therefore found numerous applications in industrial and fine chemical synthesis.

Late transition-metals, generally those from groups 8–10, have been the most commonly applied catalysts in these processes. Depending upon the oxidation-state of the transition-metal catalyst used, and the polarisation of the hydrogen-heteroatom

M. Greenhalgh, *Iron-Catalysed Hydrofunctionalisation of Alkenes and Alkynes*, Springer Theses, DOI 10.1007/978-3-319-33663-3_1

Scheme 1.1 Cross-coupling reactions and the hydrofunctionalisation of alkenes and alkynes using a hydrofunctionalisation reagent (H-ER^3_x) as alternative approaches to molecular synthesis

bond of the hydrofunctionalisation reagent, two general approaches have been used for the transition-metal-catalysed hydrofunctionalisation of alkenes and alkynes. In both cases, coordination of the alkene or alkyne to the transition-metal catalyst is essential for activation of the carbon–carbon multiple bond.

Coordination of an alkene or alkyne to a high oxidation-state late transition-metal catalyst can render the alkene or alkyne more susceptible to nucleophilic attack [4]. For hydrofunctionalisation methodologies where the hydrofunctionalisation reagent is nucleophilic in nature (hydroamination, hydroalkoxylation, etc.), addition of the hydrofunctionalisation reagent to the coordinated alkene or alkyne can give a metal-alkyl or metal-vinyl intermediate, respectively (Scheme 1.2). The hydrofunctionalisation product is then released following protolytic cleavage of the metal-carbon bond (protodemetallation). The metal-alkyl or metal-vinyl intermediate may also be formed through an inner-sphere mechanism, following insertion of the coordinated alkene or alkyne into a metal-heteroatom bond [5].

For hydrofunctionalisation methodologies where the hydrofunctionalisation reagent is not intrinsically nucleophilic (hydrosilylation, hydroboration, etc.), the main approach is to use a low oxidation-state transition-metal catalyst, which can undergo oxidative addition into the hydrogen–heteroatom bond (Scheme 1.3). Insertion of the coordinated alkene or alkyne into either the metal–hydrogen or metal–heteroatom bond gives a metal-alkyl/vinyl intermediate. Reductive elimination of the carbon-heteroatom or carbon–hydrogen bond gives the product of hydrofunctionalisation, and regenerates the low oxidation-state transition-metal catalyst. Hydrosilylation has been proposed to occur by both pathways depending upon the transition-metal catalyst used. Olefin addition into the metal–hydride bond followed by carbon–silicon bond reductive elimination is known as the ‘Chalk–

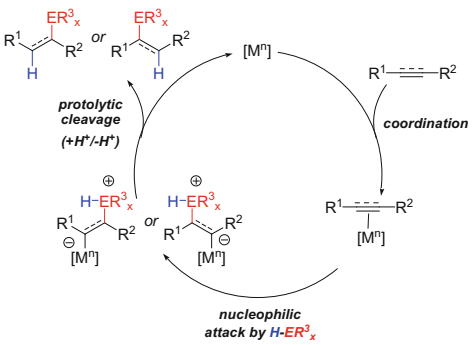

Scheme 1.2 Hydrofunctionalisation of alkenes and alkynes through coordination to a transition-metal catalyst and external attack by a nucleophilic hydrofunctionalisation reagent (H-ER^3_x)

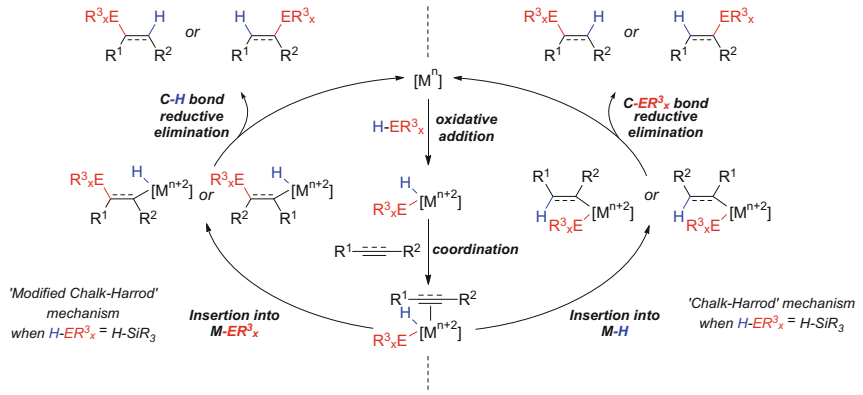

Scheme 1.3 Hydrofunctionalisation of alkenes and alkynes through oxidative addition of a transition-metal catalyst into the hydrogen–heteroatom bond of a hydrofunctionalisation reagent ($H\text{-}ER^3_x$)

Harrod' mechanism [6], whilst olefin addition into the metal–silicon bond followed by carbon–hydrogen bond reductive elimination is known as the 'modified Chalk–Harrod' mechanism (Scheme 1.3) [7]. The regioselectivity of either process is determined by the regiochemistry of the alkene/alkyne insertion into the metal–hydrogen or metal–heteroatom bond.

1.1 Hydrofunctionalisation Using Precious Late Transition-Metal Catalysts

The development of hydrofunctionalisation methodologies has, and continues to be, focused on the use of highly active catalysts based upon precious late transition-metals such as rhodium, palladium, platinum and iridium.

The hydroformylation and hydrosilylation of alkenes represent two of the largest-scale applications of homogeneous catalysis on an industrial scale, and each make use of precious transition-metal catalysts [8]. Hydroformylation is the addition of carbon monoxide and hydrogen to alkenes to give aldehyde products. The hydroformylation of propene **1** alone is performed on a one million tonne scale annually (Scheme 1.4a) [9]. The best catalytic activities, and highest regioselectivities for linear aldehyde products, have been reported using rhodium catalysts bearing phosphine ligands [8b]. The regioselectivity of hydroformylation has been attributed to the coordination geometry of the trigonal bipyramidal rhodium complex **4** or **5** prior to alkene insertion into the rhodium–hydrogen bond (Scheme 1.4b). The complex with phosphine ligands in the equatorial positions **4** (L = PR_3) can be favoured by the use of low carbon monoxide pressures, high phosphine to rhodium ratios, and wide bite-angle bidentate phosphine ligands (bite-angle close to 120°) [10].

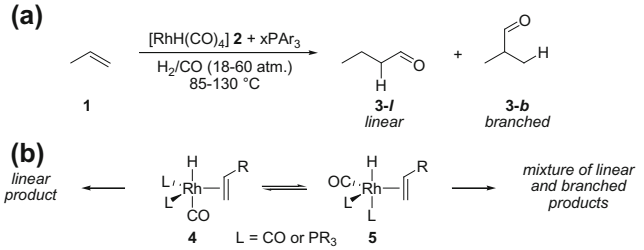

Scheme 1.4 **a** General conditions used for the hydroformylation of propene; **b** Isomeric trigonal bipyramidal rhodium complexes leading to linear and branched aldehyde products

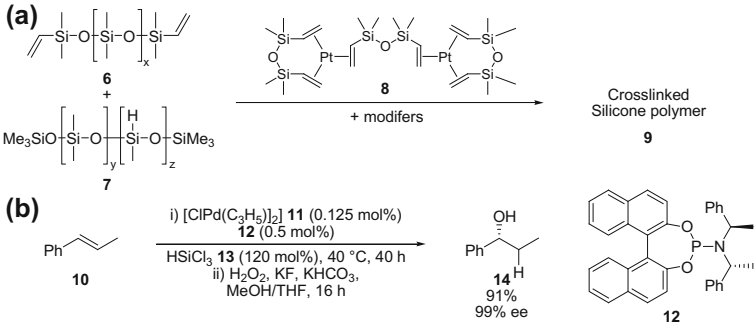

Scheme 1.5 Hydrosilylation of alkenes: **a** Industrial application of platinum-catalysed hydrosilylation for the synthesis of cross-linked silicone polymers; **b** Palladium-catalysed enantioselective hydrosilylation-oxidation of aryl alkenes

The hydrosilylation of alkenes is used industrially for the synthesis of cross-linked silicone polymers **9**, with the field currently dominated by platinum catalysts, in particular modifications of Karstedt's catalyst **8** (Scheme 1.5a) [11]. The hydrosilylation of alkenes using Karstedt's catalyst can be complicated by alkene isomerisation, which is proposed to be catalysed by colloidal platinum species formed under the reaction conditions [12]. Colloidal platinum was found to form most readily in hydrosilylation reactions using weakly coordinating olefins [12], and thus the addition of strong σ-donor ligands such as phosphines and carbenes has been found to inhibit colloidal platinum formation and decrease the extent of alkene isomerisation [13]. The hydrosilylation of alkenes and alkynes is also used in fine chemical synthesis for the preparation of alkyl, vinyl and allyl silanes, which have applications in stereospecific oxidation [14] and cross-coupling reactions [15], amongst others [16]. High enantioselectivities and complementary chemo-, stereo- and regioselectivities have been reported using platinum, rhodium, palladium and iridium catalysts. Asymmetric hydrosilylation reactions have been achieved using palladium catalysts bearing enantiopure phosphine and phosphoramidite ligands,

with excellent enantioselectivities reported for the hydrosilylation of aryl alkenes (Scheme 1.5b) [17].

Boronic acid derivatives have become ubiquitous in chemical synthesis, and can be conveniently synthesised by transition-metal-catalysed hydroboration of alkenes and alkynes [18]. Rhodium and iridium catalysts have been most commonly used for these reactions. Asymmetric variants have also been developed, with the highest enantioselectivities reported for the rhodium-catalysed hydroboration of aryl alkenes using catechol borane (Scheme 1.6a) [19]. The alkyl and vinyl boronic esters produced in these reactions can be applied in stereospecific transformations for the formation of carbon–carbon and carbon–heteroatom bonds, including oxidation, amination, homologation and Suzuki–Miyaura cross-coupling reactions [20].

The hydroamination of alkenes, alkynes and allenes is a reaction of great interest in fine chemical research for the synthesis of pharmaceutical and agrochemical products [21]. Of particular interest is the enantioselective hydroamination of alkenes to give amine products with a stereogenic centre adjacent to the amine group [22]. Palladium, rhodium and iridium catalysts bearing enantiopure phosphine ligands have been used for both inter- and intramolecular hydroamination reactions. Although highly enantioselective intermolecular hydroamination reactions have been mostly confined to styrene and norbornene derivatives, amine products have been obtained in good to excellent yields and enantioselectivities with these substrates (Scheme 1.6b) [23].

With ever-growing global demand for metal and mineral resources set to continue into the 21st century, the development of methodologies that do not rely on precious transition-metal catalysts is of paramount importance [24]. The use of

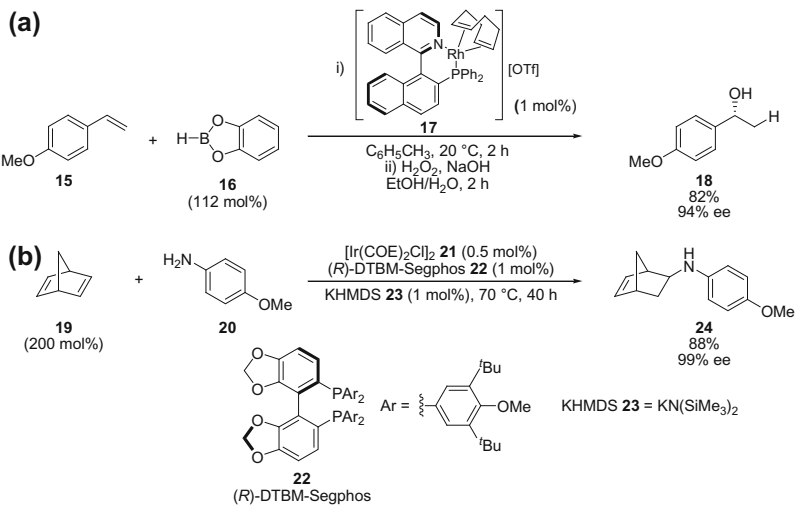

Scheme 1.6 Asymmetric hydrofunctionalisation reactions with potential application in fine chemical synthesis: **a** Rhodium-catalysed hydroboration-oxidation of aryl alkenes; **b** Iridium-catalysed hydroamination of norbornadiene

more inexpensive and earth-abundant metals in place of precious transition-metals in catalysis therefore represents an important area of research. In addition to attempts to emulate the reactivity of precious transition-metals, research into the use of alternative catalysts may also provide novel reactivity to compliment entrenched methodologies [25].

1.2 Hydrofunctionalisation Using Early Transition-Metal and Main Group Metal Catalysts

The use of early transition-metals (groups 3–5, as well as lanthanides and actinides) and main group metals (groups 1–2, 13) as catalysts in hydrofunctionalisation reactions has received increased interest in recent years [8c, 26]. In contrast to late transition-metals, the catalysts used in these reactions have a d^0 electronic configuration, and thus alkene hydrofunctionalisation takes place by alternative reaction mechanisms. Due to the d^0 electronic configuration of the catalyst, the oxidative addition of the catalyst into a hydrogen–heteroatom bond is not possible, and therefore reaction mechanisms involve alkene insertion steps, σ-bond metathesis and cycloaddition reactions, during which the oxidation-state of the catalyst remains constant (Scheme 1.7).

The hydrosilylation and hydroamination of alkenes using early transition-metal and main group metal catalysts is proposed to usually proceed by an 'alkene insertion mechanism' (Scheme 1.8a) [8c, 27]. Alkene insertion into either a metal-hydrogen or a metal–heteroatom bond gives a metal alkyl intermediate **28** or **31** which can undergo protolysis or σ-bond metathesis with another equivalent of amine or silane. For hydroamination, alkene insertion into the metal–amide bond is reported to be the turnover-limiting step (Scheme 1.8, **30** → **31**) [27a]. The resulting alkyl-metal species **31** is highly reactive, resulting in fast protolysis. For alkene hydrosilylation using early transition-metal catalysts, rapid alkene insertion into a metal–hydride bond (Scheme 1.8, **26** → **28**) is is proposed to be followed by a turnover-limiting σ-bond metathesis between the metal alkyl intermediate **28** and

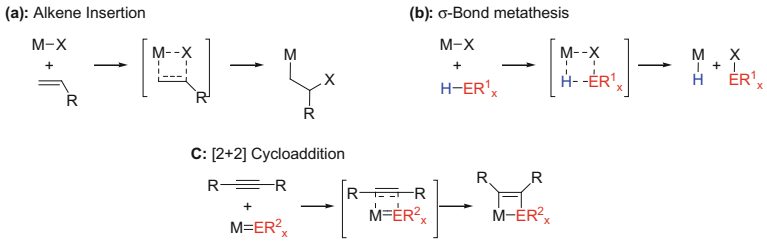

Scheme 1.7 Elementary reactions of metals with a d^0 electronic configuration: **a** Alkene insertion into a metal-X bond; **b** σ-bond metathesis between a metal-X bond and a hydrogen–heteroatom bond; **c** [2 + 2] Cycloaddition between an alkene and metal-heteroatom multiple bond

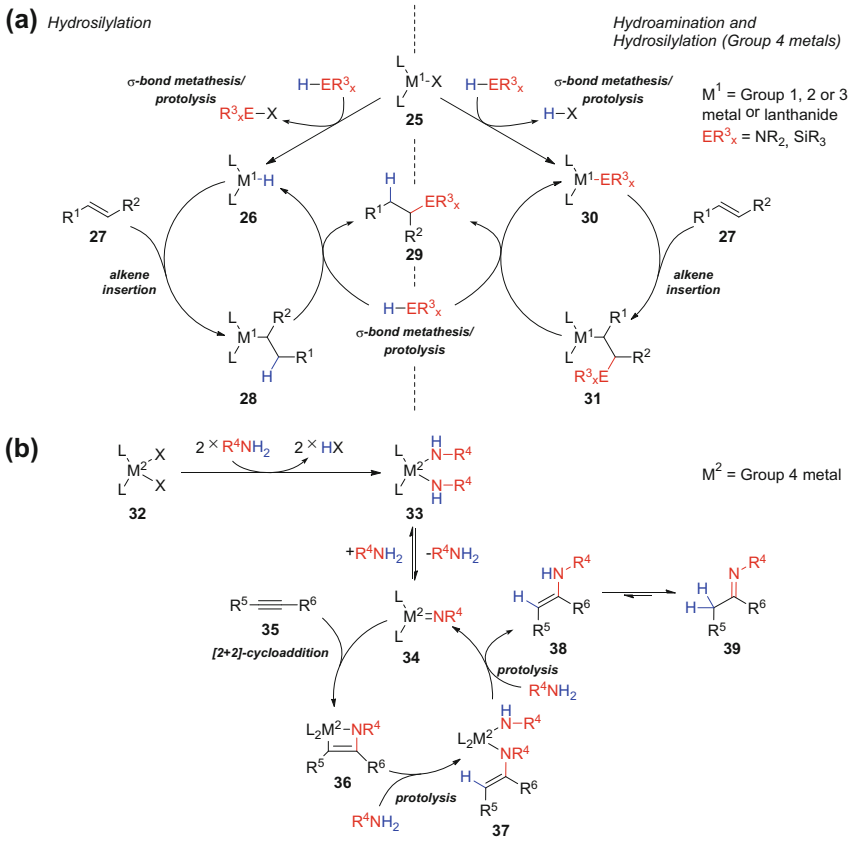

Scheme 1.8 Mechanisms of alkene and alkyne hydrofunctionalisation using metal catalysts with a d^0 electronic configuration. **a** 'Alkene insertion mechanism' proposed for the hydroamination and hydrosilylation of alkenes using groups 1–3, and lanthanide, metal catalysts; **b** 'Imido mechanism' proposed for the hydroamination of alkynes using group 4 metal catalysts

an equivalent of silane [27b]. Based upon the observation of dehydrosilylation side-products, it has been proposed that group 4 metals catalyse hydrosilylation by a mechanism involving alkene insertion into a metal–silicon bond (Scheme 1.8, **30** → **31**) rather than insertion into a metal–hydride bond (Scheme 1.8, **26** → **28**) [28].

The hydroamination of alkynes **35** using group 4 transition-metal pre-catalysts **32** has been proposed to proceed by an alternative mechanism involving the formation of a metal-imido complex **34** (Scheme 1.8b) [29]. [2 + 2]-Cycloaddition between the metal-imido complex **34** and alkyne substrate **35** gives an azametallacyclobutene intermediate **36**, which following protolysis releases the hydroamination product **38**. Evidence for this mechanism has been provided by computational modelling, the isolation of azametallacyclobutene intermediates **36**

which display catalytic activity, and the fact that only primary amines can be used in these reactions. It has been suggested that a 'metal-imido mechanism' may also be in operation for the hydroamination of alkenes using group 4 transition-metal pre-catalysts in some cases [30], however less supporting experimental and theoretical data has been reported.

The hydroamination of alkenes, alkynes, allenes and dienes is the most studied hydrofunctionalisation reaction catalysed by early transition-metals and main group metals. Low catalyst loadings and short reaction times have been reported for the intramolecular hydroamination of olefins, giving amine products in good to excellent levels of regio- and stereochemical control. Asymmetric intramolecular hydroamination reactions have been developed using a range of metals bearing enantiopure nitrogen and oxygen-based ligands (Scheme 1.9) [31]. Conducting the asymmetric hydroamination reactions at lower temperatures (<0 °C) can result in improved enantioselectivities, however much longer reaction times are required for good conversions to be obtained. The intermolecular hydroamination of alkenes has also been reported using catalysts based on early transition-metals and main group metals, however higher catalyst loadings, longer reaction times and higher reaction temperatures are required [26a].

The hydrosilylation of alkenes, alkynes and dienes has been reported by a number of groups using catalysts based on group 3 and 4 transition-metals and lanthanides, usually in the form of metallocene complexes [8c]. More recently metal amide and imine complexes have also been successfully used in these reactions. The hydrosilylation of terminal alkenes give linear silane products with good to excellent regioselectivity, whilst the hydrosilylation of styrene derivatives give benzylic silane products regioselectively. Only limited examples have been reported for the hydrosilylation of internal alkenes however, and tertiary silanes show no activity in these reactions. Asymmetric versions have been developed with good enantioselectivities reported in some cases (Scheme 1.10a, b) [27b, 32].

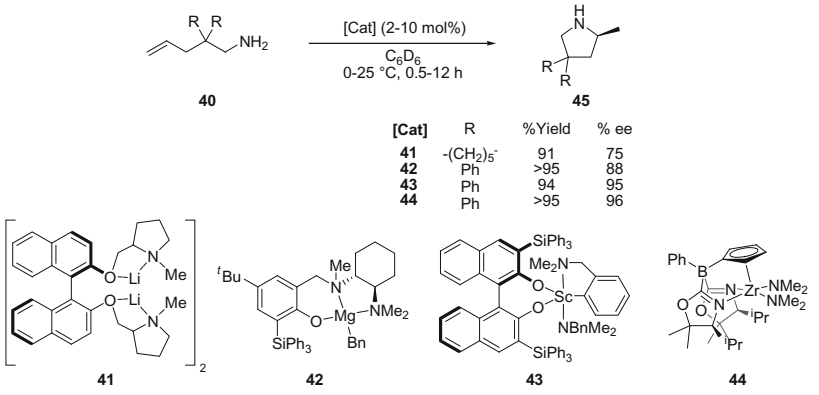

Scheme 1.9 Enantioselective intramolecular hydroamination using a selection of catalysts based upon metals from groups 1–4 bearing enantiopure nitrogen and oxygen-based ligands

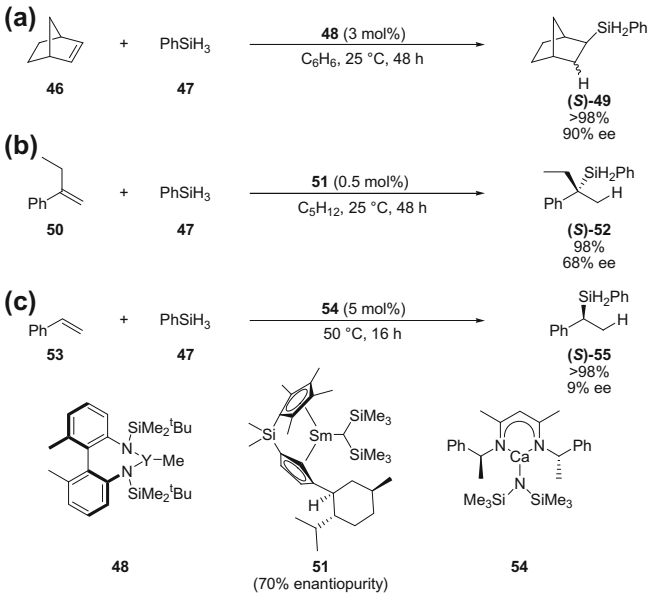

Scheme 1.10 Enantioselective hydrosilylation of alkenes using lanthanide, early transition-metal and alkaline-earth metal catalysts. **a** Yttrium-catalysed hydrosilylation of norbornene; **b** Samarium-catalysed hydrosilylation of 2-phenyl-1-butene; **c** Calcium-catalysed hydrosilylation of styrene

Alkaline-earth metal complexes have also been applied in the hydrosilylation of styrene derivatives and 1,3-dienes [8c, 26b], with an example of enantioselective hydrosilylation reported using a β-diketimide calcium hexamethyldisilazane complex **54** (Scheme 1.10c) [33].

1.3 Hydrofunctionalisation Using First-Row Transition-Metal Catalysts

1.3.1 Nickel

Found in the same group as platinum and palladium, nickel has numerous applications in catalysis. In addition to hydrogenation and cross-coupling reactions, nickel catalysts have been used for alkene and alkyne hydrofunctionalisation reactions, in particular hydrocyanation [34] and hydrovinylation [35].

The main industrial application of hydrocyanation is in the synthesis of adiponitrile **61** from 1,3-butadiene **56**, originally developed by DuPont using a nickel(0) triarylphosphite catalyst, $[Ni(P(OAr)_3)_4]$ **58** (Scheme 1.11) [36]. Adiponitrile **61** is a key precursor to nylon-6,6 and is produced annually on a scale in excess of one

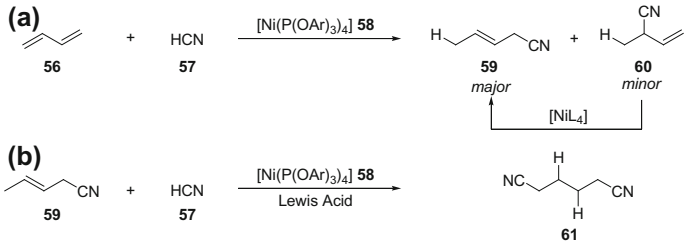

Scheme 1.11 Nickel-catalysed hydrocyanation of 1,3-butadiene **56** to give adiponitrile **61**

million tonnes [37]. The nickel-catalysed hydrocyanation of 1,3-butadiene **56** gives a separable mixture of 3-pentenenitrile **59** and 2-methyl-3-butenenitrile **60** (Scheme 1.11a). Using a similar nickel(0) catalyst, 2-methyl-3-butenenitrile **60** can be isomerised to give 3-pentenenitrile **59**, which can undergo hydrocyanation with the aid of a Lewis acid co-catalyst to give adiponitrile **61** (Scheme 1.11b). The major pathway for catalyst deactivation in this process is the formation of kinetically inert square planar dicyanonickel(II) complexes, $[Ni(OPAr_3)_2(CN)_2]$. Pringle, and later van Leeuwen and Vogt, reported that the use of a wide bite angle bidentate phosphine or phosphite ligand significantly improved catalyst lifetime by disfavouring the square planar conformation of the deactivated catalyst [38].

The asymmetric nickel-catalysed hydrocyanation of alkenes has also been extensively studied, with the highest enantioselectivities reported by RajanBabu for the hydrocyanation of 6-methoxy-2-vinylnaphthalene **62** using a sugar-derived diphosphinite ligand **64** (Scheme 1.12) [39]. Currently asymmetric hydrocyanation is not widely applicable however, with high enantioselectivities only reported for a small range of aryl alkene substrates.

The hydrovinylation of alkenes and 1,3-dienes is a synthetically useful process for the construction of carbon–carbon bonds, through the formal addition of a vinyl group and a hydrogen across an unsaturated system [35]. There are a number of challenges with this reaction. Firstly, selectivity is required for the reaction to occur between the substrates, and not with the product, as this would eventually lead to a polymerisation reaction. Secondly, the catalyst must be able to differentiate between

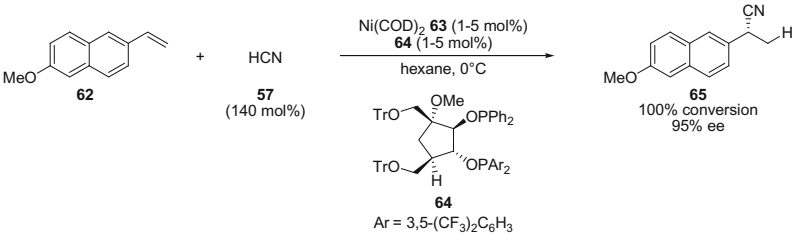

Scheme 1.12 Nickel-catalysed asymmetric hydrocyanation 6-methoxy-2-vinylnaphthalene using a sugar-derived diphosphinite ligand **64**

the two alkene substrates to give a single product. Finally, the product is commonly a terminal alkene, and thus isomerisation to internal alkene products must be avoided. These challenges are overcome by judicious choice of catalyst and by using two sterically and/or electronically differentiated alkene substrates, which give a hydrovinylation product which is sterically or electronically deactivated relative to the substrates. The majority of methodologies have therefore focussed on the 1,2-hydrovinylation of styrene (electronically activated) or norbornene (strained) derivatives using ethylene (unhindered), or the 1,4-hydrovinylation of 1,3-dienes. Using nickel catalysts, high yields and enantioselectivities have been reported for the 1,2-hydrovinylation of prochiral alkenes. Typically the best activity and highest enantioselectivities have been reported using enantiopure monodentate phosphine ligands, or bidentate ligands where one ligand is only weakly-coordinating (Scheme 1.13) [40]. Strongly chelating bidentate phosphine ligands inhibit nickel-catalysed hydrovinylation reactions by forming coordinatively-saturated, and therefore inactive, nickel complexes [35a, 41].

Nickel catalysts have also been used for the hydrocarboxylation of alkenes. Hoberg reported that in the presence of nickel(0) complexes, styrene **53** and carbon dioxide underwent oxidative coupling to give oxonickelacyclopentanone intermediates **75** [42], which following hydrolysis gave products arising from the formal hydrocarboxylation (**α-** and **β-76**) and dehydrocarboxylation (**77**) of styrene (Scheme 1.14a) [43]. By varying the reaction temperature, selectivity for either the hydrocarboxylation or dehydrocarboxylation product could be obtained, however a catalytic version of the reaction was not developed. Inspired by this work, Rovis rationalised that the addition of a stoichiometric hydride source (diethylzinc **80**) might be used to turn over the reaction (Scheme 1.14b) [44]. Using 10 mol% nickel

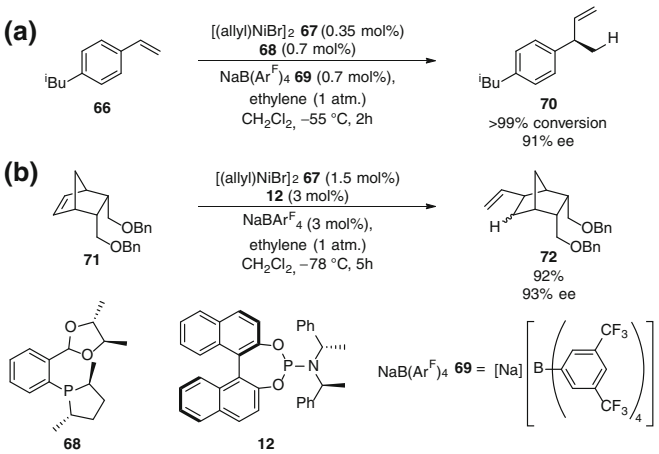

Scheme 1.13 Nickel-catalysed asymmetric hydrovinylation of styrene and norbornene derivatives using enantiopure monodentate phosphine ligands **68** and **12**

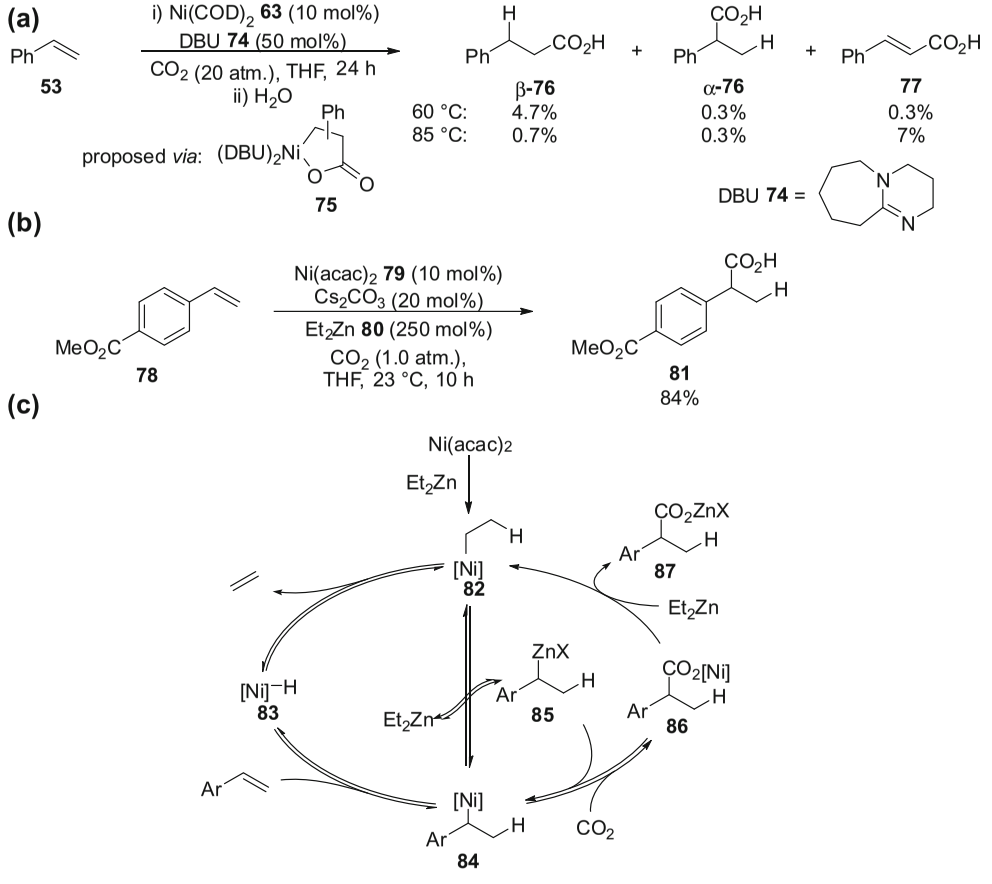

Scheme 1.14 **a** Nickel-mediated hydrocarboxylation and dehydrocarboxylation of styrene; **b** Nickel-catalysed hydrocarboxylation of styrene derivatives; **c** Proposed mechanism for nickel-catalysed hydrocarboxylation of styrene derivatives

(II) acetylacetonate **79** as pre-catalyst, styrene derivatives bearing electron-withdrawing groups underwent hydrocarboxylation to give α-aryl carboxylic acids in good to excellent yield. Although inspired by Hoberg's work, the contrast in regioselectively for the hydrocarboxylation of styrene suggested an alternative mechanism was in operation. Quenching the reaction after 1 h with D_2O resulted in a 50 % yield of ethylbenzene with deuterium incorporation in the benzylic position, suggesting the presence of a benzylic organometallic reagent in higher concentration than the nickel catalyst. It was therefore suggested that the reaction proceeded by hydrometallation of styrene to give a benzyl nickel species **84**, which following transmetallation would give a benzylic zinc reagent **85** and reform the catalyst (Scheme 1.14c). An independently synthesised benzylic zinc reagent was found to not react with carbon dioxide in the absence of nickel however, suggesting that transmetallation from zinc to nickel was required for carboxylation.

1.3.2 Cobalt

Cobalt catalysts have been used in alkene hydrofunctionalisation reactions for many decades, with the original academic and industrial hydroformylation processes utilising a cobalt carbonyl catalyst [8b]. These cobalt catalysts however have been mostly replaced by rhodium catalysts which offer improved activity and selectivity. More recently cobalt complexes have been found to be effective catalysts for hydrovinylation, hydroboration and hydrosilylation reactions.

An example of cobalt-catalysed enantioselective 1,4-hydrovinylation of 1,3-dienes was reported by RajanBabu using a combination of cobalt chloride and an enantiopure bidentate phosphine ligand (*S*, *S*)-BDPP **89** (Scheme 1.15) [45]. This is in contrast to nickel-catalysed hydrovinylation, where the hydrovinylation of 1,3-dienes usually gives 1,2-hydrovinylation products, and the use of bidentate phosphines produce catalytically inactive species [46]. Both of these differences may be attributed to the higher coordination numbers and different coordination geometries favoured by cobalt complexes.

Cobalt catalysts bearing tridentate redox-active ligands have recently been shown to be active for the hydroboration of alkenes (Scheme 1.16). Using either a bis(imino)pyridine (BIP) cobalt(I) complex [47] or a phosphino-bipyridine cobalt (II) complex **94** reduced in situ with sodium triethylborohydride [48], the hydroboration of terminal alkenes using pinacol borane **93** (HBpin) gave linear

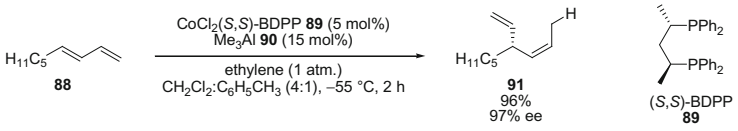

Scheme 1.15 Cobalt-catalysed asymmetric 1,4-hydrovinylation of 1,3-nonadiene **88**

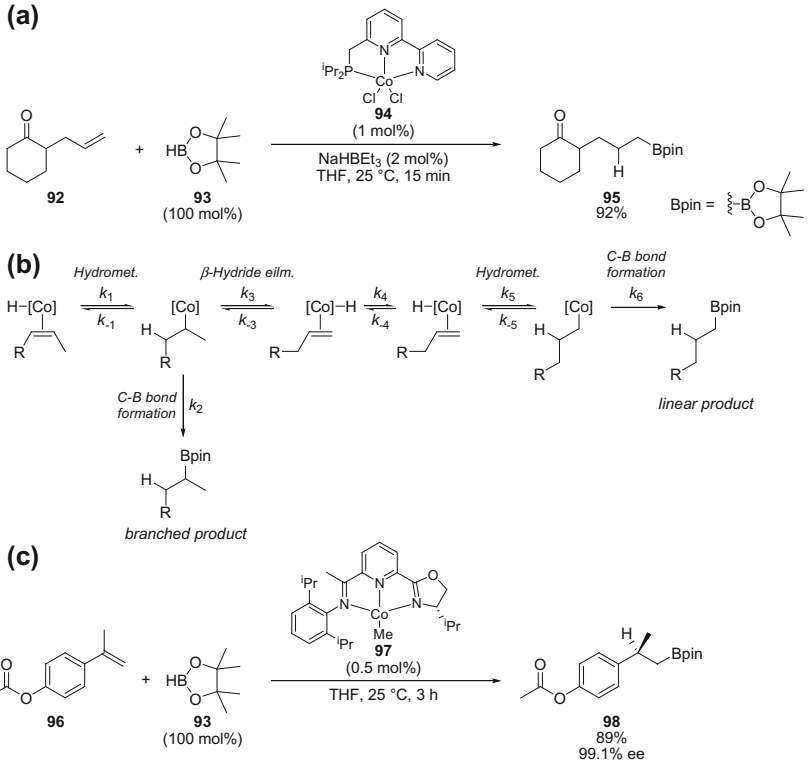

Scheme 1.16 Cobalt-catalysed hydroboration and asymmetric hydroboration of alkenes using pinacol borane

boronic esters in excellent yields (Scheme 1.16a). Internal alkenes also gave linear pinacol boronic ester products. This was explained by isomerisation of the internal alkene, where the rate of alkene isomerisation outcompeted the rate at which the hydroboration product was released (Scheme 1.16b, $k_3 > k_2$). The hydroboration of 4-octene using d_1-pinacol borane (DBpin) resulted in deuterium incorporation in multiple positions in the alkyl chain, which suggested that cobalt-catalysed hydroboration may proceed by alkene insertion into a cobalt–hydride bond followed by carbon–boron bond reductive elimination [47]. Cobalt(I) complexes bearing enantiopure iminopyridine-oxazoline ligands **97** have been applied for the asymmetric hydroboration of 1,1-disubstituted alkenes, giving hydroboration products in excellent yields and enantioselectivities (Scheme 1.16c) [49].

The applicability of cobalt carbonyl clusters as pre-catalysts for the hydrosilylation of alkenes was established over 50 years ago [50], however competitive alkene isomerisation detracted from the synthetic utility of the method in comparison to analogous reactions using platinum catalysts. Recent reports however have shown that highly active cobalt catalysts can be designed that are selective for

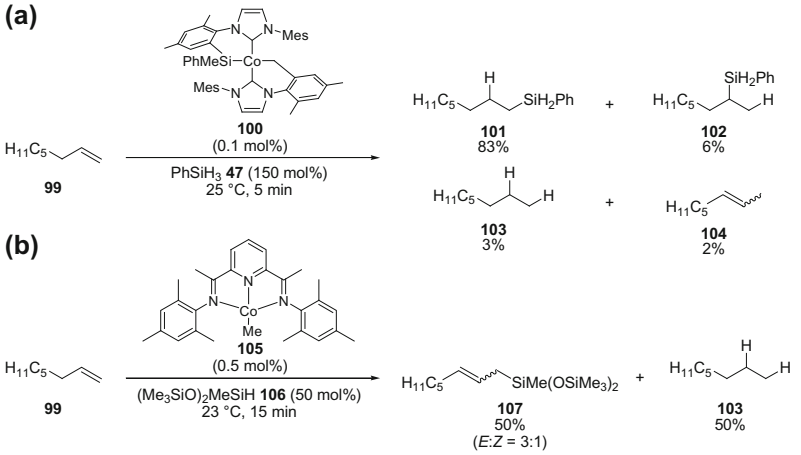

Scheme 1.17 Cobalt-catalysed hydrosilylation and dehydrosilylation of terminal alkenes

either the hydrosilylation or dehydrosilylation-hydrogenation of alkenes. Using a silyl-donor-functionalised *N*-heterocyclic carbene cobalt(II) complex **100**, Deng reported excellent yields for the hydrosilylation of 1-octene **99** at low catalyst loadings and short reaction times (Scheme 1.17a) [51]. Only minor products arising from alkene isomerisation were reported. A procedure for the dehydrosilylation of alkenes was reported by Chirik using a bis(imino)pyridine (BIP) cobalt(I) complex **105** (Scheme 1.17b) [52]. An equivalent of alkane **103** was produced from the reduction of the alkene substrate for each equivalent of dehydrosilylation product **107** formed. Excellent selectivity for the formation of allyl silane, rather than vinyl silane, products was reported.

Selectivity for dehydrosilylation over hydrosilylation using this catalyst can be explained if alkene insertion into a cobalt–silicon bond occurs rather than insertion into a cobalt–hydride bond (Scheme 1.18). Alkene insertion into the cobalt–silicon bond of cobalt–silyl complex **108** would give the cobalt–alkyl intermediate **109**, which can undergo β-hydride elimination to give an allyl silane **107**, or carbon–hydrogen bond formation to give an alkyl silane **112**. It was proposed that if the cobalt–alkyl intermediate **109** did not possess a hydride ligand, then the difference in the rate of intramolecular β-hydride elimination, relative to intermolecular carbon–hydrogen bond formation, can be used to justify the selectivity observed for the dehydrosilylation product. The cobalt–hydride complex **110**, formed following β-hydride elimination, can react with another equivalent of alkene to give cobalt alkyl complex **111**, which following reaction with another equivalent of silane can give the alkane product **103** and regenerate the cobalt–silyl complex **108**. This mechanism was suggested, and primary catalytic steps demonstrated, by Wrighton for the hydrosilylation of alkenes using cobalt carbonyl clusters [53]. The selectivity for allyl silane products, over vinyl silanes, in this example was proposed to

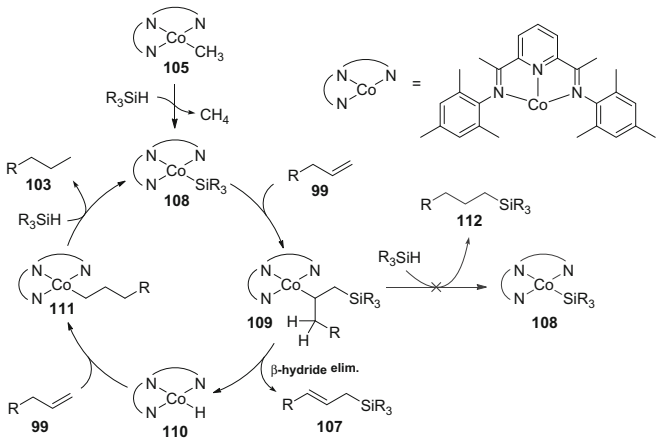

Scheme 1.18 Proposed mechanism for cobalt-catalysed dehydrosilylation of terminal alkenes

reflect an overriding steric effect of the bulky silicon group directing β-hydride elimination from the less sterically encumbered alkyl chain.

1.3.3 Iron

Iron is the most abundant transition-metal and 4th most abundant element in the earth's crust [54]. Based upon this high terrestrial abundance, iron is inexpensive, offers sustainable long-term commercial availability and is considered environmentally benign [24, 55]. Iron has many biological functions and consequentially a significantly higher concentration of iron is permitted in pharmaceuticals than precious transition-metals [56]. Iron catalysis has enjoyed a rebirth in recent decades with many methodologies developed for cross-coupling [57] and redox reactions [58]. The iron-catalysed hydrofunctionalisation of alkenes and alkynes has recently emerged as a growing area of research, with methodologies reported for hydroamination, hydroalkoxylation, hydrocarboxylation, hydrothiolation, hydrophosphination, hydrosilylation, hydroboration, hydromagnesiation and carbonylation reactions [59]. The methodologies may be broadly separated into those where the iron catalyst is either in a high (≥ +2), or a low (< +2), oxidation-state.

1.3.3.1 High Oxidation-State Iron-Catalysed Hydrofunctionalisation

Iron(III) salts are hard Lewis acids and have been used in hydrofunctionalisation reactions to increase the susceptibility of alkenes and alkynes to nucleophilic attack

[60]. Methodologies have been developed for the addition of amines, alcohols, carboxylic acids, thiols and 1,3-dicarbonyls to alkenes, alkynes and allenes, most commonly using either $FeCl_3$ **114** or $Fe(OTf)_3$ **115** (Tf = CF_3SO_2) as a (pre-) catalyst. The hydrofunctionalisation of unactivated alkenes **113** has been mostly confined to intramolecular reactions (Scheme 1.19a), with intermolecular reactions generally limited to those using either strained alkenes, such as norbornene **46**, or those capable of stabilising a cationic intermediate, such as styrene derivatives, 1,3-dienes and enol ethers (Scheme 1.19b) [59b]. Iron-catalysed hydroamination reactions using Lewis acidic iron(III) salts have relied upon the use of amines bearing electron-withdrawing groups, such as aniline and tosylamine derivatives (Scheme 1.19a, b). Amines with increased basicity, such as primary alkyl amines, are unreactive, and this has been suggested to reflect the formation of stable Lewis adducts between the amine and Lewis acidic iron(III) salt. Hannedouche recently reported the first example of an iron-catalysed hydroamination with a primary alkyl amine, using an iron(II) β-diketiminate alkyl complex **123** as a pre-catalyst (Scheme 1.19c) [61]. Based upon stoichiometric and kinetic experiments, the reaction was proposed to proceed by an 'alkene insertion mechanism' analogous to that proposed for hydroamination using early transition-metal and lanthanide catalysts (Scheme 1.8a).

Iron(III) salts have also been used to promote radical-mediated alkene hydrofunctionalisation reactions [59b, 62]. The most common approach is the reductive

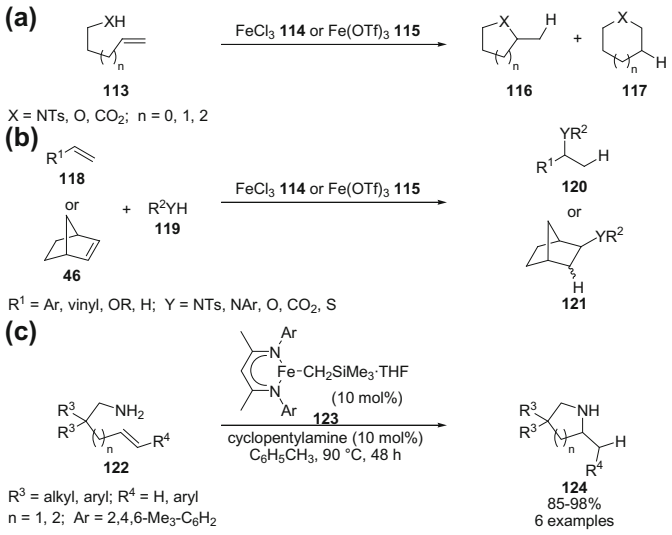

Scheme 1.19 High oxidation-state iron pre-catalysts used for the hydrofunctionalisation of alkenes. **a** Intramolecular hydroamination, hydroalkoxylation and hydrocarboxylation using iron (III) salts; **b** Intermolecular hydroamination, hydroalkoxylation, hydrocarboxylation and hydrothiolation using iron(III) salts; **c** Intramolecular hydroamination using an iron(II) β-diketiminate alkyl complex

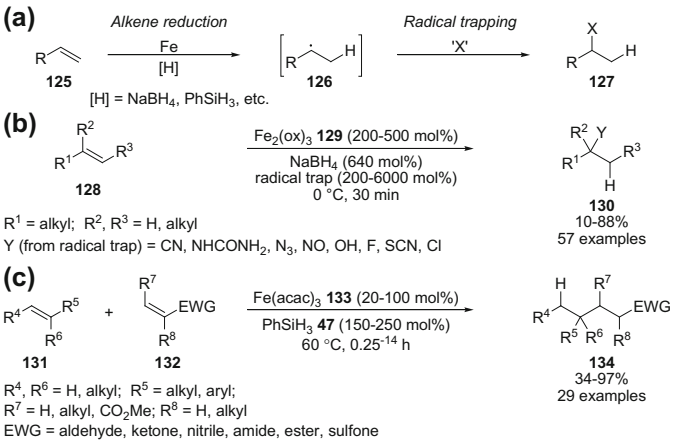

Scheme 1.20 Iron-catalysed, radical-mediated hydrofunctionalisation of alkenes. **a** General scheme; **b** Broad-scope hydrofunctionalisation using a range of radical traps; **c** Reductive cross-coupling of alkenes

formation of an alkyl radical intermediate **126** from an alkene **125** and a stoichiometric hydrogen source using an iron(III) pre-catalyst (Scheme 1.20a). The formation of an alkyl radical intermediate **126** in the presence of a suitable radical trap leads to the formation of formal hydrofunctionalisation products **127**. This approach has been used recently by Boger as a general methodology for the hydrofunctionalisation of alkenes **128** using a range of radical traps (Scheme 1.20b) [63]. Carbon–carbon and carbon–heteroatom bond formation occurred at the most substituted alkene carbon, consistent with stabilisation of an alkyl radical intermediate. Good to excellent yields were obtained, however superstoichiometric iron (III) oxalate **129** and sodium borohydride were required. Baran found that electron-deficient alkenes **132** could also be used as radical traps for this chemistry, and developed an efficient iron-catalysed reductive cross-coupling reaction between primary, 1,1-disubstituted, and tertiary alkenes **131** with electron-deficient alkenes **132** (Scheme 1.20c) [64]. The reaction of $Fe(acac)_3$ **133**, phenylsilane **47** and an alkene **131** was proposed to give a stabilised alkyl radical intermediate, which underwent conjugate addition to an intra- or intermolecular α,β-unsaturated system **132** to give the cross-coupled products **134** in generally good to excellent yields. Sub-stoichiometric quantities of iron salt could be used in this methodology.

1.3.3.2 Low Oxidation-State Iron-Catalysed Hydrofunctionalisation

Iron complexes in formal oxidation-states below +2 are highly reactive species and have been applied as catalysts for cross-coupling reactions [57] and olefin and carbonyl reductions [58a–c], amongst others [65]. There has been substantial interest in hydrofunctionalisation reactions using low oxidation-state iron catalysts

in recent years, with methodologies developed for chemo-, regio- and stereoselective hydrosilylation, hydrovinylation, hydroboration and carbonylation of alkenes and alkynes.

Iron complexes in low oxidation-states are generally air- and moisture sensitive and are readily oxidised to iron(II) and iron(III) species. Air-stable iron(0) complexes are known, however these are generally limited to iron carbonyl complexes, in which the strong bonding between iron and carbon monoxide makes the complex kinetically inert. Catalytically active species may be produced however by thermally- or photochemically-induced carbon monoxide dissociation [66].

A more general approach to a wider variety of low oxidation-state iron complexes is through the reduction of an iron(II) or iron(III) complex with a suitable reductant (Scheme 1.21) [67]. Reducing reagents must have a greater reduction potential than the low oxidation-state iron species formed, and therefore strong inorganic or organometallic reducing reagents are generally used [68]. The reduction of ferrocene **135** with lithium metal in the presence of ethylene has been shown to produce an iron-ethylene complex with two lithium counterions **137** (Scheme 1.21a) [67a]. Based upon the greater electropositivity of lithium in comparison to iron, this can be considered as a 4-electron reduction to give a formally iron(–II) complex.

Sodium amalgam **139** [67b], sodium naphthalide **142** [67c] and potassium anthrancenide **145** [67d] have also be used for 2–4 electron reductions of iron(II) complexes (Scheme 1.21b–d). Reducing agents with smaller reduction potentials can also be used, with magnesium **148** [67e], organozinc **151** [67f] and organoaluminium **153** [67f] reagents all shown to be effective for the reduction of iron(II)/(III) complexes (Scheme 1.21e–g). These low oxidation-state iron complexes have all shown activity as pre-catalysts for either cross-coupling, hydrogenation or hydrofunctionalisation reactions, however they can be challenging to synthesise and are highly air- and moisture sensitive.

Redox-active (non-innocent) ligands are commonly used for the stabilisation of reduced iron complexes (Scheme 1.21b, c, e) [69]. Redox-active ligands are able to accept electron density from the iron centre, and thus provide stabilisation to the complex. When a complex contains a potentially redox-active ligand only a formal oxidation-state of iron can be assigned without thorough analysis of the structural, electronic and spectroscopic properties of the isolated complex. Chirik has studied the electronic structures of reduced bis(imino)pyridine (BIP) iron complexes in detail [70]. The reduction of bis(imino)pyridine iron(II) dibromide (BIP) complex **156** using sodium amalgam **139** or sodium triethylborohydride resulted in a two-electron reduction to give a formally iron(0) bis(dinitrogen) complex **157** (Scheme 1.22a) [71]. This bis(imino)pyridine iron bis(dinitrogen) complex showed excellent activity as a pre-catalyst for hydrogenation and hydrofunctionalisation reactions. Due to interconversion between the bis(dinitrogen) complex **157** and the mono(dinitrogen) complex **158** in solution, the electronic structure of the related four-coordinate 4-dimethylaminopyridine (DMAP) complex **159** was investigated [72]. It was shown that rather than existing as an iron(0) complex, this complex was better described as an intermediate-spin iron(II) complex bound to a doubly reduced diradical bis(imino)pyridine ligand **159′** (Scheme 1.22b). This assignment was

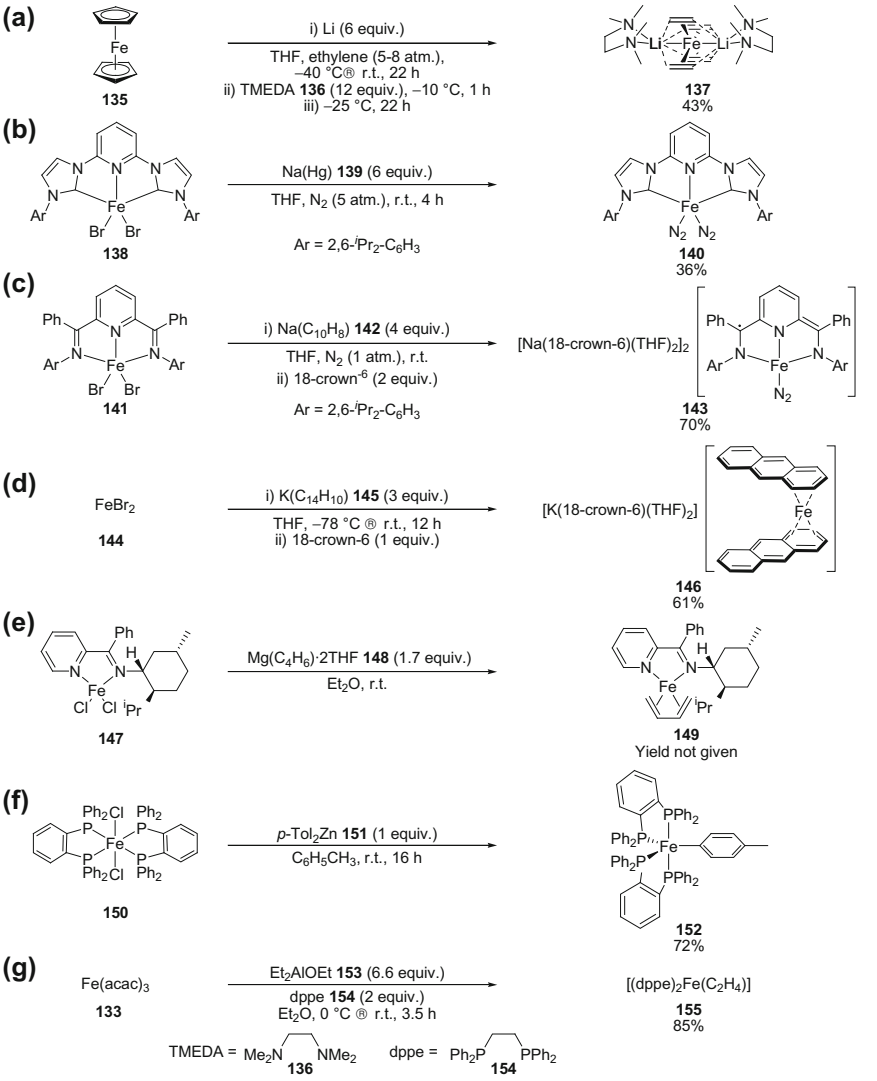

Scheme 1.21 The reduction of iron(II)/(III) species using inorganic and organometallic reductants. **a** Lithium reduction of ferrocene **135** in the presence of ethylene and *N*, *N*, *N′*, *N′*-tetramethylethylenediamine **136**; **b** Sodium amalgam **139** reduction of iron(II) bromide complex **138**; **c** Sodium naphthalide **142** reduction of iron(II) bromide complex **141**; **d** Potassium anthracenide **145** reduction of iron(II) bromide **144**; **e** Magnesium butadiene **148** reduction of iron (II) chloride complex **147**; **f** Di-*p*-tolylzinc **151** reduction of iron(II) chloride complex **150**; **g** Diethylaluminium ethoxide **153** reduction of iron(III) acetylacetonate **133** in the presence of 1,2-bis(diphenylphosphino)ethane **154**

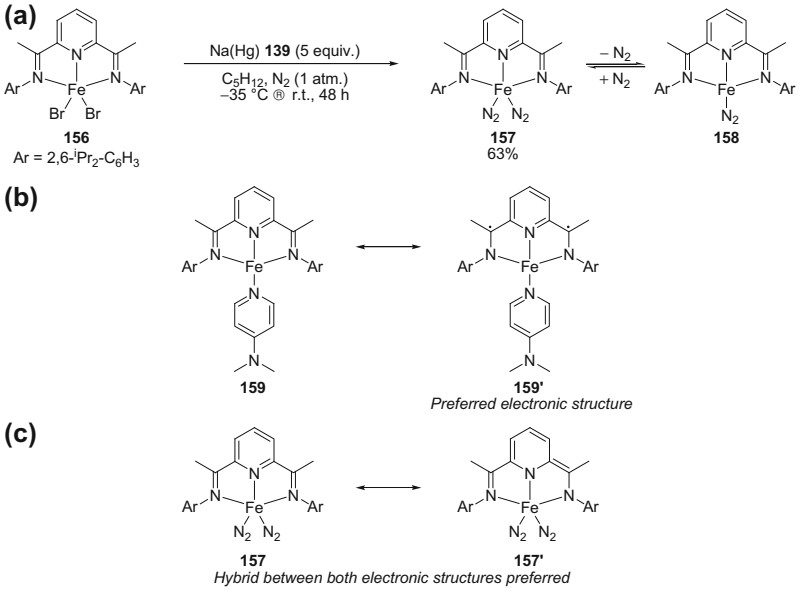

Scheme 1.22 Redox chemistry of bis(imino)pyridine (BIP) complexes. **a** Sodium amalgam **139** reduction of iron(II) bromide complex **156** to give bis(imino)pyridine iron dinitrogen complexes **157** and **158**; **b** Electronic resonance structures of four-coordinate bis(imino)pyridine iron DMAP complex **159** and **159′** (DMAP = 4-dimethylaminopyridine); **c** Electronic resonance structures of bis(imino)pyridine iron bis(dinitrogen) complex **157** and **157′**

made using single crystal X-ray analysis, X-ray absorption and emission spectroscopy, NMR spectroscopy, Mössbauer spectroscopy and computational modelling. Although this description appears to be transposable to the four-coordinate bis(imino)pyridine iron mono(dinitrogen) complex **158**, the bis(dinitrogen) analogue **157** has recently been shown to be better described as a resonance hybrid between iron(0) and iron(II), with no evidence of ligand-centred radicals (Scheme 1.22c) [73]. Although the electronic structures of these complexes should only be transposed to catalytically active species with caution due to subtle ligand and coordination geometry effects, the broad redox chemistry associated with the bis(imino)pyridine ligand framework undoubtedly contributes to the catalytic activity of these iron complexes in hydrogenation and hydrofunctionalisation reactions.

Despite the increased stability and extended catalyst lifetimes associated, reduced iron complexes bearing redox-active ligands are still highly air- and moisture sensitive and can be difficult to prepare and isolate. For more operationally-simple catalysis, low oxidation-state iron catalysts can also be formed in situ from the reduction of a bench-stable iron(II) or iron(III) pre-catalyst. Activated elemental metals, organometallic reagents and metal hydrides have all

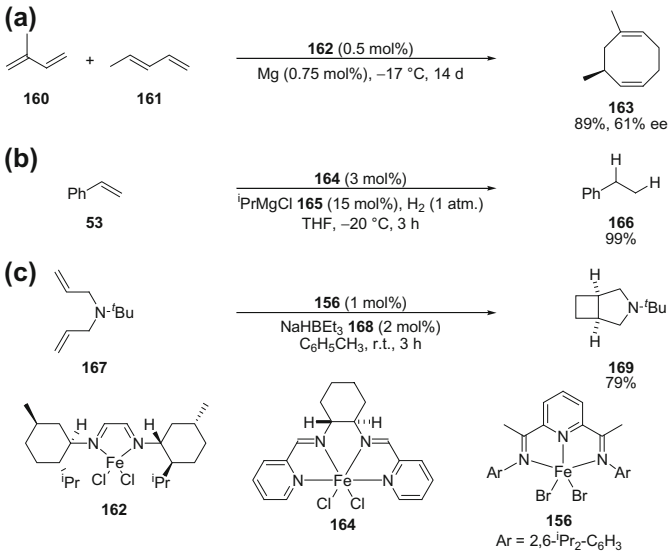

Scheme 1.23 Iron-catalysed reactions in which the active catalyst is formed in situ by reduction of an iron(II) pre-catalyst using: **a** Activated magnesium (1.5 equiv. with respect to iron); **b** Iso-Propylmagnesium chloride **165** (5 equiv. with respect to iron); **c** Sodium triethylborohydride **168** (2 equiv. with respect to iron)

been used for the reduction of iron(II)/(III) pre-catalysts in situ to give catalytically active species that are capable of catalysing reactions usually achieved using low oxidation-state iron complexes (Scheme 1.23a–c) [74]. The drawbacks of this approach include the formation of a potentially ill-defined catalytically active species and the possibility of functional group incompatibility between the substrate and the reducing agent. However, both of these issues can be addressed by using an appropriate method of pre-catalyst reduction, and understanding the mechanism of this reduction.

Research into iron-catalysed cross-coupling reactions has intensified over the past 10–15 years, with the majority of methodologies using Grignard reagents as the nucleophilic cross-coupling partner [57]. One appealing aspect of these reactions is the use of a bench-stable iron(II)/(III) pre-catalyst, which is reduced in situ by the Grignard reagent to give the catalytically-active iron species. The reduction of iron salts using Grignard reagents was originally studied in detail by Kochi [75], and has subsequently been studied both experimentally and computationally by Bogdanović [76] and Norrby [77], amongst others [78]. Depending upon the structure of the Grignard reagent a number of reduction pathways can be accessed (Scheme 1.24). For the reduction of an iron(II)/(III) salt **170** using an aryl Grignard reagent **171**, the only reduction product formed is biaryl **173**, arising from carbon–carbon bond formation by reductive elimination from a diaryliron intermediate **172** (Scheme 1.24a). Each equivalent of biaryl **171** formed therefore corresponds to a

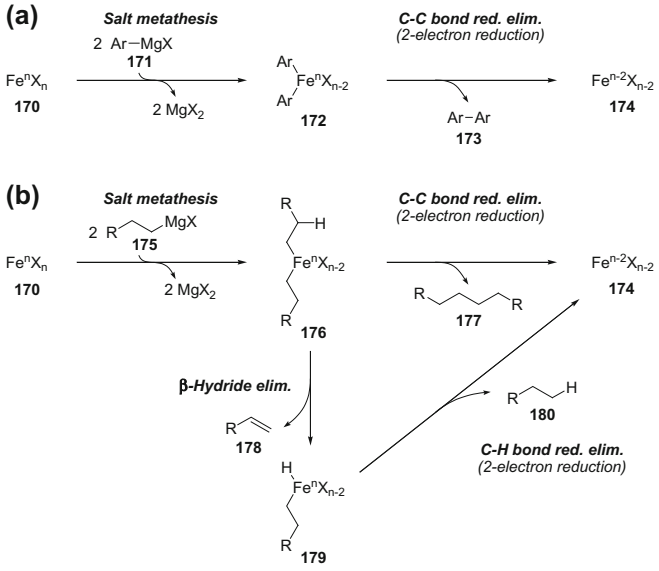

Scheme 1.24 Reduction of iron salts **170** using Grignard reagents: **a** Reduction pathway using arylmagnesium halides **171**; **b** Competing reduction pathways using alkylmagnesium halides bearing β-hydrogen atoms **175**

two-electron reduction of the iron pre-catalyst **170**. For alkyl Grignard reagents bearing β-hydrogen atoms **175** the situation is more complex, with alkane **180**, alkene **178** and alkane dimer **177** products formed (Scheme 1.24b). It has been proposed that the alkane **180** and alkene **178** products are formed following β-hydride elimination from the dialkyliron intermediate **176** to give the alkene **178** and a transient alkyliron-hydride **179**. Carbon-hydrogen bond reductive elimination then gives the alkane product **180** and results in an overall two-electron reduction of the iron pre-catalyst **170**. Although the ratio of these three by-products of reduction can vary depending upon the oxidation-state of iron pre-catalyst and structure of Grignard reagent used, the reduction of iron(II) salts using alkyl Grignard reagents bearing readily-accessible β-hydrogen atoms, such as ethylmagnesium bromide, predominately results in the formation of alkane **180** and alkene **178** products [75]. As the alkane and alkene products are formed in equimolar quantities, the reduction of the iron pre-catalyst **170** may be calculated by quantifying the amount of either the alkane **180** or alkene **178**. Bogdanović has reported that, in the absence of an electrophile/oxidant, the reaction of iron(II) chloride by heptylmagnesium bromide results in a four electron reduction to give an 'inorganic Grignard reagent', $[Fe(MgX)_2]$, where iron is formally in the (–II) oxidation state [76].

Application of Low Oxidation-State Iron Complexes in Hydrofunctionalisation Reactions

Iron-catalysed hydrosilylation was first reported over 50 years ago using iron pentacarbonyl as a pre-catalyst, however a mixture of products arising from hydrosilylation, dehydrosilylation and hydrogenation were obtained, detracting from synthetic utility [79]. The first highly selective catalyst was reported by Chirik, who showed that a formally iron(0) bis(imino)pyridine (BIP) bis(dinitrogen) complex **157** was effective for the hydrosilylation of alkenes **181** to give linear hydrosilylation products **188**, without competitive dehydrosilylation (Scheme 1.25a) [71]. This seminal report stimulated the search for further iron catalysts which featured high activity and chemoselectivity for hydrosilylation, but did not suffer from the high air- and moisture sensitivity typical of bis(imino) pyridine iron bis(dinitrogen) complexes. To date, the most active iron catalysts for the hydrosilylation of simple alkenes and alkynes have all featured the use of a redox-active tridentate ligand (Scheme 1.25a, b) [80]. The potential industrial applicability of iron-catalysed hydrosilylation has been demonstrated in the synthesis of silicone polymers [80a], which were reported to be identical to those produced with commercial platinum catalysts. The iron-catalysed hydrosilylation of

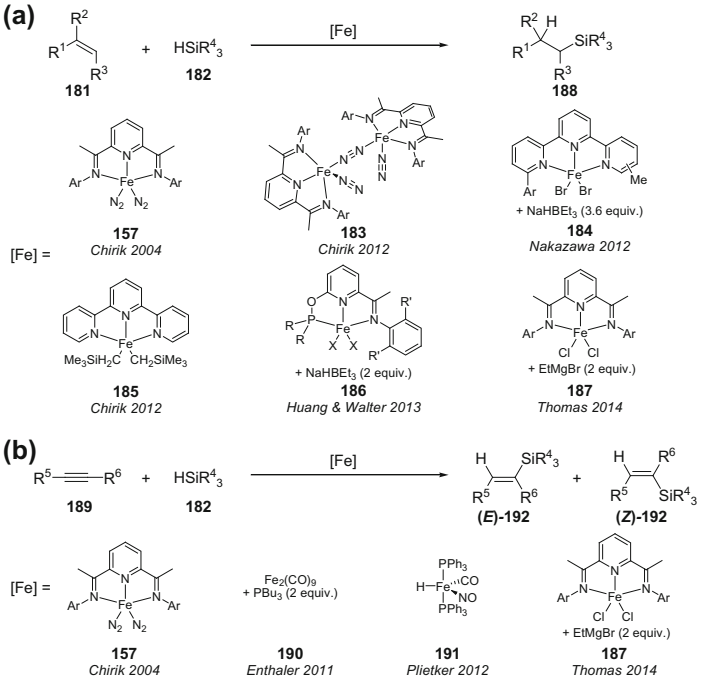

Scheme 1.25 Iron catalysts reported by different research groups for the iron-catalysed hydrosilylation of alkenes (**a**) and alkynes (**b**)

alkynes **189** has also been reported using iron carbonyl clusters **190** and a (nitroso) iron hydride complex [$FeH(CO)NO(PPh_3)_2$] **191** as pre-catalysts (Scheme 1.25b) [81]. In both cases a mixture of diastereoisomers, **(*E*)-192** and **(*Z*)-192**, were obtained however the diastereoselectivity of hydrosilylation could be controlled in some cases by judicious choice of the ligand or silane used.

Iron-catalysed hydrovinylation has also been studied for many years, with all methodologies to date reporting the 1,4-hydrovinylation of 1,3-dienes [59b]. The majority of work was conducted 40–50 years ago and focussed on the hydrovinylation of simple dienes with ethylene **193** (Scheme 1.26a). The catalytically active iron species in these reactions was proposed to be an iron(0) complex [82], which was commonly prepared in situ by the reduction of an iron(III) pre-catalyst using an organoaluminium or organomagnesium reagent. The addition of bidentate phosphine ligands was found to improve catalytic activity (Scheme 1.26b) [83]. This was attributed to the formation of an iron species with an appropriate conformation to bind the 1,3-diene substrate in an η^4-fashion and prevent side-reactions. tom Dieck developed an enantioselective iron-catalysed 1,4-hydrovinylation reaction by using iron complexes bearing enantiopure

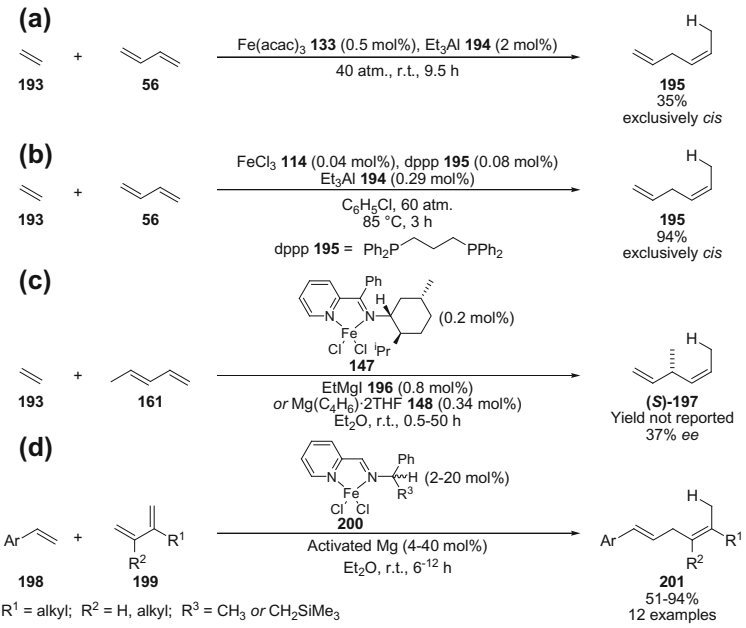

Scheme 1.26 Iron-catalysed 1,4-hydrovinylation of 1,3-dienes. **a** 1,4-hydrovinylation of 1,3-butadiene **56** with ethylene **193** using an iron pre-catalyst reduced in situ with triethylaluminium **194**; **b** Improvement in activity using a bidentate phosphine ligand **195**; **c** Enantioselective 1,4-hydrovinylation of 1,3-pentadiene **161** with ethylene **193** using an iminopyridine iron complex **147** reduced in situ with organomagnesium reagents; **d** Expansion of substrate scope for iron-catalysed 1,4-hydrovinylation of 1,3-dienes

redox-active iminopyridne ligands **147** (Scheme 1.26c) [84]. Only moderate enantioselectivities and limited examples were reported however. A broader substrate scope for iron-catalysed 1,4-hydrovinylation was subsequently reported by Ritter, using an iminopyridine iron(II) pre-catalyst **200** (Scheme 1.26d) [85]. Following pre-catalyst activation using activated magnesium, a selection of styrene derivatives **198** and allylbenzene were reacted with 2-, and 2,3-disubstituted 1,3-dienes **199**. For unsymmetrical dienes, vinylation occurred at the least sterically hindered end of the diene.

Ritter extended the work on the iron-catalysed 1,4-hydrofunctionalisation of 1,3-dienes to include hydroboration and hydrosilylation, by using similar iron complexes bearing bidentate iminopyridine ligands (Scheme 1.27) [86]. The use of bidentate ligands in these reactions is in contrast to iron-catalysed hydrosilylation of simple alkenes (Scheme 1.25), where tridentate ligands are commonly used, and presumably reflects the difference in free coordination sites on iron required for η^2-alkene, and η^4-diene binding.

The 1,4-hydroboration of 1,3-dienes **202** was achieved using pinacol borane **93** as the boron source, and provided the first example of an iron-catalysed hydroboration of an olefin (Scheme 1.27a) [86a]. Allyl boronic ester products **204** and **205**

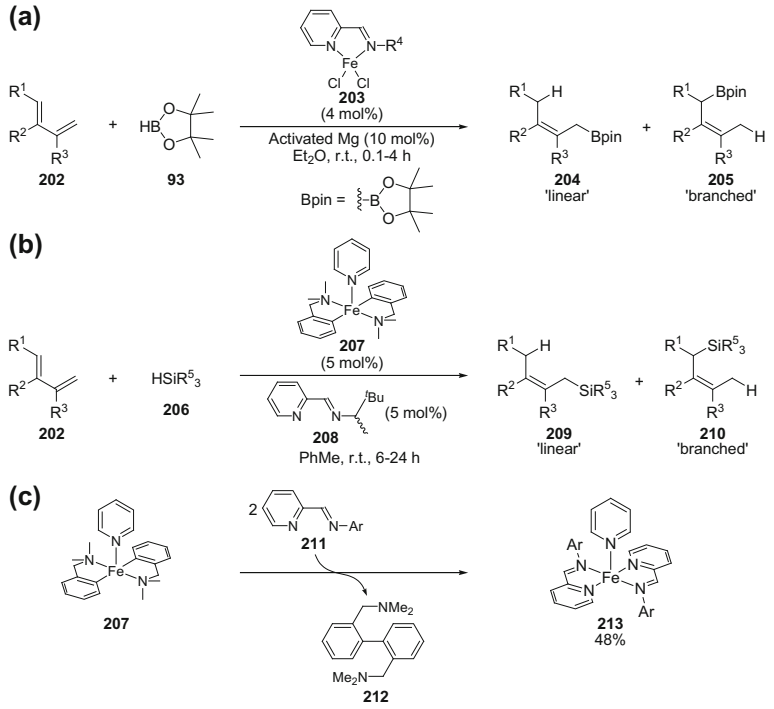

Scheme 1.27 Iron-catalysed 1,4-hydrofunctionalisation of 1,3-dienes using an iminopyridine iron catalyst. **a** Hydroboration using pinacol borane; **b** Hydrosilylation using tertiary silanes; **c** Reduction of iron(II) pre-catalyst **207** through carbon–carbon bond reductive elimination

were obtained in good to excellent yield and with control of regio- and diastereoselectivity. For the 1,4-hydrosilylation of 1,3-dienes **202**, a modified procedure was used for the formation of the low oxidation-state iron iminopyridine catalyst (Scheme 1.27b) [86b]. A bis(aryl) iron(II) pre-catalyst **207** was used, which following the addition of an iminopyridine ligand **208** was proposed to produce an iron(0) species in situ following carbon–carbon bond reductive elimination of a biaryl by-product. This proposal was supported by the stoichiometric reaction between iron(II) pre-catalyst **207** and 2 equivalents of an iminopyridine ligand **211** (Scheme 1.27c) [86b]. A formally iron(0) complex **213** was isolated along with 1 equivalent of the expected biaryl by-product **212**. Using this approach, the 1,4-hydrosilylation of 1,3-dienes **202** with tertiary silanes **206** gave allyl silanes **209** and **210** in good to excellent yields (Scheme 1.27b). The optimal iron-to-iminopyridine ligand ratio was 1:1, with an excess of iminopyridine **208** retarding the rate of the reaction, presumably by competing with the 1,3-diene **202** or silane **206** for coordination sites on iron. This indicated the active catalyst was most likely a mono-ligated low-oxidation iron complex.

The iron-catalysed hydroboration of simple alkenes **214** has recently been reported by a number of groups (Scheme 1.28) [87]. In keeping with iron-catalysed hydrosilylation [71, 80, 81], the majority of methodologies have involved the use of simple iron carbonyl complexes or iron complexes bearing tridentate redox-active ligands. In all cases excellent levels of regioselectivity for linear boronic ester products **219** has been reported. Very recently, an enantioselective iron-catalysed hydroboration of 1,1-disubstituted alkenes has been reported using an iminopyridine oxazoline iron catalyst **217** [87f]. High yields and enantioselectivities of over

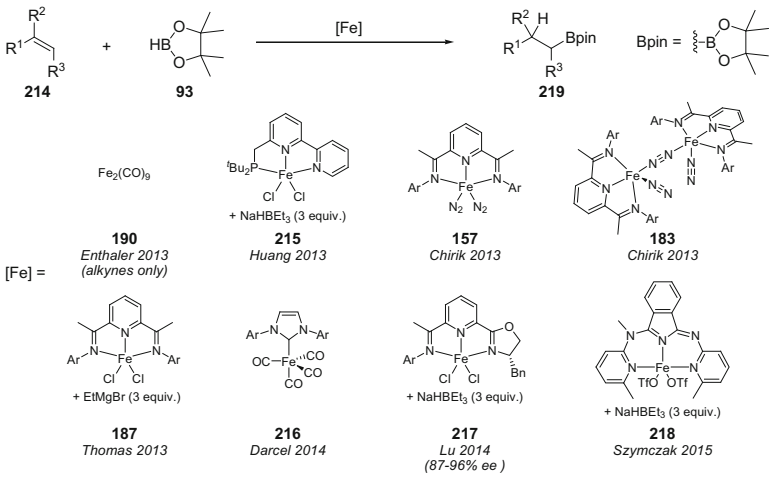

Scheme 1.28 Iron catalysts reported by different research groups for the iron-catalysed hydroboration of alkenes and alkynes

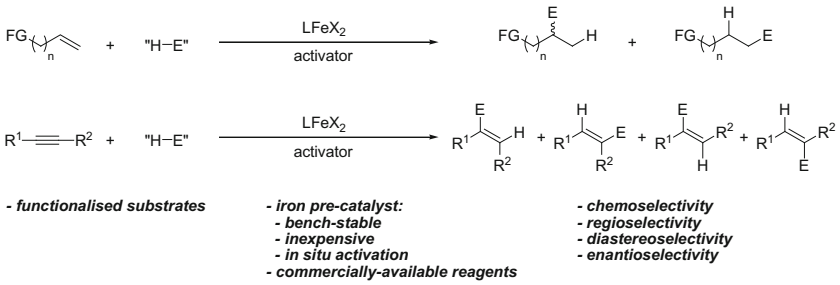

Scheme 1.29 Project aims: development of operationally-simple iron-catalysed hydrofunctionalisation methodologies using commercially-available reagents

90 % ee were generally reported, representing the first efficient iron-catalysed methodology for the enantioselective reduction of alkenes [88].

1.4 General Aims

We aimed to develop operationally-simple iron-catalysed methodologies for the hydrofunctionalisation of alkenes and alkynes which would make use of a bench-stable iron pre-catalyst and commercially-available reagents (Scheme 1.29). By in situ reduction of a bench-stable pre-catalyst we would investigate the use of low oxidation-state iron catalysts in hydrofunctionalisation reactions. Key to making the developed methodology practical for use by the synthetic chemistry community would be a thorough evaluation of the chemo-, regio- and stereoselectivity of the process. Investigation of the mechanism of any developed methodology would be used to help better understand the fundamental science involved and direct future research efforts.

References

1. *Cross-Coupling Reactions. A Practical Guide*; Miyaura, N., Ed.; Springer: Berlin, 2002.
2. (a) *Hydrofunctionalization*; Ananikov, V. P., Tanaka, M., Eds.; Topics in Organometallic Chemistry; Spinger-Verlag: Berlin, Heidelberg, 2013. (b) Zeng, X. *Chem. Rev.* **2013**, *113*, 6864.
3. *Science of synthesis: Houber-Weyl methods of molecular transformations. 47, Alkenes*; Bellus, D., de Meijere, A., Eds.; Georg Thieme: New York, 2009.
4. (a) Eisenstein, O.; Hoffmann, R. *J. Am. Chem. Soc.* **1981**, *103*, 4308. (b) Cameron, A. D.; Smith, Jr., V. H.; Baird, M. C. *J. Chem. Soc., Dalton Trans.* **1988**, 1037.
5. Hanley, P. S.; Hartwig, J. F. *Angew. Chem. Int. Ed.* **2013**, *52*, 8510.
6. Chalk, A. J.; Harrod, J. F. *J. Am. Chem. Soc.* **1965**, *87*, 16.
7. (a) Schroeder, M. A.; Wrighton, M. S. *J. Organomet. Chem.* **1977**, *128*, 345. (b) Randolph, C. L.; Wrighton, M. S. *J. Am. Chem. Soc.* **1986**, *108*, 3366.

8. (a) Bhaduri, S.; Mukesh, D. *Homogeneous Catalysis: Mechanisms and Industrial Applications;* Wiley: Hoboken, 2014; pp 131-166. (b) Franke, R.; Selent, D.; Börner, A. *Chem. Rev.* **2012**, *112*, 5675. (c) Marciniec, B. *Hydrosilylation: A Comprehensive Review on Recent Advances*; Springer: Berlin, 2009.
9. Raff, D. K. Butanals. In *Ullmann's Encyclopedia of Industrial Chemistry*; Wiley-VCH: Weinheim, 2000.
10. van Leeuwen, P. W. N. M.; Kamer, P. C. J.; Reel, J. N. H. *Pure Appl. Chem.* **1999**, *71*, 1443.
11. (a) Karstedt, B. D. (General Electric Company) Platinum complexes of unsaturated siloxanes and platinum containing organopolysiloxanes US3775452, **1973**. (b) Hitchcock, P. B.; Lappert, M. F.; Wargurst, N. J. W. *Angew. Chem. Int. Ed. Engl.* **1991**, *30*, 438.
12. Stein, J.; Lewis, L. N.; Gao, Y.; Scott, R. A. *J. Am. Chem. Soc.* **1999**, *121*, 3693.
13. (a) Markó, I. E.; Stérin, S.; Buisine, O.; Mignani, G.; Branlard, P.; Tinant, B.; Declercq, J.-P. *Science* **2002**, *298*, 204. (b) Troegel, D.; Stohrer, J. *Coord. Chem. Rev.* **2011**, *255*, 1440.
14. (a) Tamao, K.; Ishida, N.; Tanaka, T.; Kumada, M. *Organometallics* **1983**, *2*, 1694. (b) Fleming, I.; Henning, R.; Plaut, H. *J. Chem. Soc. Chem. Commun.* **1984**, 29.
15. Hatanaka, Y.; Hiyama, T. *J. Org. Chem.* **1988**, *53*, 918. (b) Denmark, S. E.; Regens, C. S. *Acc. Chem. Res.* **2008**, *41*, 1486.
16. Fleming, I.; Barbero, A.; Walter, D. *Chem. Rev.* **1997**, *97*, 2063.
17. Jensen, J. F.; Svendsen, B. Y.; la Cour, T. V.; Pedersen, H. L.; Johannsen, M. *J. Am. Chem. Soc.* **2002**, *124*, 4558.
18. *Boronic Acids: Preparation and Applications in Organic Synthesis and Medicine*; Hall, D. G., Ed.; Wiley-VCH: Weinheim, 2005.
19. (a) Burgess, K.; Ohlmeyer, M. J. *J. Org. Chem.* **1988**, *53*, 5179. (b) Hayashi, T.; Matsumoto, Y.; Ito, Y. *J. Am. Chem. Soc.* **1989**, *111*, 3426. (c) Doucet, H.; Fernandez, E.; Layzell, T. P.; Brown, J. M. *Chem. Eur. J.* **1999**, *5*, 1320.
20. Crudden, C. M.; Edwards, D. *Eur. J. Org. Chem.* **2003**, 4695.
21. Nugent, T. C. Asymmetric Reductive Amination. In *Chiral Amine Synthesis. Methods, Developments and Applications*; Nugent, T. C., Ed.; Wiley-VCH: Weinheim, 2010; pp 225-245.
22. Reznichenko, A. L.; Nawara-Hultzsch, A. J.; Hultzch, K. C. *Top. Curr. Chem.* **2014**, *343*, 191.
23. Zhou, S.; Hartwig, J. *J. Am. Chem. Soc.* **2008**, *130*, 12220.
24. (a) BGS (2012a), Risk list 2012, Nottingham, U.K., British Geological Survey. (b) *The Role of the Chemical Sciences in finding Alternatives to Critical Resources;* Friedman, D., Masciangioli, T., Olson, S. Eds.; The National Academies Press: Washington, 2012.
25. Albrecht, M.; Bedford, R. B.; Plietker, B. *Organometallics* **2014**, *33*, 5619.
26. (a) Reznichenko, A. L.; Kultzsch, K. C. In *Hydrofunctionalization*; Ananikov, V. P., Tanaka, M., Eds.; Topics in Organometallic Chemistry; Spinger-Verlag: Berlin, Heidelberg, 2013; pp 51-114. (b) Crimmin, M. R.; Hill, M. S. In *Alkaline-Earth Metal Compounds*; Harder, S. Ed.; Topics in Organometallic Chemistry; Spinger-Verlag: Berlin, Heidelberg, 2013; pp 191-241.
27. (a) Gagné, M. R.; Stern, C. L.; Marks, T. J. *J. Am. Chem. Soc.* **1992**, *114*, 275. (b) Fu, P.-F.; Brard, L.; Li, Y.; Marks, T. J. *J. Am. Chem. Soc.* **1995**, *117*, 7157.
28. Kesti, M. R.; Waymouth, R. M. *Organometallics* **1992**, *11*, 1095.
29. Walsh, P. J.; Baranger, A. M.; Bergman, R. G. *J. Am. Chem. Soc.* **1992**, *114*, 1708.
30. (a) Bexrud, J.A.; Beard, J. D.; Leitch, D. C.; Schafer, L. L. *Org. Lett.* **2005**, *7*, 1959. (b) Kim, H.; Lee P.H.; Livinghouse, T. *Chem. Commun*. **2005**, 5205.
31. (a) Martínez, P. H.; Hultzsch, K. C.; Hampel, F. *Chem. Commun.* **2006**, 2221. (b) Zhang, X.; Emge, T. J.; Hultzsch, K. C. *Angew. Chem. Int. Ed.* **2012**, *51*, 394. (c) Gribkov, D. V.; Hultzsch, K. C.; Hampel, F. *J. Am. Chem. Soc.* **2006**, *128*, 3748. (d) Manna, K.; Xu, S.; Sadow, A. D. *Angew. Chem. Int. Ed.* **2011**, *50*, 1865.
32. Gountchev, T. I.; Tilley, T. D. *Organometallics* **1999**, *18*, 5661.
33. Buch, F.; Harder, S. *Z. Naturforsch.* **2008**, *63b*, 169.
34. Bini, L.; Müller, C.; Vogt, D. *Chem. Commun.* **2010**, *46*, 8325.
35. (a) RajanBabu, T. V. *Synlett* **2009**, 853. (b) Hilt, G. *Eur. J. Org. Chem.* **2012**, 4441.

36. (a) Seidel W. C.; Tolman, C. A. Hydrocyanation of conjugated diolefins. U.S. Patent 3850973, November 26, 1974. (b) Tolman, C. A. *J. Chem. Educ.* **1986**, 6*3*, 199.
37. Musser, M. T. Adipic Acid. In *Ullmann's Encyclopedia of Industrial Chemistry*; Wiley-VCH: Weinheim, 2005.
38. (a) Baker, M. J.; Harrison, K. N.; Orpen, A. G.; Pringle, P. G.; Shaw, G. *J. Chem. Soc. Chem. Commun*. **1991**, 803. (b) Kranenburg, M.; Kamer, P. C. J.; van Leeuwen, P. W. N. M.; Vogt, D.; Keim, W. *J. Chem. Soc., Chem. Commun.* **1995**, 2177.
39. (a) T. V. RajanBabu, A. L. Casalnuovo, *J. Am. Chem. Soc.* **1992**, 114, 6265. (b) T. V. RajanBabu, A. L. Casalnuovo, *J. Am. Chem. Soc.* **1996**, *118*, 6325.
40. (a) Zhang, A.; RajanBabu, T. V. *Org. Lett.* **2004**, *6*, 1515. (b) Liu, W.; RajanBabu, T. V. *J. Org. Chem.* **2010**, *75*, 7636.
41. Ceder, R.; Muller, G.; Ordinas, J. I. *J. Mol. Catal.* **1994**, *92*, 127.
42. Hoberg, H.; Peres, Y.; Krüger, C.; Tsay, Y.-H. *Angew. Chem. Int. Ed. Engl.* **1987**, *26*, 771.
43. Hoberg, H.; Peres, Y.; Milchereit, A. *J. Organomet. Chem.* **1986**, *307*, C38.
44. Williams, C. M.; Johnson, J. B.; Rovis, T. *J. Am. Chem. Soc.* **2008**, *130*, 14936.
45. Sharma, R. K.; RajanBabu, T. V.; *J. Am. Chem. Soc.* **2010**, *132*, 3295.
46. (a) Zhang, A.; RajanBabu, T. V. *J. Am. Chem. Soc.* **2006**, *128*, 54. (b) Saha, B.; Smith, C. R.; RajanBabu, T. V. *J. Am. Chem. Soc.* **2008**, *130*, 9000.
47. Obligacion, J. V.; Chirik, P. J. *J. Am. Chem. Soc.* **2013**, *135*, 19107.
48. Zhang, L.; Zuo, Z.; Leng, X.; Huang, Z. *Angew. Chem. Int. Ed.* **2014**, *53*, 2696.
49. (a) Zhang, L.; Zuo, Z.; Wan, X.; Huang, Z. *J. Am. Chem. Soc.* **2014**, *136*, 15501. (b) Chen, J.; Xi, T.; Ren, X.; Cheng, B.; Guo, J.; Lu, Z. *Org. Chem. Front.* **2014**, *1*, 1306.
50. (a) Harrod, J. F.; Chalk, A. J. *J. Am. Chem. Soc.* **1965**, *87*, 1133. (b) Chalk, A. J.; Harrod, J. F. *J. Am. Chem. Soc.* **1967**, *89*, 1640.
51. Mo, Z.; Liu, Y.; Deng, L. *Angew. Chem. Int. Ed.* **2013**, *52*, 10845.
52. Atienza, C. C. H.; Diao, T.; Weller, K. J.; Nye, S. A.; Lewis, K. M.; Delis, J. G. P.; Boyer, J. L.; Roy, A. K.; Chirik, P. J. *J. Am. Chem. Soc.* **2014**, *136*, 12108.
53. Seitz, F.; Wrighton, M. S. *Angew. Chem. Int. Ed. Engl.* **1988**, *27*, 289.
54. Cox, P. A. *The Elements: Their Origin, Abundance, and Distribution*; Oxford University Press: Oxford, 1989.
55. Enthaler, S.; Junge, K. Beller, M. *Angew. Chem. Int. Ed.* **2008**, *47*, 3317.
56. (a) *Guidance on the specification limits for residues of metal catalysts or metal reagents*, European Medicines Agency, **2008**, Doc. Ref. EMEA/CHMP/SWP/4446/2000. (b) Venugopal, B.; Luckey, T. D. *Metal Toxicity in Mammals;* vol. 2, Plenum Press: New York, 1978.
57. (a) Leitner, A. In *Iron Catalysis in Organic Chemistry: Reactions and Applications*; Plietker, B., Ed.; Wiley-VCH: Weinheim, 2008; pp 147-176. (b) Czaplik, W. M.; Mayer, M.; Cvengroš, J.; Jacobi von Wangelin, A. *ChemSusChem* **2009**, *2*, 396.
58. (a) Le Bailly, B. A. F.; Thomas, S. P. *RSC Advances* **2011**, *1,* 1435. (b) Junge, K.; Schröder, K.; Beller, M. *Chem. Commun.* **2011**, *47*, 4849. (c) Nagashime, H.; Sunada, Y.; Nishikata, T.; Chaiyanurakkul, A. In *The Chemistry of Organoiron Compounds;* Marek, I., Ed.; Wiley: Hoboken, 2014; pp 325-378. (d) Schröder, K.; Junge, K.; Bitterlich, B.; Beller, M. *Top. Organomet. Chem.* **2011**, *33*, 83.
59. (a) Nakazawa, H.; Itazaki, M. *Top. Organomet. Chem.* **2011**, *33*, 27. (b) Greenhalgh, M. D.; Jones, A. S.; Thomas, S. P. *ChemCatChem* **2015**, *7*, 190.
60. Vrancken, E.; Campagne, J.-M. In *The Chemistry of Organoiron Compounds*; Marek, I., Ed.; Wiley-Blackwell: Hoboken, 2014; pp 419-498.
61. Bernoud, E.; Oulie, P.; Guillot, R.; Mellah, M.; Hannedouche, J. *Angew. Chem. Int. Ed.* **2014**, *53*, 4930.
62. Greenhalgh, M. D.; Thomas, S. P. *ChemCatChem* **2014**, *6*, 1520.
63. (a) Leggans, E. K.; Barker, T. J.; Duncan, K. K.; Boger, D. L. *Org. Lett*. **2012**, *14*, 1428. (b) Barker, T. J.; Boger, D. L. *J. Am. Chem. Soc.* **2012**, *134*, 13588.
64. (a) Lo, J. C.; Yabe, Y.; Baran, P. S. *J. Am. Chem. Soc.* **2014**, *136*, 1304. (b) Lo, J. C.; Gui, J.; Yabe, Y.; Pan, C.-M.; Baran, P. S. *Nature* **2015**, *516*, 343.

65. Bolm, C.; Legros, J.; Le Paih, J.; Zani, L. *Chem. Rev.* **2004**, *104*, 6217.
66. Wrighton, M. *Chem. Rev.* **1974**, *74*, 401.
67. a) Fürstner, A.; Martin, R.; Krause, H.; Seidel, G.; Goddard, R.; Lehmann, C. W. *J. Am. Chem. Soc.* **2008**, *130*, 8773. (b) Danopoulos, A. A.; Wright, J. A.; Motherwell, W. B. *Chem. Commun.* **2005**, 784. (c) Tondreau, A. M.; Stieber, S. C. E.; Milsmann, C.; Lobkovsky, E.; Weyhermüller, T.; Semproni, S. P.; Chirik, P. J. *Inorg. Chem.* **2013**, *52*, 635. (d) Brennessel, W. W.; Jilek, R. E.; Ellis, J. E. *Angew. Chem. Int. Ed.* **2007**, *46*, 6132. (e) tom Dieck, H.; Dietrich, J. *Angew. Chem. Int. Ed. Engl.* **1985**, *24*, 781. (f) Adams, C. J.; Bedford, R. B.; Carter, E.; Gower, N. J.; Haddow, M. F.; Harvey, J. N.; Huwe, M.; Cartes, M. A.; Mansell, S. M.; Mendoza, C.; Murphy, D. M.; Neeve, E. C.; Nunn, J. *J. Am. Chem. Soc.* **2012**, *134*, 10333. (g) Hata, G.; Kondo, H.; Miyake, A. *J. Am. Chem. Soc.* **1968**, *90*, 2278.
68. Connelly, N. G.; Geiger, W. E. *Chem. Rev.* **1996**, *96*, 877.
69. (a) Butin, K. P.; Beloglazkina, E. K.; Zyk, N. V. *Russ. Chem. Rev.* **2005**, *74*, 531. (b) Caulton, K. G. *Eur. J. Inorg. Chem.* **2012**, 435.
70. Chirik, P. J. In *Pincer and Pincer-Type Complexes: Applications in Organic Synthesis and Catalysis*; Szabo, K. J., Wendt, O. F., Eds.; Wiley-VCH: Weinheim, 2014; pp 189-212.
71. Bart, S. C.; Lobkovsky, E.; Chirik, P. J. *J. Am. Chem. Soc.* **2004**, *126*, 13794.
72. Bart, S. C.; Chłopek, K.; Bill, E.; Bouwkamp, M. W.; Lobkovsky, E.; Neese, F.; Wieghardt, K.; Chirik, P. J. *J. Am. Chem. Soc.* **2006**, *128*, 13901.
73. Stieber, S. C. E.; Milsmann, C.; Hoyt, J. M.; Turner, Z. R.; Finkelstein, K. D.; Wieghardt, K.; DeBeer, S.; Chirik, P. J. *Inorg. Chem.* **2012**, *51*, 3770.
74. (a) Baldenius, K.-U.; tom Dieck, H.; König, W. A.; Icheln, D.; Runge, T. *Angew. Chem. Int. Ed. Engl.* **1992**, *31*, 305. (b) Frank, D. J.; Guiet, L.; Kaslin, A.; Murphy, E.; Thomas, S. P. *RSC Adv.* **2013**, *3*, 25698. (c) Boukamp, M. W.; Bowman, A. C.; Lobkovsky, E.; Chirik, P. J. *J. Am. Chem. Soc.* **2006**, *128*, 13340.
75. (a) Tamura, M.; Kochi, J. *J. Organomet. Chem.* **1971**, *31*, 289. (b) Tamura, M.; Kochi, J. *Bull. Chem. Jpn. Soc.* **1971**, *44*, 3063.
76. Bogdanović, B.; Schwickardi, M. *Angew. Chem. Int. Ed.* **2000**, *39*, 4610.
77. (a) Kleimark, J.; Hedström, A.; Larsson, P.-F.; Johansson, C.; Norrby, P.-O. *ChemCatChem* **2009**, *1*, 152. (b) Hedström, A.; Lindstedt, E.; Norrby, P.-O. *J. Organomet. Chem.* **2013**, *748*, 51.
78. (a) Bedford, R. B.; Carter, E.; Cogswell, P. M.; Gower, N. J.; Haddow, M. F.; Harvey, J. N.; Murphy, D. M.; Neeve, E. C.; Nunn, J. *Angew. Chem. Int. Ed.* **2013**, *52*, 1285. (b) Guisán-Ceinos, M.; Tato, F.; Buñuel, E.; Calle, P.; Cárdenas, D. J. *Chem. Sci.* **2013**, *4*, 1098.
79. Nesmeyanov, A. N.; Freidlina, R. K.; Chukovskaya, E. C.; Petrova, R. G.; Belyavksy, A. B. *Tetrahedron* **1962**, *17*, 61.
80. (a) Tondreau, A. M.; Atienza, C. C. H.; Weller, K. J.; Nye, S. A.; Lewis, K. M.; Delis, J. G. P.; Chirik, P. J. *Science* **2012**, *335*, 567. (b) Atienza, C. C. H.; Tondreau, A. M.; Weller, K. J.; Lewis, K. M.; Cruse, R. W.; Nye, S. A.; Boyer, J. L.; Delis, J. G. P.; Chirik, P. J. *ACS Catal.* **2012**, *2*, 2169. (c) Kamata, K.; Suzuki, A.; Nakai, Y.; Nakazawa, H. *Organometallics* **2012**, *31*, 3825. (d) Tondreau, A. M.; Atienza, C. C. H.; Darmon, J. M.; Milsmann, C.; Hoyt, H. M.; Weller, K. J.; Nye, S. A.; Lewis, K. M.; Boyer, J.; Delis, J. G. P.; Lobkovsky, E.; Chirik, P. J.; *Organometallics* **2012**, *31*, 4886. (e) Peng, D.; Zhang, Y.; Du, X.; Zhang, L.; Leng, X.; Walter, M. D.; Huang, Z. *J. Am. Chem. Soc.* **2013**, *135*, 19154. (f) Greenhalgh, M. D.; Frank, D. J.; S. P. Thomas, *Adv. Synth. Catal.* **2014**, *356*, 584.
81. (a) Enthaler, S.; Haberberger, M.; Irran, E. *Chem. Asian J.* **2011**, *6*, 1613. (b) Haberberger, M.; Irran, E.; Enthaler, S. *Eur. J. Inorg. Chem.* **2011**, 2797. (c) Belger, C.; Plietker, B. *Chem. Commun.* **2012**, *48*, 5419.
82. Hata, G.; Kondo, H.; Miyake, A. *J. Am. Chem. Soc.* **1968**, *90*, 2278.
83. Iwamoto, M.; Yuguchi, S. *J. Org. Chem.* **1966**, *31*, 4290.
84. Ehlers, J.; König, W. A.; Lutz, S.; Wenz, G.; tom Dieck, H. *Angew. Chem. Int. Ed. Engl.* **1988**, *27*, 1556.
85. Moreau, B.; Wu, J. Y.; Ritter, T. *Org. Lett.* **2009**, *11*, 337.

86. (a) Wu, J. Y.; Moreau, B.; Ritter, T. *J. Am. Chem. Soc.* **2009**, *131*, 12915. (b) Wu, J. Y.; Stanzl, B. N.; Ritter, T. *J. Am. Chem. Soc.* **2010**, *132*, 13214.
87. (a) Haberberger, M.; Enthaler, S. *Chem. Asian J.* **2013**, *8*, 50. (b) Zhang, L.; Peng, D.; Leng, X.; Huang, Z. *Angew. Chem. Int. Ed.* **2013**, *52*, 3676. (c) Obligacion, J. V.; Chirik, P. J. *Org. Lett*. **2013**, *15*, 2680. (d) Greenhalgh, M. D.; Thomas, S. P. *Chem. Commun*. **2013**, *49*, 11230. (e) Zheng, J.; Sortais, J.-B.; Darcel, C. *ChemCatChem* **2014**, *6*, 763. (f) Chen, J.; Xi, T.; Lu, Z. *Org. Lett.* **2014**, *16*, 6452. (g) Tseng, K.-N. T.; Kampf, J. W.; Szymczak, N. K. *ACS Catal.* **2015**, *5*, 411.
88. The enantioselective iron-catalysed hydrogenation of alkenes has been reported with enantioselectivities of up to 49% ee at low conversion: (a) Hoyt, J. M.; Shevlin, M.; Margulieux, G. W.; Krska, S. W.; Tudge, M. T.; Chirik, P. J. *Organometallics* **2014**, *33*, 5781. (b) Chirik, P. J.; Monfette, S.; Hoyt, J. M.; Friedfeld, M. R. Enantiopure base-metal catalysts for asymmetric catalysis and bis(imino)pyridine iron alkyl complexes for catalysis. U.S. Patent 20130079567 A1, March 28, 2013.

Chapter 2
Iron-Catalysed Hydrosilylation of Alkenes and Alkynes

Abstract The hydrosilylation of alkenes represents one of the largest applications of homogeneous catalysis on an industrial scale, and currently uses precious transition-metal catalysts such as platinum. This chapter deals with the development of an iron-catalysed methodology for the hydrosilylation of alkenes and alkynes using a bench-stable iron(II) pre-catalyst, which could be activated in situ. The reaction scope and limitations are presented along with preliminary mechanistic studies, which lead to a discussion of possible reaction mechanisms and future work required to investigate this method further.

2.1 Introduction

The hydrosilylation of alkenes using iron pentacarbonyl was first reported over 50 years ago. High regioselectivity for linear silane products and good conversions of silane were reported, however excess alkene **220** was required and a mixture of products arising from hydrosilylation **223**, dehydrosilylation **224** and hydrogenation **225** were obtained (Scheme 2.1a) [1]. High temperatures or continual near-UV irradiation was required for pre-catalyst activation and catalyst regeneration following recombination with CO. Although the methodology was not synthetically applicable, Wrighton was intrigued to investigate the mechanism by which dehydrosilylation products were obtained. Based upon work using iron carbonyl complexes, Wrighton was the first to propose and demonstrate the primary catalytic steps of a 'modified Chalk-Harrod' mechanism for the hydrosilylation of alkenes [1c]. The significant proposal in this mechanism was alkene insertion into a metal–silicon bond, rather than alkene insertion into a metal–hydride bond (Scheme 2.1b). Following this seminal work, 'modified Chalk-Harrod' mechanisms have been proposed for cobalt- [2], rhodium- [3], and iridium-catalysed [4] hydrosilylation reactions.

Although not synthetically useful for the hydrosilylation of alkenes, iron carbonyl pre-catalysts have been used for the hydrosilylation of alkynes to give vinyl silane products. Enthaler reported that in the presence of phosphines, iron carbonyl clusters **190** could be used for the synthesis of (*E*)-vinylsilanes (*syn*-addition of Si-H), which were isolated as (*Z*)-alkenes **(*Z*)-229** following protodesilylation

M. Greenhalgh, *Iron-Catalysed Hydrofunctionalisation of Alkenes and Alkynes*, Springer Theses, DOI 10.1007/978-3-319-33663-3_2

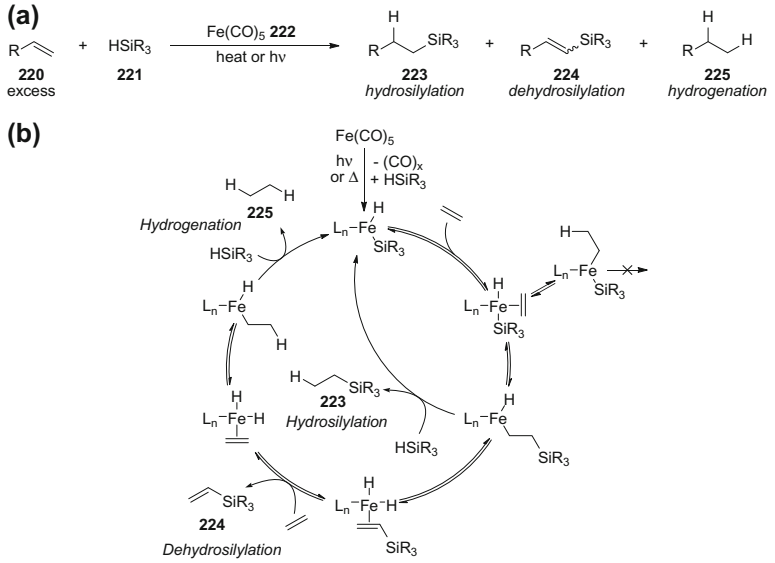

Scheme 2.1 Iron-catalysed hydrosilylation of alkenes using iron pentacarbonyl as a pre-catalyst. **a** General reaction scheme; **b** 'Modified Chalk-Harrod' mechanism proposed by Wrighton

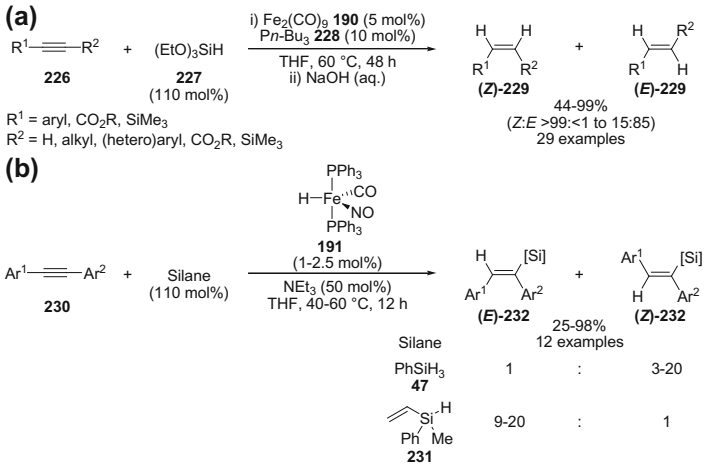

Scheme 2.2 Hydrosilylation of alkynes using iron carbonyl complexes as pre-catalysts. **a** Using a catalyst combination of $Fe_2(CO)_9$ **190** and tributylphosphine **228**; **b** using (nitroso)iron hydride complex $[FeH(CO)NO(PPh_3)_2]$ **191** as pre-catalyst

(Scheme 2.2a) [5]. A range of electronically-differentiated diarylalkynes **226** were hydrosilylated using triethoxysilane **227**, however the excellent stereoselectivity reported for the hydrosilylation of diphenylacetylene did not prove to be general, and a range of yields and stereoselectivities were reported. The hydrosilylation of

diphenylacetylene was also demonstrated in the presence of reducible functional groups, with aldimines, esters, amides, epoxides and nitriles all tolerated, however aldehydes, ketones and sulfoxides were competitively reduced.

Plietker reported a stereodivergent protocol for the hydrosilylation of alkynes **230** using (nitroso)iron hydride complex [$FeH(CO)NO(PPh_3)_2$] **191** as a pre-catalyst (Scheme 2.2b) [6]. In this case, the stereochemical outcome of the hydrosilylation of diphenylacetylene could be controlled to give either the (*Z*)-vinylsilane **(*Z*)-232** (*anti*-addition of Si–H) or (*E*)-vinylsilane **(*E*)-232** (*syn*-addition of Si–H) by varying the nature of the silane used. Phenylsilane **47** gave the (*Z*)-vinylsilane **(*Z*)-232**, arising from the formal *anti*-addition of the Si–H bond to the alkyne, whilst more sterically-demanding tertiary silanes **231** gave the (*E*)-vinylsilane **(*E*)-232** (*syn*-addition of Si–H) selectively. Regioselectivity in the hydrosilylation of unsymmetrical alkynes was not reported, as in this case the products were isolated as alkenes following protodesilylation.

The variation in diastereoselectivity in these reactions may be explained by isomerisation of a common intermediate. If a modified Chalk-Harrod mechanism were in operation then a (*Z*)-metallavinylsilane intermediate **(*Z*)-234** would be formed following alkyne insertion into an iron–silicon bond (Scheme 2.3). This metallavinylsilane may then undergo π-bond isomerisation via a zwitterionic carbenoid [3c] **235** or metallocyclopropene [4b, c] **236** intermediate. The hydrosilylation product **(*E*)-237** or **(*Z*)-237** may then be released following carbon–hydrogen bond formation. The diastereoselectivity of hydrosilylation using different catalysts and different silanes may therefore be explained by comparing the thermodynamic stability of metallavinylsilane intermediates **(*Z*)-234** and **(*E*)-234**, and the rate of isomerisation of the initially formed (*Z*)-metallavinylsilane intermediate **(*Z*)-234** relative to the rate of carbon–hydrogen bond formation to give hydrosilylation product **(*E*)-237** ($k_2 + k_3$ vs. k_1). These thermodynamic and kinetic parameters depend upon the electronic and steric properties of the silane, alkyne and ligands

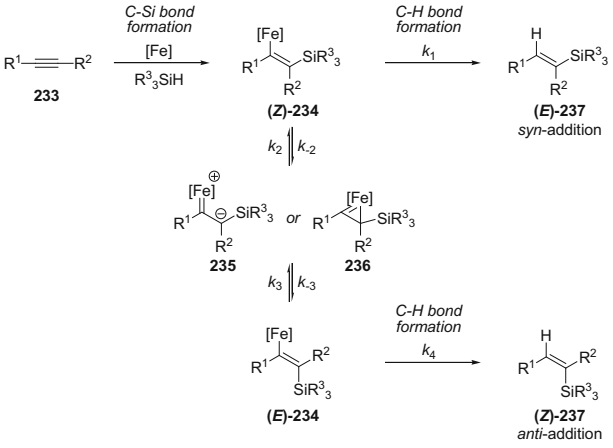

Scheme 2.3 Possible mechanism to explain the stereochemical outcome of iron-catalysed hydrosilylation of alkynes

used in the reaction, and whether carbon–hydrogen bond formation occurs by an intra- or intermolecular reaction.

According to this mechanism the most thermodynamically-favoured metallavinylsilane intermediate will be obtained if the rate of carbon–hydrogen bond formation (k_1) is slower than the rate of metallavinylsilane π-bond isomerisation, **(*Z*)-234** ⇋ **(*E*)-234**, (k_2 + k_3) [3c, 4b, c]. There are a number of factors which can increase or decrease the rate of either process. The rate of carbon–hydrogen bond formation can be slow relative to the rate of (intramolecular) π-bond isomerisation if carbon–hydrogen bond occurs by an intermolecular reaction with another equivalent of silane, through either a σ-bond metathesis or oxidative addition-reductive elimination pathway. The rate of carbon–hydrogen bond formation will also be affected by the nature of the catalyst and the structure of the silane used (e.g. silanes bearing electron-withdrawing groups undergo oxidative addition more quickly than those bearing electron-donating groups) [3c]. The rate of π-bond isomerisation between the metallavinylsilane intermediates [**(*Z*)-234** ⇋ **(*E*)-234**] can be retarded by sterically demanding silanes, alkyne substituents or iron catalysts, in particular if isomerisation occurs through a sterically-congested metallocyclopropene intermediate **236**. In both of the proposed intermediates **235** and **236** there is also significant charge separation, with a build-up of negative charge α- to silicon (and β- to R^2) and a build-up of positive charge β- to silicon (and α- to R^1). Stabilisation of these intermediates by electron-donating or electron-withdrawing substituents on the alkyne (or catalyst), in combination with the ability of silicon groups to stabilise both α-anions and β-cations [7], can be used to help rationalise the relative accessibility of these reaction intermediates.

A classic example in which this mechanism has been used to justify the stereoselectivity of hydrosilylation is in iridium- and rhodium-catalysed hydrosilylation of terminal alkynes **238** [3c, 4b, c]. In both cases the thermodynamically less favoured (*Z*)-vinylsilane product **(*Z*)-240** was obtained selectively (Scheme 2.4). Carbon–hydrogen bond formation was proposed to occur through an intermolecular reaction at a sufficiently slow rate to allow efficient isomerisation between the

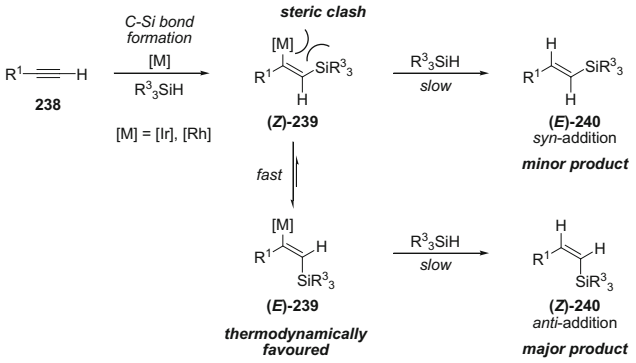

Scheme 2.4 Proposed mechanism to explain the stereochemical outcome of iridium- and rhodium-catalysed hydrosilylation of terminal alkynes

metallavinylsilane intermediates [**(*Z*)-239** ⇌ **(*E*)-239**]. The initially formed metallavinylsilane intermediate **(*Z*)-239** was proposed to be destabilised by the steric clash between the iridium/rhodium catalyst and silane group. π-Bond isomerisation would relieve this steric clash and give the more thermodynamically-stable (*E*)-metallavinylsilane intermediate **(*E*)-239**. Carbon–hydrogen bond formation from this intermediate then gives the (*Z*)-vinylsilane **(*Z*)-240** as the major product.

In 2004 Chirik reported that bis(imino)pyridine (BIP) iron(0) bis(dinitrogen) complexes **157** were active for the hydrosilylation of alkenes and alkynes (Scheme 2.5a) [8]. The hydrosilylation of terminal alkenes **241** (R^3 = H) gave linear silane products **242** (R^3 = H) with complete control of regiochemistry, and with no concurrent formation of dehydrosilylation products. Whilst primary alkenes readily underwent hydrosilylation, 1,1- and 1,2-disubstituted alkenes reacted more slowly and tri-substituted alkenes were unreactive, allowing for the chemoselective hydrosilylation of less-substituted alkenes. The hydrosilylation of diphenylacetylene using phenylsilane gave the (*E*)-vinylsilane product stereoselectively (*syn*-addition of Si–H), which is in contrast to the methodologies reported by Enthaler and Plietker, where either low diastereoselectivities or selectivities in favour of the (*Z*)-vinylsilane product (*anti*-addition of Si–H) were observed when using the same substrates. Bis(imino)pyridine ligands (BIP) are known to be redox-active (non-innocent), with the potential to accept up to three electrons [9], and it was shown that the formally iron(0) complex used in these reactions was better described as a resonance hybrid between iron(0) and iron(II) (Scheme 1.22c) [10]. The high activity and selectivity reported by Chirik in this seminal report inspired much of the work in the past decade on iron-catalysed hydrogenation and hydrofunctionalisation reactions using low oxidation-state iron catalysts.

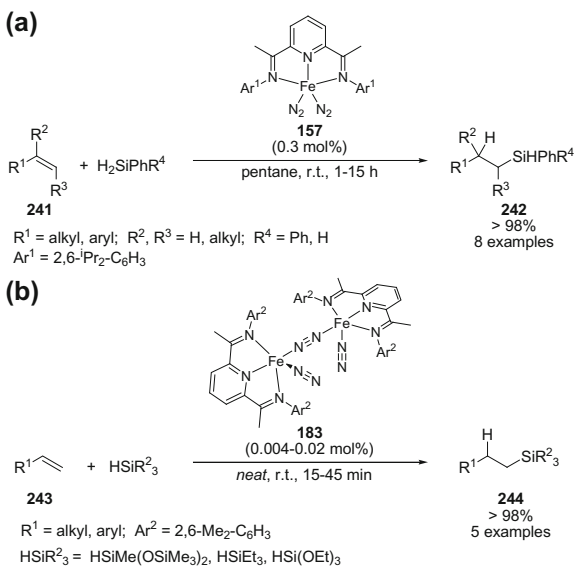

Scheme 2.5 Hydrosilylation of alkenes using bis(imino) pyridine (BIP) iron bis (dinitrogen) complexes. **a** Hydrosilylation using first-generation pre-catalyst; **b** hydrosilylation using second-generation pre-catalyst

Chirik reported a second generation catalyst **183** following the synthesis and characterisation of a number of bis(imino)pyridine iron bis(dinitrogen) complexes and related low oxidation-state iron complexes [11]. Bis(imino)pyridine (BIP) complexes with less sterically-demanding *N*-aryl substituents gave improved activity for the hydrosilylation of alkenes with tertiary silanes, with catalyst turnover frequencies of up to 100,000 mol h^{-1} reported in some examples (Scheme 2.5b) [12]. Silicone polymers prepared using this second generation catalyst were reported to be identical to those prepared using a platinum catalyst, indicating the potential for future industrial applications.

Despite the high catalytic activities reported, bis(imino)pyridine (BIP) iron bis (dinitrogen) complexes are highly air- and moisture sensitive and challenging to prepare and store. These difficulties, in addition to an absence of published work demonstrating chemoselective alkene hydrosilylation in the presence of other reducible functionalities, has stimulated research in this field from Chirik and others.

Nakazawa and Chirik independently investigated the use of tridentate terpyridine (terpy) ligands for iron-catalysed hydrosilylation of alkenes (Scheme 2.6) [13, 14]. Nakazawa prepared a range of iron(II) chloride and bromide terpyridine complexes **184**, which were reduced in situ to give an active catalyst using sodium triethylborohydride **168** (3.6 equiv. with respect to iron) (Scheme 2.6a) [13]. Primary and secondary silanes **246** reacted with terminal alkenes **245** to give linear hydrosilylation products **247**, without competitive dehydrosilylation. High reaction temperatures and long reaction times were required however, and internal alkenes and tertiary silanes were unreactive.

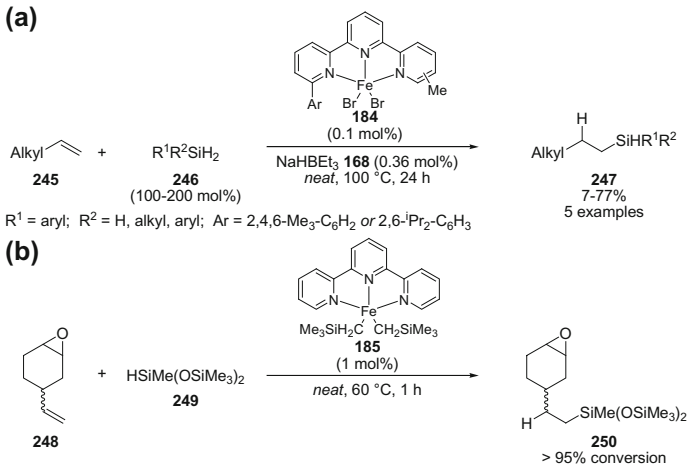

Scheme 2.6 Hydrosilylation of alkenes using iron(II) terpyridine complexes as pre-catalysts. **a** Using an iron(II) halide complex **184** reduced in situ using $NaHBEt_3$ **168**; **b** using an iron(II) dialkyl complex **185**

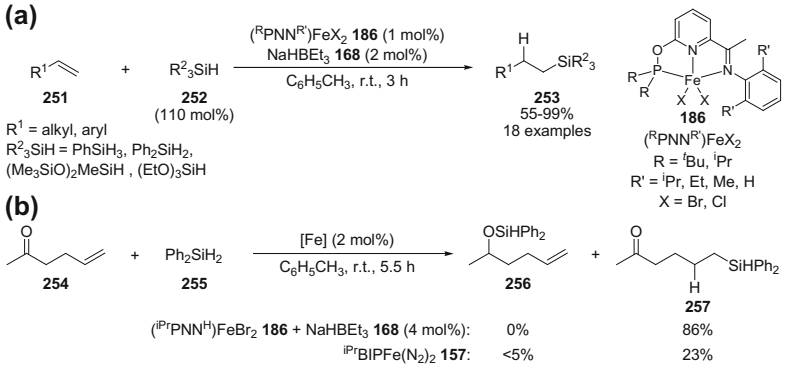

Scheme 2.7 Hydrosilylation of alkenes using a phosphinite-iminopyridine (PNN) iron complex as pre-catalyst. **a** General reaction scheme; **b** comparison of chemoselectivity for alkene and ketone hydrosilylation using iron pre-catalysts **186** and **157**

Chirik used an alternative approach to in situ pre-catalyst activation by preparing a range of iron(II) alkyl complexes bearing terpyridine (terpy), bis(imino)pyridine (BIP) and pyridine bis(oxazoline) (Pybox) ligands [14]. Pre-catalyst activation was achieved by heating at 60 °C, and although this represented a simpler approach than the isolation of formally iron(0) complexes, the iron(II) alkyl complexes used were still highly air- and moisture sensitive. Chirik focussed on hydrosilylation using previously challenging tertiary silanes, and found that the iron(II) alkyl complexes bearing terpyridine (terpy) or bis(imino)pyridine ligands bearing small *N*-aryl substituents were effective pre-catalysts, whilst the Pybox iron(II) alkyl complex was inactive. The terpyridine iron(II) dialkyl pre-catalyst **185** was chemoselective for the hydrosilylation of an industrially relevant epoxide-containing alkene substrate, vinylcyclohexene oxide **248** (Scheme 2.6b). In contrast, substantial substrate or catalyst decomposition was observed using either the bis(imino)pyridine (BIP) iron(II) alkyl pre-catalyst or Karstedt's platinum catalyst [15].

Huang and Walter have reported that phosphinite-iminopyridine (PNN) iron complexes **186** are chemoselective pre-catalysts for the hydrosilylation of alkenes in the presence of carbonyl functionalities (Scheme 2.7) [16]. The iron(II) chloride or bromide pre-catalysts were reduced in situ using sodium triethylborohydride **168** (2 equiv. with respect to iron). The chemoselective hydrosilylation of terminal alkenes **251** was demonstrated in the presence of a number of functional groups, including ethers, tertiary amines, acetals, ketones, esters and amides. Internal alkenes were unreactive however, and substrates containing nitro, nitrile, unprotected alcohol and amine, and heteroaromatic groups were not tolerated. The hydrosilylation of 5-hexan-2-one **254** using PNN iron complex **186** resulted in chemoselective hydrosilylation of the alkene, whilst the bis(imino)pyridine (BIP) iron bis(dinitrogen) complex **157**, gave a combination of alkene and ketone hydrosilylation products **257** and **256** (Scheme 2.7b). The excellent chemoselectivity for alkene

hydrosilylation in the presence of carbonyls was attributed to the electron-donating effect of the PNN ligand, rendering the iron centre less oxophilic relative to bis (imino)pyridine iron complexes.

2.2 Results and Discussion

2.2.1 State of the Art at the Outset of the Project

Bis(imino)pyridine (BIP) iron bis(dinitrogen) complexes were the only highly active pre-catalysts reported for the hydrosilylation of alkenes at the outset of this project (Scheme 2.8). Low catalyst loadings and excellent turnover-frequencies had been reported, however the difficult synthesis and isolation of the formally iron(0) bis (nitrogen) complexes not only limits their practical usage, but also limits the diversity of catalyst structures that can be examined. In addition, the chemoselectivity of the reaction had not been investigated. The hydrosilylation of alkynes had been reported using iron carbonyl complexes, however elevated reaction temperatures, long reaction times and variable diastereoselectivity could be seen to affect synthetic utility.

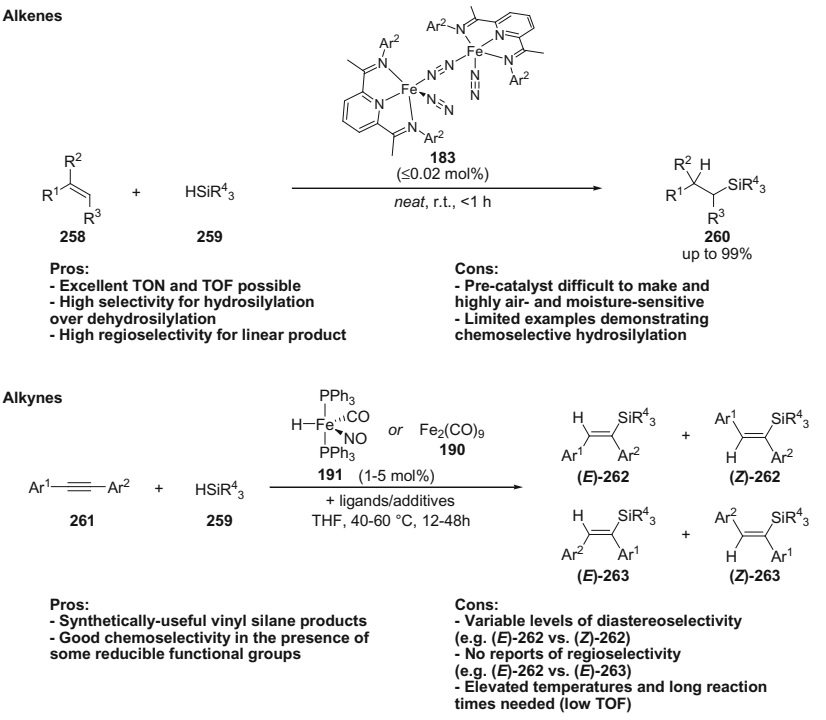

Scheme 2.8 State of the art iron-catalysed hydrosilylation methodologies in early 2012

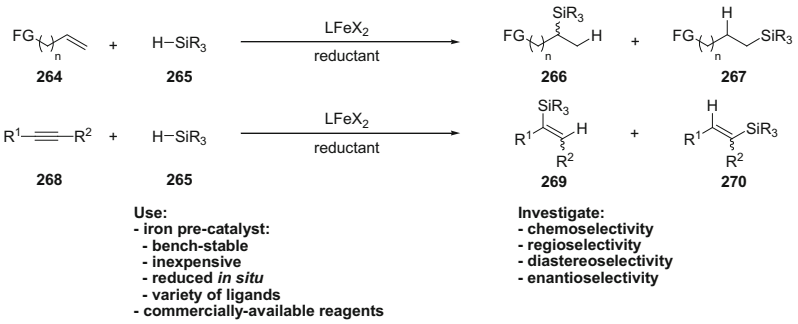

Scheme 2.9 Proposed development of iron-catalysed hydrosilylation methodology

2.2.2 *Project Aims*

The principal objective of this work was to investigate the possibility of using the in situ reduction of an iron pre-catalyst for the hydrosilylation of alkenes (Scheme 2.9). This would allow the use of a bench-stable pre-catalyst and also provide a simple approach to screen a range of different ligands and pre-catalysts. Ideally the pre-catalyst and reducing reagent used should be easy to handle and be commercially-available. The developed methodology would then be applied to the hydrosilylation of a range of alkenes and alkynes focussing on the chemo-, regio- and stereoselectivity of the process.

2.2.3 *Methodology Development*

2.2.3.1 Ligand and Pre-catalyst Synthesis

Bis(imino)pyridine (BIP) ligands **273a-c** bearing sterically-differentiated *N*-aryl substituents were synthesised by condensation of 2,6-diacetylpyridine **271** with two equivalents of an appropriate aniline derivative **272a-c** (Scheme 2.10a) [17]. The reactions were heated at reflux in toluene with *p*-toluenesulfonic acid as a catalyst and with a Dean-Stark apparatus attached [18]. (±)-*N*,*N*′-Bis(pyridin-2-ylmethylene) cyclohexane-1,2-diamine **276** was synthesised by the condensation of two equivalents of 2-pyridinecarboxaldehyde **274** with (±)-*trans*-diaminocyclohexane **275** [19]. In this case molecular sieves were used to remove water from the reaction. Iron(II) bis [1,2-bis(diphenylphosphino)ethane] complex **278** was prepared according to a literature procedure from iron(II) tetrafluoroborate hexahydrate **277** and 1,2-bis (diphenylphosphino)ethane **154** in acetonitrile (Scheme 2.10c) [20, 21].

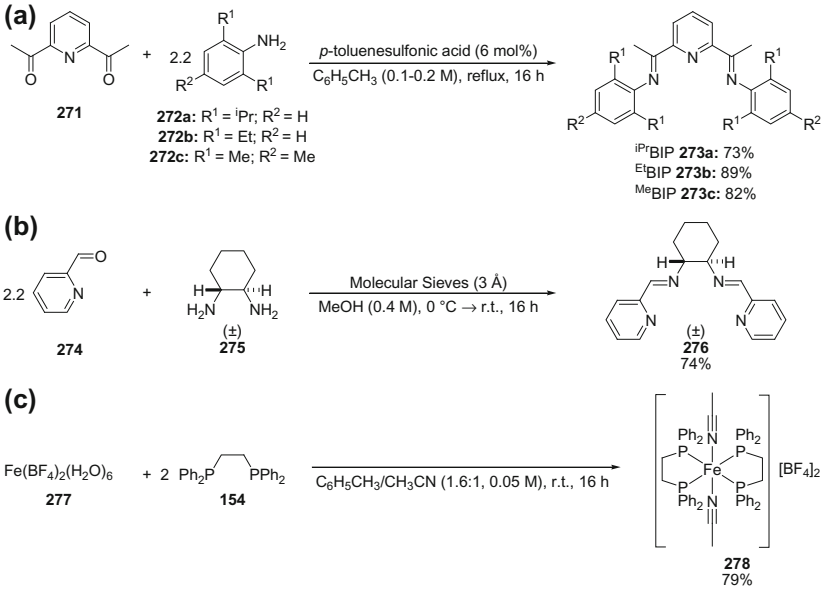

Scheme 2.10 Synthesis of iminopyridine-based ligands **273a-c** and **276** through condensation reactions (**a**, **b**) and iron(II) bis[1,2-bis(diphenylphosphino)ethane] complex **278** (**c**)

2.2.3.2 Reaction Optimisation

Initial studies focussed on the identification of a suitable reducing agent for the in situ activation of a bis(imino)pyridine iron(II) pre-catalyst, and provide a proof of concept (Table 2.1). The hydrosilylation of styrene **53** with phenylsilane **47** in tetrahydrofuran was attempted using a combination of iron(II) chloride **279** and bis (imino)pyridine ligand **273a** (^{iPr}BIP), which were complexed in situ. The use of ethylmagnesium bromide **280** as the in situ reductant was evaluated by systematically varying the quantity of ethylmagnesium bromide **280** used relative to iron pre-catalyst (Table 2.1, entries 1–6). The addition of between two and three equivalents of ethylmagnesium bromide **280** with respect to iron gave the linear hydrosilylation product **281** in quantitative yield within 1 h, without any dehydrosilylation products observed. The use of excess ethylmagnesium bromide **280** resulted in a reduction in catalytic activity, whilst the use of less than two equivalents did not result in any catalytic activity. Similar results were also obtained using *p*-tolylmagnesium bromide **282**, with either two or three equivalents giving an active catalyst (Table 2.1, entries 7–10). Sodium triethylborohydride **168** also produced an active catalyst, however only a moderate yield of hydrosilylation product **281** was obtained in addition to unidentified side-products (Table 2.1, entry 11). The use of *n*-butyllithium **283** resulted in complete conversion of styrene into an unidentified polymeric material, with no hydrosilylation products obtained (Table 2.1, entry 12). Organolithium reagents have been reported to initiate the

rapid polymerisation of styrene in tetrahydrofuran [22], and therefore we investigated the use of *n*-butyllithium as an activating reagent in toluene and hexane. Unfortunately, bis(imino)pyridine iron(II) dihalide complexes are insoluble in non-polar solvents, and so the same in situ complexation approach could not be used to assess hydrosilylation activity. Reduced bis(imino)pyridine iron complexes are reported to be soluble in non-polar solvents however [8], therefore pre-complexed bis(imino)pyridine iron(II) dibromide **156** was used in the hope that a soluble catalyst would be formed following in situ reduction. Using *n*-butyllithium **283** (3 equivalents with respect to iron) in either toluene or hexane now gave an active catalyst, with quantitative conversion to the linear silane **281** again observed within 1 h (Table 2.1, entries 13–14).

The hydrosilylation of styrene **53** with phenylsilane **47** was then investigated using a combination of iron(II) chloride **279** (1 mol%) and a range of ligands, activated in situ using ethylmagnesium bromide **280** (2 mol%) (Table 2.2). The bis(imino)pyridine class of ligands **279a-c** all gave hydrosilylation products in quantitative yield within 1 h (Table 2.2, entries 1–5). Reducing the size of the 2,6-substituents of the *N*-aryl group from ^{iPr}BIP **273a** to ^{Et}BIP **273b** resulted in a

Table 2.1 Identification of iron-catalysed hydrosilylation methodology I: activating agent[a]

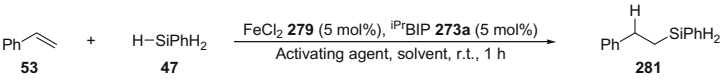

Entry	Activating agent (mol%)	Solvent	Yield (%)[b]
1	EtMgBr **280** (8)	THF	–[c]
2	EtMgBr **280** (10)	THF	>95
3	EtMgBr **280** (13)	THF	>95
4	EtMgBr **280** (16)	THF	91[c]
5	EtMgBr **280** (18)	THF	80[c]
6	EtMgBr **280** (20)	THF	41[c]
7	*p*-TolylMgBr **282** (5)	THF	–[c]
8	*p*-TolylMgBr **282** (10)	THF	>95
9	*p*-TolylMgBr **282** (15)	THF	>95
10	*p*-TolylMgBr **282** (20)	THF	21[c]
11	$NaBHEt_3$ **168** (15)	THF	44[d]
12	*n*-BuLi **283** (15)	THF	–[e]
13[f]	*n*-BuLi **283** (15)	Toluene	>95
14[f]	*n*-BuLi **283** (15)	Hexane	>95

[a]Conditions: styrene **53** (0.7 mmol), $FeCl_2$ **279** (5 mol%), ^{iPr}BIP **273a** (5 mol%), $PhSiH_3$ **47** (0.7 mmol), activating agent (5–20 mol%), solvent (0.25 M), r.t. 1 h; [b]Yield determined by ^{1}H NMR spectroscopy using 1,3,5-trimethoxybenzene as an internal standard; [c]Remaining mass balance accounted for by styrene; [d]Unidentified side-products obtained (~25 %); [e]^{1}H NMR Spectra broad, no starting material or product; [f]Pre-complexed ^{iPr}BIP$FeBr_2$ **156** (5 mol%) used in place of $FeCl_2$ **279** and ^{iPr}BIP **273a**

Table 2.2 Identification of iron-catalysed hydrosilylation methodology II: ligands[a]

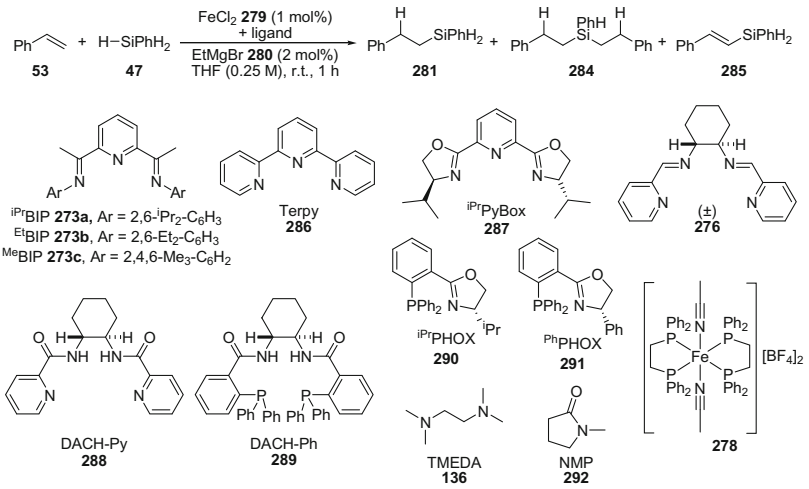

Entry	Ligand/Complex (mol%)	$PhSiH_3$ mol%	Yield (%)[b]		
			281	284[c]	285
1	^{iPr}BIP **273a** (1)	100	>95	–	–
2	^{Et}BIP **273b** (1)	100	60	40	–
3	^{Et}BIP **273b** (1)	110	>95	–	–
4	^{Et}BIP **273b** (1)	50	–	>95	–
5[#]	^{Me}BIP **273c** (1)	120	10	90	–
6	None	110	–	–	–
7[d]	^{Et}BIP **273b** (1)	110	–	–	–
8[e]	^{Et}BIP **273b** (1)	110	>95	–	–
9	Terpy **286** (1)	110	<1	–	2
10	^{iPr}Pybox **287** (1)	110	1	–	1
11	**276** (1)	110	–	–	–
12	DACH-Py **288** (1)	110	–	–	–
13	DACH-Ph **289** (1)	110	–	–	–
14	^{iPr}PHOX **290** (1)	110	<1	–	1
15[d]	^{Ph}PHOX **291** (1)	110	–	–	–
16	TMEDA **134** (4–20)	110	–	–	–
17	NMP **292** (4–20)	110	–	–	–
18	**278** (1)	110	–	–	–

[a]Conditions: styrene **53** (0.7 mmol), $FeCl_2$ **279** (1 mol%), ligand (0.007–0.14 mmol), $PhSiH_3$ **47** (0.35–0.84 mmol), EtMgBr **280** (2 mol%), tetrahydrofuran (0.25 M), r.t., 1 h; [b]Yield determined by ^{1}H NMR spectroscopy using 1,3,5-trimethoxybenzene as an internal standard; [c]Yield of bis (hydrosilylation) product **284** based upon silane; [d]No iron(II) chloride **279** added; [e]High purity iron(II) chloride **279** (99.99 %) used [23]; # = Result obtained by Dominik Frank

mixture of two hydrosilylation products (Table 2.2, entry 2). The new hydrosilylation product had formed through the reaction of the secondary silane product **281** with another equivalent of styrene to give a tertiary silane (bis-silylation product) **284**. The mono-silylation product **281** could be obtained exclusively by using 1.1 equivalents of phenylsilane **47**, whilst the bis-silylation product **284** was quantitatively formed by using 0.5 equivalents of phenylsilane **47** (Table 2.2, entries 3–4). Further reduction in the size of the 2,6-substituents of the *N*-aryl group to ^{Me}BIP **273c** gave a highly active catalyst, however a mixture of mono- and bis-silylation products **281** and **284** were obtained, even when using excess phenylsilane (Table 2.2, entry 5). This suggests that under the developed conditions, bis(imino) pyridine ligands with smaller *N*-aryl substituents form more active iron catalysts for hydrosilylation. This is in keeping with the work of Chirik using isolated bis(imino) pyridine iron bis(dinitrogen) complexes [12a]. No hydrosilylation activity was observed in the absence of either iron(II) chloride **279** or ligand (Table 2.2, entries 6–7), and the use of high purity iron(II) chloride **279** (99.99%) [23] in combination with bis(imino)pyridine ligand **273b** (^{Et}BIP) gave the hydrosilylation product **281** in quantitative yield, attesting to the catalytic activity of iron (Table 2.2, entry 8).

A selection of commercially-available, or easily prepared, bi-, tri- and tetradentate nitrogen- and phosphorous-based ligands were applied in the reaction (Table 2.2, entries 9–17). Iron(II) halide salts do not readily form complexes with phosphine ligands, and therefore the pre-formed iron(II) bis[1,2-bis (diphenylphosphino)ethane] complex **278** was used (Table 2.2, entry 18). None of the ligands or complexes tested were effective for the hydrosilylation of styrene, with only very low yields obtained in some examples. Small quantities of the dehydrosilylation product **285** were also observed. In each example the majority of the mass balance was accounted for by unreacted starting material.

The low activity observed using 2,2′;6′,2″-terpyridine **286** (Table 2.2, entry 9) is in keeping with the results of Nakazawa, who attempted in situ activation of 2,2′;6′,2″-terpyridine iron(II) halide complexes using sodium triethylborohydride for the hydrosilylation of 1-octene using phenylsilane **47** [13]. Nakazawa attributed the lack of hydrosilylation activity to the formation of catalytically inactive bis (terpyridine) iron(II) complexes, $[Fe(terpy)_2][FeX_4]_2$ [24]. The low reactivity using the iso-propyl-substituted pyridine bis(oxazoline) ligand (^{iPr}Pybox) **287** (Table 2.2, entry 10) is also comparable to the work of Chirik, who reported that ^{iPr}Pybox iron (II) dialkyl complexes were ineffective pre-catalysts for the hydrosilylation of 1-octene using tertiary silanes [14]. Chirik has also reported that the sodium amalgam **139** or sodium naphthalenide **142** reduction of ^{iPr}Pybox iron(II) chloride complex **293** gives a catalytically inactive (^{iPr}Pybox)$_2$iron(0) complex **294** (Scheme 2.11) [25]. It is therefore possible that a similar (^{iPr}Pybox)$_2$iron(0) complex is formed following reduction using ethylmagnesium bromide, and may account for the low catalytic activity observed using ^{iPr}Pybox ligand **287**. It is worthwhile noting that the reduction of bis(imino)pyridine iron(II) chloride complexes bearing less sterically demanding ligands, such as ^{Et}BIP **273b** and ^{Me}BIP **273c**, have also been reported to give catalytically-inactive bis(ligand) iron(0) complexes following reduction with sodium amalgam [26]. Sodium naphthalenide

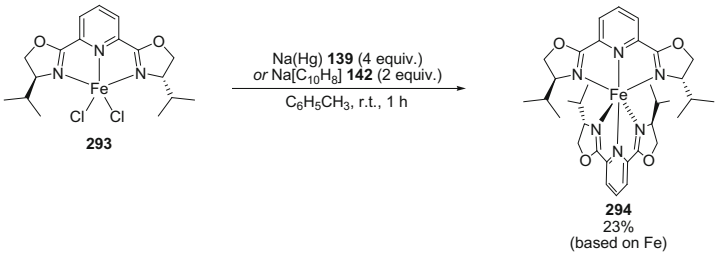

Scheme 2.11 Reduction of ^{iPr}Pybox iron(II) chloride complex **293** using sodium amalgam **139** or sodium naphthalide **142** to give catalytically-inactive (^{iPr}Pybox)$_2$Fe(0) complex **294**

reduction of the same bis(imino)pyridine (BIP) iron(II) chloride complexes was shown to give catalytically-active bis(imino)pyridine iron(0) dinitrogen complexes [11], which may indicate that the developed in situ reduction using ethylmagnesium bromide results in reduced iron species more similar to those obtained by sodium naphthalenide reduction.

The highest activities for the hydrosilylation of styrene **53** with phenylsilane **47** had been obtained using a combination of iron(II) chloride **279** and a bis(imino) pyridine ligand (^{Et}BIP **273b** or ^{Me}BIP **273c**), reduced in situ using ethylmagnesium bromide **280** (2–3 equivalents with respect to iron). The generality of this procedure was investigated to evaluate the scope and limitations in terms of silane structure, alkene and alkyne substitution, functional group tolerance and regio-, diastereo- and enantioselectivity.

2.2.4 Silane Scope and Limitations

Using a combination of iron(II) chloride **279** (1 mol%) and bis(imino)pyridine ligand **273b** (^{Et}BIP) (1 mol%), the hydrosilylation of styrene **53** using secondary silanes gave linear hydrosilylation products in quantitative yield within 1 h (Table 2.3, entries 1–2). Tertiary silanes proved to be much less reactive, giving only poor to moderate yields of the hydrosilylation product, albeit still with complete control of regioselectivity (Table 2.3, entries 3–5). Bis(imino)pyrindine ligand **273c** (^{Me}BIP) had shown high activity for the hydrosilylation of styrene using secondary silanes (Table 2.2, entry 5) and therefore this ligand was tested in the hydrosilylation of styrene using the tertiary silane dimethylphenylsilane **299**. Unfortunately no hydrosilylation product was obtained in this case (Table 2.3, entry 6).

As altering the catalyst structure had not proved effective, the alkene substrate was changed from styrene **53** to 1-hexene **306**, in the hope that the reduced steric effects would improve the efficiency of hydrosilylation. In addition, the significant difference in electronics between styrene **53** and 1-hexene **306** could also have an effect. Using a combination of iron(II) chloride **279** (1 mol%) and bis(imino)pyridine ligand **273b** (^{Et}BIP) (1 mol%), the hydrosilylation of 1-hexene **306** using

Table 2.3 Hydrosilylation of alkenes using different silanes: scope and limitations[a]

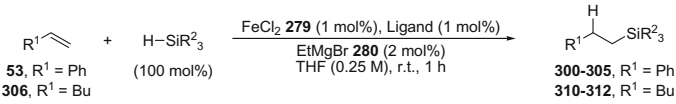

Entry	R^1	Ligand	Silane	Yield (%)[b]
1	Ph	^{Et}BIP **273b**	Ph_2SiH_2 **255**	>95
2		^{Et}BIP **273b**	Et_2SiH_2 **296**	>95
3[#]		^{Et}BIP **273b**	Me_2PhSiH **297**	14
4[#]		^{Et}BIP **273b**	$BnMe_2SiH$ **298**	38
5[#]		^{Et}BIP **273b**	$(Me_3SiO)_2MeSiH$ **249**	5
6[#]		^{Me}BIP **273c**	Me_2PhSiH **299**	–
7	Bu	^{Et}BIP **273b**	$BnMe_2SiH$ **298**	78
8		^{Et}BIP **273b**	$(Me_3SiO)_2MeSiH$ **249**	85
9		^{Et}BIP **273b**	$Me_3SiOSiMe_2H$ **307**	86
10		^{Et}BIP **273b**	Cl_3SiH **13**	–
11		^{Et}BIP **273b**	$(EtO)_3SiH$ **227**	–
12		^{Et}BIP **273b**	Et_3SiH **308**	–
13		^{Et}BIP **273b**	^{t}BuMe$_2$SiH **309**	–

[a]Conditions: alkene (0.7 mmol), $FeCl_2$ **279** (1 mol%), ligand (1 mol%), silane (0.7 mmol), EtMgBr **280** (2 mol%), tetrahydrofuran (0.25 M), r.t., 1 h; [b]Yield determined by ^{1}H NMR spectroscopy using 1,3,5-trimethoxybenzene as an internal standard; # = Result obtained by Dominik Frank

tertiary silanes gave linear hydrosilylation products **310-312** in good to excellent yield within 1 h (Table 2.3, entries 7–9). Once again, the linear hydrosilylation product was obtained with complete control of regiochemistry. The tertiary silanes heptamethyltrisiloxane **249** and pentamethyldisiloxane **307** are structurally representative of the silicon-hydrides present in silicone fluids used for the industrial synthesis of cross-linked silicone polymers. The good hydrosilylation activity observed using these silanes may therefore indicate potential industrial applicability of this catalytic system. The hydrosilylation of 1-hexene using tertiary silanes was found not to be general however, with no hydrosilylation products observed using silanes **13**, **227**, **308** and **309** (Table 2.3, entries 10–13). This lack of reactivity may be attributed to the more varied steric (e.g. ^{t}BuMe$_2$SiH **309**) or electronic (e.g. $(EtO)_3SiH$ **227** and Cl_3SiH **13**) properties of these silanes.

2.2.5 Alkene Scope and Limitations

The synthetic utility and chemoselectivity of the developed methodology was investigated using a range of alkenes bearing different substitution patterns and

functional groups. The efficiency of the screening process was maximised by using functionalised substrates which were either commercially-available or could be synthesised in a single step from commercially-available compounds.

2.2.5.1 Alkene Substrate Synthesis

A wide variety of styrene derivatives are commercially-available and these were used as a starting point for the synthesis of functionalised substrates. The amide-substituted styrene derivatives **317** and **320** were synthesised by the condensation of the appropriate benzoic acids and amines, mediated by a combination of triphenylphosphine **315** and iodine (Scheme 2.12) [27].

Conversion of 2-bromostyrene **321** and 4-vinylbenzyl chloride **324** into their respective Grignard reagents [28], followed by reaction with either allyl bromide **322** or benzonitrile **327** was used for the synthesis of alkene (**323** and **326**) or keto-functionalised (**328**) derivatives, respectively (Scheme 2.13a, b). A substrate

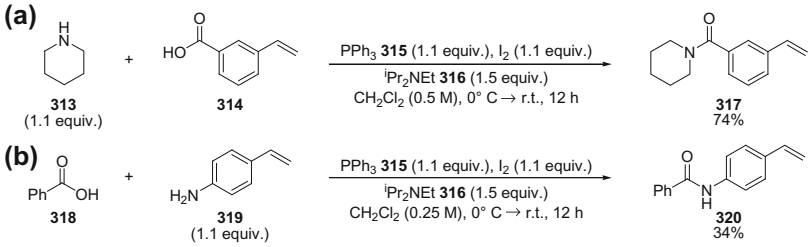

Scheme 2.12 Synthesis of ester and amide-functionalised styrene derivatives

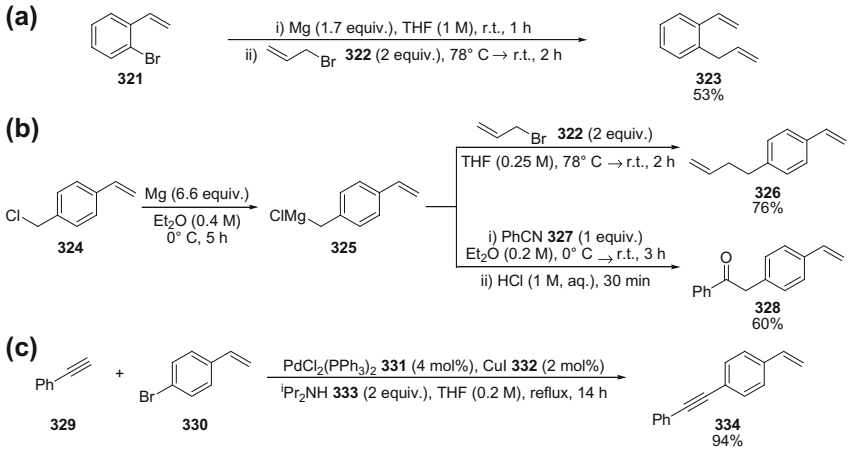

Scheme 2.13 Synthesis of allyl-, homoallyl-, keto- and alkynyl-substituted styrene derivatives by carbon–halogen bond functionalisation reactions

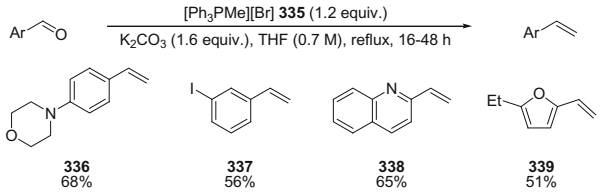

Scheme 2.14 Synthesis of styrene derivatives and vinyl-substituted heteroaromatic substrates using the Wittig reaction

containing both alkene and alkyne functional groups **334** was synthesised by the Sonagashira cross-coupling of phenylacetylene **329** and 4-bromostyrene **330** (Scheme 2.13c) [29].

A range of benzaldehyde derivatives are also commercially-available, and can be conveniently converted to styrene derivatives using the Wittig reaction. Morpholino- and iodo-substituted styrene derivatives **336** and **337**, and vinyl-substituted heteroaromatics **338** and **339** were synthesised using methyltriphenylphosphonium bromide **335** (Scheme 2.14) [30].

2.2.5.2 Hydrosilylation of Alkenes

The hydrosilylation of sterically and electronically-differentiated alkenes and alkynes was evaluated using the optimised conditions of iron(II) chloride **279** (1 mol%), bis(imino)pyridine **273b** (^{Et}BIP) (1 mol%), ethylmagnesium bromide **280** (2 mol%) and phenylsilane **47** (110 mol%). Styrene derivatives bearing a selection of both electron-donating and electron-withdrawing substituents gave hydrosilylation products **340-345** in good to excellent yields, and without a noticeable difference in activity (Table 2.4). In each case the linear silane was obtained with excellent regioselectivity. Primary amines have been reported to poison platinum hydrosilylation catalysts [15], and therefore the efficient hydrosilylation of 4-vinylaniline using this iron catalyst is notable. Chloro- and fluorostyrene derivatives gave the linear silane products **344** and **345**, with conservation of the aryl–halide bond [31]. In contrast, bromo- and iodostyrene derivatives **330** and **337** did not undergo hydrosilylation, with only starting material and small quantities (<5 %) of styrene obtained. The protodehalogenation of these substrates may arise due to cleavage of the carbon–halogen bond by the in situ generated low oxidation-state iron catalyst [32]. Heteroaromatic substrates were tolerated to some extent. 2-Vinylquinoline underwent hydrosilylation to give the linear silane product **346** in excellent yield, however the hydrosilylation of 4-vinylpyridine was accompanied by the formation of a polymeric material, limiting the yield of silane **347** to just 26 %. The attempted hydrosilylation of 2-vinylpyridine **348** gave only polymeric material, with no silane products obtained. The hydrosilylation of 2-vinylfuran **339** was also not successful, however in this case only starting material was recovered. This suggests an inherent lack of reactivity of this alkene towards

Table 2.4 Hydrosilylation of electronically-differentiated styrene derivatives and heteroaromatic substrates[a]

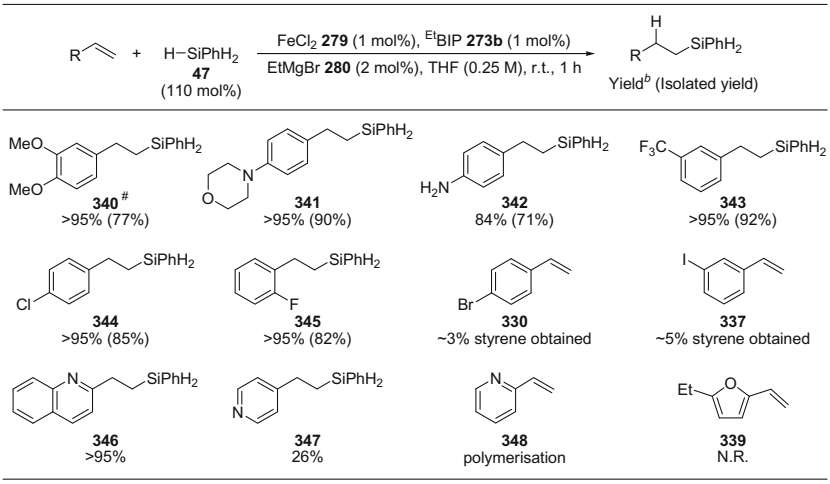

[a]Conditions: alkene (0.7 mmol), $FeCl_2$ **279** (1 mol%), [Et]BIP **273b** (1 mol%), $PhSiH_3$ **47** (0.77 mmol), EtMgBr **280** (2 mol%), tetrahydrofuran (0.25 M), r.t., 1 h; [b]Yield determined by ^1H NMR spectroscopy using 1,3,5-trimethoxybenzene as an internal standard; # = Result obtained by Dominik Frank

hydrosilylation using this catalyst, however the excellent recovery of starting material indicates the possibility that remote furan functionalities may be tolerated in the reaction.

Numerous iron-catalysed methodologies have been reported for the hydrosilylation of carbon–heteroatom multiple bonds including aldehydes, ketones, imines, esters, amides and nitriles [33]. Significant to this work, Chirik has shown that a bis(imino)pyridine iron(II) dialkyl pre-catalyst **349** is effective for the hydrosilylation of aldehydes and ketones [34]. Chirik found that the hydrosilylation of 5-hexene-2-one **254** gave the secondary alcohol product **350**, with no hydrosilylation, or reduction, or the terminal alkene reported (Scheme 2.15).

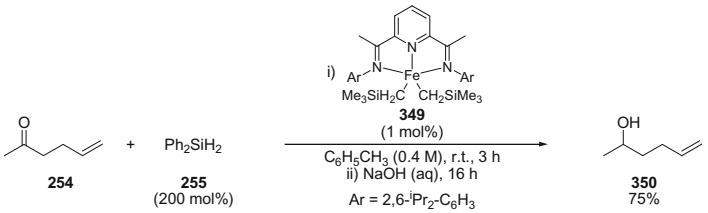

Scheme 2.15 Chemoselective hydrosilylation of the ketone functionality in 5-hexen-2-one **254** using a bis(imino)pyridine iron(II) dialkyl pre-catalyst **349**

The chemoselectivity of the developed methodology was therefore investigated for the hydrosilylation of a range of alkenes bearing functional groups containing carbon–heteroatom multiple bonds (Table 2.5). Ester-substituted alkenes were tolerated in the reaction, with linear silane products **351**, **352** and **353** obtained in quantitative yield and with no hydrosilylation of the ester was observed. Bis(imino) pyridine (BIP) iron bis(nitrogen) complexes have been shown to undergo oxidative addition into carbon–oxygen bonds of esters such as methylbenzoate and phenylacetate to give iron benzoate and phenolate complexes, respectively [35]. These complexes were catalytically inactive in hydrogenation reactions, and thus have been identified as possible decomposition products for bis(imino)pyridine iron-catalysed reactions. Under the developed hydrosilylation conditions however, no carbon–oxygen bond cleavage was observed in methylbenzoate or phenylacetate derivatives **351** and **352**. This may indicate that the rate of alkene hydrosilylation outcompetes the rate of carbon–oxygen bond cleavage, or that the reactions of isolated bis(imino)pyridine iron bis(nitrogen) complexes are not representative of the active iron catalyst formed under the developed reaction conditions.

In contrast, the amide-functionalised alkenes **317**, **320** and **354** were unreactive, with only starting material recovered in each case (Table 2.5). Similarly low activity

Table 2.5 Hydrosilylation of alkene substrates bearing reducible functional groups[a]

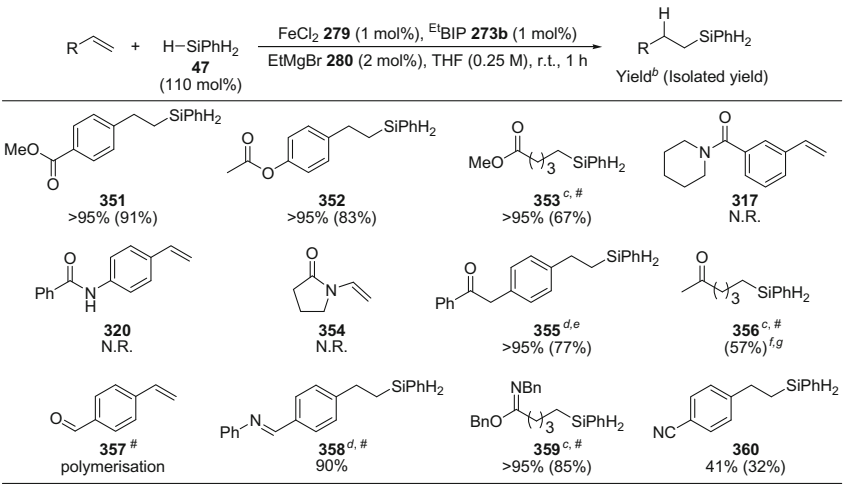

[a]Conditions: alkene (0.7 mmol), $FeCl_2$ **279** (1 mol%), [Et]BIP **273b** (1 mol%), $PhSiH_3$ **47** (0.77 mmol), EtMgBr **280** (2 mol%), tetrahydrofuran (0.25 M), r.t., 1 h; [b]Yield determined by ^1H NMR spectroscopy using 1,3,5-trimethoxybenzene as an internal standard; [c]$FeCl_2$ **279** (3 mol%), [Et]BIP **273b** (3 mol%), EtMgBr **280** (6 mol%) used; [d]$FeCl_2$ **279** (5 mol%), [Et]BIP **273b** (5 mol%), EtMgBr **280** (10 mol%) used; [e]Olefin added before the addition of EtMgBr **280**; [f]14 % of alcohol product **350** also isolated; [g]Yield using quantitative NMR spectroscopy not determined; # = Result obtained by Dominik Frank

has been reported for the hydrogenation of amide-substituted alkenes using bis(imino)pyridine iron bis(nitrogen) pre-catalysts, and this may reflect strong and inhibitive binding of the amide to the iron catalyst [35b]. Ketones have also been shown to bind strongly to bis(imino)pyridine iron bis(nitrogen) complexes [35b], and it was initially found that the hydrosilylation of 1-phenyl-2-(4-vinylbenzene)-ethanone **328** gave the hydrosilylation product **355** in only low yield. Increasing the pre-catalyst loading to 5 mol% and adding the substrate immediately after pre-catalyst reduction, rather than before, gave the hydrosilylation product **355** in quantitative yield. No reduction of the ketone functionality was observed. The hydrosilylation of 5-hexene-2-one **254** was also chemoselective for alkene hydrosilylation to give the alkyl silane product **356**. In this case the ketone was also reduced at a competitive rate, however a chemoselectivity of 4:1 in favour of alkene hydrosilylation was still achieved. This is in contrast to Chirik's work using bis(imino)pyridine iron(II) dialkyl pre-catalysts (Scheme 2.15) [34], and most likely reflects a difference in the oxidation-states of the active catalysts in each case. Bis(imino)pyridine iron(II) dialkyl complexes have been suggested to give low oxidation-state iron catalysts upon thermally-activated iron–carbon bond homolysis [14], however under the room temperature reaction conditions used for aldehyde and ketone hydrosilylation an iron catalyst in an oxidation-state of +2 is more likely [34]. The attempted hydrosilylation of an aldehyde-functionalised alkene substrate, 4-vinylbenzaldehyde **357**, was unsuccessful, with only polymeric material produced.

Chemoselectivity for the hydrosilylation of alkenes in the presence of carbon–nitrogen multiple bonds was also investigated (Table 2.5). Aldimine and imino ester functionalities were both tolerated giving linear silanes **358** and **359** as the major products, however small quantities of unidentified side-products were also obtained. The hydrosilylation of 4-cyanostyrene gave a mixture of products and polymeric material, resulting in a low mass recovery. The linear silane **360** was isolated as the major product in a modest yield of 41 %. A combined total of approximately 7 % of two aldehyde products were also observed in the crude reaction mixture by ^{1}H NMR spectroscopy. These may have been produced by competitive hydrosilylation of the nitrile group of the starting material and product to give *N*-silylated aldimine products, which were hydrolysed upon reaction work-up.

The reaction of terminal alkenes with primary silanes had consistently given hydrosilylation products (Tables 2.1, 2.2, 2.3, 2.4, 2.5), however the reaction of 4-phenylbutene **361** with diphenylsilane **255** unexpectedly gave a mixture of dehydrosilylation and hydrogenation products (Scheme 2.16a). Allylsilane **362** was obtained in close to 50 % yield, with excellent regioselectivity and in a 6:1 mixture of diastereoisomers. The hydrogenation product, butylbenzene **363**, was also obtained in a similar yield. This was in contrast to the hydrosilylation of styrene **53** using diphenylsilane **255** which had been found to give the hydrosilylation product **300** (Table 2.3, entry 1). The selectivity for dehydrosilylation in the reaction between 4-phenylbutene **361** and diphenylsilane **255** also could not be attributed to a property specific to 4-phenylbutene, as reaction with primary and tertiary silanes gave the hydrosilylation products **364** and **365**, with no dehydrosilylation products

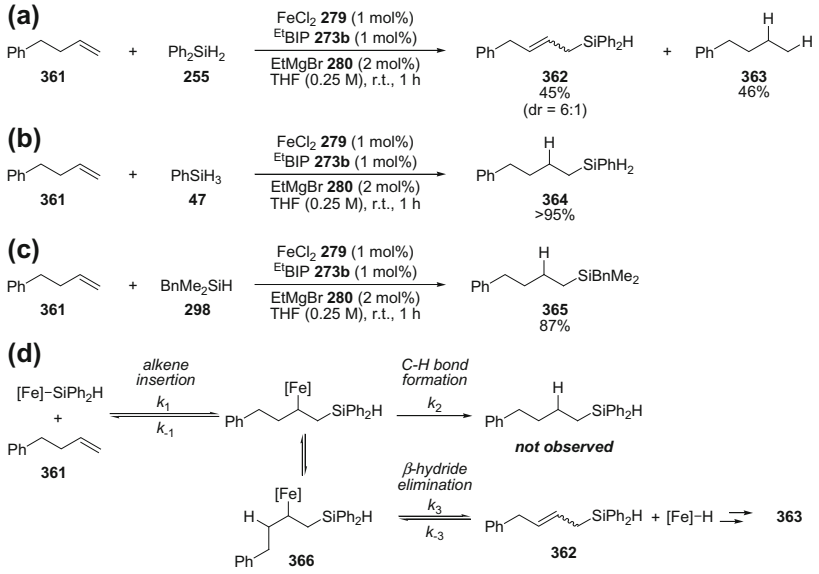

Scheme 2.16 Hydrosilylation of 4-phenylbutene **361** using primary, secondary and tertiary silanes

obtained (Scheme 2.16b, c). Although the source of this intriguing selectivity has not been identified, these results suggest that a 'modified Chalk-Harrod' mechanism [1c, 2–4] of hydrosilylation may be in operation. The formation of the allylsilane product **362** can be explained by alkene insertion into an iron–silicon bond, followed by β-hydride elimination (Scheme 2.16d). The high selectivity observed for dehydrosilylation can be explained if the rate of β-hydride elimination (k_3) is significantly faster than the rate of carbon–hydrogen bond formation (k_2) to give the hydrosilylation product. The iron–hydride species formed may then react with another equivalent of alkene to give the hydrogenation product **363**. The same product distribution cannot be explained by a mechanism in which alkene insertion into an iron–hydride bond takes place.

The scope and limitations of the methodology for the hydrosilylation of more highly-substituted alkenes was then investigated. Unfortunately, 1,1- and 1,2-disubstituted alkenes did not undergo hydrosilylation using the developed reaction conditions. It was rationalised that in comparison to primary alkenes these more sterically hindered alkenes may bind less favourably to iron, and thus coordination of the tetrahydrofuran solvent may become competitive with substrate binding. The hydrosilylation of 1,1- and 1,2-disubstituted alkenes was therefore attempted in toluene solution, using pre-complexed bis(imino)pyridine iron(II) chloride pre-catalyst ^{Et}BIPFeCl$_2$ **367** (1 mol%) and *n*-butyllithium **283** as in situ reductant (2 mol%) (Table 2.6). Under the modified conditions, α-methylstyrene

Table 2.6 Hydrosilylation of 1,1- and 1,2-disubstituted alkenes[a]

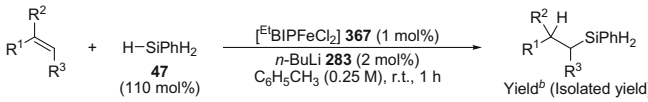

368	369	370[c]
>95% (94%)	>95% (96%) (1:1 mixture of diastereoisomers)	88% (84%)

[a]Conditions: alkene (0.7 mmol), ^{Et}BIPFeCl$_2$ **367** (1 mol%), PhSiH$_3$ **47** (0.77 mmol), *n*-BuLi **283** (2 mol%), toluene (0.25 M), r.t., 1 h; [b]Yield determined by ^{1}H NMR spectroscopy using 1,3,5-trimethoxybenzene as an internal standard; [c]Reaction in neat cyclooctene

and (*R*)-(+)-limonene both underwent hydrosilylation to give linear silanes **368** and **369** in excellent yield, with the latter obtained as a 1:1 mixture of diastereoisomers. Cyclooctene also underwent hydrosilylation, however silane **370** was obtained in only a modest yield of 24 %. Switching from toluene to neat cyclooctene improved hydrosilylation activity further, with the cyclooctyl silane product **370** obtained in an 88 % yield within 1 h.

Due to the low propensity of 1,2-disubstituted alkenes to undergo hydrosilylation in tetrahydrofuran, diene substrates **371** and **373** were used in the hope of chemoselective hydrosilylation of the terminal alkene. 4-Vinylcyclohexene **371** gave the linear silane **372** in excellent yield, with no competitive reduction of the internal alkene observed (Scheme 2.17a). The terminal alkene of *trans*-1-phenyl-1,3-butadiene **373** also underwent chemoselective hydrosilylation, however in this case a 1:1 mixture of regioisomers **374-*l*** and **374-*b*** were formed (Scheme 2.17b). This is the only reported example of an iron-catalysed hydrosilylation in which the hydrosilylation of a terminal alkene has given a secondary silane product.

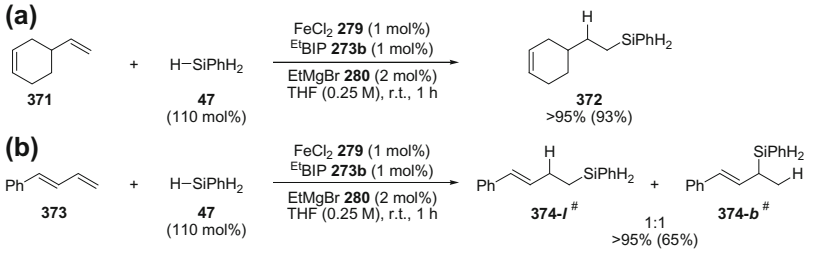

Scheme 2.17 Chemoselective hydrosilylation of the terminal alkene of diene substrates **371** and **373**

Hydrosilylation of 1,1-Disubstituted Alkenes Using Enantiopure Bis(imino) pyridine Iron(II) Pre-catalysts

The enantioselective cobalt-catalysed hydrogenation of 1,1-disubstituted aryl alkenes was recently reported by Chirik using an enantiopure cobalt(I) bis(imino) pyridine complex **376** (Scheme 2.18) [36], however the application of these ligands in enantioselective iron-catalysed reactions was not reported. This may indicate that Chirik found only low enantioinduction using the bis(imino)pyridine iron analogues, or that the bis(imino)pyridine iron(0) bis(dinitrogen) pre-catalysts favoured by Chirik were inaccessible. As the developed hydrosilylation methodology had been successfully applied to the hydrosilylation of prochiral 1,1-disubstituted alkenes, the possibility of enantioselective iron-catalysed hydrosilylation using enantiopure bis(imino)pyridine iron complexes was investigated.

A range of enantiopure C_1-symmetric bis(imino)pyridine ligands **380a-d** were synthesised from the sequential condensation of 2,6-diacetylpyridine **271** with an aniline derivative **272b-c**, followed by condensation with an enantiopure amine **379a-b** (Scheme 2.19a). The first condensation to give the mono(imino)pyridine intermediates **378a-b** was complicated by concurrent formation of the bis(imino) pyridine analogues, even when using substoichiometric quantities of the aniline derivative **272b-c**. The mono- and bis(imino)pyridine derivatives could not be separated by recrystallisation, however the bis(imino)pyridine impurity could be effectively removed by complexation with an equivalent of iron(II) chloride **279**. Condensation of the mono(imino)pyridine intermediates **378a-b** with (*S*)-(+)-3,3-dimethyl-2-butylamine **379a** gave crystalline bis(imino)pyridine derivatives ^{Et,tBu}BIP **380a** and ^{Me,tBu}BIP **380c**, which could be purified by recrystallisation. In contrast, condensation of the mono(imino)pyridine intermediates **378a-b** with (*S*)-(+)-1-cyclohexylethylamine **379b** gave the bis(imino)pyridine derivatives ^{Et,Cy}BIP **380b** and ^{Me,Cy}BIP **380d** as viscous oils, and were therefore complexed with iron (II) chloride without further purification.

The enantiopure bis(imino)pyridine iron(II) chloride complexes were initially tested for base reactivity in the hydrosilylation of styrene **53** using phenylsilane **47** (Scheme 2.20). In each case quantitative conversion to the alkyl silane was obtained, and so the hydrosilylation of prochiral 1,1-disubstituted alkenes was investigated.

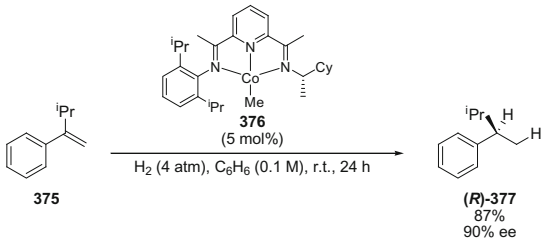

Scheme 2.18 Cobalt-catalysed enantioselective hydrogenation of prochiral 1,1-disubstituted aryl alkenes using an enantiopure cobalt(I) bis(imino)pyridine complex **376**

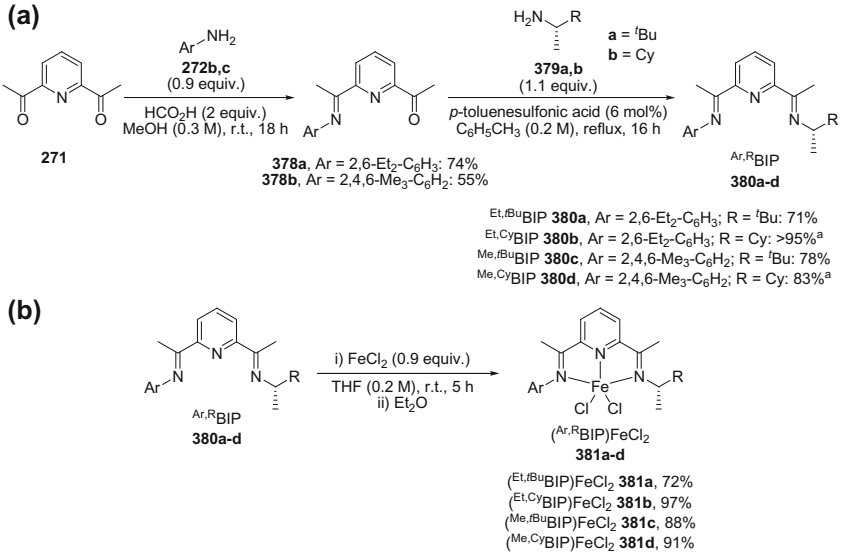

Scheme 2.19 Synthesis of enantiopure bis(imino)pyridine iron(II) chloride complexes **381a-d**. **a** Synthesis of enantiopure bis(imino)pyridine ligands **380a-d**. **b** Complexation with iron(II) chloride

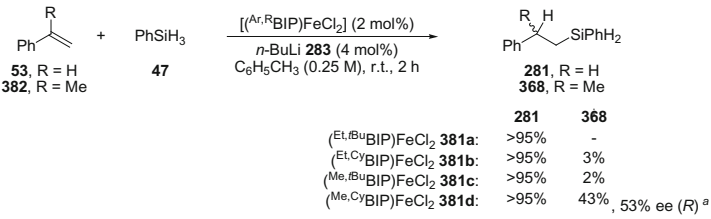

a Determined by chiral HPLC following conversion to 2-phenylpropanol 383

Scheme 2.20 Hydrosilylation of styrene **53** and α-methylstyrene **382** using enantiopure bis (imino)pyridine iron(II) pre-catalysts **381a-d**

The complex bearing the most sterically-hindered enantiopure bis(imino)pyridine ligand, (^{Et,tBu}BIP)FeCl$_2$ **381a**, was inactive for the hydrosilylation of α-methylstyrene **382**. Reduction in the size of the enantiopure amine group to the cyclohexane derivative, (^{Et,Cy}BIP)FeCl$_2$ **381b**, gave an iron catalyst with minimal activity, with the alkyl silane **368** obtained in 3 % yield. Reduction in the size of the *N*-aryl substituents was then investigated. The iron(II) complex (^{Me,tBu}BIP)FeCl$_2$ **381c** also displayed minimal activity for hydrosilylation, however further reduction in the steric bulk of the ligand to (^{Me,Cy}BIP)FeCl$_2$ **381d** produced a moderately active catalyst. The hydrosilylation product **368** was obtained in 43 % yield, and 53 % enantiomeric excess. The absolute stereochemistry of the product was determined to

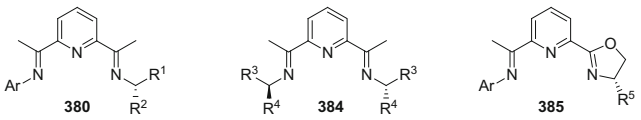

Fig. 2.1 Enantiopure C_1- and C_2-symmetric iminopyridine-based ligand structures which may be investigated for the development of asymmetric iron-catalysed hydrosilylation

be (*R*)-based upon chiral HPLC and optical rotation. The hydrosilylation of (*R*)-limonene was also tested with each of the enantiopure bis(imino)pyridine iron(II) pre-catalysts **368a-d**, however no hydrosilylation activity was observed.

It is apparent from this work that the more sterically-bulky bis(imino)pyridine ligands do not form a catalyst capable of the hydrosilylation of (prochiral) 1,1-disubstituted alkenes. Reducing the steric-hindrance of the ligand further may improve hydrosilylation activity, however enantioselectivity might be compromised if less sterically-hindered analogues also result in a wider binding cavity and lower facial selectivity. There is however good scope for further exploration of this class of C_1-symmetric enantiopure ligand **380** due to the wide variety of aniline derivatives and enantiopure amines that are commercially-available (Fig. 2.1). It would also be worthwhile investigating the use of *N*-alkyl substituted C_2-symmetric enantiopure ligands **384** for enantioselective hydrosilylation. Chirik has reported that *N*-alkyl substituted bis(imino)pyridine iron(0) bis(dinitrogen) complexes cannot be synthesised by sodium amalgam or sodium naphthalenide reduction [11, 25, 26], however the in situ reduction technique developed in this methodology may allow access to previously inaccessible catalyst structures. This work might also be extended by investigating the use of enantiopure iminopyridine oxazoline ligands **385**, following recent reports of their application in the enantioselective cobalt- [37] and iron-catalysed [38] hydroboration of 1,1-disubstituted alkenes.

Gram-Scale Hydrosilylation

The hydrosilylation reactions aimed at investigating chemo-, regioselectivity had been performed on a small scale (<1 mmol), and therefore the potential to perform the reaction on a preparative scale (10 mmol) was investigated. Performing the reaction on a larger scale also provided the opportunity to use the methodology developed for the hydrosilylation of 1,1 and 1,2-disubstituted alkenes, and conduct the reaction under 'solvent-free' conditions. From preliminary experiments, it was found that the hydrosilylation of styrene **53** using phenylsilane **47** was unselective towards multiple hydrosilylations, with a mixture of the mono-silylation product **281** and bis-silylation product **284** obtained (Scheme 2.21a). This indicated that the rate of hydrosilylation of styrene **53** by the secondary silane product **281** was competitive with the rate of hydrosilylation of styrene **53** by phenylsilane **47**. The hydrosilylation of styrene **53** was therefore investigated using diethylsilane **296**. Using just 0.07 mol% iron pre-catalyst ^{Et}BIPFeCl$_2$ **367**, the hydrosilylation of

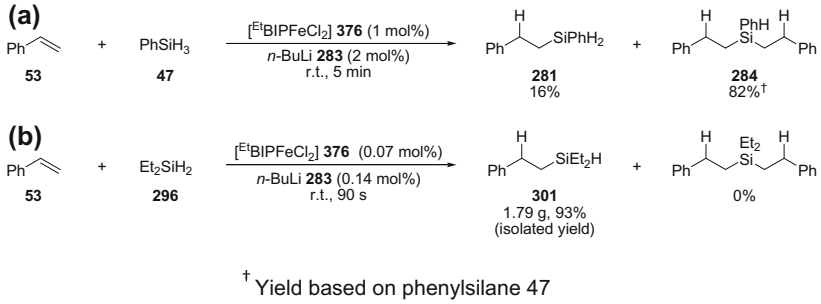

Scheme 2.21 Gram-scale hydrosilylation of styrene **53** under 'solvent-free' conditions

styrene **53** with diethylsilane **296** was complete within 90 s, giving the mono-silylation product **301** in quantitative conversion, and 93 % isolated yield (Scheme 2.21b). Under the 'solvent-free' reaction conditions it was apparent that the hydrosilylation reaction was highly exothermic, with the reaction temperature increasing almost instantaneously upon addition of the silane. The reaction was quenched when the reaction temperature ceased to increase, however the hydrosilylation reaction may have been complete much sooner. Under these unoptimised conditions, the catalyst turn-over-frequency was calculated as approximately 60,000 mol h^{-1}. Chirik has reported catalyst turn-over-frequencies of up to 100,000 mol h^{-1} using isolated bis(imino)pyridine iron bis(dinitrogen) complexes [12a]. This demonstrates that the developed methodology provides access to iron catalysts with a similarly high activity for hydrosilylation, without the need to prepare and isolate highly air- and moisture sensitive iron complexes.

2.2.6 *Hydrosilylation of Alkynes*

The developed methodology was applied to the hydrosilylation of alkynes using phenylsilane (Table 2.7). Internal alkynes underwent diastereoselective hydrosilylation to give (*E*)-vinylsilane products (*syn*-addition of Si–H), whilst terminal alkynes gave a mixture of diastereoisomers, with the major (*Z*)-vinylsilane product arising from the formal *anti*-addition of the silicon–hydrogen bond.

Diaryl- and dialkyl alkynes gave (*E*)-vinylsilanes **386** and **387** in excellent yield, and with complete diastereochemical control. The stereochemistry of the vinylsilane products was confirmed by comparison with literature data, and by stereoretentive protodesilylation using tetrabutylammonium fluoride [39]. The unsymmetrically-substituted internal alkyne, 1-phenylpropyne, also underwent hydrosilylation to give a 9:1 mixture of regioisomers **β-388** and **α-388**. Both regioisomers were obtained as a single diastereoisomer, with the major regioisomer confirmed as the (*E*)-vinyl silane **β-388** by 1D nOe NMR spectroscopy. The hydrosilylation of terminal alkynes was regioselective for the addition of the silicon group to the terminal position,

Table 2.7 Hydrosilylation of internal and terminal alkynes[a]

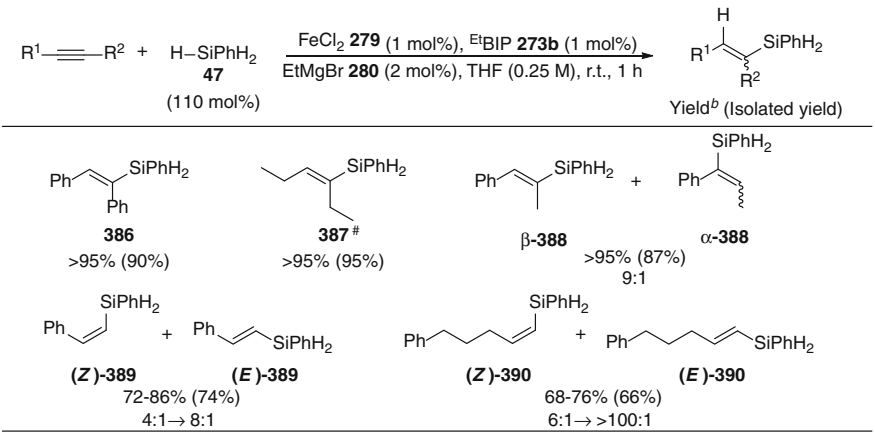

[a]Conditions: alkyne (0.7 mmol), $FeCl_2$ **279** (1 mol%), [Et]BIP **273b** (1 mol%), $PhSiH_3$ **47** (0.77 mmol), EtMgBr **280** (2 mol%), tetrahydrofuran (0.25 M), r.t., 1 h; [b]Yield determined by ^1H NMR spectroscopy using 1,3,5-trimethoxybenzene as an internal standard; # = Result obtained by Dominik Frank

however, in contrast to internal alkynes, a mixture of diastereoisomers was obtained (Table 2.7). Phenylacetylene gave vinylsilane products **(*Z*)-389** and **(*E*)-389** in good to excellent yield, with the major product **(*Z*)-389** arising from the formal *anti*-addition of the silicon–hydrogen bond. (*Z*)-Vinylsilane **(*Z*)-389** could be reproducibly obtained in 4:1 to 8:1 diastereoselectivity. The hydrosilylation of the terminal alkyl-substituted alkyne, 5-phenylpentyne, also gave a mixture of diastereoisomers, however in this case a wider range of diastereoselectivities were observed. Under the optimised conditions, diastereoselectivities ranging from 6:1 to greater than 100:1 were obtained in favour of the (*Z*)-vinylsilane **(*Z*)-390** (formal *anti*-addition of the silicon–hydrogen bond).

The formation of the thermodynamically unfavoured (*Z*)-vinylsilane products **(*Z*)-389** and **(*Z*)-390** may be explained using the mechanisms proposed by Crabtree [4b, c] and Ojima [3c] for iridium- and rhodium-catalysed hydrosilylation (Scheme 2.22). s*yn*-Silylmetallation of the terminal alkyne **329** or **391** would give the (*Z*)-metallavinylsilane intermediate **(*Z*)-392** regio- and diastereoselectively. This can undergo π-bond isomerisation via either the zwitterionic carbenoid **393** or metallocyclopropene **394** intermediate to give the (*E*)-metallavinylsilane **(*E*)-392**. If the rate of metallavinylsilane π-bond isomerisation (k_2) is significantly faster than the rate of carbon–hydrogen bond formation (k_1), then the ratio of hydrosilylation products will reflect the difference in thermodynamic stability between the (*Z*)- and (*E*)-metallavinylsilane intermediates **(*Z*)-392** and **(*E*)-392**. Assuming the iron catalyst has more steric bulk than the organic R^1 group, the (*E*)-metallavinylsilane

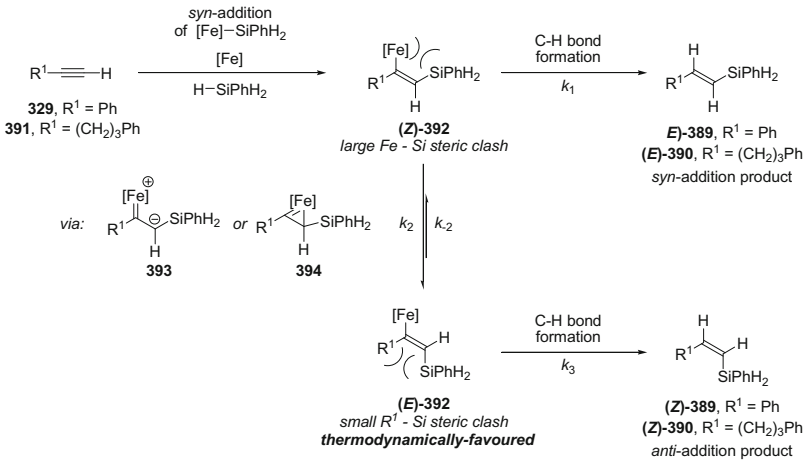

Scheme 2.22 Proposed mechanism for the hydrosilylation of terminal alkynes to explain diastereoselectivity for the formation of (*Z*)-vinylsilanes **(*Z*)-389** and **(*Z*)-390**

intermediate **(*E*)-392**, where iron is *trans*- to the silicon group, and *cis*- to the hydrogen, should be the thermodynamically-favoured metallavinylsilane intermediate. An alternative explanation could be proposed where metallavinylsilane π-bond isomerisation is fast and reversible, but the rate of carbon–hydrogen bond formation from **(*E*)-392** to give **(*Z*)-389/390** (k_3), is significantly faster than the rate of carbon–hydrogen bond formation from **(*Z*)-392** to give **(*E*)-389/390** (k_1). This may be more significant if carbon–hydrogen bond formation occurs by an intermolecular process, and the rate of this process (k_1) is retarded by the greater steric congestion around iron in (*Z*)-metallavinylsilane intermediate **(*Z*)-392** (Scheme 2.22). These justifications based upon differences in thermodynamic and kinetic parameters do not need to be mutually exclusive however, and it is likely that a combination of factors will influence the level of diastereoselectivity obtained in these reactions.

The (*Z*)-vinylsilane **(*Z*)-390**, obtained from the hydrosilylation of 5-phenylpentyne **391**, was obtained in higher diastereoselectivity than the (*Z*)-vinylsilane **(*Z*)-389** obtained from the hydrosilylation of phenylacetylene **329**. This might be explained by considering the difference in thermodynamic stability of the respective (*E*)-metallavinylsilane intermediates **(*E*)-392** (where R^1 = phenyl or an alkyl chain). When the R^1 group is phenyl (following silylmetallation of phenylacetylene **329**), there would be a larger steric clash with the silicon group in (*E*)-metallavinylsilane **(*E*)-392** than that when the R^1 group is an alkyl chain (following silylmetallation of 5-phenylpentyne **391**). This would result in a smaller difference in thermodynamic stability between the (*E*)- and (*Z*)-metallavinylsilane intermediates **(*E*)-** and **(*Z*)-392** when the R^1 group is phenyl. A lower preference for (*E*)-metallavinylsilane **(*E*)-392** would therefore lead to lower diastereoselectivity for (*Z*)-vinylsilane **(*Z*)-389**.

To investigate the inconsistent diastereoselectivities obtained for the hydrosilylation of 5-phenylpentyne, a range of variables were systematically altered,

Table 2.8 Effect of Grignard reagent loading on the diastereoselectivity of the hydrosilylation of 5-phenylpentyne[a]

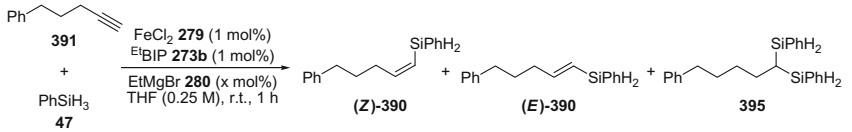

Entry	EtMgBr/mol %	Yield (%)[b,c]			*Z*: *E* diastereomeric ratio	Total yield of hydrosilylation products (%)[b,d]
		(*Z*)-390	(*E*)-390	395		
1	2	68	0.5	0	136:1	69
2	3	67	6.6	13	10:1	100
3	4	39	16	27	5:2	109

[a]Conditions: 5-phenylpentyne **391** (0.7 mmol), $FeCl_2$ **279** (1 mol%), [Et]BIP 273**b** (1 mol%), $PhSiH_3$ **47** (0.77 mmol), EtMgBr **280** (2–4 mol%), tetrahydrofuran (0.25 M), r.t., 1 h; [b]Yield determined by ^1H NMR spectroscopy using 1,3,5-trimethoxybenzene as an internal standard; [c]Yield based on 5-phenylpentyne **391** (max yield = 100 %); [d]Yield based on phenylsilane (max yield = 110 %)

including reaction concentration, equivalents of silane and amount of Grignard reagent. The only variable which resulted in a clear trend was the alteration of the amount of Grignard reagent used to activate the pre-catalyst (Table 2.8).

The standard reaction conditions gave the (*Z*)- and (*E*)-vinylsilanes **(*Z*)-390** and **(*E*)-390** in good yield and excellent diastereoselectivity for the (*Z*)-vinylsilane **(*Z*)-390** (Table 2.8, entry 1, *Z*:*E* = ~130:1). Increasing the quantity of Grignard reagent still gave the (*Z*)- and (*E*)-vinylsilanes **(*Z*)-390** and **(*E*)-390** in good yield, however the *Z*:*E* diastereoselectivity was reduced to just 10:1 (Table 2.8, entry 2). Increasing the quantity of Grignard reagent further resulted in even lower diastereoselectivity, with a preference of just 5:2 for the (*Z*)-vinylsilane **(*Z*)-390** obtained (Table 2.8, entry 3). In addition, a third product **395**, arising from the formal bis-hydrosilylation of the alkyne was obtained when increased amounts of Grignard reagent were used.

Increasing the amount of Grignard reagent used to activate the pre-catalyst resulted in an increase in the total amount of silylated products, and therefore it is possible that more active catalyst (or *a* more active catalyst) was formed under the reaction conditions. The higher proportion of (*E*)-vinylsilane **(*E*)-390** produced may be explained by the formation of a catalytic species with different diastereoselectivity, or through isomerisation of the (*Z*)-vinylsilane product **(*Z*)-390** to the thermodynamically-favoured (*E*)-vinylsilane **(*E*)-390** under the reaction conditions. The disilylated product **395** was presumably formed following the hydrosilylation of a vinylsilane product (**(*Z*)-390** or **(*E*)-390**). The formation of this product may also provide an indication to the source of the variable *Z*:*E* diastereoselectivities observed (Scheme 2.23). *syn*-Silylmetallation of the (*Z*)-vinylsilane product **(*Z*)-390** would give the iron alkyl intermediate **396**, which following C–H bond

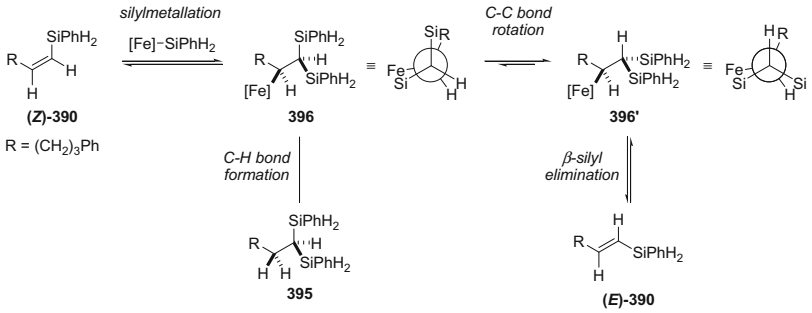

Scheme 2.23 Proposed mechanism for the isomerisation of (*Z*)-vinylsilane **(*Z*)-390** to give (*E*)-vinylsilane **(*E*)-390** via a disilylated intermediate **396**

formation would give the disilylated product **395** (Scheme 2.23). Iron alkyl intermediate **396** suffers from significant steric clashes by the eclipsed arrangement of the silicon group and alkyl chain, however this steric clash can be decreased by C–C bond rotation to give iron alkyl intermediate **396′**. β-Silyl elimination from iron alkyl intermediate **396′** would then give the (*E*)-vinylsilane product **(*E*)-390**. Further evidence would be required to support this proposition. Kinetic data would allow quantification of product formation and interconversion, and application of (*Z*)-vinylsilane **(*Z*)-390** as a substrate would support of refute the proposal that isomerisation occurs under the reaction conditions.

In contrast to the hydrosilylation of terminal alkynes, the hydrosilylation of internal alkynes gave only a single diastereoisomer arising from the *syn*-addition of the silicon–hydrogen bond (Table 2.7). It is conceivable that terminal and internal alkynes may undergo hydrosilylation by different mechanisms, however the difference in diastereoselectivity can be rationalised using the same metallavinylsilane mechanism, if when using internal alkynes the rate of metallavinylsilane π-bond isomerisation (k_2) is significantly slower than the rate of carbon–hydrogen bond formation (k_1) (Scheme 2.24). This can be justified as the presence of a second organic group at the R^2 position will increase the steric congestion in the proposed zwitterionic carbenoid **400** or metallocyclopropene **401** intermediates, and make metallavinylsilane π-bond isomerisation less favourable. An increase in steric congestion might be expected to have a greater negative effect on the stability of the more sterically hindered metallocyclopropene **401** intermediate. These results therefore indicate that metallavinylsilane π-bond isomerisation may occur via a metallocyclopropene **401** intermediate, as originally proposed by Crabtree for rhodium-catalysed hydrosilylation [4b, c].

Having established reactivity for both the hydrosilylation of alkenes and alkynes, substrates were chosen which contained both functionalities in order to investigate the chemoselectivity between these groups (Scheme 2.25). The addition of 1-phenyl-4-pent-1-yne **402** to the iron pre-catalyst in tetrahydrofuran resulted in an immediate colour change from blue to yellow. This indicated decomplexation of the bis(imino)pyridine ligand from iron, and accordingly the subsequent

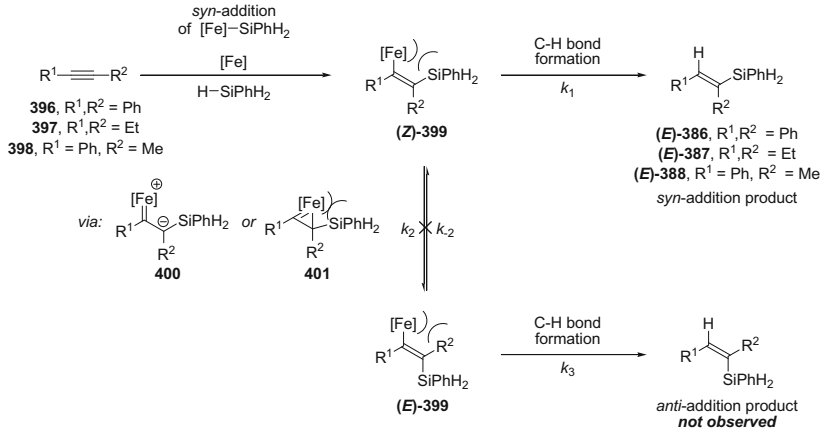

Scheme 2.24 Proposed mechanism for the hydrosilylation of internal alkynes to explain diastereoselectivity for the formation of (*E*)-vinylsilanes **(*E*)-386-388**

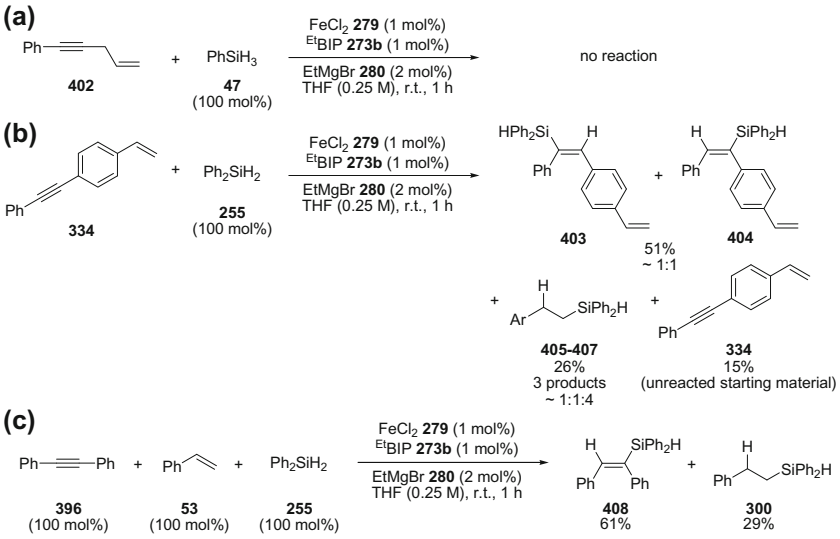

Scheme 2.25 Investigation of chemoselectivity of hydrosilylation between alkyne and alkene functionalities

hydrosilylation reaction failed (Scheme 2.25a). Ligand decomplexation was presumably caused by preferential binding between iron(II) with the excess 1-phenyl-4-pent-1-yne **402** substrate, potentially acting as a bidentate ligand.

This issue was circumvented by using 4-(phenylethynyl)styrene **334**, in which the alkene and alkyne functionalities were further apart. Initial hydrosilylation reactions using phenylsilane **47** resulted in a complex mixture of products, in which no remaining alkene functionalities were present. This complex mixture was attributed to

subsequent hydrosilylation reactions between the olefin and silane functionalities present in the secondary silane products and was therefore not informative about reaction chemoselectivity. This problem was partially solved by using a secondary silane, which would give a significantly less reactive tertiary silane product, however hydrosilylation using diphenylsilane **255** still gave a complex mixture of products (Scheme 2.25b). From ^{1}H NMR spectroscopy it was determined that three styrene derivatives were present in a 2:7:7 ratio, along with three distinguishable linear alkyl silane products in a 1:1:4 ratio. One of the styrene derivatives was identified as starting material **334**, whilst the other two products (51 % yield, approximately 1:1 ratio) were assigned as the two vinylsilane regioisomers **403** and **404**. The three alkyl silanes **405-407** could not be definitively assigned, however the major product was tentatively assigned as the product with alkyne functionality intact, with the other two, present in an approximately 1:1 ratio, assigned as being those where the alkyne had also undergone hydrosilylation. Overall this experiment indicated that alkyne hydrosilylation had occurred in 60 % of the material, whilst alkene hydrosilylation had occurred in 26 % of the material. This suggests a chemoselectivity in favour of alkyne hydrosilylation of approximately 2:1. As this product mixture had proved challenging to separate and definitively assign, diphenylacetylene and styrene were reacted with diphenylsilane in a simple competition experiment (Scheme 2.25c). Once again, chemoselectivity for alkyne hydrosilylation was observed, with vinylsilane **408** and alkylsilane **300** obtained in a ratio of approximately 2:1.

The level of chemoselectivity observed for the hydrosilylation of alkynes over alkenes could indicate that alkynes undergo hydrosilylation at a faster rate than alkenes using this catalyst. However, chemoselectivity could also arise due to a higher binding affinity between the low oxidation-state iron catalyst and the alkyne, thus preventing alkene coordination and inhibiting the rate of alkene hydrosilylation [40]. In order to delineate these possibilities, kinetic profiles for the hydrosilylation of styrene **53** and diphenylacetylene **396**, in combination and in isolation, would need to be obtained.

2.2.7 Derivatisation of Hydrosilylation Products

The majority of the alkyl and vinyl silanes produced using this methodology were secondary and tertiary silanes, and could therefore be conveniently oxidised to the corresponding alcohols or ketones, as originally described by Tamao [41]. Using hydrogen peroxide **409** and potassium bicarbonate **410** in a mixed solvent system of tetrahydrofuran and methanol, alkyl silanes **301**, **344** and **351** were oxidised to give linear alcohols **411-413** in excellent yield (Scheme 2.26a).

The original procedure recommended heating the reactions at reflux, however it was found that the alcohol products were obtained in equal yield at room temperature. The oxidation of vinyl silane **386** gave a mixture of oxidised products when the reaction was heated at reflux. These were attributed to silicon–carbon bond oxidation to give the expected ketone product **414**, followed by

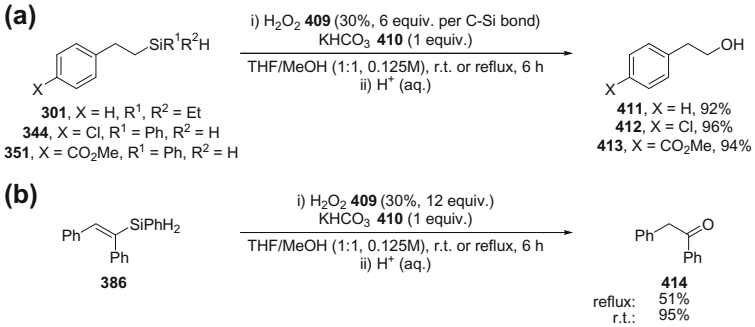

Scheme 2.26 Tamao oxidation of alkyl- and vinylsilanes **301**, **344**, **351** and **386** to give alcohol and ketone products **411-414**

Baeyer-Villiger rearrangement. The ketone product **414** could be obtained selectively by conducting the oxidation at room temperature (Scheme 2.26b).

The iron-catalysed hydrosilylation reaction was commonly conducted in tetrahydrofuran, and therefore the one-pot hydrosilylation-oxidation of alkenes was attempted by the simple addition of hydrogen peroxide **409**, potassium bicarbonate **410** and methanol following the hydrosilylation reaction. This would provide products from the formal anti-Markovnikov hydration of alkenes. Unexpectedly, the one-pot hydrosilylation-oxidation of styrene **53** did not give the linear alcohol **411**, but instead resulted in quantitative conversion to the silanol product **415** (Scheme 2.27a). This one-pot hydrosilylation-oxidation procedure was also applied to the hydrosilylation-oxidation of an alkyne, to give vinyl silanediol **417**, again in excellent yield (Scheme 2.27b). This synthetic sequence is potentially useful as alkylsilanols have numerous applications in materials chemistry [42], whilst vinylsilanols can be used as substrates in cross-coupling [43], Mizoroki–Heck [44], and carbonyl addition reactions [45].

The selectivity for silicon–hydrogen bond oxidation over silicon–carbon bond oxidation in this reaction is intriguing considering that the only difference between the isolated oxidation procedure and one-pot procedure is the presence of iron. This

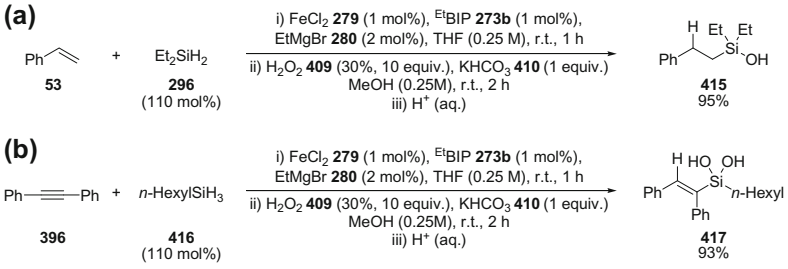

Scheme 2.27 One-pot iron-catalysed hydrosilylation-oxidation of styrene **53** and diphenylacetylene **396** to give alkyl silanol **415** and vinyl silanol **417**, respectively

difference in reactivity may be explained by iron-catalysed decomposition of hydrogen peroxide [46], if the rate of decomposition is faster than the rate of silicon–carbon bond oxidation. Silicon–hydrogen bond oxidation may therefore occur through reaction with hydrogen peroxide at a faster rate than the rate of hydrogen peroxide decomposition, or through reaction with the hydroxyl radicals or iron-peroxide intermediates proposed during the iron-catalysed decomposition of hydrogen peroxide.

2.2.8 Preliminary Mechanistic Work

The mechanism of iron-catalysed hydrosilylation was originally studied by Wrighton, focussing on hydrosilylation reactions which used iron carbonyl pre-catalysts (Scheme 2.28a) [1b, c]. The concurrent formation of dehydrosilylation **224** and hydrogenation **225** products led Wrighton to propose that iron-catalysed hydrosilylation proceeded by alkene insertion into an iron–silicon bond (Scheme 2.28b, i), rather than insertion into an iron–hydrogen bond (Scheme 2.28b, ii). Following alkene insertion into the iron–silicon bond, β-hydride elimination would give the dehydrosilylation product **224** and produce an iron(di)hydride, which could react with a further equivalent of alkene **220** to produce the hydrogenation product **225**. The same products would not be obtained by alkene insertion into the iron–hydrogen bond, as β-hydride elimination would simply reform an alkene (Scheme 2.28b, ii).

To provide support for the proposed mechanism (Scheme 2.28c), Wrighton investigated the stoichiometric reactions of pentamethylcyclopentadienyl iron carbonyl complexes to assess the feasibility of the key steps of: **A** oxidative addition; **B** alkene insertion; **C** β-hydride elimination and **D** carbon–hydrogen bond reductive elimination (Scheme 2.29) [1c]. Near-UV irradiation of the iron(silyl)dicarbonyl complex **418** in the presence of trimethylsilane gave the iron(disilyl)hydride complex **419** (Scheme 2.29a). The formation of iron(disilyl)hydride complex **419** was proposed to occur following carbon monoxide dissociation from iron(silyl) dicarbonyl complex **418** and subsequent oxidative addition into the silicon–hydrogen bond of trimethylsilane. The formation of this complex provides evidence for the oxidative addition of coordinatively-unsaturated iron carbonyl complexes into a silicon–hydrogen bond.

Near-UV irradiation of the iron(silyl)dicarbonyl complex **418** in the presence of ethylene **193** gave iron-alkyl complex **422**, which indicated the insertion of ethylene **193** into the iron–silicon bond (Scheme 2.29b). Near-UV irradiation of the isolated iron-alkyl complex **422** resulted in decomposition through β-hydride- and β-silyl elimination pathways to give iron(hydride)dicarbonyl **425** and iron(silyl) dicarbonyl **418** in 65 and 29 % yield, respectively (Scheme 2.29c). Vinylsilane **424** and ethylene **193** were released as by-products of these reactions. This experiment supported the proposed mechanism for the formation of dehydrosilylation products in iron-catalysed hydrosilylation, and also demonstrated that alkene insertion into

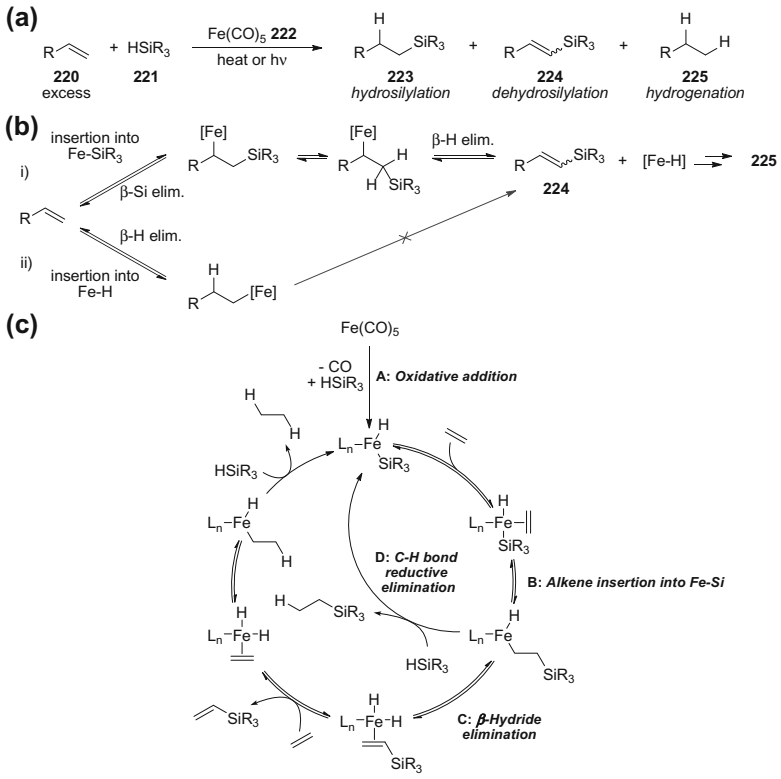

Scheme 2.28 Iron-catalysed hydrosilylation using iron pentacarbonyl as a pre-catalyst. **a** General reaction scheme. **b** Significance of alkene insertion into an iron–silicon bond for the formation of dehydrosilylation products. **c** Proposed hydrosilylation mechanism, with 'key steps' (***A–D***) highlighted

the iron–silicon bond was reversible. Finally, near-UV irradiation of iron(alkyl) dicarbonyl complex **426** in the presence of trimethylsilane resulted in the formation of methane and iron(disilyl)hydride complex **419** (Scheme 2.29d). The pentacoordinate iron(silyl)(hydride) intermediate **427** was proposed based upon UV-visible absorption spectroscopy. Significantly, tetramethylsilane ($SiMe_4$) was not observed, suggesting that carbon–hydrogen bond reductive elimination was kinetically favoured over carbon–silicon bond reductive elimination.

In-depth mechanistic studies have not been undertaken for bis(imino)pyridine iron-catalysed hydrosilylation reactions. Chirik has reported the stoichiometric reactions of bis(imino)pyridine iron bis(dinitrogen) complex **157** with diphenylacetylene **396** and phenylsilane **47** to give the isolatable acetylene- and bis(silane) complexes **429** and **430** (Scheme 2.30a, b) [8]. Both complexes were effective pre-catalysts for hydrosilylation, showing similar activity to bis(imino)pyridine iron bis(nitrogen) complexes. This demonstrates that both complexes are in equilibrium with catalytically-active species in solution, however in the absence of kinetic data further conclusions on the catalytic significance of these complexes is difficult.

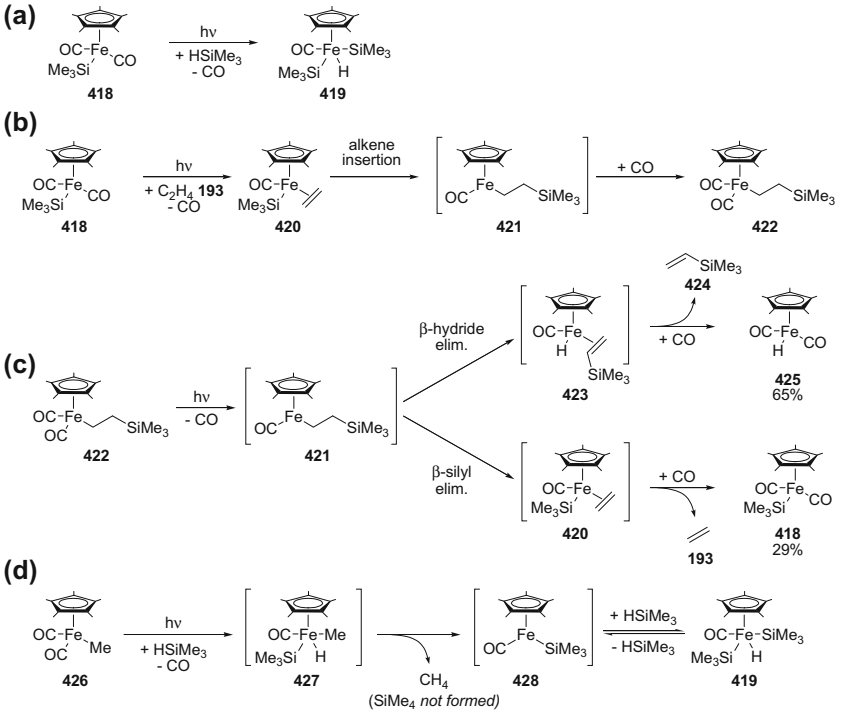

Scheme 2.29 Stoichiometric reactions of pentamethylcyclopentadienyl iron carbonyl complexes to demonstrate each of the 'key steps' (**A–D**) highlighted in Scheme 2.28c. **a** Oxidative addition of $HSiR_3$, **b** alkene insertion into Fe-SiR_3, **c** β-hydride- and β-silyl elimination from iron alkyl, **d** reductive elimination of C–H bond

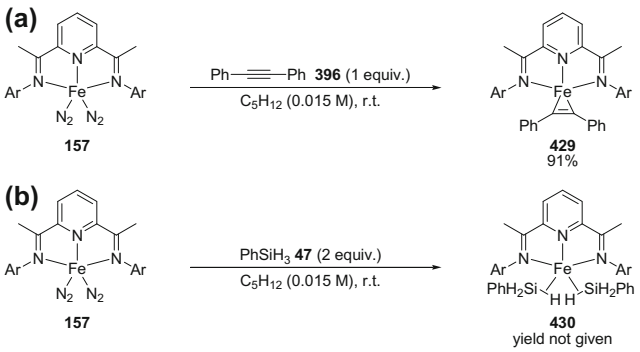

Scheme 2.30 Stoichiometric reactions of bis(imino)pyridine iron bis(dinitrogen) complex **157** with phenylacetylene **396** and phenylsilane **47** to give iron complexes **429** and **430**, respectively

Analysis of the crystal structure of the diphenylacetylene complex **429** showed pyramidalisation of the acetylenic carbons and elongation of the carbon–carbon triple bond, consistent with considerable π-back bonding from the iron centre. The (bis)silane σ-complex **430** contained two phenylsilane molecules, each bound to iron through a silicon–hydrogen σ-bond. Single crystal X-ray analysis showed significant elongation of the coordinated silicon–hydrogen σ-bond. Although the reaction of the bis(imino)pyridine iron bis(dinitrogen) complex **157** with phenylsilane **47** had given a (bis)silane σ-complex **430**, Chirik suggested that iron-catalysed hydrosilylation may instead proceed by oxidative addition of the iron catalyst into the silicon–hydrogen bond to give an iron(silyl)(hydride) intermediate. The yield was not given for the synthesis of the (bis)silane σ-complex **430**, and so it is conceivable that an iron(silyl)(hydride) complex may have also been formed, but was not isolated.

We sought to investigate some mechanistic aspects of the developed methodology for iron-catalysed hydrosilylation. Rather than focussing on the stoichiometric reactions of isolated complexes, we chose to study catalytic reactions where analysis of the reaction products and by-products could be used to provide mechanistic insight.

2.2.8.1 Reduction of Iron(II) Pre-catalyst

Using the developed in situ pre-catalyst reduction technique, we were presented with an opportunity to calculate the average oxidation-state of the iron catalyst in the reaction by using *p*-tolylmagnesium bromide as the pre-catalyst reductant. Arylation of the iron(II) pre-catalyst ^{Et}BIPFeCl$_2$ **367** by *p*-tolylmagnesium bromide **282** would give an iron(II)diaryl intermediate **431**, which following carbon–carbon bond reductive elimination would result in a two electron reduction of iron, and the formation of 4,4′-dimethylbiphenyl **432** as a by-product (Scheme 2.31) [47]. Quantification of the formation of 4,4′-dimethylbiphenyl **432** could then be used to calculate the average number of electrons that had been transferred to iron during pre-catalyst reduction (Eq. 2.1).

$$\text{Number of electrons transfered to iron} = \frac{\%\ \text{Yield of } \mathbf{432} \times 2}{\text{mol}\%\ \text{of } ^{Et}\text{BIPFeCl}_2\ \mathbf{367}\ \text{used}} \qquad (2.1)$$

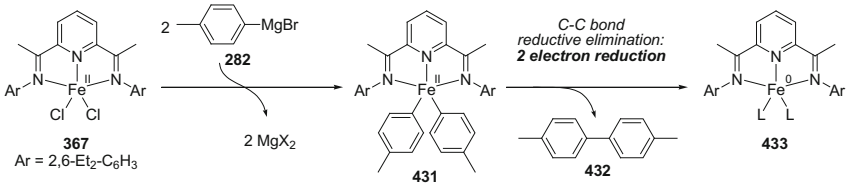

Scheme 2.31 Reduction of iron(II) pre-catalyst using *p*-tolylmagnesium bromide

Table 2.9 Quantification of the reduction of the Iron(II) pre-catalyst using *p*-tolylmagnesium bromide[a]

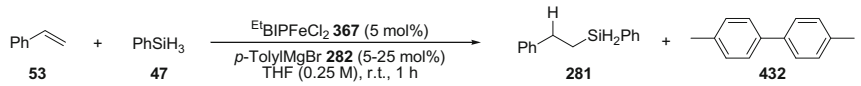

53 47 281 432

Entry	*p*-TolylMgBr/mol %	Yield (%)[b]		Number of electron reduction of iron	Average oxidation-state of iron
		281	432		
1	5	–	0.75	0.30	1.70
2	10	93	2.25	0.90	1.10
3	15	82	3.70	1.48	0.52
4	20	21	4.10	1.64	0.36
5	25	4	4.45	1.78	0.22

[a]Conditions: styrene **53** (0.7 mmol), $^{Et}BIPFeCl_2$ **367** (5 mol%), $PhSiH_3$ **47** (0.77 mmol), *p*-tolylMgBr **282** (5-25 mol%), THF (0.25 M), r.t. 1 h; [b]Yield determined by ^1H NMR spectroscopy using 1,3,5-trimethoxybenzene as an internal standard

Pre-catalyst activation using various amounts of *p*-tolylmagnesium bromide **282** was studied for the hydrosilylation of styrene **53** with phenylsilane **47** (Table 2.9). An iron(II) pre-catalyst loading of 5 mol% was used to improve the accuracy of quantification of the 4,4′-dimethylbiphenyl **432** by-product. All reactions were worked up by the addition of aqueous acid under an inert atmosphere to limit the possibility of oxidative homocoupling of any remaining Grignard reagent [48], which could lead to misleadingly high quantities of 4,4′-dimethylbiphenyl **432**. The yields of hydrosilylation product **281** and 4,4′-dimethylbiphenyl **432** were calculated by quantitative ^1H NMR spectroscopy using 1,3,5-trimethoxybenzene (20 mol%) as an internal standard. Using the same technique it was determined that the solution of *p*-tolylmagnesium bromide used in these experiments contained <0.5 % 4,4′-dimethylbiphenyl **432**, relative to the concentration of Grignard reagent.

In keeping with the initial reaction optimisation studies it was found that maximum catalytic activity was observed when two equivalents of *p*-tolylmagnesium bromide **282** were used (Table 2.9, entry 2). At this loading of Grignard reagent, 4,4′-dimethylbiphenyl **432** was obtained in a 2.25 % yield, corresponding to a 0.9 electron reduction of the iron(II) pre-catalyst to an average formal oxidation-state of 1.1. This was intriguing as the quantity of 4,4′-dimethylbiphenyl **432** obtained accounted for only half of the *p*-tolylmagnesium bromide that had been used. Use of 5 mol% *p*-tolylmagnesium bromide **282** (1 equivalent with respect to iron) did not give an active catalyst and resulted in the formation of only a trace amount of 4,4′-dimethylbiphenyl **432** (Table 2.9, entry 1). This indicates that more than one equivalent of *p*-tolylmagnesium bromide **282** is needed for the reductive elimination of 4,4′-dimethylbiphenyl **432** to take place, and is consistent with the proposed pre-catalyst reduction pathway (Scheme 2.31). The addition of more than two equivalents of *p*-tolylmagnesium bromide **282** with respect to iron resulted in

increasingly poor catalytic activity and the formation of more 4,4′-dimethylbiphenyl **432** (Table 2.9, entries 3–5). The lowest catalytic activity was observed using 25 mol% *p*-tolylmagnesium bromide **282** (5 equivalents with respect to iron). In this case, 4,4′-dimethylbiphenyl **432** was obtained in a 4.45 % yield, suggesting that reduction below iron(0) was unfavourable even in the presence of excess Grignard reagent (Table 2.9, entry 5).

These results suggest that the iron(II) pre-catalyst **367** was reduced to an iron(I) species following reaction with two equivalents of *p*-tolylmagnesium bromide **282**. Only one equivalent of the *p*-tolylmagnesium bromide **282** could be accounted by the formation of 4,4′-dimethylbiphenyl **432**, however pre-catalyst reduction with just one equivalent of *p*-tolylmagnesium bromide **282** did not give an active catalyst. This could indicate the formation of an iron(I) aryl complex, where the first equivalent of *p*-tolylmagnesium bromide **283** is needed for the one electron reduction of the iron(II) pre-catalyst **367**, and the second equivalent remains bound to iron.

These results can be explained if the reaction of *p*-tolylmagnesium bromide **282** with the iron(II) dichloride pre-catalyst ^{Et}BIPFeCl$_2$ **367** gives an iron(II)(aryl)(chloride) intermediate **434** which is arylated at a slower rate than the iron(II) dichloride complex ^{Et}BIPFeCl$_2$ **367** (Scheme 2.32a, $k_1 > k_2$). Therefore the addition of just one equivalent of *p*-tolylmagnesium bromide **282** results in a catalytically inactive iron(II) species **434** and the formation of only small quantities of 4,4′-dimethylbiphenyl **432**. Upon addition of a second equivalent of *p*-tolylmagnesium

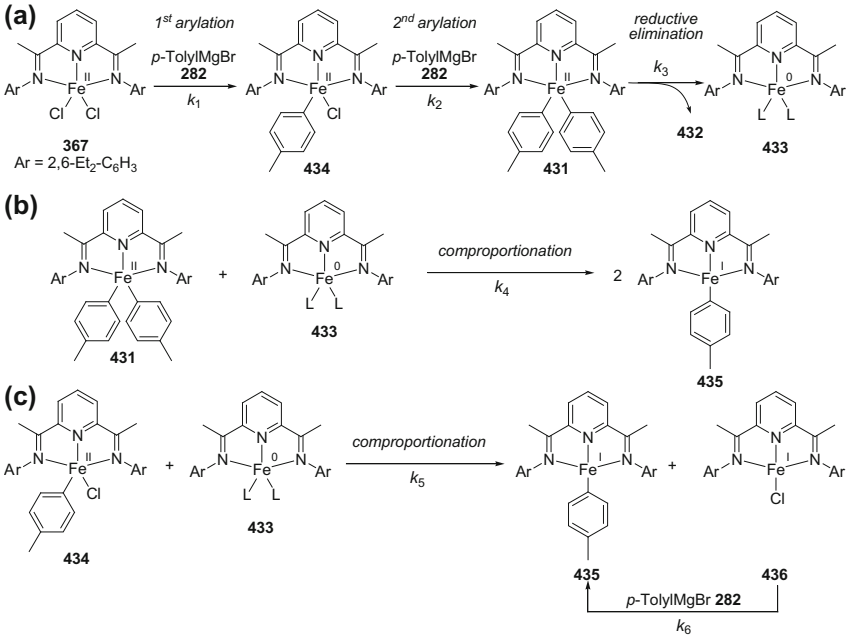

Scheme 2.32 Proposed formation of an iron(I) aryl complex **435** following the reduction of the iron(II) pre-catalyst **367** using *p*-tolylmagnesium bromide

bromide **282**, the diarylated iron(II) complex **431** is formed, which can undergo carbon–carbon bond reductive elimination to give 4,4′-dimethylbiphenyl **432** and a formally iron(0) complex **433**. Comproportionation between the formally iron(0) complex **433** and the diaryl iron(II) complex **431** would give two equivalents of the proposed iron(I) aryl complex **435** (Scheme 2.32b). The formation of an iron(I) aryl complex under the reaction conditions might suggest that the rate of comproportionation is comparable, or faster than, the rate of reductive elimination of 4,4′-dimethylbiphenyl **432** from the diaryl iron(II) complex **431** ($k_4 \geq k_3$). Alternatively, if the rate of the second arylation (k_2) is slower than all other processes, the concentration of the iron(II)(aryl)(chloride) intermediate **434** will be high. Comproportionation may therefore take place between iron(0) complex **433** and iron(II)(aryl)(chloride) intermediate **434** to give the iron(I) aryl complex **435** and the iron(I) chloride complex **436**. The iron(I) chloride complex **436** may then be converted to the iron(I) aryl complex **435** following reaction with another equivalent of *p*-tolylmagnesium bromide (Scheme 2.32c). According to either reduction pathway, two equivalents of *p*-tolylmagnesium bromide **282** would be required to give the iron(I) aryl complex **435**.

Chirik has shown that the analogous reaction of a bis(imino)pyridine iron(II) dibromide complex with two equivalents of phenyllithium also results in a one electron reduction to give a bis(imino)pyridine iron(I) phenyl complex, with concurrent formation of half an equivalent of biphenyl [49]. Chirik has also recently reported that bis(imino)pyridine iron(I) methyl complexes are suitable pre-catalysts for the hydrogenation of alkenes, without the need for any further reductant [50]. Although formally assigned as an iron(I) complex it is important to consider the redox-activity of the bis(imino)pyridine ligand. The reduction of the iron(II) pre-catalyst may in reality result in a one-electron reduction of the bis(imino) pyridine ligand to leave the iron centre in an oxidation-state of +2. Chirik has reported this effect with analogous bis(imino)pyridine iron (mono)alkyl complexes, where the electronic structures were determined to be high spin iron(II) centres coupled to bis(imino)pyridine radical anions [51].

The lower formal oxidation-states calculated when using excess *p*-tolylmagnesium bromide **282** (Table 2.9, entries 3–5) suggests that a larger quantity of the iron (0) complex **433** was formed. This could indicate that the rate of the second arylation (k_2) is the rate limiting process, and therefore an increase in the concentration of *p*-tolylmagnesium bromide **282** leads to an increase in the concentration of the diaryl iron(II) complex **431**. This would increase the rate of reductive elimination (k_3) to give iron(0) complex **433**. Based upon Chirik's work however it would be expected that an iron(0) complex, such as **433**, should also be an effective pre-catalyst for the hydrosilylation of alkenes. The reduction in catalytic activity observed upon the use of excess *p*-tolylmagnesium bromide **282** might therefore be attributed to further arylation of the iron(0) or iron(I) complexes formed to give catalytically inactive aryl-ferrate species **437** (Scheme 2.33a) [49]. Reductive elimination from iron(0) aryl complexes to give lower oxidation-state iron complexes has not been reported, and therefore coordinatively saturated aryl-ferrate species, such as **437**, may be the dominant species in solution in the presence of excess *p*-tolylmagnesium bromide

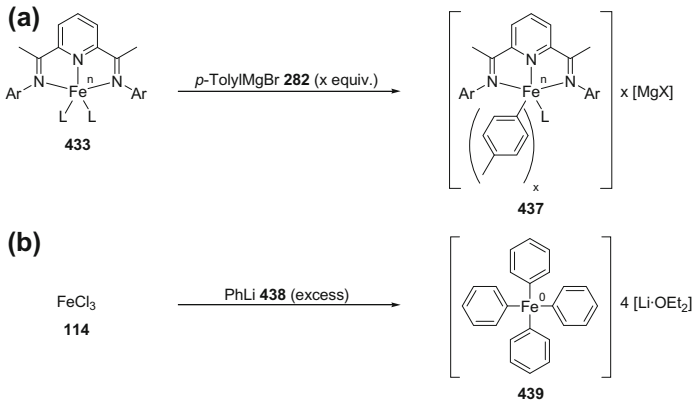

Scheme 2.33 Exhaustive arylation of iron species by aryl-metal reagents. **a** Proposed deactivation of iron (pre-)catalyst in the presence of excess *p*-tolylmagnesium bromide **282**. **b** Reported reaction of iron(III) chloride **114** with phenyllithium **438** to give iron(0) tetraphenylferrate **439** [52]

282. This is supported by the reaction of iron(III) chloride **114** with excess phenyllithium **438**, which leads to the formation of the highly arylated square-planar iron(0) tetraphenylferrate complex **439** (Scheme 2.33b) [52].

2.2.8.2 Hydrosilylation Using Deuterium-Labelled Silane

The deuterium-labelled silane, diphenyl(silane-d_2) ***d*$_2$-255**, was conveniently prepared by lithium aluminium deuteride ***d*$_4$-441** reduction of dichlorodiphenylsilane **440** (Scheme 2.34).

The hydrosilylation of styrene **53** using diphenyl(silane-d_2) ***d*$_2$-255** was investigated to ascertain if any useful mechanistic insight could be gained from this simple reaction (Scheme 2.35). The expected addition product ***d*$_1$-300** with a single deuterium incorporated at the benzylic position was obtained as the major product, however addition products with two deuteriums ***d*$_2$-300** and two hydrogens **300** in the benzylic position were also obtained. In addition, mono-deuterated diphenyl (silane-d_1) ***d*$_1$-255** and non-deuterated diphenylsilane **255** were also recovered, where deuterium–hydrogen exchange had occurred on silicon. The hydrosilylation products ***d*$_{0\text{-}2}$-300** were also obtained as a mixture, where the silyl group contained

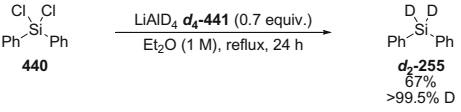

Scheme 2.34 Reduction of dichlorodiphenylsilane **440** with lithium aluminium deuteride ***d*$_4$-441** to give diphenyl(silane-d_2) ***d*$_2$-255**

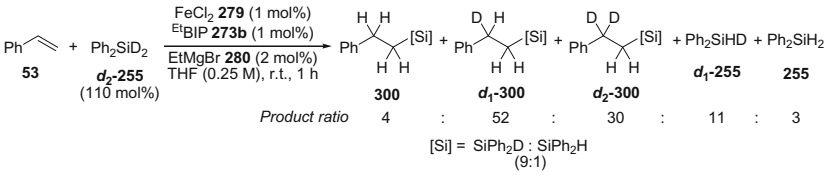

Scheme 2.35 Hydrosilylation of styrene **53** using diphenyl(silane-d_2) ***d*$_2$-255**

either a silicon–deuterium or silicon–hydrogen bond. Significantly, ^{2}H NMR spectroscopy confirmed the presence of deuterium only on silicon and in the benzylic position, with no deuterium incorporation observed at the homobenzylic position (α- to the silyl group).

The observation of H–D transfer between the benzylic position of styrene and the silane can be most easily explained by reversible styrene insertion into an iron–hydride/deuteride bond and reversible oxidative addition/reductive elimination of the silane (Scheme 2.36a). Insertion of styrene into the iron–deuterium bond of iron complex **442** would give the iron-alkyl intermediate **443**, which contains both a hydrogen and deuterium atom β- to iron. β-Deuteride elimination would reform the original iron–deuteride complex **442**, however β-hydride elimination would give iron–hydride complex **444** and α-deuteriostyrene ***α*-*d*$_1$-53**. Diphenyl(silane-d_1) ***d*$_1$-255** could also be formed following silicon–hydrogen bond reductive elimination. The formation of these two products represents the formal hydrogen transfer from styrene to diphenylsilane, and deuterium transfer from diphenylsilane to styrene, and could therefore be used to account for the mixture of products obtained (Scheme 2.35). A possible weakness with this mechanism is that no deuterium incorporation was observed in the homobenzylic position of the hydrosilylation products ***d*$_{0\text{-}2}$-300**. This would imply that alkene insertion into the iron–deuteride bond of iron complex **442** would need to be 100 % regioselective. If styrene insertion took place with the opposite regioselectivity, iron-benzyl intermediate **445** would be formed, which would lead to products with deuterium incorporation in the

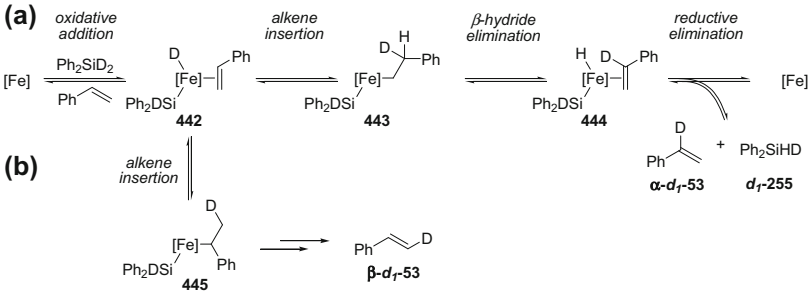

Scheme 2.36 Reversible β-hydride elimination mechanism to explain hydrogen–deuterium exchange in the hydrosilylation of styrene using deuterium-labelled silane

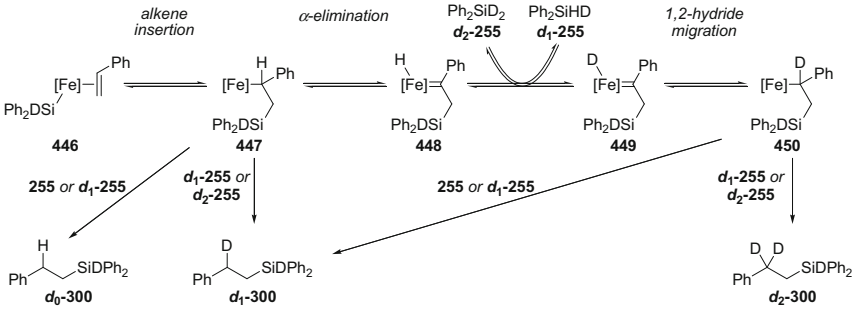

Scheme 2.37 Reversible α-elimination mechanism, via iron carbenoid intermediates **448** and **449**, to explain hydrogen–deuterium exchange in the hydrosilylation of styrene **53** using Ph_2SiD_2 ***d*$_2$-255**

homobenzylic position (Scheme 2.36b). Iron-alkyl complexes have been shown to rearrange to the most thermodynamically-favoured species [53], and therefore it would be expected that formation of the iron-benzyl species **445**, and not iron-alkyl species **443**, would be more favourable.

An alternative proposal which involves the intermediacy of iron carbenoid species [54] could be used to account for the regioselectivity of deuterium incorporation in hydrosilylation products ***d*$_{0\text{-}2}$-300** (Scheme 2.37). Alkene insertion into the iron–silicon bond of iron–silyl complex **446** would give the iron–benzyl intermediate **447**. Carbon–hydrogen bond formation from this intermediate would give hydrosilylation product ***d*$_1$-300**. If iron-benzyl intermediate **447** also had a deuteride ligand this product could be formed by reductive elimination, however in the absence of a deuteride ligand an intermolecular reaction with another equivalent of silane would be required to release the hydrosilylation product ***d*$_1$-300**. Alternatively, iron–benzyl intermediate **447** may decompose by an α-elimination pathway to give the (hydrido)iron carbenoid intermediate **448**. Hydride–deuteride ligand exchange could take place by reaction with another equivalent of silane ***d*$_2$-255**, through an oxidative addition-reductive elimination or σ-bond metathesis process. A 1,2-deuteride migration of iron carbenoid intermediate **449** would give the iron-benzyl intermediate **448** with deuterium incorporation in the benzylic position. Carbon–deuterium bond formation from this intermediate would give hydrosilylation product ***d*$_2$-300** with two deuterium in the benzylic position. Although β-hydride elimination is probably the most commonly considered decomposition pathway for metal-alkyl species, α-elimination processes are also thermodynamically favourable through the conversion of a metal-alkyl into a relatively more stable metal carbenoid complex [55]. The proposed iron carbenoid intermediate **448** might be classified as a Fischer carbene, based upon the low oxidation-state of iron and strong π-accepting abilities of the bis(imino)pyridine ligand [56]. It would therefore be expected that the formation of the iron carbenoid complex **448** would be favoured by the stabilising effects of the adjacent aromatic ring and silane group [57].

2.2.8.3 Proposed Mechanism for Iron-Catalysed Hydrosilylation Using a Bis(imino)pyridine Iron(II) Pre-catalyst

During this work a number of observations were made that provide some mechanistic insight, and allow a possible mechanism to be proposed (Scheme 2.38). In the proposed mechanism the formal oxidation-state of iron has been given in each instance,

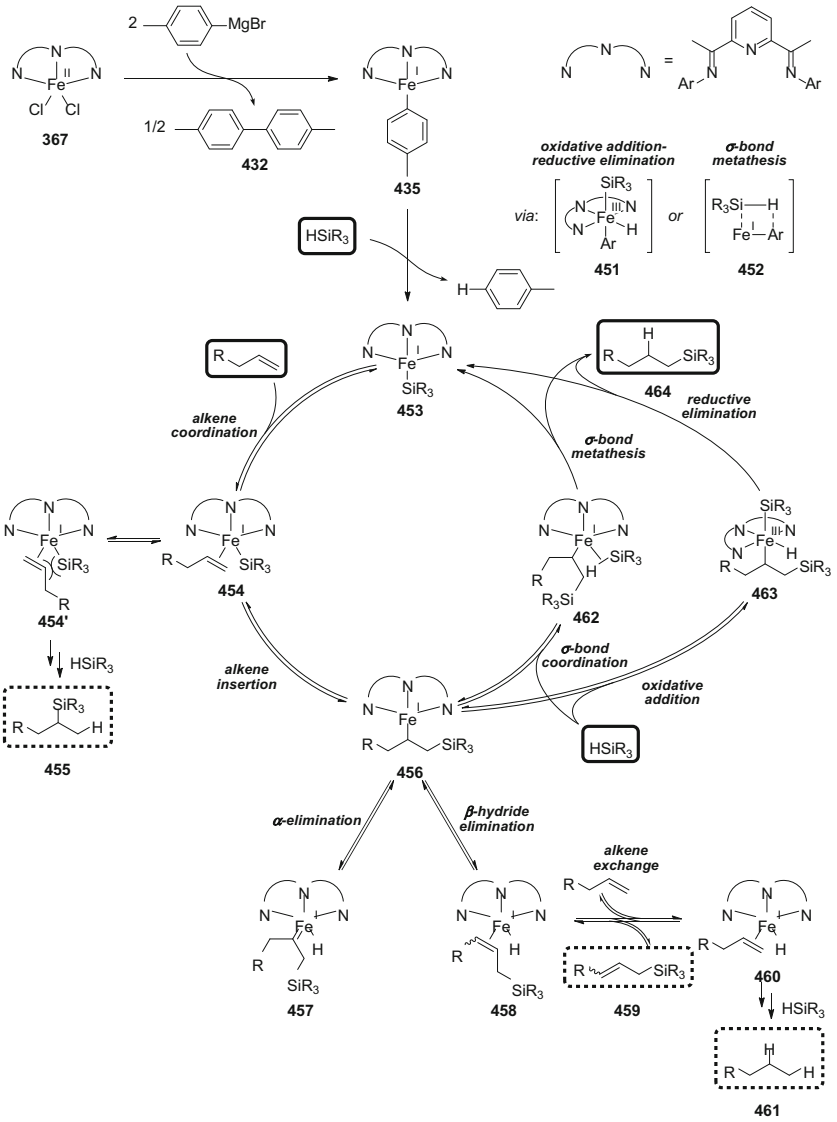

Scheme 2.38 Proposed mechanism for the iron-catalysed hydrosilylation of alkenes using an iron (II) pre-catalyst

for iron complexes bearing a neutral bis(imino)pyridine ligand. It is important to appreciate that the bis(imino)pyridine ligand can also exist in reduced forms, meaning that the true oxidation-state of iron in these complexes could be higher.

The oxidation-state studies show that the iron(II) pre-catalyst ^{Et}BIPFeCl$_2$ **367** reacts with two equivalents of *p*-tolylmagnesium bromide **282** to give half an equivalent of 4,4′-dimethylbiphenyl **432**. This accounts for just half of the *p*-tolylmagnesium bromide **282** used, and indicates a one electron reduction of the pre-catalyst. These two observations together suggest the formation of the iron(I)-*p*-tolyl complex **435**. This species would still be only a pre-catalyst, and require conversion to an active catalyst. The diastereoselective hydrosilylation of terminal alkynes to give (*Z*)-vinylsilane products (Table 2.7), and the dehydrosilylation of 4-phenylbutene **361** using secondary silanes (Scheme 2.16), suggests that alkene/alkyne insertion into an iron–silicon bond takes place. It is therefore plausible that iron(I)-*p*-tolyl complex **435** is converted to an active iron(I) silyl complex **453** following reaction with an equivalent of silane. This may take place by an oxidative addition-reductive elimination pathway, via an iron(III) complex **451**, or by a σ-bond metathesis between the iron–aryl and silicon–hydrogen bonds **452**. In the latter process, the silane may first coordinate to iron to give a silane σ-bond complex, similar to those reported by Chirik [8].

As the hydrosilylation of terminal alkenes gave linear silane products exclusively using this methodology, alkene insertion into the iron–silicon bond must take place regioselectively to give the iron alkyl complex **456**. This regioselectivity could arise from a preference for alkene coordination with the large alkyl group orientated away from the large silyl group to reduce steric hindrance in iron complex **454**. Following formation of iron alkyl complex **456** a number of processes can take place. Reversible α-elimination would give the iron carbenoid complex **457**, proposed based upon the reactions using deuterium-labelled silane, whilst β-hydride elimination would give iron–hydride **458**. Alkene exchange would release the dehydrosilylation product **459** and give an iron–hydride alkene complex **460**, which could lead to the hydrogenation product **461**, following alkene insertion and reaction with a further equivalent of silane.

Iron alkyl complex **456** may alternatively react with a further equivalent of silane to give the hydrosilylation product **464**. This may take place by oxidative addition of iron into the silicon–hydrogen bond to give an iron(III) intermediate **463**. Regioselective oxidative addition of the silicon–hydrogen bond should give the iron complex with the silicon and alkyl groups *trans*- to one another in order to limit steric clashes. The resulting *cis*- relationship between the hydride and alkyl groups would be suitable for carbon–hydrogen bond reductive elimination. The strong *trans*- influence of the silicon group would be expected to weaken the iron–carbon bond and favour reductive elimination of the hydrosilylation product **464** [58]. Alternatively, carbon–hydrogen bond formation may take place by a σ-bond metathesis process [59]. Transition-metal-silane σ-complexes are well known [60], and the reaction of a bis(imino)pyridine iron bis(dinitrogen) complex has been shown to give a bis(silane) σ-complex [8], where the silicon–hydrogen bonds were significantly elongated. Silane σ-bond complexation to iron alkyl complex **456**

would give the iron(alkyl)(silane) complex **462**. Elongation and weakening of the coordinated silicon–hydrogen bond would activate it to σ-bond metathesis with the iron–alkyl bond to release the hydrosilylation product **464**. Although formally proposed as a redox-neutral process, it is possible that the transition-state structure of the σ-bond metathesis process may be asynchronous. This could result in a transition-state structure for σ-bond metathesis that may resemble the iron(III) intermediate **463**. The two mechanisms may therefore be distinguished by whether an iron(III) complex, such as **463**, is a reaction intermediate or a transition-state structure (local minima or saddle point on a potential energy surface).

2.2.8.4 Future Directions for Further Elucidation of the Hydrosilylation Mechanism

The mechanism of the developed methodology may be investigated further by a combination of studying the kinetic profile of catalytic reactions and by using the stoichiometric reactions of isolated iron complexes as evidence for the suggested primary steps of the catalytic cycle.

Following the kinetic profile of the hydrosilylation of alkenes will provide information about the rate of catalyst formation during pre-catalyst reduction and the rate of catalyst decomposition in the presence of different quantities of activating agents and functionalised substrates. A range of electronically-differentiated styrene derivatives were applicable in the reaction, providing an opportunity to assess the effect of these groups on the rate of reaction and perform a Hammett analysis. The hydrosilylation of electronically unsymmetrical diarylalkynes would also be interesting to assess not only the rate of reaction, but also the regio- and diastereoselectivity of the process. The source of diastereoselectivity in the hydrosilylation of terminal alkynes could also be investigated more thoroughly through a kinetic analysis approach. Significantly the diastereoselectivity of the reaction could be assessed at all points of the reaction, potentially providing evidence on whether the two diastereoisomers are formed concurrently and in a consistent ratio. It is possible that the formation of each diastereoisomer may give independent kinetic profiles, which could indicate isomerisation between the two diastereoisomers or the presence of multiple catalytically-active species in the reaction.

Key to the suggested catalytic cycle was the formation of an iron(I) aryl pre-catalyst **435**. This complex can be independently synthesised through the reaction of a bis(imino)pyridine iron(II) bromide complex **156** and *p*-tolyllithium **465** (Scheme 2.39a) [49]. The reaction of this complex with a silane could provide evidence to support or refute the suggested pre-catalyst conversion to an iron(I) silyl complex **453** (Scheme 2.39b). Using a deuterium-labelled silane may aid analysis of the reaction products and by-products. Applying both of these complexes as (pre-) catalysts in hydrosilylation reactions would provide data on the catalytic competence of the two complexes. Kinetic analysis would provide quantification of the relative induction periods. Isolation of an iron alkyl complex **456** following alkene insertion into an iron–silicon bond may be challenging due to the various decomposition

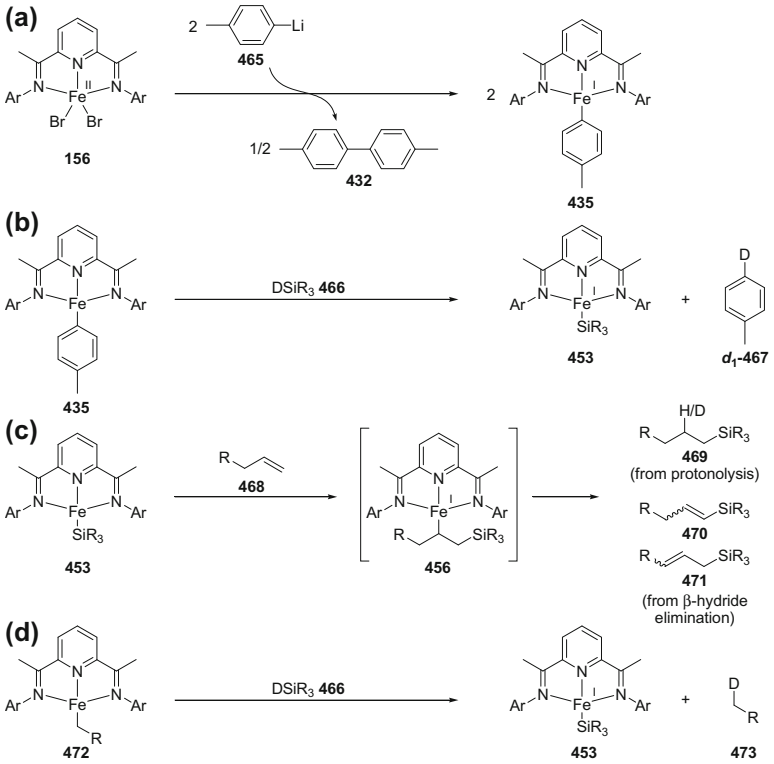

Scheme 2.39 Proposed stoichiometric reactions of isolated iron complexes to validate or disprove each step of the proposed catalytic cycle

pathways identified (Scheme 2.39c). If isolation of the iron alkyl intermediate **456** did prove overly-challenging then analysis of the decomposition products could still be sufficiently informative to provide mechanistic insight. The synthesis of iron alkyl complexes has been reported however [49], therefore if isolation of iron alkyl complex **456** was not possible, an independently synthesised iron alkyl complex **472** could be used as a model complex to validate the final step through reaction with another equivalent of deuterium-labelled silane (Scheme 2.39d).

2.3 Conclusions

A methodology for the iron-catalysed hydrosilylation of alkenes and alkynes using primary, secondary and tertiary silanes has been developed, using the in situ activation of a bench-stable bis(imino)pyridine iron(II) pre-catalyst with an organometallic reagent (Scheme 2.40). This provides a convenient approach to iron-catalysed hydrosilylation, without the need to synthesise and isolate air- and

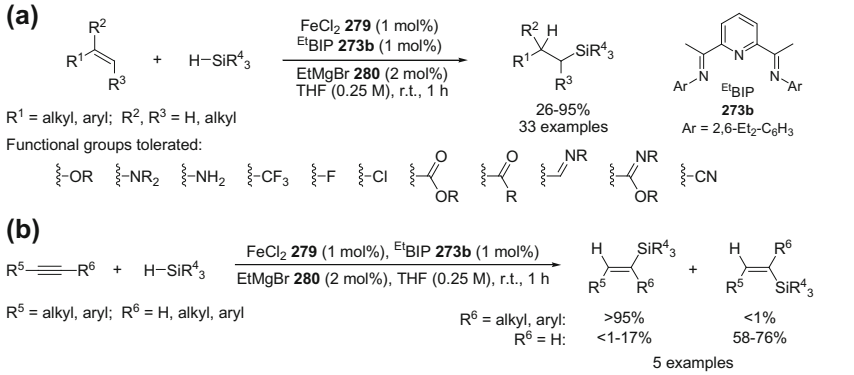

Scheme 2.40 Iron-catalysed hydrosilylation of alkenes and alkynes using in situ reduction of an iron(II) pre-catalyst with ethylmagnesium bromide

moisture sensitive iron complexes. Oxidation of the alkyl- and vinyl silane products using hydrogen peroxide in the presence of the iron catalyst resulted in chemoselective silicon–hydrogen bond oxidation to give alkyl- and vinyl silan(edi)ol products. This serendipitously-discovered one-pot process provides simple access to these synthetically-useful products.

Terminal, 1,1- and 1,2-disubstituted alkenes underwent hydrosilylation to give linear silane products in good to excellent yield and with complete control of regioselectivity (Scheme 2.40a). A range of potentially reducible functional groups were tolerated, and catalyst turnover frequencies of up to 60,000 mol h^{-1} were recorded. The first example of enantioselective iron-catalysed hydrosilylation was obtained using an enantiopure C_1-symmetric bis(imino)pyridine iron(II) pre-catalyst. The hydrosilylation of α-methylstyrene gave the linear silane product in 43 % yield and 53 % ee. During this work, Huang reported an iron-catalysed hydrosilylation methodology displaying a similar range of functional group tolerance [16]. Higher levels of chemoselectivity for the hydrosilylation of alkenes in the presence of ketones were reported, however the methodology was only applicable to terminal alkenes, and the phosphinite-iminopyridine iron(II) pre-catalysts used were air-sensitive, and prepared by a 5-step synthesis.

The hydrosilylation of internal alkynes gave (*E*)-vinyl silanes with complete control of diastereoselectivity, whilst the hydrosilylation of terminal alkynes gave (*Z*)-vinyl silanes in a range of diastereoselectivities (*Z*:*E* = 4:1 → 100:1) (Scheme 2.40b). Further work could focus on the regio- and diastereoselectivity of the hydrosilylation of unsymmetrical di-substituted alkynes. This work would extend the synthetic utility of the process, and may provide further mechanistic insight. Previous iron-catalysed methodologies for the hydrosilylation of alkynes developed by either Enthaler [5] or Plietker [6], have only reported diastereoselectivities for the hydrosilylation of internal alkynes. These methodologies were applied to a much broader range of alkynes, however variable levels of diastereo- and regioselectivity were reported.

Preliminary mechanistic studies indicated that a one-electron reduction of the iron(II) pre-catalyst takes place to give an active catalyst in the formal oxidation-state of iron(I). The use of deuterium-labelled diphenylsilane, Ph_2SiD_2, resulted in a mixture of deuterated- and non-deuterated hydrosilylation products, which may indicate the intermediacy of an iron-carbenoid species (on- or off-cycle). Further mechanistic studies could focus on stoichiometric reactions using isolated iron-complexes to provide support for, or refute, the proposed steps of the catalytic cycle. Kinetic analysis of the hydrosilylation reactions should be undertaken using a range of electronically-differentiated styrene- and diaryl alkyne derivatives. The hydrosilylation reaction profile using these substrates could be obtained in isolation (to provide absolute rates) and in competition experiments (to provide information about competitive binding and reaction inhibition).

Having developed a methodology in which a highly-active low oxidation-state iron catalyst was formed in situ, the potential to extend the process to other hydrofunctionalisation reactions was investigated.

References

1. (a) Nesmeyanov, A. N.; Freidlina, R. K.; Chukovskaya, E. C.; Petrova, R. G.; Belyavksy, A. B. *Tetrahedron* **1962**, *17*, 61. (b) Schroeder, M. A.; Wrighton, M. S. *J. Organomet. Chem.* **1977**, *128*, 345. (c) Randolph, C. L.; Wrighton, M. S. *J. Am. Chem. Soc.* **1986**, *108*, 3366.
2. Seitz, F.; Wrighton, M. S. *Angew. Chem. Int. Ed. Engl.* **1988**, *27*, 289.
3. (a) Onopchenko, A.; Sabourin, E. T.; Beach, D. L. *J. Org. Chem.* **1983**, *48*, 5101. (b) Millan, A.; Fernandez, M.-J.; Bentz, P.; Maitlis, O. M. *J. Mol. Catal.* **1984**, *26*, 89. (c) Ojima, I.; Clos, N.; Donovan, R. J.; Ingallina, P. *Organometallics* **1990**, *9*, 3127. (d) Duckett, S. B.; Perutz, R. N. *Organometallics* **1992**, *11*, 90. (e) Sakaki, S.; Sumimoto, M.; Fukuhara, M.; Sugimoto, M.; Fujimoto, H.; Matsuzaki, S. *Organometallics* **2002**, *21*, 3788.
4. (a) Oro, L. A.; Fernandez, M. J.; Esteruelas, M. A.; Jimenez, M. S. *J. Mol. Catal.* **1986**, *37*, 151. (b) Tanke, R. S.; Crabtree, R. H. *J. Am. Chem. Soc.* **1990**, *112*, 7984. (c) Jun, C.-H.; Crabtree, R. H. *J. Organomet. Chem.* **1993**, *447*, 177.
5. (a) Enthaler, S.; Haberberger, M.; Irran, E. *Chem. Asian J.* **2011**, *6*, 1613. (b) Haberberger, M.; Irran, E.; Enthaler, S. *Eur. J. Inorg. Chem.* **2011**, 2797.
6. Belger, C.; Plietker, B. *Chem. Commun.* **2012**, *48*, 5419.
7. Colvin, E. W. *Chem. Soc. Rev.* **1978**, *7*, 15.
8. Bart, S. C.; Lobkovsky, E.; Chirik, P. J. *J. Am. Chem. Soc.* **2004**, *126*, 13794.
9. Chirik, P. J. In *Pincer and Pincer-Type Complexes: Applications in Organic Synthesis and Catalysis*; Szabo, K. J., Wendt, O. F., Eds.; Wiley-VCH: Weinheim, 2014; pp 189-212.
10. Stieber, S. C. E.; Milsmann, C.; Hoyt, J. M.; Turner, Z. R.; Finkelstein, K. D.; Wieghardt, K.; DeBeer, S.; Chirik, P. J. *Inorg. Chem.* **2012**, *51*, 3770.
11. Russell, S. K.; Darmon, J. M.; Lobkovsky, E.; Chirik, P. J. *Inorg. Chem.* **2010**, *49*, 2782.
12. (a) Tondreau, A. M.; Atienza, C. C. H.; Weller, K. J.; Nye, S. A.; Lewis, K. M.; Delis, J. G. P.; Chirik, P. J. *Science* **2012**, *335*, 567. (b) Atienza, C. C. H.; Tondreau, A. M.; Weller, K. J.; Lewis, K. M.; Cruse, R. W.; Nye, S. A.; Boyer, J. L.; Delis, J. G. P.; Chirik, P. J. *ACS Catal.* **2012**, *2*, 2169.
13. Kamata, K.; Suzuki, A.; Nakai, Y.; Nakazawa, H. *Organometallics* **2012**, *31*, 3825.
14. Tondreau, A. M.; Atienza, C. C. H.; Darmon, J. M.; Milsmann, C.; Hoyt, H. M.; Weller, K. J.; Nye, S. A.; Lewis, K. M.; Boyer, J.; Delis, J. G. P.; Lobkovsky, E.; Chirik, P. J.; *Organometallics* **2012**, *31*, 4886.

15. (a) Markó, I. E.; Stérin, S.; Buisine, O.; Mignani, G.; Branlard, P.; Tinant, B.; Declercq, J.-P. *Science* **2002**, *298*, 204. (b) Troegel, D.; Stohrer, J. *Coord. Chem. Rev.* **2011**, *255*, 1440.
16. Peng, D.; Zhang, Y.; Du, X.; Zhang, L.; Leng, X.; Walter, M. D.; Huang, Z. *J. Am. Chem. Soc.* **2013**, *135*, 19154.
17. (a) Small, B. L.; Brookhart, M.; Bennett, A. M. A. *J. Am. Chem. Soc.* **1998**, *120*, 4049. (b) Britovsek, G. J. P.; Bruce, M.; Gibson, V. C.; Kimberley, B. S.; Maddox, P. J.; Mastroianni, S.; McTavish, S. J.; Redshaw, C.; Solan, G. A.; Strömberg, S.; White, A. J. P.; Williams, D. J. *J. Am. Chem. Soc.* **1999**, *121*, 8728.
18. Esteruelas, M. A.; López, A. M.; Méndez, L.; Oliván, M.; Oñate E. *Organometallics* **2003**, *22*, 395.
19. Cristau, H.-J.; Ouali, A.; Spindler, J.-F.; Taillefer, M. *Chem. Eur. J.* **2005**, *11*, 2483.
20. DuBois, D. L.; Miedaner, A. *Inorg. Chem.* **1986**, *25*, 4642.
21. Bedford, R. B.; Carter, E.; Cogswell, P. M.; Gower, N. J.; Haddow, M. F.; Harvey, J. N.; Murphy, D. M.; Neeve, E. C.; Nunn, J. *Angew. Chem. Int. Ed.* **2013**, *52*, 1285.
22. (a) Waack, R.; Doran, M. A. *J. Org. Chem.* **1967**, *32*, 3395. (b) Wei, X.; Taylor, R. J. K. *Chem. Commun.* **1996**, 187.
23. See experimental chapter for further details.
24. Nakayama, Y.; Baba, Y.; Yasuda, H.; Kawakita, K.; Ueyama, N. *Macromolecules* **2003**, *36*, 7953.
25. Tondreau, A. M.; Darmon, J. M.; Wile, B. M.; Floyd, S. K.; Lobkovsky, E.; Chirik, P. J. *Organometallics* **2009**, *28*, 3928.
26. Wile, B. M.; Trovitch, R. J.; Bart, S. C.; Tondreau, A. M.; Lobkovsky, E.; Milsmann, C.; Bill, E.; Wieghardt, K.; Chirik, P. J. *Inorg. Chem.* **2009**, *48*, 4190.
27. Kumar, A.; Akula, H. K.; Lakshman, M. K. *Eur. J. Org. Chem.* **2010**, 2709.
28. (a) Mirviss, S. B. *J. Org. Chem.* **1989**, *54*, 1948. (b) Baker, K. V.; Brown, J. M.; Hughes, N.; Skarnulis, A. J.; Sexton, A. *J. Org. Chem.* **1991**, *56*, 698.
29. Chinchilla, R.; Nájera, C. *Chem. Rev.* **2007**, *107*, 874.
30. Gülak, S.; Jacobi von Wangelin, A. *Angew. Chem. Int. Ed.* **2012**, *51*, 1357.
31. Gülak, S.; Gieshoff, T. N.; Jacobi von Wangelin, A. *Adv. Synth. Catal.* **2014**, *355*, 2197.
32. (a) Fürstner, A.; Leitner, A. *Angew. Chem. Int. Ed.* **2002**, *41*, 609. (b) Czaplik, W. M.; Grupe, S.; Mayer, M.; Jacobi von Wangelin, A. *Chem. Commun.* **2010**, *46*, 6350.
33. For reviews see: references 58a-b. For recent examples see: (a) Das, S.; Wendt, B.; Möller, K.; Junge, K.; Beller, M. *Angew. Chem. Int. Ed.* **2012**, *51*, 1662. (b) Bézier, D.; Venkanna, G. T.; Mistal Castro, L. C.; Zheng, J.; Roisnel, T.; Sortais, J.-B.; Darcel, C. *Adv. Synth. Catal.* **2012**, *354*, 1879. (c) Misal Castro, L. C.; Sortais, J.-B.; Darcel, C. *Chem. Commun.* **2012**, *48*, 151. (d) Volkov, A.; Buitrago, E.; Adolfsson, H. *Eur. J. Org. Chem.* **2013**, 2066.
34. Tondreau, A. M.; Lobkovsky, E.; Chirik, P. J. *Org. Lett.* **2008**, *10*, 2789.
35. (a) Trovitch, R. J.; Lobkovsky, E.; Bill, E.; Chirik, P. J. *Organometallics* **2008**, *27*, 1470. (b) Trovitch, R. J.; Lobkovsky, E.; Bouwkamp, M. W.; Chirik, P. J. *Organometallics* **2008**, *27*, 6264.
36. Monfette, S.; Turner, Z. R.; Semproni, S. P.; Chirik, P. J. *J. Am. Chem. Soc.* **2012**, *134*, 4561.
37. (a) Zhang, L.; Zuo, Z.; Wan, X.; Huang, Z. *J. Am. Chem. Soc.* **2014**, *136*, 15501. (b) Chen, J.; Xi, T.; Ren, X.; Cheng, B.; Guo, J.; Lu, Z. *Org. Chem. Front.* **2014**, *1*, 1306.
38. Chen, J.; Xi, T.; Lu, Z. *Org. Lett.* **2014**, *16*, 6452.
39. Fleming, I.; Dunoguès, J.; Smithers, R. In *Organic Reactions*. Wiley: Weinheim, 1989, vol. 37; pp 57-575.
40. (a) Yu, Y.; Smith, L. M.; Flaschenriem, C. J.; Holland, P. L. *Inorg. Chem.* **2006**, *45*, 5742. (b) Casitas, A.; Krause, H.; Goddard, R.; Fürstner, A. *Angew. Chem. Int. Ed.* **2015**, *54*, 1521.
41. (a) Tamao, K.; Ishida, N.; Tanaka, T.; Kumada, M. *Organometallics* **1983**, *2*, 1694. (b) Tamao, K.; Ishida, N. *J. Organomet. Chem.* **1984**, *269*, C37. (c) Fleming, I.; Henning, R.; Plaut, H. *J. Chem. Soc. Chem. Commun.* **1984**, 29.
42. (a) Marciniec, B. *Hydrosilylation: A Comprehensive Review on Recent Advances*; Springer: Berlin, 2009. (b) Lickiss, P. D. *Adv. Inorg. Chem.* **1995**, *42*, 147.

43. (a) Hirabayashi, K.; Mori, A.; Kawashijma, J.; Suguro, M.; Nishihara, Y.; Hiyama, T. *J. Org. Chem.* **2000**, *65*, 5342. (b) Denmark, S. E.; Neuville, L.; Christy, M. E. L.; Tymonko, S. A. *J. Org. Chem.* **2006**, *71*, 8500.
44. Mori, A. Danda, Y.; Fujii, T.; Hirabayashi, K.; Osakada, K. *J. Am. Chem. Soc.* **2001**, *123*, 10774.
45. Fujii, T.; Koike, T.; Mori, A.; Osakada, K. *Synlett* **2002**, 298.
46. (a) Ya Sychev, A.; Isak, V. G. *Russ. Chem. Rev.* **1995**, *12*, 1105. (b) Walling, C. *Acc. Chem. Res.* **1975**, *8*, 125.
47. (a) Tamura, M.; Kochi, J. *Bull. Chem. Jpn. Soc.* **1971**, *44*, 3063. (b) Hedström, A.; Lindstedt, E.; Norrby, P.-O. *J. Organomet. Chem.* **2013**, *748*, 51.
48. Kharasch, M. S.; Fields, E. K. *J. Am. Chem. Soc.* **1941**, *63*, 2316.
49. Fernández, I.; Trovitch, R. J.; Lobkovsky, E.; Chirik, P. J. *Organometallics* **2008**, *27*, 109.
50. Chirik, P. J.; Monfette, S.; Hoyt, J. M.; Friedfeld, M. R. Enantiopure base-metal catalysts for asymmetric catalysis and bis(imino)pyridine iron alkyl complexes for catalysis. U.S. Patent 20130079567 A1, March 28, 2013.
51. Trovitch, R. J.; Lobkovsky, E.; Chirik, P. J. *J. Am. Chem. Soc.* **2008**, *130*, 11631.
52. Bazhenova, T. A.; Lobkovskaya, R. M.; Shibaeya, R. P.; Shilov, A. E.; Shilova, A. K.; Gruselle, M.; Leny, G.; Tchoubar, B. *J. Organomet. Chem.* **1983**, *244*, 265.
53. (a) Vela, J.; Smith, J. M.; Lachicotte, R. J.; Holland, P. L. *Chem. Commun.* **2002**, 2886. (b) Vela, J.; Vaddadi, S.; Cundari, T. R.; Smith, J. M.; Gregory, E. A.; Lachicotte, R. J.; Flaschenriem, C. J.; Holland, P. L. *Organometallics* **2004**, *23*, 5226.
54. Russell, S. K.; Hoyt, J. M.; Bart, S. C.; Milsmann, C.; Stieber, S. C. E.; Semproni, S. P.; DeBeer, S.; Chirik, P. J. *Chem. Sci.* **2014**, *5*, 1168.
55. Kochi, J. K. *Organometallic Mechanisms and Catalysis*; Academic Press: New York, 1978; pp 285-288.
56. Occhipinti, G.; Jensen, V. R. *Organometallics* **2011**, *30*, 3522.
57. Frenking, G.; Solà, M.; Vyboishchikov, S. F. *J. Organomet. Chem.* **2005**, *690*, 6178.
58. (a) Chatt, J.; Eaborn, C.; Ibekwe, S. D.; Kapoor, P. N. *J. Chem. Soc. A* **1970**, 1343. (b) Dioumaev, V. K.; Procopio, L. J.; Carroll, P. J.; Berry, D. H. *J. Am. Chem. Soc.* **2003**, *125*, 8043.
59. Waterman, R. *Organometallics* **2013** *32*, 7249.
60. Lin, Z. *Chem. Soc. Rev.* **2002**, *31*, 239.

Chapter 3
Iron-Catalysed Hydroboration of Alkenes and Alkynes

Abstract Boronic acid derivatives have become ubiquitous in chemical synthesis, and can be conveniently synthesised by transition-metal-catalysed hydroboration of alkenes and alkynes, with rhodium and iridium catalysts most commonly used. This chapter deals with the development of an iron-catalysed methodology for the hydroboration of alkenes and alkynes using a bench-stable iron(II) pre-catalyst, which could be activated in situ. The reaction scope and limitations were investigated and a discussion of possible reaction mechanisms is presented.

3.1 Introduction

In 2009 Ritter reported the 1,4-hydroboration of 1,3-dienes to produce synthetically useful allyl boronic esters **204/205** (Scheme 3.1a) [1]. Reduction of an iminopyridine iron(II) pre-catalyst **474/475** using activated magnesium gave an active catalyst for the addition of pinacol borane **93** to 1,3-dienes **202**. Most of the substrates used were 2-substituted 1,3-dienes, however, examples of 1,2-, 1,4- and 2,3- disubstituted dienes were also reported. In no case was 1,2-hydroboration observed. By changing the iminopyridine ligand used, regioselectivity for either allyl boronic ester product **204** or **205** could be obtained. Good to excellent yields of allyl boronic esters were obtained; however, only a limited range of functional groups were shown to be tolerated in the reaction. Recently Huang showed that following the examination of a range of iminopyridine iron(II) pre-catalysts, the 1,4-hydroboration of 1-aryl-substituted 1,3-dienes **476** gave α-aryl secondary allyl boronic esters **478** in good to excellent yields and regioselectivities (Scheme 3.1b) [2]. The highest regioselectivities were obtained using an iron complex bearing an iminopyridine ligand **477** with a bulky diphenylphosphinomethyl group in a remote position relative to the iron centre. Single crystal X-ray analysis confirmed that this phosphine group was not involved in binding to the iron centre, and it was proposed that the effect on regioselectivity was due to increased rigidity of the ligand through restricted rotation of the *N*-aryl substituent.

Iron-catalysed methodologies for the hydroboration of simple alkenes and alkynes have only been reported in the past two years, with numerous groups now working in

M. Greenhalgh, *Iron-Catalysed Hydrofunctionalisation of Alkenes and Alkynes*, Springer Theses, DOI 10.1007/978-3-319-33663-3_3

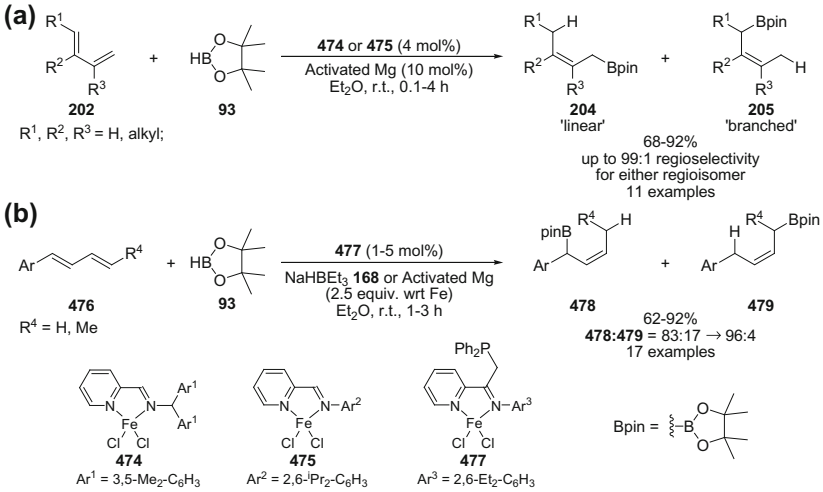

Scheme 3.1 1,4-Hydroboration of 1,3-dienes using iron(II) iminopyridine pre-catalysts. **a** Regiodivergent hydroboration of aliphatic 1,3-dienes **202** using iron pre-catalysts **474** and **475**; **b** regioselective hydroboration of 1-aryl-1,3-dienes **476** using iron pre-catalyst **477**

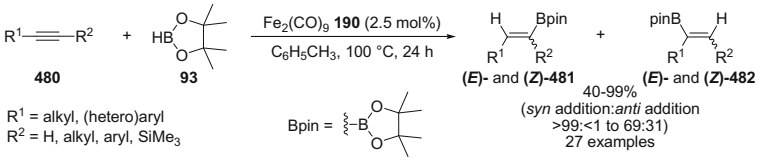

Scheme 3.2 Hydroboration of terminal and internal alkynes **480** using an iron carbonyl cluster pre-catalyst $Fe_2(CO)_9$ **190**

this rapidly expanding area. In 2013, Enthaler reported that iron carbonyl clusters **190** were effective pre-catalysts for the hydroboration of terminal and internal alkynes **480**, giving vinyl boronic esters **481** and **482** in good to excellent yields (Scheme 3.2) [3]. The reactions were heated at 100 °C to activate the iron carbonyl clusters through the dissociation of CO. In contrast to Enthaler's work on the hydrosilylation of alkynes [4], it was found that the addition of nitrogen- and phosphorous-based ligands had no beneficial effect on the reaction. The hydroboration of terminal alkynes (R^2 = H) gave (*E*)-vinylboronic esters **(*E*)-481** (*syn*-addition of B–H) in high regio- and diastereoselectivity, however the hydroboration of unsymmetrical internal alkynes generally gave a mixture of regio- and diastereoisomers.

Huang reported the first example of the iron-catalysed hydroboration of simple alkenes **483** using pinacol borane **93** (Scheme 3.3) [5]. A selection of iron(II) pre-catalysts, which were activated in situ using sodium triethylborohydride **168** (3 equiv. with respect to iron), were assessed for hydroboration activity. Iron(II) chloride alone and iron(II) pre-catalysts with bidentate phosphino- and

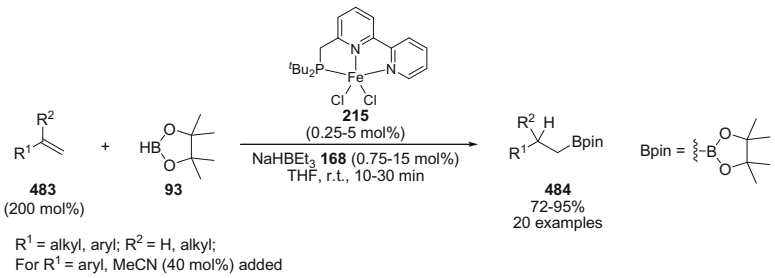

Scheme 3.3 Hydroboration of terminal and 1,1-disubstituted alkenes **483** using a PNN iron(II) pre-catalyst **215** reduced in situ using sodium triethylborohydride **168**

iminopyridine ligands gave hydroboration products in only very low yields, however those bearing tridentate ligands showed much improved activity. The highest yields were obtained using a phosphino-bipyridine (PNN) iron(II) complex **215**, however the multi-step synthesis of the ligand, coupled with its air-sensitivity may be seen to detract from synthetic applicability. The hydroboration of terminal and 1,1-disubstituted alkenes **483** gave linear alkyl boronic esters **484** in good to excellent yields, although an excess amount of the alkene (2 equiv.) was required. Functional groups including a tertiary amine, benzyl ether, tosyl-protected alcohol and an acetal were tolerated. The hydroboration of styrene gave a mixture of hydroboration, dehydroboration and hydrogenation products, which was attributed to β-hydride elimination from an iron–alkyl intermediate. Selectivity for hydroboration was obtained by the addition of acetonitrile (40 mol%), which was suggested to inhibit β-hydride elimination by coordination to free sites on iron.

Chirik showed that bis(imino)pyridine iron bis(dinitrogen) complexes **157** and **183**, previously used for the hydrosilylation and hydrogenation of alkenes [6], were also effective pre-catalysts for the hydroboration of terminal, 1,1- and 1,2-disubstituted alkenes [7]. In general the reactions were conducted in neat alkene and pinacol borane **93** in a 1:1 ratio. Similar reactivity was observed for both pre-catalysts for the hydroboration of terminal aliphatic alkenes, however the hydroboration of internal alkenes and styrene derivatives with each pre-catalyst showed significant differences (Scheme 3.4). Using the bis(imino)pyridine iron complex **183**, with less sterically-demanding *N*-aryl groups, a mixture of hydroboration, dehydroboration and hydrogenation products were observed for the hydroboration of styrene **53** and cyclohexene **489**. In contrast, the bis(imino)pyridine iron complex bearing more sterically-demanding *N*-aryl groups **157**, gave the hydroboration product selectively in each case. The hydroboration of *cis*-oct-4-ene **493** using iron pre-catalyst **157** gave a mixture of 4- and 1-octylboronic esters **494** and **495** in a 1:5 ratio, however pre-catalyst **183** gave only the 1-octylboronic ester **495**, again highlighting the subtle difference in reactivity between these two structurally similar pre-catalysts. Hydroboration of *cis*-oct-4-ene using d_1-pinacolborane resulted in deuterium incorporation in multiple positions along the alkyl chain, which was suggested to reflect a fast rate of alkene isomerisation relative to carbon–boron bond formation.

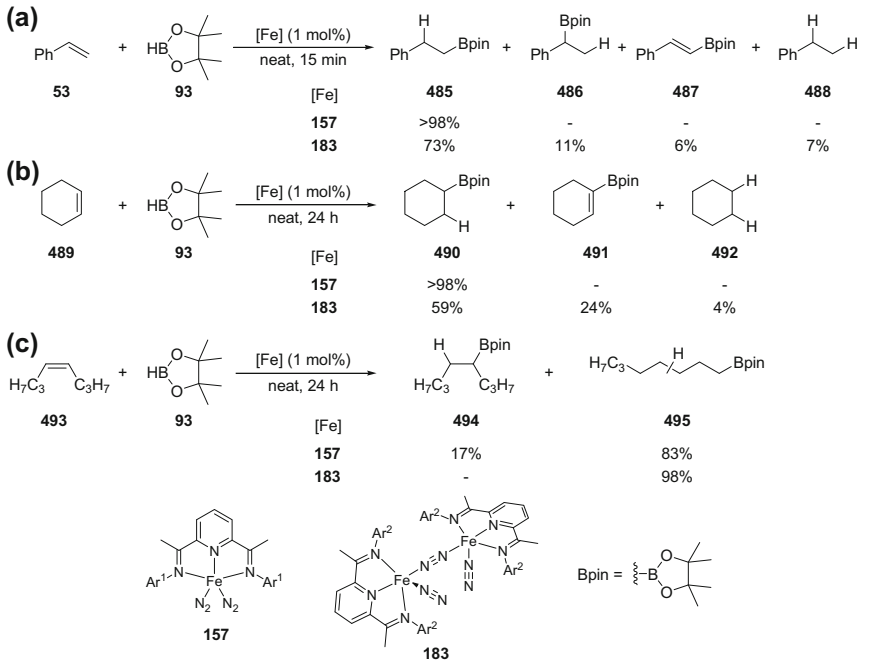

Scheme 3.4 Selectivity differences in the hydroboration of styrene and 1,2-disubstituted alkenes using bis(imino)pyridine iron bis(dinitrogen) complexes **157** and **183**

Szymczak recently reported preliminary results for the hydroboration of terminal and 1,2-disubstituted alkenes and alkynes using an iron(II) complex bearing an *N*,*N*,*N*-bMepi pincer ligand (bMepi = 1,3-bis(6′-methyl-2′-pyridylimino)isoindolate), which was activated in situ by reduction using sodium triethylborohydride **168** (Scheme 3.5) [8]. Methylation of the ligand backbone of *N*,*N*,*N*-bMepi iron(II) complex **497** provided simple access to the iron(II) complex **218**, bearing a neutral tridentate ligand. The methylated iron complex **218** displayed improved activity for hydroboration, which was attributed to an increase in the electrophilicity of the iron centre and a decrease in the reduction potential of the complex, relative to the unmodified iron complex **497**. The hydroboration of an internal alkyne gave the (*Z*)-vinyl boronic ester **500** (*syn*-addition of B–H) diastereoselectivity, whilst the hydroboration of a terminal alkyne gave a mixture of (*E*)-vinyl boronic ester **500** (*syn*-addition of B–H) and (*Z*)-vinyl boronic ester **501** (*anti*-addition of B–H) in an 85:15 ratio (Scheme 3.5b).

Darcel found that the iron carbene tetracarbonyl complex [(IMes)Fe(CO)$_4$] **216** [IMes = 1,3-bis(2,4,6-trimethylphenyl)imidazol-2-ylidene] was an effective pre-catalyst for the hydroboration of terminal alkenes **502** with pinacol borane **93** to give linear boronic esters **503** (Scheme 3.6) [9]. In contrast, the use of $Fe_2(CO)_9$ **190** as a pre-catalyst resulted in low yields of the hydroboration product, along with

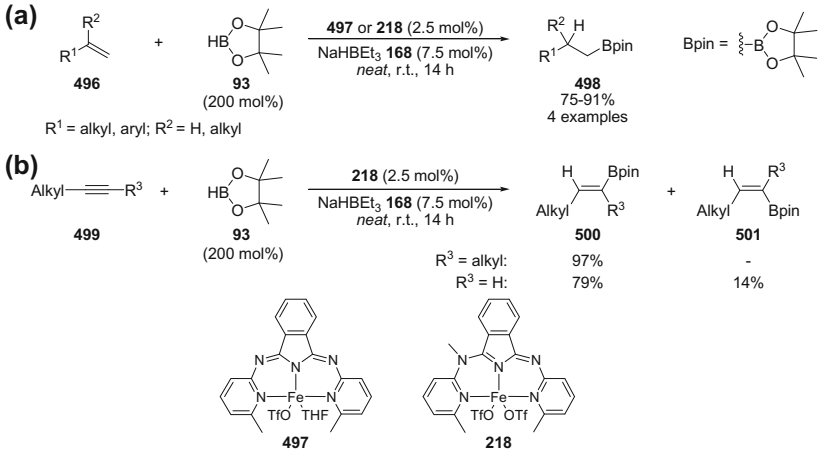

Scheme 3.5 Hydroboration of terminal and 1,2-disubstituted alkenes and alkynes using *N*,*N*,*N*-bMepi iron complexes **497** and **218**, reduced in situ using sodium triethylborohydride

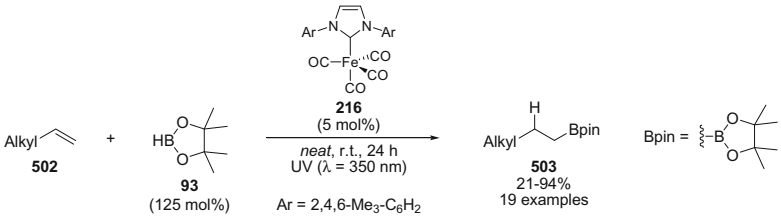

Scheme 3.6 Hydroboration of terminal alkenes using iron carbene tetracarbonyl complex [(IMes)$Fe(CO)_4$] **216**, activated using continual near-UV irradiation (λ = 350 nm)

extensive double-bond isomerisation [10]. Continuous near-UV irradiation (λ = 350 nm) was required for hydroboration activity, which was attributed to the need for CO dissociation in pre-catalyst activation and regeneration following catalyst recombination with CO [11]. A range of functionalised substrates were used, including those containing halide, acetal, ether, ester, epoxide and nitrile groups; however, in some cases only moderate yields were obtained.

Very recently Lu reported the enantioselective hydroboration of 1,1-disubstituted aryl alkenes **504** using an iron(II) pre-catalyst **217** bearing an enantiopure iminopyridine oxazoline ligand, activated in situ using sodium triethylborohydride **168** (Scheme 3.7) [12]. Linear boronic esters **505** were obtained in good to excellent yield and with generally high enantioselectivity. Iminopyridine oxazoline ligands had been independently developed and used by both Lu and Huang for enantioselective cobalt-catalysed hydroboration [13]. α-Alkyl-substituted styrene derivatives bearing electron-donating and electron-withdrawing groups were tolerated, however application of the methodology using β-substituted styrene derivatives and aliphatic

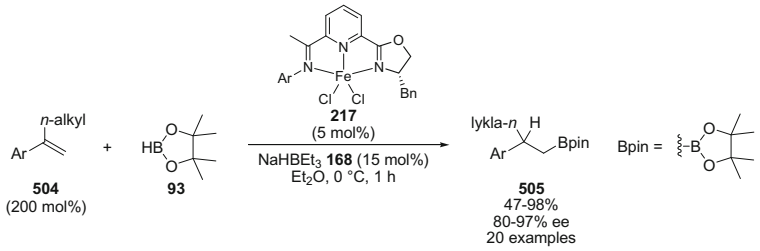

Scheme 3.7 Enantioselective hydroboration 1,1-disubstituted alkenes using an iminopyridine oxazoline iron(II) pre-catalyst **217** reduced in situ using sodium triethylborohydride

1,1-disubstituted alkenes has yet to be reported. This work represents not only the first example of enantioselective iron-catalysed hydroboration, but more broadly the first efficient iron-catalysed process for the enantioselective reduction of alkenes [14].

3.2 Results and Discussion

3.2.1 State of the Art at the Outset of the Project

In 2012, iron-catalysed hydroboration was limited to a single methodology for the hydroboration of 1,3-dienes (Scheme 3.8) [1]. The hydroboration of simple alkenes and alkynes had not been reported.

3.2.2 Project Aims

Building upon positive preliminary results using the in situ reduction of an iron pre-catalyst for the hydrosilylation of alkenes, the potential to extend this methodology to hydroboration was explored (Scheme 3.9). Upon identification of a

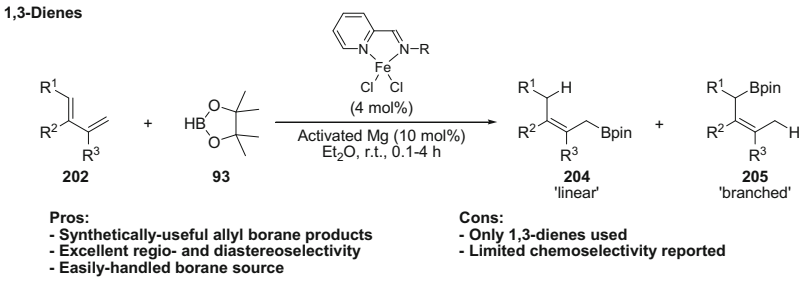

Scheme 3.8 State of the art iron-catalysed hydroboration in early 2012

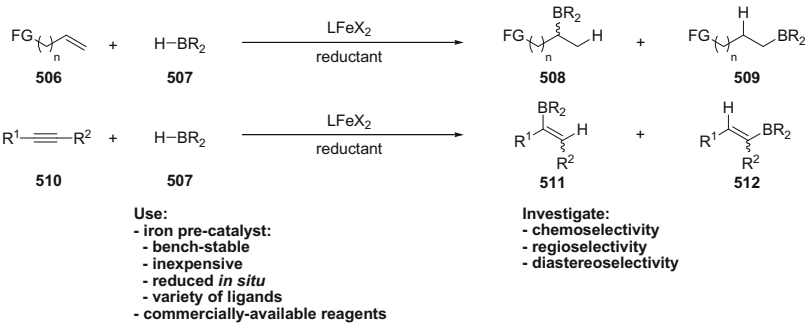

Scheme 3.9 Proposed development of iron-catalysed hydroboration methodology

suitable methodology, the hydroboration of a range of alkenes and alkynes would be investigated, focussing on the chemo-, regio- and stereoselectivity of the process.

3.2.3 *Methodology Development*

Using the conditions developed for hydrosilylation, the iron-catalysed hydroboration of alkenes was evaluated using pinacol borane **93** (110 mol%) in place of a silane (Table 3.1). The hydroboration of styrene **53** gave the linear pinacol boronic

Table 3.1 Identification of iron-catalysed hydroboration methodology I[a]

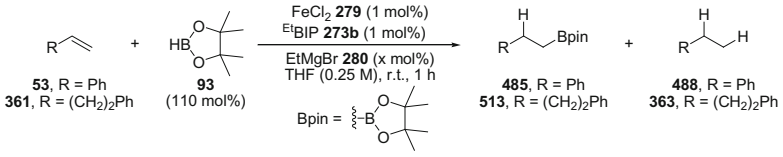

Entry	R	EtMgBr mol%	Yield (%)[b]	
			485/513	**488/363**
1	Ph	2	12	7[c]
2	$(CH_2)_2Ph$	2	88	–[d]
3	$(CH_2)_2Ph$	1	14	–[c]
4	$(CH_2)_2Ph$	3	90	–[d]
5	$(CH_2)_2Ph$	4	86	–[d]
6	$(CH_2)_2Ph$	5	46	–[d]

[a]Conditions: alkene (0.7 mmol), $FeCl_2$ **279** (1 mol%), [Et]BIP **273b** (1 mol%), pinacol borane **93** (0.77 mmol), EtMgBr **280** (1–5 mol%), tetrahydrofuran (0.25 M), r.t., 1 h; [b]Yield determined by ^{1}H NMR spectroscopy using 1,3,5-trimethoxybenzene as an internal standard; [c]Remaining mass balance accounted for by unreacted alkene; [d]Remaining mass balance accounted for by internal alkenes 1-phenyl-2-butene **514** and 1-phenyl-1-butene **515**

ester **485** in only a low yield (Table 3.1, entry 1). Ethylbenzene **488**, arising from the hydrogenation of styrene **53**, was also obtained as a minor side-product, however the majority of the alkene substrate was recovered as unreacted starting material. Increasing the reaction time to 16 h did not improve the yield of the hydroboration product. The hydroboration of alkyl-substituted alkenes was therefore investigated. Under identical reaction conditions, 4-phenylbutene **361** underwent hydroboration to give the linear boronic ester **513** in excellent yield within 1 h (Table 3.1, entry 2). The remaining mass balance was accounted for by a mixture of internal alkenes, presumably formed by the isomerisation of 4-phenylbutene **361**. Reducing the quantity of ethylmagnesium bromide **280** to 1 mol% (1 equivalent with respect to iron), resulted in a significantly lower yield of the linear boronic ester **513**, with the remaining mass balance accounted for by recovered starting material (Table 3.1, entry 3). Using either 3 or 4 mol% ethylmagnesium bromide **280** (3 or 4 equivalents with respect to iron) gave yields of the linear boronic ester **513** which were comparable to those using 2 mol% ethylmagnesium bromide **280** (Table 3.1, entries 4–5). The use of 5 mol% ethylmagnesium bromide (5 equivalents with respect to iron) gave the linear boronic ester **513** in a yield of just 46 %, with the remaining material recovered as a mixture of internal alkene products (Table 3.1, entry 6). As ethylmagnesium bromide **280** loadings of between 2 and 4 mol% had proved equally effective for pre-catalyst activation, the subsequent reaction optimisation and substrate scope experiments were conducted using the intermediate quantity of 3 mol% ethylmagnesium bromide **280**.

The hydroboration of 4-phenylbutene **361** with pinacol borane **93** was investigated using iron(II) chloride **279** (1 mol%) and a range of ligands, activated in situ with ethylmagnesium bromide **280** (3 mol%) (Table 3.2). The linear boronic ester **513** was only obtained when using the bis(imino)pyridine ligand **273b** (^{Et}BIP) (Table 3.2, entry 1). All other mono-, bi-, tri- and tetradentate nitrogen- and phosphorous-based ligands tested gave only a combination of the hydrogenation product **363** and alkene isomerisation products **514** and **515**, along with recovered starting material. The internal alkene isomers **514** and **515** were most likely formed through an iron-catalysed isomerisation of 4-phenylbutene **361**. The iron-catalysed isomerisation of terminal alkenes to give internal alkenes has been reported using iron carbonyl pre-catalysts [10], or using an iron(III) pre-catalyst, reduced in situ using a Grignard reagent [15]. In both cases an iron(0) species was suggested to be the active catalyst. The source of the hydrogenation product **363** is less obvious, and could not be attributed to concurrent dehydroboration of 4-phenylbutene **361** as no vinyl or allyl boronic ester products were observed. It is possible that the hydrogenation product may arise from iron-catalysed disproportionation of pinacol borane to give bis(pinacolato)diboron (B_2pin_2) and dihydrogen, followed by iron-catalysed alkene hydrogenation. The application of d_1-pinacol borane (DBpin) and analysis of the reaction products by ^{11}B NMR spectroscopy could provide evidence for the source of the hydrogenation product **363**, however as this side-product was not observed using bis(imino)pyridine ligand **273b** no further investigations were undertaken.

Table 3.2 Identification of iron-catalysed hydroboration methodology II: ligands[a]

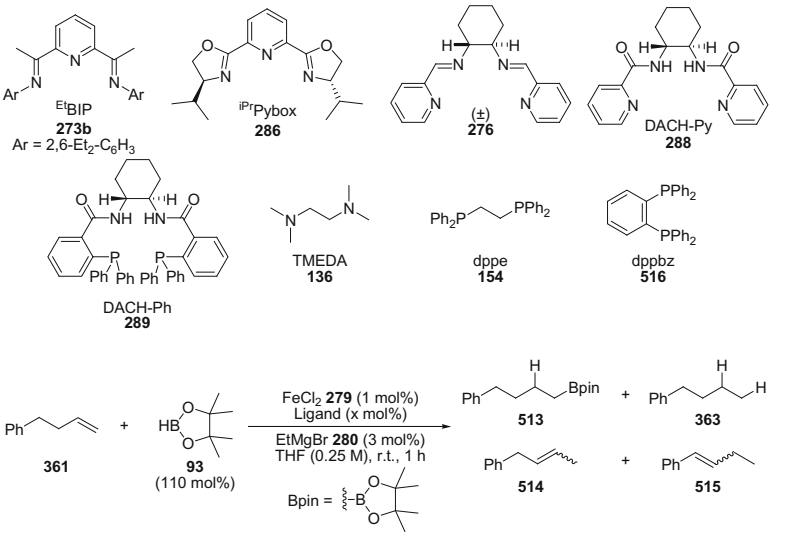

Entry	Ligand/complex (mol%)	Yield (%)[b]			
		513	**363**	**514**	**515**
1	^{Et}BIP **273b** (1)	90	–	6	3
2	^{iPr}Pybox **286** (1)	–	14	57	4
3	**276** (1)	–	10	15	–
4	DACH-Py **288** (1)	–	7	52	2
5	DACH-Ph **289** (1)	–	5	20	2
6	TMEDA **136** (4–20)	–	5	25	2
7	dppe **154** (1.5 mol%)	–	15	39	2
8	dppbz **516** (1.5 mol%)	–	–	–	–
9	PPh_3 **315** (3 mol%)	–	3	56	10
10	PCy_3 **517** (3 mol%)	–	6	54	10
11	P^nBu_3 **518** (3 mol%)	–	10	34	2
12	no $FeCl_2$, no ligand	–	–	–	–

[a]Conditions: 4-phenylbutene **361** (0.7 mmol), $FeCl_2$ **279** (1 mol%), ligand (0.007–0.14 mmol), pinacol borane **93** (0.77 mmol), EtMgBr **280** (3 mol%), tetrahydrofuran (0.25 M), r.t., 1 h; [b]Yield determined by ^{1}H NMR spectroscopy using 1,3,5-trimethoxybenzene as an internal standard. Remaining mass balance accounted for by recovered starting material

3.2.4 Hydroboration of Alkenes and Alkynes

The synthetic utility and chemoselectivity of the developed methodology was investigated using a range of alkenes and alkynes bearing different functional groups. Only a limited number of functionalised terminal alkenes were

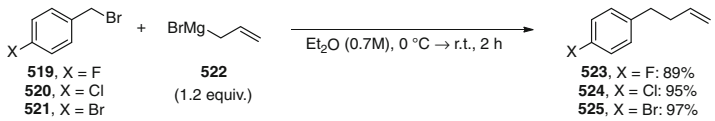

519, X = F
520, X = Cl
521, X = Br

522
(1.2 equiv.)

523, X = F: 89%
524, X = Cl: 95%
525, X = Br: 97%

Scheme 3.10 Synthesis of halide-substituted 4-phenylbutene derivatives **523-525**

commercially-available therefore a divergent synthesis to provide a range of functionalised 4-phenylbutene derivatives was used.

3.2.4.1 Substrate Synthesis

Halide-functionalised 4-phenylbutene derivatives **523-525** were synthesised by the reaction of the corresponding benzyl bromide derivative **519-521** with allylmagnesium bromide **522** (Scheme 3.10).

The bromide-substituted 4-phenylbutene derivative, 1-bromo-4-(3-butenyl)-benzene **525**, was then used for the synthesis of all other 4-phenylbutene derivatives **526-530**, **532**, **533**, **535**, **538** and **540-542** (Scheme 3.11). Conversion of 1-bromo-4-(3-butenyl)-benzene **525** to the corresponding aryl Grignard reagent and subsequent reaction with an appropriate electrophile gave carboxylic acid, aldehyde and keto-functionalised derivatives **526-529** (Scheme 3.11a) [16]. The low yield of the methylketone derivative **528** was due to competitive deprotonation of dimethylacetamide to give 4-phenylbutene **361** as a major side-product. The carboxylic derivative **526** was converted to the methylbenzoate derivative **530** by acid-catalysed esterification [17], and into the amide-substituted derivatives **532** and **533** following condensation with either *tert*-butylamine **531** or piperidine **313**, mediated by a combination of triphenylphosphine **315** and iodine (Scheme 3.11b) [18]. Reduction of the aldehyde **527** with sodium borohydride **534** gave alcohol **535**, whilst a modified Schmidt reaction provided the benzonitrile derivative **538** (Scheme 3.11c) [19]. The acidic conditions used for the synthesis of benzonitrile derivative **538** also resulted in isomerisation of the alkene to give internal alkene products in ~15 % yield. These could not be separated and therefore benzonitrile derivative **538** was used in subsequent hydroboration reactions as a mixture of isomers. Condensation of the aldehyde **527** with aniline **539** gave the aldimine product **540**, which was also reduced using sodium borohydride **534** to give the secondary amine product **541** (Scheme 3.11c). A substrate containing both alkene and alkyne functional groups **542** was synthesised by a Sonagashira cross-coupling reaction between 1-bromo-4-(3-butenyl)-benzene **525** and phenylacetylene **329** (Scheme 3.11d) [20].

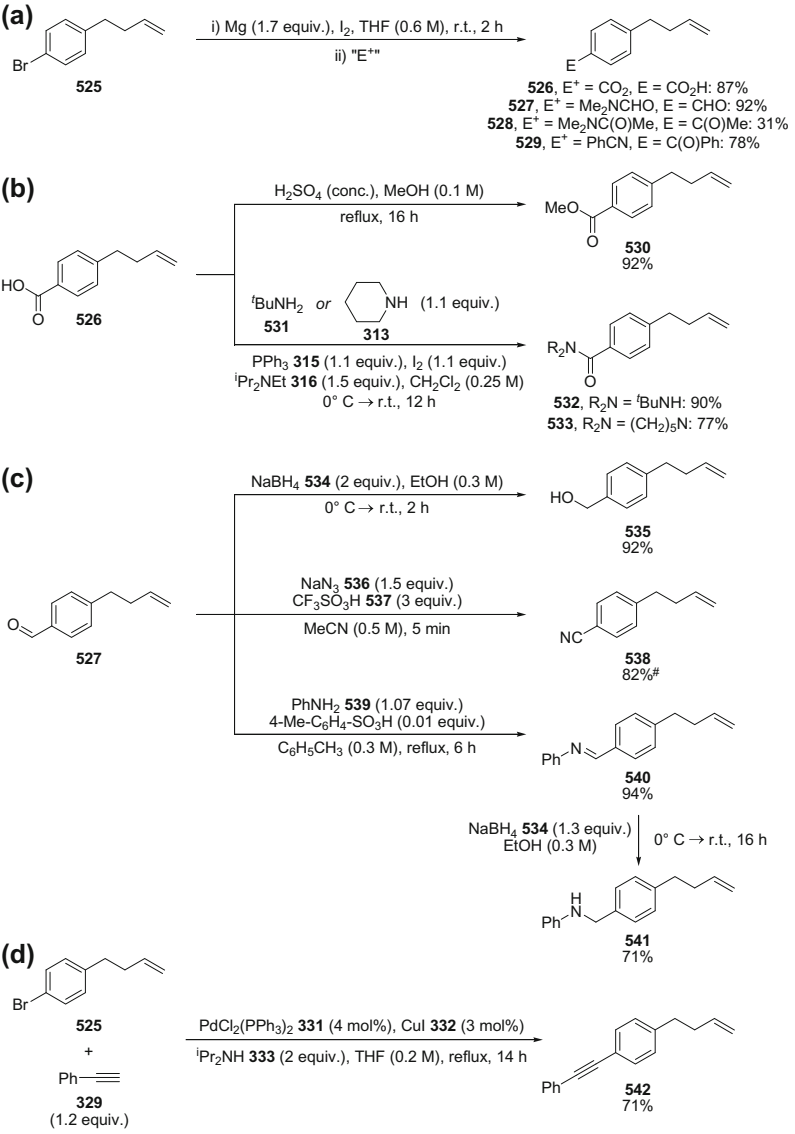

approx. 15 % internal alkene isomers also obtained

Scheme 3.11 Synthesis of 4-phenylbutene derivatives **526-530**, **532**, **533**, **535**, **538** and **540-542**.

3.2.4.2 Hydroboration Substrate Scope: Chemo-, Regio- and Diastereoselectivity

The hydroboration of alkenes **523-525** bearing aryl fluoride-, chloride- and bromide groups gave the linear boronic esters **543-545** in excellent yield (Table 3.3). In contrast to the attempted hydrosilylation of 4-bromostyrene **330** (Sect. 2.2.5.2, Table 2.4), the hydroboration of 1-bromo-4-(3-butenyl)-benzene **525** did not result in any protodehalogenation of the aryl bromide functionality. This difference in reactivity may indicate that the catalytic species formed in each reaction displays different chemoselectivity, or that there is a fundamental difference in reactivity between the two aryl bromide substrates. The alkene and aryl bromide functionalities of 4-bromostyrene **330** are linked through a conjugated π-system, whilst in 1-bromo-4-(3-butenyl)-benzene **525** the two functionalities are remote. A significant effect of aryl–chloride bond activation has been reported for iron-catalysed cross-coupling reactions using chlorostyrene derivatives [21]. Carbon–chlorine bond cleavage was suggested to occur following initial coordination of the iron catalyst to the alkene functional group followed by haptotropic migration [22] through the conjugated π-system. A similar effect may explain the difference in carbon–bromine bond reactivity in this methodology using 4-bromostyrene **330** and 1-bromo-4-(3-butenyl)-benzene **525**.

The secondary amine-functionalised substrate **541** underwent efficient hydroboration to give linear boronic ester **546** in excellent yield (Table 3.3). The unprotected alcohol-functionalised substrate **535** was also applied to the hydroboration conditions, however a stoichiometric amount of Grignard reagent was required to deprotonate the alcohol and, subsequently, activate the iron(II) pre-catalyst. 4-Vinylcyclohexene **371** underwent chemoselective hydroboration of the terminal alkene to give the linear boronic ester **549** in excellent yield, with no hydroboration

Table 3.3 Hydroboration of alkenes bearing functional groups[a]

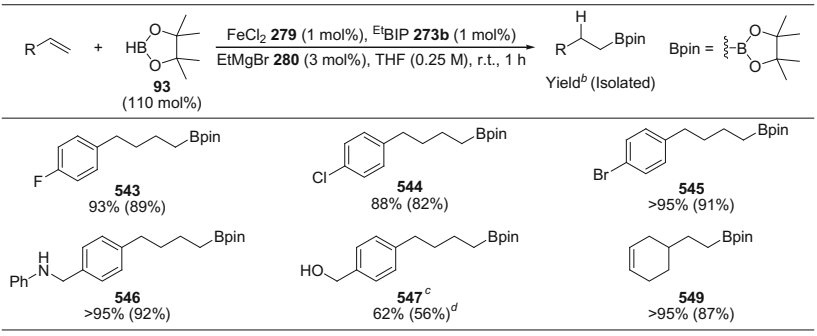

[a]Conditions: alkene (0.7 mmol), $FeCl_2$ **279** (1 mol%), [Et]BIP **273b** (1 mol%), pinacol borane **93** (0.77 mmol), EtMgBr **280** (3 mol%), tetrahydrofuran (0.25 M), r.t., 1 h; [b]Yield determined by ^1H NMR spectroscopy using 1,3,5-trimethoxybenzene as an internal standard; [c]Pinacol borane **93** (1.5 mmol) used and *p*-tolylMgBr **282** (105 mol%) used in place of EtMgBr **280**; [d]Product isolated as a diol (4-(4-hydroxymethylphenyl)butan-1-ol **548**) following oxidation of alkyl pinacol boronic ester **547**

of the internal alkene observed. In contrast, the hydroboration of 4-vinylcyclohexene **371** using Wilkinson's catalyst, $[Rh(PPh_3)_3Cl]$, has been reported to give a mixture of pinacol boronic ester products, consisting of six different regio- and stereoisomers [5].

The hydroboration of alkene substrates bearing functional groups containing potentially reducible carbon–heteroatom multiple bonds was then investigated (Table 3.4). The ester-functionalised substrate **530** underwent chemoselective hydroboration of the alkene, with no C–O bond cleavage or reduction of the ester observed [23]. The secondary amide-functionalised substrate **532** gave the pinacol boronic ester **551** in moderate yield, however a higher pre-catalyst loading of 5 mol% was required. Hydroboration of the tertiary amide-functionalised substrate **533** was unsuccessful however, with only unreacted starting material recovered, even when using a pre-catalyst loading of 5 mol%. This is in keeping with work on hydrosilylation, where amide-functionalised substrates showed low reactivity, and may indicate strong and inhibitive binding between the amide and the iron catalyst [24].

The keto-functionalised substrates **528** and **529** were not tolerated under the reaction conditions, with chemoselective reduction of the ketone observed in each case (Table 3.4). No alkene hydroboration was observed. Due to the incompatibility of these keto-functionalised substrates, the aldehyde-functionalised substrate **527** was not tested in these reactions. Instead, the corresponding aldimine-functionalised alkene substrate **540** was applied in the hydroboration reaction, giving the linear pinacol boronic ester **554** in good yield. The aldimine group was also reduced in approximately 10 % of the material to give a mixture of secondary amine products **541** and **546**. The alkene of the benzonitrile derivative **538** did not undergo successful hydroboration, however some reduction of the nitrile was observed. The primary amine **555** was obtained in just under 30 % yield, and was presumably formed following two successive hydroboration reactions *via* an imine

Table 3.4 Hydroboration of alkene substrates bearing functional groups containing unsaturated carbon–heteroatom bonds[a]

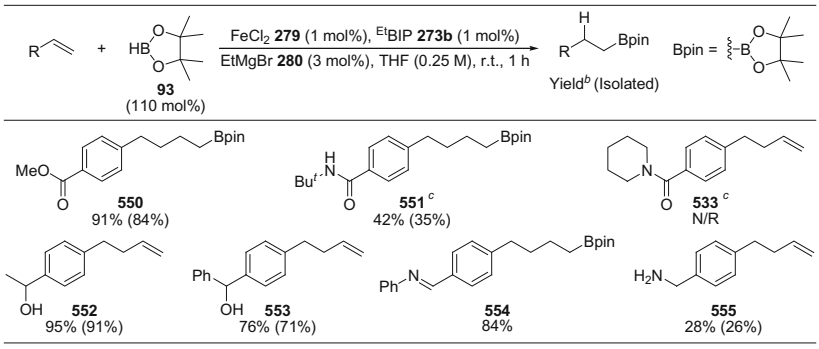

[a]Conditions: alkene (0.7 mmol), $FeCl_2$ **279** (1 mol%), [Et]BIP **273b** (1 mol%), pinacol borane **93** (0.77 mmol), EtMgBr **280** (3 mol%), tetrahydrofuran (0.25 M), r.t., 1 h; [b]Yield determined by ^1H NMR spectroscopy using 1,3,5-trimethoxybenzene as an internal standard; [c]$FeCl_2$ **279** (5 mol%), [Et]BIP **273b** (5 mol%), EtMgBr **280** (15 mol%)

Table 3.5 Hydroboration of 1,1- and 1,2-disubstituted alkenes[a]

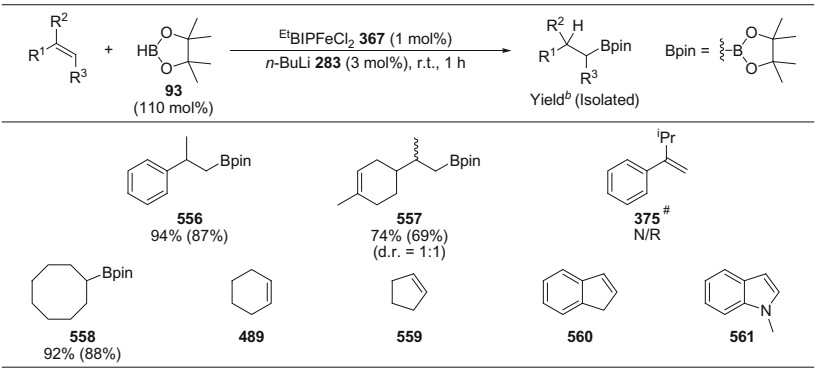

[a]Conditions: alkene (0.7 mmol), $^{Et}BIPFeCl_2$ **367** (1 mol%), pinacol borane **93** (0.77 mmol), *n*-BuLi **283** (3 mol%), r.t., 1 h; [b]Yield determined by ^1H NMR spectroscopy using 1,3,5-trimethoxybenzene as an internal standard. # Substrate synthesised by Dominik Frank

intermediate. Based upon ^1H NMR spectroscopy, an imine product may have been present in the crude reaction mixture in approximately 10 % yield, however isolation and characterisation of this product was not possible.

In keeping with the hydrosilylation methodology, it was found that 1,1- and 1,2-disubstituted alkenes did not undergo hydroboration in tetrahydrofuran. Only minimal activity was observed in toluene, however by conducting the reactions in the absence of an added solvent, good to excellent yields were obtained (Table 3.5). α-Methylstyrene and (*R*)-limonene underwent hydroboration to give the linear pinacol boronic esters **556** and **557** in 94 and 74 % yield, respectively. The more sterically-hindered 1,1-disubstituted alkene **375** was unreactive. Cyclooctene underwent hydroboration to give cyclooctyl pinacol boronic ester **558** in excellent yield, however cyclohexene **489**, cyclopentene **559**, indene **560** and *N*-methylindole **561** were unreactive under the reaction conditions.

The potential to perform the hydroboration methodology on a preparative scale was then investigated. The gram-scale hydroboration of 4-phenylbutene **361** using pinacol borane **93** was conducted under 'solvent-free' conditions, using *n*-butyllithium **283** as the iron(II) pre-catalyst reductant. Using 0.1 mol% iron(II) pre-catalyst, the blue suspension turned yellow following addition of 4-phenylbutene **361**, suggesting decomplexation of the bis(imino)pyridine ligand. This may be attributed to competitive binding with 4-phenylbutene **361**, or through reaction with an impurity present in the alkene substrate. The use of 0.2 mol% iron (II) pre-catalyst proved effective however, with the linear pinacol boronic ester **513** obtained in 94 % yield within 60 s (Scheme 3.12). This corresponds to a catalyst turn-over frequency of 30,000 mol h^{-1}, and therefore represents the most efficient iron catalyst for hydroboration reported to date.

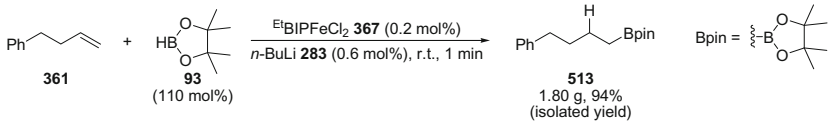

Scheme 3.12 Gram-scale hydroboration of 4-phenylbutene **361** under 'solvent-free' conditions

Table 3.6 Hydroboration of alkynes[a]

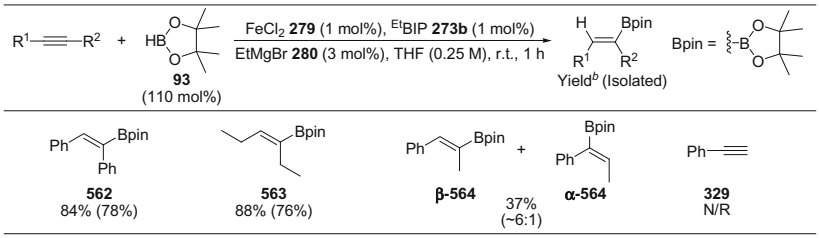

[a]Conditions: alkyne (0.7 mmol), $FeCl_2$ **279** (1 mol%), EtBIP **273b** (1 mol%), pinacol borane **93** (0.77 mmol), EtMgBr **280** (3 mol%), tetrahydrofuran (0.25 M), r.t., 1 h; [b]Yield determined by ^1H NMR spectroscopy using 1,3,5-trimethoxybenzene as an internal standard

Finally, the developed methodology was applied to the hydroboration of alkynes (Table 3.6). Diphenylacetylene and 3-hexyne both underwent hydroboration to give (*Z*)-vinylboronic esters **562** and **563** in good yield and with complete control of diastereoselectivity. The reactions frequently did not reach completion, even with extended reaction times, suggesting that strong binding of the alkyne to the iron catalyst may inhibit reactivity, or that catalyst decomposition takes place using this combination of substrates. The high diastereoselectivity for the *syn*-addition product however represents an improvement upon the hydroboration of internal alkynes using iron carbonyl pre-catalysts, where a range of diastereoselectivities were reported [4]. Surprisingly the unsymmetrically-substituted internal alkyne, 1-phenylpropyne, only gave the vinylboronic esters **β-564** and **α-564** in low to moderate yield. In keeping with the hydrosilylation of 1-phenylpropyne, the β-aryl vinylboronic ester **β-564** was obtained as the major regioisomer (~6:1 regioselectivity). The terminal alkyne, phenylacetylene **329** did not undergo hydroboration. It is possible that in this case the relatively acidic acetylenic proton of phenylacetylene may cause catalyst deactivation resulting in the lack of hydroboration activity.

Having established reactivity for the hydroboration of both alkenes and alkynes, substrates were chosen which contained two different carbon–carbon multiple bonds in order to investigate the chemoselectivity between these groups (Scheme 3.13). The hydroboration of the diene **326**, containing both an alkyl- and

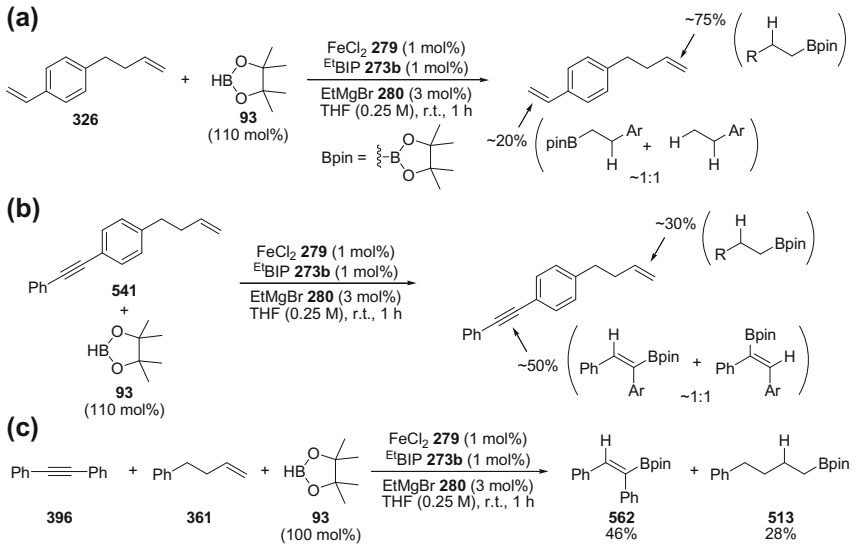

Scheme 3.13 Hydroboration of substrates containing multiple alkene/alkyne functionalities

an aryl alkene gave a mixture of hydroboration and hydrogenation products (Scheme 3.13a). The complex mixture obtained was analysed by quantification of the unreacted alkene functional groups. It was determined that the alkyl alkene had undergone chemoselective hydroboration, to give linear alkyl boronic ester products in approximately 75 % yield. By comparison the styrene group had been reduced to give a combination of alkyl boronic ester and alkane products in a combined yield of approximately 20 %.

The hydroboration of a substrate containing both alkene and alkyne functional groups **541** again gave a complex mixture of mono- and dihydroboration regioisomers (Scheme 3.13b). Quantification of the unreacted functional groups was used to determine that both functional groups had undergone hydroboration, with a slight preference for hydroboration of the alkyne functionality (~ 5:3 chemoselectivity for alkyne hydroboration). The situation was simplified by a competition reaction between diphenylacetylene **396** and 4-phenylbutene **361** with one equivalent of pinacol borane **93** (Scheme 3.13c). A similar chemoselectivity in favour of alkyne hydroboration was observed (approximately 5:3). Once again, the reaction did not reach completion, suggesting that alkynes may cause catalyst deactivation [25]. To gain further insight, kinetic data for the hydroboration of diphenylacetylene **396** and 4-phenylbutene **361**, in combination and in isolation, could be obtained.

3.2.5 *Iron-Catalysed Functionalisation of Alkenes Using Alternative (Hydro)Functionalisation Reagents*

Having developed methodologies for the iron-catalysed hydrosilylation and hydroboration of alkenes, the use of alternative hydrofunctionalisation and heterofunctionalisation reagents was briefly investigated (Table 3.7).

The hydrofunctionalisation of styrene **53** and 4-phenylbutene **361** using alternative group 14 hydrides, triethylgermanium hydride **565** and tributyltin hydride **568**, gave linear alkyl germane products **566** and **567** and alkyl stannane products **569** and **570** in variable yield. Whilst the hydrogermylation of styrene **53** proceeded in close to quantitative yield, the hydrogermylation of 4-phenylbutene **361** gave the hydrofunctionalisation product **567** in only moderate yield. The reaction of styrene **53** or 4-phenylbutene **361** with tributyltin hydride **568** gave only trace quantities of hydrofunctionalisation products, even when conducted in neat alkene. Due to the low yields observed by ^{1}H NMR spectroscopy, and likely acute toxicity of the products, the tetraalkyltin products **569** and **570** were not isolated.

The potential to use the in situ generated iron catalyst to activate carbon–hydrogen bonds was then investigated. Cycloheptatriene **571** and xanthene **572** were chosen as potentially suitable hydrofunctionalisation reagents, due to similar hydride donor abilities with phenylsilane, based upon nucleophilic reactivity parameters [26]. No reaction was observed with either styrene **53** or 4-phenylbutene **371**, with both starting materials recovered in quantitative yield. The heterofunctionalisation of styrene was also tested using both trimethylsilyl cyanide **573** and (dimethylphenylsilyl)boronic acid pinacol ester **574** [27], however in both cases

Table 3.7 Hydrofunctionalisation and heterofunctionalisation reactions using alternative functionalisation reagents[a]

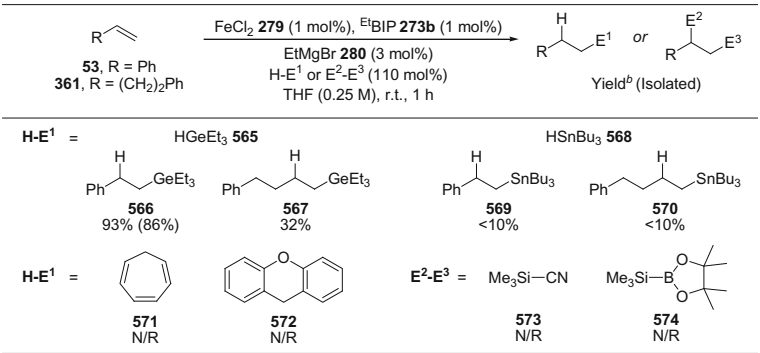

[a]Conditions: alkene (0.7 mmol), $FeCl_2$ **279** (1 mol%), ^{Et}BIP **273b** (1 mol%), hydrofunctionalisation reagent (0.77 mmol), EtMgBr **280** (3 mol%), tetrahydrofuran (0.25 M), 1 h, r.t; [b]Yield determined by ^{1}H NMR spectroscopy using 1,3,5-trimethoxybenzene as an internal standard

only starting material was recovered. Considering the significantly lower hydrosilylation activity using tertiary silanes, it is possible that these reactions were unsuccessful due to the extra steric bulk of these heterofunctionalisation reagents.

3.2.6 *Preliminary Mechanistic Investigations*

The iron-catalysed hydroboration of alkenes and alkynes has only been reported very recently, and therefore only preliminary mechanistic studies have been disclosed to date. However, based upon experiments of our own, and by considering the data presented by others, some features of the mechanism can be discussed.

Using the developed in situ pre-catalyst reduction technique, we were able to calculate the average oxidation-state of the iron catalyst in the reaction by using *p*-tolylmagnesium bromide **282** as the pre-catalyst reductant. Arylation of the iron(II) pre-catalyst ^{Et}BIPFeCl$_2$ **367** by *p*-tolylmagnesium bromide **282** would give an iron (II)diaryl intermediate **431**, which following carbon–carbon bond reductive elimination would result in a two electron reduction of iron, and the formation of 4,4′-dimethylbiphenyl **432** as a by-product (Scheme 3.14) [28]. Quantification of the formation of 4,4′-dimethylbiphenyl **432** could then be used to calculate the average number of electrons that had been transferred to iron during pre-catalyst reduction (Eq. 3.1).

$$\text{Number of electrons transferred to iron} = \frac{\%\ \text{Yield of } \mathbf{432} \times 2}{\text{mol}\%\ \text{of } ^{Et}\text{BIPFeCl}_2\ \mathbf{367}\ \text{used}} \quad (3.1)$$

Pre-catalyst activation using various amounts of *p*-tolylmagnesium bromide **282** was studied for the hydroboration of 4-phenylbutene **361** with pinacol borane **93** (Table 3.8). Iron(II) pre-catalyst loadings of both 5 and 10 mol% were used to test the reproducibility of the quantification of the 4,4′-dimethylbiphenyl **432** by-product. All reactions were worked up by the addition of aqueous acid under an inert atmosphere to limit the possibility of oxidative homocoupling of any remaining Grignard reagent [29]. The yields of hydroboration product **513** and 4,4′-dimethylbiphenyl **432** were calculated by quantitative ^{1}H NMR spectroscopy using 1,3,5-trimethoxybenzene (20 mol%) as an internal standard. Using the same

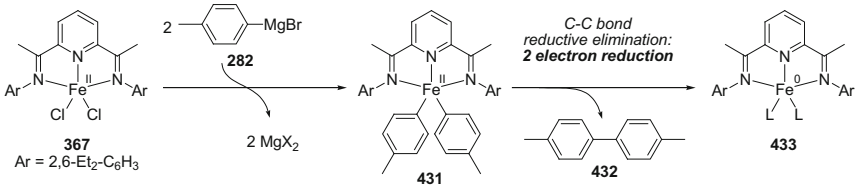

Scheme 3.14 Reduction of iron(II) pre-catalyst using *p*-tolylmagnesium bromide

Table 3.8 Quantification of the reduction of the iron(II) pre-catalyst using *p*-tolylmagnesium bromide[a]

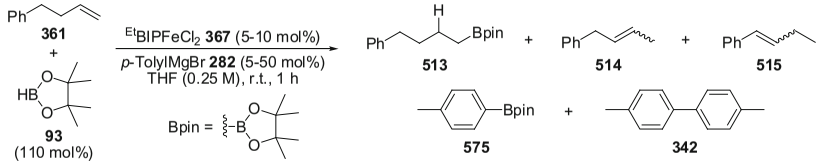

Entry	$^{Et}BIPFeCl_2$/mol %	*p*-TolylMgBr/mol %	Yield[b] (%)				Number of electron reduction of Fe	Average oxidation-state of Fe
			513	**514/515**	**575**	**342**		
1	5	5	18	–/–	–	0.90	0.36	1.64
2	5	10	92	–/6	2	2.35	0.94	1.06
3	5	15	91	–/6	5	2.55	1.02	0.98
4	5	20	84	7/7	11	3.75	1.50	0.50
5	5	25	52	34/8	18	3.85	1.54	0.46
6	10	10	40	4/–	–	3.65	0.73	1.27
7	10	20	92	–/5	9	5.15	1.03	0.97
8	10	30	76	5/10	17	6.70	1.34	0.66
9	10	40	60	22/12	24	7.55	1.51	0.49
10	10	50	18	52/12	33	7.80	1.56	0.44

[a]Conditions: 4-phenylbutene **361** (0.7 mmol), $^{Et}BIPFeCl_2$ **367** (5–10 mol%), pinacol borane **93** (0.77 mmol), *p*-tolylMgBr **282** (5–50 mol%), tetrahydrofuran (0.25 M), 1 h, r.t; [b]Yield determined by ^1H NMR spectroscopy using 1,3,5-trimethoxybenzene as an internal standard

technique it was determined that the solution of *p*-tolylmagnesium bromide used in these experiments contained <0.5 % 4,4′-dimethylbiphenyl **342**, relative to the concentration of Grignard reagent.

At a 5 mol% loading of iron(II) pre-catalyst, maximum catalytic activity was obtained when using between two and three equivalents of *p*-tolylmagnesium bromide **282** (Table 3.8, entry 2–3). At this loading of Grignard reagent, 4,4′-dimethylbiphenyl **342** was obtained in a 2.35–2.55 % yield, corresponding to a 0.94–1.02 electron reduction of the iron(II) pre-catalyst **367** to an average formal oxidation-state of approximately iron(I). This was in keeping with the work on hydrosilylation, where a similar one electron reduction of the iron(II) pre-catalyst was observed. Once again, only one equivalent of the added *p*-tolylmagnesium bromide **282** could be accounted for based upon the formation of 4,4′-dimethyl-biphenyl **342**. The reaction between a bis(imino)pyridine iron(II) complex with two equivalents of phenyllithium has been reported to give half an equivalent of biphenyl and an iron(I) phenyl complex [30]. It is therefore plausible that the 'missing equivalent' of *p*-tolylmagnesium bromide **282** might be explained by the formation of an iron(I) aryl complex **345** (Scheme 3.15a, and see Sect. 2.2.8.1). The iron(I) aryl complex **345** would most likely still be a pre-catalyst, which could be converted to an active catalyst through reaction with an equivalent of pinacol borane **93** to give an iron(I) hydride complex **576** or iron(I) boryl complex **577** (Scheme 3.15b).

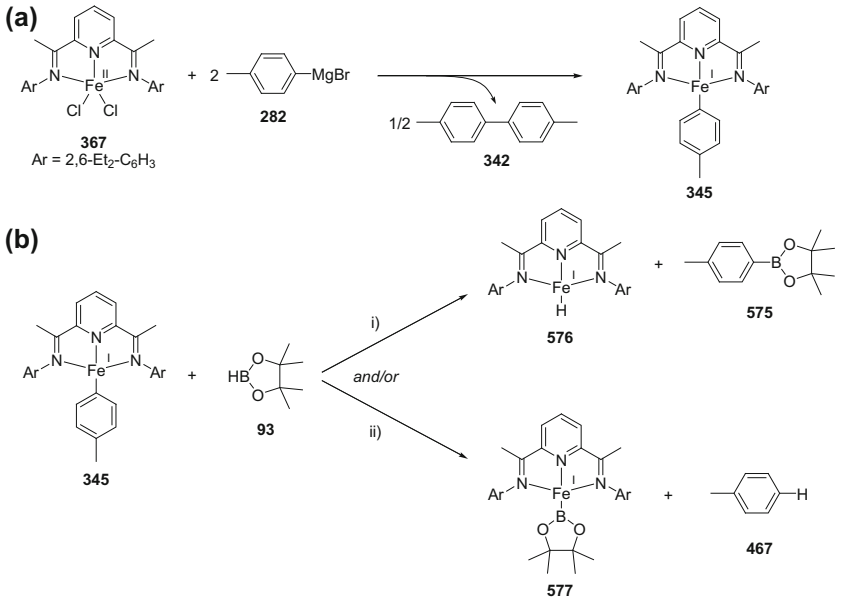

Scheme 3.15 **a** Reduction of iron(II) pre-catalyst ^{Et}BIPFeCl$_2$ **367** using *p*-tolylmagnesium bromide **282** to give iron(I) aryl complex **345**; **b** possible reaction of iron(I) aryl complex **345** with pinacol borane **93** to give iron(I) hydride or boryl complexes **576** and **577**

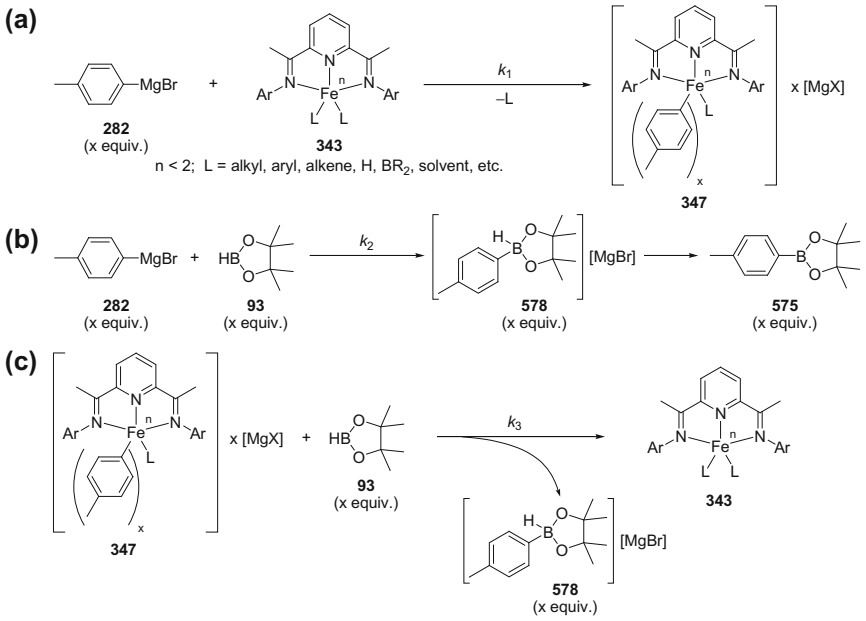

Scheme 3.16 **a** Formation of proposed catalytically-inactive iron-ate complex **347** in the presence of excess *p*-tolylmagnesium bromide **282**; **b** reaction of *p*-tolylmagnesium bromide **282** with pinacol borane **93**; **c** regeneration of 'active catalyst' **343** through reaction of iron-ate complex **347** with pinacol borane **93**

It was found that moderate hydroboration activity was still observed even when excess *p*-tolylmagnesium bromide **282** was used (Table 3.8, entry 5). This was in contrast to the analogous hydrosilylation experiment (Sect. 2.2.8.1, Table 2.9, entry 5), where the hydrosilylation product was obtained in only 4 % yield. This low activity had been proposed to reflect the formation of a catalytically-inactive iron-ate complex **347** from the reaction between *p*-tolylmagnesium bromide **282** and a low oxidation-state catalytically-active iron complex **343** (Scheme 3.16a) [30]. A clue to the difference in activity may be the formation of significant quantities of the *p*-tolyl pinacol boronic ester by-product **575** at higher *p*-tolylmagnesium bromide concentrations (Table 3.8). Pinacol borane readily reacts with alkyl- and aryl Grignard reagents at room temperature to give alkyl- and aryl pinacol esters in excellent yield within 1 h [31]. In contrast, the reaction of phenylsilane with phenylmagnesium bromide produces diphenylsilane in only moderate yield after extended reaction times [32].

The formation of the *p*-tolyl pinacol boronic ester by-product **575** may therefore indicate that the presence of pinacol borane **93** can prevent iron-ate complex formation, or mediate catalyst regeneration following iron-ate complex formation (Scheme 3.16b, c). The formation of the proposed catalytically-inactive iron-ate complex **347** may be prevented if the rate of reaction between *p*-tolylmagnesium

bromide **282** with pinacol borane **93** (k_2) is faster than the rate of iron-ate complex **347** formation (k_1) (Scheme 3.16a, b). Alternatively iron-ate complex formation may still occur, but the greater electrophilicity of pinacol borane **93**, in comparison to phenylsilane, may allow catalyst regeneration through the reaction of the iron-ate complex **347** with pinacol borane **93** (Scheme 3.16c). Both scenarios would result in formation of the same products, and therefore in order to distinguish these pathways, kinetic data would be required for the formation of *p*-tolyl pinacol boronic ester **375** under the reaction conditions, and by the independent reactions of *p*-tolylmagnesium bromide **282** and the iron-ate complex **347** with pinacol borane **93**.

Repeating the same analysis of iron(II) pre-catalyst **367** reduction using a 10 mol % pre-catalyst loading gave comparable results (Table 3.8, entries 6–10). The highest catalytic activity was obtained when using two equivalents of *p*-tolylmagnesium bromide **282** (Table 3.8, entry 7). 4,4′-Dimethylbiphenyl **342** was obtained in a 5.15 % yield, approximately corresponding to a one-electron reduction of the iron(II) pre-catalyst **367** to an average formal oxidation-state of iron(I).

Deuterium-labelling studies can also be used to provide further mechanistic details. Although we have not undertaken these studies, Chirik has reported the hydroboration of terminal and internal alkenes using d_1-pincol borane ***d*$_1$-93** (DBPin) [7]. The reaction of 1-octene **99** or allyltrimethylsilane **579** with d_1-pinacol borane ***d*$_1$-93** (DBPin) was reported to give the linear boronic esters ***d*$_1$-495** and ***d*$_1$-580** with deuterium incorporation exclusively in the 2-position (Scheme 3.17a). This was suggested to indicate that the rate of hydroboration was significantly faster than the rate of alkene isomerisation. However, through inspection of the supporting information supplied by Chirik, it appears that low levels of deuterium were observed in other positions in the alkyl chain, especially when using bis(imino)pyridine iron pre-catalyst **183** bearing the less sterically-demanding ligand (Scheme 3.17c). This suggests that the terminal alkene can undergo reversible hydrometallation/β-hydride elimination prior to the formation of the hydroboration product. No internal boronic esters were reported, which indicates that alkene isomerisation was significantly faster than the rate of hydroboration of an internal alkene. In keeping with this suggestion, the hydroboration of *cis*-4-octene **493** with d_1-pinacol borane ***d*$_1$-93** (DBPin) using iron pre-catalyst **183** gave the linear boronic ester ***d*$_1$-495** with deuterium incorporation observed in all positions on the alkyl chain (Scheme 3.17b, c).

One aspect of the hydroboration mechanism which still needs to be addressed if whether iron-catalysed hydroboration proceeds by alkene insertion into an iron–hydride bond followed by carbon–boron bond formation [33], or by alkene insertion into an iron–boron bond followed by carbon–hydrogen bond formation [34]. The results of the deuterium-labelling studies could be explained by either mechanism (Scheme 3.18). The isomerisation of internal alkenes to give linear boronic ester hydroboration products indicates that alkene insertion into an iron–hydride bond is fast and reversible (Scheme 3.18a). The selectivity for linear boronic ester products could be explained if the rate of carbon–boron bond formation from a secondary alkyl–iron species (k_2) is significantly slower than β-hydride elimination (k_{-1} or k_3), whilst carbon–boron bond formation from a primary alkyl–iron species (k_6) occurs at a competitive rate (Scheme 3.18a).

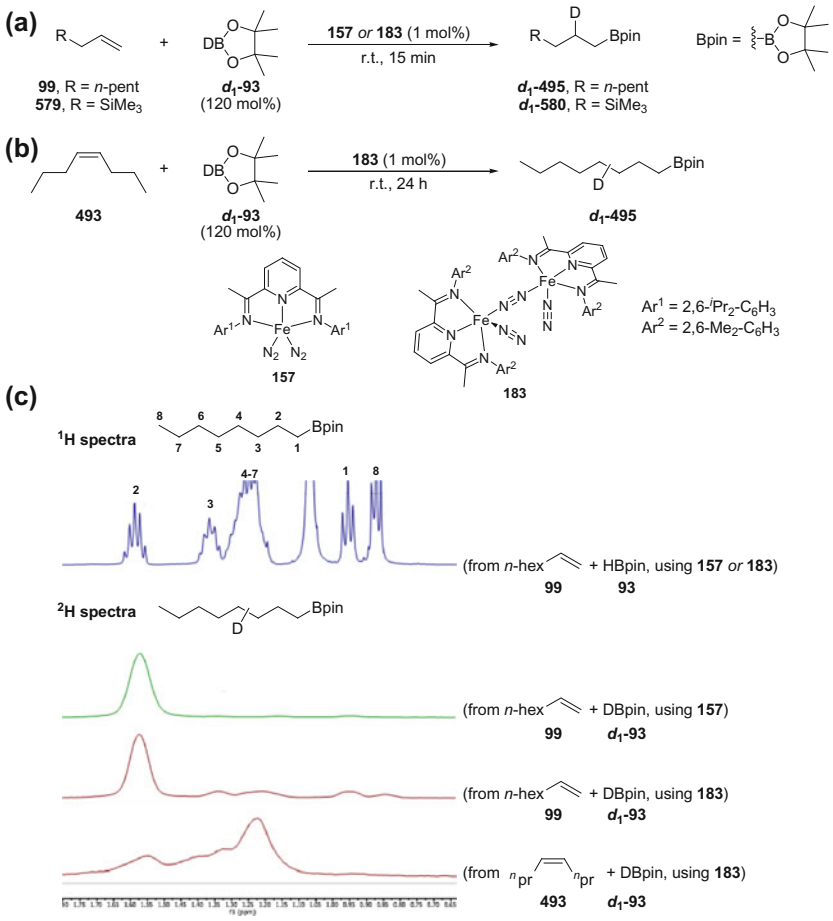

Scheme 3.17 Hydroboration of terminal (**a**) and internal (**b**) alkenes using d_1-pinacol borane ***d*$_1$-93** and bis(imino)pyridine iron pre-catalysts **157** and **183**; **c** ^{1}H and ^{2}H NMR spectra of 1-octyl pinacol boronic ester ***d*$_1$-495** from the reaction of 1-octene **99** or 4-*cis*-octene **493** using pinacol borane **93** or d_1-pinacol borane ***d*$_1$-93** and bis(imino)pyridine iron pre-catalyst **157** or **183**—spectra obtained from supporting information of reference 87c

However this data does not rule out a hydroboration mechanism in which alkene insertion into an iron–boron bond takes place (Scheme 3.18b, c). The deuterium-labelling studies demonstrate alkene isomerisation most likely proceeds through a hydrometallation/β-hydride elimination pathway, however this may only be a competitive side-reaction (Scheme 3.18 **Bi** and **Ci**). Alkene insertion into an iron–boron bond could still be the productive pathway for hydroboration (Scheme 3.18 **Bii** and **Cii**). The selectivity for linear boronic ester products could be explained if the rate of insertion of an internal alkene into an iron–hydride bond is significantly faster than the rate of insertion of an internal alkene into an iron–boron

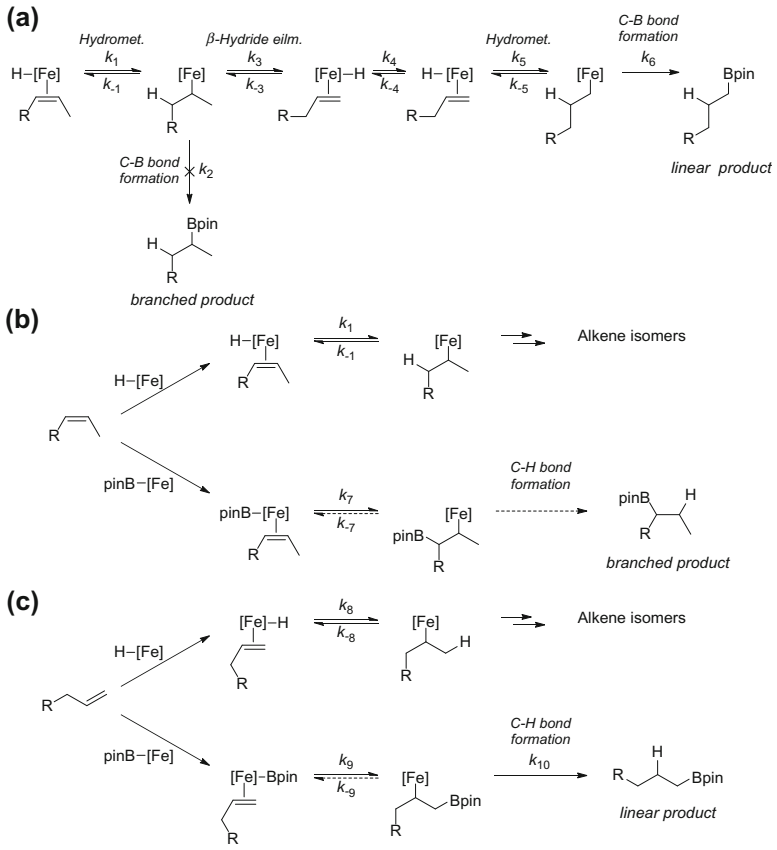

Scheme 3.18 Possible mechanisms to explain the formation of linear boronic ester products from the hydroboration of internal and terminal alkenes. **a** By alkene insertion into an iron–hydride bond followed by carbon–boron bond formation; **b** and **c** by alkene insertion into an iron–boron bond followed by carbon–hydrogen bond formation

bond (Scheme 3.18b $k_1 \gg k_7$). Alkene isomerisation would therefore dominate. Due to the reduced steric hindrance of a terminal alkene, insertion into either an iron–hydride or iron–boron bond may take place at a competitive rate (Scheme 3.18c k_5 or $k_8 \approx k_9$). Internal alkenes would therefore need to be isomerised to the terminal alkene before hydroboration could take place. Isomerisation of an internal alkene to a terminal alkene product is thermodynamically unfavourable, therefore only small quantities of a terminal alkene might be expected to form. This may not be significant however if insertion of the terminal alkene into the iron–boron bond was irreversible, or the subsequent rate of carbon–hydrogen bond formation was fast (k_{10}). For either proposed mechanism, a terminal alkene must be a reaction intermediate in order to give linear pinacol boronic ester products.

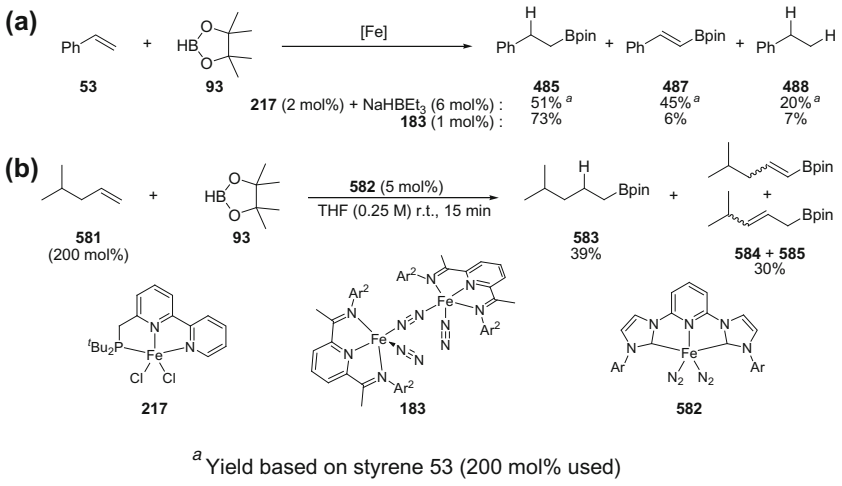

[a] Yield based on styrene 53 (200 mol% used)

Scheme 3.19 The formation of vinyl boronic ester side-products in iron-catalysed hydroboration of alkenes using a selection of different iron pre-catalysts.

Both Huang and Chirik have reported that the iron-catalysed hydroboration of styrene **53** with pinacol borane **93** gave the vinyl pinacol boronic ester **487** as a side-product arising from the formal dehydroboration of styrene (Scheme 3.19a, b) [5, 7]. The dehydroboration of an alkyl alkene, 4-methyl-1-pentene **581**, was also been reported using a bis(*N*-heterocyclic carbene)pyridine iron bis(dinitrogen) complex **582** [7]. These dehydroboration products could be obtained by alkene insertion into an iron–boron bond followed by β-hydride elimination. Alternatively, dehydrogenation of the alkene to give an alkyne could be followed by hydroboration. For this latter pathway, the observation of alkyne side-products might be expected. These dehydroboration products cannot be explained however by a mechanism which involves the insertion of an alkene into an iron–hydride bond.

The formation of dehydroboration products means it is probable that alkene insertion into an iron–boron bond can take place, however it is possible that this is simply a side reaction. The productive reaction to give hydroboration products could still proceed by alkene insertion into an iron–hydride bond, followed by carbon–boron bond formation. Based upon the available evidence it is therefore not currently possible to confirm or rule out either possible pathway.

In order to obtain sufficient evidence for either of these processes, stoichiometric reactions between isolated iron complexes could be used to investigate the feasibility of the possible catalytic steps. As alkene insertion into both iron–hydride and iron–boron bonds appears to be possible (based upon alkene isomerisation and dehydroboration products), the most significant reaction to focus on may be the feasibility of carbon–hydrogen or carbon–boron bond formation following the reaction of an iron–alkyl intermediate **472** with pinacol borane **93** (Scheme 3.20a). Other important stoichiometric reactions would be the reaction of the proposed iron (I) aryl pre-catalyst **345** with pinacol borane **93** (Scheme 3.15b), and the reaction of

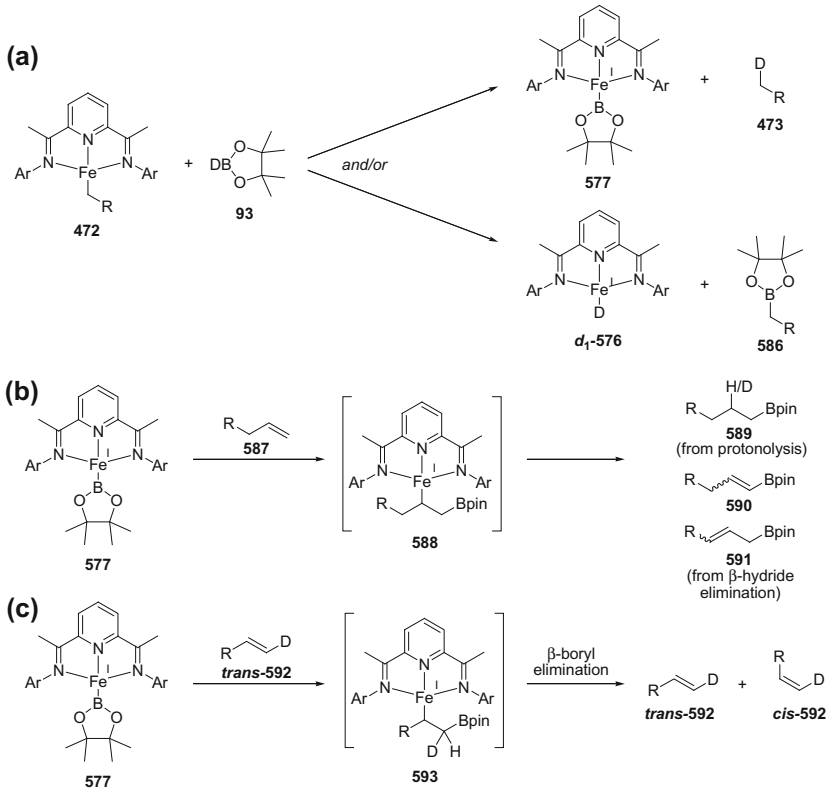

Scheme 3.20 Proposed reactions of isolated iron complexes to provide further evidence for elucidation of the mechanism of iron-catalysed hydroboration

an alkene with an iron–boryl complex **577** (Scheme 3.20b). The latter reaction could provide evidence for the feasibility of alkene insertion into an iron–boron bond, and although isolation of the proposed iron–alkyl intermediate **588** may be challenging, its formation would be indicated if alkyl, vinyl or allyl boronic ester products **589-591** were obtained. The reversibility of alkene insertion into an iron–boron bond (β-boryl elimination) [35] could be investigated by the reaction of a single diastereoisomer of an isotopically-labelled alkene **592** with an iron–boryl complex **577** (Scheme 3.20c). The iron–carbon bond of the intermediate iron–alkyl complex **593** may be expected to be configurationally unstable [36], therefore any erosion of the diastereomeric ratio of the alkene could indicate a reversible alkene insertion/β-boryl elimination process.

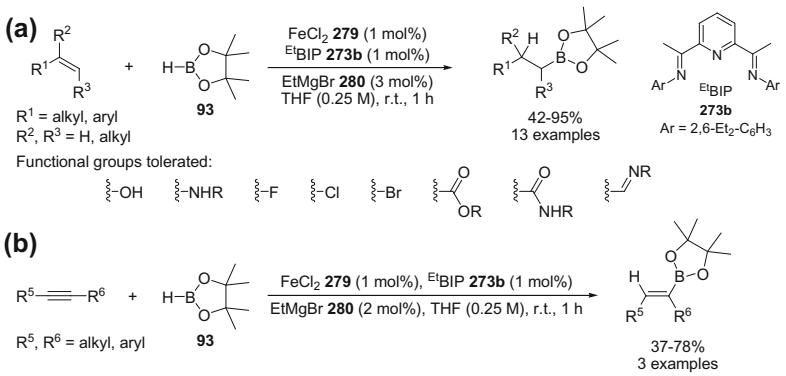

Scheme 3.21 Iron-catalysed hydroboration of alkenes and alkynes using in situ reduction of an iron(II) pre-catalyst with ethylmagnesium bromide

3.3 Conclusions

The iron-catalysed hydroboration of alkenes and alkynes using pinacol borane **93** has been developed, using the in situ activation of a bench-stable bis(imino)pyridine iron(II) pre-catalyst with an organometallic reagent (Scheme 3.21). This provides a convenient approach to iron-catalysed hydroboration, without the need to synthesise and isolate air- and moisture sensitive iron complexes. During the development of this methodology, two other methodologies for the hydroboration of alkenes were reported by Huang and Chirik, however in each case an air- and moisture sensitive iron pre-catalyst was used.

Terminal, 1,1- and 1,2-disubstituted alkenes underwent hydroboration to give linear pinacol boronic esters in good to excellent yield and with complete control of regioselectivity (Scheme 3.21a). Whilst the hydroboration of terminal alkenes was achieved in tetrahydrofuran or toluene solution, or in the absence of solvent, the hydroboration of disubstituted alkenes was only efficient in the absence of added solvent. A range of functional groups were tolerated, and catalyst turnover frequencies of up to 30,000 mol h^{-1} were recorded. This represents the most efficient iron catalyst for the hydroboration of alkenes reported to date.

Internal alkyl- and aryl alkynes underwent hydrosilylation to give (*Z*)-vinyl boronic esters diastereoselectively (Scheme 3.21b). Terminal alkynes were found to be unsuitable substrates. The yields obtained using alkynes were generally lower than those obtained using alkenes. It is possible that this may be explained by catalyst decomposition, or deactivation through inhibitive binding, in the presence of alkynes. Obtaining kinetic data by following the reaction profile for the hydroboration of alkenes and alkynes in isolation, and in competition, may allow differentiation between these possibilities.

Further work could also focus on the regioselectivity (and diastereoselectivity) of the hydroboration of unsymmetrical di-substituted alkynes. These reactions would extend the synthetic utility of the process, and may provide some mechanistic insight. The only previously reported iron-catalysed methodology for the hydroboration of alkynes reported variable levels of regio- and diastereoselectivity using unsymmetrical alkynes [4].

Preliminary mechanistic studies have indicated that a one-electron reduction of the iron(II) pre-catalyst takes place to give an active catalyst in the formal oxidation-state of iron(I). Although experiments using d_1-pinacol borane have been reported by Chirik, conducting these experiments using the developed methodology would allow further analysis of the products obtained. Other mechanistic studies could focus on stoichiometric reactions using isolated iron-complexes to provide support for, or refute, the proposed steps of the catalytic cycle. Kinetic analysis of the hydroboration reaction should be undertaken using a range of electronically-differentiated styrene- and diaryl alkyne derivatives. The hydroboration reaction profile using these substrates could be obtained in isolation (to provide absolute rates) and in competition experiments (to provide information about competitive binding and reaction inhibition).

References

1. Wu, J. Y.; Moreau, B.; Ritter, T. *J. Am. Chem. Soc.* **2009**, *131*, 12915.
2. Cao, Y.; Zhang, Y.; Zhang, L.; Zhang, D.; Leng, X.; Huang, Z. *Org. Chem. Front.* **2014**, *1*, 1101.
3. Haberberger, M.; Enthaler, S. *Chem. Asian J.* **2013**, *8*, 50.
4. (a) Enthaler, S.; Haberberger, M.; Irran, E. *Chem. Asian J.* **2011**, *6*, 1613. (b) Haberberger, M.; Irran, E.; Enthaler, S. *Eur. J. Inorg. Chem.* **2011**, 2797.
5. Zhang, L.; Peng, D.; Leng, X.; Huang, Z. *Angew. Chem. Int. Ed.* **2013**, *52*, 3676.
6. (a) Bart, S. C.; Lobkovsky, E.; Chirik, P. J. *J. Am. Chem. Soc.* **2004**, *126*, 13794. (b) Tondreau, A. M.; Atienza, C. C. H.; Weller, K. J.; Nye, S. A.; Lewis, K. M.; Delis, J. G. P.; Chirik, P. J. *Science* **2012**, *335*, 567. (c) Atienza, C. C. H.; Tondreau, A. M.; Weller, K. J.; Lewis, K. M.; Cruse, R. W.; Nye, S. A.; Boyer, J. L.; Delis, J. G. P.; Chirik, P. J. *ACS Catal.* **2012**, *2*, 2169. (d) Russell, S. K.; Darmon, J. M.; Lobkovsky, E.; Chirik, P. J. *Inorg. Chem.* **2010**, *49*, 2782.
7. Obligacion, J. V.; Chirik, P. J. *Org. Lett*. **2013**, *15*, 2680.
8. Tseng, K.-N. T.; Kampf, J. W.; Szymczak, N. K. *ACS Catal.* **2015**, *5*, 411.
9. Zheng, J.; Sortais, J.-B.; Darcel, C. *ChemCatChem* **2014**, *6*, 763.
10. (a) Crivello J. V.; Kong, S. *J. Org. Chem.* **1998**, *63*, 6745. (b) Tooley, P. A.; Arndt L. W.; Darensbourg, M. Y. *J. Am. Chem. Soc.* **1985**, *107*, 2422. (c) Jennerjahn, R.; Jackstell, R.; Piras, I.; Franke, R.; Jiao, H.; Bauer M.; Beller, M. *ChemSusChem* **2012**, *5*, 734.
11. Wrighton, M. *Chem. Rev.* **1974**, *74*, 401.
12. Chen, J.; Xi, T.; Lu, Z. *Org. Lett.* **2014**, *16*, 6452.
13. (a) Zhang, L.; Zuo, Z.; Wan, X.; Huang, Z. *J. Am. Chem. Soc.* **2014**, *136*, 15501. (b) Chen, J.; Xi, T.; Ren, X.; Cheng, B.; Guo, J.; Lu, Z. *Org. Chem. Front.* **2014**, *1*, 1306.
14. The enantioselective iron-catalysed hydrogenation of alkenes has been reported with enantioselectivities of up to 49% ee at low conversion: (a) Hoyt, J. M.; Shevlin, M.; Margulieux, G. W.; Krska, S. W.; Tudge, M. T.; Chirik, P. J. *Organometallics* **2014**, *33*, 5781.

(b) Chirik, P. J.; Monfette, S.; Hoyt, J. M.; Friedfeld, M. R. Enantiopure base-metal catalysts for asymmetric catalysis and bis(imino)pyridine iron alkyl complexes for catalysis. U.S. Patent 20130079567 A1, March 28, 2013.
15. Mayer, M.; Welther A.; Jacobi von Wangelin, A. *ChemCatChem* **2011**, *3*, 1567.
16. (a) Mirviss, S. B. *J. Org. Chem.* **1989**, *54*, 1948. (b) Baker, K. V.; Brown, J. M.; Hughes, N.; Skarnulis, A. J.; Sexton, A. *J. Org. Chem.* **1991**, *56*, 698. (c) Ortiz-Marciales, M.; Tirado, L. M.; Colón, R.; Ufret, M. L.; Figueroa, R.; Lebrón, M.; DeJesús, M.; Martínez, J.; Malavé, T. *Synth. Commun.* **1998**, *28*, 4067.
17. Webb, S. J.; Sanders, J. K. M. *Inorg. Chem.* **2000**, *39*, 5920.
18. Kumar, A.; Akula, H. K.; Lakshman, M. K. *Eur. J. Org. Chem.* **2010**, 2709.
19. Rokade, B. V.; Prabhu, K. R. *J. Org. Chem.* **2012**, *77*, 5364.
20. Chinchilla, R.; Nájera, C. *Chem. Rev.* **2007**, *107*, 874.
21. (a) Gülak, S.; Jacobi von Wangelin, A. *Angew. Chem. Int. Ed.* **2012**, *51*, 1357. (b) Gülak, S.; Gieshoff, T. N.; Jacobi von Wangelin, A. *Adv. Synth. Catal.* **2014**, *355*, 2197.
22. Gridnev, I. D. *Coord. Chem. Rev.* **2008**, *252*, 1798.
23. Trovitch, R. J.; Lobkovsky, E.; Bouwkamp, M. W.; Chirik, P. J. *Organometallics* **2008**, *27*, 6264.
24. Trovitch, R. J.; Lobkovsky, E.; Bill, E.; Chirik, P. J. *Organometallics* **2008**, *27*, 1470.
25. Casitas, A.; Krause, H.; Goddard, R.; Fürstner, A. *Angew. Chem. Int. Ed.* **2015**, *54*, 1521.
26. (a) Mayr, H.; Lang, G.; Ofial, A. R. *J. Am. Chem. Soc.* **2002**, *124*, 4076. (b) Hom, M.; Schappele, L. H.; Lang-Wittkowski, G.; Mayr, H.; Ofial, A. R. *Chem. Eur. J.* **2013**, *19*, 249.
27. Oestreich, M.; Hartmann, E.; Mewald, M. *Chem. Rev.* **2013**, *113*, 402.
28. (a) Tamura, M.; Kochi, J. *Bull. Chem. Jpn. Soc.* **1971**, *44*, 3063. (b) Hedström, A.; Lindstedt, E.; Norrby, P.-O. *J. Organomet. Chem.* **2013**, *748*, 51.
29. Kharasch, M. S.; Fields, E. K. *J. Am. Chem. Soc.* **1941**, *63*, 2316.
30. Fernández, I.; Trovitch, R. J.; Lobkovsky, E.; Chirik, P. J. *Organometallics* **2008**, *27*, 109.
31. Clary, J. W.; Rettenmaier, T. J.; Snelling, R.; Bryks, W.; Banwell, J.; Wipke, W. T.; Singaram, B. *J. Org. Chem.* **2011**, *76*, 9602.
32. (a) Gilman, H.; Zuech, E. A. *J. Am. Chem. Soc.* **1957**, *79*, 4560. (b) Gilman, H.; Zuech, E. A. *J. Am. Chem. Soc.* **1959**, *81*, 5925.
33. (a) Männing, D.; Nöth, H. *Angew. Chem. Int. Ed. Engl.* **1985**, *24*, 878. (b) Evans, D. A.; Fu, G. C.; Anderson, B. A. *J. Am. Chem. Soc.* **1992**, *114*, 6679.
34. (a) Brown, J. M.; Lloyd-Jones, G. C. *J. Chem. Soc., Chem. Commun.* **1992**, 710. (b) Burgess, K.; van der Donk, W. A.; Westcott, S. A.; Marder, T. B.; Baker, R. T.; Calabrese, J. C. *J. Am. Chem. Soc.* **1992**, *114*, 9350. (c) Westcott, S. A.; Marder, T. B.; Baker, R. T. *Organometallics* **1993**, *12*, 975.
35. Lam, K. C.; Lin, Z.; Marder, T. B. *Organometallics* **2007**, *26*, 3149.
36. Hölzer, B.; Hoffmann, R. W. *Chem. Commun.* **2003**, 732.

Chapter 4
Iron-Catalysed Hydromagnesiation of Styrene Derivatives

4.1 Introduction

Grignard reagents are highly versatile organometallic reagents, which can be used for the formation of a range of carbon–carbon and carbon–heteroatom bonds, through reaction with electrophiles, or by cross-coupling methodologies [1]. Conventionally, Grignard reagents are synthesised by the insertion of magnesium into a carbon–halogen bond (Scheme 4.1a); however difficulties can arise due to competitive side-reactions, or if the alkyl halide is not readily accessible or contains functional groups which are incompatible with the conditions used for Grignard reagent formation. In these instances alternative methods for the synthesis of Grignard reagents are required. Methods have been developed for the synthesis of functionalised aryl Grignard reagents through halogen-magnesium exchange, direct magnesiation and magnesium insertion in the presence of lithium chloride [2]. The hydromagnesiation of alkenes, dienes and alkynes can be used for the synthesis of alkyl-, allyl and vinyl Grignard reagents, respectively [3]. The hydromagnesiation reaction involves the formal addition of a magnesium–hydrogen bond across an olefin, and provides an alternative method for access to a range of Grignard reagents (Scheme 4.1b).

The hydromagnesiation of alkenes is a particularly synthetically-useful process for the synthesis of Grignard reagents which cannot be prepared easily by conventional methods. Benzylic Grignard reagents are challenging to synthesise by the insertion of magnesium in carbon–halogen bonds due to competitive Wurtz homo-coupling leading to 1,2-diarylethane side-products [4]. Methods to circumvent this side-reaction involve the slow addition of a benzyl chloride at low temperature and high dilution to highly-dispersed magnesium [5] or magnesium anthracene [6]. The hydromagnesiation of styrene derivatives is therefore an attractive option for the synthesis of benzylic Grignard reagents.

M. Greenhalgh, *Iron-Catalysed Hydrofunctionalisation of Alkenes and Alkynes*, Springer Theses, DOI 10.1007/978-3-319-33663-3_4

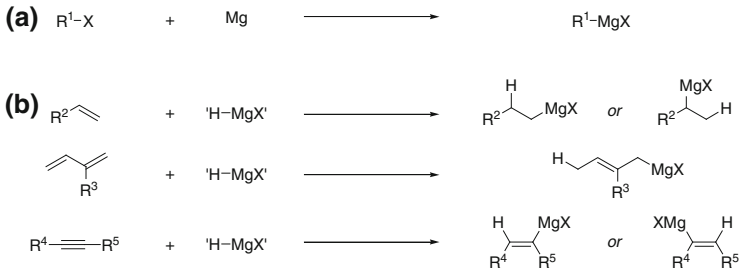

Scheme 4.1 Methods for the synthesis of Grignard reagents. **a** Insertion of magnesium in a carbon–halide bond; **b** hydromagnesiation of alkenes, dienes and alkynes

4.1.1 Hydromagnesiation Using Magnesium Hydride

The addition of magnesium hydride to alkenes takes place at high temperature, however due to a number of side-reactions the organomagnesium species are obtained in only low yield [7]. The addition of transition-metal salts can catalyse this reaction to give organomagnesium reagents in good to excellent yield. In addition to the choice of transition-metal catalyst the method of magnesium hydride preparation is crucial, with good activity only observed with freshly prepared highly-dispersed magnesium hydride.

Ashby first reported that the reaction of magnesium hydride **595** with alkenes could be catalysed by the addition of bis(cyclopentadienyl)titanium dichloride **594** (Cp_2TiCl_2) [8]. Terminal alkenes **593** and internal and terminal alkynes gave hydromagnesiation products in high yield within 1 h (Scheme 4.2a). The identity of the organomagnesium product was indicated by deuterium incorporation in the product following reaction with deuterium oxide. Terminal alkenes gave linear organomagnesium reagents, whilst styrene gave a mixture of benzylic and homobenzylic

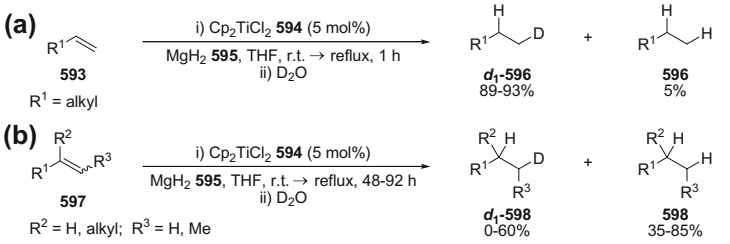

Scheme 4.2 Hydromagnesiation of terminal alkenes (**a**) and disubstituted alkenes (**b**) using magnesium hydride **595** and bis(cyclopentadienyl)titanium dichloride **594** (Cp_2TiCl_2)

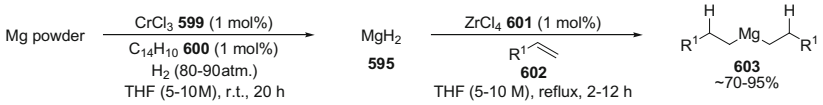

Scheme 4.3 Hydrogenation of magnesium using a mixed pre-catalyst system of chromium(III) chloride **599** and anthracene **600** to give activated magnesium hydride **595**, and subsequent hydromagnesiation of terminal alkenes **602** using zirconium(IV) chloride **601** as a pre-catalyst

organomagnesium reagents in a 9:1 ratio. Internal and 1,1-disubstituted alkenes **597** were also reduced to alkanes **598** over extended reactions periods, however upon quenching the reaction with deuterium oxide, little or no deuterium incorporation was observed in some cases (Scheme 4.2b). This was attributed to decomposition of the organomagnesium product over extended reaction times. Ashby noted the method of magnesium hydride preparation was significant and obtained the best yields when magnesium hydride was freshly prepared from diethylmagnesium and lithium aluminium hydride [9].

Bogdanović developed a method for the synthesis of highly active magnesium hydride **595** by the hydrogenation of magnesium powder in the presence of a chromium or titanium pre-catalyst and anthracene **600** [10]. It was suggested that this reaction proceeded by formation of magnesium anthracene [11], followed by hydrogenation to give magnesium hydride and reform anthracene. Only small quantities of 9,10-dihydroanthracene, arising from the hydrogenation of anthracene, were observed. The magnesium hydride **595** produced was highly pyrophoric, however it was found that the same catalytic system, containing chromium or titanium, was also effective for the addition of the magnesium hydride **595** to alkenes **602** to give dialkylmagnesium reagents **603** (Scheme 4.3) [12]. The addition of further transition-metal salts and complexes was found to be beneficial for the hydromagnesiation reaction, with the highest yields obtained using zirconium tetrahalide **601** salts. Terminal alkenes **602** underwent hydromagnesiation to give linear dialkylmagnesium reagents **603**, as determined by reaction with various electrophiles, whilst the hydromagnesiation of styrene gave a mixture of benzylic and homobenzylic organomagnesium reagents in 75 % yield and 20:1 regioselectivity. The hydromagnesiation of styrene and isoprene were complicated by competing oligomerisation reactions, whilst disubstituted alkenes were found to be unreactive.

4.1.2 Hydromagnesiation Using Grignard Reagents Bearing β-Hydrogen Atoms

The most common approach for the hydromagnesiation of alkenes **604** and alkynes is the use of a Grignard reagent bearing β-hydrogen atoms **605** as a superficial source of 'HMgX' (Scheme 4.4a) [3]. An equivalent of alkene **607** is produced as a

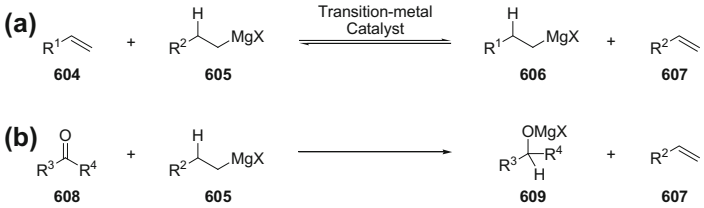

Scheme 4.4 **a** Transition-metal-catalysed hydromagnesiation of alkenes **604** using a Grignard reagent bearing β-hydrogen atoms **605**; **b** Meerwein-Ponndorf-Verley-type reduction of ketones **608** using a Grignard reagent bearing β-hydrogen atoms **605**

by-product, and thus the reaction is generally reversible and thermodynamically driven. Titanium and nickel catalysts have been most frequently used for this reaction, however examples using iron, cobalt, vanadium and zirconium salts have also been reported. The analogous "hydromagnesiation" of ketones **608** using alkyl Grignard reagents bearing β-hydrogen atoms **605**, in which an "HMgX" unit is formally transferred from the Grignard reagent to the ketone, is also known (Scheme 4.4b). This Meerwein–Ponndorf–Verley-type (MPV) reduction is a common side reaction in Grignard addition reactions [1].

In 1961, Cooper and Finkbeiner reported that titanium tetrachloride **611** was an effective pre-catalyst for the isomerisation of iso-propylmagnesium bromide **610** (Scheme 4.5a) [13]. Quenching the reaction with deuterium oxide gave a mixture of 1- and 2-deuteriopropane **612** and **613**, indicating isomerisation of iso-propylmagnesium bromide **610** to give the linear Grignard reagent, *n*-propylmagnesium bromide in situ. It was proposed that isomerisation of the Grignard reagent took place through a β-hydride elimination/hydrometallation pathway, going via a titanium-hydride intermediate **614**.

It was rationalised that the addition of an alkene could compete for coordination sites on titanium with the alkene formed in situ, and thus could result in the formation of a Grignard reagent derived from the added alkene. The reaction of 1-pentene **615** and *n*-propylmagnesium bromide **616** in the presence of titanium tetrachloride **611** (3 mol%) resulted in the formation of *n*-pentylmagnesium bromide, determined by the formation of 1-hexanol **618** following reaction with formaldehyde **617** (Scheme 4.5b). Cooper and Finkbeiner extended the methodology to a range of terminal alkenes, including styrene derivatives, however 1,1- and 1,2-disubstituted alkenes were unreactive. The identity and structure of the Grignard reagent formed in situ was inferred by reaction with a variety of electrophiles, including oxygen, carbon dioxide, aldehydes and ketones. Terminal alkyl alkenes gave linear alkyl Grignard reagents, whilst styrene derivatives gave branched benzylic Grignard reagents. The regioselectivity in both cases was attributed to the formation of the thermodynamically-favoured Grignard reagent.

Cooper and Finkbeiner proposed a mechanism for titanium-catalysed hydromagnesiation (Scheme 4.6a). Alkylation of the titanium pre-catalyst would give an alkyl-titanium species **619**, which could undergo β-hydride elimination to give a

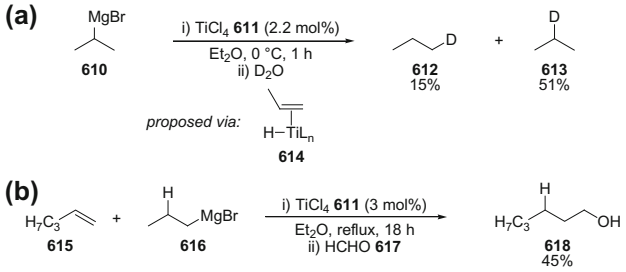

Scheme 4.5 **a** Titanium-catalysed isomerisation of alkyl Grignard reagents bearing β-hydrogen atoms. **b** Titanium-catalysed hydromagnesiation of 1-pentene **615** using *n*-propylmagnesium bromide **616**

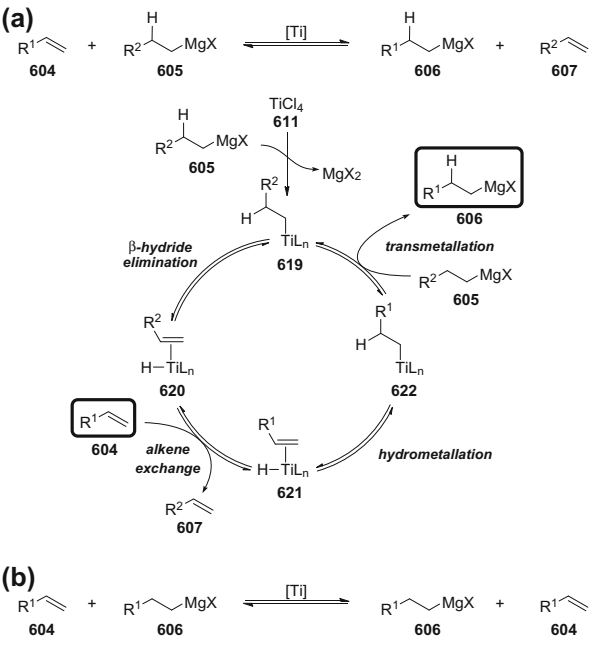

Scheme 4.6 **a** Proposed mechanism for titanium-catalysed hydromagnesiation of alkenes **604** using alkyl Grignard reagents bearing β-hydrogen atoms **605**. **b** 'Unproductive' hydromagnesiation reaction between an alkene **604** and a Grignard reagent bearing β-hydrogen atoms **606**

titanium-hydride intermediate **620**. Alkene exchange followed by hydrometallation would give an alkyl-titanium intermediate **622**. Transmetallation with another equivalent of Grignard reagent **605** would release the alkyl Grignard reagent product **606** and reform the initial alkyl-titanium species **619**.

Cooper and Finkbeiner commonly used *n*-propylmagnesium bromide as the 'hydromagnesiation reagent' on the premise that removal of the volatile propene by-product from the reaction would drive the reaction towards completion. The alkyl Grignard reagent formed in the reaction can also act as a 'hydromagnesiation reagent' however, and therefore the unproductive hydromagnesiation reaction between the alkyl Grignard reagent product **606** and alkene starting material **604**

would become increasingly significant as the reaction proceeded (Scheme 4.6b). This, in combination with catalyst decomposition and alkene isomerisation to give unreactive internal alkenes, can be used to explain the moderate yields obtained using this methodology.

Ashby studied the hydromagnesiation of 1-octene with a range of organomagnesium reagents and magnesium hydrides using bis(cyclopentadienyl)titanium dichloride **594** (Cp_2TiCl_2) [14]. The kinetic profile of the reaction was obtained for each hydromagnesiation reagent, with quantification of octylmagnesium bromide inferred based upon the amount of octane produced following hydrolysis. The reaction of an alkyl Grignard reagent or magnesium hydride with bis(cyclopentadienyl)titanium dichloride (Cp_2TiCl_2) resulted in the formation of a titanium hydride species, $[Cp_2TiH_2]^-$, identified based upon by electron spin resonance (ESR) spectroscopy [14, 15]. Coordination of an alkene to $[Cp_2TiH_2]^-$ would give a 19-electron complex, therefore it was suggested that the active catalyst was a neutral titanium monohydride species [Cp_2TiH], in equilibrium with the observed $[Cp_2TiH_2]^-$. The use of ethylmagnesium bromide resulted in only low yields of octylmagnesium bromide (<20 %) after 1 h, with a large amount of starting material remaining. In contrast, *n*-propyl- and *n*-butylmagnesium bromide gave octylmagnesium bromide in 50–60 % yield within the same time period. The low activity observed using ethylmagnesium bromide was attributed to the formation of a catalytically-inactive titanium ate complex $[Cp_2TiEt_2]^-$. The increased steric bulk of *n*-propyl- and *n*-butylmagnesium bromide was suggested to disfavour the analogous titanium ate complexes $[Cp_2TiR_2]^-$ and favour the catalytically-active monoalkyl titanium complex [Cp_2TiR]. Magnesium hydrides (MgH_2, MgHBr, MeMgH) were also effective for the hydromagnesiation of 1-octene, providing further evidence to suggest the reaction proceeded via a titanium hydride intermediate. In all cases internal alkene isomerisation products were obtained in 30–40 % yield. This mechanistic work supported the general mechanism proposed by Cooper and Finkbeiner (Scheme 4.6a), and corroborated the steps of pre-catalyst activation to a give a titanium(III)alkyl complex [15, 16], followed by β-hydride elimination to give a titanium hydride species.

Titanium-catalysed hydromagnesiation has been extended to include dienes and internal alkynes, giving allyl and vinyl Grignard reagents, respectively [17]. Sato reported that bis(cyclopentadienyl)titanium dichloride **594** (Cp_2TiCl_2) catalysed the 1,4-hydromagnesiation of 1,3-dienes to give allyl Grignard reagents (Scheme 4.7) [17a]. The hydromagnesiation of isoprene **623** using *n*-propylmagnesium bromide **616** gave the primary Grignard reagent **624** regioselectively, as determined by subsequent reaction with water or acetone. The allylic alkylation of acetone **627** gave the tertiary alcohol **628** as a single regioisomer [18]. The high yields obtained for the hydromagnesiation of 1,3-dienes were attributed to the greater stability of the allyl Grignard reagent **624**, relative to *n*-propylmagnesium bromide **616**, providing a thermodynamic driving force for the reaction.

The titanium-catalysed hydromagnesiation of disubstituted alkynes **629a-d** using iso-butylmagnesium bromide **630** gave (*E*)-vinyl Grignard reagents **631a-d** and **632a-d** (*syn* addition of 'HMgX') with excellent diastereoselectivity in some cases

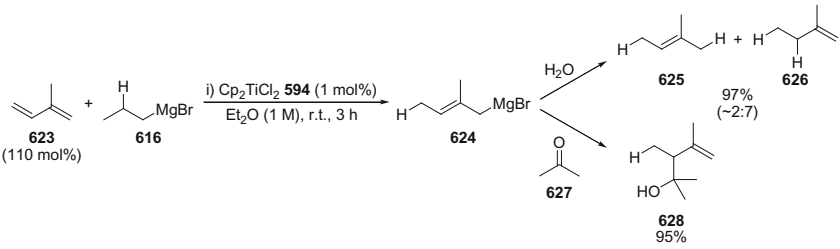

Scheme 4.7 Titanium-catalysed hydromagnesiation of isoprene **623** and subsequent reaction with electrophiles

(Scheme 4.8) [17b]. The diastereo- and regioselectivity of the reaction was determined based upon the products formed following the reaction of the intermediate vinyl Grignard reagent with an electrophile.

Whilst the hydromagnesiation of unsymmetrically-substituted dialkylalkynes **629a**, was not regioselective, the hydromagnesiation of aryl- and silyl-substituted alkynes showed excellent levels of regioselectivity. 1-Phenylpropyne **629b** underwent hydromagnesiation to give the α-aryl (*E*)-vinyl Grignard reagent **631b** in 9:1 regioselectivity. 1-Trimethylsilylhexyne **629c** showed similarly high levels of regioselectivity for the α-silyl (*E*)-vinyl Grignard reagent **632c**. These regioselectivities might be predicted based upon the increased thermodynamic stability of α-aryl and α-silyl anions. Interestingly, the hydromagnesiation of 1-trimethylsilyl-2-phenylacetylene **629d** gave the α-aryl (*E*)-vinyl Grignard reagent **631d** in excellent regioselectivity, demonstrating that the aromatic group has a greater directing effect in this reaction. The mechanism proposed by Sato for the titanium-catalysed hydromagnesiation of 1,3-dienes and disubstituted alkynes [19] was based upon those previously proposed by Cooper and Finkbeiner, and corroborated by Ashby, for the hydromagnesiation of alkenes.

Although much less well developed, nickel salts have also been used as pre-catalysts for the hydromagnesiation of alkenes and alkynes [20]. In 1967 Markó reported the nickel-catalysed hydromagnesiation of terminal alkenes using alkyl Grignard reagents bearing β-hydrogen atoms (Scheme 4.9a) [20a]. Terminal alkenes underwent hydromagnesiation to give alkyl Grignard reagents as a mixture of

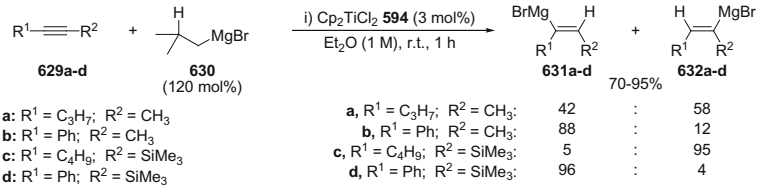

Scheme 4.8 Regioselectivity in the titanium-catalysed hydromagnesiation of unsymmetrically-substituted alkynes **629a-d**. Ratio of vinyl Grignard reagents **631a-d** and **632a-d** inferred by analysis of products formed following reaction with electrophiles (I_2, D_2O, CH_3I)

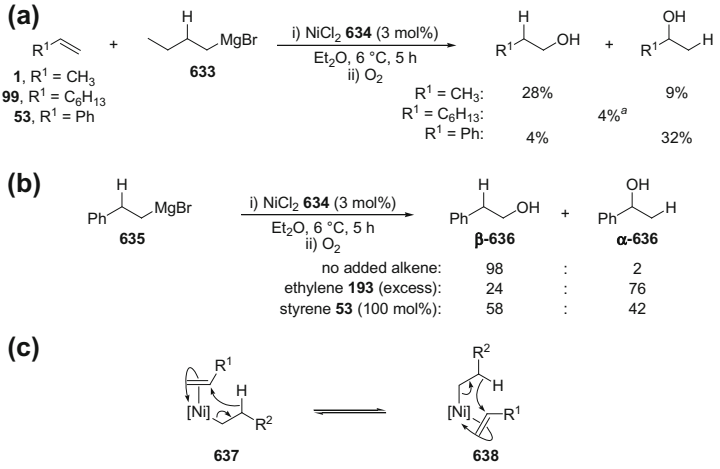

Scheme 4.9 Nickel-catalysed hydromagnesiation. **a** Hydromagnesiation of terminal alkenes using *n*-butylmagnesium bromide **633**. **b** Isomerisation of (2-phenylethyl)magnesium bromide **635** using nickel chloride **634** in the absence and presence of alkenes. **c** Proposed direct β-hydride transfer between alkyl and alkene ligands on nickel. [a]Regioselectivity not reported

regioisomers. For alkyl-substituted alkenes, linear primary Grignard reagents were predominantly produced, whilst styrene **53** gave the secondary benzylic Grignard reagent selectively. Short-chain alkenes, and those unable to undergo isomerisation, such as propene **1**, were successfully applied in the reaction, however long-chain terminal alkenes, such as 1-octene **99**, preferentially underwent isomerisation to give unreactive internal alkenes.

Although the yields obtained using this methodology were inferior to those obtained using titanium catalysts, Markó studied the reaction in detail and proposed an alternative mechanism for nickel-catalysed hydromagnesiation. In contrast to titanium catalysts, Markó noted that the isomerisation of Grignard reagents bearing β-hydrogen atoms using nickel chloride was inefficient in the absence of an added alkene (Scheme 4.9b) [20]. The addition of ethylene **193** or styrene **53** significantly increased the amount of product **α-636** obtained following Grignard reagent isomerisation. Secondly, Markó reported that the addition of a Grignard reagent and an alkene to nickel chloride resulted in a black homogeneous solution. Centrifugation of this mixture was used to remove insoluble material, however the black solution maintained catalytic activity. Centrifugation of the reaction mixture *before* the addition of either the Grignard reagent or the alkene resulted in a solution with significantly reduced catalytic activity [20b]. Markó suggested that these results indicated that the catalyst was homogeneous and required both an alkene ligand, and an alkyl ligand (from the Grignard reagent). Based upon these experiments Markó suggested that nickel-catalysed hydromagnesiation might proceed by a direct β-hydride transfer between alkyl and alkene ligands on nickel (Scheme 4.9c). It was suggested that hydrogen transfer could be facilitated by the non-bonding orbitals of nickel without the formation of a discrete nickel hydride.

The proposal that a nickel hydride intermediate was not involved in the mechanism of hydromagnesiation was based upon the observation that Grignard reagents did not undergo isomerisation in the absence of an alkene (Scheme 4.9b). Markó also demonstrated that an active catalyst was not formed in the absence of an alkene. An alternative explanation for the lack of Grignard reagent isomerisation in the absence of an alkene would therefore be that the alkene was simply required to stabilise the active catalyst. The fact that an active catalyst was not formed in the absence of an alkene could therefore invalidate the conclusions made based upon the Grignard reagent isomerisation experiments.

4.1.3 Iron-Catalysed Hydromagnesiation

In the early 1970s, Kochi conducted a series of fundamental investigations into the reactions of Grignard reagents with transition-metal salts, resulting in the seminal work on iron-catalysed cross-coupling reactions [21]. In one study, Kochi aimed to determine the oxidation-state of the transition-metal species formed following reaction with various Grignard reagents by analysis of the by-products of reduction [22]. Styrene was added to a number of these reactions with the intention of trapping possible alkyl radical intermediates. Instead, ethylbenzene was obtained in reasonable yield when an alkyl Grignard reagent bearing β-hydrogen atoms was used. This was attributed to the hydromagnesiation of styrene. Nickel, cobalt and iron salts gave ethylbenzene in moderate yields, and this reaction was further investigated using iron(III) chloride. The hydromagnesiation of alkenes using iron (III) chloride was most efficient in diethyl ether at low temperature or in tetrahydrofuran at room temperature (Scheme 4.10a, b). Following the hydromagnesiation of styrene **53** using ethylmagnesium bromide **280**, reaction with deuterium oxide

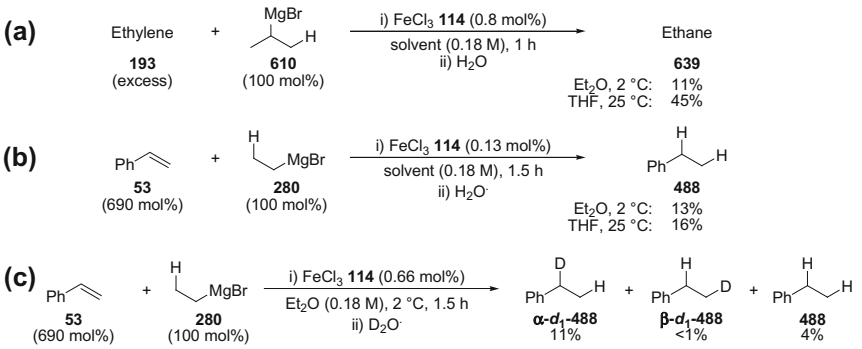

Scheme 4.10 Iron-catalysed hydromagnesiation using iron(III) chloride **114**. **a** Hydromagnesiation of ethylene **193** using iso-propylmagnesium bromide **610**; **b** hydromagnesiation of styrene **43** using ethylmagnesium bromide **280**; **c** hydromagnesiation of styrene **53** using ethylmagnesium bromide **280** followed by reaction with deuterium oxide

gave a mixture of d_1-ethylbenzene regioisomers **α-d_1-488** and **β-d_1-488** (Scheme 4.10c). The major regioisomer **α-d_1-488** contained deuterium at the benzylic position (~14:1 regioselectivity). Kochi suggested the reaction could proceed via an iron-hydride intermediate, however in-depth mechanistic studies were not conducted, and the synthetic utility of the reaction was not developed further.

In 2008, Shirakawa and Hayashi reported that 2-alkyl Grignard reagents **640** bearing β-hydrogen atoms underwent isomerisation to give the more thermodynamically-stable 1-alkyl Grignard reagents **643** using a combination of iron and copper halide salts (Scheme 4.11a) [23]. A homobenzylic Grignard reagent **646** was also isomerised to give the more thermodynamically-stable benzylic Grignard reagent **647** (Scheme 4.11b). In the absence of either iron or copper only minimal isomerisation was observed, indicating the essential role of both metals (Scheme 4.11a). The reaction of 2-octylmagnesium bromide **649** (6 equiv.) with copper(I) bromide **641** followed by reaction with deuterium oxide indicated that no isomerisation of the Grignard reagent had taken place (Scheme 4.11c). The reaction of 2-octylmagnesium bromide **649** (6 equiv.) with iron(III) chloride **114** resulted in

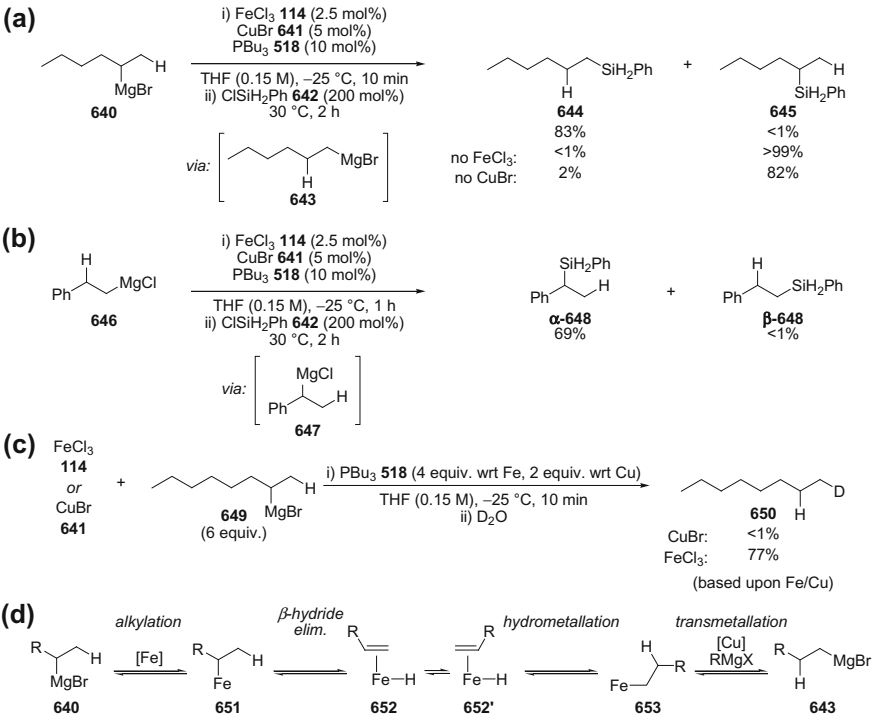

Scheme 4.11 Isomerisation of alkyl Grignard reagents using iron-copper cooperative catalysis. **a** Isomerisation of a 2-alkyl Grignard reagent **640** to a 1-alkyl Grignard reagent **643**; **b** isomerisation of a homobenzylic Grignard reagent **646** to a benzylic Grignard reagent **647**; **c** stoichiometric reactions of iron and copper salts with 2-octylmagnesium bromide **649**. **d** Proposed mechanism of alkyl Grignard reagent isomerisation

isomerisation to give the linear alkyl silane product **650** in close to quantitative conversion, with respect to iron (Scheme 4.11c). These experiments indicated that iron was responsible for the isomerisation of the alkyl Grignard reagent. This presumably occurred by alkylation of iron by the 2-alkyl Grignard reagent, followed by isomerisation to the thermodynamically-favoured 1-alkyliron species [24]. The minimal catalytic activity observed in the absence of copper (Scheme 4.11a) demonstrated that copper was necessary for reaction turn-over, and therefore it was proposed that copper was needed to assist transmetallation from iron to magnesium.

Based upon these experiments it was proposed that alkyl isomerisation occurred by β-hydride elimination of the 2-alkyliron intermediate **651** to give an iron-hydride **652** and an alkene (Scheme 4.11d). Reinsertion of the alkene into the iron–hydride bond would give the thermodynamically-favoured 1-alkyliron species **653** [24]. Under the developed conditions, 3-alkyl Grignard reagents were not isomerised to 1-alkyl Grignard reagents; however, formation of internal alkene products and catalyst decomposition were observed. It was therefore proposed that internal alkenes could not undergo insertion into the iron-hydride intermediate. In support of this proposal, when an extra equivalent of a terminal alkene was added to the reaction mixture, hydromagnesiation of the added alkene to give a 1-alkyl Grignard reagent was observed.

Shirakawa and Hayashi developed this result into a synthetically useful methodology for the hydromagnesiation of alkenes [25]. A combination of iron(III) chloride **114** (2.5 mol%), copper(I) bromide **641** (5 mol%) and tributylphosphine **518** (10 mol%) was effective for the hydromagnesiation of terminal aliphatic alkenes **654** using cyclopentylmagnesium bromide **655** as the stoichiometric source of 'H-MgX' (Scheme 4.12a). Internal alkenes were unreactive under the reaction

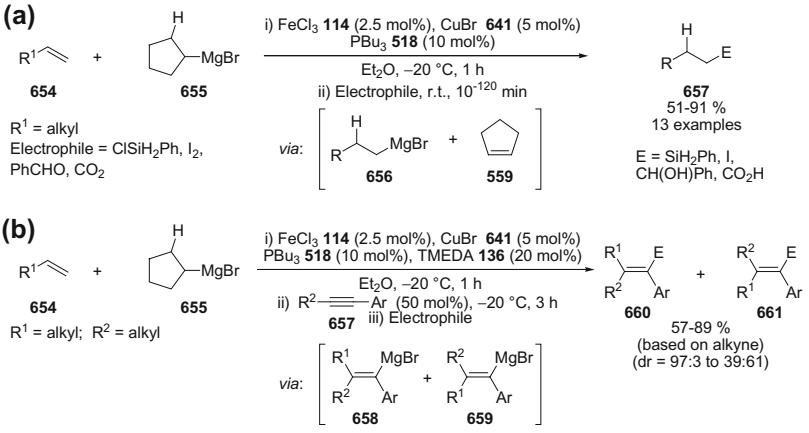

Scheme 4.12 Iron-catalysed hydromagnesiation of terminal alkenes **654** to give primary alkyl Grignard reagents **656**. **a** Subsequent reaction with electrophiles to give hydrofunctionalised products **657**. **b** Subsequent iron-catalysed addition to alkynes **657** to give tri- and tetra-substituted alkenes **660** and **661**

conditions, therefore the formation of cyclopentene **559** following "HMgX" transfer from cyclopentylmagnesium bromide **655** effectively removed this alkene by-product and made the reaction irreversible. The 1-alkyl Grignard reagent products **656** were reacted with a number of electrophiles, including chlorosilanes, carbon dioxide, benzaldehyde and iodine, to give a range of hydrofunctionalised products **657** in good to excellent yield. Functional groups that may not be compatible, or may cause complications, with standard Grignard reagent formation techniques such as alcohols and alkyl and aryl halides were tolerated.

The alkyl Grignard reagents **656** formed in the reaction were also applied in a subsequent iron-catalysed carbomagnesiation of alkynes **657** to give vinyl Grignard reagent intermediates **658** and **659** (Scheme 4.12b). These were reacted with electrophiles to give tri- and tetra-substituted alkene products **660** and **661**. The carbomagnesiation of 1-arylalkynes **657** proceeded with high regioselectivity to give the α-aryl vinyl Grignard reagent, however the diastereoselectivity of the reaction was low. When the reaction was quenched 1 min after the addition of the alkyne, comparable diastereoselectivities were obtained. This suggested that the low diastereoselectivity was an inherent result of the carbomagnesiation reaction, and did not result from a subsequent isomerisation of the vinyl Grignard reagent. Interestingly, despite using alkyl Grignard reagents bearing β-hydrogen atoms, no hydromagnesiation of the disubstituted alkynes **657** was reported.

Ready reported the iron-catalysed carbomagnesiation of propargylic and homopropargylic alcohols **662** using alkyl and aryl Grignard reagents (Scheme 4.13) [26]. The vinyl Grignard reagent intermediates **664** were reacted with electrophiles to give alkene products **666** in good to excellent yield, and in excellent regio- and diastereoselectivity. The majority of examples used methylmagnesium bromide **663** as the Grignard reagent. It was noted that the use of ethylmagnesium bromide **280** led to minor side-products **667** arising from competitive hydromagnesiation of the propargylic alcohol. *N*-Methylpyrrolidinone (NMP) was used as a co-solvent in the examples using ethylmagnesium bromide **280**, presumably in an attempt to limit β-hydride elimination and favour the carbomagnesiation product **666** [27]. The use of iso-propylmagnesium bromide **610** was reported to give the hydromagnesiation product **667** in moderate yield, although quantification of this product was not given.

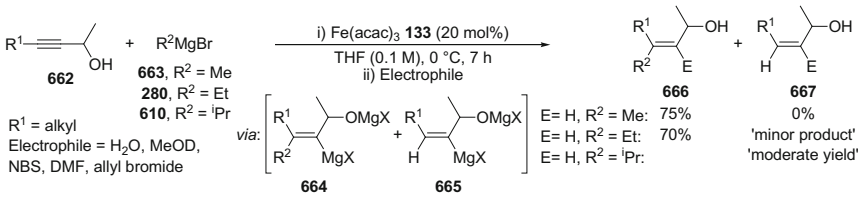

Scheme 4.13 Iron-catalysed carbo- and hydromagnesiation of propargylic alcohols **662** using methyl- **663**, ethyl- **280** and iso-propylmagnesium bromide **610**

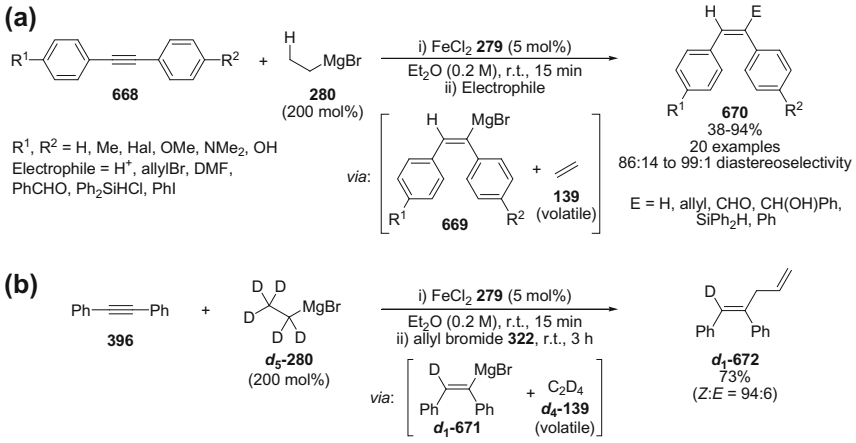

Scheme 4.14 Iron-catalysed hydromagnesiation diarylalkynes **668** using ethylmagnesium bromide **280**, and subsequent reaction with electrophiles to give tri-substituted alkenes **670**

Iron-catalysed hydromagnesiation of diarylalkynes **668** and 1,3-diynes was reported by Nakamura using iron(II) chloride **279** (5 mol%) and ethylmagnesium bromide **280** (200 mol%) to give (*E*)-vinyl Grignard reagents **669** in high yield and diastereoselectivity (Scheme 4.14) [28]. In contrast to the work of Shirakawa and Hayashi [25] and Ready [26] only minor products (<2 %) arising from the carbomagnesiation of the alkynes were observed. It is unclear whether this difference in product distribution was due to a difference in the catalytic species formed, or an inherent difference in the reactivities of the alkyne substrates used in each methodology. Nakamura commented that alkyl-substituted alkynes reacted poorly under the reaction conditions, but did not elaborate further.

A variety of diarylalkynes **668** bearing both electron-donating and electron-withdrawing substituents gave *syn*-addition products **669** with good to excellent control of stereochemistry. The intermediate (*E*)-vinyl Grignard reagents **669** were reacted with a range of electrophiles, such as allyl bromide, benzaldehyde, *N*,*N*-dimethylformamide and chlorosilanes, to give hydrofunctionalised products **670** in good to excellent yields. The (*E*)-vinyl Grignard reagents **669** were also applied in subsequent nickel- and iron-catalysed coupling reactions. The reaction was chemoselective for the hydromagnesiation of diarylalkynes in the presence of other alkynes or alkenes; however, there was no control of regiochemistry in the hydromagnesiation of unsymmetrically-substituted diarylalkynes. Nakamura suggested that this lack of regioselectivity might indicate a radical process instead of a pure organometallic mechanism. Although no ligands were added to the reaction, it was suggested that the ethylene by-product produced during the reaction might act as a stabilising ligand on iron [29]. The use of d_5-ethylmagnesium bromide ***d*$_5$-280** gave the (*Z*)-alkene product ***d*$_1$-672** with 99 % deuterium incorporation.

This demonstrated that the added hydride originated from ethylmagnesium bromide, and provided evidence that the products were formed through a hydromagnesiation reaction.

4.2 Results and Discussion

4.2.1 State of the Art at the Outset of the Project

At the beginning of 2011, very little had been reported on iron-catalysed hydromagnesiation. The work of Kochi from 1971 had demonstrated the feasibility of using iron catalysts for hydromagnesiation [22], however only low yields of Grignard reagents had been reported. The hydromagnesiation of styrene gave the benzylic Grignard reagent in approximately 10 % yield and 14:1 regioselectivity. Ready had noted the hydromagnesiation of propargylic alcohols using alkyl Grignard reagents bearing β-hydrogen atoms as an unwanted side-reaction [26]. Shirakawa and Hayashi had used the hydromagnesiation of a terminal alkene to support their suggestion that the iron-catalysed isomerisation of alkyl Grignard reagents proceeded via an iron hydride intermediate [23], however the development of this result into a synthetically-useful methodology was not reported until 2012 [25].

4.2.2 Project Aims

The objective of this work was to develop an operationally-simple iron-catalysed methodology for the hydromagnesiation of styrene derivatives to give benzylic Grignard reagents (Scheme 4.15). This substrate class was targeted as benzylic Grignard reagents are challenging to access by alternative methods [4–6]. Key to this methodology would be the use of a bench-stable iron pre-catalyst and easy to handle, commercially-available reagents. The developed methodology would be applied to the hydromagnesiation of a range of styrene derivatives to determine the

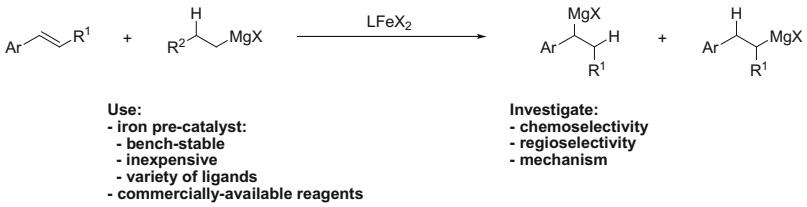

Scheme 4.15 Proposed development of iron-catalysed hydromagnesiation methodology

chemo- and regioselectivity of the process. As the only thorough mechanistic work on hydromagnesiation had been undertaken using titanium catalysts, the mechanism of the developed iron-catalysed process would be investigated.

4.2.3 Methodology Development

The hydromagnesiation of styrene **53** was initially investigated using carbon dioxide as an electrophile to give formal hydrocarboxylation products. This would allow simple product purification and provide access to α-aryl carboxylic acids from styrene derivatives [30]. Initial studies focussed on the hydromagnesiation of styrene **53** using simple iron salts (2.5 mol%) and iso-propylmagnesium chloride **165** in tetrahydrofuran (Table 4.1). In keeping with iron-catalysed cross-coupling methodologies, the Grignard reagent was added slowly over the course of approximately 10 min. The reactions were stirred for 1 h before reaction with carbon dioxide. Using a range of different iron(II) and iron(III) salts gave very low quantities of the carboxylic acids **α-76** and **β-76**. These results indicated only minimal hydromagnesiation activity, which was in contrast to the work of Kochi where moderate yields were obtained under apparently similar conditions [22]. Heating the reactions at reflux gave the carboxylic acids **α-76** and **β-76** in much improved yields. Close to 60 % yield was obtained using iron(II) triflate (Table 4.1, entry 4). A moderate regioselectivity for the α-aryl carboxylic acid product **α-76** was also obtained (~14:1). The addition of simple ligands (NMP **292**, TMEDA **136**, PPh_3 **315**) and increasing the reaction time did not improve the yield or regioselectivity of the reaction.

Table 4.1 Identification of iron-catalysed hydromagnesiation methodology I: iron salts[a]

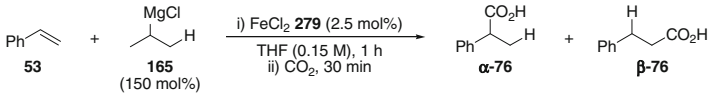

Entry	$FeX_{2/3}$	Yield (%)[b] (room temperature)		Yield (%)[b] (heating at reflux)	
		α-76	β-76	α-76	β-76
1	$FeCl_2$ **279**	<1	–	8	<1
2	$FeBr_2$ **144**	2	–	–	–
3	$Fe(OAc)_2$ **673**	1	–	12	<1
4	$Fe(OTf)_2$ **674**	<1	–	55	4
5	$FeCl_3$ **114**	2	–	7	<1
6	$Fe(acac)_3$ **133**	–	–	10	<1

[a]Conditions: (i) styrene **53** (0.7 mmol), iron salt (2.5 mol%), i-PrMgCl **165** (150 mol%), tetrahydrofuran (0.15 M), r.t., 1 h. (ii) CO_2, 30 min; [b]Yield determined by ^1H NMR spectroscopy using 1,3,5-trimethoxybenzene as an internal standard

As only moderate yields and regioselectivities had been obtained, optimisation of the reaction at room temperature was investigated through the addition of ligands. It was expected that a low oxidation-state iron species would be produced under the highly reducing conditions of the reaction [21, 22, 29a, c, 31], and therefore the use of an appropriate ligand could provide stabilisation to this species. The formal hydrocarboxylation of styrene using ethylmagnesium bromide and carbon dioxide was therefore investigated using iron(II) chloride (5 mol%), and a range of nitrogen- and phosphorus-based ligands (Table 4.2). The use of *N*-methylpyrrolidone **292** (NMP) (30 mol%) gave significantly improved catalytic activity, with the hydrocarboxylation products obtained in close to 30 % yield (Table 4.2, entry 1). Increasing the loading of NMP **292** to 300 mol% was not beneficial (Table 4.2, entry 2). The use of *N*,*N*,*N*′,*N*′-tetramethylethylenediamine **136** (TMEDA) (5–25 mol%) gave carboxylic acids **α-76** and **β-76** in 80 % yield, and with high regioselectivity for the α-aryl carboxylic acid **α-76** (Table 4.2, entries 3–4). Tri(*n*-butyl)phosphine **518** was also an effective ligand, with carboxylic acids **α-76** and **β-76** obtained in 68 % yield (Table 4.2, entry 5).

In an attempt to improve catalyst stability, the use of multi-dentate and redox-active ligands was investigated [32]. The use of ^{iPr}Pybox **287**, DACH-py **288**, and the tetradentate iminopyridine ligand **276** did not improve upon the yields obtained using TMEDA **136** (Table 4.2, entries 6–8). The use of bis(imino)pyridine ligand **273a** (^{iPr}BIP) however, produced a highly active catalyst with full conversion of starting material and quantitative yield of the carboxylic acids **α-76** and **β-76** obtained (Table 4.2, entry 9). Excellent regioselectively for the α-aryl carboxylic acid **α-76** was observed (α:β, ~60:1). Reducing the pre-catalyst loading to 0.1 mol %, and the quantity of ethylmagnesium bromide **280** to 120 mol%, gave a comparable yield, albeit following a slightly extended reaction time of 3 h (Table 4.2, entry 10).

In the absence of iron, no reaction was observed. The addition of trace amounts of other transition-metal salts to the standard reaction conditions did not improve the yield of the hydrocarboxylation products **α-76** and **β-76** [33]. Copper, nickel, cobalt, iridium, rhodium, palladium and ruthenium salts were tested at a 1000 ppm concentration, with respect to iron. The use of these transition-metal salts in the absence of iron showed no catalytic activity. The use of high purity iron(II) chloride (99.99 %) gave carboxylic acids **α-76** and **β-76** in near-quantitative yield (Table 4.2, entry 11). These results suggest that the active catalyst is an iron species.

When the reaction was conducted at 0 °C, the carboxylic acid product **α-76** was obtained in only 2 % yield (Table 4.2, entry 12). At −15 °C no catalytic activity was observed (Table 4.2, entry 13). In diethyl ether or toluene solution at room temperature no catalytic activity was observed, with only recovered starting material and propanoic acid obtained (Table 4.2, entries 14–15).

Table 4.2 Identification of iron-catalysed hydromagnesiation methodology I: iron salts[a]

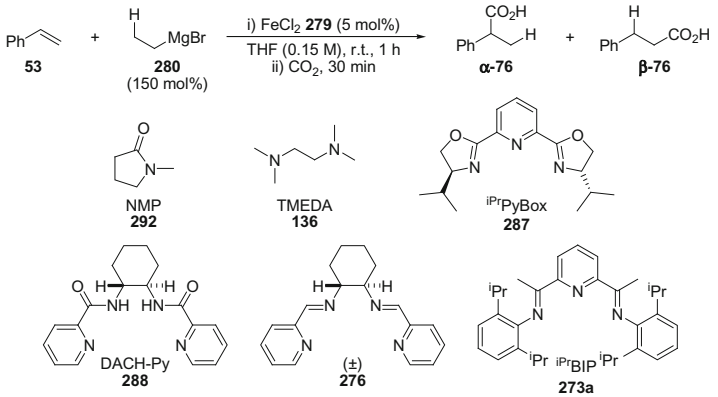

Entry	Ligand (mol%)	Yield (%)[b]	
		α-76	β-76
1	NMP **292** (30)	27	2
2	NMP **292** (300)	–	–
3	TMEDA **136** (5)	79	1
4	TMEDA **136** (25)	77	1
5	*n*-Bu_3P **518** (20)	66	2
6	^{iPr}Pybox **287** (5)	39	2
7	DACH-py **288** (5)	66	1
8	**276** (5)	76	<1
9	^{iPr}BIP **273a** (5)	98	1
10[c]	^{iPr}BIP **273a** (0.1)	97	1
11[d]	^{iPr}BIP **273a** (1)	97	1
12[e]	^{iPr}BIP **273a** (1)	2	–
13[f]	^{iPr}BIP **273a** (1)	–	–
14[g]	^{iPr}BIP **273a** (1)	–	–
15[h]	^{iPr}BIP **273a** (1)	–	–

[a]Conditions: (i) styrene **53** (0.7 mmol), $FeCl_2$ **279** (5 mol%), EtMgBr **280** (150 mol%), tetrahydrofuran (0.15 M), r.t., 1 h. (ii) CO_2, 30 min; [b]Yield determined by ^{1}H NMR spectroscopy using 1,3,5-trimethoxybenzene as an internal standard; [c]$FeCl_2$ **279** (0.1 mol%), EtMgBr **280** (120 mol%) used, 3 h reaction time; [d]$FeCl_2$ **279** (99.99 % purity, 1 mol%) used; [e]Reaction temperature = 0 °C; [f]Reaction temperature = −15 °C; [g]Et_2O (0.15 M) used in place of THF; [h]Toluene (0.15 M) used in place of THF

4.2.3.1 Substrate Scope and Limitations

The synthetic utility and chemoselectivity of the developed methodology was investigated using a range of styrene derivatives bearing different substitution patterns and functional groups. Styrene derivatives which were not commercially-available were synthesised from benzaldehyde derivatives using the Wittig reaction (Table 4.3).

Table 4.3 Preparation of styrene derivatives using the Wittig reaction

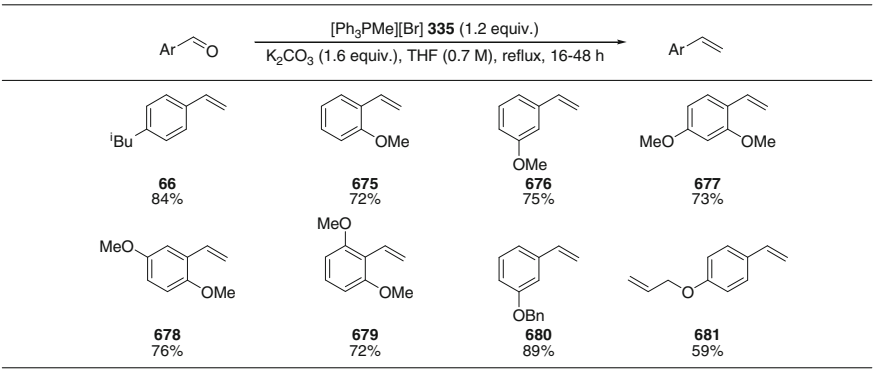

Alkyl-substituted styrene derivatives were tolerated in the reaction, giving carboxylic acids in generally high yield (Table 4.4). Alkyl substitution in the *meta*- and *para*- positions gave α-aryl carboxylic acids with excellent regioselectivity, however 2-methylstyrene gave the α-aryl carboxylic acid **α-682** in only 10:1 regioselectivity. The regioselectivity of hydromagnesiation using 2,4- and 2,5-dimethylstyrene derivatives was even lower, with carboxylic acids **687** and **688** obtained in a roughly 1:1 mixture of α- and β-aryl regioisomers. The use of the more sterically-hindered alkyl Grignard reagent, cyclopentylmagnesium bromide **655**, in place of ethylmagnesium bromide **280**, gave the carboxylic acids **687** and **688** with increased regioselectivity for the β-aryl carboxylic acids **β-687** and **β-688**. It would be expected that the α-aryl Grignard reagent would still be the thermodynamically-favoured Grignard reagent in these cases, therefore the β-aryl carboxylic acids **β-687** and **β-688** must be the kinetically-favoured products. This may be attributed to a steric effect imposed by these substrates which results in a transition-state structure or binding conformation that leads to formation of the β-aryl Grignard reagent. The more sterically-hindered styrene derivative 2,4,6-trimethylstyrene **689** did not undergo hydromagnesiation and was recovered in quantitative yield.

Methyl ether-substituted styrene derivatives were also suitable substrates, giving carboxylic acids in generally good to excellent yield (Table 4.4). Unlike 2-methylstyrene, 2-methoxystyrene gave the α-aryl carboxylic acid **α-690** in excellent yield and with high regioselectivity (α:β, >100:1). The difference in regioselectivity might be explained by a binding interaction between the *ortho*-methoxy group and the iron (or magnesium) centre, which may enhance the preference for the transition-state structure or binding conformation that leads to the α-product (Fig. 4.1). 3-Methoxystyrene gave the α-aryl carboxylic acid **α-691** in excellent yield and regioselectivity (α:β, >100:1), however 4-methoxystyrene gave **α-692** in only moderate yield and with comparably low regioselectivity (α:β, 18:1).

Table 4.4 Hydromagnesiation of styrene derivatives: substrate scope and limitations I[a]

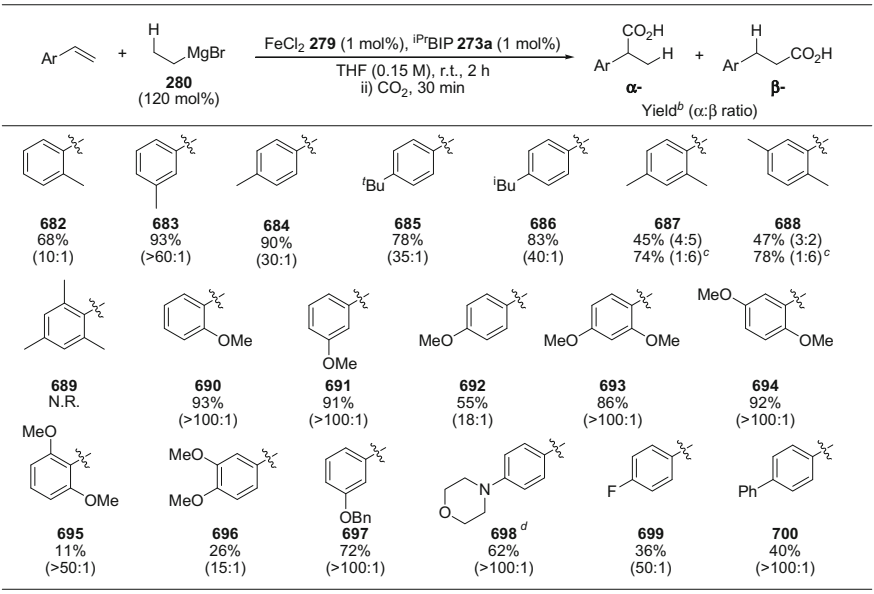

[a]Conditions: (i) styrene derivative (0.7 mmol), $FeCl_2$ **279** (1 mol%), [iPr]BIP **273a** (1 mol%), EtMgBr **280** (120 mol%), THF (0.15 M), r.t., 2 h, (ii) CO_2, 30 min; [b]Isolated yield; [c]Cyclopentylmagnesium bromide **655** (120 mol%) used in place of EtMgBr **280**. [d]Isolated as methyl ester—conditions: (i) HCl (0.9 mmol, 2 M in Et_2O). (ii) $(COCl)_2$ (10 mmol). (iii) MeOH (0.1 M), NEt_3 (3 mmol), r.t., 2 h

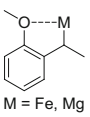

Fig. 4.1 Possible bonding interaction in an *ortho*-methoxy-substituted benzylic organometallic species

In contrast to 2,4- and 2,5-dimeththylstyrene, 2,4- and 2,5-dimethoxystyrene gave the α-aryl carboxylic acids **α-693** and **α-694** in excellent yield and regioselectivity (α:β, >100:1). This is again indicative of a significant directing or activating effect of the *ortho*-methoxy group. The sterically-hindered styrene derivative 2,6-dimethoxystyrene **679** also showed some activity, with the α-aryl carboxylic acid **α-695** obtained in 11 % yield (α:β, 50:1).

3,4-Dimethoxystyrene gave the α-aryl carboxylic acid **α-696** in only 28 % yield (Table 4.4). In addition to recovered 3,4-dimethoxystyrene, two further styrene derivatives were obtained, which might be explained by demethylation of the starting material. The Grignard reagent-mediated cleavage of ethers has been reported to be accelerated by the presence of iron and cobalt salts [34]. Although demethylation was not observed in any of the other examples, the rate of

demethylation may be enhanced in this case by co-ordination to the adjacent methoxy group. The benzyl ether-functionalised styrene derivative **680** underwent hydromagnesiation to give the α-aryl carboxylic acid **α-697** in good yield and with high regioselectivity (α:β, >100:1). No products arising from the cleavage of the phenyl benzyl ether were observed.

Tertiary amine-substituted styrene derivatives could also be applied in the methodology (Table 4.4). The zwitterionic amino acid products proved challenging to isolate, therefore the carboxylic acid was converted to the corresponding methyl ester. The highest yield of methyl ester **698** was obtained by conversion of the crude reaction product to the corresponding acid chloride using oxalyl chloride followed by reaction with methanol. The α-aryl ester **α-698** was obtained in good yield and with high regioselectivity (α:β, >100:1). 4-Fluorostyrene and 4-phenylstyrene also underwent hydromagnesiation, however the α-aryl carboxylic acids **α-699** and **α-700** were obtained in only moderate yield. The hydromagnesiation of 4-fluorostyrene also resulted in the formation of small quantities of styrene, presumably formed by protodehalogenation of 4-fluorostyrene.

A number of styrene derivatives were found to be incompatible with the developed methodology (Table 4.5). Styrene derivatives **10**, **382**, **560** and **711** bearing substitution in the α- or β-position were unreactive, resulting in quantitative recovery of starting material in each case. This is in keeping with previous

Table 4.5 Hydromagnesiation of styrene derivatives: substrate scope and limitations II[a]

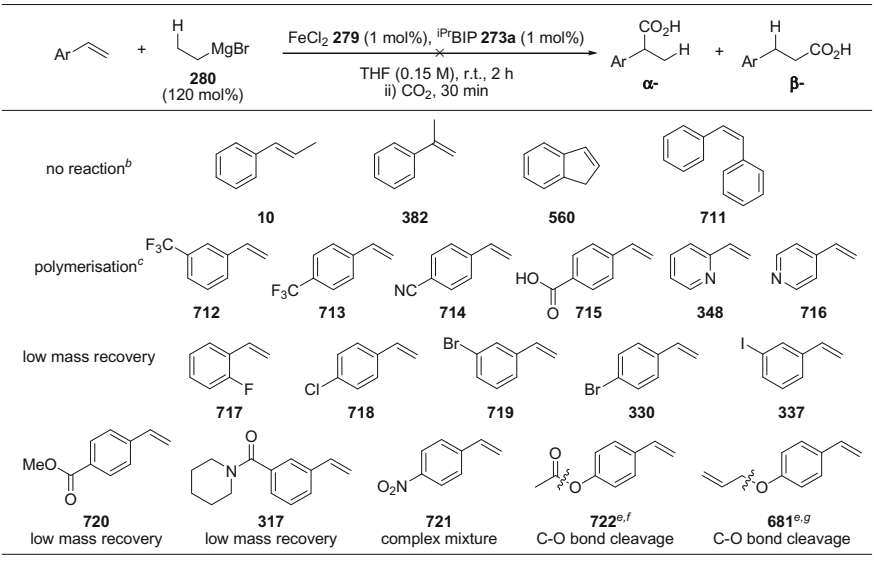

[a]Conditions: (i) styrene derivative (0.7 mmol), $FeCl_2$ **279** (1 mol%), [iPr]BIP **273a** (1 mol%), EtMgBr **280** (120 mol%), THF (0.15 M), r.t. 2 h, (ii) CO_2, 30 min; [b]Quantitative recovery of starting material; [c]Insoluble solid produced; [d]Small quantities of styrene **53** observed (< 5 %); [e]4-Vinylphenol obtained in quantitative yield; [f]EtMgBr (350 mol%) gave same result; [g]EtMgBr (250 mol%) gave same result

hydromagnesiation methodologies using alkyl Grignard reagents bearing β-hydrogen atoms, where internal alkenes have been reported to be either unreactive or give hydromagnesiation products in only very low yield. Styrene derivatives **712-715** bearing electron-withdrawing groups and vinylpyridines **348** and **716** did not give any hydromagnesiation products. The formation of a gummy material which was insoluble in diethyl ether was observed. This was attributed to polymerisation of the styrene substrates [35].

In contrast to 4-fluorostyrene, 2-fluorostyrene **717** did not undergo hydromagnesiation, with mostly starting material and styrene recovered (Table 4.5). This indicated that cleavage of the carbon–fluorine bond had taken place in preference to hydromagnesiation of the vinyl group. 2-Chlorostyrene derivatives have been shown to undergo chemoselective iron-catalysed cross-coupling, with the *ortho*-vinyl group suggested to activate the carbon–chlorine bond to cleavage by the low oxidation-state iron catalyst [36]. Carbon–chlorine bond cleavage was suggested to occur following initial coordination of the iron catalyst to the *ortho*-vinyl group followed by haptotropic migration [37] through the conjugated π-system. This effect was reported to be much less pronounced for 3- and 4-chlorostyrene derivatives. The difference in reactivity of 2- and 4-fluorostyrene in the hydromagnesiation reaction may be attributed to a similar effect. The lack of hydromagnesiation activity might be attributed to a catalytically-inactive iron-fluoride complex, formed following cleavage of the carbon–fluorine bond of 2-fluorostyrene. Carbon–fluorine bond cleavage to give an iron-fluoride complex has previously been suggested as a potential cause of catalyst deactivation in iron-catalysed cross-coupling reactions [38].

Chloro-, bromo- and iodostyrene derivatives **717-719**, **330** and **337** did not undergo hydromagnesiation, with only small quantities of styrene derivatives recovered (Table 4.5). Based upon ^{1}H NMR spectroscopy it appeared that the styrene substrates had undergone polymerisation to give soluble polymeric material. Small quantities of styrene **53** were also obtained suggesting competitive protodehalogenation [39].

The use of ester and amide-substituted styrene derivatives **720** and **317** also resulted in no product formation (Table 4.5). The expected carbonyl-addition products were not obtained, however broad features in the ^{1}H NMR spectra may again be indicative of competitive polymerisation. No propanoic acid was obtained suggesting that all of the Grignard reagent had been consumed. This may imply that Grignard addition to the carbonyl groups had occurred. This may have taken place before or after polymerisation of the vinyl group. The reaction using 4-nitrostyrene **721** gave a complex mixture, however no hydromagnesiation products were observed. Nitroarenes readily react with Grignard reagents at room temperature (and below) to give *C*- and *N*-alkylated nitro, nitroso and amine products [40], potentially explaining the incompatibility of 4-nitrostyrene **721** with the developed methodology.

4-Acetoxystyrene **722** and 4-allyloxystyrene **681** underwent carbon–oxygen bond cleavage to give 4-vinylphenol in quantitative yield (Table 4.5). The iron-catalysed cleavage of phenyl allyl ethers has been reported using a

combination of iron(II) chloride **279** (1 mol%) and ethylmagnesium bromide **280** (105 mol%) [41]. In each case at least one equivalent of ethylmagnesium bromide **280** would be consumed in the cleavage of the carbon–oxygen bond, and therefore the hydromagnesiation of 4-acetoxystyrene **722** and 4-allyloxystyrene **681** was attempted using excess ethylmagnesium bromide **280**. In both cases 4-vinylphenol was again obtained in quantitative yield, indicating that the magnesium phenolate, presumably formed following carbon–oxygen bond cleavage, was not a suitable substrate for hydromagnesiation.

The hydromagnesiation of other unsaturated carbon–carbon multiple bonds was also investigated. The alkyl-substituted alkene, 4-phenylbutene **361**, underwent hydromagnesiation to give the linear carboxylic acid **723** in 28 % yield (Scheme 4.16a). The regioselectivity observed for the linear hydrocarboxylation product is consistent with formation of the thermodynamically-favoured 1-alkyl Grignard reagent. In addition to the hydrocarboxylation product **723**, internal alkenes **514** and **515** were obtained, along with unreacted starting material. The yield obtained was somewhat lower than the yield of 72 % reported by Shirakawa and Hayashi for the hydromagnesiation of the same substrate [25]. Applying the hydromagnesiation conditions developed by Shirakawa and Hayashi to the hydrocarboxylation of styrene resulted in a 20 % yield of carboxylic acids with low regioselectivity (~4:1). This demonstrated that the developed methodologies were complementary for the hydromagnesiation of either alkyl- or aryl alkenes, respectively.

Due to the low hydromagnesiation activity observed using alkyl alkenes, the chemoselectivity of the developed methodology was tested using a substrate containing both aryl- and alkyl alkene functional groups **326** (Scheme 4.16b). α-Aryl carboxylic acids **α-724** and **α-725** were obtained in a combined yield of approximately 40 %, whilst the alkyl carboxylic acid **726** was obtained in 9 % yield. This corresponded to a chemoselectivity of approximately 4:1 for hydromagnesiation of the aryl alkene.

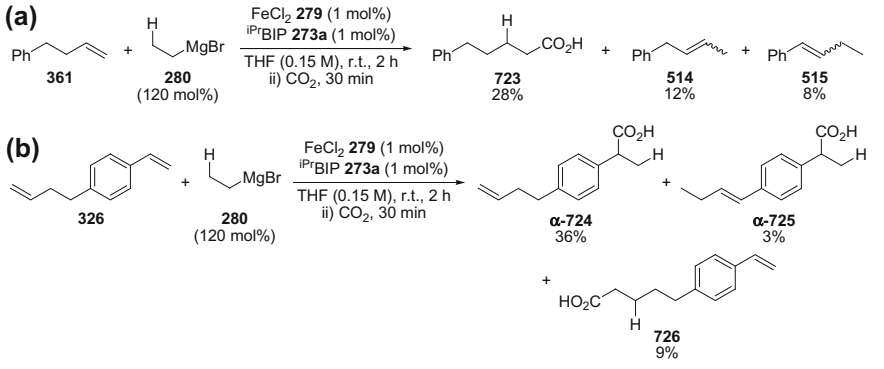

Scheme 4.16 **a** Hydromagnesiation of 4-phenylbutene **361**, followed by reaction with CO_2. **b** Investigation of the chemoselectivity of hydromagnesiation between aryl- and alkyl alkenes

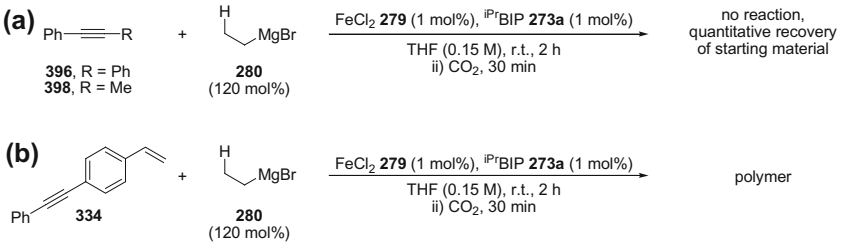

Scheme 4.17 **a** Unsuccessful hydromagnesiation of internal alkynes **396** and **398**. **b** Investigation of the chemoselectivity of hydromagnesiation between an alkyne and an aryl alkene

Hydromagnesiation reactions using diphenylacetylene **396** and 1-phenylpropyne **398** were unsuccessful, with only starting material and propanoic acid obtained (Scheme 4.17a). The hydromagnesiation of 4-(phenylethynyl)styrene **334** was therefore investigated in the hope of chemoselective hydromagnesiation of the styrene group (Scheme 4.17b). Full conversion of the starting material was observed, but no hydromagnesiation products were obtained. Based upon ^{1}H NMR spectroscopy it appeared that the styrene substrate had undergone polymerisation to give a soluble polymeric material.

All of the hydromagnesiation reactions had been conducted on a small scale (~1 mmol), therefore the potential to perform the reaction on a preparative scale was investigated. This work was undertaken for the final step of a synthesis of ibuprofen, in which only iron-catalysed reactions were used. With the intention to make the methodology more industrially-applicable, the inexpensive catalyst combination of iron(III) acetylacetonate **133** and *N*,*N*,*N*′,*N*′-tetramethylethylenediamine **136** (TMEDA) was used for reaction development. The progress of the reaction was monitored by periodically removing aliquots, which were reacted with chlorotrimethylsilane **727** to give the α-aryl silane **α-728** (Fig. 4.2).

Using 1 mol% iron(III) acetylacetonate **133** and TMEDA **136** (1 mol%), over 60 % yield was obtained within the first 10 min, with full conversion reached within 2 h (Fig. 4.2 ●). When the scale of the reaction was increased tenfold, a similar initial rate of reaction was observed, however the rate significantly decreased beyond 50 % conversion, with only 63 % yield obtained after 2 h (Fig. 4.2 ●). It was rationalised that the production of the ethylene **193** by-product may inhibit the reaction, through competition with styrene **53** for binding sites on iron and by increasing the reversibility of the reaction. It therefore seemed possible that inefficient loss of ethylene **193** from solution could be responsible for the retardation in the rate of reaction. A faster rate of ethylene **193** loss from solution on a small scale might be expected due to the larger surface area of the solution and more efficient stirring. To aid the loss of ethylene **193** on a large scale, the reaction was continuously sparged with nitrogen. High catalyst activity was recovered and a yield of 92 % was obtained within 2 h (Fig. 4.2 ●). These results indicate that on a preparative scale efficient loss of ethylene **193** from solution is of paramount importance in order to obtain hydromagnesiation products in high yield.

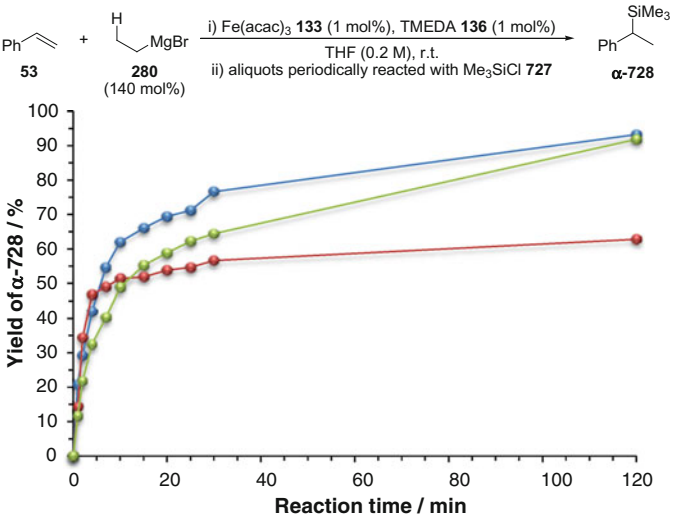

Fig. 4.2 Kinetic analysis of the hydromagnesiation of styrene on a preparative scale. Conditions: $Fe(acac)_3$ **133** (1 mol%), TMEDA **136** (1 mol%), styrene **53** (0.7 or 7 mmol), EtMgBr **280** (140 mol%), THF (0.2 M). Key: ● = 0.7 mmol scale; ● = 7 mmol scale; ● = 7 mmol scale, with continual N_2 sparge

The developed methodology was applied, on scale, to the three-step synthesis of ibuprofen **α-686** using iron-catalysed reactions for each step (Scheme 4.18). Starting from 4-chlorophenyl trifluoromethanesulfonate **729**, sequential iron-catalysed alkyl-aryl and aryl-vinyl cross-coupling reactions gave 4-iso-butylstyrene **66** in 74 % yield over two steps. Without purification, 4-iso-butylstyrene **66** could be used in the subsequent hydromagnesiation-carboxylation step to give ibuprofen **α-686**. In keeping with the trial experiments using styrene (Fig. 4.2), the 10 mmol-scale

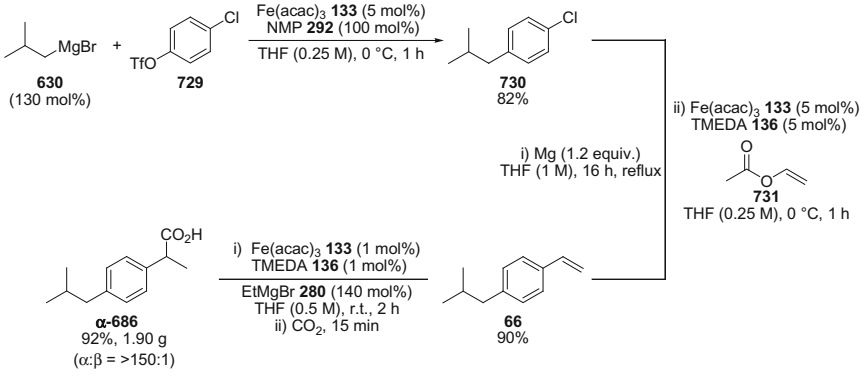

Scheme 4.18 Three-step synthesis of ibuprofen **α-686**, using iron-catalysed reactions for each step. In collaboration with Adam Kolodziej and Fern Sinclair

hydromagnesiation of 4-iso-butylstyrene **66** could be driven to completion by sparging the reaction with nitrogen. Regioselectivity for the α-aryl carboxylic acid was approximately 40:1, however recrystallisation of the crude reaction product from hexane provided ibuprofen **α-686** in a 92 % isolated yield and with high regioisomeric purity (α:β, >150:1). Optimisation of the sequential iron-catalysed alkyl-aryl and aryl-vinyl cross-coupling reactions to give 4-iso-butylstyrene **66** was carried out in collaboration with undergraduate students, Adam Kolodziej and Fern Sinclair.

4.2.4 Investigation of Reaction Mechanism

The first question to address was whether the formal hydrocarboxylation reaction did in fact proceed by hydromagnesiation to give a benzylic Grignard reagent. Addition of carbon dioxide from the start of the reaction had resulted in significantly lower yields, indicating that a period of time was required for a reactive intermediate to accumulate. Quenching the hydromagnesiation of styrene using deuterated methanol gave d_1-ethylbenzene in quantitative yield, with deuterium incorporation at the benzylic position. This indicated the presence of a stoichiometric quantity of a benzylic organometallic reagent. As magnesium was the only metal present in a stoichiometric quantity, this benzylic organometallic reagent was likely to be the benzylic Grignard reagent.

The preparation of Grignard reagents in all previous hydromagnesiation methodologies had been inferred by similar observations based upon the analysis of the products formed following the addition of an electrophile [3, 8, 12–14, 17, 20, 25, 28]. We aimed to observe the intermediate benzylic Grignard reagent directly by multinuclear and 2D NMR spectroscopy. In tetrahydrofuran (at concentrations below 3 M) the composition of organomagnesium species in solution can be expressed by the simplified Schlenk equilibrium, where only monomeric magnesium species are present (Eq. 1) [42]. The observation and characterisation of discrete Grignard reagents (monoalkylmagnesium, RMgBr) and dialkylmagnesium species (R_2Mg) by NMR spectroscopy can often be challenging due to rapid interconversion between the species on the NMR timescale. The rate of interconversion between organomagnesium species is highly dependent upon the structure of the organic group. Ashby reported that whilst methyl Grignard reagent required cooling to −100 °C to observe MeMgX and Me_2Mg, *tert*-butyl Grignard reagent was observed as discrete mono- and dialkylmagnesium species at room temperature [43].

$$MgBr_2 + R_2Mg \rightleftharpoons 2 \times RMgBr \quad (1)$$

Conducting the iron-catalysed hydromagnesiation of styrene in d_8-tetrahydrofuran gave a mixture of the benzylic Grignard reagent, 1-phenylethylmagnesium bromide **734** and the dibenzylmagnesium species, bis(1-phenylethyl)magnesium **733**. At room

temperature, these species were present in a ratio of 1:1.5, corresponding to an equilibrium constant (K_{eq}) of 0.44 for the Schlenk equilibrium (Scheme 4.19). Characterisation of each organomagnesium species was aided by perturbation of the Schlenk equilibrium to favour either organomagnesium species (Fig. 4.3). Addition of 1,4-dioxane resulted in the precipitation of $MgBr_2$·dioxane to give a majority of the

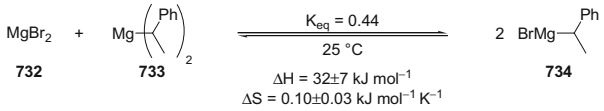

732 733 734

Scheme 4.19 Schlenk equilibrium between dibenzylmagnesium species **733** and magnesium bromide **732**, and benzylic Grignard reagent **734**

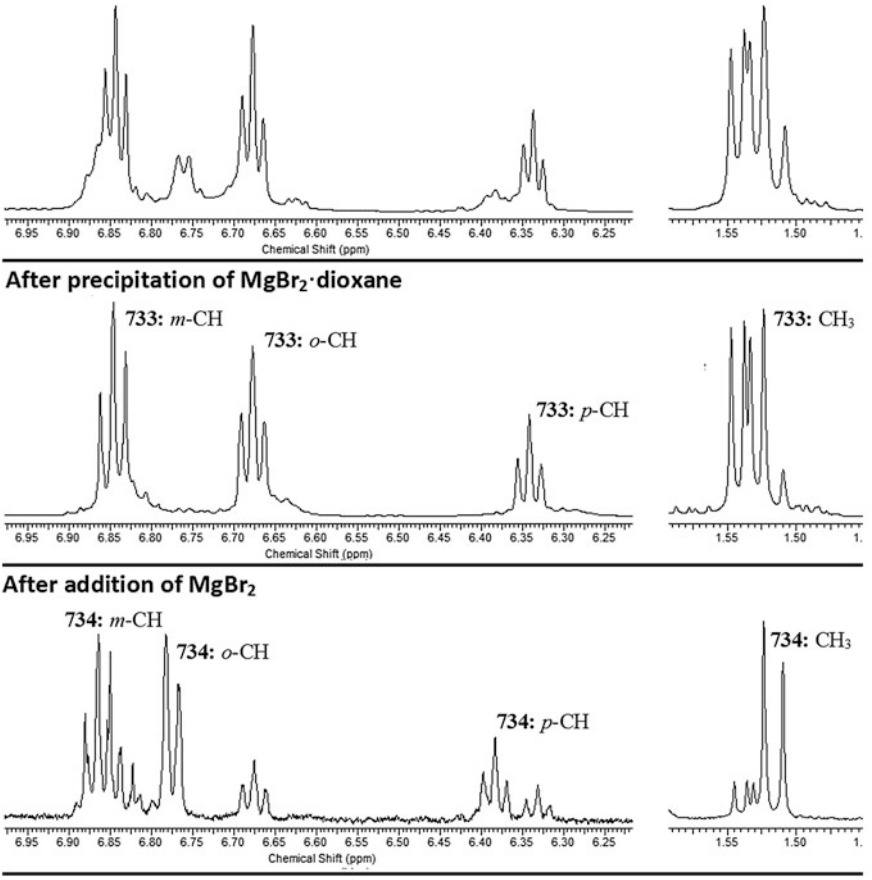

Fig. 4.3 ^{1}H NMR spectra of benzylic Grignard regent **734** and dibenzylmagnesium **733** at room temperature

dibenzylmagnesium species **733** [44], whilst addition of $MgBr_2$ led to an increase in the concentration of the Grignard reagent **734** (Fig. 4.3). The dibenzylmagnesium species **733** was observed as a 1:1 mixture of diastereoisomers.

As a quantifiable mixture of the benzylic Grignard reagent **734** and dibenzylmagnesium species **733** was observed at room temperature, we were presented with an opportunity to determine the thermodynamic parameters of alkyl exchange between these species. This would provide data on the entropy and enthalpy of formation of the Grignard reagent **734** from $MgBr_2$ **732** and the dibenzylmagnesium species **733**. These parameters would reflect the fundamental properties of the organomagnesium species in solution, but not provide information about the iron-catalysed hydromagnesiation reaction.

Alkyl exchange between the benzylic Grignard reagent **734** and dibenzylmagnesium species **733** was sufficiently slow that equilibrium constants could be measured using variable temperature NMR spectroscopy (5–55 °C). ^{13}C NMR Spectroscopy was used to determine the equilibrium constant at each temperature by integration of equivalent carbons of the Grignard reagent **734** and the dibenzylmagnesium species **733** over 5 resonances. Upon increasing the temperature, a decrease in the concentration of the dibenzylmagnesium species **733** was accompanied by an increase in the concentration of the Grignard reagent **734** (Fig. 4.4).

Using the calculated equilibrium constants, a van't Hoff plot was constructed (Fig. 4.5, where gradient = $-\Delta H/R$, and intercept = $\Delta S/R$). From this analysis the enthalpy and entropy of formation of the Grignard reagent **734** from $MgBr_2$ **732** and the dibenzylmagnesium species **733** were calculated as 32 ± 7 kJ mol^{-1} and 0.10 ± 0.03 kJ mol^{-1} K^{-1}, respectively (Fig. 4.5 and Scheme 4.19). A positive value for the enthalpy of formation (ΔH) in tetrahydrofuran is common, and has been proposed to reflect the increased solvation of $MgBr_2$ **732** compared to the organomagnesium species [42]. These data show that the benzylic organomagnesium species formed in this reaction exhibits a particularly large preference to exist as the dibenzylmagnesium species **733** in tetrahydrofuran. The values calculated for

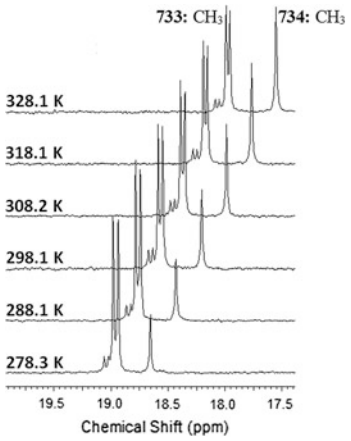

Fig. 4.4 Variable temperature ^{13}C NMR spectra of methyl carbons of benzylic Grignard reagent **734** and dibenzylmagnesium **733**

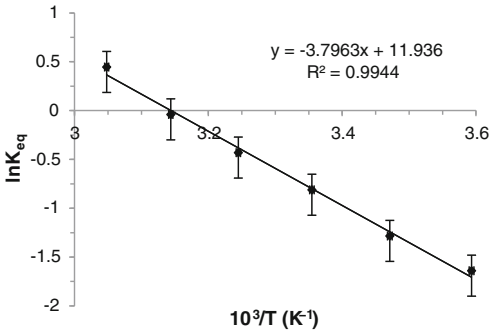

Fig. 4.5 van't Hoff plot of $\ln K_{eq}$ versus $10^3/T$ for the reaction $MgBr_2$ **732** + R_2Mg **733** ⇌ 2 × RMgBr **734** (R = $CH(CH_3)Ph$)

the enthalpy and entropy of formation were comparable to those reported for the formation of *tert*-butylmagnesium chloride from *tert*-Bu_2Mg and $MgCl_2$ in tetrahydrofuran [43]. The benzylic organomagnesium species was found to be relatively stable, with 95 % of the active species remaining two weeks after synthesis.

Research within our group has since shown that the intermediate organomagnesium reagent can be reacted with a variety of electrophiles to give a range of hydrofunctionalised products in good to excellent yield (Scheme 4.20) [45]. The methodology has also been used by Yang for the formal hydroamination of styrene derivatives using *O*-benzoyl-*N*,*N*-dialkylhydroxylamines as the electrophilic nitrogen source [46].

Having confirmed that the developed methodology proceeded by iron-catalysed hydromagnesiation, the mechanism was investigated. Mechanistic studies have been reported for titanium- and nickel-catalysed hydromagnesiation, however no detailed studies had been undertaken using iron. Mechanistic investigations of

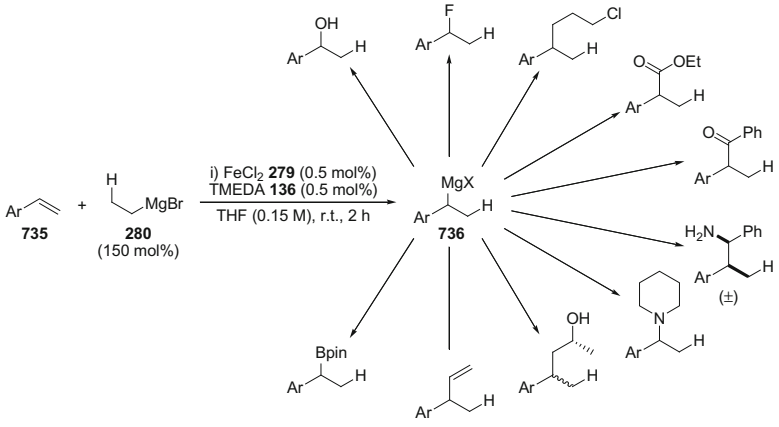

Scheme 4.20 Iron-catalysed formal hydrofunctionalisation of styrene derivatives using a variety of electrophiles to give a range of functionalised products

iron-catalysed processes involving Grignard reagents have been, in general, focussed on cross-coupling reactions [21c, 47]. Based upon this literature, and the mechanisms proposed for titanium- and nickel-catalysed hydromagnesiation [13, 20], a reasonable mechanism for iron-catalysed hydromagnesiation can be proposed (Scheme 4.21). Alkylation and reduction of the iron(II) pre-catalyst by ethylmagnesium bromide **280** would give a low oxidation-state alkyliron species **737**. Coordination of the styrene derivative **735**, before, after or during reduction of the pre-catalyst would give an alkyliron-olefin complex **738**. Formal β-hydride exchange between the two ligands can then take place to give the benzyliron species **740**. This hydride transfer has previously been suggested to proceed by a β-hydride elimination/hydrometallation pathway going through an iron-hydride intermediate **739**. The intermediacy of an iron-hydride has been proposed based upon the isomerisation of 3-coordinate iron(II)-alkyl complexes [24c, d], and the fact that iron catalyses the isomerisation of alkyl Grignard reagents in the absence of an added alkene [23]. Alternatively β-hydride transfer may take place by a direct β-hydride transfer mechanism, similar to the mechanism proposed for nickel-catalysed hydromagnesiation [20]. Following formation of the benzyliron species **740**, transmetallation with another equivalent of ethylmagnesium bromide **280** would release the benzylic Grignard reagent product **736** and reform the original alkyliron species **737**.

There were a number of questions about the proposed mechanism (Scheme 4.21) which we wished to address with this mechanistic work:

(i) What is the mechanism of hydride transfer (Scheme 4.21, β-hydride elimination/hydrometallation on **A** or direct β-hydride transfer **B**)?
(ii) What factors dictate which styrene derivatives are suitable substrates?
(iii) What is the rate equation of the reaction?
(iv) What is the nature of the iron catalyst—role of the ligand, homo/heterogeneity and oxidation-state?

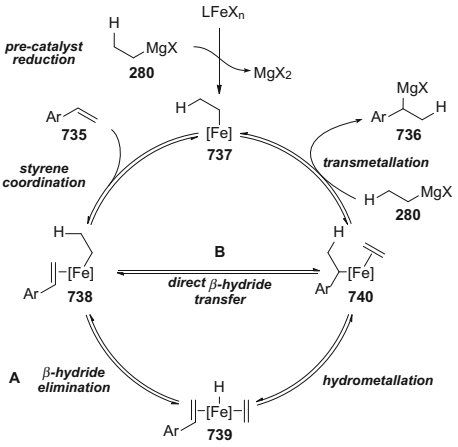

Scheme 4.21 Proposed mechanism of iron-catalysed hydromagnesiation

4.2.4.1 Mechanism of Hydride Transfer

A range of Grignard reagents have been used for the optimisation of iron-catalysed hydromagnesiation methodologies [3], however this has always been approached with the objective of obtaining the highest yield of product with the best control of regio- and/or stereochemistry. Significantly, the Grignard reagents which have shown the best activity for hydromagnesiation are those which generate an alkene by-product which cannot undergo hydromagnesiation (an internal alkene or a gas). We were interested in quantifying the differences in the efficiency and regioselectivity of hydromagnesiation using different alkyl Grignard reagents. This was done by following the kinetic profiles of these reactions. Using this approach, any change in the rate or regioselectivity of hydromagnesiation over the course of the reaction could be quantified.

Ethylmagnesium bromide **280** proved to be the most efficient Grignard reagent tested for the hydromagnesiation of 2-methoxystyrene **675**, giving the highest overall yield, initial rate of reaction and α:β regioselectivity (Table 4.6, entry 1).

Table 4.6 Hydromagnesiation of 2-methoxystyrene using different Grignard reagents

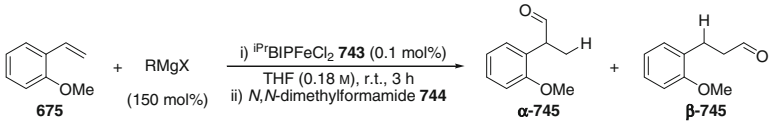

Entry	RMgX	Initial rate of reaction (%/min)	% yield (α + β)-**745** after 3 h	α:β ratio[a]	
				Start	End
1	 **280**	40	99[b]	80:1	100:1
2	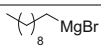 **741**	7	78	35:1	60:1
3	 **630**	0.5[d]	23	15:1	21:1
4	 **655**	5	85	10:1	16:1
5	 **610**	1	62	11:1	22:1
6	 **742**	0.1[d]	4	N/D[e]	
7	MgH_2 **595**	0	0 (8)[f]	N/A[g]	
8	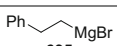 **635**	15	82	4:1	10:1

[a]α:β Ratio at start of reaction, and after 3 h; [b]% Yield obtained within 1 h; [c]1 mol% Pre-catalyst **743**; [d]Initial rate using 1 mol% catalyst; [e]Not determined; [f]10 mol% EtMgBr **280** added, maximum yield of 8 % obtained within first 5 min; [g]Not applicable

Over the course of the reaction the α:β regioselectivity improved moderately from 80:1 at the outset, to 100:1 at completion. Using *n*-decylmagnesium bromide **741** the initial rate of reaction was around 5–6 times slower than that observed using ethylmagnesium bromide **280**. The α:β regioselectivity was also lower, with an initial regioselectivity of 35:1 rising to 60:1 over the course of the reaction (Table 4.6, entry 2). iso-Butylmagnesium bromide **630** was much less reactive. The pre-catalyst loading had to be increased 10-fold in order to obtain reasonable reactivity (Table 4.6, entry 3). The α:β regioselectivity using iso-butylmagnesium bromide **630** was also lower (α:β, 15:1 → 21:1). This reactivity trend was in stark contrast to the titanium-catalysed hydromagnesiation of 1-octene, where iso-butylmagnesium bromide **630** proved to be the best choice of Grignard reagent for hydromagnesiation [14].

The rate of hydromagnesiation using secondary Grignard reagents, cyclopentylmagnesium bromide **655** and iso-propylmagnesium bromide **610**, was also slower than that when using ethyl- or *n*-decylmagnesium bromide (Tables 4.6, entries 4 and 5). The regioselectivity of hydromagnesiation was also much lower in these cases, with α:β regioselectivities rising from about 10:1 to 20:1 during the course of the reaction. It should be noted that cyclopentylmagnesium bromide **655** gave a higher overall yield after 3 h than was obtained using *n*-decylmagnesium bromide **741**. This may be explained by considering the ability of the respective alkene by-products to undergo competitive hydromagnesiation. Whilst it would be expected that 1-decene could undergo competitive hydromagnesiation (and isomerisation), cyclopentene would not, and would therefore be effectively removed from the catalytic cycle. *tert*-Butylmagnesium chloride **742** was the least effective Grignard reagent tested, with only 4 % yield of the hydromagnesiation products obtained after 3 h using 1 mol% pre-catalyst (Table 4.6, entry 6). Magnesium hydride **595** was not a suitable hydride source for iron-catalysed hydromagnesiation, either in isolation, or in combination with a sub-stoichiometric quantity of ethylmagnesium bromide **280** (10 mol%), added to facilitate reduction of the iron (II) pre-catalyst **743** (Table 4.6, entry 7).

For all alkyl Grignard reagents tested, the α:β ratio of hydromagnesiation products increased over the course of the reaction. The α-aryl Grignard reagent would be expected to be the thermodynamically-favoured product based on anion stability. The increase in the α:β ratio during the reaction could therefore be explained if the β-aryl Grignard reagent, formed as a minor product, was isomerised to the thermodynamically-favoured α-aryl Grignard reagent during the reaction. When a representative β-aryl Grignard reagent **635** was used in the reaction, an efficient rate of hydromagnesiation of 2-methoxystyrene **675** was observed, albeit with low regioselectivity (Table 4.6, entry 8). The increase in α:β regioselectivity observed over time using all Grignard reagents can therefore be explained by the competitive rate of hydromagnesiation by the in situ generated β-aryl Grignard reagent. In all cases however, an initial preference for the α-aryl Grignard reagent was also observed, suggesting that the α-aryl Grignard reagent is both the thermodynamically- and kinetically-favoured product.

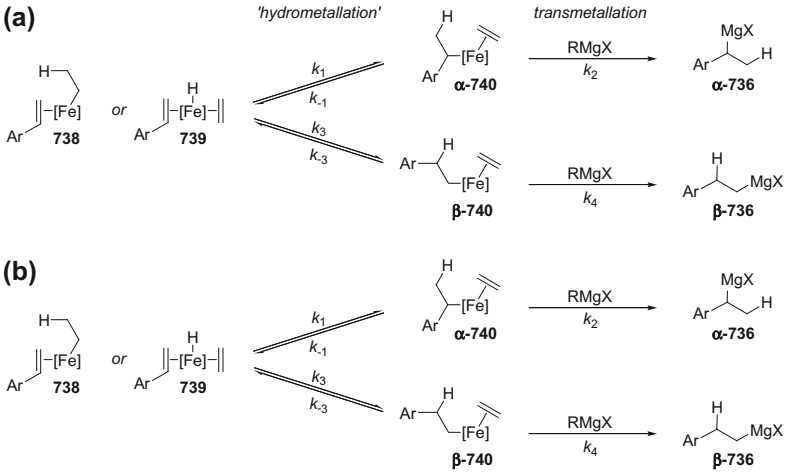

Scheme 4.22 Proposals to explain the kinetic preference for the formation the α-aryl Grignard reagent **α-736**

The kinetic preference for the formation of the α-aryl Grignard reagent could be potentially explained in two ways (Scheme 4.22). The simplest explanation would be that the 'hydrometallation' of the styrene derivative (by either a β-hydride elimination/hydrometallation or direct β-hydride transfer mechanism) is regioselective to give an α-aryl iron species **α-740** ($k_1 > k_3$). Transmetallation would then give the α-aryl Grignard reagent **α-736** (Scheme 4.22a). Alternatively, the 'hydrometallation' process could be reversible but not regioselective ($k_1 \approx k_3$), with the kinetic preference for the α-aryl Grignard reagent **α-736** arising due to a faster rate of transmetallation from the α-aryl iron species **α-740**, in comparison to the rate of transmetallation from the β-aryl iron species **β-740** ($k_2 > k_4$) (Scheme 4.22b). The use of a deuterium-labelled Grignard reagent would distinguish between these pathways. If the 'hydrometallation' of styrene was regioselective for the formation of the α-aryl iron species **α-736** ($k_1 > k_3$), then deuterium incorporation would only be expected in the β-position of the α-aryl Grignard reagent **α-736**. If the 'hydrometallation' of styrene was highly reversible but not regioselective ($k_1 \approx k_3$) then deuterium incorporation would be expected in both positions of the α-aryl Grignard reagent **α-736**.

The hydromagnesiation of 2-methoxystyrene **675** using d_5-ethylmagesium bromide ***d*$_5$−280** gave a mixture of deuterated products (Fig. 4.6). Aliquots were removed from the reaction periodically and reacted with *N*,*N*-dimethylformamide **744** (DMF) to give a mixture of aldehyde products. These products were analysed by ^{1}H, ^{2}H and ^{13}C NMR spectroscopy. The α-aryl aldehyde products with 0 or 1 deuterium in the β-position were observed from the outset of the reaction, whilst those with 2 or 3 deuterium in the β-position were observed only as the reaction progressed. The yield of each α-aryl aldehyde product increased throughout the reaction before reaching a plateau, suggesting that once formed, the α-aryl Grignard

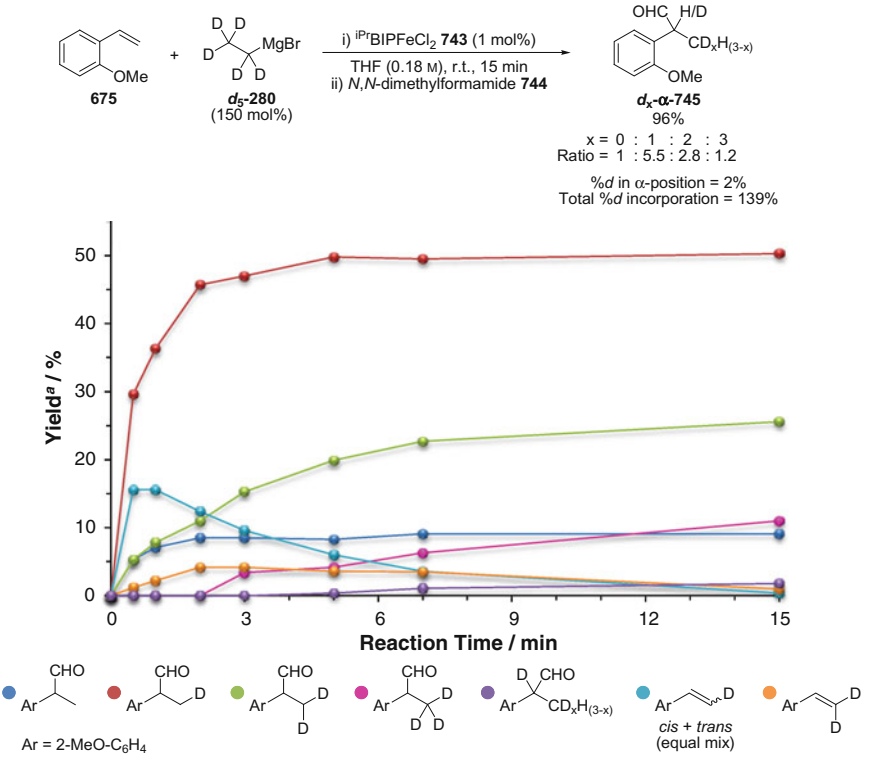

Fig. 4.6 Hydromagnesiation of 2-methoxystyrene **675** using d_5-ethylmagnesium bromide ***d*$_5$-280**. [a]Yield determined by ^{1}H NMR spectroscopy using 1,3,5-trimethoxybenzene as an internal standard

reagent did not re-enter the catalytic cycle. Styrene derivatives with either 1 or 2 deuterium in the β-position were also observed during the reaction, but were consumed as the reaction progressed. This suggests that the multiply-deuterated products arise from a step-wise mechanism involving reversible deuteride and hydride transfers between alkyl and alkene ligands on iron, along with reversible alkene association and dissociation.

α-Aryl aldehyde products with deuterium incorporation at the α-position were only observed towards the end of the reaction (>80 % conversion). The hydromagnesiation of styrene using d_5-ethylmagesium bromide ***d*$_5$-280** would also result in the formation of low quantities of the α-deuterated β-aryl Grignard reagent **α-*d*$_1$-746**. Towards the end of the reaction the concentration of d_5-EtMgBr would be low, and therefore the rate of hydromagnesiation using the in situ generated α-deuterated β-aryl Grignard reagent **α-*d*$_1$-746** would become competitive (Scheme 4.23a). This reaction could result in the formation of the α-deuteriostyrene derivative **α-*d*$_1$-675**. Hydromagnesiation of the α-deuteriostyrene derivative **α-*d*$_1$-675** would then

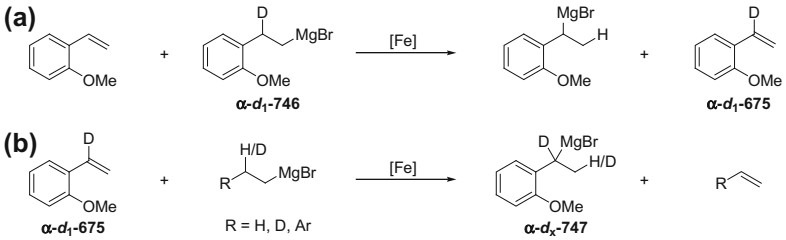

Scheme 4.23 Proposed pathway to explain the formation of an α-aryl Grignard reagent **α-d_x-747** with deuterium incorporation in the α-aryl position

produce an α-aryl Grignard reagent **α-d_x-747** with deuterium incorporation at the α-position (Scheme 4.23b).

The low quantity of deuterium incorporation in the α-position therefore indicates that the α-aryl Grignard reagent is the kinetic product due to regioselective 'hydrometallation' of the styrene substrate (Scheme 4.22a). In total, more than 100 % deuterium incorporation was observed in the reaction products, which indicates that hydride transfer from benzyl to ethylene ligands on iron takes place ('hydrometallation' is reversible). The formal loss of protons/protides from the reaction can be accounted for by the formation, and loss from solution, of d_x-ethylene (where $x < 4$).

The same analysis was then applied to the hydromagnesiation of 2-methoxystyrene **675** using d_7-iso-propylmagnesium bromide ***d_7*-610** (Fig. 4.7). Once again it appeared that the α-aryl Grignard reagents formed in the reaction were not consumed, and those with 0 or 1 deuterium in the β-position were formed initially, whilst those with 2 or 3 deuterium were formed slowly throughout the reaction. The distribution of deuterated products was significantly different to that when d_5-EtMgBr ***d_5*-280** was used however, with the major products being those with 0 or 1 deuterium in the β-position. α-Aryl Grignard reagents with deuterium incorporation at the α-position were formed early in the reaction (<30 % conversion), and continued to increase in concentration throughout the reaction. The probable intermediate leading to this product, the α-deuteriostyrene derivative **α-d_1-675**, was also observed.

The higher quantities of α-deuterated products formed using d_7-iso-propylmagnesium bromide ***d_7*-610** can be explained if the rate of hydromagnesiation using the in situ generated α-deuterated β-aryl Grignard reagent **α-d_1-746** was competitive much earlier in the reaction with the rate of hydromagnesiation using d_7-iso-propylmagnesium bromide ***d_7*-610**, thus leading to a higher concentration of the α-deuteriostyrene derivative **α-d_1-675**. Two factors may contribute to this effect. The lower regioselectivity of hydromagnesiation using iso-propylmagnesium bromide would lead to a higher concentration of the α-deuterated β-aryl Grignard reagent in the reaction (Table 4.6, entry 5), and the rate constant for hydromagnesiation using the α-deuterated β-aryl Grignard reagent **α-d_1-746** would be expected to be larger than the rate constant for hydromagnesiation using d_7-iso-propylmagnesium bromide ***d_7*-610** (Table 4.6, entries 5 and 8).

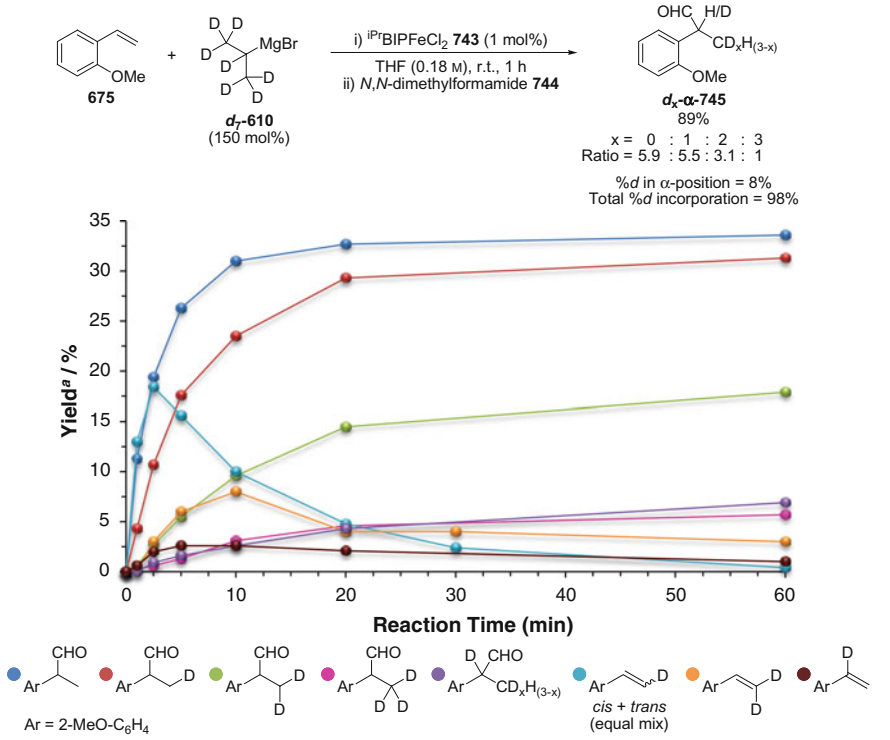

Fig. 4.7 Hydromagnesiation of 2-methoxystyrene **675** using d_7-iso-propylmagnesium bromide ***d*$_7$-610**. [a]Yield determined by ^{1}H NMR spectroscopy using 1,3,5-trimethoxybenzene as an internal standard

Using d_7-iso-propylmagnesium bromide ***d*$_7$-610**, a near stoichiometric quantity of deuterium was incorporated into the reaction products. This suggests that the mixture of deuterated products arise mostly from hydride (protide) or deuteride transfer between (homo)benzyl and styrene ligands on iron. Hydride transfer to the in situ generated d_6-propene was comparatively insignificant. This could be explained if the rate of d_6-propene/styrene exchange was significantly faster than the rate of hydride transfer to d_6-propene.

Based upon the studies using deuterium-labelled Grignard reagents it was confirmed that the regioselectivity for the formation of the α-aryl Grignard reagent arises from the regioselective 'hydrometallation' of the styrene derivative (Scheme 4.22a). In addition it was shown that when ethylmagnesium bromide **280** was used, this 'hydrometallation' process was reversible.

Two mechanisms for hydride transfer had been proposed (Scheme 4.21). The regioselectivity of the process has been shown to depend on the structure of the

Grignard reagent (Table 4.6), and the process was found to be reversible when using ethylmagnesium bromide **280** (Fig. 4.6). A β-hydride elimination-hydrometallation pathway could only account for these observations if hydride transfer involved the formation of a 6-coordinate iron-hydride intermediate such as species **739** (Scheme 4.21). If dissociation of the alkene by-product (following β-hydride elimination) took place *prior* to hydrometallation, then a common iron-hydride intermediate would be formed regardless of the alkyl Grignard reagent used. In this scenario, the differences in regioselectivity using different Grignard reagents would be difficult to justify. Considering the alternative direct β-hydride transfer mechanism (Scheme 4.21, **738** → **740**), both an alkyl and alkene ligand on iron would be required, therefore the regioselectivity of the process would be expected to be much more dependent upon the steric bulk of the Grignard reagent used. It would also be expected that a direct β-hydride transfer mechanism could be reversible.

In order to distinguish between these reaction pathways the isomerisation of the β-aryl Grignard reagent, (2-phenylethyl)magnesium bromide **635**, was investigated. If an iron-hydride was the active species for hydromagnesiation, it would be expected that (2-phenylethyl)magnesium bromide **635** could isomerise to the corresponding α-aryl Grignard reagent **734** in the presence of the iron catalyst (Scheme 4.24a). If hydromagnesiation proceeded by a direct β-hydride transfer mechanism, then isomerisation would only be expected in the presence of a styrene (or alkene) derivative capable of undergoing hydromagnesiation (Scheme 4.24b).

The isomerisation of (2-phenylethyl)magnesium bromide **635** in the presence of iron(II) chloride (0.1 mol%) and bis(imino)pyridine **273a** (0.1 mol%) was followed over the course of 5 h (Fig. 4.8). Aliquots were taken from the reaction periodically and reacted with *N*,*N*-dimethylformamide **744** (DMF) to give a mixture of the α- and β-aryl aldehyde products **α-748** and **β-748**. In the absence of an added alkene, just 1 % isomerisation to give the α-aryl aldehyde product **α-748** was observed over 5 h (Fig. 4.8 ●). The addition of styrene (10 mol%) resulted in isomerisation to give α-aryl aldehyde **α-748** in a 23 % yield in the same time period (Fig. 4.8 ●). The addition of 1-octene **99** (100 mol%) also catalysed the isomerisation of (2-phenylethyl)magnesium bromide **635** to give the α-aryl aldehyde **α-748**

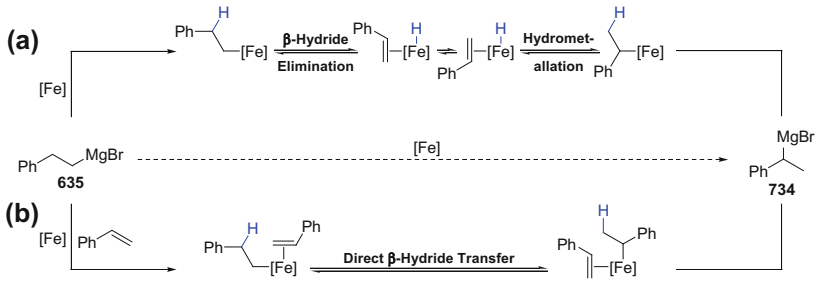

Scheme 4.24 Possible mechanisms for the iron-catalysed isomerisation of (2-phenylethyl)-magnesium bromide **635**

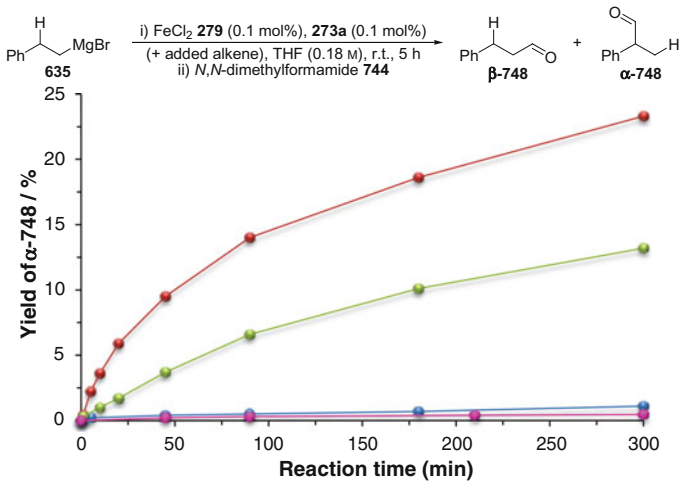

Fig. 4.8 Isomerisation of β-aryl Grignard reagent **635** in the absence and presence of alkenes. ● = no alkene added (0.5 mol% styrene **53** present in Grignard reagent solution); ● = styrene **53** (10 mol%) added; ● = 1-octene **99** (100 mol%) added. ● = cyclopentene **559** (10 mol%), indene **560** (10 mol%), α-methylstyrene **382** (10 mol%) or β-methylstyrene **10** (10 mol%) added [48]

(Fig. 4.8 ●). To ascertain if an alkene was simply required for catalyst stabilisation, alkenes (including styrene derivatives) unable to undergo hydromagnesiation were added to the reaction. The addition of cyclopentene **559**, indene **560**, α-methylstyrene **382** or β-methylstyrene **10** (all 10 mol%) did not facilitate isomerisation, with <1 % α-aryl aldehyde **α-748** obtained after 5 h in each case (Fig. 4.8 ●). 2-Methoxystyrene **675** underwent hydromagnesiation using ethylmagnesium bromide **280** in the presence of these alkenes (all 10 mol%) indicating that these alkenes do not inhibit the hydromagnesiation reaction.

Based upon these experiments it is most likely that iron-catalysed hydromagnesiation follows a direct β-hydride transfer mechanism, without the formation of a discrete iron-hydride intermediate. The formation of an off-cycle iron-hydride cannot be ruled out. A similar mechanism has been suggested, based upon computational modelling, as the main chain transfer mechanism in bis(imino)pyridine iron complex-catalysed alkene polymerisation [49]. In this case an agostic bonding interaction between iron and the 'hydride' was identified, whilst the formation of a discrete iron-hydride was found to be unfavourable. In these calculations an iron(II) species was used and therefore may not be transposable to our system, however a similar computational modelling approach might be used to provide support for, or against, the proposed mechanism.

Hayashi and Shirakawa previously reported the isomerisation of 2-alkyl and homobenzylic Grignard reagents to give the thermodynamically-favoured 1-alkyl and benzylic Grignard reagents in the absence of an added alkene (Scheme 4.11b) [23].

Significantly, 2.5–5 mol% of an iron(III) pre-catalyst was used in these experiments. The reaction of iron salts with alkyl Grignard reagents bearing β-hydrogen atoms results in the reduction of the iron salt and the formation of alkene and alkane by-products [22, 50]. It is therefore possible that it is the in situ formation of these alkene by-products, which allow the isomerisation of the alkyl Grignard reagent. In order to confirm this proposal, mechanistic work using Hayashi and Shirakawa's system would have to be undertaken.

The possibility that the reaction proceeded by a radical mechanism was also considered. The most common approach to identify the intermediacy of an alkyl radical involves the addition of a radical trap or radical inhibitor to the standard reaction conditions. Alkyl radicals readily add to styrene [51], and therefore the formation of polymeric products may indicate the formation of a benzyl radical in the reaction. Polymeric material was obtained, but only in reactions using styrene derivatives bearing electron-withdrawing groups (Table 4.5). Using these substrates, no hydromagnesiation products were obtained however and therefore it cannot be concluded whether the two products are formed via a common intermediate. In addition, the polymeric material obtained could also form through an anionic polymerisation mechanism. Ideally a radical trap could be added to a (usually) successful hydromagnesiation reaction. Common radical traps such as (2,2,6,6-tetramethyl-piperidin-1-yl)oxyl (TEMPO), 2,2-diphenyl-1-picrylhydrazyl (DPPH) and galvinoxyl, would be expected to react directly with the Grignard reagent [40, 52] or iron (pre-)catalyst [53], and therefore were not thought appropriate for use in this case. It was considered that γ-terpinene **749**, which reacts with radical species through hydrogen abstraction to give *para*-cymene **751** [54], might be compatible with the reaction conditions. The hydromagnesiation of 2-methoxystyrene **675** in the presence of γ-terpinene **749** (50 mol%) gave the benzylic Grignard reagent in quantitative yield, as determined following reaction with *N*,*N*-dimethylformamide **744** (DMF) (Scheme 4.25a). γ-Terpinene **749** was recovered quantitatively, indicating that no hydrogen abstraction reaction had taken place. Based upon these observations it would appear that a benzyl radical intermediate is not involved, or is not sufficiently long-lived to undergo an intermolecular addition or abstraction reaction. A substrate which could undergo an intramolecular radical reaction was therefore targeted [55]. Due to the necessity of using a terminal styrene derivative the choice of possible substrates was limited. The hydromagnesiation of 2-allylstyrene **323** was investigated, as it was expected that a benzyl radical intermediate may undergo 5-*exo*-*trig* cyclisation onto the pendant alkene. Interestingly, no hydromagnesiation reaction occurred, with only small quantities of the internal alkene products **(*E*)-** and **(*Z*)-752** formed from the isomerisation of the allyl group (Scheme 4.25b). The lack of hydromagnesiation activity may be attributed to increased steric hindrance disfavouring coordination of iron to the vinyl group. Unfortunately this experiment does not provide any support for, or against, a radical intermediate in this reaction.

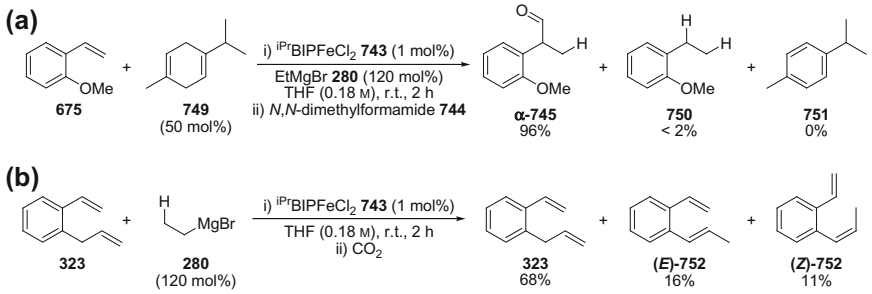

Scheme 4.25 Investigations into the possibility of a benzyl radical intermediate in the hydromagnesiation of styrene derivatives

4.2.4.2 Kinetic Analysis

The developed methodology was most efficient for the hydromagnesiation of styrene derivatives bearing electron-donating (Me, OMe), electron-neutral (H, Ph) or slightly electron-withdrawing (F) groups (Table 4.4). In contrast, styrene derivatives bearing more strongly electron-withdrawing groups (CF_3, CO_2Me, NO_2, CN) were not tolerated (Table 4.5). Although substrates bearing electron-donating groups generally gave the best yields of hydromagnesiation products, this reactivity could not be correlated to the Hammett sigma constants for each substrate [56]. In the formal hydrocarboxylation of styrene derivatives, the substrate bearing the most electron-donating group, 4-methoxystyrene ($\sigma = -0.27$, $\sigma^{\cdot} = 0.018$), underwent hydromagnesiation to give the α-aryl carboxylic acid **α-692** in only a moderate yield of 55 %. In contrast, 3-methoxystyrene ($\sigma = 0.12$, $\sigma^{\cdot} = -0.001$), in which the *meta*-methoxy group is slightly electron-withdrawing relative to the vinyl group, gave the corresponding α-aryl carboxylic acid **α-691** in 91 % yield. 4-Fluorostyrene ($\sigma = 0.06$, $\sigma^{\cdot} = -0.011$) which should have a similar electronic effect to 3-methoxystyrene, gave the α-aryl carboxylic acid **α-699** in a yield of just 36 %.

In order to assess the electronic influence of different substituents on the hydromagnesiation of styrene derivatives in more detail, the kinetic profiles for the hydromagnesiation of a series of *para*- and *meta*-substituted styrene derivatives were obtained (Fig. 4.9).

The hydromagnesiation of 4-methoxystyrene occurred at a high initial rate of reaction, which rapidly decreased as the reaction progressed (Fig. 4.9 ●). A similar, but less pronounced effect was observed for 4-*tert*-butylstyrene and 4-methylstyrene (Fig. 4.9 ● and ●). The initial rates of hydromagnesiation using styrene or 3-methoxystyrene were much slower, however with these substrates the rate of reaction remained relatively constant for the majority of the reaction (until ~70–80 % yield) (Fig. 4.9 ● and ●). The initial rate of hydromagnesiation of 4-fluorostyrene was similar to that of 3-methoxystyrene, however the rate of reaction quickly decreased, with a complete loss in catalytic activity within 30 min

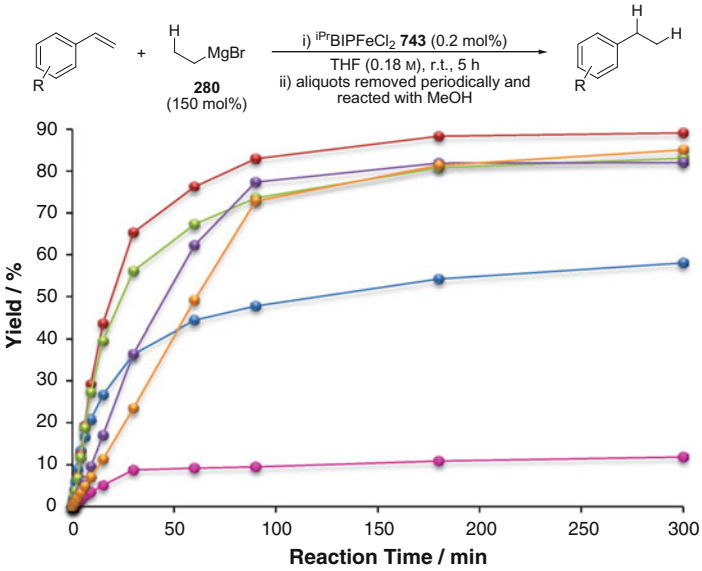

Fig. 4.9 Kinetic profiles for the hydromagnesiation of a selection of electronically-differentiated styrene derivatives. ● = 4-Methoxystyrene; ● = 4-*tert*-butylstyrene; ● = 4-methylstyrene; ● = styrene; ● = 4-fluorostyrene; ● = 3-methoxystyrene

(Fig. 4.9 ●). The loss in catalytic activity was accompanied by the formation of styrene, indicating cleavage of the carbon–fluorine bond of 4-fluorostyrene. This could result in the formation of a catalytically-inactive iron complex with a kinetically inert iron–fluoride bond [38].

This data shows that styrene derivatives bearing electron-donating groups undergo hydromagnesiation at a fast initial rate, which rapidly decreases as the reaction progresses. This could be attributed to catalyst decomposition or reaction inhibition. Styrene derivatives bearing electron-donating groups would be expected to bind less strongly to a low oxidation-state iron catalyst [29b, d], which could lead to a faster rate of catalyst decomposition. Alternatively, inhibition of the reaction could occur following the formation of a product. For the hydromagnesiation of styrene derivatives bearing electron-donating groups no side-products were observed in the reaction, therefore this inhibition might be attributed to the formation of the benzylic Grignard reagent. The presence of an electron-donating group on a benzylic Grignard reagent would be expected to increase the nucleophilicity of the Grignard reagent [57], and therefore could lead to reaction inhibition through over-alkylation of iron. For a productive hydromagnesiation reaction, the iron catalyst must be alkylated by the 'sacrificial' alkyl Grignard reagent (e.g. ethylmagnesium bromide), therefore competitive alkylation by the benzylic Grignard reagent would inhibit this productive cycle. Alkylation by the benzylic Grignard reagent may lead to a catalytically-inactive iron species, or one which only catalyses a 'non-productive' hydromagnesiation reaction. This latter

situation would be one in which hydride transfer takes place between a benzyl and styrene ligand, to give the same products and result in no overall change.

The effect of reaction inhibition by product formation could be investigated by the addition of an independently-synthesised benzylic Grignard reagent to a standard hydromagnesiation reaction. A benzylic Grignard reagent was synthesised by the slow addition of (1-bromoethyl)benzene to highly-dispersed magnesium at low temperature and high dilution [5]. Addition of this Grignard reagent to the hydromagnesiation reaction resulted in complete inhibition of the reaction, even in the presence of excess ethylmagnesium bromide. This inhibition could therefore not be attributed to the Grignard reagent itself, and was most likely due to an impurity in the Grignard reagent produced as a side-product during Grignard reagent formation.

By measuring the maximum initial rate of reaction using each styrene derivative, a Hammett plot was constructed (Fig. 4.10). The best correlation was obtained using standard Hammett sigma constants [56a]. A negative ρ value ($\rho = -2.2$) was obtained, signifying that styrene derivatives bearing electron-donating groups underwent hydromagnesiation most rapidly (Fig. 4.10).

Explaining this ρ value is difficult without knowing the turnover-limiting step of the reaction. A large negative ρ value would generally indicate the stabilisation of a developing positive charge at the benzylic position of the styrene derivative in the transition-state structure of the turnover-limiting step. This analysis may not correlate to the hydride transfer step as an increase in negative charge at the benzylic position would be expected.

Styrene derivatives bearing electron-withdrawing groups would be expected to bind more strongly to a low oxidation-state iron complex through an increased contribution from back-bonding [29b, d]. It is therefore possible that styrene derivatives bearing electron-donating groups may react more quickly because styrene dissociation is required to produce an active catalyst (Scheme 4.26a). The increased back-bonding between styrene derivatives bearing electron-withdrawing groups and iron would also result in increased pyramidalisation of the vinylic carbons. This may disfavour a direct β-hydride transfer process by increased steric

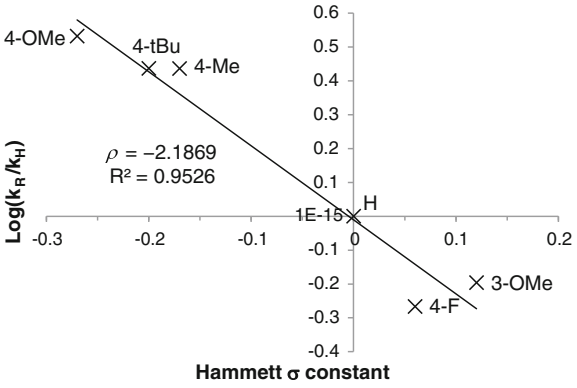

Fig. 4.10 Hammett plot using electronically-differentiated 4- and 3-substituted styrene derivatives

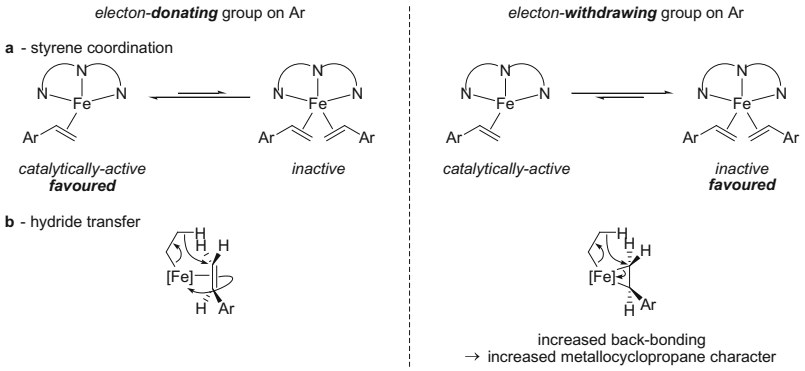

Scheme 4.26 Two possible explanations for the negative ρ value calculated for the hydromagnesiation of electronically-differentiated styrene derivatives

hindrance imposed by a reduced metal-alkene distance and a lower availability of the necessary non-bonding orbitals needed for hydride transfer to take place (Scheme 4.26b). Finally, it may be possible that an electron-donating group could destabilise the iron-benzyl intermediate and increase the rate of transmetallation to give the α-aryl Grignard reagent.

Styrene derivatives with α- or β-substitution were unreactive under the developed hydromagnesiation conditions. This lack of reactivity could be explained if either substrate binding; β-hydride transfer; or transmetallation were unfavourable. The addition of α- or β-methylstyrene to the hydromagnesiation of 2-methoxystyrene **675** was found to slightly reduce the rate of reaction. This suggests that α- and β-methylstyrene bind to iron competitively with 2-methoxystyrene. When d_5-ethylmagnesium bromide ***d*$_5$-280** was used for the attempted hydromagnesiation of α- and β-substituted styrene derivatives, all substrates were recovered with no deuterium incorporation (Scheme 4.27). These experiments indicate that α- and β-substituted styrene derivatives bind to the active iron catalyst, but do not undergo hydrometallation. These substrates have been successfully applied in iron-catalysed hydrogenation reactions, which may provide further support for a mechanism for hydromagnesiation which does not involve an iron-hydride intermediate.

In order to obtain further information about the turnover-limiting step, the reaction order with respect to each reagent was obtained by using different initial

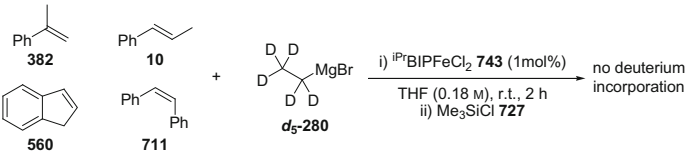

Scheme 4.27 Attempted hydromagnesiation of disubstituted styrene derivatives using deuterated ethylmagnesium bromide ***d*$_5$-280**

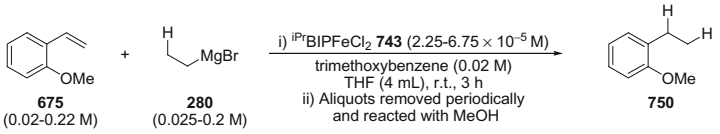

Scheme 4.28 Conditions used for initial rates approach for the hydromagnesiation of 2-methoxystyrene **675** using ethylmagnesium bromide **280** at different initial concentrations of each reagent

concentrations of iron pre-catalyst, styrene derivative and Grignard reagent. For the hydromagnesiation of 2-methoxystyrene using ethylmagnesium bromide, overall reaction orders were difficult to obtain due to the presence of an induction period and the possibility of reaction inhibition following product formation. An initial rates approach was therefore adopted, where the initial maximum rate (following the induction period) was measured at different initial concentrations of each reactant (Scheme 4.28).

The reaction was found to be first order with respect to iron pre-catalyst (Fig. 4.11). The reaction order with respect to 2-methoxystyrene **675** and ethylmagnesium bromide **280** was more complex (Figs. 4.12 and 4.13). When the concentration of 2-methoxystyrene **675** was lower than the concentration of ethylmagnesium bromide **280**, a first order relationship was observed (Fig. 4.12). At 2-methoxystyrene **675** concentrations above the concentration of ethylmagnesium bromide **280** there was a zero order rate dependence on changing the concentration of 2-methoxystyrene **675**. Measuring the initial rate of reaction at different initial concentrations of ethylmagnesium bromide **280** resulted in a similar relationship (Fig. 4.13). The initial rate of reaction was first order in ethylmagnesium bromide **280** when it was the limiting reagent, however when ethylmagnesium bromide **280** was in excess there was a zero order rate dependence on ethylmagnesium bromide **280** concentration.

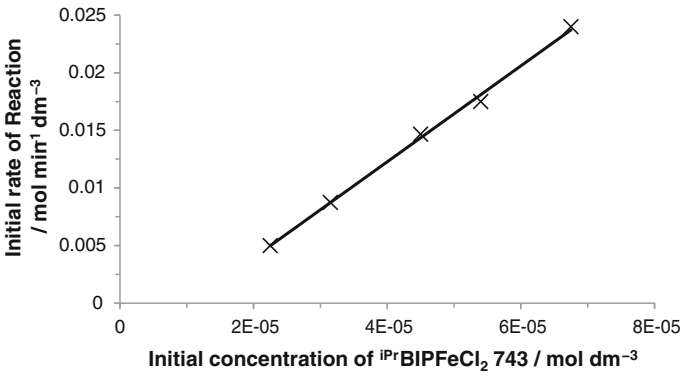

Fig. 4.11 Initial rate of reaction dependence on concentration of iron pre-catalyst **743**

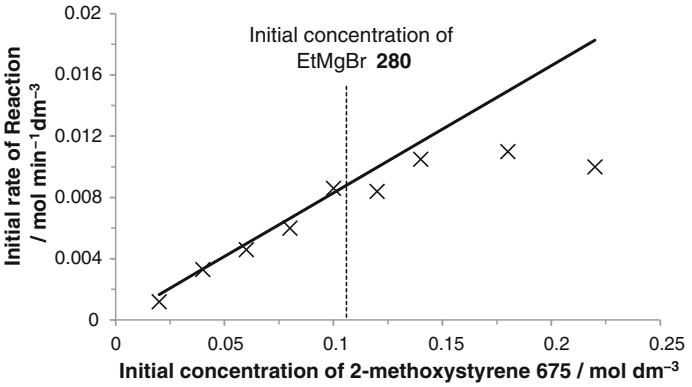

Fig. 4.12 Initial rate of reaction dependence on concentration of 2-methoxystyrene **675**

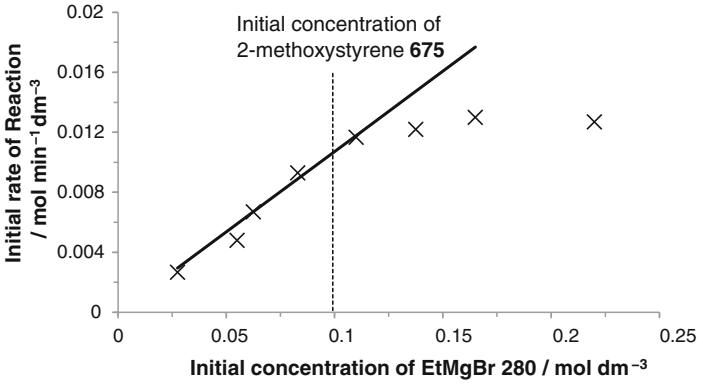

Fig. 4.13 Initial rate of reaction dependence on concentration of ethylmagnesium bromide **280**

This data is not easily explained. The first order relationship with respect to iron pre-catalyst concentration suggests an iron catalyst is involved in the turnover-limiting step. The observation that the rate of reaction is first order in either 2-methoxystyrene or ethylmagnesium bromide concentration, depending on which is limiting, suggests a pre-complexation between these two reagents prior to the turnover-limiting step. This pre-complexation would not involve the iron catalyst. If this analysis is correct, and not a product of an uncontrolled source of experimental error, then it may be interesting to investigate further. It is possible that it may be substrate-specific to 2-methoxystyrene however, and therefore the same kinetic analysis should be repeated using different styrene derivatives. As the use of different styrene derivatives gave different overall reaction profiles (Fig. 4.9), kinetic data should be acquired for two styrene derivatives which display apparently disparate reaction profiles to determine the rate equation in each case.

4.2.4.3 Nature of the Catalyst

The role and influence of ligands used in iron-catalysed processes is still an area of intense debate. Iron-catalysed cross-coupling reactions, and more recently hydrogenation reactions, have been most commonly studied, with the addition of ligands proposed to stabilise low oxidation-state or coordinatively-unsaturated iron species, inhibit catalyst deactivation and aggregation, or simply be spectators.

Following the seminal publications by Kharasch [58] and Kochi [21, 22] on the reaction of Grignard reagents with iron salts, numerous iron-catalysed cross-coupling methodologies have been developed using Grignard reagents as the nucleophilic coupling partner [47]. These reactions commonly operate under 'ligand-free' conditions, or with the addition of a simple amine ligand or co-solvent.

During the optimisation studies it was found that the iron-catalysed hydromagnesiation of styrene derivatives could be improved by the addition of a number of ligands. Particularly high yields were obtained using bis(imino)pyridine ligand **273a** (^{iPr}BIP) and *N*,*N*,*N*′,*N*′-tetramethylethylenediamine **136** (TMEDA). These two ligands are very different in nature. Bis(imino)pyridine **273a** (^{iPr}BIP) is a redox-active tridentate ligand with the ability to accept electron density from the iron centre [32, 59], whilst TMEDA **136** is a simple bidentate tertiary amine, with no reported π-acceptor abilities. The role of each of these ligands in the reaction was therefore investigated.

Using the concentration of iron pre-catalyst commonly used in these reactions (1.8×10^{-3} M, 1 mol%, 2.5 mL of THF), kinetic profiles for the hydromagnesiation of 2-methoxystyrene **273** were obtained (Fig. 4.14). Using iron(II) chloride **279** in the absence of a ligand, < 5 % yield was obtained after 1 h (Fig. 4.14 ●), however using a combination of iron(II) chloride **279** and bis(imino)pyridine ligand **273a** (1 mol%) gave 99 % yield within 10 min (Fig. 4.14 ●). The addition of TMEDA **136** to iron(II) chloride **279** was also found to increase reactivity, with progressively improved activity observed by increasing the loading of TMEDA **136** (0.5–10 mol%) (Fig. 4.14 ●, ●, ● and ●). In addition, longer induction periods were observed at higher concentrations of TMEDA **136**, suggesting that TMEDA **136** may reduce the rate of formation of the active catalyst.

When the concentration of iron pre-catalyst was reduced by a factor of 10, to 1.8×10^{-4} M (0.15 mol%, 3.75 mL of THF) (Fig. 4.15 ●), a combination of iron (II) chloride **279** and bis(imino)pyridine ligand **273a** now gave the hydromagnesiation product in 95 % yield after 2 h. Interestingly, under these more dilute conditions, iron(II) chloride **279** alone was a competent catalyst for hydromagnesiation, giving 80 % yield after 2 h (Fig. 4.15 ●). When the Grignard reagent was added *before* the styrene derivative however no catalytic activity was observed. It is therefore likely that, in the absence of additional ligands, the styrene derivative coordinates to iron to stabilise the low oxidation-state catalyst [21, 25, 29, 36, 47c]. This shows that iron(II) chloride **279** can be used as a pre-catalyst, but suggests that at iron concentrations $\geq 1.8 \times 10^{-3}$ M, or in the absence of a styrene derivative, rapid catalyst deactivation occurs [21, 47, 60]. In Kochi's original report on iron-catalysed hydromagnesiation, an iron concentration of 2.3×10^{-4} M was used

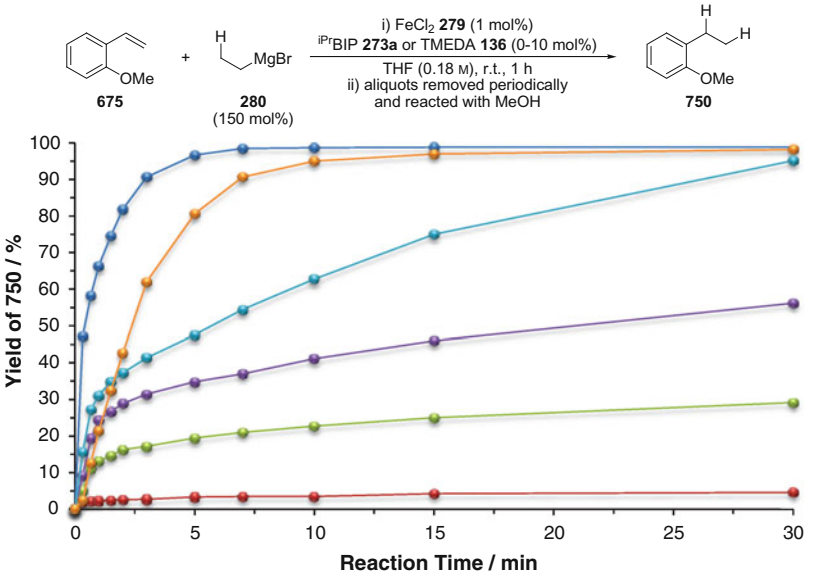

Fig. 4.14 Hydromagnesiation of 2-methoxystyrene **675** using different iron pre-catalysts ([Fe] = 1.8 × 10^{-3} M). ● = $FeCl_2$ **279** + ^{iPr}BIP **273a** (1 mol%); ● = $FeCl_2$ **279**; ● = $FeCl_2$ **279** + TMEDA **136** (0.5 mol%); ● = $FeCl_2$ **279** + TMEDA **136** (1 mol%); ● = $FeCl_2$ **279** + TMEDA **136** (2 mol%); ● = $FeCl_2$ **279** + TMEDA **136** (10 mol%)

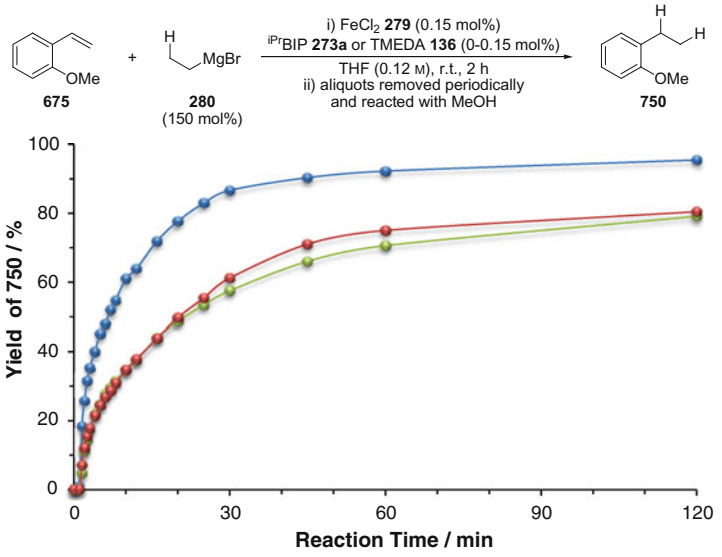

Fig. 4.15 Hydromagnesiation of 2-methoxystyrene **675** using different iron pre-catalysts ([Fe] = 1.8 × 10^{-3} M). ● = $FeCl_2$ **279** + ^{iPr}BIP **273a** (0.15 mol%); ● = $FeCl_2$ **279**; ● = $FeCl_2$ **279** + TMEDA **136** (0.15 mol%)

[22]. The lack of catalytic activity observed using iron salts in early optimisation studies (Table 4.1) may therefore be attributed to the high concentration of iron pre-catalyst used in these experiments (3.8×10^{-3} M).

The addition of TMEDA **136** to these reactions had no observable effect on catalyst activity (Fig. 4.15 ●). This result, in combination with the lack of an optimal stoichiometry between the iron(II) chloride **279** and TMEDA **136** at higher iron pre-catalyst concentration (Fig. 4.14), suggests that TMEDA **136** may not be involved in the primary catalytic cycle, but instead play a role in preventing catalyst deactivation. The combination of iron(II) chloride **279** and bis(imino)pyridine **273a** gave a catalyst with higher activity at both reaction dilutions, which suggests that this ligand may remain bound to the catalytically-active iron species. The higher rates of reaction using the bis(imino)pyridine iron complex (Figs. 4.14 and 4.15) cannot be used to claim ligand-enhanced reactivity however, as the faster rates of reaction observed could simply reflect enhanced stability of the complex towards catalyst deactivation leading to a higher concentration of active catalyst.

Due to the highly reducing conditions necessary for the hydromagnesiation of alkenes, the possibility for pre-catalyst reduction to form colloidal or bulk metal was a serious consideration [33b, 61]. To better understand the activity of the catalyst, determination of the homo- or heterogeneity of the active species is important. The reduction of iron(II) or iron(III) salts by organometallic reagents, including Grignard reagents, to give iron nanoparticles has been reported by a number of groups [62]. The mercury drop test [63] and Maitlis' hot filtration test [64] have been applied to a number of transition-metal-catalysed reactions, however due to the low propensity of iron to form amalgams with mercury [65], and the high air- and moisture sensitivity and small size of iron nanoparticles [66] we chose to use alternative tests.

Collman has shown that two modifications of the three-phase test [67] can be used to distinguish between homo- and heterogeneous hydrogenation catalysts [68]. Using a polymer-bound substrate, only homogeneous catalysts, which could permeate the polymer matrix showed hydrogenation activity. Collman also showed that a polymer-bound catalyst poison would selectively poison homogeneous catalysts, and therefore in the presence of a polymer-bound poison the hydrogenation of a solution-phase substrate was only observed using a heterogeneous catalyst. The diolefinic ligand dibenzo[*a*,*e*]cyclooctatetraene **761** (DCT) [69] has been shown to form remarkably stable complexes with a variety of transition-metals [70]. Crabtree applied DCT **761** as a test to determine catalyst homogeneity, and found that DCT **761** inhibited homogeneous hydrogenation catalysts, but did not affect heterogeneous catalysts [71].

These tests were used to determine the homogeneity of the iron catalyst in the developed methodology. A polymer-bound styrene substrate **756**, for use in the three-phase test, and dibenzo[*a*,*e*]cyclooctatetraene (DCT) **761** were synthesised according to literature procedures (Scheme 4.29) [68, 72, 73].

The polymer-bound styrene substrate **756** was applied to the hydromagnesiation conditions using 1 mol% iron(II) chloride **279** and bis(imino)pyridine ligand **273a**. Following reaction with *N*,*N*-dimethylformamide **744** none of the expected aldehyde product **763** was obtained (Scheme 4.30). When a solution-phase styrene

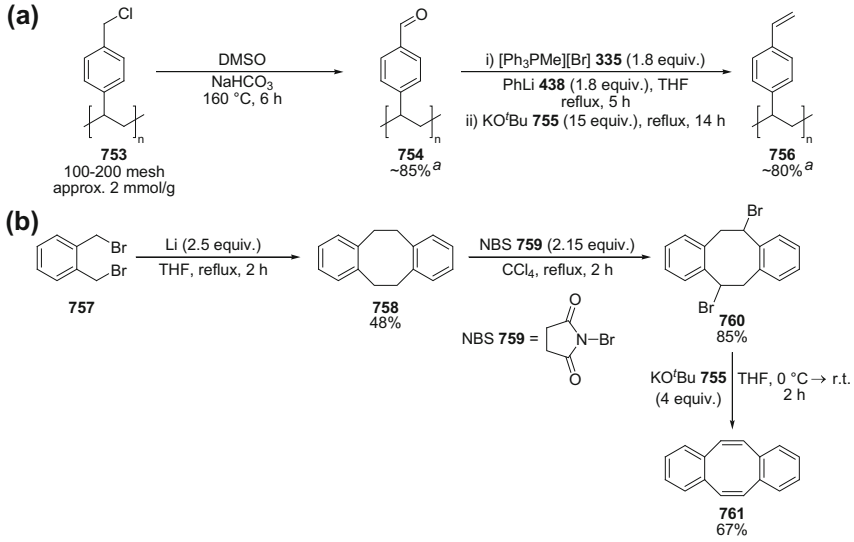

[a] Determined using high resolution magic angle spinning (HRMAS) NMR spectroscopy.

Scheme 4.29 Synthesis of polymer-bound styrene **756** and dibenzo[*a*,*e*]cyclooctatetraene **761**

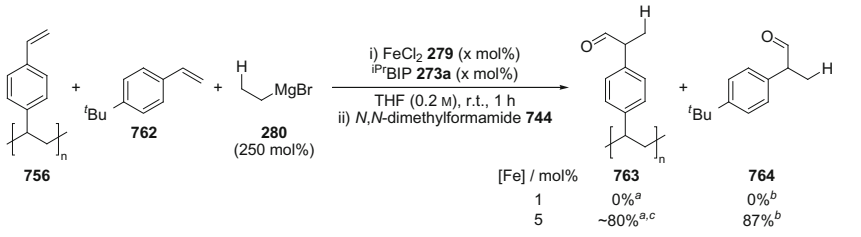

[a] Formation determined by IR spectroscopy; [b] Yield determined by ^{1}H NMR spectroscopy using 1,3,5-trimethoxybenzene as an internal standard; [c] Conversion determined using high resolution magic angle spinning (HRMAS) NMR spectroscopy.

Scheme 4.30 Hydromagnesiation of polymer-bound styrene **756** using ethylmagnesium bromide **280**, in the presence of *tert*-butylstyrene **762**

substrate **762** was also added to this reaction however, no hydromagnesiation activity was observed indicating that an active catalyst was not present in the reaction. When the catalyst loading was increased to 5 mol%, hydromagnesiation activity was observed for both the polymer-bound and solution-phase styrene substrates **756** and **762**. These results are indicative of a homogeneous catalyst, where the polymer-bound substrate **756** also contains a low quantity of a polymer-bound catalyst poison (between 1 and 5 mol% poison).

It is conceivable that small soluble iron nanoparticles could display similar activity in the three-phase test, and therefore Crabtree's selective poisoning experiment using

dibenzo[*a*,*e*]cyclooctatetraene **761** (DCT) was applied. The addition of DCT **761** has been shown not to cause the inhibition of a nanoparticulate iron hydrogenation catalyst [74], and has very recently been shown to cause the slow inhibition of an iron hydrogenation catalyst thought to be homogeneous [75].

Due to the use of an homogeneous iron(II) pre-catalyst **743** in this methodology, DCT **761** was added 2 min after the start of the reaction to avoid the possibilty of DCT **761** binding to the iron pre-catalyst **743**. The addition of DCT **761** (1 or 2 equivalents with respect to ^{iPr}BIPFeCl$_2$ **743**) resulted in complete and almost instantaneous inhibition of the reaction (Fig. 4.16 ● and ●). When 0.5 equivalents of DCT **761** was added (with respect to iron pre-catalyst **743**), reduced activity was observed, but the reaction was not fully inhibited (Fig. 4.16 ●). This suggested that close to one equivalent of DCT **761** was required to inhibit the reaction. It would be expected that a heterogeneous catalyst would require much less than one equivalent of a catalyst poison due to the low surface area of metal sites available relative to the pre-catalyst [33b, 61]. The 1:1 stoichiometry between DCT **761** and iron needed for catalyst inhibition therefore provides good evidence for a homogeneous catalyst in this reaction. Further, independently synthesised iron nanoparticles [76], which were active for the hydrogenation of allylbenzene [76b], were inactive for the hydromagnesiation of 2-methoxystyrene **675** using ethylmagnesium bromide **280**.

The close to 1:1 stoichiometry between DCT **761** and iron pre-catalyst **743** needed for inhibition of reactivity also indicated a close to quantitative conversion of pre-catalyst to an active catalyst, or a species in equilibrium with an active

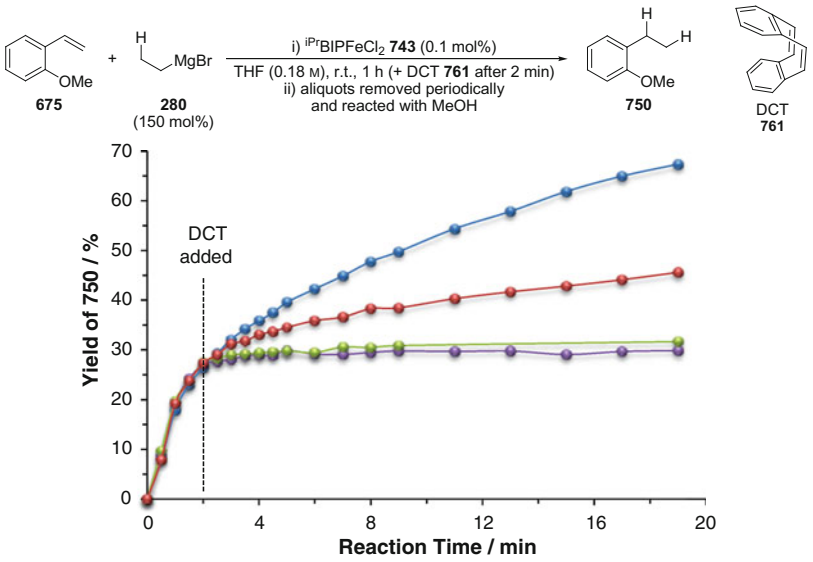

Fig. 4.16 Hydromagnesiation of 2-methoxystyrene **675** in the absence and presence of DCT **761**. ● = no DCT **761** added; ● = DCT **761** (0.05 mol%) added after 2 min; ● = DCT **761** (0.1 mol%) added after 2 min; ● = DCT **761** (0.2 mol%) added after 2 min

catalyst. The apparent efficiency of pre-catalyst-to-catalyst conversion could allow the possibility to accurately quantify pre-catalyst reduction, by measuring the amount of by-products formed from the reduction of the iron(II) pre-catalyst.

A common area of uncertainty in low oxidation-state iron catalysis is the oxidation-state of the active iron species. The reaction of an iron salt with an alkyl Grignard reagent bearing β-hydrogen atoms has been proposed to generate low oxidation-state iron species with oxidation states ranging from iron(−II) to iron(I) [21b, 22, 47c, 50]. The major reduction pathway for an iron(II) salt **170** involves disproportionation of the alkyl group of the Grignard reagent **175** to give alkane **180** and alkene **178** by-products in equal amounts (Scheme 4.31) [22, 47d, e]. Experimental evidence using aryl organometallic reagents and alkyl Grignard reagents, which do not undergo β-hydride elimination, indicate iron(I) is a kinetically viable catalyst for cross-coupling reactions [47e, g, 77]. This evidence was based upon analysis of the by-products of the reduction of iron, with the only by-products in these cases arising by carbon–carbon bond formation through homocoupling of the Grignard reagent (e.g. product **177**).

In order to quantify pre-catalyst reduction using an alkyl Grignard reagent bearing β-hydrogen atoms, the amount of alkane **180** and alkene **178** by-products would need to be quantified. As these should be formed in equal amounts [22], quantification of either by-product could be used to determine pre-catalyst reduction. As a stoichiometric quantity of alkene by-product is formed in the hydromagnesiation reaction, quantification of the alkane by-product was targeted instead. In order to achieve an accurate analysis for the reduction of the iron pre-catalyst, a high molecular weight alkyl Grignard reagent **765** was chosen where all reaction products and by-products **766-770** were non-volatile and could be uniquely identified and quantified by ^{1}H NMR spectroscopy (Fig. 4.17). The background quantity of alkane **767** present in the Grignard reagent was determined, and parallel control reactions were conducted (in triplicate) in the absence of iron(II) chloride

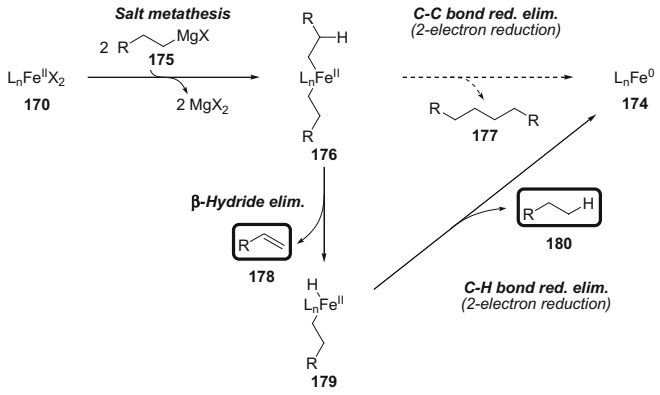

Scheme 4.31 Reduction pathway for an iron(II) pre-catalyst **170** using an alkyl Grignard reagent **175** bearing β-hydrogen atoms

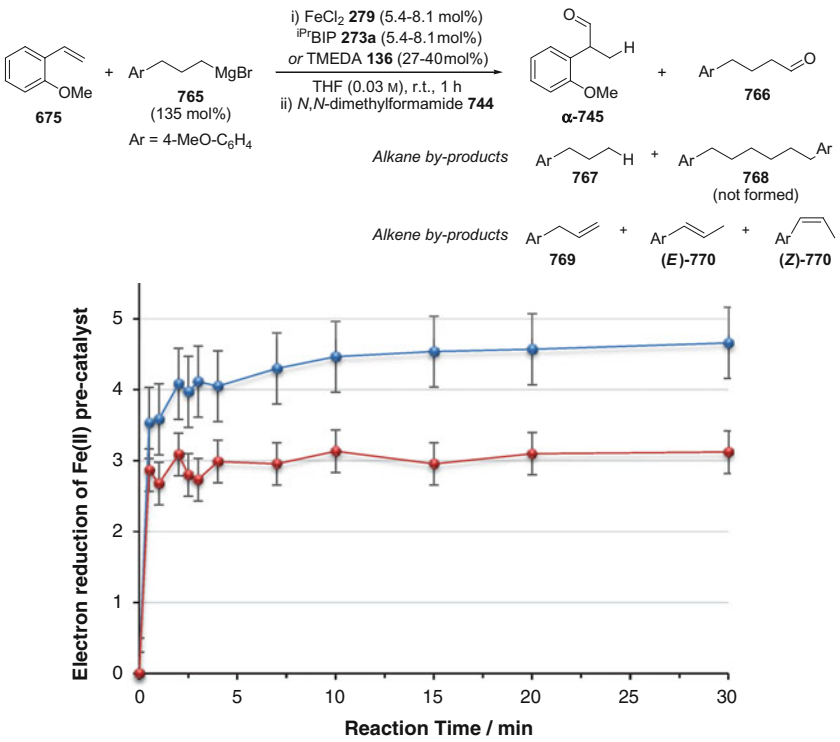

Fig. 4.17 Quantification of the reduction of iron(II) pre-catalysts using alkyl Grignard reagent **765** ● = ^{iPr}BIPFeCl$_2$ **734**; ● = FeCl$_2$ **279** + TMEDA **136** (5 equiv. w.r.t. Fe)

279 to ascertain the amount of alkane by-product formed from protonation of the Grignard reagent **765** by species present in the reaction medium and during aliquot quenching.

Using iron(II) chloride **279** and bis(imino)pyridine ligand **273a**, a catalytically-active species was formed within 30 s and was accompanied by the formation of by-products from the reduction of the iron(II) pre-catalyst corresponding to a 3–4 electron reduction (Fig. 4.17). The quantity of products from the reduction of the pre-catalyst slowly increased for the following 10 min, stabilising at a quantity that corresponded to a 4–5 electron reduction of the pre-catalyst. The same analysis was applied to a pre-catalyst combination of iron(II) chloride **279** and TMEDA **136** (5 equivalents with respect to iron). In this case, a 3-electron reduction was calculated at the outset of the reaction, with no further reduction observed over the course of the reaction. Each experiment was repeated three times and at different loadings of iron pre-catalyst.

The quantity of by-products formed from the reduction of either iron(II) pre-catalyst suggests that the active catalyst in this reaction may be in a formal oxidation-state below iron(0). As a note of caution, the presence of any species in

the reaction capable of oxidising the low oxidation-state iron catalyst could result in the formation of a misleadingly large quantity of by-products from reduction [58a]. Conducting the reaction at different dilutions and using different concentrations of 2-methoxystyrene **675** produced matching data however, suggesting that this potential source of error could probably be discounted. The iron pre-catalyst bearing bis(imino)pyridine ligand **273a** (^{iPr}BIP) was reduced by approximately 1-2 electrons more than iron(II) chloride **279** in the presence of TMEDA **136**. This can be explained by the fact that bis(imino)pyridine (BIP) ligands are redox-active, with the ability to accept up to three electrons [59, 78]. The 4-5 electron reduction of the iron pre-catalyst bearing bis(imino)pyridine ligand **273a** (^{iPr}BIP) would result in an iron species in a formal oxidation-state of −2 or −3. Iron(−III) is not possible as this would correspond to a d^{11} electron configuration. This implies that the redox-activity of the bis(imino)pyridine ligand is significant for the stabilisation of the active iron catalyst, and provides further evidence to suggest that the bis(imino) pyridine ligand **273a** (^{iPr}BIP) may remain bound to iron in the active state.

4.2.4.4 Proposed Mechanism

Based upon this work a mechanism for the iron-catalysed hydromagnesiation of styrene derivatives **735** using ethylmagnesium bromide **280** can be proposed (Scheme 4.32). Reduction of the iron(II) pre-catalyst by ethylmagnesium bromide **280** gives a low oxidation-state iron catalyst **737**. The iron catalyst is a homogeneous species with the iron centre in a formal oxidation-state of zero, or below. When using low concentrations of iron pre-catalyst ($\leq 1.8 \times 10^{-4}$ M) the styrene substrate is a sufficiently good ligand to stabilise the active catalyst to give high yields of hydromagnesiation product. This effect could be substrate dependant however. At higher concentrations of iron other stabilising ligands are needed.

Scheme 4.32 Proposed mechanism for the iron-catalysed hydromagnesiation of styrene derivatives **735** using ethylmagnesium bromide **280**

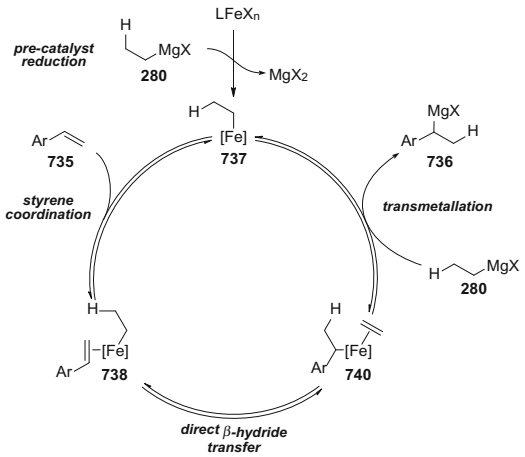

The use of TMEDA **136** has a beneficial effect in preventing catalyst deactivation, however it is unclear whether TMEDA **136** has a role in binding to iron in the primary catalytic cycle.

The highest activities for hydromagnesiation are obtained when using a redox-active bis(imino)pyridine ligand (BIP). It appears that the bis(imino)pyridine (BIP) binds to iron to form the active catalyst and plays an active role in stabilisation of the low oxidation-state by accepting electron density from the iron centre. The high activity observed using bis(imino)pyridine (BIP) ligands may not necessarily reflect an enhanced or modified reactivity of iron in these complexes, but may simply be attributed to an exceptional ability of the ligand to prevent catalyst deactivation, leading to extended catalyst lifetimes and higher concentrations of active catalyst.

Following the formation of an ethyliron-styrene complex **738**, a direct β-hydride transfer takes place to produce a benzyliron-ethylene complex **740**. It is possible that an agostic bond between iron and the transferring hydride may be required, but there is no evidence for the formation of a discrete iron-hydride intermediate. The direct β-hydride transfer is regioselective to add the hydride to the β-position of the styrene derivative. The direct β-hydride transfer process is reversible. Transmetallation between benzyliron-ethylene complex **740** and another equivalent of ethylmagnesium bromide **280** releases the hydromagnesiation product **736** and reforms the ethyliron complex **737**.

The reaction can be inhibited following the formation of an α-aryl Grignard reagent bearing an electron-donating group. This may be due to competitive alkylation of iron by these species resulting in a lower concentration of the ethyliron complex **737**. The reaction is also inhibited following the cleavage of carbon–fluorine bonds, and may be attributed to the formation of a catalytically-inactive iron-fluoride complex.

The turnover-limiting step of the reaction has not yet been determined. The use of deuterium-labelled alkyl Grignard reagents resulted in extensive deuterium-scrambling. As the formed benzylic Grignard reagents do not appear to re-enter the cycle, this suggests that the rate of alkene-styrene exchange and subsequent hydride transfer between the benzyl and styrene ligands is faster than the rate of transmetallation. It may therefore be tempting to suggest that transmetallation could be the turnover-limiting step.

The Hammett plot analysis demonstrated that styrene derivatives bearing electron-donating groups undergo hydromagnesiation most rapidly. This would be difficult to explain if the direct β-hydride transfer was the turnover-limiting step. An increase in negative (and not positive) charge at the benzylic position would be expected in the transition-state structure (late transition state). The trend could potentially be explained by a difference in bonding between iron and the electronically-differentiated styrene derivatives (early transition state). Stronger back-bonding between iron and styrene derivatives bearing electron-withdrawing groups may disfavour the direct β-hydride transfer by a change in the stereoelectronic nature of the iron complex. The lower electron density at iron may also decrease the contribution of an agostic iron–hydrogen bond which may be

significant for the direct β-hydride transfer process. Kinetic experiments using 2-methoxystyrene **675** and ethylmagnesium bromide **280** indicate a first order rate dependence on the concentration of iron, and a first order rate dependence on the limiting reagent (2-methoxystyrene **675** or ethylmagnesium bromide **280**). A zero order rate dependence was found for the reagent in excess. More experimental and theoretical work would be needed to explain this kinetic data and help identify the turnover-limiting step.

4.2.4.5 Future Mechanistic Work

Further work on the reaction kinetics could be undertaken using different styrene substrates. Different overall reaction profiles were observed using different styrene derivatives (Fig. 4.9), therefore it is possible that different rate equations may be obtained depending on the substrate. Kinetic data could be obtained using both 4-*tert*-butylstyrene and 3-methoxystyrene, as these two substrates display very different reaction profiles. As all data currently obtained relates to absolute rates of reaction, competition experiments could be conducted using two different styrene derivatives, to provide information about differences in substrate binding and reaction inhibition following product formation. Experiments using d_5-ethylmagnesium bromide should also be undertaken to determine whether there is a kinetic isotope effect. This could provide information about the turnover-limiting step. As both zero and first order rate dependences have been observed depending upon the limiting reagent, these kinetic isotope experiments should be undertaken with the Grignard reagent both in excess, and as the limiting reagent.

Although an independently-synthesised benzylic Grignard reagent was not applicable in the reaction, an estimate of the extent at which the benzylic Grignard reagent formed in situ re-enters the catalytic cycle could be measured using a pseudo-isotope/deuterium-labelling experiment (Scheme 4.33). The hydromagnesiation of two styrene derivatives, which give distinguishable products, would need to be undertaken, where one styrene derivative contained deuterium labels in the β-position. When using cyclopentylmagnesium bromide **655** as the 'sacrificial' Grignard reagent, any deuterium transfer could be attributed to transfer from the in situ produced benzylic Grignard reagent (or benzylic iron species) to a styrene derivative. If the extent of deuterium transfer increased when using ethylmagnesium

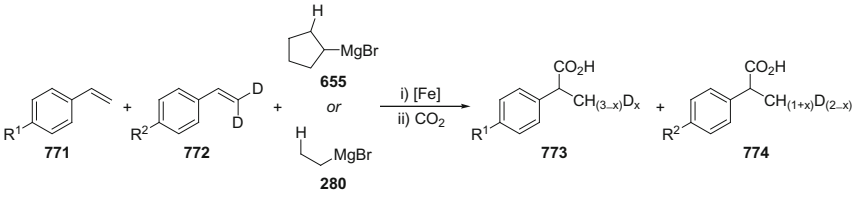

Scheme 4.33 Proposed deuterium scrambling in pseudo isotope/deuterium labelling experiment

bromide **280** as the 'sacrificial' Grignard reagent, the contribution from hydride transfer from a benzyl to an ethene ligand could also be quantified. A range of deuterium-labelled styrene derivatives could be synthesised by Wittig reactions using benzaldehyde derivatives and d_3-methyltriphenylphosphonium iodide (prepared from d_3-iodomethane).

The complexation of dibenzo[*a*,*e*]cyclooctatetraene **761** (DCT) with iron has not been reported, therefore isolation of a low oxidation-state iron-DCT complex would be a useful contribution to support past, current and future mechanistic investigations using DCT **761**. Attempts were made to obtain a bis(imino)pyridine iron-DCT complex, however ^{1}H NMR spectroscopy was uninformative and a crystal suitable for single crystal X-ray analysis could not be obtained. Red-brown crystals were grown at −35 °C from a hexane-diethyl ether solution, following reduction of the iron(II) pre-catalyst, ^{iPr}BIPFeCl$_2$ **743**, in the presence of DCT **761** using ethylmagnesium bromide **280** in tetrahydrofuran. Although the crystals had the expected unit cell volume, desolvation during crystal preparation meant that a structure could not be obtained. Attempts to obtain crystals suitable for single crystal X-ray analysis could be continued using this approach. Chirik has reported the synthesis and structures of bis(imino)pyridine iron-diene complexes, formed from the reaction between a bis(imino)pyridine iron bis(dinitrogen) complex and a diene [79]. Although this may not be representative of the reaction conditions used for hydromagnesiation, it may provide a more convenient route to the synthesis of a low oxidation-state iron-DCT complex. Synthesis by this route would still provide a useful precedent for the binding of iron with DCT. Upon isolation of the complex, alkene/ligand exchange studies could be conducted to determine the lability of the iron-DCT complex.

Finally, the methods that have been used here to investigate the mechanism of the iron-catalysed hydromagnesiation of styrene derivatives could be applied to the methodologies reported by Hayashi and Shirakawa [25] and Nakamura [28]. Subtle differences in solvent, reaction temperature and choice of ligand appear to be significant for the difference in substrate scope between the methodologies. It would be interesting to investigate and compare the mechanisms of all three methodologies to see if there are any common elementary steps that provide insight into the fundamental reactions of iron alkyl complexes and alkyl Grignard reagents.

4.3 Conclusions

The iron-catalysed hydromagnesiation of styrene derivatives has been developed using ethylmagnesium bromide **280** as the 'sacrificial' Grignard reagent ('hydride' source), and a bench-stable bis(imino)pyridine iron(II) pre-catalyst (Scheme 4.34). Styrene derivatives bearing electron-donating substituents underwent hydromagnesiation to give benzylic Grignard reagents, which were reacted with carbon dioxide to give α-aryl carboxylic acids in generally high yield and regioselectivity (α:β, up to 100:1). This represents the first thorough evaluation of the synthetic

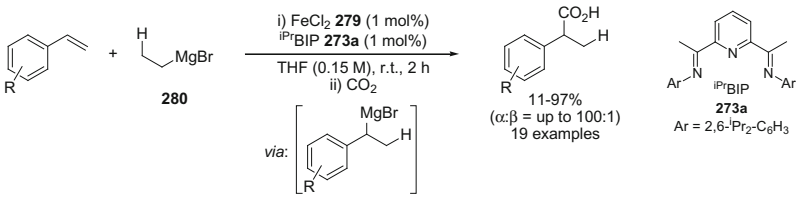

Scheme 4.34 Iron-catalysed hydromagnesiation of styrene derivatives, used for the synthesis of α-aryl carboxylic acids

utility of hydromagnesiation for the synthesis of benzylic Grignard reagents. Under the developed reaction conditions, disubstituted alkenes, alkynes and terminal alkyl-substituted alkenes showed reduced reactivity, potentially providing an opportunity for chemoselective hydromagnesiation of aryl alkenes. Shirakawa and Hayashi [25] and Nakamura [28] have reported complementary iron-catalysed methodologies for the hydromagnesiation of alkyl-substituted alkenes and diaryl alkynes, respectively.

The intermediate Grignard reagent has been observed and characterised spectroscopically. The methodology has recently been extended to a more general hydrofunctionalisation methodology, through the reaction of the intermediate benzylic Grignard reagent with a range of electrophiles. The synthetic utility of the reaction on a preparative scale (10 mmol) has also been highlighted in the key final step of the synthesis of ibuprofen using only iron-catalysed reactions.

Mechanistic investigations suggest that the iron pre-catalyst is reduced by ethylmagnesium bromide **280** to a low oxidation-state homogeneous iron species. Coordination of the styrene derivative, and alkylation of iron by ethylmagnesium bromide **280** produces an ethyliron-styrene complex. Hydride transfer to styrene is proposed to take place through a direct β-hydride transfer process, without the formation of a discrete iron hydride intermediate, to give a benzyliron-ethene species. Based upon deuterium-labelling studies this process has been shown to be

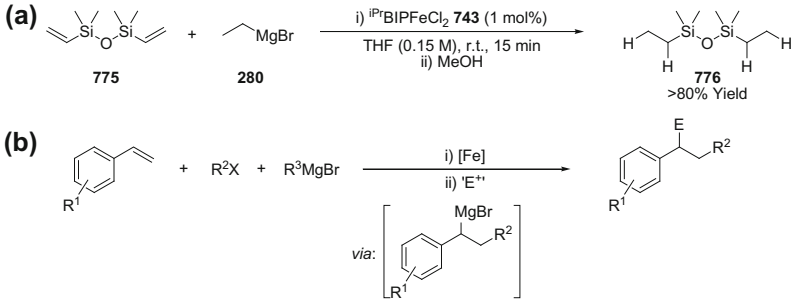

Scheme 4.35 Extensions to the iron-catalysed hydromagnesiation methodology, which could be investigated

reversible. Transmetallation between the benzyliron species and ethylmagnesium bromide **280** then releases the benzylic Grignard reagent and regenerates the iron catalyst. Further experimental and theoretical mechanistic investigations could be undertaken to better understand this reaction (see Sect. 4.2.4.5).

The methodology is currently only applicable to terminal styrene derivatives, and therefore provides access to only a limited range of benzylic Grignard reagents. Preliminary experiments suggest that vinyl silanes can also be applied in the reaction, however the regioselectivity and substrate scope and limitations of the reaction have not been evaluated (Scheme 4.35a). The hydromagnesiation of other alkenes which possess an α-substituent capable of stabilising a negative charge could also be investigated. Titanium-catalysed alkyl- and arylmagnesiation of alkenes has been reported, using an alkyl- or aryl halide as a stoichiometric alkyl- or aryl radical source (R^2), and *n*-butylmagnesium bromide as a 'sacrificial' source of magnesium [80]. The aptitude of low oxidation-state iron catalysts to produce alkyl- and aryl radicals from alkyl- and aryl halides [81] may allow a similar carbomagnesiation reaction to be developed using an iron catalyst (Scheme 4.35b). This would provide access to a wide range of β-substituted benzylic Grignard reagents.

References

1. *Handbook of Grignard Reagents*; Silverman, G. S., Rakita, P. E., Eds.; Marcel Decker: New York, 1996.
2. (a) Knochel, P.; Dohle, W.; Gommermann, N.; Kneisel, F. F.; Kopp, F.; Korn, T.; Sapountzis, I.; Vu, V. A. *Angew. Chem. Int. Ed.* **2003**, *42*, 4302. (b) Krasovskiy, A.; Konchel, P. *Angew. Chem. Int. Ed.* **2004**, *43*, 3333. (c) Clososki, G. C.; Rohbogner, C. J.; Knochel, P. *Angew. Chem. Int. Ed.* **2007**, *46*, 7681. (d) Piller, F. M.; Appukkuttan, P.; Gavryushin, A.; Helm, M.; Knochel, P. *Angew. Chem. Int. Ed.* **2008**, *47*, 6802.
3. (a) Felkin, H.; Swierczewski, G. *Tetrahedron* **1975**, *31*, 2735. (b) Sato, F. *J. Organomet. Chem.* **1985**, *285*, 53. (c) Sato, F.; Urabe, H. In *Handbook of Grignard Reagents*; Silverman, G. S., Rakita, P. E., Eds.; Marcel Decker: New York, 1996; pp 23-52. (d) Greenhalgh, M. D.; Thomas, S. P. *Synlett* **2013**, *24*, 531.
4. (a) Stobbe, H.; Posnjak, G. *Justus Liebigs Ann. Chem.* **1909**, *371*, 287. (b) Cohen, H. L.; Wright, G. F. *J. Org. Chem.* **1953**, *18*, 432.
5. Baker, K. V.; Brown, J. M.; Hughes, N.; Skarnulis, A. J.; Sexton, A. *J. Org. Chem.* **1991**, *56*, 698.
6. Bogdanović, B. *Acc. Chem. Res.* **1988**, *21*, 261.
7. Podall, H. E.; Foster, W. E. *J. Org. Chem.* **1958**, *23*, 1848.
8. Ashby, E. C.; Smith, T. *J. Chem. Soc., Chem. Commun.* **1978**, 30.
9. Barbaras, G. D.; Dillard, C.; Finholt, A. E.; Wartik, T.; Wilzbach, K. E.; Schlesinger, H. I. *J. Am. Chem. Soc.* **1951**, *73*, 4585.
10. (a) Bogdanović, B.; Liao, S.-t.; Schwickardi, M.; Sikorsky, P.; Spliethoff, B. *Angew. Chem. Int. Ed. Engl.* **1980**, *19*, 818. (b) Bogdanović, B.; Bons, P.; Schwickardi, M.; Seevogel, K. *Chem. Ber.* **1991**, *124*, 1041.
11. (a) Ramsden, H. E. U.S. Patent 3354190, November 21, 1967. (b) Bogdanović, B. *Acc. Chem. Res.* **1988**, *21*, 261.
12. (a) Bogdanović, B.; Schwickardi, M.; Sikorsky, P.; *Angew. Chem. Int. Ed. Engl.* **1982**, *21*, 199. (b) Bogdanović, B.; Maruthamuthu, M. *J. Organomet. Chem.* **1984**, *272*, 115.

(c) Bogdanović, B.; Bons, P.; Konstantinović, S.; Schwickardi, M.; Westeppe, U. *Chem. Ber.* **1993**, *126*, 1371.
13. (a) Finkbeiner, H. L.; Cooper, G. D. *J. Org. Chem*. **1961**, *26*, 4779. (b) Cooper, G. D.; Finkbeiner, H. L. *J. Org. Chem*. **1962**, *27*, 1493. (c) Finkbeiner, H. L.; Cooper, G. D. *J. Org. Chem*. **1962**, *27*, 3395.
14. Ashby, E. C.; Ainslie, R. D. *J. Organomet. Chem.* **1983**, *250*, 1.
15. Brintzinger, H. H. *J. Am. Chem. Soc.* **1967**, *89*, 6871.
16. Martin, H. A.; Jellinek, M. F. *J. Organomet. Chem.* **1968**, *12*, 149.
17. (a) Sato, F.; Ishikawa, H.; Sato, M. *Tetrahedron Lett.* **1980**, *21*, 365. (b) Sato, F.; Ishikawa, H.; Sato, M. *Tetrahedron Lett.* **1981**, *22*, 85. (c) Sato, F.; Watanabe, H.; Tanaka, Y.; Yamaji, T.; Sato, M. *Tetrahedron Lett.* **1983**, *24*, 1041. (d) Sato, F.; Katsuno, H. *Tetrahedron Lett.* **1983**, *24*, 1809.
18. Benkeser, R. A.; Young, W. G.; Broxterman, W. E.; Jones, Jr., D. A.; Piaseczynski, S. J. *J. Am. Chem. Soc.* **1969**, *91*, 132.
19. Gao, Y.; Sato, F. *J. Chem. Soc. Chem. Commun.* **1995**, 659.
20. (a) Farády, L.; Bencze, L.; Markó, L. *J. Organomet. Chem.* **1967**, *10*, 505. (b) Farády, L.; Bencze, L.; Markó, L. *J. Organomet. Chem.* **1969**, *17*, 107. (c) Farády, L.; Markó, L. *J. Organomet. Chem.* **1971**, *28*, 159. (d) Snider,B. B.; Karras, M.; Conn, R. S. E. *J. Am. Chem. Soc.* **1978**, *100*, 4624.
21. (a) Tamura, M.; Kochi, J. *J. Am. Chem. Soc.* **1971**, *93*, 1487. (b) Neumann, S. M.; Kochi, J. K.; *J. Org. Chem.* **1975**, *40*, 599. (c) Smith, R. S.; Kochi, J. K. *J. Org. Chem.* **1976**, *41*, 502.
22. (a) Tamura, M.; Kochi, J. *J. Organomet. Chem.* **1971**, *31*, 289. (b) Tamura, M.; Kochi, J. *Bull. Chem. Jpn. Soc.* **1971**, *44*, 3063.
23. Shirakawa, E.; Ikeda, D.; Yamaguchi, S.; Hayashi, T. *Chem. Commun*. **2008**, 1214.
24. (a) Reger, D. L.; Culbertson, E. C. *Inorg. Chem.* **1977**, *16*, 3104. (b) Harvey, J. N. *Organometallics* **2001**, *20*, 4887. (c) Vela, J.; Smith, J. M.; Lachicotte, R. J.; Holland, P. L. *Chem. Commun.* **2002**, 2886. (d) Vela, J.; Vaddadi, S.; Cundari, T. R.; Smith, J. M.; Gregory, E. A.; Lachicotte, R. J.; Flaschenriem, C. J.; Holland, P. L. *Organometallics* **2004**, *23*, 5226.
25. Shirakawa, E.; Ikeda, D.; Masui, S.; Yoshida, M.; Hayashi, T. *J. Am. Chem. Soc.* **2012**, *134*, 272.
26. Zhang, D.; Ready, J. M. *J. Am. Chem. Soc.* **2006**, *128*, 15050.
27. (a) Cahiez, G.; Marquais, S. *Synlett* **1993**, 45. (b) Cahiez, G.; Marquais, S. *Tetrahedron Lett.* **1996**, *37*, 1773.
28. Ilies, L.; Yoshida, T.; Nakamura, E. *J. Am. Chem. Soc.* **2012**, *134*, 16951.
29. (a) Jonas, K.; Schieferstein, L.; Krüger, C.; Tsay, T.-H. *Angew. Chem. Int. Ed. Engl.* **1979**, *18*, 550. (b) Yu, Y.; Smith, L. M.; Flaschenriem, C. J.; Holland, P. L. *Inorg. Chem.* **2006**, *45*, 5742. (c) Fürstner, A.; Majima, K.; Martín, R.; Krause, H.; Kattnig, E.; Goddard, R.; Lehmann, C. W. *J. Am. Chem. Soc.* **2008**, *130*, 1992. (d) Casitas, A.; Krause, H.; Goddard, R.; Fürstner, A. *Angew. Chem. Int. Ed.* **2015**, *54*, 1521.
30. El Ali, B.; Alper, H. Hydrocarboxylation and Hydroesterification Reactions Catalyzed by Transition Metal Complexes. In *Transition Metals for Organic Synthesis*; Beller, M., Bolm, C., Eds.; Wiley-VCH: Weinheim, 2004; pp 113-132.
31. Connelly, N. G.; Geiger, W. E. *Chem. Rev.* **1996**, *96*, 877.
32. (a) Butin, K. P.; Beloglazkina, E. K.; Zyk, N. V. *Russ. Chem. Rev.* **2005**, *74*, 531. (b) Caulton, K. G. *Eur. J. Inorg. Chem.* **2012**, 435.
33. (a) Thomé, I.; Nijs, A.; Bolm, C. *Chem. Soc. Rev.* **2012**, *41*, 979. (b) Crabtree, R. H. *Chem. Rev.* **2012**, *112*, 1536.
34. Kharasch, M. S.; Huang, R. L. *J. Org. Chem.* **1952**, *17*, 669.
35. (a) Hirao, A.; Loykulnant, S.; Ishizone, T. *Prog. Polym. Sci.* **2002**, *27*, 1399. For reviews on the use of bis(imino)pyridine iron complexes for polymerisation see: (b) Gibson, V. C.; Redshaw, C.; Solan, G. A. *Chem. Rev.* **2007**, *107*, 1745.
36. (a) Gülak, S.; Jacobi von Wangelin, A. *Angew. Chem. Int. Ed.* **2012**, *51*, 1357. (b) Gülak, S.; Gieshoff, T. N.; Jacobi von Wangelin, A. *Adv. Synth. Catal.* **2014**, *355*, 2197.
37. Gridnev, I. D. *Coord. Chem. Rev.* **2008**, *252*, 1798.

38. Hatakeyama, T.; Kondo, Y.; Fujiwara, Y.; Takaya, H.; Ito, S.; Nakamura, E.; Nakamura, M. *Chem. Commun.* **2009**, 1216.
39. (a) Fürstner, A.; Leitner, A. *Angew. Chem. Int. Ed.* **2002**, *41*, 609. (b) Czaplik, W. M.; Grupe, S.; Mayer, M.; Jacobi von Wangelin, A. *Chem. Commun.* **2010**, *46*, 6350.
40. (a) Bartoli, G. *Acc. Chem. Res.* **1984**, *17*, 109. (b) Ricci, A.; Fochi, M. *Angew. Chem., Int. Ed.* **2003**, *42*, 1444.
41. Gästner, D.; Konnerth, H.; Jacobi von Wangelin, A. *Catal. Sci. Technol.* **2013**, *3*, 2541.
42. Ashby, E. C.; Laemmle, J.; Neumann, H. M. *Acc. Chem. Res.* **1974**, *7*, 272.
43. Parris, G. E.; Ashby, E. C. *J. Am. Chem. Soc.* **1971**, *93*, 1206.
44. (a) Schlenk, W.; Schlenk, W. *Ber. dtsch. Chem. Ges.* **1929**, *62*, 920. (b) Noller, C. R.; White, W. R. *J. Am. Chem. Soc.* **1937**, *59*, 1354.
45. Jones, A. S.; Paliga, J. F.; Greenhalgh, M. D.; Quibell, J. M.; Steven, A.; Thomas, S. P. *Org. Lett.* **2014**, *16*, 5964.
46. Huehls, C. B.; Lin, A.; Yang, J. *Org. Lett.* **2014**, *16*, 3620.
47. For reviews see: (a) Leitner, A. In *Iron Catalysis in Organic Chemistry: Reactions and Applications*; Plietker, B., Ed.; Wiley-VCH: Weinheim, 2008; pp 147-176. (b) Czaplik, W. M.; Mayer, M.; Cvengroš, J.; Jacobi von Wangelin, A. *ChemSusChem* **2009**, *2*, 396. For selected examples see: (c) Fürstner, A.; Martin, R.; Krause, H.; Seidel, G.; Goddard, R.; Lehmann, C. W. *J. Am. Chem. Soc.* **2008**, *130*, 8773. (d) Kleimark, J.; Hedström, A.; Larsson, P.-F.; Johansson, C.; Norrby, P.-O. *ChemCatChem* **2009**, *1*, 152. (e) Hedström, A.; Lindstedt, E.; Norrby, P.-O. *J. Organomet. Chem.* **2013**, *748*, 51. (f) Bedford, R. B.; Carter, E.; Cogswell, P. M.; Gower, N. J.; Haddow, M. F.; Harvey, J. N.; Murphy, D. M.; Neeve, E. C.; Nunn, J. *Angew. Chem. Int. Ed.* **2013**, *52*, 1285. (g) Guisán-Ceinos, M.; Tato, F.; Buñuel, E.; Calle, P.; Cárdenas, D. J. *Chem. Sci.* **2013**, *4*, 1098.
48. See experimental chapter for further details.
49. Deng, L.; Margl, P.; Ziegler, T. *J. Am. Chem. Soc.* **1999**, *121*, 6479.
50. Bogdanović, B.; Schwickardi, M. *Angew. Chem. Int. Ed.* **2000**, *39*, 4610.
51. Giese, B. *Angew. Chem. Int. Ed. Engl.* **1983**, *22*, 753.
52. Davies, A. G.; Roberts, B. P. *J. Chem. Soc. B* **1968**, 1074.
53. (a) Van Humbeck, J. F.; Simonovich, S. P.; Knowles, R. R.; MacMillan, D. W. C. *J. Am. Chem. Soc.* **2010**, *132*, 10012. (b) Smith, J. M.; Mayberry, D. E.; Margarit, C. G.; Sutter, J.; Wang, H.; Meyer, K.; Bontchev, R. P. *J. Am. Chem. Soc.* **2012**, *134*, 6516.
54. Aschmann, S. M.; Arey, J.; Atkinson, R. *Atmos. Environ.* **2011**, *45*, 4408.
55. Griller, D.; Ingold, K. U. *Acc. Chem. Res.* **1980**, *13*, 317.
56. (a) McDaniel, D. H.; Brown, H. C. *J. Org. Chem.* **1958**, *23*, 420. (b) Wayner, D. D. M.; Arnold, D. R. *Can. J. Chem.* **1984**, *62*, 1164.
57. To the best of my knowledge there are no systematic studies on the nucleophilicities of *para*- and *meta*-substituted benzylic Grignard reagents. For nucleophilicity studies of benzylic anions see: (a) Berger, S. T. A.; Ofial, A. R.; Mayr, H. *J. Am. Chem. Soc.* **2007**, *129*, 9753. (b) Seeliger, F.; Mayr, H. *Org. Biomol. Chem.* **2008**, *6*, 3052. (c) Francisco, C.-B.; Mayr, H. *Eur. J. Org. Chem.* **2013**, 4255.
58. (a) Kharasch, M. S.; Fields, E. K. *J. Am. Chem. Soc.* **1941**, *63*, 2316. (b) Kharasch, M. S.; Lewis, D. W.; Reynolds, W. B.; *J. Am. Chem. Soc.* **1943**, *65*, 498. (c) Kharasch, M. S.; Fuchs, C. F. *J. Org. Chem.* **1945**, *10*, 292.
59. Chirik, P. J. In *Pincer and Pincer-Type Complexes: Applications in Organic Synthesis and Catalysis*; Szabo, K. J., Wendt, O. F., Eds.; Wiley-VCH: Weinheim, 2014; pp 189-212.
60. Kleimark, J.; Larsson, P.-F.; Emany, P.; Hedström, A.; Norrby, P.-O. *Adv. Synth. Catal.* **2011**, *354*, 448.
61. Widegren, J. A.; Finke, R. G. *J. Mol. Catal., A.* **2003**, *198*, 317.
62. Welther, A.; Jacobi von Wangelin, A. *Curr. Org. Chem.* **2013**, *17*, 236.
63. (a) Paal, C.; Hartmann, W. *Chem. Ber.* **1918**, *51*, 711. (b) Whitesides, G. M.; Hackett, M.; Brainard, R. L.; Lavalleye, J.-P. P. M.; Sowinski, A. F.; Izumi, A. N.; Moore, S. S.; Brown, D. W.; Staudt, E. M. *Organometallics* **1985**, *4*, 1819.
64. Hamlin, J. E.; Hirai, K.; Millan, A. Maitlis, P. M. *J. Mol. Catal.* **1980**, *7*, 543.

65. (a) Mørup, S.; Linderoth, S.; Jacobsen J.; Holmblad, M. *Hyperfine Interact.* **1991**, *69*, 489. (b) Linderoth S.; Mørup, S. *J. Phys.: Condens. Matter* **1992**, *4*, 8627.
66. Laine, R. M. *J. Mol. Catal.* **1982**, *14*, 137.
67. Rebek, J.; Gavina, F. *J. Am. Chem. Soc.* **1974**, *96*, 7112.
68. Collman, J. P.; Kosydar, K. M.; Bressan, M.; Lamanna, W.; Garrett, T. *J. Am. Chem. Soc.* **1984**, *106*, 2569.
69. Fieser, L. F.; Pechet, M. M. *J. Am. Chem. Soc.* **1946**, *68*, 2577.
70. Douglas, A. R.; Crabtree, R. H. *Organometallics* **1983**, *2*, 621.
71. Douglas, A. R.; Crabtree, R. H. *Organometallics* **1983**, *2*, 855.
72. Frechet, J. M.; Schuerch, C. *J. Am. Chem. Soc.* **1971**, *93*, 492.
73. Franck, G.; Brill, M.; Helmchen, G. *Org. Synth.* **2012**, *89*, 55.
74. Gieshoff, T. N.; Welther, A.; Kessler, M. T.; Prechtl, M. H. G.; Jacobi von Wangelin, A. *Chem. Commun.* **2014**, *50*, 2261.
75. Gieshoff, T. N.; Villa, M.; Welther, A.; Plois, M.; Chakraborty, U.; Wolf, R.; Jacobi von Wangelin, A. *Green Chem.* **2015**, *17*, 1408.
76. (a) Phua, P.-H.; Lefort, L.; Boogers, J. A. F.; Trisany, M.; de Vries, J. G. *Chem. Commun.* **2009**, 3747. (b) Welther, A.; Bauer, M.; Mayer, M.; Jacobi von Wangelin, A. *ChemCatChem* **2012**, *4*, 1088.
77. Adams, C. J.; Bedford, R. B.; Carter, E.; Gower, N. J.; Haddow, M. F.; Harvey, J. N.; Huwe, M.; Cartes, M. A.; Mansell, S. M.; Mendoza, C.; Murphy, D. M.; Neeve, E. C.; Nunn, J. *J. Am. Chem. Soc.* **2012**, *134*, 10333.
78. Tondreau, A. M.; Stieber, S. C. E.; Milsmann, C.; Lobkovsky, E.; Weyhermüller, T.; Semproni, S. P.; Chirik, P. J. *Inorg. Chem.* **2013**, *52*, 635.
79. (a) Boukamp, M. W.; Bowman, A. C.; Lobkovsky, E.; Chirik, P. J. *J. Am. Chem. Soc.* **2006**, *128*, 13340. (b) Russell, S. K.; Lobkovsky, E.; Chirik, P. J. *J. Am. Chem. Soc.* **2011**, *133*, 8858.
80. Nii, S.; Terao, J.; Kambe, N. *J. Org. Chem.* **2004**, *69*, 573.
81. Greenhalgh, M. D.; Thomas, S. P. *ChemCatChem* **2014**, *6*, 1520.

Chapter 5
Experimental

Abstract Detailed experimental procedures and full characterisation data for all novel compounds in this thesis are presented in this chapter.

5.1 General Experimental

All air- and moisture sensitive reactions were carried out using standard vacuum line and Schlenk techniques, or in a glovebox with a purified nitrogen atmosphere. All solvents for air- and moisture sensitive techniques were obtained from an anhydrous solvent system (Innovative Technology). Anhydrous d_8-tetrahydrofuran was distilled from sodium/benzophenone. All glassware was cleaned using base (KOH, ^{i}PrOH) and acid (HCl_{aq}) baths.

Iron(II) chloride was purchased from Strem Chemicals Inc. (UK); anhydrous iron chloride, 98 % (product number 93-2631. Lot 19226800, 44.00000 % Fe, expect 44.059 %). Iron(II) chloride 99.99 % was purchased from Sigma Aldrich (UK); anhydrous beads, ~10 mesh, 99.99 % (product number 450936). All reagents were purchased from Sigma Aldrich, Alfa Aesar, Acros organics, Tokyo Chemical Industries UK, and Apollo Scientific or synthesised within the laboratory. Carbon dioxide was purchased from BOC LTD (UK) (C40-VB—carbon dioxide cylinder, vapour, B-size 10).

Thin layer chromatography was performed on aluminium-backed silica plates (Merck 60 F_{254}). Pet. ether refers to petroleum ether 40–60. Product spots were visualised by UV light at 254 nm, and subsequently developed using potassium permanganate solution if appropriate. Flash column chromatography was performed on silica gel (Merck Kieselgel 60, 40–63 μm). Gas chromatography was performed on an VG Trio 1000 GCMS, equipped with a Zebron ZB-5HTcolumn (30.0 m × 0.25 mm), or an Agilent HP6890 gas chromatograph equipped with an

M. Greenhalgh, *Iron-Catalysed Hydrofunctionalisation of Alkenes and Alkynes*, Springer Theses, DOI 10.1007/978-3-319-33663-3_5

Agilent J&W DB-5 ms capillary column (15 m × 0.25 mm × 0.25 μm). Method used: [70-1]: Injector temp. 250, 70 °C for 3 min, ramps 25 °C/min to 200 °C, ramps 45 °C/min to 250 °C, holds for 3 min, ramps 45 °C/min to 300 °C, holds for 3 min. Chiral HPLC analysis was performed on an Agilent 1100 instrument using 4.6 × 250 mm columns.

^{1}H, ^{2}H, ^{11}B, ^{13}C, ^{19}F and ^{29}Si NMR spectra were recorded on Bruker Avance III 400 and 500 MHz; Bruker AVI 400 MHz; Bruker Avance I 600 MHz; Varian VNMR 400 and 500 MHz; or Jeol Eclipse 300 and 400 MHz spectrometers. High resolution magic angle spinning was acquired using a TXI-HRMAS probe, optimised using a KBr standard. All spectra were obtained at ambient temperature, unless otherwise stated. The chemical shifts (δ) were recorded in parts per million (ppm) and the coupling constants (*J*) in Hertz (Hz). ^{1}H and ^{13}C NMR multiplicities and coupling constants are reported where applicable. Abbreviations used in the description of multiplicities are: app. (apparent), br. (broad), s (singlet), d (doublet), t (triplet), q (quartet), quin. (quintet), sext. (sextet), sept. (septet), non. (nonet). ^{1}H and ^{13}C NMR spectra were referenced to the residual deuterated solvent peak ($CHCl_3$: 7.27 ppm, 77.00 ppm; CH_2Cl_2: 5.32 ppm, 54.00 ppm; d_8-THF: 1.73 ppm, 25.37; CD_3CN: 1.94 ppm, 1.39 ppm).

Infra-red spectra were recorded on a Perkin-Elmer Spectrum One FT-IR, or Shimadzu IRAffinity-1 spectrometer (serial no. A213749) spectrometer. Optical rotations were recorded on an Optical Activity POLAAR 20 polarimeter with a path length of 1 dm. Concentrations are quoted in g/100 mL. Melting points were determined using a Stuart Scientific SMP10, or Griffin Gallankamp, melting point apparatus and were uncorrected. High resolution mass spectra were recorded on a VG autospec, or Thermo/Finnigan MAT 900, mass spectrometer.

5.2 General Procedures

General Procedure A: Hydrosilylation of olefins in tetrahydrofuran

An olefin (0.7 mmol) was added to a solution of iron(II) chloride **279** (0.9 mg, 0.007 mmol) and 2,6-bis-[1-(2,6-diethylphenylimino)ethyl]pyridine **273b** (0.007 mmol) in anhydrous tetrahydrofuran (3 mL) at room temperature under an atmosphere of nitrogen. Ethylmagnesium bromide **280** (1.5 M in Et_2O, 10 μL, 2 drops, 0.015 mmol) was added, followed by a silane (0.77 mmol) and the reaction was stirred at room temperature for 1 h. Aqueous sulfate buffer (10 mL) was added and the aqueous phase extracted with diethyl ether (3 × 20 mL). The combined organic extracts were washed with water and brine, dried ($MgSO_4$) and concentrated in vacuo. Trimethoxybenzene (23.5 mg, 0.14 mmol) was added as an internal standard, and a yield for the reaction determined by ^{1}H NMR spectroscopy.

Known compounds were identified by ^{1}H NMR spectroscopy, and characterised by comparison with authentic samples of spectral data. Isolated yields were determined following purification by flash silica chromatography.

General Procedure B: Hydrosilylation of olefins in toluene and 'solvent-free' conditions

An olefin was added to a suspension of 2,6-bis-[1-(2,6-diethylphenylimino)ethyl] pyridine iron(II) chloride **367** (^{Et}BIPFeCl$_2$) (3.9 mg, 0.007 mmol) in anhydrous toluene (3 mL), or in the absence of solvent at room temperature under an atmosphere of nitrogen. *n*-Butyllithium **283** (1 M in hexane, 3 drops, 0.015 mmol) was added, followed by a silane (1.1 equiv. with respect to olefin) and the reaction stirred at room temperature. Aqueous sulfate buffer (10 mL) was added and the aqueous phase extracted with diethyl ether (3 × 20 mL). The combined organic extracts were washed with water and brine, dried ($MgSO_4$) and concentrated in vacuo. Trimethoxybenzene (23.5 mg, 0.14 mmol) was added as an internal standard, and a yield for the reaction determined by ^{1}H NMR spectroscopy.

Known compounds were identified by ^{1}H NMR spectroscopy, and characterised by comparison with authentic samples of spectral data. Isolated yields were determined following purification by flash silica chromatography.

General Procedure C: Hydroboration of olefins in tetrahydrofuran

An olefin (0.7 mmol) was added to a solution of iron(II) chloride **279** (0.9 mg, 0.007 mmol) and 2,6-bis-[1-(2,6-diethylphenylimino)ethyl]pyridine **273b** (3.0 mg, 0.007 mmol) in anhydrous tetrahydrofuran (3 mL) at room temperature under an atmosphere of nitrogen. Ethylmagnesium bromide **280** (1.5 M in Et_2O, 15 μL, 3 drops, 0.023 mmol) was added, followed by pinacol borane **93** (110 μL, 0.77 mmol) and the reaction stirred at room temperature for 1 h. Water (10 mL) was added and the aqueous phase extracted with diethyl ether (3 × 20 mL). The combined organic extracts were washed with water and brine, dried ($MgSO_4$) and concentrated in vacuo. Trimethoxybenzene (23.5 mg, 0.14 mmol) was added as an internal standard, and a yield for the reaction determined by ^{1}H NMR spectroscopy.

Known compounds were identified by ^{1}H NMR spectroscopy, and characterised by comparison with authentic samples of spectral data. Isolated yields were determined following purification by flash silica chromatography.

General Procedure D: Hydroboration of olefins using 'solvent-free' conditions

An olefin (0.7 mmol) was added to 2,6-bis-[1-(2,6-diethylphenylimino)ethyl]pyridine iron(II) chloride **367** (^{Et}BIPFeCl$_2$) (3.9 mg, 0.007 mmol) at room temperature under an atmosphere of nitrogen. *n*-Butyllithium **283** (1.1 M in hexane, 20 μL, 4 drops, 0.021 mmol) was added, followed by pinacol borane **93** (110 μL, 0.77 mmol) and the reaction stirred at room temperature for 1 h. Water (10 mL) was added and the aqueous phase extracted with diethyl ether (3 × 20 mL). The combined organic extracts were washed with water and brine, dried ($MgSO_4$) and concentrated in vacuo. Trimethoxybenzene (23.5 mg, 0.14 mmol) was added as an internal standard, and a yield for the reaction determined by ^{1}H NMR spectroscopy.

Known compounds were identified by ^{1}H NMR spectroscopy, and characterised by comparison with authentic samples of spectral data. Isolated yields were determined following purification by flash silica chromatography.

General procedure E: Formal hydrocarboxylation of styrene derivatives
A styrene derivative (0.7 mmol) was added to a solution of iron(II) chloride **279** (0.9 mg, 0.007 mmol) and 2,6-bis-[1-(2,6-diisoprpylphenylimino)ethyl]pyridine **273a** (3.4 mg, 0.007 mmol) in anhydrous tetrahydrofuran (5 mL) at room temperature. Ethylmagnesium bromide **280** (0.3 mL, 3 M in Et_2O, 0.9 mmol) was added dropwise over 10 min and the reaction stirred at room temperature under an atmosphere of nitrogen for 2 h. Carbon dioxide was bubbled through the reaction *via* a needle for 30 min. Aqueous sulphate buffer solution (10 mL) was added and the aqueous phase was extracted with diethyl ether (3 × 20 mL). The combined organic extracts were washed sequentially with water and brine, dried ($MgSO_4$) and concentrated in vacuo to give the crude reaction products.

Known products were identified by ^{1}H NMR spectroscopy, and characterised by comparison with authentic samples of spectral data.

To determine isolated yields, sodium hydroxide (1 M aqueous) was added to the crude reaction products and extracted with diethyl ether (3 × 20 mL). The organic phases were discarded. The aqueous phase was acidified to pH 1 with concentrated hydrochloric acid, and extracted with diethyl ether (3 × 20 mL). The combined organic phases were washed sequentially with water and brine, dried ($MgSO_4$) and concentrated in vacuo to give the carboxylic acid product. If necessary, the product was further purified by flash silica chromatography.

5.3 Compound Preparation and Characterisation Data

4-iso-Butylstyrene **66** (*by* Wittig reaction)

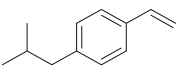

4-iso-Butylbenzaldehyde (0.83 mL, 5 mmol) was added to potassium carbonate (1.1 g, 8 mmol) and methyltriphenylphosphonium bromide **335** (2.1 g, 6 mmol) in anhydrous tetrahydrofuran (5 mL), and heated at reflux for 16 h. The reaction mixture was cooled, filtered and concentrated in vacuo. The residue was dissolved in hot *n*-pentane, cooled to 0 °C, filtered, and washed with cold *n*-pentane. The filtrate was dried ($MgSO_4$) and concentrated in vacuo to give 4-iso-butylstyrene **66** as a colourless oil (666 mg, 84 %).

^{1}H NMR (400 MHz, $CDCl_3$) 7.37-7.32 (m, 2H, ArH), 7.15-7.10 (m, 2H, ArH), 6.72 (dd, J = 17.5, 11.0 Hz, 1H, CH), 5.72 (dd, J = 17.5, 1.0 Hz, 1H, CH), 5.21 (dd, J = 11.0, 1.0 Hz, 1H, CH), 2.48 (d, J = 7.0 Hz, 2H, CH_2), 1.88 (app. non, J = 7.0 Hz, 1H, CH), 0.92 (d, J = 6.5 Hz, 6H, CH_3). **^{13}C NMR** (100 MHz, $CDCl_3$) 141.5 (C), 136.8 (CH), 135.1 (C), 129.3 (2 × CH), 125.9 (2 × CH), 112.8 (CH), 45.2 (CH_2), 30.2 (CH), 22.3 (2 × CH_3). **IR** (neat) ν_{max} cm^{-1} 3086, 3019, 2954, 2920, 2847, 1631, 1511, 1464, 1405, 1383, 1366.

Data were in accordance with those previously reported [1].

4-iso-Butylstyrene **66** (*by* iron-catalysed cross-coupling reaction)

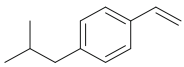

4-Chloro-(2-methylpropyl)benzene **730** (1.69 g, 10 mmol) was added to magnesium turnings (290 mg, 12 mmol) in anhydrous tetrahydrofuran (10 mL). A single crystal of iodine was added, and the reaction mixture was heated at reflux for 16 h. The reaction mixture was cooled to room temperature, transferred to an oven-dried J. Young's tube, and made up to 15 mL with anhydrous tetrahydrofuran. The concentration of the Grignard reagent (4-isobutylphenyl)magnesium chloride was determined to be 0.65 M by titration using 2-hydroxybenzaldehyde phenylhydrazone.

(4-Isobutylphenyl)magnesium chloride (8 mL, 0.65 M in tetrahydrofuran, 5.2 mmol) was added to a solution of iron(III) acetylacetonate **133** (70 mg, 0.2 mmol) and *N*,*N*,*N*′,*N*′-tetramethylethylenediamine **136** (0.12 mL, 0.8 mmol) in anhydrous tetrahydrofuran (15 mL) at 0 °C over 2 min. The reaction was stirred for a further 2 min before vinyl acetate (0.37 mL, 4 mmol) was added in one portion. The reaction was stirred at 0 °C for 1 h. Aqueous sulfate buffer solution (10 mL) was added, and the aqueous phase was extracted with diethyl ether (3 × 30 mL). The combined organic phases were washed sequentially with water and brine, dried ($MgSO_4$), and concentrated in vacuo to give the crude reaction product as a colourless oil, which could be used without further purification. Purification by flash silica chromatography (hexane) gave spectroscopically pure 4-iso-butylstyrene (see above).

2-Phenylpropanoic acid **α-76**

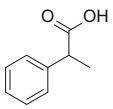

According to general procedure **E**, styrene **53** (80 μL, 0.7 mmol), iron(II) chloride **279** (0.9 mg, 0.007 mmol), 2,6-bis-[1-(2,6-diisopropylphenylimino)ethyl]pyridine **273a** (3.4 mg, 0.007 mmol), ethylmagnesium bromide **280** (3 M in Et_2O, 0.3 mL, 0.9 mmol) and carbon dioxide were reacted in anhydrous tetrahydrofuran to give the crude reaction product, which was purified by acid-base work-up to give 2-phenylpropanoic acid **α-76** as a colourless oil (101 mg, 0.67 mmol, 96 %).

^{1}H NMR (400 MHz, $CDCl_3$) 11.38 (s, br, 1H, CO_2H), 7.40-7.26 (m, 5H, ArH), 3.75 (q, J = 7.0 Hz, 1H, CH), 1.53 (d, J = 7.0 Hz, 3H, CH_3). **^{13}C NMR** (100 MHz, $CDCl_3$) 180.9 (C=O), 139.7 (C), 128.7 (2 × CH), 127.6 (2 × CH), 127.4 (CH), 45.3 (CH), 18.1 (CH_3). **IR** (neat) ν_{max} cm^{-1} 3030, 2980, 2937, 1702, 1496, 1453, 1413, 1230. **GC-MS** [70-1] (M^+, relative abundance): 5.75 min (150, 99 %).

Data were in accordance with those previously reported [2].

Diphenyl(silane-d_2) ***d*$_2$-255**

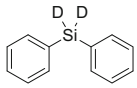

Dichlorodiphenylsilane **440** (6.60 g, 26 mmol) was added dropwise to a stirred suspension of lithium aluminium deuteride ***d*$_4$-441** (790 mg, 19 mmol) in anhydrous diethyl ether (25 mL) under a nitrogen atmosphere. The reaction was heated at reflux for 24 h, cooled to room temperature, and *iso*-propanol (0.5 mL) added slowly, followed by water (5 mL), and aqueous sulfate buffer (25 mL). The mixture was filtered through a short column of Celite, which was washed with diethyl ether (50 mL). The aqueous layer was separated, and extracted with diethyl ether (2 × 20 mL). The organic fractions were combined, dried ($MgSO_4$) and concentrated in vacuo to give a mixture of an oil and a colourless precipitate. Pentane (25 mL) was added, and the suspension was filtered through a short column of Celite, which was washed with pentane (50 mL). The filtrate was dried ($MgSO_4$) and concentrated in vacuo to give diphenyl(silane-d_2) ***d*$_2$-255** as a colourless oil (3.25 g, 17.4 mmol, 67%, >99.5 atom % D).

^{1}H NMR (500 MHz, $CDCl_3$) 7.66-7.61 (m, 4H, ArH), 7.47-7.43 (m, 2H, ArH), 7.43-7.38 (m, 4H, ArH). **^{13}C NMR** (126 MHz, $CDCl_3$) 135.7 (4 × CH), 131.4 (2 × C), 129.9 (2 × CH), 128.1 (4 × CH). **^{2}H NMR** (61 MHz, $CHCl_3$) 4.97. **^{29}Si NMR** (79 MHz, $CDCl_3$) −33.9 (quin., J = 30.5 Hz). **IR** (neat) ν_{max} cm^{-1} 3069, 3011, 1545, 1427, 1121, 997, 741, 714, 692, 634, 613.

Data were in accordance with those previously reported [3].

2,6-Bis-[1-(2,6-diisopropylphenylimino)ethyl]pyridine **273a**

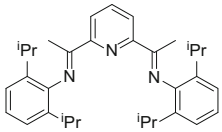

2,6-Diisopropylaniline **272a** (10.9 mL, 58 mmol) was added to a stirred suspension of 2,6-diacetylpyridine **271** (4.2 g, 26 mmol) and *p*-toluenesulfonic acid (0.3 g, 1.5 mmol) in anhydrous toluene (350 mL) and heated at reflux under Dean-Stark conditions for 16 h. The solvent was removed in vacuo and the yellow solid recrystallised from hot dichloromethane to give 2,6-bis-[1-(2,6-diisopropylphenylimino) ethyl]pyridine **273a** (9.1 g, 19.0 mmol, 73 %) as yellow needles.

m.p. 298–299 °C (CH_2Cl_2). **^{1}H NMR** (400 MHz, $CDCl_3$) 8.50 (d, J = 8.0 Hz, 2H, pyH), 7.95 (t, J = 8.0 Hz, 1H, pyH), 7.21-7.17 (m, 4H, ArH), 7.15-7.09

(m, 2H, ArH), 2.79 (sept., J = 7.0 Hz, 4H, CH), 2.29 (s, 6H, CH_3), 1.18 (d, J = 7.0 Hz, 24H, CH_3). **^{13}C NMR** (126 MHz, $CDCl_3$) 166.9 (2 × C), 155.1 (2 × C), 146.5 (2 × C), 136.8 (CH), 135.8 (4 × C), 123.6 (2 × CH), 123.0 (4 × CH), 122.2 (2 × CH), 28.3 (2 × CH), 23.2 (4 × CH_3), 22.9 (4 × CH_3), 17.1 (2 × CH_3). **IR** (neat) ν_{max} cm^{-1} 3060, 2959, 2925, 2867, 1643, 1570, 1455, 1435, 1364.

Data were in accordance with those previously reported [4].

2,6-Bis-[1-(2,6-diethylphenylimino)ethyl]pyridine **273b**

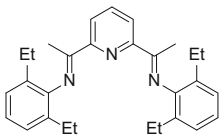

2,6-Diethylaniline **272b** (4.66 mL, 28.3 mmol) was added to a stirred suspension of 2,6-diacetylpyridine **271** (2.1 g, 13 mmol) and *p*-toluenesulfonic acid (0.14 g, 0.75 mmol) in anhydrous toluene (60 mL) and heated at reflux under Dean-Stark conditions for 16 h. The solvent was removed in vacuo and the yellow solid recrystallised from hot dichloromethane to give 2,6-bis-[1-(2,6-diethylphenylimino) ethyl]pyridine **273b** (4.9 g, 11.5 mmol, 89 %) as yellow needles.

m.p. 185–186 °C (CH_2Cl_2). **^{1}H NMR** (500 MHz, $CDCl_3$) 8.51 (d, J = 8.0 Hz, 2H, pyH), 7.95 (t, J = 8.0 Hz, 1H, pyH), 7.17-7.13 (m, 4H, ArH), 7.09-7.05 (m, 2H, ArH), 2.50-2.34 (m, 8H, CH_2), 2.28 (s, 6H, CH_3), 1.18 (t, J = 7.5 Hz, 12H, CH_3). **^{13}C NMR** (126 MHz, $CDCl_3$) 167.0 (2 × C), 155.1 (2 × C), 147.7 (2 × C), 136.9 (CH), 131.2 (4 × C), 125.9 (4 × CH), 123.3 (2 × CH), 122.2 (2 × CH), 24.6 (4 × CH_2), 16.8 (2 × CH_3), 13.7 (4 × CH_3). **IR** (neat) ν_{max} cm^{-1} 2970, 2930, 2874, 1638, 1587, 1568, 1452, 1366, 1242, 1198, 1121, 1101, 1076.

Data were in accordance with those previously reported [5].

2,6-Bis-[1-(2,4,6-trimethylphenylimino)ethyl]pyridine **273c**

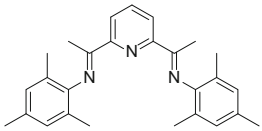

2,4,6-Trimethylaniline **272c** (3.86 mL, 27.5 mmol) was added to a stirred suspension of 2,6-diacetylpyridine **271** (2.04 g, 12.5 mmol) and *p*-toluenesulfonic acid (0.14 g, 0.75 mmol) in anhydrous toluene (60 mL) and heated at reflux under Dean-Stark conditions for 16 h. The solvent was removed in vacuo and the yellow solid recrystallised from hot dichloromethane to give 2,6-bis-[1-(2,4,6-trimethylphenylimino)ethyl]pyridine **273c** (4.1 g, 10.3 mmol, 82 %) as yellow needles.

m.p. 167–168 °C (CH_2Cl_2). **^{1}H NMR** (400 MHz, $CDCl_3$) 8.51 (d, J = 8.0 Hz, 2H, pyH), 7.93 (t, J = 8.0 Hz, 1H, pyH), 6.92 (s, 4H, ArH), 2.32 (s, 6H, CH_3), 2.26 (s, 6H, CH_3), 2.04 (s, 12H, CH_3). **^{13}C NMR** (126 MHz, $CDCl_3$) 167.4 (2 × C), 155.2 (2 × C), 146.2 (2 × C), 136.8 (CH), 132.2 (2 × C), 128.5 (4 × CH), 125.2 (4 × C), 122.2 (2 × CH), 20.7 (2 × CH_3), 17.9 (4 × CH_3), 16.4 (2 × CH_3). **IR** (neat) ν_{max} cm^{-1} 2911, 2857, 1636, 1568, 1476, 1450, 1364, 1294, 1250, 1213, 1119, 1074, 854, 816, 789, 739, 721.

Data were in accordance with those previously reported [6].

(±)-*N*,*N*′-Bis(pyridin-2-ylmethylene)cyclohexane-1,2-diamine **276**

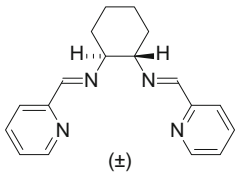

2-Pyridinecarboxaldehyde **274** (2.52 mL, 26.4 mmol) in anhydrous methanol (30 mL) was added to a solution of (±)-*trans*-diaminocyclohexane **275** (1.44 mL, 12 mmol) in anhydrous methanol (30 mL) and molecular sieves (3 Å) at 0 °C under an atmosphere of nitrogen. The reaction mixture was shaken for 16 h, allowing the reaction to warm to room temperature. The solution was filtered through Celite and the solvent removed in vacuo to give the crude product which was recrystallised from hot ethanol to give (±)-*N*,*N*′-bis(pyridin-2-ylmethylene) cyclohexane-1,2-diamine **276** (2.6 g, 8.9 mmol, 74 %) as colourless needles.

m.p. 139–141 °C (EtOH). **^{1}H NMR** (300 MHz, $CDCl_3$) 8.56 (ddd, J = 5.0, 1.5, 1.0 Hz, 2H, pyH), 8.32 (s, 2H N=CH), 7.89 (dt, J = 8.0, 1.0 Hz, 2H, pyH), 7.65 (ddd, J = 8.0, 1.5, 0.5 Hz, 2H, pyH), 7.23 (ddd, J = 7.5, 5.0, 1.0 Hz, 2H, pyH), 3.60-3.49 (m, 2H, CH), 1.95-1.78 (m, 6H, CH_2), 1.58-1.46 (m, 2H, CH_2). **^{13}C NMR** (100 MHz, $CDCl_3$) 161.4, 154.6, 149.2, 136.4, 124.5, 121.3, 73.5, 32.7, 24.3. **IR** (neat) ν_{max} cm^{-1} 3053, 3007, 2936, 2851, 1644, 1586, 1567, 1467, 1436, 1370.

Data were in accordance with those previously reported [7].

Bis[1,2-bis(diphenylphosphino)ethane]iron bis(acetonitrile) ditetrafluoroborate **278**

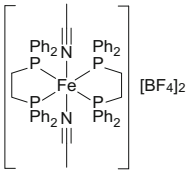

Bis(diphenylphosphino)ethane **154** (2.4 g, 6 mmol) in toluene (40 ml) was added to a solution of iron(II)tetrafluoroborate hexahydrate **277** (1.0 g, 3 mmol) in acetonitrile (25 ml) and stirred overnight at room temperature. The solvent was removed in vacuo and the solid was washed with dichloromethane (2 × 20 ml) and recrystallised from a 1:1 mixture of hot acetone/acetonitrile to give bis[1,2-bis (diphenylphosphino)ethane]iron bis(acetonitrile) ditetrafluoroborate **278** (2.6 g, 2.4 mmol, 79 %) as a bright red solid.

^{1}H NMR (400 MHz, CD_3CN) 7.53 (t, J = 7.5 Hz, 8H, ArH), 7.30 (t, J = 7.5 Hz, 16H, ArH), 7.01-6.86 (m, 16H, ArH), 3.01-2.89 (m, 8H, CH_2), 1.96 (s, 6H, CH_3). **^{13}C NMR** (100 MHz, CD_3CN) 142.1, 133.7 (CH), 132.6 (CH), 130.9 (app. quin., J = 9.0 Hz, C), 130.5 (CH), 29.4 (app. quin., J = 10.5 Hz, CH_2), 1.84 (CH_3). **^{31}P NMR** (162 MHz, CD_3CN) 56.4.

Data were in accordance with those previously reported [8].

d_5-Ethylmagnesium bromide ***d*$_5$-280**

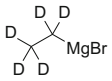

Magnesium turnings (1.3 g, 53 mmol) and anhydrous diethyl ether (15 mL) were added to an oven-dried multi-necked round-bottomed flask with a reflux condenser attached, under a nitrogen atmosphere. d_5-Bromoethane (0.3 mL, 0.5 g, 4.4 mmol) was added, followed by a single crystal of iodine. The remaining d_5-bromoethane (3.0 mL, 4.5 g, 39.6 mmol) was added over the course of an hour at a rate to maintain reflux. The reaction was stirred for a further 90 min, allowed settle, and the prepared Grignard reagent transferred by syringe to an oven-dried J. Young's sample flask. The concentration of d_5-ethylmagnesium bromide ***d*$_5$-280** was determined to be 3.0 M by titration using 2-hydroxybenzaldehyde phenylhydrazone.

1-Phenyl-2-(phenylsilyl)ethane **281**

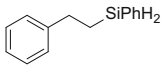

According to General Procedure **A**, styrene **53** (80 μL, 0.7 mmol), phenylsilane **47** (95 μL, 0.77 mmol), iron(II) chloride **279** (0.9 mg, 0.007 mmol), 2,6-bis-[1-(2,6-diethylphenylimino)ethyl]pyridine **273b** (3.0 mg, 0.007 mmol) and ethylmagnesium bromide **280** (2 drops, 0.015 mmol) were reacted in anhydrous tetrahydrofuran (3 mL) to give the crude reaction product, which was purified by filtration through a plug of silica using 0.5 % ethyl acetate/petroleum ether to give 1-phenyl-2-(phenylsilyl)ethane **281** as a colourless oil (140 mg, 0.66 mmol, 94 %).

^{1}H NMR (400 MHz, $CDCl_3$) 7.63-7.58 (m, 2H, ArH), 7.46-7.37 (m, 3H, ArH), 7.34-7.28 (m, 2H, ArH), 7.25-7.18 (m, 3H, ArH), 4.36 (t, J = 3.5 Hz, 2H, SiH_2), 2.84-2.77 (m, 2H, $ArCH_2$), 1.38-1.31 (m, 2H, $SiCH_2$). **^{13}C NMR** (101 MHz, $CDCl_3$) 144.0 (C), 135.2 (2 × CH), 132.1 (C), 129.6 (CH), 128.3 (2 × CH), 128.0 (2 × CH), 127.9 (2 × CH), 125.8 (CH), 31.1 (CH_2), 12.1 (CH_2). **^{29}Si NMR** (79 MHz, $CDCl_3$) −31.0. **IR** (neat) ν_{max} cm^{-1} 3024, 2965, 2922, 2129, 1495, 1452, 1429, 1260, 1115, 1057, 1032, 1013, 934, 843, 814, 696.

Data were in accordance with those previously reported [9].

Di(phenylethyl)phenylsilane **284**

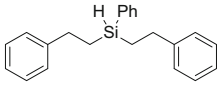

According to General Procedure **A**, styrene **53** (80 μL, 0.7 mmol), phenylsilane **47** (43 μL, 0.35 mmol), iron(II) chloride **279** (0.9 mg, 0.007 mmol), 2,6-bis-[1-(2,6-diethylphenylimino)ethyl]pyridine **273b** (3.0 mg, 0.007 mmol) and ethylmagnesium bromide **280** (2 drops, 0.015 mmol) were reacted in anhydrous tetrahydrofuran (3 mL) to give the crude reaction product, which was purified by filtration through a plug of silica using 0.5 % ethyl acetate/petroleum ether to give *di(phenylethyl)phenylsilane* **284** as a colourless oil (102 mg, 0.32 mmol, 91 % based on silane).

^{1}H NMR (400 MHz, $CDCl_3$) 7.59-7.54 (m, 2H, ArH), 7.44-7.36 (m, 3H, ArH), 7.31-7.25 (m, 4H, ArH), 7.21-7.15 (m, 6H, ArH), 4.37 (quin., J = 3.5 Hz, 1H, SiH), 2.75-2.67 (m, 2H, $ArCH_2$), 1.29-1.20 (m, 2H, $SiCH_2$). **^{13}C NMR** (101 MHz, $CDCl_3$) 144.4 (2 × C), 134.8 (C), 134.7 (2 × CH), 129.4 (CH), 128.3 (4 × CH), 128.0 (2 × CH), 127.8 (4 × CH), 125.7 (2 × CH), 30.5 (2 × CH_2), 13.9 (2 × CH_2). **^{29}Si NMR** (79 MHz, $CDCl_3$) −9.6. **IR** (neat) ν_{max} cm^{-1} 3025, 2965, 2922, 2110, 1603, 1495, 1452, 1427, 1260, 1112, 1057, 1032, 1011. **HRMS** (EI) calculated for $C_{22}H_{24}Si$ 316.16418. Found 316.16417.

1-Phenyl-2-(diphenylsilyl)ethane **300**

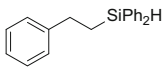

According to General Procedure **A**, styrene **53** (80 μL, 0.7 mmol), diphenylsilane **255** (130 μL, 0.7 mmol), iron(II) chloride **279** (0.9 mg, 0.007 mmol), 2,6-bis-[1-(2,6-diethylphenylimino)ethyl]pyridine **273b** (3.0 mg, 0.007 mmol) and ethylmagnesium bromide **280** (2 drops, 0.015 mmol) were reacted in anhydrous tetrahydrofuran (3 mL) to give the crude reaction product, which was purified by filtration through a plug of silica using 0.5 % ethyl acetate/petroleum ether to give 1-phenyl-2-(diphenylsilyl)ethane **300** as a colourless oil (184 mg, 0.64 mmol, 91 %).

^{1}H NMR (400 MHz, $CDCl_3$) 7.64-7.57 (m, 4H, ArH), 7.45-7.38 (m, 6H, ArH), 7.33-7.27 (m, 2H, ArH), 7.24-7.18 (m, 3H, ArH), 4.94 (t, J = 3.5 Hz, 1H, SiH), 2.84-2.77 (m, 2H, $ArCH_2$), 1.59-1.52 (m, 2H, $SiCH_2$). **^{13}C NMR** (101 MHz, $CDCl_3$) 144.3 (C), 135.1 (4 × CH), 134.1 (2 × C), 129.6 (2 × CH), 128.3 (2 × CH), 128.0 (4 × CH), 127.8 (2 × CH), 125.7 (CH), 30.4 (CH_2), 14.3 (CH_2). **^{29}Si NMR** (79 MHz, $CDCl_3$) −14.1.

Data were in accordance with those previously reported [10].

1-Phenyl-2-(diphenylsilyl)(ethane-d_n) ***d*$_n$-300**

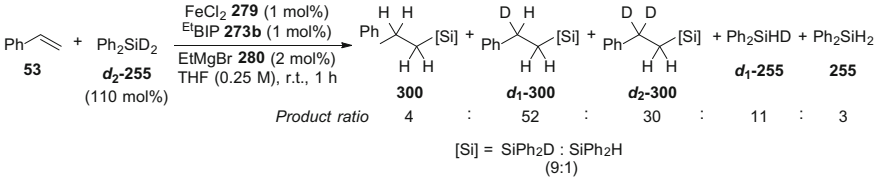

According to General Procedure **A**, styrene **53** (80 μL, 0.7 mmol), diphenyl(silane-d_2) ***d*$_2$-255** (143 mg, 0.77 mmol), iron(II) chloride **279** (0.9 mg, 0.007 mmol), 2,6-bis-[1-(2,6-diethylphenylimino)ethyl]pyridine **273b** (3.0 mg, 0.007 mmol) and ethylmagnesium bromide **280** (2 drops, 0.015 mmol) were reacted in anhydrous tetrahydrofuran (3 mL) to give the crude reaction product, which was purified by filtration through a plug of silica using 0.5 % ethyl acetate/petroleum ether to give a mixture of silanes: 1-phenyl-2-(diphenylsilyl)(ethane-d_n) ***d*$_n$-300**; diphenyl(silane-d_1) ***d*$_1$-255**; and diphenylsilane **255** as a colourless oil (201 mg).

All protons were accounted for in ^{1}H NMR spectra of crude reaction material. Around 30–35 % of the protons from the benzylic position of styrene had formally transferred to silicon, with deuterium transfer in the opposite direction (see ^{1}H spectra of crude reaction). No deuterium incorporation in homobenzylic (alpha to silicon) position, by ^{1}H, ^{2}H and ^{13}C NMR spectroscopy.

1-Phenyl-2-(diphenylsilyl)(ethane-d_n) ***d*$_n$-300**: **^{1}H NMR** (500 MHz, $CDCl_3$) 7.60-7.57 (m, 4H, ArH), 7.44-7.36 (m, 6H, ArH), 7.30-7.25 (m, 2H, ArH), 7.21-7.15 (m, 3H, ArH), 4.90 (t, J = 3.6 Hz, 0.11H, SiH), 2.80-2.72 (m, 0.67H, $ArCH_2$), 1.54-1.49 (m, 2H, $SiCH_2$). **^{13}C NMR** (126 MHz, $CDCl_3$)—selected peaks: 30.5 (s, **300**, $ArCH_2$), 30.2 (t, J = 19.5 Hz, ***d*$_1$-300**, ArCHD), 29.8 (quin., J = 19.5 Hz, ***d*$_2$-300**, $ArCD_2$), 14.3 (**300**, $SiCH_2$), 14.2 (***d*$_1$-300**, $SiCH_2$), 14.1 (***d*$_2$-300**, $SiCH_2$). **^{2}H NMR** (61 MHz, $CHCl_3$) 4.93-4.78 (br, SiD), 2.75-2.53 (br, ArCD (H/D)).

1-Phenyl-2-(diphenylsilyl)(ethane-d_n) ***d*$_n$-300**: NMR spectra

^{1}H NMR spectra: 500 MHz—crude reaction mixture:

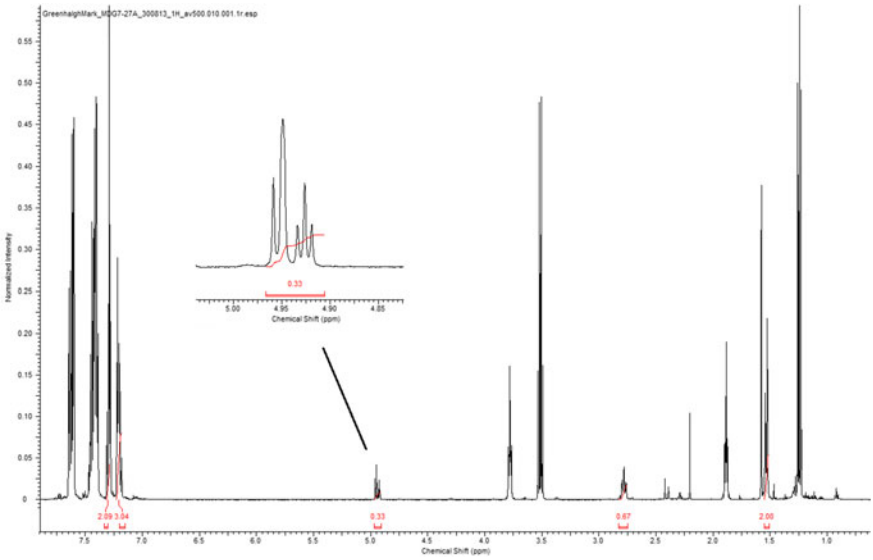

^{1}H NMR spectra: 500 MHz

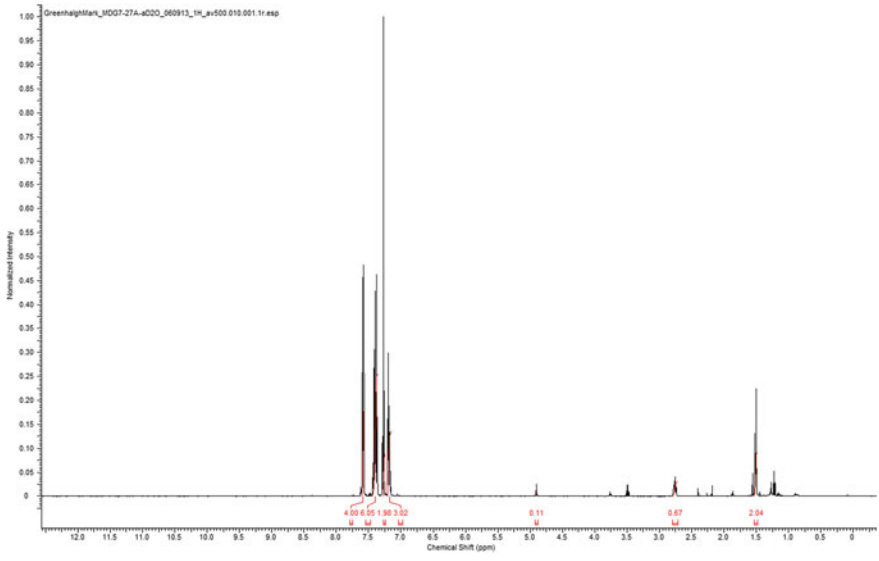

^{13}C NMR spectra: 126 MHz

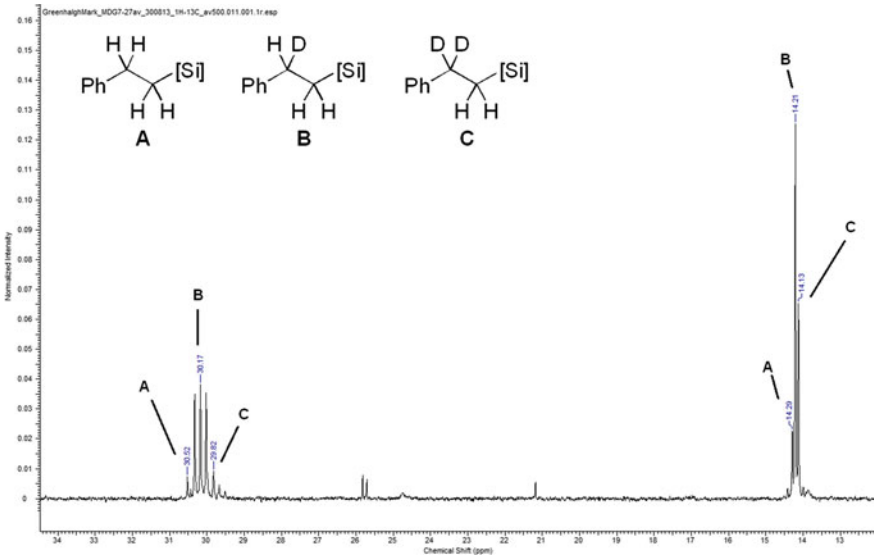

^{2}H NMR spectra: 61 MHz

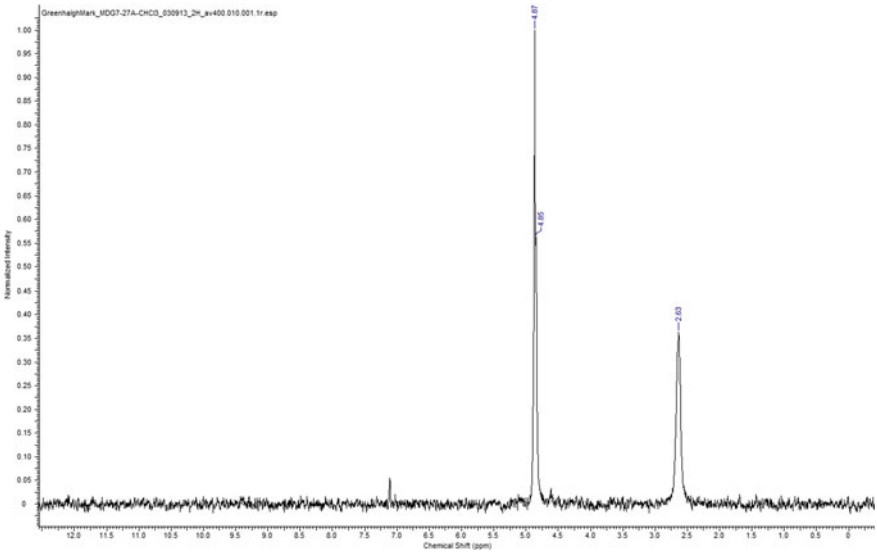

1-Phenyl-2-(diethylsilyl)ethane **301**

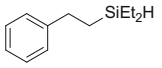

According to General Procedure **A**, styrene **53** (80 μL, 0.7 mmol), diethylsilane **296** (91 μL, 0.7 mmol), iron(II) chloride **279** (0.9 mg, 0.007 mmol), 2,6-bis-[1-(2,6-diethylphenylimino)ethyl]pyridine **273b** (3.0 mg, 0.007 mmol) and ethylmagnesium bromide **280** (2 drops, 0.015 mmol) were reacted in anhydrous tetrahydrofuran (3 mL) to give the crude reaction product, which was purified by filtration through a plug of silica using 0.5 % ethyl acetate/petroleum ether to give *1-phenyl-2-(diethylsilyl)ethane* **301** as a colourless oil (120 mg, 0.63 mmol, 89 %).

^{1}H NMR (400 MHz, $CDCl_3$) 7.36-7.28 (m, 2H, ArH), 7.25-7.18 (m, 3H, ArH), 3.73 (sept., J = 3.0 Hz, 1H, SiH), 2.75-2.68 (m, 2H, $ArCH_2$), 1.04 (t, J = 8.0 Hz, 6H, CH_3), 1.06-1.00 (m, 2H, $SiCH_2CH_2$), 0.65 (qd, J = 8.0, 3.0 Hz, 4H, $SiCH_2CH_3$). **^{13}C NMR** (101 MHz, $CDCl_3$) 145.0 (C), 128.3 (2 × CH), 127.8 (2 × CH), 125.6 (CH), 30.8 (CH_2), 12.8 (CH_2), 8.2 (2 × CH_3), 2.8 (2 × CH_2). **^{29}Si NMR** (79 MHz, $CDCl_3$) −1.9. **IR** (neat) ν_{max} cm^{-1} 3026, 2953, 2911, 2873, 2098, 1495, 1454, 1413, 1014, 970, 799, 727, 696. **MS** (EI, 70 eV) *m/z* (%) 192 (M^+, 9), 163 (56), 135 (47), 107 (100), 59 (35). **HRMS** (ESI^+) calculated for $C_{12}H_{20}Si$ 192.13343. Found 192.13288.

Gram-scale, solvent-free hydrosilylation of styrene

n-Butyllithium **283** (1.5 M in hexanes, 10 μL, 3 drops, 0.015 mmol) was added to a suspension of 2,6-bis-[1-(2,6-diethylphenylimino)ethyl]pyridine iron(II) chloride **367** (^{Et}BIPFeCl_2) (3.9 mg, 0.007 mmol) in styrene **53** (1.04 g, 10 mmol) under an atmosphere of nitrogen. Diethylsilane **296** (1.4 mL, 10.8 mmol) was added resulting in an instantaneous increase in the reaction temperature. Within 90 s the reaction temperature began to decrease, and the reaction was quenched with aqueous sulfate buffer (10 mL). The aqueous phase was extracted with diethyl ether (3 × 20 mL). The combined organic extracts were washed with water and brine, dried ($MgSO_4$) and concentrated in vacuo. The resulting oil was passed through a plug of silica (0.5 % ethyl acetate/hexane) and concentrated in vacuo to give 1-phenyl-2-(diethylsilyl)ethane **301** as a colourless oil (1.79 g, 9.32 mmol, 93 %). (For data see above)

Benzyldimethylhexylsilane **310**.

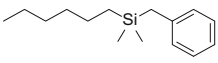

According to General Procedure **A**, 1-hexene **306** (87 μL, 0.7 mmol), benzyldimethylsilane **298** (110 μL, 0.7 mmol), iron(II) chloride **279** (0.9 mg, 0.007 mmol), 2,6-bis-[1-(2,6-diethylphenylimino)ethyl]pyridine **273b** (3.0 mg,

0.007 mmol) and ethylmagnesium bromide **280** (2 drops, 0.015 mmol) were reacted in anhydrous tetrahydrofuran (3 mL) to give the crude reaction product, which was purified by filtration through a plug of silica using 0.5 % ethyl acetate/petroleum ether to give benzyldimethylhexylsilane **310** as a colourless oil (118 mg, 0.50 mmol, 72 %).

^{1}H NMR (400 MHz, $CDCl_3$) 7.24-7.19 (m, 2H, ArH), 7.10-7.04 (m, 1H, ArH), 7.03-6.98 (m, 2H, ArH), 2.09 (s, 2H, $ArCH_2$), 1.35-1.23 (m, 8H, CH_2), 0.91 (t, J = 7.0 Hz, 3H, CH_3), 0.54-0.47 (m, 2H, $SiCH_2$), −0.04 (s, 6H, $SiCH_3$). **^{13}C NMR** (101 MHz, $CDCl_3$) δ_C (101 MHz, $CDCl_3$) 140.5 (C), 128.09 (2 × CH), 128.05 (2 × CH), 123.8 (CH), 33.3 (CH_2), 31.6 (CH_2), 25.6 (CH_2), 23.7 (CH_2), 22.6 (CH_2), 14.8 (CH_2), 14.2 (CH_3), −3.6 (2 × $SiCH_3$). **^{29}Si NMR** (79 MHz, $CDCl_3$) 2.3. **IR** (neat) ν_{max} cm^{-1} 2955, 2920, 2857, 1601, 1493, 1452, 1248, 1206, 1153, 1055, 1034, 825. **HRMS** (EI) calculated for $C_{15}H_{26}Si$ 234.17983. Found 234.17953.

Data were in accordance with those previously reported [11].

3-Hexyl-1,1,1,3,5,5,5-heptamethyltrisiloxane **311**

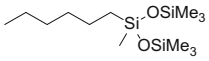

According to General Procedure **A**, 1-hexene **306** (87 μL, 0.7 mmol), 1,1,1,3,5,5,5-heptamethyltrisiloxane **249** (190 μL, 0.7 mmol), iron(II) chloride **279** (0.9 mg, 0.007 mmol), 2,6-bis-[1-(2,6-diethylphenylimino)ethyl]pyridine **273b** (3.0 mg, 0.007 mmol) and ethylmagnesium bromide **280** (2 drops, 0.015 mmol) were reacted in anhydrous tetrahydrofuran (3 mL) to give the crude reaction product, which was purified by filtration through a plug of silica using 0.5 % ethyl acetate/petroleum ether to give 3-hexyl-1,1,1,3,5,5,5-heptamethyltrisiloxane **311** as a colourless oil (180 mg, 0.59 mmol, 84 %).

^{1}H NMR (400 MHz, $CDCl_3$) 1.36-1.23 (m, 8H, CH_2), 0.91 (t, J = 7.0 Hz, 3H, CH_3), 0.50-0.43 (m, 2H, $SiCH_2$), 0.09 (s, 18H, $SiCH_3$), 0.00 (s, 3H, $SiCH_3$). **^{13}C NMR** (101 MHz, $CDCl_3$) 32.9 (CH_2), 31.6 (CH_2), 23.0 (CH_2), 22.6 (CH_2), 17.6 (CH_2), 14.1 (CH_3), 1.9 (6 × CH_3), −0.3 (CH_3). **^{29}Si NMR** (79 MHz, $CDCl_3$) 6.8. **HRMS** (EI) calculated for $C_{13}H_{34}O_2Si_3$ 306.18612. Found 306.18657.

Data were in accordance with those previously reported [12].

Hexylpentamethyldisiloxane **312**

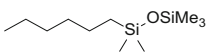

According to General Procedure **A**, 1-hexene **306** (87 μL, 0.7 mmol), pentamethyldisiloxane **307** (137 μL, 0.7 mmol), iron(II) chloride **298** (0.9 mg, 0.007 mmol), 2,6-bis-[1-(2,6-diethylphenylimino)ethyl]pyridine **273b** (3.0 mg, 0.007 mmol) and ethylmagnesium bromide **280** (2 drops, 0.015 mmol) were

reacted in anhydrous tetrahydrofuran (3 mL) to give the crude reaction product, which was purified by filtration through a plug of silica using 0.5 % ethyl acetate/petroleum ether to give hexylpentamethyldisiloxane **312** as a colourless oil (137 mg, 0.59 mmol, 84 %).

^{1}H NMR (400 MHz, $CDCl_3$) 1.34-1.26 (m, 8H, CH_2), 0.90 (t, J = 7.0 Hz, 3H, CH_3), 0.55-0.48 (m, 2H, $SiCH_2$), 0.07 (s, 9H, $SiCH_3$), 0.04 (s, 6H, $SiCH_3$). **^{13}C NMR** (151 MHz, $CDCl_3$) 33.1 (CH_2), 31.6 (CH_2), 23.2 (CH_2), 22.6 (CH_2), 18.4 (CH_2), 14.1 (CH_3), 2.0 (2 × CH_3), 0.3 (CH_3). **^{29}Si NMR** (99 MHz, $CDCl_3$) 7.5, 6.9. **IR** (neat) ν_{max} cm^{-1} 2957, 2922, 2857, 1252, 1053, 839.

Data were in accordance with those previously reported [13].

1-(3-Vinylbenzoyl)piperidine **317**

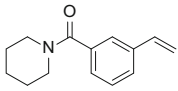

Prepared according to a literature procedure [14].

Triphenylphosphine **315** (polymer bound, 1.83 g, 5.5 mmol) and iodine (1.40 g, 5.5 mmol) were added to anhydrous dichloromethane (10 mL) and stirred at 0 °C for 5 min under nitrogen. A solution of 3-vinylbenzoic acid **314** (740 mg, 5 mmol) in anhydrous dichloromethane (10 mL) was added followed by the dropwise addition of diisopropylethylamine **316** (1.3 mL, 7.5 mmol) and piperidine **313** (0.55 mL, 5.5 mmol). The reaction was allowed to warm to room temperature over 12 h. The reaction was filtered and the residue washed with dichloromethane (3 × 20 mL). The organic fraction was washed with saturated sodium thiosulfate, water, and brine, dried ($MgSO_4$) and concentrated in vacuo to give the crude product, which was purified by flash silica chromatography (20 % EtOAc/hexane) to give *1-(3-vinylbenzoyl)piperidine* **317** as a yellow oil (797 mg, 3.7 mmol, 74 %).

^{1}H NMR (500 MHz, $CDCl_3$) 7.46-7.42 (m, 2H, ArH), 7.35 (t, J = 8.0 Hz, 1H, ArH), 7.28-7.24 (m, 1H, ArH), 6.72 (dd, J = 17.5, 11.0 Hz, 1H, CH), 5.78 (dd, J = 17.5, 0.5 Hz, 1H, CH), 5.30 (dd, J = 11.0, 0.5 Hz, 1H, CH), 3.72 (br, 2H, CH_2), 3.35 (br, 2H, CH_2), 1.69 (br, 4H, CH_2), 1.52 (br, 2H, CH_2). **^{13}C NMR** (100 MHz, $CDCl_3$) 170.1 (C=O), 137.9 (C), 136.8 (C), 136.2 (CH), 128.5 (CH), 127.1 (CH), 126.0 (CH), 124.6 (CH), 114.8 (CH), 48.8 (br, CH_2), 43.1 (br, CH_2), 26.6 (br, CH_2), 25.6 (br, CH_2), 24.6 (CH_2). **IR** (neat) ν_{max} cm^{-1} 2936, 2855, 1626, 1441, 1277, 1206, 1109, 997, 903. **HRMS** (EI^+) calculated for $C_{14}H_{17}NO$ 215.13047. Found 215.12992.

N-Benzoyl-4-vinylaniline **320**

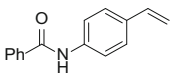

Triphenylphosphine **315** (1.44 g, 5.5 mmol) and iodine (1.40 g, 5.5 mmol) were added to anhydrous dichloromethane (18 mL) and stirred at 0 °C for 5 min under nitrogen. Benzoic acid **318** (611 mg, 5 mmol) was added followed by the dropwise addition of diisopropylethylamine **316** (1.3 mL, 7.5 mmol) and a solution of 4-vinylaniline **319** (0.65 mL, 5.5 mmol) in anhydrous dichloromethane (2 mL). The reaction was allowed to warm to room temperature over 12 h. The reaction was filtered and the residue washed with dichloromethane (3 × 20 mL). The organic fraction was washed with saturated sodium thiosulfate, water, and brine, dried ($MgSO_4$) and concentrated in vacuo to give the crude product, which was purified by flash chromatography (15 % EtOAc/Hexane) to give *N*-benzoyl-4-vinylaniline **320** as a colourless solid (380 mg, 1.7 mmol, 34 %).

m.p. 163-165 °C. $\mathbf{R_f}$ 0.5 (25 % EtOAc/Hex). $^{\mathbf{1}}$**H NMR** (500 MHz, $CDCl_3$) 7.91-7.86 (m, 2H, ArH), 7.82 (br, 1H, NH), 7.65-7.61 (m, 2H, ArH), 7.59-7.55 (m, 1H, ArH), 7.54-7.48 (m, 2H, ArH), 7.46-7.41 (m, 2H, ArH), 6.71 (dd, J = 17.5, 11.0 Hz, 1H, CH), 5.73 (dd, J = 17.5, 0.5 Hz, 1H, CH), 5.23 (dd, J = 11.0, 0.5 Hz, 1H, CH). $^{\mathbf{13}}$**C NMR** (126 MHz, $CDCl_3$) 165.6 (C=O), 137.5 (C), 136.1 (CH), 134.9 (C), 134.0 (C), 131.9 (CH), 128.8 (2 × CH), 227.0 (2 × CH), 126.9 (2 × CH), 120.1 (2 × CH), 113.2 (2 × CH). **IR** (neat) ν_{max} cm^{-1} 3335, 3053, 2995, 1649, 1626, 1601, 1587, 1508, 1498, 1422, 1400, 1319, 1248, 1180, 897, 835, 792.

Data were in accordance with those previously reported [15].

2-Allylstyrene **323**

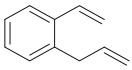

2-Bromostyrene **321** (0.18 g, 1 mmol) was added to magnesium turnings (413 mg, 17 mmol) in anhydrous tetrahydrofuran (10 mL) in a flask equipped with a reflux condenser, at room temperature and under a nitrogen atmosphere. A single iodine crystal was added to initiate the reaction. Within 1 min the iodine colour disappeared and the reaction temperature began to increase. The reaction was periodically cooled in ice and the remaining 2-bromostyrene **321** (1.62 g, 9 mmol) was added in portions over 30 min at a rate to prevent the reaction temperature increasing excessively. The reaction was stirred for an additional 30 min at 0 °C, and then allowed to settle at room temperature for 1 h. The freshly prepared Grignard reagent was added to allyl bromide **322** (1.73 mL, 20 mmol) in anhydrous tetrahydrofuran (20 mL) at −78 °C over the course of 5 min. The reaction was stirred at −78 °C for an additional 1 h, and then allowed to warm to room temperature over 1 h. Aqueous sulfate buffer (20 mL) was added and the aqueous phased extracted with diethyl ether (3 × 25 mL). The combined organic phases were dried ($MgSO_4$) and concentrated in vacuo to give the crude product, which was purified by flash silica chromatography (hexane) to give 2-allylstyrene **323** as a colourless oil (761 mg, 5.28 mmol, 53 %).

^{1}H NMR (400 MHz, $CDCl_3$) 7.56-7.50 (m, 1H, ArH), 7.27-7.21 (m, 2H, ArH), 7.21-7.16 (m, 1H, ArH), 6.99 (dd, *J* = 17.5, 11.0 Hz, 1H, CH), 5.99 (ddt, *J* = 17.0, 10.0, 6.0 Hz, 1H, CH), 5.67 (dd, *J* = 17.5, 1.5 Hz, 1H, CH), 5.23 (dd, *J* = 11.0, 1.5 Hz, 1H, CH), 5.09 (app. dq, *J* = 10.0, 1.5 Hz, 1H, CH), 5.00 (app. dq, *J* = 17.0, 1.5 Hz, 1H, CH), 3.48 (app. dt, *J* = 6.0, 1.5 Hz, 2H, CH_2). **^{13}C NMR** (101 MHz, $CDCl_3$) 137.0 (C), 136.8 (CH), 136.7 (C), 134.6 (CH), 129.7 (CH), 127.9 (CH), 126.6 (CH), 125.7 (CH), 115.8 (CH), 115.5 (CH), 37.4 (CH_2).

Data were in accordance with those previously reported [16].

4-(3-Butenyl)-styrene **326**

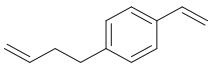

4-Vinylbenzylmagnesium chloride **325** was prepared according to a procedure reported by Brown [17].

Magnesium turnings (1.6 g, 66 mmol) were added to an oven-dried Schlenk tube with a magnetic stirrer bar and sealed with a pressure-equalising dropping funnel. The vessel was back-filled 3 times with nitrogen and the magnesium turnings were stirred vigorously overnight under a nitrogen atmosphere. After stirring overnight the magnesium turnings appeared dark grey, and the bottom of the flask and stirrer bar had a metallic coating. Anhydrous diethyl ether was added to cover the magnesium, and the reaction cooled to 0 °C. 4-Vinylbenzylchloride **324** (1.53 g, 10 mmol) in anhydrous diethyl ether (15 mL) was added dropwise over 3 h. The reaction was stirred for a further 2 h at 0 °C. The solution was transferred by syringe to a clean, oven-dried Schlenk tube, made up to 20 mL with extra anhydrous diethyl ether and stored under a nitrogen atmosphere. The concentration of the Grignard reagent was determined to be 0.5 M by titration against 2-hydroxybenzaldehyde phenylhydrazone.

The freshly prepared Grignard reagent **325** was added to allyl bromide **322** (1.73 mL, 20 mmol) in anhydrous tetrahydrofuran (20 mL) at −78 °C over the course of 5 min. The reaction was stirred at −78 °C for an additional 1 h, and then allowed to warm to room temperature over 1 h. Aqueous sulfate buffer (20 mL) was added and the aqueous phased extracted with diethyl ether (3 × 25 mL). The combined organic phases were dried ($MgSO_4$) and concentrated in vacuo to give the crude product, which was purified by flash silica chromatography (hexane) to give *4-(3-butenyl)-styrene* **326** as a colourless oil (1.20 g, 7.58 mmol, 76 %).

^{1}H NMR (400 MHz, $CDCl_3$) 7.40-7.33 (m, 2H, ArH), 7.21-7.14 (m, 2H, ArH), 6.72 (dd, *J* = 17.5, 11.0 Hz, 1H, CH), 5.88 (ddt, *J* = 17.0, 10.0, 6.5 Hz, 1H, CH), 5.74 (dd, *J* = 17.5, 1.0 Hz, 1H, CH), 5.22 (dd, *J* = 11.0, 1.0 Hz, 1H, CH), 5.07 (app. dq, *J* = 17.0, 1.5 Hz, 1H, CH), 5.03-4.98 (m, 1H, CH), 2.76-2.69 (m, 2H, $ArCH_2$), 2.44-2.35 (m, 2H, CH_2). **^{13}C NMR** (101 MHz, $CDCl_3$) 141.6 (C), 138.0 (CH), 136.6 (CH), 135.2 (C), 128.6 (2 × CH), 126.1 (2 × CH), 115.0 (CH), 112.9 (CH), 35.4 (CH_2), 35.1 (CH_2). **IR** (neat) ν_{max} cm^{-1} 3082, 2978, 2926, 2855, 1639,

1630, 1512, 1439, 1406, 1119, 1016, 989, 903, 841, 826. **HRMS** (EI) calculated for $C_{12}H_{14}$ 158.10900. Found 158.10828.

1-Phenyl-2-(4-vinylbenzene)-ethanone **328**

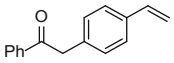

4-Vinylbenzylmagnesium chloride **325** (prepared as above, 8 mL, 0.5 M in diethyl ether, 4 mmol) was added to benzonitrile **327** (0.4 mL, 4 mmol) in anhydrous diethyl ether (15 mL) at 0 °C under an atmosphere of nitrogen. The reaction was allowed to warm to room temperature over 90 min. Aqueous HCl (5 mL, 1 M) was added and the reaction was stirred vigorously for 30 min. The aqueous phase was extracted with diethyl ether (3 × 20 mL), and the combined organic phases dried ($MgSO_4$) and concentrated in vacuo. The crude product was purified by flash silica chromatography (7 % EtOAc/Hexane) to give *1-phenyl-2-(4-vinylbenzene)-ethanone* **328** as a colourless amorphous solid (535 mg, 2.41 mmol, 60 %).

m.p. 139–141 °C. **^{1}H NMR** (500 MHz, $CDCl_3$) 8.04-8.00 (m, 2H, ArH), 7.59-7.54 (m, 1H, ArH), 7.50-7.45 (m, 2H, ArH), 7.40-7.36 (m, 2H, ArH), 7.26-7.22 (2H, m, ArH), 6.70 (dd, J = 17.5, 11.0, 1H, CH), 5.73 (dd, J = 17.5, 1.0 Hz, 1H, CH), 5.23 (dd, J = 11.0, 1.0 Hz, 1H, CH), 4.29 (s, 2H, CH_2). **^{13}C NMR** (126 MHz, $CDCl_3$) 197.5 (C=O), 136.6 (C), 136.4 (CH), 136.3 (C), 134.1 (C), 133.2 (CH), 129.6 (2 × CH), 128.64 (2 × CH), 128.60 (2 × CH), 126.5 (2 × CH), 113.7 (CH), 42.3 (CH_2). **IR** (neat) ν_{max} cm^{-1} 3059, 2905, 1688, 1595, 1512, 1447, 1410, 1333, 1219, 1200, 1115, 995, 903, 874, 831, 800, 752, 689, 657. **HRMS** (EI) calculated for $C_{16}H_{14}O$ 222.10392. Found 222.10391.

4-(Phenylethynyl)styrene **334**

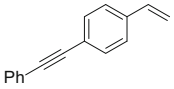

Diisopropylamine **333** (2.8 mL, 20 mmol) was added to a solution of bis(triphenylphosphine) palladium(II) dichloride **331** (280 mg, 0.4 mmol), copper(I) iodide **332** (38 mg, 0.2 mmol), 4-bromostyrene **330** (1.3 mL, 10 mmol) and phenylacetylene **329** (1.3 mL, 12 mmol) in anhydrous tetrahydrofuran (50 mL) and the reaction was heated at reflux for 16 h. The reaction was cooled, filtered and the residue washed with diethyl ether (2 × 10 mL). The organic phase was washed with water and brine, dried ($MgSO_4$) and concentrated in vacuo to give the crude product, which was purified by flash silica chromatography (1 % EtOAc/hexane) to give *4-(phenylethynyl)styrene* **334** as a colourless solid, which rapidly turned yellow upon aging (1.91 g, 9.35 mmol, 94 %).

m.p. 81–83 °C. **^{1}H NMR** (500 MHz, $CDCl_3$) 7.57-7.53 (m, 2H, ArH), 7.52-7.48 (m, 2H, ArH), 7.43-7.38 (m, 2H, ArH), 7.39-7.32 (m, 2H, ArH), 6.73 (dd, *J* = 17.5, 11.0 Hz, 1H, CH), 5.80 (dd, *J* = 17.5, 0.5 Hz, 1H, CH), 5.31 (dd, *J* = 11.0, 0.5 Hz, 1H, CH). **^{13}C NMR** (126 MHz, $CDCl_3$) 137.4 (C), 136.3 (CH), 131.8 (2 × CH), 131.6 (2 × CH), 128.3 (2 × CH), 128.3 (CH), 126.2 (2 × CH), 123.3 (C), 122.6 (C), 114.7 (CH), 90.0 (C), 89.4 (C). **IR** (neat) ν_{max} cm^{-1} 2981, 1815, 1625, 1506, 1483, 1440, 1404, 1177, 1056, 993, 903, 843, 752, 691. **HRMS** (EI) calculated for $C_{16}H_{14}$ 204.09335. Found 204.09348.

4-Morpholinostyrene **336**

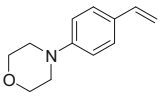

4-Morpholinobenzaldehyde (1.91 g, 10 mmol) was added to potassium carbonate (2.2 g, 16 mmol) and methyltriphenylphosphonium bromide **335** (4.2 g, 12 mmol) in anhydrous 1,4-dioxane (15 mL), and heated at reflux for 16 h. The reaction mixture was cooled, filtered and concentrated in vacuo. The residue was purified by flash silica chromatography (10 % EtOAc/Hex) to give *4-morpholinostyrene* **336** as white needles (1.29 g, 6.82 mmol, 68 %).

m.p. 98–99 °C. **^{1}H NMR** (400 MHz, $CDCl_3$) 7.38-7.33 (m, 2H, ArH), 6.91-6.86 (m, 2H, ArH), 6.66 (dd, *J* = 17.5, 11.0 Hz, 1H, CH), 5.62 (dd, *J* = 17.5, 1.0 Hz, 1H, CH), 5.12 (dd, *J* = 11.0, 1.0 Hz, 1H, CH), 3.90-3.85 (m, 4H, CH_2), 3.21-3.16 (m, 4H, CH_2). **^{13}C NMR** (101 MHz, CDCl3) 150.8 (C), 136.2 (CH), 129.5 (C), 127.1 (2 × CH), 115.4 (2 × CH), 111.0 (CH), 66.8 (CH_2), 49.1 (CH_2). **IR** (neat) ν_{max} cm^{-1} 2963, 2851, 2828, 1601, 1514, 1447, 1379, 1331, 1261, 1238, 1190, 1121, 1051, 922, 901, 826. **HRMS** (EI) calculated for $C_{12}H_{15}ON$ 189.11482. Found 189.11500.

3-Iodostyrene **337**

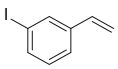

3-Iodobenzaldehyde (1.16 g, 5 mmol) was added to potassium carbonate (1.1 g, 8 mmol) and methyltriphenylphosphonium bromide **335** (2.1 g, 6 mmol) in anhydrous tetrahydrofuran (5 mL) and heated at reflux for 16 h. The reaction mixture was cooled, filtered and concentrated in vacuo. The residue was dissolved in hot *n*-pentane, cooled to 0 °C, filtered, and washed with cold *n*-pentane. The filtrate was dried ($MgSO_4$) and concentrated in vacuo to give *3-iodostyrene* **337** as a colourless oil (645 mg, 2.80 mmol, 56 %).

^{1}H NMR (400 MHz, $CDCl_3$) 7.80-7.76 (m, 1H, ArH), 7.62-7.56 (m, 1H, ArH), 7.40-7.34 (m, 1H, ArH), 7.07 (t, *J* = 8.0 Hz, 1H, ArH), 6.63 (dd, *J* = 17.5,

11.0 Hz, 1H, CH), 5.76 (dd, J = 17.5, 0.5 Hz, 1H, CH), 5.30 (dd, J = 11.0, 0.5 Hz, 1H, CH). **^{13}C NMR** (101 MHz, $CDCl_3$) 139.7 (C), 136.6 (CH), 135.4 (CH), 135.1 (CH), 130.2 (CH), 125.4 (CH), 115.3 (CH), 94.6 (C). **IR** (neat) ν_{max} cm^{-1} 3086, 3053, 3007, 1687, 1585, 1555, 1470, 1408, 1198, 1067, 986, 910, 881, 808, 785. **HRMS** (EI) calculated for C_8H_7I 229.95870. Found 229.95938.

2-Vinylquinoline **338**

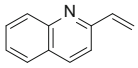

Quinoline-2-carboxaldehyde (1.57 g, 10 mmol) was added to potassium carbonate (2.2 g, 16 mmol) and methyltriphenylphosphonium bromide **335** (4.2 g, 12 mmol) in anhydrous tetrahydrofuran (15 mL), and heated at reflux for 16 h. The reaction mixture was cooled, filtered and concentrated in vacuo. The residue was purified by flash chromatography (15 % EtOAc/Hex) to give 2-vinylquinoline **338** as a yellow oil (1.01 g, 6.52 mmol, 65 %).

^{1}H NMR (400 MHz, $CDCl_3$) 8.12 (d, J = 8.5 Hz, 1H, ArH), 8.08 (dd, J = 8.5, 1.0 Hz, 1H, ArH), 7.79 (dd, J = 8.5, 1.5 Hz, 1H, ArH), 7.71 (td, J = 8.5, 1.5 Hz, 1H, ArH), 7.62 (d, J = 8.5 Hz, 1H, ArH), 7.51 (td, J = 8.5, 1.0 Hz, 1H, ArH), 7.05 (dd, J = 17.5, 11.0 Hz, 1H, CH), 6.29 (dd, J = 17.5, 1.0 Hz, 1H, CH), 5.68 (dd, J = 11.0, 1.0 Hz, 1H, CH). **^{13}C NMR** (101 MHz, $CDCl_3$) 156.1 (C), 148.0 (C), 138.0 (CH), 136.3 (CH), 129.6 (CH), 129.4 (CH), 127.5 (C), 127.4 (CH), 126.3 (CH), 119.8 (CH), 118.4 (CH).

Data were in accordance with those previously reported [18].

2-Vinyl-5-ethylfuran **339**

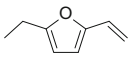

5-Ethyl-2-furfural (1.18 mL, 10 mmol) was added to potassium carbonate (2.2 g, 16 mmol) and methyltriphenylphosphonium bromide **335** (4.2 g, 12 mmol) in anhydrous tetrahydrofuran (15 mL), and heated at reflux for 16 h. The reaction mixture was cooled, filtered and concentrated in vacuo. The residue was dissolved in hot *n*-pentane, cooled to 0 °C, filtered, and washed with cold *n*-pentane. The filtrate was dried ($MgSO_4$) and concentrated in vacuo to give 2-vinyl-5-ethylfuran **339** as a colourless oil (624 mg, 5.11 mmol, 51 %).

^{1}H NMR (400 MHz, $CDCl_3$) 6.46 (dd, J = 17.5, 11.0 Hz, 1H, CH), 6.16 (d, J = 3.0 Hz, 1H, ArH), 5.98 (dt, J = 3.0, 1.0 Hz, 1H, ArH), 5.59 (dd, J = 17.5, 1.5 Hz, 1H, CH), 5.08 (dd, J = 11.0, 1.5 Hz, 1H, CH), 2.67 (qd, J = 7.5, 1.0 Hz, 2H, CH_2), 1.26 (t, J = 7.5 Hz, 3H, CH_3). **^{13}C NMR** (101 MHz, $CDCl_3$) 157.7 (C), 151.5 (C), 125.2 (CH), 110.5 (CH), 108.9 (CH), 105.7 (CH), 21.5 (CH_2), 12.1 (CH_3).

1-(4-Morpholinophenyl)-2-(phenylsilyl)ethane **341**

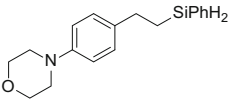

According to General Procedure **A**, 4-morpholinostyrene **336** (132 mg, 0.7 mmol), phenylsilane **47** (95 μL, 0.77 mmol), iron(II) chloride **279** (0.9 mg, 0.007 mmol), 2,6-bis-[1-(2,6-diethylphenylimino)ethyl]pyridine **273b** (3.0 mg, 0.007 mmol) and ethylmagnesium bromide **280** (2 drops, 0.015 mmol) were reacted in anhydrous tetrahydrofuran (3 mL) to give the crude reaction product, which was purified by flash silica column chromatography (10 % EtOAc/hexane) to give *1-(4-morpholinophenyl)-2-(phenylsilyl)ethane* **341** as a yellow oil (187 mg, 0.63 mmol, 90 %).

^{1}H NMR (400 MHz, $CDCl_3$) 7.63-7.58 (m, 2H, ArH), 7.47-7.37 (m, 3H, ArH), 7.18-7.12 (m, 2H, ArH), 6.92-6.86 (m, 2H, ArH), 4.36 (t, J = 3.5 Hz, 2H, SiH_2), 3.93-3.86 (m, 4H, CH_2), 3.19-3.12 (m, 4H, CH_2), 2.79-2.72 (m, 2H, $ArCH_2$), 1.36-1.28 (m, 2H, $SiCH_2$). **^{13}C NMR** (101 MHz, $CDCl_3$) 149.4 (C), 135.7 (C), 135.2 (2 × CH), 132.2 (C), 129.5 (CH), 128.5 (2 × CH), 128.0 (2 × CH), 115.9 (2 × CH), 66.9 (2 × CH_2), 49.7 (2 × CH_2), 30.1 (CH_2), 12.1 (CH_2). **^{29}Si NMR** (79 MHz, $CDCl_3$) −31.1. **IR** (neat) ν_{max} cm^{-1} 2959, 2920, 2853, 2127, 1611, 1514, 1449, 1427, 1377, 1330, 1260, 1233, 1119, 930. **HRMS** (EI) calculated for $C_{18}H_{23}ONSi$ 297.15434. Found 297.15445.

1-(4-Aminophenyl)-2-(phenylsilyl)ethane **342**

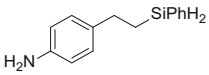

According to General Procedure **A**, 4-aminostyrene **319** (137 μL, 0.7 mmol), phenylsilane **47** (95 μL, 0.77 mmol), iron(II) chloride **279** (0.9 mg, 0.007 mmol), 2,6-bis-[1-(2,6-diethylphenylimino)ethyl]pyridine **273b** (3.0 mg, 0.007 mmol) and ethylmagnesium bromide **280** (2 drops, 0.015 mmol) were reacted in anhydrous tetrahydrofuran (3 mL) to give the crude reaction product, which was purified by flash silica column chromatography (10 % EtOAc/hexane) to give *1-(4-aminophenyl)-2-(phenylsilyl)ethane* **342** as a yellow oil (113 mg, 0.50 mmol, 71 %).

^{1}H NMR (400 MHz, $CDCl_3$) 7.61-7.55 (m, 2H, ArH), 7.45-7.35 (m, 3H, ArH), 7.04-6.97 (m, 2H, ArH), 6.67-6.61 (m, 2H, ArH), 4.32 (t, J = 3.5 Hz, 2H, SiH_2), 3.6 (s, br., 2H, NH_2), 2.75-2.65 (m, 2H, $ArCH_2$), 1.33-1.23 (m, 2H, $SiCH_2$). **^{13}C NMR** (101 MHz, $CDCl_3$) 144.2 (C), 135.2 (2 × CH), 134.1 (C), 132.3 (C), 129.5 (CH), 128.7 (2 × CH), 128.0 (2 × CH), 115.2 (2 × CH), 30.2 (CH_2), 12.3 (CH_2).

^{29}Si NMR (79 MHz, $CDCl_3$) −31.1. **IR** (neat) ν_{max} cm^{-1} 3447, 3370, 3001, 2922, 2845, 2127, 1618, 1514, 1427, 1275, 1177, 1117, 1057, 934, 914, 826. **HRMS** (EI) calculated for $C_{14}H_{17}NSi$ 227.11248. Found 227.11251.

1-(3-(Trifluoromethyl)phenyl)-2-(phenylsilyl)ethane **343**

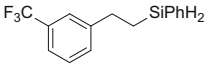

According to General Procedure **A**, 3-trifluoromethylstyrene (104 μL, 0.7 mmol), phenylsilane **47** (95 μL, 0.77 mmol), iron(II) chloride **279** (0.9 mg, 0.007 mmol), 2,6-bis-[1-(2,6-diethylphenylimino)ethyl]pyridine **273b** (3.0 mg, 0.007 mmol) and ethylmagnesium bromide **280** (2 drops, 0.015 mmol) were reacted in anhydrous tetrahydrofuran (3 mL) to give the crude reaction product, which was purified by filtration through a plug of silica using 0.5 % ethyl acetate/petroleum ether to give *1-(3-(trifluoromethyl)phenyl)-2-(phenylsilyl)ethane* **343** as a colourless oil (180 mg, 0.64 mmol, 92 %).

^{1}H NMR (500 MHz, $CDCl_3$) 7.60-7.56 (m, 2H, ArH), 7.47-7.35 (m, 7H, ArH), 4.35 (t, J = 3.5 Hz, 2H, SiH_2), 2.87-2.81 (m, 2H, $ArCH_2$), 1.37-1.30 (m, 2H, $SiCH_2$). **^{13}C NMR** (126 MHz, $CDCl_3$) 144.7 (C), 135.2 (2 × CH), 131.7 (C), 131.3 (q, J = 1 Hz, CH), 130.4 (q, J = 32 Hz, C), 129.8 (CH), 128.7 (CH), 128.1 (2 × CH), 124.6 (q, J = 4 Hz, CH), 124.2 (q, J = 272 Hz, CF_3), 122.7 (q, J = 4 Hz, CH), 30.9 (CH_2), 12.0 (CH_2). **^{19}F NMR** (376 MHz, $CDCl_3$) −62.6. **IR** (neat) ν_{max} cm^{-1} 2922, 2133, 1450, 1429, 1325, 1163, 1117, 1072, 934, 875, 833, 799, 734, 698. **^{29}Si NMR** (79 MHz, $CDCl_3$) −31.0. **HRMS** (EI) calculated for $C_{15}H_{15}F_3Si$ 280.08897. Found 280.08896.

1-(4-Chlorophenyl)-2-(phenylsilyl)ethane **344**

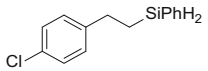

According to General Procedure **A**, 4-chlorostyrene (84 μL, 0.7 mmol), phenylsilane **47** (95 μL, 0.77 mmol), iron(II) chloride **279** (0.9 mg, 0.007 mmol), 2,6-bis-[1-(2,6-diethylphenylimino)ethyl]pyridine **273b** (3.0 mg, 0.007 mmol) and ethylmagnesium bromide **280** (2 drops, 0.015 mmol) were reacted in anhydrous tetrahydrofuran (3 mL) to give the crude reaction product, which was purified by filtration through a plug of silica using 0.5 % ethyl acetate/petroleum ether to give *1-(4-chlorophenyl)-2-(phenylsilyl)ethane* **344** as a colourless oil (147 mg, 0.60 mmol, 85 %).

^{1}H NMR (400 MHz, $CDCl_3$) 7.61-7.55 (m, 2H, ArH), 7.47-7.35 (m, 3H, ArH), 7.28-7.23 (m, 2H, ArH), 7.16-7.10 (m, 2H, ArH), 4.34 (t, J = 3.5 Hz, 2H, SiH_2),

2.79-2.72 (m, 2H, $ArCH_2$), 1.33-1.26 (m, 2H, $SiCH_2$). **^{13}C NMR** (101 MHz, $CDCl_3$) 142.3 (C), 135.2 (2 × CH), 131.9 (C), 131.5 (C), 129.7 (CH), 129.2 (2 × CH), 128.4 (2 × CH), 128.1 (2 × CH), 30.5 (CH_2), 12.1 (CH_2). **^{29}Si NMR** (79 MHz, $CDCl_3$) −31.1. **IR** (neat) ν_{max} cm^{-1} 2922, 2129, 1489, 1429, 1406, 1115, 1092, 1014, 934, 918, 845, 827, 800, 698. **HRMS** (EI) calculated for $C_{14}H_{15}ClSi$ 246.06261. Found 246.06287.

1-(2-Fluorophenyl)-2-(phenylsilyl)ethane **345**

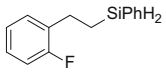

According to General Procedure **A**, 2-fluorostyrene (83 μL, 0.7 mmol), phenylsilane **47** (95 μL, 0.77 mmol), iron(II) chloride **279** (0.9 mg, 0.007 mmol), 2,6-bis-[1-(2,6-diethylphenylimino)ethyl]pyridine **273b** (3.0 mg, 0.007 mmol) and ethylmagnesium bromide **280** (2 drops, 0.015 mmol) were reacted in anhydrous tetrahydrofuran (3 mL) to give the crude reaction product, which was purified by filtration through a plug of silica using 0.5 % ethyl acetate/petroleum ether to give *1-(2-fluorophenyl)-2-(phenylsilyl)ethane* **345** as a colourless oil (113 mg, 0.50 mmol, 82 %).

^{1}H NMR (400 MHz, $CDCl_3$) 7.63-7.57 (m, 2H, ArH), 7.46-7.36 (m, 3H, ArH), 7.24-7.14 (m, 2H, ArH), 7.10-7.05 (m, 1H, ArH), 7.05-6.98 (m, 1H, ArH), 4.36 (t, J = 3.5 Hz, 2H, SiH_2), 2.87-2.79 (m, 2H, $ArCH_2$), 1.37-1.29 (m, 2H, $SiCH_2$). **^{13}C NMR** (101 MHz, $CDCl_3$) 160.9 (d, J = 245 Hz, CF), 135.2 (2 × CH), 131.9 (C), 130.7 (d, J = 16 Hz, C), 129.9 (d, J = 5 Hz, CH), 129.7 (CH), 128.0 (2 × CH), 127.5 (d, J = 8 Hz, CH), 123.9 (d, J = 4 Hz, CH), 115.2 (d, J = 22 Hz, CH), 24.4 (d, J = 3 Hz, CH_2), 10.8 (CH_2). **^{19}F NMR** (376 MHz, $CDCl_3$) −118.9. **^{29}Si NMR** (79 MHz, $CDCl_3$) −31.1. **IR** (neat) ν_{max} cm^{-1} 2936, 2922, 2131, 1585, 1489, 1454, 1429, 1227, 1180, 1134, 1117, 1034, 934, 918, 752, 698. **HRMS** (EI) calculated for $C_{14}H_{15}FSi$ 230.09216. Found 230.09220.

1-(2′-Quinolyl)-2-(phenylsilyl)ethane **346**

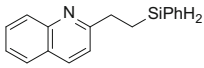

According to General Procedure **A**, 2-vinylquinoline **338** (109 mg, 0.7 mmol), phenylsilane **47** (95 μL, 0.77 mmol), iron(II) chloride **280** (0.9 mg, 0.007 mmol), 2,6-bis-[1-(2,6-diethylphenylimino)ethyl]pyridine **273b** (3.0 mg, 0.007 mmol) and ethylmagnesium bromide **280** (2 drops, 0.015 mmol) were reacted in anhydrous tetrahydrofuran (3 mL) to give the crude reaction product, *1-(2′-quinolyl)-2-(phenylsilyl)ethane* **346**, as a yellow oil (>95 % by NMR). Attempts to purify the product resulted in decomposition.

^{1}H NMR (400 MHz, $CDCl_3$) 8.12-8.02 (m, 2H, ArH), 7.80-7.76 (m, 1H, ArH), 7.72-7.66 (m, 1H, ArH), 7.63-7.59 (m, 2H, ArH), 7.53-7.47 (m, 1H, ArH), 7.41-7.34 (m, 3H, ArH), 7.32-7.28 (m, 1H, ArH), 4.42 (t, J = 3.5 Hz, 2H, SiH_2), 3.18-3.11 (m, 2H, $ArCH_2$), 1.54-1.37 (m, 2H, $SiCH_2$).

1-(4′-Pyridyl)-2-(phenylsilyl)ethane **347**

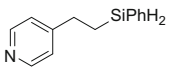

According to General Procedure **A**, 4-vinylpyridine (76 μL, 0.7 mmol), phenylsilane **47** (95 μL, 0.77 mmol), iron(II) chloride **279** (0.9 mg, 0.007 mmol), 2,6-bis-[1-(2,6-diethylphenylimino)ethyl]pyridine **273b** (3.0 mg, 0.007 mmol) and ethylmagnesium bromide **280** (2 drops, 0.015 mmol) were reacted in anhydrous tetrahydrofuran (3 mL) to give the crude reaction product, *1-(4′-pyridyl)-2-(phenylsilyl)ethane* **347**, as a yellow oil (26 % by NMR). Attempts to purify the product resulted in decomposition.

^{1}H NMR (400 MHz, $CDCl_3$) 8.47-8.39 (m, 2H, ArH), 7.60-7.55 (m, 2H, ArH), 7.44-7.36 (m, 3H, ArH), 7.11-7.06 (m, 2H, ArH), 4.35 (t, J = 3.5 Hz, 2H, SiH_2), 2.78-2.71 (m, 2H, $ArCH_2$), 1.33-1.25 (m, 2H, $SiCH_2$).

Methyl 4-[2-(phenylsilyl)ethyl]benzoate **351**

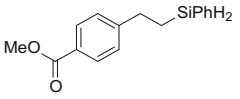

According to General Procedure **A**, methyl 4-vinylbenzoate (114 mg, 0.7 mmol), phenylsilane **47** (95 μL, 0.77 mmol), iron(II) chloride **279** (0.9 mg, 0.007 mmol), 2,6-bis-[1-(2,6-diethylphenylimino)ethyl]pyridine **273b** (3.0 mg, 0.007 mmol) and ethylmagnesium bromide **280** (2 drops, 0.015 mmol) were reacted in anhydrous tetrahydrofuran (3 mL) to give the crude reaction product, which was purified by flash silica column chromatography (7 % EtOAc/Hexane) to give methyl *4-[2-(phenylsilyl)ethyl]benzoate* **351** as a colourless oil (172 mg, 0.64 mmol, 91 %).

^{1}H NMR (500 MHz, $CDCl_3$) 7.99-7.95 (m, 2H, ArH), 7.60-7.56 (m, 2H, ArH), 7.45-7.36 (m, 3H, ArH), 7.28-7.24 (m, 2H, ArH), 4.34 (t, J = 3.5 Hz, 2H, SiH_2), 3.92 (s, 3H, CH_3), 2.86-2.80 (m, 2H, $ArCH_2$), 1.36-1.29 (m, 2H, $SiCH_2$). **^{13}C NMR** (126 MHz, CDCl3) 167.1 (C=O), 149.4 (C), 135.2 (2 × CH), 131.7 (C), 129.7 (2 × CH), 129.7 (CH), 128.1 (2 × CH), 127.9 (2 × CH), 127.8 (C), 51.9 (CH_3), 31.1 (CH_2), 11.8 (CH_2). **^{29}Si NMR** (79 MHz, CDCl3) −31.0. **IR** (neat) ν_{max} cm^{-1} 2949, 2131, 1717, 1609, 1429, 1414, 1308, 1275, 1179, 1109. **HRMS** (EI) calculated for $C_{16}H_{18}O_2Si$ 270.10706. Found 270.10687.

1-(4-Acetoxyphenyl)-2-(phenylsilyl)ethane **352**

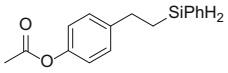

According to General Procedure **A**, 4-acetoxystyrene (107 μL, 0.7 mmol), phenylsilane **47** (95 μL, 0.77 mmol), iron(II) chloride **279** (0.9 mg, 0.007 mmol), 2,6-bis-[1-(2,6-diethylphenylimino)ethyl]pyridine **273b** (3.0 mg, 0.007 mmol) and ethylmagnesium bromide **280** (2 drops, 0.015 mmol) were reacted in anhydrous tetrahydrofuran (3 mL) to give the crude reaction product, which was purified by flash silica column chromatography (7 % EtOAc/Hexane) to give *1-(4-acetoxyphenyl)-2-(phenylsilyl)ethane* **352** as a colourless oil (157 mg, 0.58 mmol, 83 %).

^{1}H NMR (400 MHz, $CDCl_3$) 7.61-7.56 (m, 2H, ArH), 7.45-7.36 (m, 3H, ArH), 7.23-7.18 (m, 2H, ArH), 7.03-6.98 (m, 2H, ArH), 4.35 (t, J = 3.5 Hz, 2H, SiH_2), 2.82-2.75 (m, 2H, $ArCH_2$), 2.31 (s, 3H, CH_3), 1.35-1.28 (m, 2H, $SiCH_2$). **^{13}C NMR** (101 MHz, $CDCl_3$) 169.6 (C=O), 148.7 (C), 141.5 (C), 135.2 (2 × CH), 132.0 (C), 129.7 (CH), 128.8 (2 × CH), 128.0 (2 × CH), 121.3 (2 × CH), 30.5 (CH_2), 21.1 (CH_3), 12.0 (CH_2). **^{29}Si NMR** (79 MHz, $CDCl_3$) −31.0. **IR** (neat) ν_{max} cm^{-1} 2935, 2922, 2129, 1761, 1601, 1506, 1477, 1454, 1429, 1368, 1192, 1152. **HRMS** (EI) calculated for $C_{16}H_{18}O_2Si$ 270.10706. Found 270.10732.

1-Phenyl-2-(4-(phenylsilylethyl)benzene)-ethanone **355**

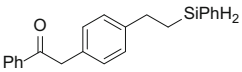

According to an adaptation to General Procedure **A**, ethylmagnesium bromide **280** (10 drops, 0.07 mmol) and phenylsilane **47** (95 μL, 0.77 mmol) were added to a solution of iron(II) chloride **279** (4.4 mg, 0.035 mmol) and 2,6-bis-[1-(2,6-diethylphenylimino)ethyl]pyridine **273b** (14.9 mg, 0.035 mmol) in anhydrous tetrahydrofuran (3 mL), followed by 1-phenyl-2-(4-vinylbenzene)-ethanone **328** (155 mg, 0.7 mmol) in tetrahydrofuran (1 mL). The reaction stirred for 1 h and worked up according to General Procedure **A** to give the crude reaction product, which was purified by flash silica column chromatography (7 % EtOAc/hexane) to give *1-phenyl-2-(4-(phenylsilylethyl)benzene)-ethanone* **355** as a colourless amorphous solid (178 mg, 0.54 mmol, 77 %).

^{1}H NMR (400 MHz, $CDCl_3$) 8.05-8.00 (m, 2H, ArH), 7.60-7.53 (m, 3H, ArH), 7.50-7.43 (m, 2H, ArH), 7.42-7.33 (m, 3H, ArH), 7.22-7.13 (m, 4H, ArH), 4.32 (t, J = 3.5 Hz, 2H, SiH_2), 4.26 (s, 2H, CH_2), 2.79-2.71 (m, 2H, $ArCH_2$), 1.34-1.26 (m, 2H, $SiCH_2$). **^{13}C NMR** (126 MHz, $CDCl_3$) 197.7 (C=O), 142.5 (C), 136.6 (C), 135.2 (2 × CH), 133.1 (CH), 132.1 (C), 131.9 (C), 129.6 (CH), 129.4 (2 × CH), 128.6 (2 × CH), 128.6 (2 × CH), 128.2 (2 × CH), 128.0 (2 × CH), 45.1 (CH_2),

30.7 (CH_2), 11.9 (CH_2). **^{29}Si NMR** (79 MHz, $CDCl_3$) −31.0. **IR** (neat) ν_{max} cm^{-1} 3053, 2922, 2903, 2131, 2110, 1689, 1595, 1514, 1447, 1427, 1332, 1204, 1152, 1117. **HRMS** (EI) calculated for $C_{22}H_{22}OSi$ 330.14345. Found 330.14389.

1-(4-Cyanophenyl)-2-(phenylsilyl)ethane **360**

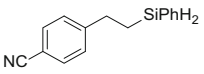

According to General Procedure **A**, 4-cyanostyrene (90 μL, 0.7 mmol), phenylsilane **47** (95 μL, 0.77 mmol), iron(II) chloride **279** (0.9 mg, 0.007 mmol), 2,6-bis-[1-(2,6-diethylphenylimino)ethyl]pyridine **273b** (3.0 mg, 0.007 mmol) and ethylmagnesium bromide **280** (2 drops, 0.015 mmol) were reacted in anhydrous tetrahydrofuran (3 mL) to give the crude reaction product, which was purified by flash silica column chromatography (7 % EtOAc/Hexane) to give *1-(4-cyanophenyl)-2-(phenylsilyl)ethane* **360** as a brown oil (53 mg, 0.22 mmol, 32 %).

^{1}H NMR (400 MHz, $CDCl_3$) 7.62-7.54 (m, 2H, ArH), 7.49-7.36 (m, 3H, ArH), 7.33-7.27 (m, 2H, ArH), 4.36 (t, J = 3.5 Hz, 2H, SiH_2), 2.89-2.81 (m, 2H, $ArCH_2$), 1.37-1.28 (m, 2H, $SiCH_2$). **^{13}C NMR** (101 MHz, $CDCl_3$) 149.5 (C), 135.2 (2 × CH), 132.2 (2 × CH), 131.4 (C), 129.9 (CH), 128.7 (2 × CH), 128.1 (2 × CH), 119.1 (C), 109.7 (C), 31.3 (CH_2), 11.7 (CH_2). **^{29}Si NMR** (79 MHz, $CDCl_3$) −31.0. **IR** (neat) ν_{max} cm^{-1} 2937, 2864, 2843, 2226, 2133, 1605, 1477, 1456, 1427, 1204, 1150. **HRMS** (EI) calculated for $C_{15}H_{15}NSi$ 237.09683. Found 237.09651.

1-Phenyl-4-(diphenylsilyl)but-2-ene **362** (6:1 mixture of diastereoisomers)

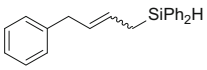

According to General Procedure **A**, phenylbutene **361** (105 μL, 0.7 mmol), diphenylsilane **255** (130 μL, 0.7 mmol), iron(II) chloride **279** (0.9 mg, 0.007 mmol), 2,6-bis-[1-(2,6-diethylphenylimino)ethyl]pyridine **273b** (3.0 mg, 0.007 mmol) and ethylmagnesium bromide **280** (2 drops, 0.015 mmol) were reacted in anhydrous tetrahydrofuran (3 mL) to give the crude reaction product, which was purified by flash silica chromatography (hexane) to give *1-phenyl-4-(diphenylsilyl)but-2-ene* **362** (6:1 mixture of diastereoisomers) as a colourless oil (99 mg, 0.31 mmol, 45 %).

Major diastereoisomer: **^{1}H NMR** (500 MHz, $CDCl_3$) 7.60-7.55 (m, 4H, ArH), 7.44-7.39 (m, 2H, ArH), 7.39-7.34 (m, 4H, ArH) 7.26-7.21 (m, 2H, ArH), 7.20-7.15 (m, 1H, ArH), 7.07-7.03 (m, 2H, ArH), 5.62-5.51 (m, 1H, CH), 5.59-5.47 (m, 1H, CH), 4.90 (t, J = 3.5 Hz, 2H, SiH_2), 3.30 (d, J = 6.5 Hz, 2H, $ArCH_2$), 2.13 (ddd, J = 7.5, 3.5, 1.0 Hz, 2H, $SiCH_2$). **^{13}C NMR** (126 MHz, $CDCl_3$) 141.0 (C), 135.3 (4 × CH), 133.8 (2 × C), 129.6 (2 × CH), 128.4 (2 × CH), 128.2 (2 × CH), 128.0 (4 × CH), 129.3 (CH) 126.4 (CH), 125.7 (CH), 39.1 ($ArCH_2$), 18.0 ($SiCH_2$). **^{29}Si NMR** (79 MHz, $CDCl_3$) −16.1.

Minor diastereoisomer: **^{1}H NMR** (500 MHz, $CDCl_3$) 7.63-7.60 (m, 4H, ArH), 7.44-7.39 (m, 2H, ArH), 7.38-7.34 (m, 4H, ArH), 7.29-7.25 (m, 2H, ArH), 7.17-7.13 (m, 1H, ArH), 7.11-7.07 (m, 2H, ArH), 5.67-5.60 (m, 1H, CH), 5.55-5.49 (m, 1H, CH), 4.92 (t, J = 3.5 Hz, 2H, SiH_2), 3.28 (d, J = ~7 Hz, 2H, $ArCH_2$), 2.24-2.21 (br. dd, J = 8.0, 3.5 Hz, 2H, $SiCH_2$). **^{13}C NMR** (126 MHz, $CDCl_3$) 141.0 (C), 135.2 (4 × CH), 133.8 (2 × C), 129.7 (2 × CH), 128.4 (2 × CH), 128.3 (2 × CH), 128.02 (CH), 128.01 (4 × CH), 127.8 (CH) 124.9 (CH), 33.3 ($ArCH_2$), 14.1 ($SiCH_2$). **^{29}Si NMR** (79 MHz, $CDCl_3$) −16.8.

Combined: **IR** (neat) ν_{max} cm^{-1} 3067, 3022, 2120, 1493, 1427, 1155, 1115, 1031, 964, 804, 731. **HRMS** (EI) calculated for $C_{22}H_{22}Si$ 314.14853. Found 314.14954.

1-Phenyl-4-(phenylsilyl)butane **364**

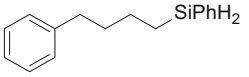

According to General Procedure **A**, phenylbutene **361** (105 μL, 0.7 mmol), phenylsilane **47** (95 μL, 0.77 mmol), iron(II) chloride **279** (0.9 mg, 0.007 mmol), 2,6-bis-[1-(2,6-diethylphenylimino)ethyl]pyridine **273b** (3.0 mg, 0.007 mmol) and ethylmagnesium bromide **280** (2 drops, 0.015 mmol) were reacted in anhydrous tetrahydrofuran (3 mL) to give the crude reaction product, which was purified by filtration through a plug of silica using 0.5 % ethyl acetate/petroleum ether to give *1-phenyl-4-(phenylsilyl)butane* **364** as a colourless oil (148 mg, 0.62 mmol, 88 %).

^{1}H NMR (400 MHz, $CDCl_3$) 7.59-7.55 (m, 2H, ArH), 7.42-7.35 (m, 3H, ArH), 7.31-7.25 (m, 2H, ArH), 7.21-7.14 (m, 3H, ArH), 4.30 (t, J = 3.0 Hz, 2H, SiH_2), 2.65-2.59 (m, 2H, $ArCH_2$), 1.75-1.66 (m, 2H, $SiCH_2$), 1.57-1.48 (m, 2H), 1.03-0.96 (m, 2H). **^{13}C NMR** (100 MHz, $CDCl_3$) 142.6 (C), 135.2 (2 × CH), 132.6 (C), 129.5 (CH), 128.4 (2 × CH), 128.2 (2 × CH), 128.0 (2 × CH), 125.6 (CH), 35.6 (CH_2), 34.6 (CH_2), 24.7 (CH_2), 9.9 (CH_2). **^{29}Si NMR** (79 MHz, $CDCl_3$) −30.9. **IR** (neat) ν_{max} cm^{-1} 3066, 3025, 2923, 2854, 2127, 1496, 1453, 1428, 1116, 935, 872, 835, 696. **HRMS** (EI) calculated for $C_{16}H_{20}Si$ 240.13343. Found 240.13378.

1-Benzyldimethylsilyl-4-phenylbutane **365**

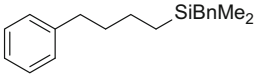

According to General Procedure **A**, phenylbutene **361** (105 μL, 0.7 mmol), benzyldimethylsilane **398** (110 μL, 0.7 mmol), iron(II) chloride **279** (0.9 mg, 0.007 mmol), 2,6-bis-[1-(2,6-diethylphenylimino)ethyl]pyridine **273b** (3.0 mg, 0.007 mmol) and ethylmagnesium bromide **280** (2 drops, 0.015 mmol) were reacted in anhydrous tetrahydrofuran (3 mL) to give the crude reaction product, which was purified by filtration through a plug of silica using 0.5 % ethyl

acetate/petroleum ether to give *1-phenyl-4-(phenylsilyl)butane* **365** as a colourless oil (172 mg, 0.61 mmol, 87 %).

^{1}H NMR (500 MHz, $CDCl_3$) 7.34-7.29 (m, 2H, ArH), 7.26-7.18 (m, 5H, ArH), 7.12-7.08 (m, 1H, ArH), 7.07-6.99 (m, 2H, ArH), 2.66-2.60 (m, 2H, $ArCH_2$), 1.70-1.62 (m, 2H, CH_2), 1.42-1.34 (m, 2H, CH_2), 0.61-0.55 (m, 2H, $SiCH_2$), 0.00 (s, 6H, $SiCH_3$). **^{13}C NMR** (126 MHz, $CDCl_3$) 142.8 (C), 140.4 (C), 128.4 (2 × CH), 128.2 (2 × CH), 128.11 (2 × CH), 128.05 (2 × CH), 125.6 (CH), 123.8 (CH), 35.6 (CH_2), 35.3 (CH_2), 25.6 (CH_2), 23.4 (CH_2), 14.6 (CH_2), −3.6 ($SiCH_3$). **^{29}Si NMR** (99 MHz, $CDCl_3$) 2.3. **IR** (neat) ν_{max} cm^{-1} 3024, 2922, 2855, 1601, 1483, 1452, 1246, 1205, 1153, 1055, 1032, 827, 740. **HRMS** (EI) calculated for $C_{19}H_{26}Si$ 282.17983. Found 282.17914.

2,6-Bis-[1-(2,6-diethylphenylimino)ethyl]pyridine iron(II) chloride **367** (^{Et}BIPFeCl_2)

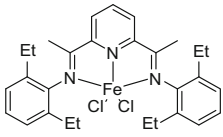

Prepared according to a literature procedure [4].

2,6-Bis-[1-(2,6-diethylphenylimino)ethyl]pyridine **273b** (852 mg, 2 mmol) and iron(II) chloride **279** (254 mg, 2 mmol) were stirred in anhydrous tetrahydrofuran (20 mL) under a nitrogen atmosphere at room temperature for 6 h. Anhydrous diethyl ether (60 mL) was added and the resulting suspension stirred for 10 min. The reaction was filtered to give a blue solid, which was washed with diethyl ether (2 × 20 mL) and dried under high vacuum for 3 h. The blue solid was dissolved in anhydrous dichloromethane (30 mL) and filtered to remove unreacted iron(II) chloride. The solvent was removed in vacuo and the blue complex dried under high vacuum for 10 h to give 2,6-bis-[1-(2,6-diethylphenylimino)ethyl]pyridine iron(II) chloride **367** (^{Et}BIPFeCl_2) as a blue solid (1.06 g, 1.92 mmol, 96 %).

^{1}H NMR (600 MHz, CD_2Cl_2) 81.1 (2H), 50.4 (1H), 15.5 (4H), 5.7 (2H), 5.0 (2H), 1.5 (4H), −4.0 (12H), −10.5 (2H), −26.0 (6H).

Data were in accordance with those previously reported [19].

1-(Phenylsilyl)-2-phenylpropane **368**

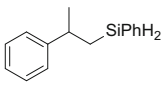

According to General Procedure **B**, α-methylstyrene **382** (91 μL, 0.7 mmol), phenylsilane **47** (95 μL, 0.77 mmol), 2,6-bis-[1-(2,6-diethylphenylimino)ethyl] pyridine iron(II) chloride **367** (^{Et}BIPFeCl_2) (3.9 mg, 0.007 mmol) and *n*-butyl-lithium **283** (3 drops, 0.015 mmol) were reacted in anhydrous toluene (3 mL) to

give the crude reaction product, which was purified by filtration through a plug of silica using 0.5 % ethyl acetate/petroleum ether to give *1-(phenylsilyl)-2-phenyl-propane* **368** as a colourless oil (149 mg, 0.66 mmol, 94 %).

^{1}H NMR (400 MHz, $CDCl_3$) 7.55-7.50 (m, 2H, ArH), 7.46-7.28 (m, 5H, ArH), 7.25-7.18 (m, 3H, ArH), 4.28-4.20 (m, 2H, SiH_2), 2.98 (app. sext., J = 7.0 Hz, 1H, ArCH), 1.43-1.31 (m, 2H, $SiCH_2$) 1.37 (d, J = 7.0 Hz, 3H, CH_3). **^{13}C NMR** (101 MHz, $CDCl_3$) 148.6 (C), 135.2 (2 × CH), 132.4 (C), 129.5 (CH), 128.4 (2 × CH), 127.9 (2 × CH), 126.6 (2 × CH), 126.0 (CH), 36.7, 24.9, 20.3. **^{29}Si NMR** (79 MHz, $CDCl_3$) −33.3. **IR** (neat) ν_{max} cm^{-1} 2957, 2922, 2129, 1493, 1452, 1429, 1115, 1057, 1034, 1007, 937, 860, 845. **HRMS** (EI) calculated for $C_{15}H_{18}Si$ 226.11723. Found 226.11714.

(4*R*)-1-Methyl-4-[(1*R*/*S*)-1-methyl-2-(phenylsilyl)ethyl]-cyclohex-1-ene **369** (1:1 mixture of diastereoisomers)

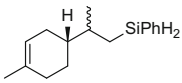

According to General Procedure **B**, (*R*)-limonene (113 μL, 0.7 mmol), phenylsilane **47** (95 μL, 0.77 mmol), 2,6-bis-[1-(2,6-diethylphenylimino)ethyl]pyridine iron(II) chloride **367** (^{Et}BIPFeCl_2) (3.9 mg, 0.007 mmol) and *n*-butyllithium **283** (3 drops, 0.015 mmol) were reacted in anhydrous toluene (3 mL) to give the crude reaction product, which was purified by filtration through a plug of silica using 0.5 % ethyl acetate/petroleum ether to give (4*R*)-1-methyl-4-[(1*R*/*S*)-1-methyl-2-(phenylsilyl) ethyl]-cyclohex-1-ene **369** as a colourless oil (164 mg, 0.67 mmol, 96 %).

^{1}H NMR (400 MHz, $CDCl_3$) 7.62-7.56 (m, 2H, ArH), 7.43-7.33 (m, 3H, ArH), 5.42-5.35 (m, 1H, CH), 4.39-4.30 (m, 2H, SiH_2), 2.06-1.88 (m, 3H, CH_2), 1.84-1.62 (m, 3H, CH_2, CH), 1.65 (s, 3H, CH_3), 1.48-1.36 (m, 1H, CH), 1.34-1.22 (m, 1H, CH_2), 1.19-1.08 (m, 1H, CH_2), 0.98 (d, J = 7.0 Hz, 1.5 H, CH_3), 0.97 (d, J = 7.0 Hz, 1.5 H, CH_3), 0.91-0.81 (m, 1H, CH_2). **^{13}C NMR** (101 MHz, $CDCl_3$) 135.2 (2 × CH), 134.0 (C), 133.0 (C), 129.4 (CH), 127.9 (2 × CH), 120.88 (0.5 × CH), 120.85 (0.5 × CH), 40.7 (0.5 × CH), 40.6 (0.5 × CH), 34.6 (0.5 × CH), 34.4 (0.5 × CH), 30.9 (0.5 × CH_2), 30.8 (0.5 × CH_2), 29.0 (0.5 × CH_2), 27.9 (0.5 × CH_2), 26.8 (0.5 × CH_2), 25.5 (0.5 × CH_2), 23.4 (CH_3), 18.9 (0.5 × CH_3), 18.5 (0.5 × CH_3), 15.4 (0.5 × CH_2), 15.0 (0.5 × CH_2). **^{29}Si NMR** (79 MHz, $CDCl_3$) −32.4, −32.6. **IR** (neat) ν_{max} cm^{-1} 2959, 2912, 2129, 1449, 1429, 1375, 1115, 1053, 1034, 933, 845, 698.

Data were in accordance with those previously reported [20].

Cyclooctylphenylsilane **370**

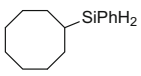

According to General Procedure **B**, cyclooctene (0.65 mL, 5 mmol), phenylsilane **47** (86 μL, 0.7 mmol), 2,6-bis-[1-(2,6-diethylphenylimino)ethyl]pyridine iron(II) chloride **367** (^{Et}BIPFeCl$_2$) (3.9 mg, 0.007 mmol) and *n*-butyllithium **283** (3 drops, 0.015 mmol) were reacted to give the crude reaction product, which was purified by filtration through a plug of silica using 0.5 % ethyl acetate/petroleum ether to give *cyclooctylphenylsilane* **370** as a colourless oil (128 mg, 0.59 mmol, 84 %).

^{1}H NMR (400 MHz, $CDCl_3$) 7.62-7.57 (m, 2H, ArH), 7.44-7.34 (m, 3H, ArH), 4.22 (d, J = 3.5 Hz, 2H, SiH_2), 1.88-1.78 (m, 2H, CH_2), 1.76-1.66 (m, 2H, CH_2), 1.65-1.43 (m, 10H, CH_2), 1.34-1.24 (m, 1H, CH). **^{13}C NMR** (101 MHz, $CDCl_3$) 135.6 (2 × CH), 132.6 (C), 129.4 (CH), 127.9 (2 × CH), 28.6 (2 × CH_2), 27.4 (2 × CH_2), 26.9 (CH_2), 26.5 (2 × CH_2), 20.1 (CH). **^{29}Si NMR** (79 MHz, $CDCl_3$) −22.9. **IR** (neat) ν_{max} cm^{-1} 2916, 2845, 2124, 1466, 1444, 1427, 1115, 1055, 11034, 923, 837, 731, 696. **HRMS** (EI) calculated for $C_{14}H_{22}Si$ 218.14853. Found 218.14906.

4-[2-(Phenylsilyl)ethyl]cyclohex-1-ene **372**

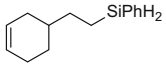

According to General Procedure **A**, 4-vinylcyclohexene **371** (91 μL, 0.7 mmol), phenylsilane **47** (95 μL, 0.77 mmol), iron(II) chloride **379** (0.9 mg, 0.007 mmol), 2,6-bis-[1-(2,6-diethylphenylimino)ethyl]pyridine **273b** (3.0 mg, 0.007 mmol) and ethylmagnesium bromide **280** (2 drops, 0.015 mmol) were reacted in anhydrous tetrahydrofuran (3 mL) to give the crude reaction product, which was purified by filtration through a plug of silica using 0.5 % ethyl acetate/petroleum ether to give 4-[2-(phenylsilyl)ethyl]cyclohex-1-ene **372** as a colourless oil (141 mg, 0.65 mmol, 93 %).

^{1}H NMR (400 MHz, $CDCl_3$) 7.62-7.56 (m, 2H, ArH), 7.44-7.35 (m, 3H, ArH), 5.71-5.63 (m, 2H, CH), 4.31 (t, J = 4.0 Hz, 2H, SiH_2), 2.19-2.09 (m, 1H, CH_2), 2.08-2.01 (m, 2H, CH_2), 1.82-1.74 (m, 1H, CH_2), 1.70-1.60 (m, 1H, CH_2), 1.58-1.48 (m, 1H, CH), 1.48-1.40 (m, 2H, CH_2), 1.27-1.15 (m, 1H, CH_2), 1.02-0.95 (m, 2H, $SiCH_2$). **^{13}C NMR** (101 MHz, $CDCl_3$) 135.2 (2 × CH), 132.7 (C), 129.5 (CH), 128.0 (2 × CH), 127.1 (CH), 126.5 (CH), 36.1 (CH), 31.8 (CH_2), 31.5 (CH_2), 28.4 (CH_2), 25.3 (CH_2), 7.2 ($SiCH_2$). **^{29}Si NMR** (79 MHz, $CDCl_3$) −30.1. **IR** (neat) ν_{max} cm^{-1} 3021, 2911, 2127, 1429, 1115, 1055, 1034, 1011, 934, 883, 835, 727, 698.

Data were in accordance with those previously reported [21].

2-Acetyl-6-[1-(2,6-diethylphenylimino)ethyl]pyridine **378a**

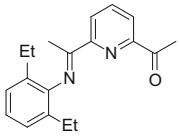

2,6-Diethylaniline **272b** (2.9 mL, 18 mmol) was added to 2,6-diacetylpyridine **271** (3.26 g, 20 mmol) and formic acid (0.3 mL) in anhydrous methanol (50 mL) and stirred under a nitrogen atmosphere for 16 h. The solvent was removed in vacuo to give a mixture of 2-acetyl-6-[1-(2,6-diethylphenylimino)ethyl]pyridine **378a** and 2,6-bis-[1-(2,6-diethylphenylimino)ethyl]pyridine **273b**. Recrystallisation from dichloromethane gave the same mixture of products. The mixture was added to tetrahydrofuran and iron(II) chloride **279** (1.1 equiv. with respect to quantity of bis(imino)pyridine **273b** contaminant, as determined by NMR) and stirred for 6 h. Diethyl ether was added to precipitate the bis(imino)pyridine iron(II) chloride complex **367**, which was filtered, and the filtrate passed through a short column of Celite. The solvent was removed in vacuo to give *2-acetyl-6-[1-(2,6-diethylphenylimino)ethyl]pyridine* **378a** as a yellow solid (3.92 g, 13.3 mmol, 74 %).

m.p. 146–148 °C (CH_2Cl_2). **^{1}H NMR** (500 MHz, $CDCl_3$) 8.57 (dd, J = 8.0, 1.0 Hz, 1H, pyH), 8.15 (dd, J = 8.0, 1.0 Hz, 1H, pyH), 7.96 (t, J = 8.0 Hz, 1H, pyH), 7.14 (app. d, J = 7.5 Hz, 2H, ArH), 7.06 (dd, 1H, J = 8.5, 6.5 Hz, ArH), 2.80 (s, 3H, $(CO)CH_3$), 2.48-2.29 (m, 4H, CH_2), 2.26 (s, 3H, $(CN)CH_3$), 1.15 (t, J = 7.5 Hz, 6H, CH_3). **^{13}C NMR** (126 MHz, $CDCl_3$) 200.1 (C=O), 166.3 (C=N), 155.5 (C), 152.5 (C), 147.5 (C), 137.3 (CH), 131.0 (2 × C), 126.0 (2 × CH), 124.5 (CH), 123.5 (CH), 122.5 (CH), 25.6 (CH_3), 24.6 (2 × CH_2), 16.7 (CH_3), 13.7 (2 × CH_3). **IR** (neat) ν_{max} cm^{-1} 2963, 2930, 2870, 1699, 1645, 1580, 1452, 1413, 1364, 1315, 1302, 1238, 1198, 1121, 1101, 1076, 993, 955, 872, 825, 799, 766. **HRMS** (EI) calculated for $C_{19}H_{22}ON_2$ 294.17267. Found 294.17325.

2-Acetyl-6-[1-(2,4,6-trimethylphenylimino)ethyl]pyridine **378b**

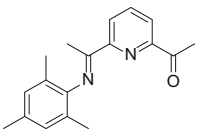

According to the method given above, 2,4,6-trimethylaniline **272c** (2.5 mL, 18 mmol) and 2,6-diacetylpyridine **271** (3.26 g, 20 mmol) were reacted to give 2-acetyl-6-[1-(2,4,6-trimethylphenylimino)ethyl]pyridine **378b** as a yellow solid (2.78 g, 9.92 mmol, 55 %).

m.p. 139–141 °C (CH_2Cl_2). **^{1}H NMR** (500 MHz, $CDCl_3$) 8.57 (dd, J = 8.0, 1.0 Hz, 1H, pyH), 8.14 (dd, J = 8.0, 1.0 Hz, 1H, pyH), 7.96 (t, J = 8.0 Hz, 1H, pyH), 6.91 (s, 2H, ArH), 2.80 (s, 3H, $(CO)CH_3$), 2.31 (s, 3H, CH_3), 2.24 (s, 3H, $(CN)CH_3$), 2.01 (s, 3H, CH_3). **^{13}C NMR** (126 MHz, $CDCl_3$) 200.0 (C=O), 166.8 (C=N), 155.6 (C), 152.4 (C), 146.0 (C), 137.2 (CH), 132.3 (C), 128.6 (2 × CH), 125.1 (2 × C), 124.5 (CH), 122.5 (CH), 25.6 (CH_3), 20.7 (CH_3), 17.81 (2 × CH_3), 16.2 (CH_3). **IR** (neat) ν_{max} cm^{-1} 2965, 2911, 1695, 1634, 1580, 1476, 1354, 1314, 1298, 1242, 1213, 1117, 1099, 1074, 993, 953, 849, 822. **HRMS** (EI) calculated for $C_{18}H_{20}ON_2$ 280.15701. Found 280.15619

Data were in accordance with those previously reported [22].

2-{1-[(1*S*)-1-Methyl-2,2-dimethylpropylimino]ethyl}-6-[1-(2,6-diethylphenylimino) ethyl]pyridine **380a** (^{Et,tBu}BIP)

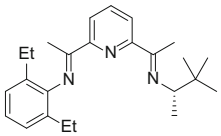

(*S*)-(+)-3,3-Dimethyl-2-butylamine **379a** (0.66 mL, 4.85 mmol) was added to a solution of 2-acetyl-6-[1-(2,6-diethylphenylimino)ethyl]pyridine **378a** (1.3 g, 4.4 mmol) and *p*-toluenesulfonic acid (30 mg, 0.16 mmol) in anhydrous toluene (15 mL) and heated at reflux under Dean-Stark conditions for 16 h. The solvent was removed in vacuo and the yellow solid recrystallised from hot dichloromethane to give *2-{1-[(1S)-1-methyl-2,2-dimethylpropylimino]ethyl}-6-[1-(2,6-diethylphenylimino)ethyl]pyridine* **380a** (^{Et,tBu}BIP) (1.18 g, 3.12 mmol, 71 %) as yellow cuboids.

m.p. 86–87 °C. **^{1}H NMR** (500 MHz, $CDCl_3$) 8.36 (dd, J = 8.0, 1.0 Hz, 1H, pyH), 8.29 (dd, J = 8.0, 1.0 Hz, 1H, pyH), 7.81 (t, J = 8.0 Hz, 1H, pyH), 7.13 (app. d, J = 7.5 Hz, 2H, ArH), 7.04 (dd, 1H, J = 8.5, 6.5 Hz, ArH), 3.48 (q, J = 6.5 Hz, 1H, CH), 2.49-2.30 (m, 4H, CH_2), 2.42 (s, 3H, (CN)CH_3), 2.25 (s, 3H, (CN)CH_3), 1.15 (t, J = 7.5 Hz, 3H, CH_3), 1.14 (t, J = 7.5 Hz, 3H, CH_3), 1.08 (d, J = 6.5 Hz, 3H, CH_3), 0.99 (s, 9H, CH_3). **^{13}C NMR** (126 MHz, $CDCl_3$) 167.1 (C), 162.9 (C), 157.2 (C), 154.7 (C), 147.9 (C), 136.5 (CH), 131.3 (C), 131.2 (C), 125.90 (CH), 125.89 (CH), 123.2 (CH), 122.0 (CH), 121.1 (CH), 64.7 (NCH), 34.8 (C), 26.5 (3 × CH_3), 24.6 (2 × CH_2), 16.8 (CH_3), 15.6 (CH_3), 13.70 (CH_3), 13.68 (CH_3), 12.9 (CH_3). **IR** (neat) ν_{max} cm^{-1} 2965, 2934, 2864, 1701, 1639, 1566, 1452, 1364, 1240, 1200, 1121, 1099, 1076, 1034, 993, 824. **HRMS** (EI) calculated for $C_{18}H_{20}ON_2$ 377.28255. Found 377.28418.

2-{1-[(1*S*)-1-Cyclohexylethylimino]ethyl}-6-[1-(2,6-diethylphenylimino)ethyl]pyridine **380b** (^{Et,Cy}BIP)

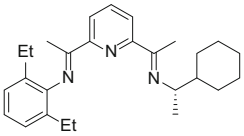

According to the method given above, (*S*)-(+)-1-cyclohexylethylamine **379b** (0.72 mL, 4.85 mmol) and 2-acetyl-6-[1-(2,6-diethylphenylimino)ethyl]pyridine **378a** (1.3 g, 4.4 mmol) were reacted to give *2-{1-[(1S)-1-cyclohexylethylimino] ethyl}-6-[1-(2,6-diethylphenylimino)ethyl]pyridine* **380b** (^{Et,Cy}BIP) as a yellow oil (1.70 g, 4.22 mmol, 96 %). The oil was used without further purification.

^{1}H NMR (600 MHz, $CDCl_3$) 8.36 (dd, J = 8.0, 1.0 Hz, 1H, pyH), 8.24 (dd, J = 8.0, 1.0 Hz, 1H, pyH), 7.81 (t, J = 8.0 Hz, 1H, pyH), 7.12 (app. d, J = 7.5 Hz, 2H, ArH), 7.04 (dd, 1H, J = 8.5, 6.5 Hz, ArH), 3.52 (quin., J = 6.5 Hz, 1H, NCH),

2.47-2.31 (m, 4H, CH_2), 2.41 (s, 3H, (CN)CH_3), 2.25 (s, 3H, (CN)CH_3), 1.92-1.85 (m, 1H, CH_2), 1.83-1.76 (m, 2H, CH_2), 1.76-1.66 (m, 2H, CH_2), 1.58-1.51 (m, 1H, CH), 1.29 (app. sext.t., J = 12.5, 3.5 Hz, 2H, CH_2), 1.22-1.14 (m, 1H, CH_2), 1.17 (d, J = 6.5 Hz, 3H, CH_3), 1.15 (td, J = 7.5, 3.5 Hz, 6H, CH_3), 1.01 (app. sext.d, J = 12.5, 3.5 Hz, 2H, CH_2). **^{13}C NMR** (151 MHz, $CDCl_3$) 167.1 (C), 163.4 (C), 157.2 (C), 154.7 (C), 147.9 (C), 136.6 (CH), 131.23 (C), 131.21 (C), 125.89 (CH), 125.88 (CH), 123.2 (CH), 122.0 (CH), 121.1 (CH), 61.3 (NCH), 44.6 (CH), 29.9 (CH_2), 29.8 (CH_2), 26.7 (CH_2), 26.5 (CH_2), 26.4 (CH_2), 24.58 (CH_2), 24.57 (CH_2), 18.4 (CH_3), 16.8 (CH_3), 13.69 (CH_3), 13.68 (CH_3), 13.4 (CH_3). **IR** (neat) ν_{max} cm^{-1} 2951, 2922, 2853, 1639, 1452, 1375, 1364, 820. **HRMS** (EI) calculated for $C_{27}H_{37}N_3$ 403.29820. Found 403.29754.

2-{1-[(1*S*)-1-Methyl-2,2-dimethylpropylimino]ethyl}-6-[1-(2,4,6-trimethylphenylimino)ethyl]pyridine **380c** ($^{Me,t Bu}$BIP)

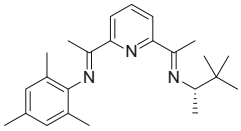

According to the method given above, (*S*)-(+)-3,3-dimethyl-2-butylamine **379a** (0.66 mL, 4.85 mmol) and 2-acetyl-6-[1-(2,4,6-trimethylphenylimino)ethyl]pyridine **378b** (1 g, 3.6 mmol) were reacted to give a the crude product, which was recrystallised from hot dichloromethane to give *2-{1-[(1S)-1-methyl-2,2-dimethylpropylimino]ethyl}-6-[1-(2,4,6-trimethylphenylimino)ethyl]pyridine* **380c** ($^{Me,t Bu}$BIP) as yellow cuboids (1.02 g, 2.81 mmol, 78 %).

m.p. 80–83 °C. **^{1}H NMR** (500 MHz, $CDCl_3$) 8.35 (dd, J = 8.0, 1.0 Hz, 1H, pyH), 8.28 (dd, J = 8.0, 1.0 Hz, 1H, pyH), 7.80 (t, J = 8.0 Hz, 1H, pyH), 6.91 (s, 2H, ArH), 3.48 (q, J = 6.5 Hz, 1H, CH), 2.42 (s, 3H, (CN)CH_3), 2.31 (s, 3H, CH_3), 2.23 (s, 3H, (CN)CH_3), 2.02 (s, 3H, CH_3), 2.02 (s, 3H, CH_3), 1.08 (d, J = 6.5 Hz, 3H, CH_3), 0.98 (s, 9H, CH_3).**^{13}C NMR** (126 MHz, $CDCl_3$) 167.7 (C), 162.9 (C), 157.2 (C), 154.8 (C), 146.4 (C), 136.5 (CH), 132.1 (C), 128.54 (CH), 128.53 (CH), 125.34 (C), 125.31 (C), 122.0 (CH), 121.1 (CH), 64.8 (NCH), 34.8 (C), 26.5 (3 × CH_3), 20.8 (CH_3), 17.87 (CH_3), 17.85 (CH_3), 16.4 (CH_3), 15.6 (CH_3), 12.9 (CH_3). **IR** (neat) ν_{max} cm^{-1} 2959, 2866, 1699, 1638, 1568, 1476, 1451, 1366, 1315, 1244, 1213, 1119, 1095, 1072, 853, 818, 789, 741. **HRMS** (EI) calculated for $C_{24}H_{33}N_3$ 363.26690. Found 363.26830.

2-{1-[(1*S*)-1-Cyclohexylethylimino]ethyl}-6-[1-(2,4,6-trimethylphenylimino)ethyl] pyridine **380d** (^{Me,Cy}BIP)

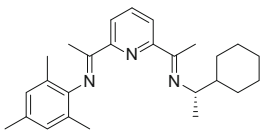

According to the method given above, (*S*)-(+)-1-cyclohexylethylamine **379b** (0.28 mL, 1.85 mmol) and 2-acetyl-6-[1-(2,4,6-trimethylphenylimino)ethyl]pyridine **378b** (463 mg, 1.65 mmol) were reacted to give *2-{1-[(1S)-1-cyclohexylethylimino]ethyl}-6-[1-(2,4,6-trimethylphenylimino)ethyl]pyridine* **380d** (^{Me,Cy}BIP) as a yellow oil, which solidified following 3 days under high vacuum (534 mg, 1.37 mmol, 83 %).

m.p. 76–78 °C. **^{1}H NMR** (500 MHz, $CDCl_3$) 8.35 (dd, J = 8.0, 1.0 Hz, 1H, pyH), 8.22 (dd, J = 8.0, 1.0 Hz, 1H, pyH), 7.80 (t, J = 8.0 Hz, 1H, pyH), 6.90 (s, 2H, ArH), 3.51 (quin., J = 6.5 Hz, 1H, CH), 2.40 (s, 3H, (CN)CH_3), 2.30 (s, 3H, CH_3), 2.22 (s, 3H, (CN)CH_3), 2.01 (s, 3H, CH_3), 2.01 (s, 3H, CH_3), 1.92-1.83 (m, 1H, CH_2), 1.82-1.66 (m, 4H, CH_2), 1.58-1.48 (m, 1H, CH), 1.35-1.18 (m, 3H, CH_2), 1.16 (d, J = 6.5 Hz, 3H, CH_3), 1.08-0.93 (m, 2H, CH_2).**^{13}C NMR** (126 MHz, $CDCl_3$) 167.6 (C), 163.4 (C), 157.2 (C), 154.8 (C), 146.3 (C), 136.5 (CH), 132.1 (C), 128.50 (CH), 128.50 (CH), 125.30 (C), 125.28 (C), 122.0 (CH), 121.1 (CH), 61.3 (NCH), 44.6 (CH), 29.9 (CH_2), 29.8 (CH_2), 26.7 (CH_2), 26.5 (CH_2), 26.4 (CH_2), 20.7 (CH_3), 18.4 (CH_3), 17.84 (CH_3), 17.83 (CH_3), 16.4 (CH_3), 13.4 (CH_3). **IR** (neat) ν_{max} cm^{-1} 2918, 2851, 1638, 1570, 1476, 1449, 1362, 1319, 1248, 1213, 1117, 1034, 854, 818, 785, 741, 679, 635. **HRMS** (EI) calculated for $C_{26}H_{35}N_3$ 389.28255. Found 389.28232. **$[\alpha]_D$** +64.0 (conc. 1.00, $CHCl_3$).

Enantiopure bis(imino)pyridine iron(II) chloride complexes **381a-d**

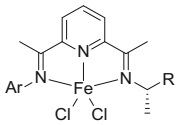

Prepared according to a literature procedure [4].

An enantiopure bis(imino)pyridine ligand **380a-d** and iron(II) chloride (1.1 equiv.) were stirred in anhydrous tetrahydrofuran (0.1 M) under a nitrogen atmosphere at room temperature for 6 h. Anhydrous diethyl ether (5 equiv. with respect to tetrahydrofuran) was added and the resulting suspension stirred for 10 min. The reaction was filtered to give the bis(imino)pyridine iron(II) chloride complex **381a-d**, which was washed with diethyl ether (2 × 20 mL) and dried under high vacuum for 3 h. The complex was dissolved in anhydrous dichloromethane and filtered to remove unreacted iron(II) chloride. The solvent was removed in vacuo and the complex dried under high vacuum for 10 h.

2-{1-[(1S)-1-Methyl-2,2-dimethylpropylimino]ethyl}-6-[1-(2,6-diethylphenylimino)ethyl]pyridine iron(II) chloride **381a** (^{Et,tBu}BIPFeCl_2): blue solid (72 %). **^{1}H NMR** (600 MHz, CD_2Cl_2) 96.7 (1H), 58.5 (1H), 45.2 (3H), 34.2 (1H), 27.6 (1H), 21.6 (1H), 20.4 (1H), 11.5 (1H), −6.2 (3H), −10.4 (1H), −14.9 (9H), −37.3 (3H), −50.2 (3H). Overlapping signals in the range of 0–4 ppm may account for unassigned 5–6 protons. **IR** (neat) ν_{max} cm^{-1} 2963, 2870,1585, 1456, 1447, 1340, 1261, 1202, 1057, 1034, 806, 775.

2-{1-[(1S)-1-Cyclohexylethylimino]ethyl}-6-[1-(2,6-diethylphenylimino)ethyl] pyridine iron(II) chloride **381b** (^{Et,Cy}BIPFeCl$_2$): blue solid (97 %). **^{1}H NMR** (600 MHz, CD_2Cl_2) 91.4 (1H), 66.6 (1H), 34.3 (1H), 23.7 (1H), 21.5 (3H), 19.9 (1H), 16.0 (1H), 9.1 (1H), 3.7 (2H), 1.8 (2H), −1.0 (1H), −2.26 (1H), −2.34 (1H), −3.1 (1H), −3.6 (1H), −3.7 (1H), −4.2 (3H), −4.6 (1H), −4.7 (1H), −5.9 (1H), −7.7 (1H), −8.9 (1H), −16.3 (1H), −26.0 (3H), −34.8 (1H), −43.4 (3H). (1H assignment missing) **IR** (neat) ν_{max} cm^{-1} 2968, 2922, 2845, 1585, 1447, 1369, 1364, 1260, 1204, 1063, 1034, 1016.

2-{1-[(1S)-1-Methyl-2,2-dimethylpropylimino]ethyl}-6-[1-(2,4,6-trimethylphenylimino)ethyl]pyridine iron(II) chloride **381c** (^{Me,tBu}BIPFeCl$_2$): blue solid (88 %). **^{1}H NMR** (600 MHz, CD_2Cl_2) 147.7 (1H), 96.1 (1H), 58.6 (1H), 43.8 (3H), 32.2 (1H), 26.8 (1H), 24.3 (3H), 20.9 (1H), 18.2 (3H), −2.9 (3H), −14.9 (9H), −35.1 (3H), −50.5 (3H). **IR** (neat) ν_{max} cm^{-1} 2967, 2922, 2864, 1580, 1477, 1371, 1260, 1215, 1055, 1034, 1016, 864, 808, 737.

2-{1-[(1S)-1-Cyclohexylethylimino]ethyl}-6-[1-(2,4,6-trimethylphenylimino) ethyl]pyridine iron(II) chloride **381d** (^{Me,Cy}BIPFeCl$_2$): blue solid (91 %). **^{1}H NMR** (600 MHz, CD_2Cl_2) 91.0 (1H), 67.3 (1H), 30.4 (1H), 23.0 (4H), 20.6 (3H), 19.0 (1H), 16.2 (3H), 4.9 (3H), 3.7 (1H), 3.4 (1H), −2.1 (1H), −2.7 (1H), −3.2 (2H), −4.3 (2H), −5.3 (1H), −7.2 (1H), −8.1 (1H), −14.5 (1H), −24.1 (3H), −31.8 (1H), −43.2 (3H). **IR** (neat) ν_{max} cm^{-1} 2968, 2920, 2845, 1628, 1587, 1474, 1445, 1371, 1261, 1217, 1055, 1034, 1022, 856, 804, 737.

Enantioselective Hydrosilylation of α-Methylstyrene **382**

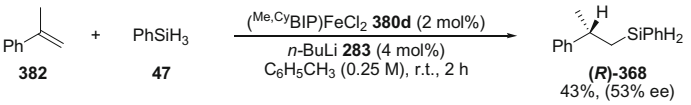

n-Butyllithium **283** (1 M in hexane, 0.26 mL, 0.26 mmol) was added to a suspension of 2,6-bis-[1-(2,6-diethylphenylimino)ethyl]pyridine iron(II) chloride **367** (^{Et}BIPFeCl$_2$) (72 mg, 0.13 mmol) in α-methylstyrene **382** (1.1 mL, 8.4 mmol) and toluene (2 mL) at room temperature under an atmosphere of nitrogen. Phenylsilane **47** (1.3 mL, 10.5 mmol) was added and the reaction stirred for 2 h. Aqueous sulfate buffer (10 mL) was added and the aqueous phase extracted with diethyl ether (3 × 20 mL). The combined organic extracts were washed with water and brine, dried ($MgSO_4$) and concentrated in vacuo to give 1-(phenylsilyl)-2-phenylpropane **368** as a colourless oil (43 %—based upon quantitative ^{1}H NMR spectroscopy using trimethoxybenzene as an internal standard).

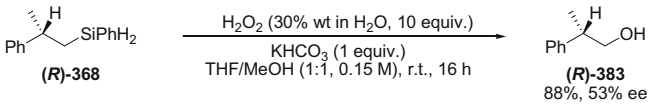

The crude product (~3.6 mmol) was added to a suspension of potassium hydrogen carbonate (360 mg, 3.6 mmol) in a mixture of tetrahydrofuran (14 mL) and methanol (14 mL). Hydrogen peroxide (4.8 mL, 30 % aqueous solution, 42 mmol) was added and the reaction stirred for 16 h at room temperature. Aqueous sulfate buffer (10 mL) was added and the aqueous phase extracted with diethyl ether (3 × 20 mL). The combined organic extracts were washed sequentially with water and brine, dried ($MgSO_4$) and concentrated in vacuo. The crude product was purified by flash silica chromatography (20 % EtOAc/hexane) to give 2-phenylpropanol **383** as a colourless oil (431 mg, 3.16 mmol, 88 %).

^{1}H NMR (500 MHz, $CDCl_3$) 7.39-7.34 (m, 2H, ArH), 7.29-7.25 (m, 3H, ArH), 3.72 (d, J = 7.0 Hz, 2H, CH_2), 2.98 (app. sext., J = 7.0 Hz, 2H, CH), 1.50 (br. s, 1H, OH), 1.31 (d, J = 7.0 Hz, 3H, CH_3). **^{13}C NMR** (126 MHz, $CDCl_3$) 143.6 (C), 128.6 (2 × CH), 127.4 (2 × CH), 126.6 (CH), 68.7 (CH_2), 42.4 (CH), 17.5 (CH_3). **Chiral HPLC** (chiralpak-IA, hexane/^{i}PrOH 99/1, 1.0 mL/min, 254 nm) 53.4 % ee: minor (23.27 %) retention time = 24.42 min; major (76.73 %) retention time = 28.26 min. **$[\alpha]_D$** +12.7 (conc. 0.79, $CHCl_3$)

Data were in accordance with those previously reported, with the major enantiomer determined to be (*R*)-2-phenylpropanol based upon retention time and direction of optical rotation [23].

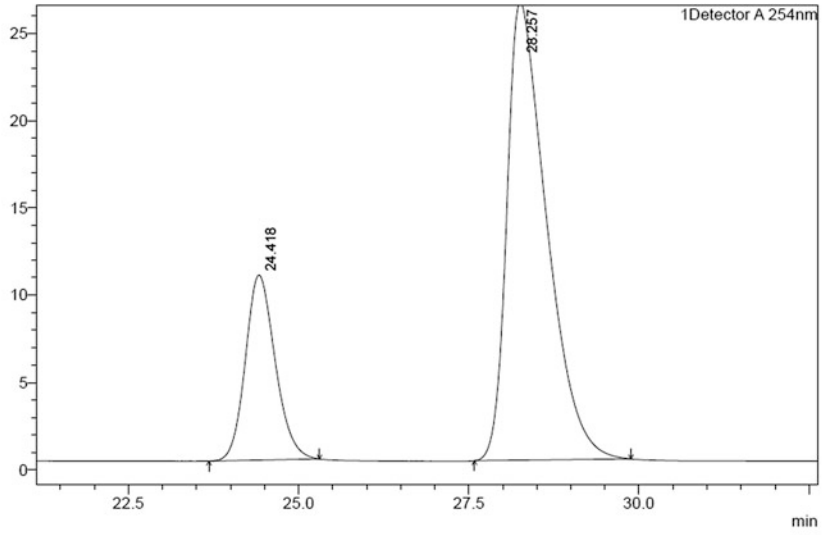

<Peak Table>

Detector A 254nm

Peak#	Ret. Time	Area	Height	Mark	Name	Area%
1	24.418	323348	10584	M		23.269
2	28.257	1066286	26242	M		76.731
Total		1389635	36826			100.000

An authentic sample of racemic 2-phenylpropanol was prepared by lithium aluminium hydride reduction of 2-phenylpropionic acid. **Chiral HPLC** (chiralpak-IA, hexane/^{i}PrOH 99/1, 1.0 mL/min, 254 nm) 0.8 % ee: minor (49.10 %) retention time = 23.99 min; major (50.90 %) retention time = 27.98 min.

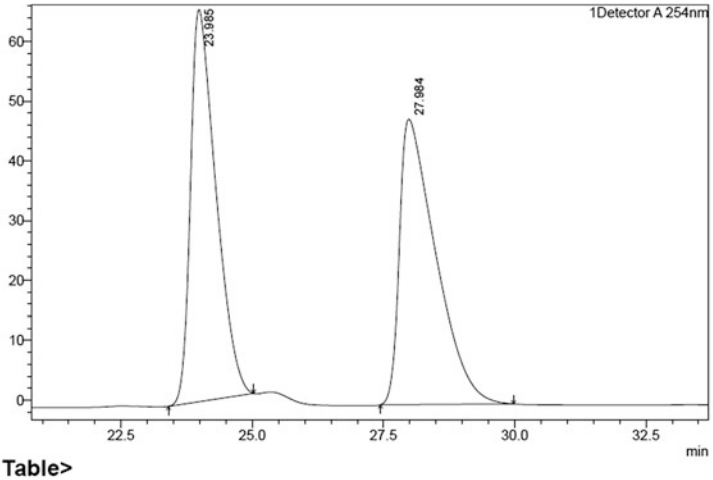

<Peak Table>

Detector A 254nm

Peak#	Ret. Time	Area	Height	Mark	Name	Area%
1	23.985	2212468	65634	M		49.096
2	27.984	2293939	47761	M		50.904
Total		4506407	113395			100.000

(*E*)-1-Phenyl-2-phenyl-2-(phenylsilyl)ethene **(*E*)-386**

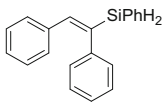

According to General Procedure **A**, diphenylacetylene **396** (125 mg, 0.7 mmol), phenylsilane **47** (95 μL, 0.77 mmol), iron(II) chloride **279** (0.9 mg, 0.007 mmol), 2,6-bis-[1-(2,6-diethylphenylimino)ethyl]pyridine **273b** (3.0 mg, 0.007 mmol) and ethylmagnesium bromide **280** (2 drops, 0.015 mmol) were reacted in anhydrous tetrahydrofuran (3 mL) to give the crude reaction product, which was purified by filtration through a plug of silica using 0.5 % ethyl acetate/petroleum ether to give *(E)-1-phenyl-2-phenyl-2-(phenylsilyl)ethene* **(*E*)-386** as a colourless solid (180 mg, 0.63 mmol, 90 %).

m.p. 55–56 °C. **^{1}H NMR** (400 MHz, $CDCl_3$) 7.64-7.58 (m, 2H, ArH), 7.47-7.35 (m, 3H, ArH), 7.32-7.26 (m, 2H, ArH), 7.25-7.19 (m, 1H, ArH), 7.17-7.12 (m, 3H, ArH), 7.12-7.08 (m, 3H, ArH), 7.07-7.04 (m, 2H, ArH) 4.83 (s, 2H, CH). **^{13}C NMR** (101 MHz, $CDCl_3$) 142.3 (CH), 141.4 (C), 138.5 (C), 136.8 (C), 135.7 (2 × CH), 131.3 (C), 129.9 (CH), 129.5 (2 × CH), 128.8 (2 × CH), 128.04 (2 × CH), 127.96 (2 × CH), 127.8 (2 × CH), 127.6 (CH), 126.3 (CH). **^{29}Si NMR** (79 MHz, $CDCl_3$) −27.9. **IR** (neat) ν_{max} cm^{-1} 3051, 3021, 2133, 1597, 1489, 1447, 1429, 1115, 1072, 1032, 957, 924, 835, 692. **HRMS** (EI) calculated for $C_{20}H_{18}Si$ 286.11723. Found 286.11740.

Protodesilylation using tetra(*n*-butyl)ammonium fluoride [24] gave cis-stilbene exclusively, as determined by ^{1}H NMR spectroscopy and GCMS.

(*E*)-1-Phenyl-2-(phenylsilyl)propene **(*E*)-β-388** and 1-phenyl-1-(phenylsilyl)propene **α-388.**

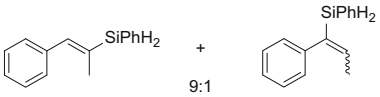

According to General Procedure **A**, 1-phenylpropyne **398** (87 μL, 0.7 mmol), phenylsilane **47** (95 μL, 0.77 mmol), iron(II) chloride **279** (0.9 mg, 0.007 mmol), 2,6-bis-[1-(2,6-diethylphenylimino)ethyl]pyridine **273b** (3.0 mg, 0.007 mmol) and ethylmagnesium bromide **280** (2 drops, 0.015 mmol) were reacted in anhydrous tetrahydrofuran (3 mL) to give the crude reaction product, which was purified by filtration through a plug of silica using 0.5 % ethyl acetate/petroleum ether to give a 9:1 mixture of (*E*)-1-phenyl-2-(phenylsilyl)propene **(*E*)-β-388** and *1-phenyl-1-(phenylsilyl)propene* **α-388** as a colourless oil (138 mg, 0.62 mmol, 88 %).

(*E*)-1-Phenyl-2-(phenylsilyl)propene **(*E*)-β-388**: **^{1}H NMR** (400 MHz, $CDCl_3$) 7.70-7.63 (m, 2H, ArH), 7.48-7.25 (m, 8H, ArH), 7.04 (q, J = 2.0 Hz, 1H, CH), 4.69 (s, 2H, SiH_2), 2.06 (d, J = 2.0 Hz, 3H, CH_3). **^{13}C NMR** (101 MHz, $CDCl_3$) 142.4 (CH), 137.8 (C), 135.6 (2 × CH), 132.7 (C), 131.6 (C), 129.8 (CH), 129.0 (2 × CH), 128.12 (2 × CH), 128.09 (2 × CH), 127.0 (CH), 17.5 (CH_3). **^{29}Si NMR** (79 MHz, $CDCl_3$) −27.6.

1-Phenyl-1-(phenylsilyl)propene **α-388**: **^{1}H NMR** (400 MHz, $CDCl_3$) 7.57-7.53 (m, 2H, ArH), 7.48-7.25 (m, 5H, ArH), 7.24-7.18 (m, 1H, ArH), 7.11-7.07 (m, 2H, ArH), 6.39 (q, J = 6.5 Hz, 1H, CH), 4.71 (s, 2H, SiH_2), 1.75 (d, J = 6.5 Hz, 3H, CH_3). **^{13}C NMR** (101 MHz, $CDCl_3$) 141.5 (CH), 140.8 (C), 137.3 (C), 135.6 (2 × CH), 131.9 (C), 129.6 (CH), 128.21 (2 × CH), 128.17 (2 × CH), 127.9 (2 × CH), 126.0 (CH), 16.3 (CH_3). **^{29}Si NMR** (79 MHz, $CDCl_3$) −30.7.

Combined: **IR** (neat) ν_{max} cm^{-1} 3019, 2924, 2127, 1597, 1489, 1429, 1115, 1032, 926, 833, 760, 714, 694. **HRMS** (EI) calculated for $C_{15}H_{16}Si$ 224.10158. Found 224.10146.

Stereochemistry of major isomer confirmed by 1D nOe:

Irradiation of SiH_2 peak at 4.69 ppm, strong positive nOe observed for peaks at 7.04 ppm (vinyl CH) and 2.06 ppm (CH_3). (peak at 7.70 ppm = *ortho* CH on phenyl group on silane—expected for both stereoisomers)

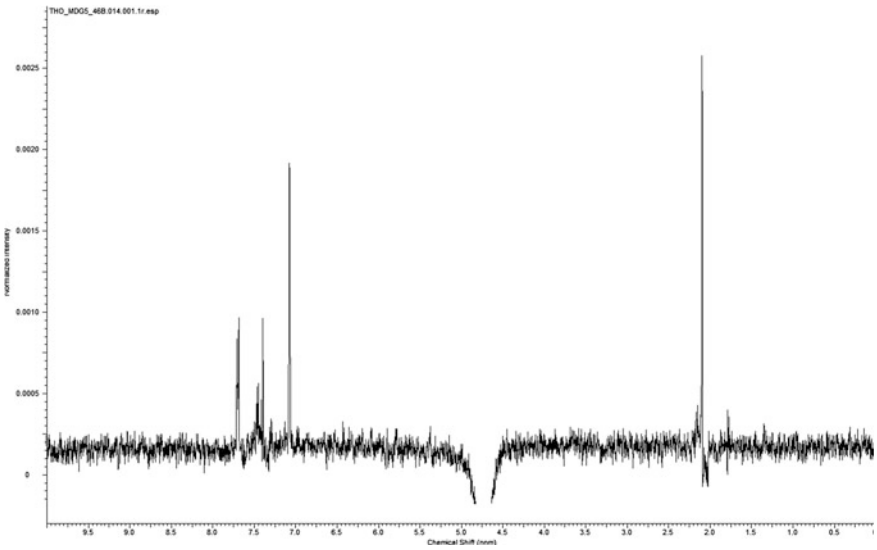

(*E*)-isomer

$SiH_2 \rightarrow$ vinyl CH = 2.5Å - nOe expected

$SiH_2 \rightarrow CH_3$ = 2.8Å - nOe expected

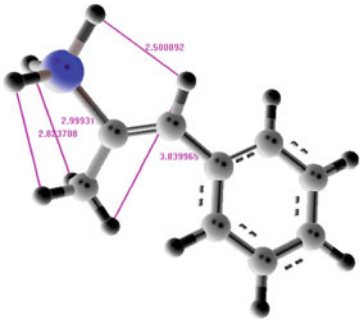

(*Z*)-isomer

$SiH_2 \rightarrow$ vinyl CH = 4.5Å - nOe ***not*** expected

$SiH_2 \rightarrow CH_3$ = 2.8Å - nOe expected

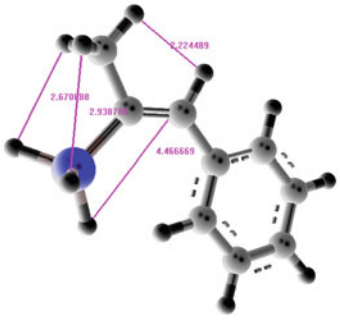

Therefore assigned as **(*E*)-isomer**

(*Z*)- and (*E*)-1-Phenyl-2-(phenylsilyl)ethene **(*Z*)-** and **(*E*)-389** (*Z*:*E* = 4:1 → 6:1)

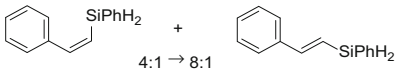

According to General Procedure **A**, phenylacetylene **329** (77 μL, 0.7 mmol), phenylsilane **47** (95 μL, 0.77 mmol), iron(II) chloride **279** (0.9 mg, 0.007 mmol), 2,6-bis-[1-(2,6-diethylphenylimino)ethyl]pyridine **273b** (3.0 mg, 0.007 mmol) and ethylmagnesium bromide **280** (2 drops, 0.015 mmol) were reacted in anhydrous tetrahydrofuran (3 mL) to give the crude reaction product, which was purified by filtration through a plug of silica using 0.5 % ethyl acetate/petroleum ether to give an 8:1 mixture of *(Z)- and (E)-1-phenyl-2-(phenylsilyl)ethene* **(*E*)-** and **(*Z*)-389** as a colourless oil (109 mg, 0.52 mmol, 74 %).

Major diastereoisomer, **(*Z*)-389**: **^{1}H NMR** (500 MHz, $CDCl_3$) 7.64-7.60 (m, 2H, ArH), 7.60 (d, *J* = 14.5 Hz, 1H, CH), 7.43-7.33 (m, 7H, ArH), 7.33-7.28 (m, 1H, ArH), 6.03 (dt, *J* = 14.5, 4.5 Hz, 1H, CH), 4.73 (d, *J* = 4.5 Hz, 2H, SiH_2). **^{13}C NMR** (126 MHz, $CDCl_3$) 150.4 (CH), 138.8 (C), 135.2 (2 × CH), 132.1 (C), 129.7 (CH), 128.3 (2 × CH), 128.2 (2 × CH), 128.09 (2 × CH), 128.05 (CH), 121.9 (CH). **^{29}Si NMR** (99 MHz, $CDCl_3$) −46.9.

Minor diastereoisomer, **(*E*)-389**: **^{1}H NMR** (500 MHz, $CDCl_3$) 7.66-7.63 (m, 2H, ArH), 7.49-7.46 (m, 2H, ArH), 7.43-7.33 (m, 6H, ArH), 7.18 (d, *J* = 19.0 Hz, 1H, CH), 6.53 (dt, *J* = 19.0, 3.5 Hz, 1H, CH), 4.72 (d, *J* = 3.5 Hz, 2H, SiH_2). **^{13}C NMR** (126 MHz, $CDCl_3$) 149.3 (CH), 137.7 (C), 135.5 (2 × CH), 131.6 (C), 129.8 (CH), 128.6 (CH), 128.6 (2 × CH), 128.1 (2 × CH), 126.7 (2 × CH), 119.4 (CH). **^{29}Si NMR** (99 MHz, $CDCl_3$) −36.5.

Combined: **IR** (neat) ν_{max} cm^{-1} 3067, 3021, 2129, 1589, 1568, 1493, 1445, 1429, 1115, 934, 845, 820, 777, 735, 696. **HRMS** (EI) calculated for $C_{14}H_{14}Si$ 210.08593. Found 210.08685.

(*Z*)- and (*E*)-5-Phenyl-1-(phenylsilyl)pent-1-ene **(*Z*)-** and **(*E*)-390** (*Z*:*E* = 6:1 → >100:1)

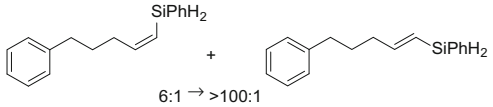

According to General Procedure **A**, 5-phenylpentyne **391** (101 mg, 0.7 mmol), phenylsilane **47** (95 μL, 0.77 mmol), iron(II) chloride **279** (0.9 mg, 0.007 mmol), 2,6-bis-[1-(2,6-diethylphenylimino)ethyl]pyridine **273b** (3.0 mg, 0.007 mmol) and ethylmagnesium bromide **280** (2 drops, 0.015 mmol) were reacted in anhydrous tetrahydrofuran (3 mL) to give the crude reaction product, which was purified by

filtration through a plug of silica using 0.5 % ethyl acetate/petroleum ether to give a 60:1 mixture of *(Z)- and (E)-5-phenyl-1-(phenylsilyl)pent-1-ene* **(*Z*)-** and **(*E*)-390** as a colourless oil (114 mg, 0.46 mmol, 66 %).

Major diastereoisomer, **(*Z*)-390**: **^{1}H NMR** (500 MHz, $CDCl_3$) 7.63-7.58 (m, 2H, ArH), 7.43-7.36 (m, 3H, ArH), 7.34-7.28 (m, 2H, ArH), 7.24-7.16 (m, 2H, ArH), 6.66 (dt, J = 13.5, 7.5 Hz, 1H, CH), 5.76 (dtt, J = 13.5, 4.0, 1.0 Hz, 1H, CH), 4.61 (d, J = 4.0 Hz, 2H, SiH_2), 2.66-2.61 (m, 2H, $ArCH_2$), 2.32 (app. qd, J = 7.5, 1.0 Hz, 2H, (CH=CH)C***H*****$_2$**), 1.80-1.71 (m, 2H, CH_2). **^{13}C NMR** (126 MHz, $CDCl_3$) 153.0 (CH), 142.2 (C), 135.3 (2 × CH), 132.2 (C), 129.5 (CH), 128.4 (2 × CH), 128.3 (2 × CH), 128.0 (2 × CH), 125.7 (CH), 119.6 (CH), 35.4 ($ArCH_2$), 33.0 ((CH=CH)***C***H_2), 31.0 (CH_2). **^{29}Si NMR** (99 MHz, $CDCl_3$) −50.4.

Minor diastereoisomer, **(*E*)-390**: **^{1}H NMR** (500 MHz, $CDCl_3$) 7.63-7.58 (m, 2H, ArH), 7.45-7.39 (m, 3H, ArH), 7.34-7.28 (m, 2H, ArH), 7.24-7.16 (m, 2H, ArH), 6.41 (dt, J = 18.5, 6.5 Hz, 1H, CH), 5.82-5.75 (m, 1H, CH), 4.58 (d, J = 3.0 Hz, 2H, SiH_2), 2.70-2.64 (m, 2H, $ArCH_2$), 2.26 (app. q, J = 7.0 Hz, 2H, (CH=CH)C***H*****$_2$**), 1.84-1.77 (m, 2H, CH_2). **^{13}C NMR** (126 MHz, $CDCl_3$) 153.4 (CH), 142.2 (C), 135.3 (2 × CH), 132.2 (C), 129.6 (CH), 128.4 (2 × CH), 128.3 (2 × CH), 128.0 (2 × CH), 125.8 (CH), 120.5 (CH), 36.3 ((CH=CH)***C***H_2), 35.3 ($ArCH_2$), 30.1 (CH_2). **^{29}Si NMR** (99 MHz, $CDCl_3$) −38.0.

Combined: **IR** (neat) ν_{max} cm^{-1} 3024, 2934, 2857, 2131, 1603, 1497, 1452, 1429, 1115, 1032, 935, 841, 737, 696. **HRMS** (EI) calculated for $C_{17}H_{20}Si$ 252.13288. Found 252.13280.

5-Phenyl-1,1-di(phenylsilyl)pentane **395**

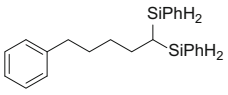

^{1}H NMR (500 MHz, $CDCl_3$) 7.55-7.50 (m, 4H, ArH), 7.42-7.37 (m, 2H, ArH), 7.37-7.31 (m, 4H, ArH), 7.28-7.24 (m, 2H, ArH), 7.20-7.15 (m, 1H, ArH), 7.12-7.08 (m, 2H, ArH), 4.41 (dd, J = 6.0, 3.5 Hz, 2H, SiH_2), 4.36 (dd, J = 6.0, 4.0 Hz, 2H, SiH_2), 2.51 (app. t, J = 7.5 Hz, 2H, $ArCH_2$), 1.69-1.62 (m, 2H, CH_2), 1.58-1.50 (m, 2H, CH_2), 1.50-1.42 (m, 2H, CH_2), 0.68 (app. non., J = 3.5 Hz, 1H, CH). **^{13}C NMR** (126 MHz, $CDCl_3$) 142.5 (C), 135.5 (4 × CH), 132.2 (2 × C), 129.6 (2 × CH), 128.4 (2 × CH), 128.2 (2 × CH), 128.0 (4 × CH), 125.7 (CH), 35.6 ($ArCH_2$), 31.2 (CH_2), 31.0 (CH_2), 27.7 (CH_2), 4.19 (CH). **^{29}Si NMR** (99 MHz, $CDCl_3$) −28.2. **IR** (neat) ν_{max} cm^{-1} 3024, 2924, 2853, 2127, 1494, 1452, 1427, 1115, 1032, 1018, 932, 826, 731. **HRMS** (EI) calculated for $C_{23}H_{28}Si_2$ 360.17241. Found 360.17134.

2-Phenylethanol **411**

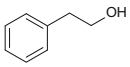

Potassium hydrogen carbonate **410** (50 mg, 0.5 mmol) and 30 % aqueous H_2O_2 **409** (1.02 mL, 9 mmol) were added to a solution of 1-phenyl-2-(diethylsilyl)ethane **301** (96 mg, 0.5 mmol) in tetrahydrofuran (2 mL) and methanol (2 mL) and stirred at room temperature for 16 h. Aqueous sulfate buffer (10 mL) was added and the aqueous phase extracted with diethyl ether (3 × 20 mL). The combined organic extracts were washed with water and brine, dried ($MgSO_4$) and concentrated in vacuo to give 2-phenylethanol **411** as a colourless oil (56 mg, 0.46 mmol, 92 %).

^{1}H NMR (400 MHz, $CDCl_3$) 7.36-7.30 (m, 2H, ArH), 7.27-7.22 (m, 3H, ArH), 3.88 (t, J = 6.5 Hz, 2H, C***H***$_2$OH), 2.89 (t, J = 6.5 Hz, 2H, $ArCH_2$), 1.76 (br. s, 1H, OH). **^{13}C NMR** (101 MHz, $CDCl_3$) 138.4 (C), 129.0 (2 × CH), 128.6 (2 × CH), 126.5 (CH), 63.7 (CH_2OH), 39.2 ($ArCH_2$).

Data were in accordance with those previously reported [25].

d_n-2-Phenylethanol ***d*$_n$-411**

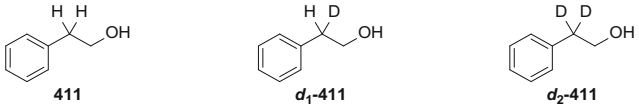

411 4%

***d*$_1$-411** 58%

***d*$_2$-411** 38%

Potassium hydrogen carbonate **410** (35 mg, 0.35 mmol) and 30 % aqueous H_2O_2 **409** (0.65 mL, 5.8 mmol) were added to a solution of 1-phenyl-2-(diphenylsilyl) (ethane-d_n) ***d*$_n$-300** (92 mg, 0.32 mmol) in tetrahydrofuran (1.5 mL) and methanol (1.5 mL) and stirred at room temperature for 16 h. Aqueous sulfate buffer (10 mL) was added and the aqueous phase extracted with diethyl ether (3 × 20 mL). The combined organic extracts were washed with water and brine, dried ($MgSO_4$) and concentrated in vacuo to give 2-phenylethanol **411** and the deuterated derivatives ***d*$_1$-411** and ***d*$_2$-411** in an approximate ratio of 4:58:38 respectively.

^{1}H NMR (400 MHz, $CDCl_3$) 7.36-7.30 (m, 2H, ArH), 7.27-2.22 (m, 3H, ArH), 7.33-7.27 (m, 2H, ArH), 3.91-3.84 (br., 2H, CH_2OH), 2.91-2.84 (m, 0.65H, $ArCH_2$) **^{13}C NMR** (126 MHz, $CDCl_3$)—selected peaks: 63.67 (**411**, CH_2OH), 63.63 (***d*$_1$-411**, CH_2OH), 63.58 (***d*$_2$-411**, CH_2OH), 39.2 (**411**, $ArCH_2$), 38.8 (t, J = 19.5 Hz, ***d*$_1$-411**, ArCHD), 38.5 (quin., J = 19.5 Hz, ***d*$_2$-411**, $ArCD_2$). **^{2}H NMR** (61 MHz, $CHCl_3$) 2.66-2.47 (br, ArCD(H/D)).

***d*$_2$-411** also confirmed by **HRMS** (EI) calculated for $C_8H_8D_2O$ 124.08517. Found 124.08510.

2-Phenylethanol d_n-**411** NMR spectra

^{1}H NMR spectra: 400 MHz

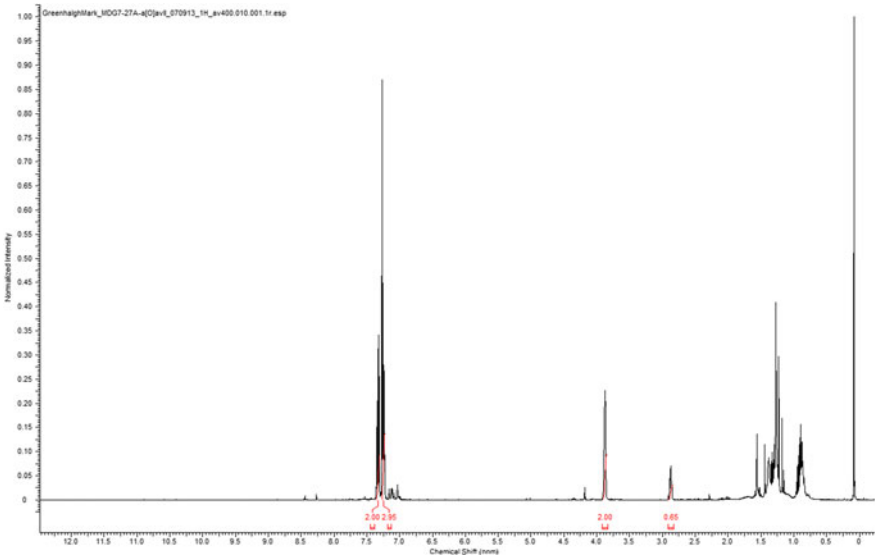

^{13}C NMR spectra: 126 MHz

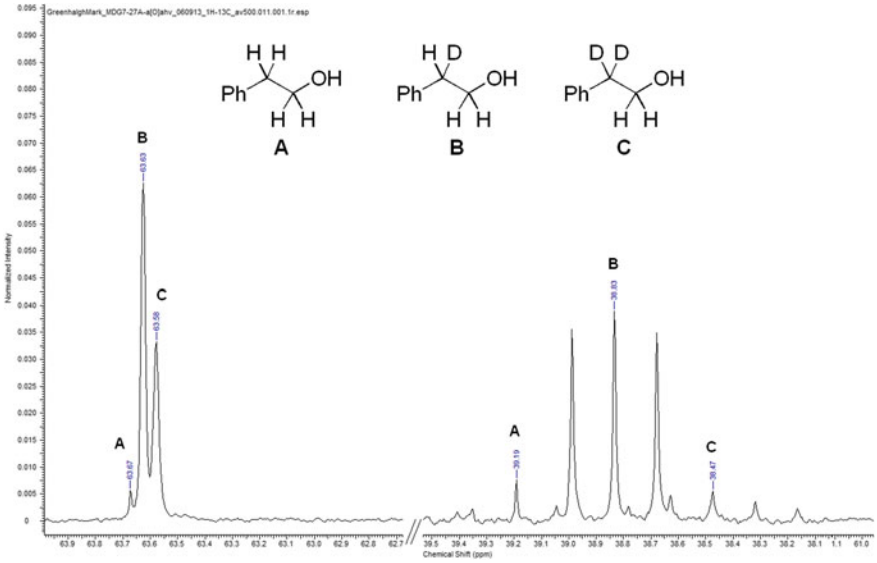

^{2}H NMR spectra: 61 MHz:

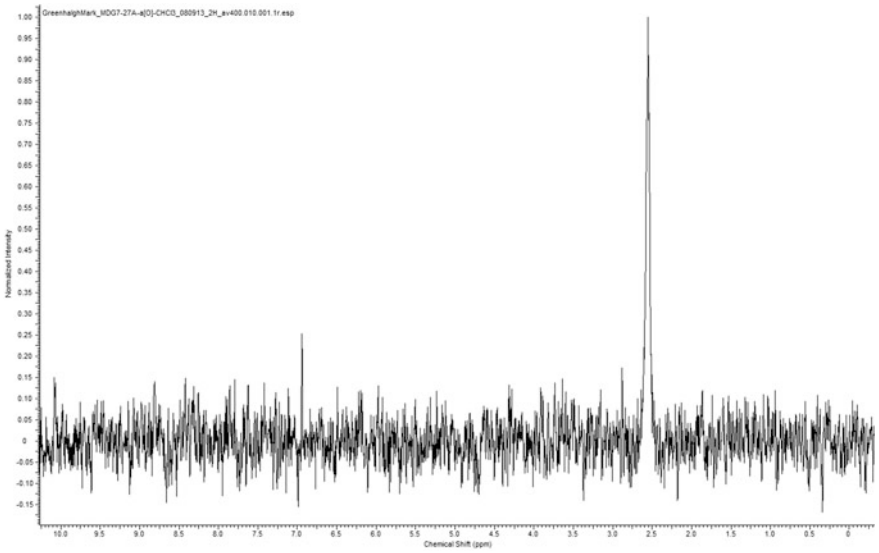

2-(4-Chlorophenyl)ethanol **412**

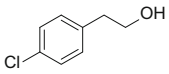

Potassium hydrogen carbonate **410** (34 mg, 0.34 mmol) and 30 % aqueous H_2O_2 **409** (0.46 mL, 4 mmol) were added to a solution of 1-(4-chlorophenyl)-2-(phenylsilyl)ethane **344** (84 mg, 0.34 mmol) in tetrahydrofuran (1.5 mL) and methanol (1.5 mL) and stirred at room temperature for 16 h. Aqueous sulfate buffer (10 mL) was added and the aqueous phase extracted with diethyl ether (3 × 20 mL). The combined organic extracts were washed with water and brine, dried ($MgSO_4$) and concentrated in vacuo to give 2-(4-chlorophenyl)ethanol **412** as a colourless oil (51 mg, 0.33 mmol, 96 %).

^{1}H NMR (400 MHz, $CDCl_3$) 7.31-7.28 (m, 2H, ArH), 7.19-7.15 (m, 3H, ArH), 3.86 (t, J = 6.5 Hz, 2H, C***H***$_2$OH), 2.85 (t, J = 6.5 Hz, 2H, $ArCH_2$), 1.91 (br. s, 1H, OH). **^{13}C NMR** (101 MHz, $CDCl_3$) 136.9 (C), 132.3 (C), 130.3 (2 × CH), 128.7 (2 × CH), 63.4 (CH_2OH), 38.4 ($ArCH_2$).

Data were in accordance with those previously reported [26].

Methyl 4-(2-hydroxyethyl)benzoate **413**

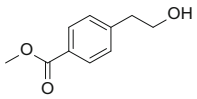

Potassium hydrogen carbonate **410** (19 mg, 0.19 mmol) and 30 % aqueous H_2O_2 **409** (0.25 mL, 2.2 mmol) were added to a solution of methyl 4-[2-(phenylsilyl) ethyl]benzoate **351** (50 mg, 0.19 mmol) in tetrahydrofuran (1 mL) and methanol (1 mL) and stirred at room temperature for 16 h. Aqueous sulfate buffer (10 mL) was added and the aqueous phase extracted with diethyl ether (3 × 20 mL). The combined organic extracts were washed with water and brine, dried ($MgSO_4$) and concentrated in vacuo to give methyl 4-(2-hydroxyethyl)benzoate **413** as a colourless oil (32 mg, 0.18 mmol, 94 %).

^{1}H NMR (500 MHz, $CDCl_3$) 8.01-7.97 (m, 2H, ArH), 7.33-7.29 (m, 2H, ArH), 3.91 (s, 3H, CH_3), 3.90 (t, J = 6.5 Hz, 2H, C***H*****$_2$**OH), 2.94 (t, J = 6.5 Hz, 2H, $ArCH_2$), 1.68 (br s., 1H, OH). **^{13}C NMR** (126 MHz, $CDCl_3$) 167.1 (C=O), 144.1 (C), 129.9 (2 × CH), 129.0 (2 × CH), 128.4 (C), 63.3 (CH_2OH), 52.0 (CH_3), 39.1 ($ArCH_2$). **IR** (neat) ν_{max} cm^{-1} 3431, 2951, 1717, 1608, 1595, 1435, 1277, 1179, 1101, 1061, 1018, 756, 700.

Data were in accordance with those previously reported [27].

2-Phenylacetophenone **414**

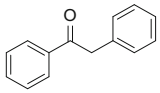

Potassium hydrogen carbonate **410** (35 mg, 0.35 mmol) and 30 % aqueous H_2O_2 **409** (0.48 mL, 4.2 mmol) were added to a solution of (*E*)-1-phenyl-2-phenyl-2-(phenylsilyl)ethene **(*E*)-386** (100 mg, 0.35 mmol) in tetrahydrofuran (1.5 mL) and methanol (1.5 mL) and stirred at room temperature for 16 h. Aqueous sulfate buffer (10 mL) was added and the aqueous phase extracted with diethyl ether (3 × 20 mL). The combined organic extracts were washed with water and brine, dried ($MgSO_4$) and concentrated in vacuo to give 2-phenylacetophenone **414** as a colourless solid (65 mg, 0.33 mmol, 95 %).

m.p. 59–61 °C. **^{1}H NMR** (500 MHz, $CDCl_3$) 8.05-8.01 (m, 2H, ArH), 7.59-7.55 (m, 1H, ArH) 7.50-7.45 (m, 2H, ArH), 7.37-7.32 (m, 2H, ArH), 7.30-7.24 (m, 3H, ArH), 4.30 (s, 2H, CH_2). **^{13}C NMR** (126 MHz, $CDCl_3$) 197.6 (C=O), 136.6 (C), 134.5 (C), 133.2 (CH), 129.4 (2 × CH), 128.66 (2 × CH), 128.63 (2 × CH), 128.60 (2 × CH), 126.9 (CH), 45.5 (CH_2). **IR** (neat) ν_{max} cm^{-1} 3057, 3026, 1682, 1595, 1497, 1449, 1429, 1335, 1070, 1028, 752, 727, 694.

Data were in accordance with those previously reported [28].

Diethyl(phenylethenyl)silanol **415**

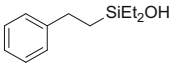

According to General Procedure **A**, styrene **53** (80 μL, 0.7 mmol), diethylsilane **296** (91 μL, 0.7 mmol), iron(II) chloride **279** (0.9 mg, 0.007 mmol), 2,6-bis-[1-(2,6-diethylphenylimino)ethyl]pyridine **273b** (3.0 mg, 0.007 mmol) and ethylmagnesium bromide **280** (2 drops, 0.015 mmol) were reacted in anhydrous tetrahydrofuran (3 mL) for 1 h. Methanol (3 mL), potassium bicarbonate **410** (80 mg, 0.8 mmol) and 30 % aqueous hydrogen peroxide **409** (0.8 mL, 7 mmol) were added and the reaction stirred at room temperature for 2 h. Aqueous sulfate buffer (10 mL) was added and the aqueous phase extracted with diethyl ether (3 × 20 mL). The combined organic extracts were washed with water and brine, dried ($MgSO_4$) and concentrated in vacuo to give *diethyl(phenylethyl)silanol* **415** as a yellow oil (139 mg, 0.67 mmol, 95 %).

^{1}H NMR (500 MHz, $CDCl_3$) 7.32-7.27 (m, 2H, ArH), 7.25-7.21 (m, 2H, ArH), 7.21-7.16 (m, 1H, ArH), 2.75-2.70 (m, 2H, $ArCH_2$), 1.41 (br. s, 1H, SiOH), 1.04-0.98 (m, 2H, CH_2Si), 1.00 (t, J = 8.0 Hz, 6H, CH_3), 0.64 (q, J = 8.0 Hz, 4H, CH_2CH_3). **^{13}C NMR** (126 MHz, $CDCl_3$) 144.9 (C), 128.4 (2 × CH), 127.8 (2 × CH), 125.7 (CH), 29.2 ($ArCH_2$), 16.1 ($SiCH_2$), 6.6, 6.2. **^{29}Si NMR** (79 MHz, $CDCl_3$) 18.1. **IR** (neat) ν_{max} cm^{-1} 3306, 2953, 2911, 2876, 1495, 1454, 1412, 1236, 1175, 1009, 825, 735, 696. **HRMS** (EI) calculated for $C_{12}H_{20}OSi$ 208.12780. Found 208.12805.

Hexyl[(*E*)-1,2-diphenylethenyl)silanediol **417**

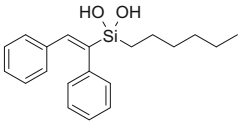

According to general procedure **A**, diphenylacetylene **396** (125 mg, 0.7 mmol), hexylsilane **416** (125 μL, 0.77 mmol), iron(II) chloride **279** (0.9 mg, 0.007 mmol), 2,6-bis-[1-(2,6-diethylphenylimino)ethyl]pyridine **273b** (3.0 mg, 0.007 mmol) and ethylmagnesium bromide **280** (2 drops, 0.015 mmol) were reacted in anhydrous tetrahydrofuran (3 mL) for 1 h. Methanol (3 mL), potassium bicarbonate **410** (80 mg, 0.8 mmol) and 30 % aqueous hydrogen peroxide **409** (0.8 mL, 7 mmol) were added and the reaction stirred at room temperature for 2 h. Aqueous sulfate buffer (10 mL) was added and the aqueous phase extracted with diethyl ether (3 × 20 mL). The combined organic extracts were washed with water and brine, dried ($MgSO_4$) and concentrated in vacuo to give *hexyl[(E)-1,2-diphenylethenyl) silanediol* **417** as a yellow oil (213 mg, 0.65 mmol, 93 %).

^{1}H NMR (400 MHz, $CDCl_3$) 7.35-7.28 (m, 2H, ArH), 7.26-7.20 (m, 1H, ArH), 7.16-7.07 (m, 6H, ArH, CH), 7.04-6.98 (m, 2H, ArH), 2.90 (br. s, 2H, SiOH), 1.48-1.38 (m, 2H, CH_2), 1.36-1.20 (m, 6H, CH_2), 0.87 (t, J = 7.0 Hz, 3H, CH_3), 0.81-0.74 (m, 2H, $SiCH_2$). **^{13}C NMR** (101 MHz, $CDCl_3$) 141.6 (C), 140.9 (C), 140.4 (CH), 136.7 (C), 129.84 (2 × CH), 128.94 (2 × CH), 127.94 (2 × CH), 127.84 (2 × CH), 127.64 (CH), 126.3 (CH), 32.8 (CH_2), 31.5 (CH_2), 22.7 (CH_2), 22.5 (CH_2), 14.1 ($SiCH_2$), 13.8 (CH_3). **^{29}Si NMR** (79 MHz, $CDCl_3$) −18.4. **IR** (neat) ν_{max} cm^{-1} 3321, 2955, 2924, 2857, 1599, 1491, 1447, 1072, 962, 829, 692. **HRMS** (EI) calculated for $C_{20}H_{27}O_2Si$ 327.17748. Found 327.17965.

2-(4-Phenylbutyl)-4,4,5,5-tetramethyl-1,3,2-dioxaborolane **513**

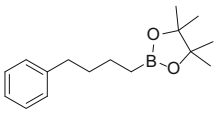

According to General Procedure **C**, 4-phenylbutene **361** (105 μL, 0.7 mmol), pinacol borane **93** (110 μL, 0.77 mmol), iron(II) chloride **279** (0.9 mg, 0.007 mmol), 2,6-bis-[1-(2,6-diethylphenylimino)ethyl]pyridine **273b** (3.0 mg, 0.007 mmol) and ethylmagnesium bromide **280** (3 drops, 0.021 mmol) were reacted in anhydrous tetrahydrofuran (3 mL) to give the crude reaction product, which was purified by flash silica column chromatography (2 % EtOAc/hexane) to give *2-(4-phenylbutyl)-4,4,5,5-tetramethyl-1,3,2-dioxaborolane* **513** as a colourless oil (159 mg, 0.61 mmol, 87 %).

^{1}H NMR (400 MHz, $CDCl_3$) 7.30-7.24 (m, 2H, ArH), 7.21-7.14 (m, 3H, ArH), 2.65-2.59 (m, 2H, $ArCH_2$), 1.69-1.60 (m, 2H, CH_2), 1.53-1.44 (m, 2H, CH_2) 1.25 (s, 12H, CH_3), 0.86-0.79 (m, 2H, BCH_2). **^{13}C NMR** (101 MHz, $CDCl_3$) 142.9 (C), 128.4 (2 × CH), 128.2 (2 × CH), 125.5 (CH), 82.9 (2 × C), 35.8 (CH_2), 34.2 (CH_2), 24.8 (4 × CH_3), 23.8 (CH_2). **^{11}B NMR** (128 MHz, $CDCl_3$) 34.4. **IR** (neat) ν_{max} cm^{-1} 2978, 2930, 2859, 1452, 1371, 1317, 1215, 1144, 966, 881, 847, 745, 698. **HRMS** (EI) calculated for $C_{16}H_{25}BO_2$ 260.19421. Found 260.19430.

1-Fluoro-4-(3-butenyl)-benzene **5230**

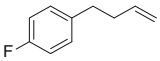

Allylmagnesium bromide **522** (9 mL, 1 M in tetrahydrofuran, 9 mmol) was added to a solution of 4-fluorobenzyl bromide **519** (1.32 g, 7 mmol) in anhydrous diethyl ether (10 mL) at 0 °C under a nitrogen atmosphere. The reaction was allowed to warm to room temperature over 2 h. Aqueous sulfate buffer solution (10 mL) was added slowly and the aqueous phase extracted with diethyl ether (3 × 20 mL). The combined organic extracts were washed with water and brine, dried ($MgSO_4$) and concentrated in vacuo to give *1-fluoro-4-(3-butenyl)-benzene* **523** as a colourless oil (933 mg, 6.22 mmol, 89 %).

^{1}H NMR (400 MHz, $CDCl_3$) 7.18-7.12 (m, 2H, ArH), 7.01-6.94 (m, 2H, ArH), 5.85 (ddt, *J* = 17.0, 10.0, 6.5 Hz, 1H, CH), 5.08-4.97 (m, 2H, CH), 2.73-2.67 (m, 2H, $ArCH_2$), 2.40-2.32 (m, 2H, CH_2). **^{13}C NMR** (101 MHz, $CDCl_3$) 161.2 (d, *J* = 243 Hz, CF), 137.8 (CH), 137.4 (d, *J* = 3 Hz, C), 129.7 (d, *J* = 8 Hz, 2 × CH), 115.1 (d, *J* = 6 Hz, 2 × CH), 114.9 (CH), 35.6 (CH_2), 34.5 (CH_2). **^{19}F NMR** (376 MHz, $CDCl_3$) −117.8. **IR** (neat) ν_{max} cm^{-1} 2926, 2859, 1641, 1601, 1508, 1439, 1221, 1157, 995, 912, 824. **HRMS** (EI) calculated for $C_{10}H_{11}F$ 150.08393. Found 150.08373.

1-Chloro-4-(3-butenyl)-benzene **524**

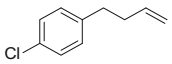

Allylmagnesium bromide **522** (9 mL, 1 M in tetrahydrofuran, 9 mmol) was added to a solution of 4-chlorobenzyl bromide **520** (1.44 g, 7 mmol) in anhydrous diethyl ether (10 mL) at 0 °C under a nitrogen atmosphere. The reaction was allowed to warm to room temperature over 2 h. Aqueous sulfate buffer solution (10 mL) was added slowly and the aqueous phase extracted with diethyl ether (3 × 20 mL). The combined organic extracts were washed with water and brine, dried ($MgSO_4$) and concentrated in vacuo to give *1-chloro-4-(3-butenyl)-benzene* **524** as a colourless oil (1.10 g, 6.63 mmol, 95 %).

^{1}H NMR (400 MHz, $CDCl_3$) 7.28-7.23 (m, 2H, ArH), 7.14-7.10 (m, 2H, ArH), 5.84 (ddt, *J* = 17.0, 10.0, 6.5 Hz, 1H, CH), 5.07-4.97 (m, 2H, CH), 2.72-2.66 (m, 2H, $ArCH_2$), 2.40-2.32 (m, 2H, CH_2). **^{13}C NMR** (101 MHz, $CDCl_3$) 140.2 (C), 137.6 (CH), 131.5 (C), 129.8 (2 × CH), 128.3 (2 × CH), 115.3 (CH), 35.3 (CH_2), 34.7 (CH_2). **IR** (neat) ν_{max} cm^{-1} 2980, 2926, 1642, 1491, 1452, 1439, 1406, 1092, 1015, 995, 912, 829, 806. **HRMS** (EI) calculated for $C_{10}H_{11}Cl$ 166.0530. Found 166.05438.

1-Bromo-4-(3-butenyl)-benzene **525**

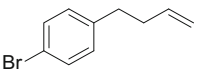

Allylmagnesium bromide **522** (30 mL, 1 M in tetrahydrofuran, 30 mmol) was added to a solution of 4-bromobenzyl bromide **521** (6.32 g, 25 mmol) in anhydrous diethyl ether (20 mL) at 0 °C under a nitrogen atmosphere. The reaction was allowed to warm to room temperature over 2 h. Aqueous sulfate buffer solution (10 mL) was added slowly and the aqueous phase extracted with diethyl ether (3 × 20 mL). The combined organic extracts were washed with water and brine, dried ($MgSO_4$) and concentrated in vacuo to give 1-bromo-4-(3-butenyl)-benzene **525** as a colourless oil (5.10 g, 24.2 mmol, 97 %).

^{1}H NMR (400 MHz, CDCl3) 7.43-7.38 (m, 2H, ArH), 7.10-7.04 (m, 2H, ArH), 5.85 (ddt, *J* = 17.0, 10.0, 6.5 Hz, 1H, CH), 5.07-4.96 (m, 2H, CH), 2.71-2.64 (m, 2H, $ArCH_2$), 2.40-2.32 (m, 2H, CH_2). **^{13}C NMR** (101 MHz, CDCl3) 140.7 (C), 137.6 (CH), 131.3 (2 × CH), 130.2 (2 × CH), 119.5 (C), 115.3 (CH), 35.3 (CH_2), 34.7 (CH_2). **IR** (neat) ν_{max} cm^{-1} 2978, 2926, 1641, 1487, 1452, 1439, 1402, 1072, 1011, 995, 912, 802.

Data were in accordance with those previously reported [29].

4-(3-Butenyl)-benzoic acid **526**

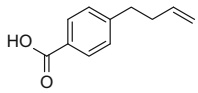

1-Bromo-4-(3-butenyl)-benzene **525** (0.21 g, 1 mmol) was added to magnesium turnings (413 mg, 17 mmol) in anhydrous tetrahydrofuran (15 mL) in a flask equipped with a reflux condenser, at room temperature and under a nitrogen atmosphere. A single iodine crystal was added to initiate the reaction. Within 1 min the iodine colour disappeared and the reaction temperature began to increase. The reaction was periodically cooled in ice to maintain the reaction temperature below reflux, and the remaining 1-bromo-4-(3-butenyl)-benzene (1.8 g, 8.7 mmol) was added in portions over 30 min. The reaction was stirred for an additional 30 min at 0 °C, and then allowed to settle at room temperature for 1 h. Carbon dioxide was bubbled through the solution, resulting in a rapid increase in reaction temperature to cause reflux. After 5 min the reaction was quenched with saturated sodium hydrogen carbonate solution and the aqueous phase washed with hexane (2 × 20 mL). The aqueous phase was acidified to pH 1 with HCl (conc.) and extracted with diethyl ether (3 × 20 mL). The combined organic phases were dried ($MgSO_4$) and concentrated in vacuo to give *4-(3-butenyl)-benzoic acid* **526** as a colourless amorphous solid (1.48 g, 8.41 mmol, 87 %).

m.p. 124–127 °C. **^{1}H NMR** (400 MHz, $CDCl_3$) 12.16 (br. s, 1H, CO_2H), 8.07-8.02 (m, 2H, ArH), 7.33-7.28 (m, 2H, ArH), 5.85 (ddt, *J* = 17.0, 10.0, 6.5 Hz, 1H, CH), 5.09-4.98 (m, 2H, CH), 2.84-2.77 (m, 2H, $ArCH_2$), 2.46-2.38 (m, 2H, CH_2). **^{13}C NMR** (101 MHz, $CDCl_3$) 171.8 (CO_2H), 148.4 (C), 137.4 (CH), 130.3 (2 × CH), 128.6 (2 × CH), 126.9 (C), 115.4 (CH), 35.4 (CH_2), 35.0 (CH_2). **IR** (neat) ν_{max} cm^{-1} 2943, 2887, 2544, 1680, 1609, 1574, 1423, 1179, 1128, 1101, 1016, 991, 935, 910, 856, 762. **HRMS** (EI) calculated for $C_{11}H_{12}O_2$ 176.08318. Found 176.08294.

4-(3-Butenyl)-benzaldehyde **527**

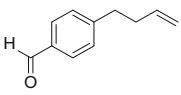

4-(3-Butenyl)-phenylmagnesium bromide was prepared from 1-bromo-4-(3-butenyl)-benzene **525** (4.4 g, 20 mmol) and magnesium turnings (1.05 g, 43 mmol) as described above for the synthesis of 4-(3-butenyl)-benzoic acid **526**.

The reaction was cooled to 0 °C, and *N,N*-dimethylformamide (1.53 g, 21 mmol in 10 mL Et_2O) was added dropwise over 2 min. The reaction was allowed to warm to room temperature over 1 h. Aqueous sulfate buffer (10 mL) was added and the aqueous phase extracted with diethyl ether (3 × 20 mL). The combined organic extracts were washed with water and brine, dried ($MgSO_4$) and concentrated in vacuo to give *4-(3-butenyl)-benzaldehyde* **527** as a yellow oil (3.08 g, 19.3 mmol, 92 %).

^{1}H NMR (400 MHz, $CDCl_3$) 9.99 (s, 1H, CHO), 7.84-7.79 (m, 2H, ArH), 7.38-7.33 (m, 2H, ArH), 5.84 (ddt, *J* = 17.0, 10.0, 6.5 Hz, 1H, CH), 5.09-4.98 (m, 2H, CH), 2.84-2.77 (m, 2H, $ArCH_2$), 2.46-2.38 (m, 2H, CH_2). **^{13}C NMR** (101 MHz, $CDCl_3$) 192.0 (CHO), 149.3 (C), 137.2 (CH), 134.5 (C), 129.9 (2 × CH), 129.1 (2 × CH), 115.5 (CH), 35.5 (CH_2), 35.0 (CH_2). **IR** (neat) ν_{max} cm^{-1} 2926, 1686, 1607, 1576, 1423, 1317, 1290, 1213, 1169, 1103, 1016, 991, 910, 853, 841, 824.

4-(3-Butenyl)-acetophenone **528**

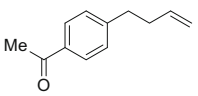

4-(3-Butenyl)-phenylmagnesium bromide was prepared from 1-bromo-4-(3-butenyl)-benzene **525** (2.53 g, 12 mmol) and magnesium turnings (352 mg, 14.5 mmol) as described above for the synthesis of 4-(3-butenyl)-benzoic acid **526**, except that diethyl ether (15 mL) was used as the solvent in place of tetrahydrofuran.

The Grignard reagent was made up to a total volume of 40 mL using anhydrous diethyl ether and cooled to 0 °C. *N,N*-Dimethylacetamide (1.2 mL, 13 mmol, in 15 mL Et_2O) was added over 10 min. The reaction was allowed to warm to room temperature over 2 h. Aqueous sulfate buffer (10 mL) was added and the aqueous phase extracted with diethyl ether (3 × 20 mL). The combined organic extracts were washed with water and brine, dried ($MgSO_4$) and concentrated in vacuo, which was purified by flash silica chromatography (5 % EtOAc/hexane) to give *4-(3-butenyl)-acetophenone* **528** as a yellow oil (648 mg, 3.72 mmol, 31 %).

^{1}H NMR (400 MHz, $CDCl_3$) 7.92-7.87 (m, 2H), 7.31-7.26 (m, 2H), 5.84 (ddt, *J* = 17.0, 10.0, 6.5 Hz, 1H), 5.08-4.98 (m, 2H), 2.82-2.75 (m, 2H), 2.59 (s, 3H), 2.44-2.37 (m, 2H). **^{13}C NMR** (101 MHz, $CDCl_3$) 197.8 (C=O), 147.6 (C), 137.4 (CH), 135.1 (C), 128.6 (2 × CH), 128.5 (2 × CH), 115.4 (CH), 35.3 (CH_2), 35.0 (CH_2), 26.5 (CH_3). **IR** (neat) ν_{max} cm^{-1} 3001, 2926, 2857, 1680, 1641, 1607, 1570, 1142, 1358, 1265, 1182, 1016, 995, 955, 912, 839, 818. **HRMS** (EI) calculated for $C_{12}H_{14}O$ 174.10392. Found 174.10395.

4-(3-Butenyl)-benzophenone **529**

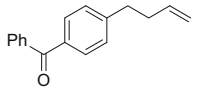

Prepared according to a literature procedure [30]. The uncatalysed reaction was found to be inefficient.

4-(3-Butenyl)-phenylmagnesium bromide was prepared from 1-bromo-4-(3-butenyl)-benzene **525** (3.16 g, 15 mmol) and magnesium turnings (437 mg, 18 mmol) as described above for the synthesis of 4-(3-butenyl)-benzoic acid **526**.

The Grignard reagent was made up to a total volume of 40 mL using anhydrous tetrahydrofuran and cooled to −78 °C. A solution of benzonitrile (1.54 g, 15 mmol), *tert*-butyldimethylsilyl chloride (2.4 g, 16 mmol) and copper bromide (50 mg, 0.35 mmol) in anhydrous tetrahydrofuran (20 mL) was added dropwise over 5 min. A further portion of copper bromide (50 mg, 0.35 mmol) was added due to the low solubility of copper bromide in tetrahydrofuran resulting in uncertainty over the quantity of copper bromide which had been added to the reaction. The reaction was allowed to warm to room temperature over 2 h. Water was added and the aqueous phase extracted with diethyl ether (3 × 20 mL). The combined organic extracts were dried ($MgSO_4$) and concentrated in vacuo. The crude product was loaded onto silica using ethyl acetate and left for 16 h. The silica was washed using ethyl acetate to give the crude product which was purified by flash silica chromatography (5 % EtOAc/hexane) to give 4-(3-butenyl)-benzophenone **529** as a yellow oil (2.76 g, 11.7 mmol, 78 %).

The literature procedure reported that hydrolysis of the *N*-silyl imine derivative of benzophenone took place rapidly upon contact with silica, however it was found that in this case extended times were required for the hydrolysis to take place.

^{1}H NMR (400 MHz, $CDCl_3$) 7.83-7.78 (m, 2H, ArH) 7.78-7.74 (m, 2H, ArH), 7.62-7.56 (m, 1H, ArH), 7.52-7.46 (m, 2H, ArH), 7.33-7.29 (m, 2H, ArH), 5.87 (ddt, J = 17.0, 10.5, 6.5 Hz, 1H, CH), 5.11-5.00 (m, 2H, CH), 2.85-2.78 (m, 2H, $ArCH_2$), 2.48-2.38 (m, 2H, CH_2). **^{13}C NMR** (101 MHz, $CDCl_3$) 196.5 (C=O), 147.0 (C), 137.9 (C), 137.5 (CH), 135.3 (C), 132.2 (CH), 130.3 (2 × CH), 129.9 (2 × CH), 128.4 (2 × CH), 128.2 (2 × CH), 115.4 (CH), 35.4 ($ArCH_2$), 35.1 (CH_2). **IR** (neat) ν_{max} cm^{-1} 3076, 2928, 2857, 1655, 1605, 1447, 1412, 1308, 1275, 1177, 1148, 999, 937, 920, 847, 789, 741, 698.

Data were in accordance with those previously reported [31].

4-(3-Butenyl)-benzoic acid methyl ester **530**

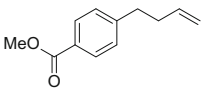

Sulfuric acid (conc., 15 drops) was added to a solution of 4-(3-butenyl)-benzoic acid **526** (528 mg, 3 mmol) in anhydrous methanol (30 mL), and the reaction heated at reflux for 16 h. The solution was cooled, saturated sodium hydrogen carbonate solution (30 mL) added, and the aqueous phase extracted with diethyl ether (3 × 20 mL). The combined organic extracts were washed with water and brine, dried ($MgSO_4$) and concentrated in vacuo to give *4-(3-butenyl)-benzoic acid methyl ester* **530** as a pale yellow oil (522 mg, 2.75 mmol, 92 %).

^{1}H NMR (400 MHz, $CDCl_3$) 7.99-7.94 (m, 2H, ArH), 7.29-7.24 (m, 2H, ArH), 5.84 (ddt, *J* = 17.0, 10.0, 6.5 Hz, 1H, CH), 5.08-4.97 (m, 2H, CH), 3.91 (s, 3H, CH_3), 2.81-2.74 (m, 2H, $ArCH_2$), 2.44-2.36 (m, 2H, CH_2). **^{13}C NMR** (101 MHz, $CDCl_3$) 167.1 (C=O), 147.3 (C), 137.5 (CH), 129.7 (2 × CH), 128.5 (2 × CH), 127.9 (CH), 115.3 (CH), 52.0 (CH_3), 35.4 (CH_2), 35.0 (CH_2). **IR** (neat) ν_{max} cm^{-1} 2951, 2849, 1719, 1611, 1435, 1416, 1275, 1179, 1107, 1020, 912, 852, 762, 704. **HRMS** (EI) calculated for $C_{12}H_{14}O_2$ 190.09883. Found 190.09903.

N-(*tert*-Butyl)-4-(3-butenyl)-benzamide **532**

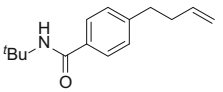

Prepared according to a literature procedure [14].

Triphenylphosphine **315** (865 mg, 3.3 mmol) and iodine (838 mg, 3.3 mmol) were added to anhydrous dichloromethane (11 mL) at 0 °C and stirred for 5 min under a nitrogen atmosphere. 4-(3-Butenyl)-benzoic acid **526** (528 mg, 3 mmol) was added followed by the concurrent dropwise addition of both diisopropylethylamine **316** (0.78 mL, 4.5 mmol) and *tert*-butylamine **531** (0.35 mL, 3.3 mmol) over 5 min. The reaction was stirred under a nitrogen atmosphere and allowed to warm to room temperature over 16 h. Water was added and the aqueous phase extracted using dichloromethane (3 × 20 mL). The organic phase was washed sequentially with saturated aqueous sodium thiosulfate solution and brine, dried ($MgSO_4$) and concentrated in vacuo. The crude reaction product was purified by flash chromatography (7 % EtOAc/hexane) to give *N-(tert-butyl)-4-(3-butenyl)-benzamide* **532** as a colourless solid (622 mg, 2.69 mmol, 90 %).

m.p. 91–92 °C. **^{1}H NMR** (400 MHz, $CDCl_3$) 7.67-7.62 (m, 2H, ArH), 7.25-7.20 (m, 2H, ArH), 5.93 (br s, 1H, NH), 5.83 (ddt, *J* = 16.5, 10.0, 6.5 Hz, 1H, CH), 5.06-4.96 (m, 2H, CH), 2.78-2.72 (m, 2H, $ArCH_2$), 2.42-2.34 (m, 2H, CH_2), 1.47 (s, 9H, CH_3). **^{13}C NMR** (101 MHz, $CDCl_3$) 166.8 (C=O), 145.2 (C), 137.5 (CH), 133.5 (C), 128.5 (2 × CH), 126.7 (2 × CH), 115.3 (CH), 51.5 (C), 35.2 (CH_2), 35.1 (CH_2), 28.9 (3 × CH_3). **IR** (neat) ν_{max} cm^{-1} 3360, 2974, 2932, 1634, 1612, 1539, 1504, 1454, 1393, 1360, 1333, 1308, 1221, 1190, 1018, 989, 912, 876, 854. **HRMS** (EI) calculated for $C_{15}H_{21}NO$ 231.16177. Found 231.16145.

1-(4-(3-Butenyl)benzoyl)piperidine **533**

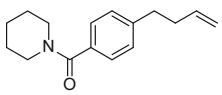

Prepared according to a literature procedure [14].

Triphenylphosphine **315** (865 mg, 3.3 mmol) and iodine (838 mg, 3.3 mmol) were added to anhydrous dichloromethane (11 mL) at 0 °C and stirred for 5 min under a nitrogen atmosphere. 4-(3-Butenyl)-benzoic acid **526** (528 mg, 3 mmol) was added followed by the concurrent dropwise addition of both diisopropylethylamine **316** (0.78 mL, 4.5 mmol) and piperidine **313** (0.33 mL, 3.3 mmol) over 5 min. The reaction was stirred under a nitrogen atmosphere and allowed to warm to room temperature over 16 h. Water was added and the aqueous phase extracted using dichloromethane (3 × 20 mL). The organic phase was washed sequentially with saturated aqueous sodium thiosulfate solution and brine, dried ($MgSO_4$) and concentrated in vacuo. The crude reaction product was purified by flash chromatography (7 % EtOAc/hexane) to give *1-(4-(3-butenyl)benzoyl)piperidine* **533** as a colourless solid (565 mg, 2.32 mmol, 77 %).

^{1}H NMR (400 MHz, $CDCl_3$) 7.34-7.29 (m, 2H, ArH), 7.23-7.18 (m, 2H, ArH), 5.85 (ddt, *J* = 17.0, 10.0, 6.5 Hz, 1H, CH), 5.08-4.96 (m, 2H, CH), 3.70 (br s, 2H, NCH_2), 3.37 (br s, 2H, NCH_2), 2.77-2.69 (m, 2H, $ArCH_2$), 2.42-2.33 (m, 2H, $ArCH_2C\boldsymbol{H_2}$), 1.76-1.45 (br m, 6H, CH_2). **^{13}C NMR** (101 MHz, $CDCl_3$) 170.4 (C=O), 143.3 (C), 137.7 (CH), 134.0 (C), 128.4 (2 × CH), 126.9 (2 × CH), 115.1 (CH), 48.8 (br., NCH_2), 43.1 (br., NCH_2), 35.3 (CH_2), 35.2 (CH_2), 26.5 (br., CH_2), 25.6 (br., CH_2), 24.6 (CH_2). **IR** (neat) ν_{max} cm^{-1} 2934, 2855, 1626, 1427, 1273, 1258, 1236, 1107, 1026, 1001, 908, 885, 851. **HRMS** (EI) calculated for $C_{16}H_{21}NO$ 243.16177. Found 243.16178.

4-(3-Butenyl)-benzyl alcohol **535**

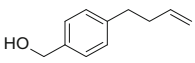

4-(3-Butenyl)-benzaldehyde **527** (480 mg, 3 mmol) was added to a suspension of sodium borohydride **534** (230 mg, 6 mmol) in anhydrous ethanol (10 mL) at 0 °C. and the reaction was allowed to warm to room temperature over 2 h. Ethanol was removed under vacuum, and saturated aqueous sodium hydrogen carbonate was added. The aqueous phase was extracted with dichloromethane (3 × 25 mL), dried ($MgSO_4$) and concentrated in vacuo to give a colourless oil, which was purified by flash silica chromatography (20 % EtOAc/hexane) to give *4-(3-butenyl)-benzyl alcohol* **535** as a colourless oil (462 mg, 2.85 mmol, 95 %).

^{1}H NMR (400 MHz, $CDCl_3$) 7.38-7.28 (m, 2H, ArH), 7.23-7.18 (m, 2H, ArH), 5.87 (ddt, *J* = 17.0, 10.0, 6.5 Hz, 1H, CH), 5.09-4.97 (m, 2H, CH), 4.67 (d,

J = 5.5 Hz, 2H, C***H***$_2$OH), 2.76-2.70 (m, 2H, ArCH$_2$), 2.42-2.35 (m, 2H, CH$_2$), 1.65 (t, *J* = 5.5 Hz, 1H OH). **^{13}C NMR** (101 MHz, $CDCl_3$) 141.4 (C), 138.4 (C), 138.0 (CH), 128.6 (2 × CH), 127.1 (2 × CH), 115.0 (CH), 65.3 (CH_2OH), 35.5 (CH_2), 35.0 (CH_2). **IR** (neat) ν_{max} cm^{-1} 3327, 2924, 2859, 1639, 1514, 1474, 1200, 1034, 1007, 997, 910, 885, 806. **HRMS** (EI) calculated for $C_{11}H_{14}O$ 162.10392. Found 162.10392.

4-(3-Butenyl)-benzonitrile **538**

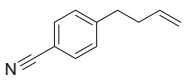

Prepared according to a literature procedure [32].

Trifluoromethanesulfonic acid **537** (1.3 mL, 15 mmol) was added to a solution of 4-(3-butenyl)-benzaldehyde **527** (800 mg, 5 mmol) and sodium azide **536** (490 mg, 7.5 mmol) in anhydrous acetonitrile (10 mL) at room temperature, and the reaction stirred for 5 min. Water was added and the aqueous phase extracted with diethyl ether (3 × 20 mL). The combined organic extracts were washed with water and brine, dried ($MgSO_4$) and concentrated in vacuo to give the crude product, which was purified by flash silica chromatography (dry loaded on Celite, column eluted using 5 % EtOAc/hexane) to give 4-(3-butenyl)-benzonitrile **538** (648 mg, 4.12 mmol, 82 %) as a yellow oil.

^{1}H NMR (400 MHz, $CDCl_3$) 7.61-7.55 (m, 2H, ArH), 7.32-7.27 (m, 2H, ArH), 5.81 (ddt, *J* = 17.0, 10.0, 6.5 Hz, 1H, CH), 5.07-4.98 (m, 2H, CH), 2.81-2.74 (m, 2H, ArCH$_2$), 2.43-2.35 (m, 2H, CH$_2$). **^{13}C NMR** (101 MHz, $CDCl_3$) 147.4 (C), 137.0 (CH), 132.1 (2 × CH), 129.3 (2 × CH), 119.1 (C), 115.7 (CH), 109.8 (C), 35.4 (CH_2), 34.8 (CH_2). **IR** (neat) ν_{max} cm^{-1} 2980, 2932, 2860, 2228, 1639, 1607, 1505, 1439, 1416, 1177, 1055, 1020, 995, 914, 841, 822.

Data were in accordance with those previously reported [33].

N-Phenyl-4-(3-butenyl)-benzaldimine **540**

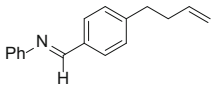

4-(3-Butenyl)-benzaldehyde **527** (2.4 g, 15 mmol), aniline (1.45 mL, 16 mmol) and *para*-toluenesulfonic acid (20 mg) were added to toluene (45 mL) and heated at reflux for 6 h under Dean-Stark conditions. The cooled mixture was filtered through a plug of silica (hexane/EtOAc/triethylamine (90:10:1)) and evaporated to give *N-phenyl-4-(3-butenyl)-benzaldimine* **540** as a yellow oil (3.32 g, 14.1 mmol, 94 %). The product was used without further purification.

^{1}H NMR (400 MHz, $CDCl_3$) 8.45 (s, 1H, CHN), 7.87-7.82 (m, 2H, ArH), 7.44-7.38 (m, 2H, ArH), 7.34-7.29 (m, 2H, ArH), 7.27-7.20 (m, 3H, ArH), 5.88

(ddt, J = 17.0, 10.0, 6.5 Hz, 1H, CH), 5.11-4.99 (m, 2H, CH), 2.83-2.77 (m, 2H, $ArCH_2$), 2.47-2.39 (m, 2H, CH_2). **^{13}C NMR** (101 MHz, $CDCl_3$) 160.3 (C=N), 152.3 (C), 145.7 (C), 137.6 (CH), 134.1 (C), 129.1 (2 × CH), 128.9 (2 × CH), 128.8 (2 × CH), 125.7 (CH), 120.8 (2 × CH), 115.3 (CH), 35.4 (CH_2), 35.2 (CH_2). **IR** (neat) ν_{max} cm^{-1} 3061, 2930, 2880, 1624, 1607, 1589, 1568, 1483, 1449, 1418, 1192, 1169, 1072, 997, 974, 912, 876, 839, 826, 762, 694. **HRMS** (EI) calculated for $C_{17}H_{17}N$ 235.13555. Found 235.13607.

N-Phenyl-4-(3-butenyl)-benzylamine **541**

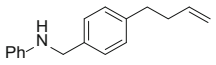

N-Phenyl-4-(3-butenyl)-benzaldimine **540** (1 g, 4.25 mmol) was added to a suspension of sodium borohydride **534** (210 mg, 5.5 mmol) in anhydrous ethanol (10 mL) at 0 °C, and the reaction stirred overnight. Ethanol was removed under vacuum, and saturated aqueous sodium hydrogen carbonate was added. The aqueous phase was extracted with diethyl ether (3 × 25 mL), dried ($MgSO_4$) and concentrated in vacuo to give a yellow oil, which was purified by flash silica chromatography (4 % EtOAc/hexane) to give *N-phenyl-4-(3-butenyl)-benzylamine* **541** as a pale yellow oil (719 mg, 3.03 mmol, 71 %).

^{1}H NMR (400 MHz, $CDCl_3$) 7.34-7.29 (m, 2H, ArH), 7.23-7.16 (m, 4H, ArH), 6.77-6.71 (m, 1H, ArH), 6.69-6.64 (m, 2H, ArH), 5.89 (ddt, J = 17.0, 10.0, 6.5 Hz, 1H, CH), 5.11-4.99 (m, 2H, CH), 4.31 (s, 2H, CH_2N), 4.01 (br. s, 1H, NH), 2.77-2.70 (m, 2H, $ArCH_2$), 2.44-2.36 (m, 2H, CH_2). **^{13}C NMR** (101 MHz, $CDCl_3$) 148.2 (C), 140.9 (C), 138.0 (CH), 136.8 (C), 129.2 (2 × CH), 128.7 (2 × CH), 127.6 (2 × CH), 117.5 (CH), 114.9 (CH), 112.8 (2 × CH), 48.1 (NCH_2), 35.5 (CH_2), 34.0 (CH_2). **HRMS** (EI) calculated for $C_{17}H_{19}N$ 237.15120. Found 237.15074.

4-(3-Butenyl)-diphenylacetylene **542**

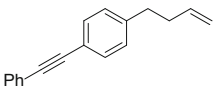

Diisopropylamine **333** (2.8 mL, 20 mmol) was added to a solution of bis(triphenylphosphine) palladium(II) dichloride **331** (280 mg, 0.4 mmol), copper(I) iodide **332** (57 mg, 0.3 mmol), 1-bromo-4-(3-butenyl)-benzene **525** (2.11 g, 10 mmol) and phenylacetylene **329** (1.3 mL, 12 mmol) in anhydrous tetrahydrofuran (40 mL) and the reaction heated at reflux for 16 h. The reaction was cooled, filtered and the residue washed with diethyl ether (2 × 10 mL). The organic phase was washed with water and brine, dried ($MgSO_4$) and concentrated in vacuo to give the crude product, which was purified by flash silica chromatography (1 % EtOAc/hexane) to give *4-(3-butenyl)-diphenylacetylene* **542** as a yellow oil (1.65 g, 7.06 mmol, 71 %).

^{1}H NMR (400 MHz, $CDCl_3$) 7.56-7.52 (m, 2H, ArH) 7.49-7.45 (m, 2H, ArH), 7.39-7.32 (m, 3H, ArH), 7.21-7.17 (m, 2H, ArH), 5.86 (ddt, *J* = 17.0, 10.0, 6.5 Hz, 1H, CH), 5.09-4.98 (m, 2H, CH), 2.77-2.71 (m, 2H, $ArCH_2$), 2.44-2.36 (m, 2H, CH_2). **^{13}C NMR** (101 MHz, $CDCl_3$) 142.3 (C), 137.7 (CH), 131.6 (2 × CH), 128.5 (2 × CH), 128.3 (2 × CH), 128.1 (CH), 123.4 (C), 120.7 (C), 115.2 (CH), 89.5 (C), 88.8 (C), 35.3 (CH_2), 35.2 (CH_2). **IR** (neat) ν_{max} cm^{-1} 3059, 2924, 2857, 2216, 1639, 1595, 1510, 1487, 1443, 1068, 997, 912, 829, 754, 689. **HRMS** (EI) calculated for $C_{18}H_{16}$ 232.12465. Found 232.12463.

2-(4-(4-Fluorophenyl)butyl)-4,4,5,5-tetramethyl-1,3,2-dioxaborolane **543**

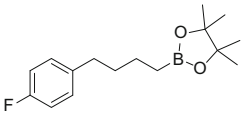

According to General Procedure **C**, 1-fluoro-4-(3-butenyl)-benzene **523** (105 mg, 0.7 mmol), pinacol borane **93** (110 μL, 0.77 mmol), iron(II) chloride **279** (0.9 mg, 0.007 mmol), 2,6-bis-[1-(2,6-diethylphenylimino)ethyl]pyridine **273b** (3.0 mg, 0.007 mmol) and ethylmagnesium bromide **280** (3 drops, 0.021 mmol) were reacted in anhydrous tetrahydrofuran (3 mL) to give the crude reaction product, which was purified by flash silica column chromatography (2 % EtOAc/hexane) to give *2-(4-(4-fluorophenyl)butyl)-4,4,5,5-tetramethyl-1,3,2-dioxaborolane* **543** as a colourless oil (173 mg, 0.62 mmol, 89 %).

^{1}H NMR (400 MHz, $CDCl_3$) 7.16-7.08 (m, 2H, ArH), 6.99-6.90 (m, 2H, ArH), 2.62-2.54 (m, 2H, $ArCH_2$), 1.66-1.55 (m, 2H, CH_2), 1.51-1.41 (m, 2H, CH_2) 1.25 (s, 12H, CH_3), 0.85-0.76 (m, 2H, BCH_2). **^{13}C NMR** (101 MHz, $CDCl_3$) 161.1 (d, *J* = 243 Hz, CF), 138.4 (d, *J* = 3 Hz, C), 129.6 (d, *J* = 8 Hz, 2 × CH), 114.8 (d, *J* = 21 Hz, 2 × CH), 82.9 (2 × C), 34.9 (CH_2), 34.2 (CH_2), 24.8 (4 × CH_3), 23.6 (CH_2). **^{11}B NMR** (128 MHz, $CDCl_3$) 34.3. **^{19}F NMR** (376 MHz, $CDCl_3$) −118.4. **IR** (neat) ν_{max} cm^{-1} 2980, 2930, 2860, 1601, 1508, 1371, 1317, 1273, 1219, 1144, 1055, 1034, 1016, 966, 847, 822. **HRMS** (EI) calculated for $C_{16}H_{24}BO_2F$ 278.18479. Found 278.18485.

2-(4-(4-Chlorophenyl)butyl)-4,4,5,5-tetramethyl-1,3,2-dioxaborolane **544**

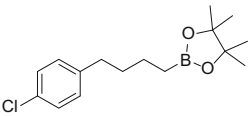

According to General Procedure **C**, 1-chloro-4-(3-butenyl)-benzene **524** (116 mg, 0.7 mmol), pinacol borane **93** (110 μL, 0.77 mmol), iron(II) chloride **279** (0.9 mg,

0.007 mmol), 2,6-bis-[1-(2,6-diethylphenylimino)ethyl]pyridine **273b** (3.0 mg, 0.007 mmol) and ethylmagnesium bromide **280** (3 drops, 0.021 mmol) were reacted in anhydrous tetrahydrofuran (3 mL) to give the crude reaction product, which was purified by flash silica column chromatography (2 % EtOAc/hexane) to give *2-(4-(4-chlorophenyl)butyl)-4,4,5,5-tetramethyl-1,3,2-dioxaborolane* **544** as a colourless oil (169 mg, 0.57 mmol, 82 %).

^{1}H NMR (400 MHz, $CDCl_3$) 7.26-7.20 (m, 2H, ArH), 7.13-7.07 (m, 2H, ArH), 2.62-2.54 (m, 2H, CH_2), 1.66-1.56 (m, 2H, CH_2), 1.51-1.41 (m, 2H, CH_2) 1.25 (s, 12H, CH_3), 0.85-0.77 (m, 2H, CH_2). **^{13}C NMR** (101 MHz, $CDCl_3$) 141.3 (C), 131.2 (C), 129.7 (2 × CH), 128.2 (2 × CH), 82.9 (2 × C), 35.0 (CH_2), 34.0 (CH_2), 24.8 (4 × CH_3), 23.6 (CH_2). **^{11}B NMR** (128 MHz, $CDCl_3$) 34.4. **IR** (neat) ν_{max} cm^{-1} 2978, 2932, 2860, 1603, 1491, 1458, 1406, 1371, 1317, 1026, 1144, 1092, 1061, 1034, 1015, 966, 846, 820, 802. **HRMS** (EI) calculated for $C_{16}H_{24}BO_2Cl$ 294.15524. Found 294.15534.

2-(4-(4-Bromophenyl)butyl)-4,4,5,5-tetramethyl-1,3,2-dioxaborolane **545**

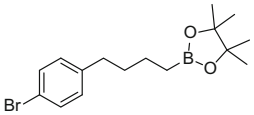

According to General Procedure **C**, 1-bromo-4-(3-butenyl)-benzene **525** (148 mg, 0.7 mmol), pinacol borane **93** (110 μL, 0.77 mmol), iron(II) chloride **279** (0.9 mg, 0.007 mmol), 2,6-bis-[1-(2,6-diethylphenylimino)ethyl]pyridine **273b** (3.0 mg, 0.007 mmol) and ethylmagnesium bromide **280** (3 drops, 0.021 mmol) were reacted in anhydrous tetrahydrofuran (3 mL) to give the crude reaction product, which was purified by flash silica column chromatography (2 % EtOAc/hexane) to give *2-(4-(4-bromophenyl)butyl)-4,4,5,5-tetramethyl-1,3,2-dioxaborolane* **545** as a colourless oil (216 mg, 0.64 mmol, 91 %).

^{1}H NMR (400 MHz, $CDCl_3$) 7.41-7.35 (m, 2H, ArH), 7.08-7.03 (m, 2H, ArH), 2.59-2.53 (m, 2H, $ArCH_2$), 1.66-1.56 (m, 2H, CH_2), 1.50-1.40 (m, 2H, CH_2), 1.25 (s, 12H, CH_3), 0.85-0.77 (m, 2H, BCH_2). **^{13}C NMR** (101 MHz, $CDCl_3$) 141.8 (C), 131.2 (2 × CH), 130.2 (2 × CH), 119.2 (C), 82.9 (2 × C), 35.1 (CH_2), 33.9 (CH_2), 24.8 (CH_2), 23.6 (CH_2). **^{11}B NMR** (128 MHz, $CDCl_3$) 34.3. **HRMS** (EI) calculated for $C_{16}H_{24}BO_2Br$ 338.10472. Found 338.10550.

2-(4-(*N*-Phenylbenzylamine)butyl)-4,4,5,5-tetramethyl-1,3,2-dioxaborolane **546**

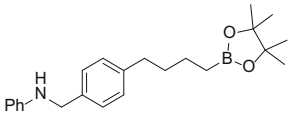

According to General Procedure **C**, *N*-phenyl-4-(3-butenyl)-benzylamine **541** (166 mg, 0.7 mmol), pinacol borane **93** (110 μL, 0.77 mmol), iron(II) chloride **279** (0.9 mg, 0.007 mmol), 2,6-bis-[1-(2,6-diethylphenylimino)ethyl]pyridine **273b** (3.0 mg, 0.007 mmol) and ethylmagnesium bromide **280** (3 drops, 0.021 mmol) were reacted in anhydrous tetrahydrofuran (3 mL) to give the crude reaction product, which was purified by flash silica chromatography (5 % EtOAc/hexane) to give *2-(4-(N-phenylbenzaldimine)butyl)-4,4,5,5-tetramethyl-1,3,2-dioxaborolane* **546** as a bright yellow oil (236 mg, 0.65 mmol, 92 %).

^{1}H NMR (400 MHz, $CDCl_3$) 7.30-7.26 (m, 2H, ArH), 7.22-7.14 (m, 4H, ArH), 6.75-6.69 (m, 1H, ArH), 6.68-6.63 (m, 2H, ArH), 4.29 (s, 2H, NCH), 3.98 (br. s, 1H, NH), 2.64-2.58 (m, 2H, $ArCH_2$), 1.68-1.58 (m, 2H, CH_2), 1.53-1.43 (m, 2H, CH_2), 1.25 (s, 12H, CH_3), 0.86-0.80 (m, 2H, CH_2). **^{13}C NMR** (101 MHz, $CDCl_3$) 148.3 (C), 142.0 (C), 136.5 (C), 129.2 (2 × CH), 128.6 (2 × CH), 127.5 (2 × CH), 117.4 (CH), 112.8 (2 × CH), 82.9 (2 × C), 48.1 (NCH_2), 35.4 (CH_2), 34.2 (CH_2), 24.8 (4 × CH_3), 23.7 (CH_2). **^{11}B NMR** (128 MHz, $CDCl_3$) 34.4. **IR** (neat) ν_{max} cm^{-1} 3431, 2936, 2922, 2230, 1639, 1609, 1504, 1414, 1258, 1055, 1034, 1016, 912, 816, 795, 733. **HRMS** (EI) calculated for $C_{23}H_{32}BNO_2$ 365.25206. Found 365.25212.

4-(4-Hydroxymethylphenyl)butan-1-ol **548**

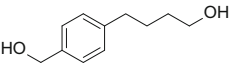

According to a modification of General Procedure **C**, 4-(3-butenyl)-benzyl alcohol **535** (113 mg, 0.7 mmol), pinacol borane **93** (220 μL, 1.54 mmol), iron(II) chloride **279** (0.9 mg, 0.007 mmol), 2,6-bis-[1-(2,6-diethylphenylimino)ethyl]pyridine **273b** (3.0 mg, 0.007 mmol) and tolylmagnesium bromide **282** (1 M in tetrahydrofuran, 0.75 mL, 0.75 mmol) were reacted in anhydrous tetrahydrofuran (3 mL) to give the crude reaction product, which was purified by flash silica chromatography (15 % EtOAc/hexane) to give 2-(4-(4-hydroxymethylphenyl)butyl)-4,4,5,5-tetramethyl-1,3,2-dioxaborolane **547** along with remaining starting material as a colourless oil. The mixture was dissolved in tetrahydrofuran (5 mL) and cooled to 0 °C. Aqueous sodium hydroxide (3 M) and 30 % hydrogen peroxide [0.5 mL, 1:1 volume ratio, with 1gL^{-1} ethylenediaminetetraacetic acid (EDTA)] was added and the mixture stirred for 20 min at room temperature. Water (10 mL) was added, and the product extracted with diethyl ether (3 × 25 mL), dried ($MgSO_4$) and concentrated in vacuo to give a colourless oil, which was purified by flash silica chromatography (4 % methanol/dichloromethane) to give 4-(4-hydroxymethylphenyl)buan-1-ol **548** as a colourless oil (71 mg, 0.39 mmol, 56 %).

^{1}H NMR (500 MHz, $CDCl_3$) 7.31-7.27 (m, 2H, ArH), 7.21-7.17 (m, 2H, ArH), 4.66 (s, 2H, ArCH_2OH), 3.66 (t, J = 6.5 Hz, 2H, CH_2OH), 2.65 (t, J = 7.5 Hz, 2H, $ArCH_2$), 1.76 (br. s., 1H, OH), 1.74-1.66 (m, 2H, CH_2), 1.65-1.57 (m, 2H,

CH_2), 1.38 (br. s., 1H, OH). **^{13}C NMR** (126 MHz, $CDCl_3$) 141.8 (C), 138.3 (C), 128.6 (2 × CH), 127.1 (2 × CH), 65.2 ($ArCH_2OH$), 62.8 (CH_2OH), 35.3 (CH_2), 32.3 (CH_2), 27.5 (CH_2). **IR** (neat) ν_{max} cm^{-1} 3306, 2932, 2859, 1514, 1458, 1420, 1209, 1202, 1026, 1017, 806, 756. **HRMS** (EI) calculated for $C_{11}H_{16}O_2$ 180.11448. Found 180.11494.

Data were in accordance with those previously reported [34].

2-(2-(Cyclohex-3-en-1-yl)ethyl)-4,4,5,5-tetramethyl-1,3,2-dioxaborolane **549**

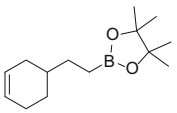

According to General Procedure **C**, 4-vinylcyclohexene **371** (91 μL, 0.7 mmol), pinacol borane **93** (110 μL, 0.77 mmol), iron(II) chloride **279** (0.9 mg, 0.007 mmol), 2,6-bis-[1-(2,6-diethylphenylimino)ethyl]pyridine **273b** (3.0 mg, 0.007 mmol) and ethylmagnesium bromide **280** (3 drops, 0.021 mmol) were reacted in anhydrous tetrahydrofuran (3 mL) to give the crude reaction product, which was purified by flash silica column chromatography (2 % EtOAc/hexane) to give 2-(2-(cyclohex-3-en-1-yl)ethyl)-4,4,5,5-tetramethyl-1,3,2-dioxaborolane **549** as a colourless oil (144 mg, 0.61 mmol, 87 %).

^{1}H NMR (400 MHz, $CDCl_3$) 5.67-5.59 (m, 2H, CH), 2.13-2.04 (m, 1H, CH_2), 2.04-1.97 (m, 2H, CH_2), 1.78-1.69 (m, 1H, CH_2), 1.66-1.55 (m, 1H, CH_2), 1.50-1.31 (m, 3H, CH_2, CH), 1.23 (s, 12H, CH_3), 1.20-1.11 (m, 1H, CH_2), 0.82-0.75 (m, 2H, BCH_2). **^{13}C NMR** (101 MHz, $CDCl_3$) 126.9 (CH), 126.7 (CH), 82.8 (2 × C), 35.7 (CH), 31.6 (CH_2), 30.6 (CH_2), 28.5 (CH_2), 25.3 (CH_2), 24.8 (4 × CH_3). **^{11}B NMR** (128 MHz, $CDCl_3$) 34.0.

Data were in accordance with those previously reported [35].

2-(4-(4-Methylbenzoate)butyl)-4,4,5,5-tetramethyl-1,3,2-dioxaborolane **550**

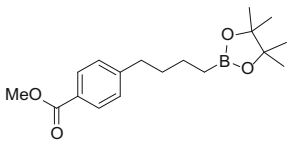

According to General Procedure **C**, 4-(3-butenyl)-benzoic acid methyl ester **530** (133 mg, 0.7 mmol), pinacol borane **93** (110 μL, 0.77 mmol), iron(II) chloride **279** (0.9 mg, 0.007 mmol), 2,6-bis-[1-(2,6-diethylphenylimino)ethyl]pyridine **273b** (3.0 mg, 0.007 mmol) and ethylmagnesium bromide **280** (3 drops, 0.021 mmol) were reacted in anhydrous tetrahydrofuran (3 mL) to give the crude reaction product, which was purified by flash silica column chromatography (7 % EtOAc/hexane) to give *2-(4-(4-methylbenzoate)butyl)-4,4,5,5-tetramethyl-1,3,2-dioxaborolane* **550** as a colourless oil (187 mg, 0.59 mmol, 84 %).

^{1}H NMR (400 MHz, $CDCl_3$) 7.96-7.91 (m, 2H, ArH), 7.26-7.21 (m, 2H, ArH), 3.89 (s, 3H, OCH_3), 2.69-2.62 (m, 2H, $ArCH_2$), 1.69-1.59 (m, 2H, CH_2), 1.52-1.42 (m, 2H, CH_2), 1.24 (s, 12H, CH_3), 0.85-0.78 (m, 2H, BCH_2). **^{13}C NMR** (101 MHz, $CDCl_3$) 167.2 (C=O), 148.5 (C), 129.6 (2 × CH), 128.4 (2 × CH), 127.5 (C), 82.9 (2 × C), 51.9 (OCH_3), 35.8 (CH_2), 33.7 (CH_2), 24.8 (4 × CH_3), 23.6 (CH_2). **^{11}B NMR** (128 MHz, $CDCl_3$) 34.4. **IR** (neat) ν_{max} cm^{-1} 2978, 2936, 2862, 1721, 1611, 1435, 1371, 1317, 1275, 1179, 1144, 1107. **HRMS** (EI) calculated for $C_{18}H_{27}BO_4$ 318.19969. Found 318.19941.

2-(4-(4-*N*-*tert*-Butylbenzamide)butyl)-4,4,5,5-tetramethyl-1,3,2-dioxaborolane **551**

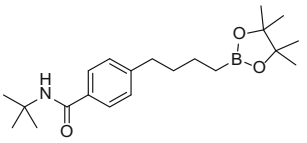

According to General Procedure **C**, *N*-(*tert*-butyl)-4-(3-butenyl)-benzamide **532** (162 mg, 0.7 mmol), pinacol borane **93** (110 μL, 0.77 mmol), iron(II) chloride **279** (2.6 mg, 0.035 mmol), 2,6-bis-[1-(2,6-diethylphenylimino)ethyl]pyridine **273b** (8.9 mg, 0.035 mmol) and ethylmagnesium bromide **280** (15 drops, 0.105 mmol) were reacted in anhydrous tetrahydrofuran (3 mL) to give the crude reaction product, which was purified by flash silica column chromatography (7 % EtOAc/hexane) to give *2-(4-(4-N-tert-butylbenzamide)butyl)-4,4,5,5-tetramethyl-1,3,2-dioxaborolane* **551** as a colourless solid (89 mg, 0.25 mmol, 35 %).

m.p. 99–101 °C. **^{1}H NMR** (400 MHz, $CDCl_3$) 7.66-7.59 (m, 2H, ArH), 7.24-7.18 (m, 2H, ArH), 5.91 (br s, 1H, NH), 2.68-2.60 (m, 2H, $ArCH_2$), 1.67-1.58 (m, 2H, CH_2), 1.51-1.41 (m, 2H, CH_2), 1.47 (s, 9H, CH_3), 1.24 (s, 12H, CH_3), 0.84-0.78 (m, 2H, BCH_2). **^{13}C NMR** (101 MHz, $CDCl_3$) 166.9 (C=O), 146.4 (C), 133.2 (C), 128.5 (2 × CH), 126.7 (2 × CH), 82.9 (2 × C), 51.5 (NC), 35.5 (CH_2), 33.9 (CH_2), 28.9 (3 × CH_3), 24.8 (4 × CH_3), 23.6 (CH_2). **^{11}B NMR** (128 MHz, $CDCl_3$) 34.5. **IR** (neat) ν_{max} cm^{-1} 3364, 2965, 2928, 2829, 1634, 1611, 1535, 1504, 1456, 1364, 1304, 1219, 1144. **HRMS** (EI) calculated for $C_{21}H_{34}BNO_3$ 359.26263. Found 359.26257.

4-(3-Butenyl)-α-methyl-benzyl alcohol **552**

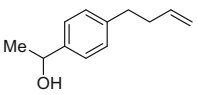

According to General Procedure **C**, 4-(3-butenyl)-acetophenone **528** (123 mg, 0.7 mmol), pinacol borane **93** (110 μL, 0.77 mmol), iron(II) chloride **279** (0.9 mg, 0.007 mmol), 2,6-bis-[1-(2,6-diethylphenylimino)ethyl]pyridine **273b** (3.0 mg, 0.007 mmol) and ethylmagnesium bromide **280** (3 drops, 0.021 mmol) were reacted in anhydrous tetrahydrofuran (3 mL) to give the crude reaction product,

which was purified by flash silica column chromatography (20 % EtOAc/hexane) to give *4-(3-butenyl)-α-methyl-benzyl alcohol* **552** as a colourless oil (113 mg, 0.64 mmol, 91 %).

^{1}H NMR (500 MHz, $CDCl_3$) 7.33-7.29 (m, 2H, ArH), 7.21-7.17 (m, 2H, ArH), 5.87 (ddt, *J* = 17.0, 10.0, 6.5 Hz, 1H, CH), 5.07 (app. dq, *J* = 17.0, 1.5 Hz, 1H, CH), 5.02-4.97 (m, 1H, CH), 4.89 (q, *J* = 6.5 Hz, 1H, C***H***(Me)OH), 2.74-2.70 (m, 2H, $ArCH_2$), 2.42-2.35 (m, 2H, CH_2), 1.78 (br. s, 1H, OH), 1.51 (d, *J* = 6.5 Hz, 3H CH_3). **^{13}C NMR** (126 MHz, $CDCl_3$) 143.3 (C), 141.2 (C), 138.0 (CH), 128.5 (2 × CH), 125.4 (2 × CH), 114.9 (CH), 70.3 (CHOH), 35.5 (CH_2), 35.0 (CH_2), 25.0 (CH_3). **IR** (neat) ν_{max} cm^{-1} 3354, 2968, 2926, 1639, 1514, 1416, 1369, 1258, 1072, 1009, 907, 791. **HRMS** (EI) calculated for $C_{12}H_{16}O$ 176.11957. Found 176.11967.

4-(3-Butenyl)-benzhydrol **553**

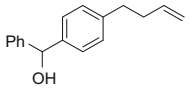

According to General Procedure **C**, 4-(3-butenyl)-benzophenone **529** (167 mg, 0.7 mmol), pinacol borane **93** (110 μL, 0.77 mmol), iron(II) chloride **279** (0.9 mg, 0.007 mmol), 2,6-bis-[1-(2,6-diethylphenylimino)ethyl]pyridine **273b** (3.0 mg, 0.007 mmol) and ethylmagnesium bromide **280** (3 drops, 0.021 mmol) were reacted in anhydrous tetrahydrofuran (3 mL) to give the crude reaction product, which was purified by flash silica column chromatography (20 % EtOAc/hexane) to give *4-(3-butenyl)-benzhydrol* **553** as a colourless oil (119 mg, 0.50 mmol, 71 %).

^{1}H NMR (500 MHz, $CDCl_3$) 7.42-7.38 (m, 2H, ArH), 7.37-7.32 (m, 2H, ArH), 7.32-7.25 (m, 3H, ArH), 7.19-7.15 (m, 2H, ArH), 6.69-6.64 (m, 2H, ArH), 5.86 (ddt, *J* = 17.0, 10.0, 6.5 Hz, 1H, CH), 5.84 (d, *J* = 3.5, 1H, Ar_2C***H***OH), 5.05 (app. dq, *J* = 17.0, 1.5 Hz, 1H, CH), 5.00-4.96 (m, 1H, CH), 2.73-2.66 (m, 2H, $ArCH_2$), 2.40-2.33 (m, 2H, CH_2), 2.16 (d, *J* = 3.5 Hz, OH). **^{13}C NMR** (126 MHz, $CDCl_3$) 143.9 (C), 141.4 (C), 141.3 (C), 138.0 (CH), 128.6 (2 × CH), 128.5 (2 × CH), 127.5 (CH), 126.6 (2 × CH), 126.5 (2 × CH), 114.9 (CH), 76.1 (CH), 35.4 (CH_2), 35.0 (CH_2). **IR** (neat) ν_{max} cm^{-1} 3375, 2974, 2922, 1639, 1512, 1493, 1452, 1416, 1379, 1325, 1260, 1177, 1076, 1015, 908, 853, 797, 731, 698. **HRMS** (EI) calculated for $C_{17}H_{18}O$ 238.13522. Found 238.13576.

2-(4-(*N*-Phenylbenzaldimine)butyl)-4,4,5,5-tetramethyl-1,3,2-dioxaborolane **554**

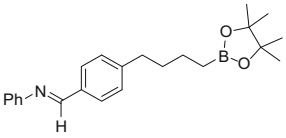

According to General Procedure **C**, *N*-phenyl-4-(3-butenyl)-benzaldimine **540** (164 mg, 0.7 mmol), pinacol borane **93** (110 μL, 0.77 mmol), iron(II) chloride **279**

(0.9 mg, 0.007 mmol), 2,6-bis-[1-(2,6-diethylphenylimino)ethyl]pyridine **273b** (3.0 mg, 0.007 mmol) and ethylmagnesium bromide **280** (3 drops, 0.021 mmol) were reacted in anhydrous tetrahydrofuran (3 mL) to give *2-(4-(N-phenylbenzaldimine)butyl)-4,4,5,5-tetramethyl-1,3,2-dioxaborolane* **554** as a yellow oil. Purification of the product by flash silica chromatography resulted mostly in hydrolysis of the product to the aldehyde. A small amount of spectroscopically pure material was obtained however.

^{1}H NMR (500 MHz, CDC_{l3}) 8.43 (s, 1H, CHN), 7.84-7.79 (m, 2H, ArH), 7.42-7.37 (m, 2H, ArH), 7.31-7.27 (m, 2H, ArH), 7.25-7.19 (m, 3H, ArH), 2.71-2.65 (m, 2H, $ArCH_2$), 1.71-1.63 (m, 2H, CH_2), 1.53-1.45 (m, 2H, CH_2), 1.26 (s, 12H, CH_3), 0.86-0.81 (m, 2H, BCH_2). **^{13}C NMR** (126 MHz, $CDCl_3$) 160.4 (C=N), 152.3 (C), 146.9 (C), 133.8 (C), 129.1 (2 × CH), 128.9 (2 × CH), 128.8 (2 × CH), 125.7 (CH), 120.9 (2 × CH), 82.9 (2 × C), 35.8 (CH_2), 33.9 (CH_2), 24.8 (4 × CH_3), 23.7 (CH_2). **^{11}B NMR** (128 MHz, $CDCl_3$) 34.5. **IR** (neat) ν_{max} cm^{-1} 2976, 2928, 2855, 1701, 1626, 1607, 1589, 1570. 1485, 1462, 1450, 1371. 1317, 1167, 1144. **HRMS** (EI) calculated for $C_{23}H_{30}BNO_2$ 363.23641. Found 363.23688.

4-(3-Butenyl)-benzyl amine **555**

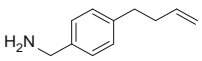

According to General Procedure **C**, 4-(3-Butenyl)-benzonitrile **538** (110 mg, 0.7 mmol), pinacol borane **93** (110 μL, 0.77 mmol), iron(II) chloride **279** (0.9 mg, 0.007 mmol), 2,6-bis-[1-(2,6-diethylphenylimino)ethyl]pyridine **273b** (3.0 mg, 0.007 mmol) and ethylmagnesium bromide **280** (3 drops, 0.021 mmol) were reacted in anhydrous tetrahydrofuran (3 mL) to give the crude reaction product, which was purified by flash silica column chromatography (7 % EtOAc/hexane) to give *4-(3-butenyl)-benzyl amine* **555** as a yellow oil (29 mg, 0.18 mmol, 26 %).

^{1}H NMR (500 MHz, $CDCl_3$) 7.26-7.22 (m, 2H, ArH), 7.19-7.15 (m, 2H, ArH), 5.87 (ddt, *J* = 17.0, 10.0, 6.5 Hz, 1H, CH), 5.06 (app. dq, *J* = 17.0, 1.5 Hz, 1H, CH), 5.01-4.97 (m, 1H, CH), 3.85 (s, 2H, CH_2NH_2), 2.74-2.68 (m, 2H, $ArCH_2$), 2.41-2.34 (m, 2H, CH_2), 1.45 (br. s, 2H, NH_2). **^{13}C NMR** (126 MHz, $CDCl_3$) 140.9 (C), 140.4 (C), 138.1 (CH), 128.6 (2 × CH), 127.0 (2 × CH), 114.9 (CH), 46.3 (CH_2NH_2), 35.5 (CH_2), 35.0 (CH_2). **IR** (neat) ν_{max} cm^{-1} 3366, 3294, 2976, 2922, 2855, 1639, 1578, 1512, 1452, 1439, 1418, 1379, 1331, 1053, 1034, 1018, 995, 908, 804. **HRMS** (EI) calculated for $C_{11}H_{15}N$ 161.11990. Found 161.12058.

2-(2-Phenyl-propyl)-4,4,5,5-tetramethyl-1,3,2-dioxaborolane **556**

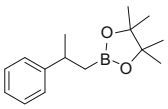

According to General Procedure **D**, α-methylstyrene (91 μL, 0.7 mmol), pinacol borane **93** (110 μL, 0.77 mmol), 2,6-bis-[1-(2,6-diethylphenylimino)ethyl]pyridine iron(II) chloride **367** (^{Et}BIP) (3.9 mg, 0.007 mmol) and *n*-BuLi **283** (4 drops, 0.021 mmol) were reacted to give the crude reaction product, which was purified by flash silica column chromatography (2 % EtOAc/Hexane) to give 2-(2-phenyl-propyl)-4,4,5,5-tetramethyl-1,3,2-dioxaborolane **556** as a colourless oil (150 mg, 0.61 mmol, 87 %).

^{1}H NMR (500 MHz, $CDCl_3$) 7.31-7.25 (m, 4H, ArH), 7.20-7.15 (m, 1H, ArH), 3.06 (app. sext., *J*= 7.0 Hz, 1H, CH), 1.31 (d, *J*= 7.0 Hz, 3H, CH_3), 1.24-1.13 (m, 2H, CH_2), 1.19 (s, 12H, CH_3). **^{13}C NMR** (126 MHz, $CDCl_3$) 149.2 (C), 128.1 (2 × CH), 126.6 (2 × CH), 125.6 (CH), 83.0 (2 × C), 35.8 (CH), 24.9 (CH_3), 24.8 (2 × CH_3), 24.7 (2 × CH_3), (21.2, BCH_2). **^{11}B NMR** (128 MHz, $CDCl_3$) 33.1.

Data were in accordance with those previously reported [35].

2-(2-((*R*)-4-Methylcyclohex-3-en-1-yl)-propyl)-
4,4,5,5-tetramethyl-1,3,2-dioxaborolane **557** (1:1 mixture of diastereoisomers)

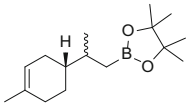

According to General Procedure **D**, (*R*)-limonene (113 μL, 0.7 mmol), pinacol borane **93** (110 μL, 0.77 mmol), 2,6-bis-[1-(2,6-diethylphenylimino)ethyl]pyridine iron(II) chloride **367** (^{Et}BIP) (3.9 mg, 0.007 mmol) and *n*-BuLi **283** (4 drops, 0.021 mmol) were reacted to give the crude reaction product, which was purified by flash silica column chromatography (2 % EtOAc/Hexane) to give 2-(2-((*R*)-4-methylcyclohex-3-en-1-yl)-propyl)-4,4,5,5-tetramethyl-1,3,2-dioxaborolane **557** (1:1 mixture of diastereoisomers) as a colourless oil (127 mg, 0.48 mmol, 69 %).

^{1}H NMR (500 MHz, $CDCl_3$) 5.39-5.35 (m, 1H, CH), 2.03-1.88 (m, 3H, CH_2), 1.78-1.60 (m, 3H, CH_2, CH), 1.64 (s, 3H, CH_3), 1.36-1.14 (m, 2H, CH_2, CH), 1.26 (s, 6H, $C(CH_3)_2$), 1.25 (s, 6H, $C(CH_3)_2$), 0.93-0.87 (m, 4H, CH_3, BCH_2), 0.65 (dd, *J*= 15.3, 9.9 Hz, 1H, BCH_2). **^{13}C NMR** (126 MHz, $CDCl_3$) 133.88 (0.5 × CH), 133.85 (0.5 × CH), 121.10 (0.5 × CH), 121.07 (0.5 × CH), 82.8 (2 × C), 40.63 (0.5 × CH), 40.55 (0.5 × CH), 33.9 (0.5 × CH), 33.7 (0.5 × CH), 31.0 (0.5 × CH_2), 30.9 (0.5 × CH_2), 29.2 (0.5 × CH_2), 28.4 (0.5 × CH_2), 26.8 (0.5 × CH_2), 25.9 (0.5 × CH_2), 24.92 (CH_3), 24.90 (CH_3), 24.71 (CH_3), 24.71 (CH_3), 23.5 (CH_3), 19.3 (0.5 × CH_3), 19.0 (0.5 × CH_3), (16.6, BCH_2). **^{11}B NMR** (128 MHz, $CDCl_3$) 33.7.

Data were in accordance with those previously reported [35].

2-Cyclooctyl-4,4,5,5-tetramethyl-1,3,2-dioxaborolane **558**

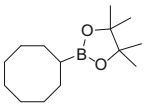

According to General Procedure **D**, cyclooctene (91 μL, 0.7 mmol), pinacol borane **93** (110 μL, 0.77 mmol), 2,6-bis-[1-(2,6-diethylphenylimino)ethyl]pyridine iron(II) chloride **367** (^{Et}BIP) (3.9 mg, 0.007 mmol) and *n*-BuLi **283** (4 drops, 0.021 mmol) were reacted to give the crude reaction product, which was purified by flash silica column chromatography (2 % EtOAc/Hexane) to give 2-cyclooctyl-4,4,5,5-tetrame thyl-1,3,2-dioxaborolane **558** as a colourless oil (147 mg, 0.62 mmol, 88 %).

^{1}H NMR (500 MHz, $CDCl_3$) 1.77-1.69 (m, 2H, CH_2), 1.68-1.61 (m, 2H, CH_2), 1.60-1.43 (m, 10H, CH_2), 1.24 (s, 12H, CH_3), 1.15-1.09 (m, 1H, CH). **^{13}C NMR** (126 MHz, $CDCl_3$) 82.7 (2 × C), 27.6 (2 × CH_2), 27.0 (2 × CH_2), 26.8 (2 × CH_2), 26.6 (CH_2), 24.7 (4 × CH_3), (21.3, BCH). **^{11}B NMR** (128 MHz, $CDCl_3$) 34.1.

Data were in accordance with those previously reported [36].

(*Z*)-2-(1,2-Diphenylvinyl)-4,4,5,5-tetramethyl-1,3,2-dioxaborolane **562**

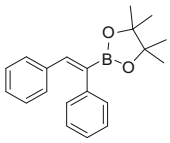

According to General Procedure **C**, diphenylacetylene (125 mg, 0.7 mmol), pinacol borane **93** (110 μL, 0.77 mmol), iron(II) chloride **279** (0.9 mg, 0.007 mmol), 2,6-bis-[1-(2,6-diethylphenylimino)ethyl]pyridine **273b** (3.0 mg, 0.007 mmol) and ethylmagnesium bromide **280** (3 drops, 0.021 mmol) were reacted in anhydrous tetrahydrofuran (3 mL) to give the crude reaction product, which was purified by flash silica column chromatography (2 % EtOAc/Hexane) to give (*Z*)-2-(1,2-diphenylvinyl)-4,4,5,5-tetramethyl-1,3,2-dioxaborolane **562** as a colourless solid (167 mg, 0.55 mmol, 78 %).

^{1}H NMR (400 MHz, $CDCl_3$) 7.39 (br s, 1H, CH), 7.31-7.26 (m, 2H, ArH), 7.25-7.17 (m, 3H, ArH), 7.16-7.11 (m, 3H, ArH), 7.10-7.06 (m, 2H, ArH), 1.33 (s, 12H, CH_3). **^{13}C NMR** (101 MHz, $CDCl_3$) 143.1 (CH), 140.4 (C), 137.0 (C), 129.9 (2 × CH), 128.8 (2 × CH), 128.2 (2 × CH), 127.8 (2 × CH), 127.6 (CH), 126.2 (CH), 83.8 (2 × C), 24.8 (4 × CH_3). **^{11}B NMR** (128 MHz, $CDCl_3$) 30.8.

Data were in accordance with those previously reported [37].

(*Z*)-2-(1-Ethyl-1-buten-1-yl)-4,4,5,5-tetramethyl-1,3,2-dioxaborolane **563**

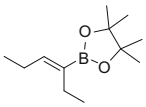

According to General Procedure **C**, 3-hexyne (79 μL, 0.7 mmol), pinacol borane **93** (110 μL, 0.77 mmol), iron(II) chloride **279** (0.9 mg, 0.007 mmol), 2,6-bis-[1-(2,6-diethylphenylimino)ethyl]pyridine **273b** (3.0 mg, 0.007 mmol) and ethylmagnesium bromide **280** (3 drops, 0.021 mmol) were reacted in anhydrous tetrahydrofuran (3 mL) to give the crude reaction product, which was purified by flash silica column chromatography (2 % EtOAc/Hexane) to give (*Z*)-2-(1-ethyl-1-buten-1-yl)-4,4,5,5-tetramethyl-1,3,2-dioxaborolane **563** as a colourless oil (112 mg, 0.53 mmol, 76 %).

^{1}H NMR (400 MHz, $CDCl_3$) 6.26 (t, J = 7.0 Hz, 1H, CH), 2.19-2.10 (m, 4H, CH_2), 1.27 (s, 12H, $C(CH_3)_2$), 1.01 (t, J = 7.5 Hz, 3H, CH_3), 0.95 (t, J = 7.5 Hz, 3H, CH_3). **^{13}C NMR** (101 MHz, $CDCl_3$) 146.9 (CH), 82.9 (2 × C), 24.7 (4 × CH_3), 21.6 (CH_2), 21.4 (CH_2), 14.8 (CH_3), 13.8 (CH_3). **^{11}B NMR** (128 MHz, $CDCl_3$) 30.8.

Data were in accordance with those previously reported [38].

1-Phenyl-2-(triethylgermyl)ethane **566**

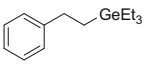

Styrene **53** (80 μL, 0.7 mmol) was added to a solution of iron(II) chloride **279** (0.9 mg, 0.007 mmol) and 2,6-bis-[1-(2,6-diethylphenylimino)ethyl]pyridine **273b** (3.0 mg, 0.007 mmol) in anhydrous tetrahydrofuran (3 mL) at room temperature under an atmosphere of nitrogen. Ethylmagnesium bromide **280** (1.5 M in Et_2O, 15 μL, 3 drops, 0.023 mmol) was added, followed by triethylgermanium hydride **565** (120 μL, 0.75 mmol) and the reaction stirred at room temperature for 1 h. Water (10 mL) was added and the aqueous phase extracted with diethyl ether (3 × 20 mL). The combined organic extracts were washed with water and brine, dried ($MgSO_4$) and concentrated in vacuo. Trimethoxybenzene (23.5 mg, 0.14 mmol) was added as an internal standard, and a yield for the reaction determined by ^{1}H NMR spectroscopy. Purification by filtration through a plug of silica using 0.5 % ethyl acetate/petroleum ether gave *1-phenyl-2-(triethylgermyl)ethane* **566** as a colourless oil (160 mg, 0.60 mmol, 86 %).

^{1}H NMR (400 MHz, $CDCl_3$) 7.34-7.28 (m, 2H, ArH), 7.26-7.17 (m, 3H, ArH), 2.74-2.67 (m, 2H, $ArCH_2$), 1.13-1.06 (m, 2H, $ArCH_2C\boldsymbol{H_2}Ge$), 1.06 (t, J = 8.0 Hz, 9H, CH_3), 0.78 (q, J = 8.0 Hz, 6H, $C\boldsymbol{H_2}CH_3$). **^{13}C NMR** (101 MHz, $CDCl_3$) 145.5 (C), 128.3 (2 × CH), 127.7 (2 × CH), 125.5 (CH), 31.3 ($ArCH_2$), 13.5 (CH_2), 9.0

(3 × CH_3), 3.9 (3 × CH_2). **IR** (neat) ν_{max} cm^{-1} 2947, 2903, 2870, 1603, 1495, 1454, 1425, 1377, 1018, 968, 746, 690. **HRMS** (EI) calculated for $C_{14}H_{24}Ge$ 266.10843. Found 266.10812.

1-Phenyl-4-(triethylgermyl)butane **567**

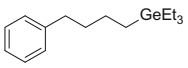

4-Phenylbutene **361** (105 μL, 0.7 mmol) was added to a solution of iron(II) chloride **279** (0.9 mg, 0.007 mmol) and 2,6-bis-[1-(2,6-diethylphenylimino)ethyl] pyridine **273b** (3.0 mg, 0.007 mmol) in anhydrous tetrahydrofuran (3 mL) at room temperature under an atmosphere of nitrogen. Ethylmagnesium bromide **280** (1.5 M in Et_2O, 15 μL, 3 drops, 0.023 mmol) was added, followed by triethylgermanium hydride **565** (120 μL, 0.75 mmol) and the reaction stirred at room temperature for 1 h. Water (10 mL) was added and the aqueous phase extracted with diethyl ether (3 × 20 mL). The combined organic extracts were washed with water and brine, dried ($MgSO_4$) and concentrated in vacuo. Trimethoxybenzene (23.5 mg, 0.14 mmol) was added as an internal standard, and a yield for the reaction determined by ^{1}H NMR spectroscopy. Purification by filtration through a plug of silica using petroleum ether gave *1-phenyl-4-(triethylgermyl)butane* **567** as a colourless oil (65 mg, 0.22 mmol, 32 %).

^{1}H NMR (600 MHz, $CDCl_3$) 7.32-7.27 (m, 2H, ArH), 7.21-7.17 (m, 3H, ArH), 2.66-2.60 (m, 2H, $ArCH_2$), 1.69-1.61 (m, 2H, CH_2), 1.47-1.40 (m, 2H, CH_2), 1.02 (t, J = 8.0 Hz, 9H, CH_3), 0.78-0.74 (m, 2H, CH_2GeEt_3), 0.72 (q, J = 8.0 Hz, 6H, $GeCH_2CH_3$). **^{13}C NMR** (151 MHz, $CDCl_3$) 142.9 (C), 128.4 (2 × CH), 128.2 (2 × CH), 125.5 (CH), 35.6 (CH_2), 35.4 (CH_2), 24.9 (CH_2), 11.3 (CH_2), 9.0 (3 × CH_3), 3.9 (3 × CH_2). **IR** (neat) ν_{max} cm^{-1} 2947, 2924, 2905, 2870, 1497, 1454, 1425, 1259, 1096, 1016, 966, 804, 743, 696.

d_7-iso-Propylmagnesium bromide ***d*$_7$-610**

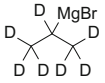

Magnesium turnings (280 mg, 11.5 mmol) and anhydrous diethyl ether (8 mL) were added to an oven-dried multi-necked round-bottomed flask with a reflux condenser attached, under a nitrogen atmosphere. d_7-2-Bromopropane (0.1 mL, 1.1 mmol) was added, followed by a single crystal of iodine. The remaining d_5-bromoethane (0.62 mL, 6.6 mmol) was added over the course of 30 min at a rate to maintain reflux. The reaction was heated at reflux for 1 h, and was then allowed to cool and settle. The prepared Grignard reagent was transferred by syringe to an oven-dried J. Young's sample flask. The concentration of d_7-iso-propylmagnesium bromide ***d*$_7$-610** was determined to be 1.5 M by titration using 2-hydroxyben zaldehyde phenylhydrazone.

(2-Phenylethyl)magnesium bromide **635**

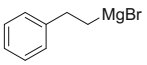

Magnesium turnings (970 mg, 40 mmol) were added to an oven-dried multi-necked round-bottomed flask with a reflux condenser attached, under a nitrogen atmosphere. Anhydrous diethyl ether (22 mL) was added, followed by approximately 10 % of the (2-bromoethyl)benzene (approx. 0.46 g, 2.5 mmol). The reaction was stirred at room temperature, however the reaction temperature did not increase, therefore a small crystal of iodine was added. Within 1 min, the brown colouration from iodine disappeared and the reaction temperature began to increase. The remaining (2-bromoethyl)benzene (4.14 g 22.5 mmol) was added over 30 min. The solution was stirred for an additional 90 min, before being allowed to cool and settle. The prepared Grignard reagent, (2-phenylethyl)magnesium bromide **635**, was transferred by syringe to an oven-dried J. Young's sample flask. The concentration of the Grignard reagent was determined to be 1 M by titration using 2-hydroxybenzaldehyde phenylhydrazone.

The prepared Grignard reagent contained approximately 1.5 % styrene **53** [relative to (2-phenylethyl)magnesium bromide **635**]. In order to remove this, the solvent was removed from the Grignard reagent under high vacuum and the solid Grignard reagent was heated gently for 10 min. Anhydrous diethyl ether (10 mL) was added to dissolve the Grignard reagent, and was removed again under high vacuum. This procedure was repeated 3 times. Anhydrous diethyl ether (15 mL) was added and the concentration of (2-phenylethyl)magnesium bromide **635** was determined to be 1.15 M by titration using 2-hydroxybenzaldehyde phenylhydrazone. Following this procedure the amount of styrene **53** in the Grignard reagent was reduced to $\sim$0.4 % [relative to (2-phenylethyl)magnesium bromide **635**].

2-Methoxystyrene **675**

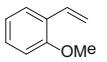

2-Methoxybenzaldhyde (670 mg, 5 mmol) was added to potassium carbonate (1.1 g, 8 mmol) and methyltriphenylphosphonium bromide **335** (2.1 g, 6 mmol) in anhydrous tetrahydrofuran (5 mL), and heated at reflux for 16 h. The reaction mixture was cooled, filtered and concentrated in vacuo. The residue was dissolved in hot *n*-pentane, cooled to 0 °C, filtered, and washed with cold *n*-pentane. The filtrate was dried ($MgSO_4$) and concentrated in vacuo to give 2-methoxystyrene **675** as a colourless oil (476 mg, 72 %).

^{1}H NMR (400 MHz, $CDCl_3$) 7.52-7.48 (m, 1H, ArH), 7.30-7.24 (m, 1H, ArH), 7.09 (dd, *J*= 17.5, 11.0 Hz, 1H, CH), 6.99-6.94 (m, 1H, ArH), 6.92-6.88 (m, 1H, ArH), 5.77 (dd, *J* = 17.5, 1.5 Hz, 1H, CH), 5.30 (dd, *J* = 11.0, 1.5 Hz, 1H, CH), 3.87 (s, 3H, CH_3). **^{13}C NMR** (100 MHz, $CDCl_3$) 156.7 (C), 131.8 (CH), 128.8 (CH), 126.7 (C), 126.5 (CH), 120.6 (CH), 114.4 (CH), 110.8 (CH), 55.4 (CH_3).

Data were in accordance with those previously reported [39].

3-Methoxystyrene **676**

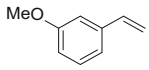

3-Methoxybenzaldhyde (670 mg, 5 mmol) was added to potassium carbonate (1.1 g, 8 mmol) and methyltriphenylphosphonium bromide **335** (2.1 g, 6 mmol) in anhydrous tetrahydrofuran (5 mL), and heated at reflux for 48 h. The reaction mixture was cooled, filtered and concentrated in vacuo. The residue was dissolved in hot *n*-pentane, cooled to 0 °C, filtered, and washed with cold *n*-pentane. The filtrate was dried ($MgSO_4$) and concentrated in vacuo to give 3-methoxystyrene **676** as a colourless oil (495 mg, 75 %).

^{1}H NMR (400 MHz, $CDCl_3$) 7.30-7.24 (m, 1H, ArH), 7.05-7.02 (m, 1H, ArH), 6.99-6.96 (m, 1H, ArH), 6.86-6.82 (m, 1H, ArH), 6.72 (dd, *J* = 17.5, 11.0 Hz, 1H, CH), 5.77 (dd, *J* = 17.5, 1.0 Hz, 1H, CH), 5.27 (dd, *J* = 11.0 Hz, 1.0 Hz, 1H, CH), 3.84 (s, 3H, CH_3). **^{13}C NMR** (100 MHz, $CDCl_3$) 159.8 (C), 139.0 (C), 136.8 (CH), 129.5 (CH), 118.9 (CH), 114.1 (CH), 113.4 (CH), 111.5 (CH), 55.2 (CH_3).

Data were in accordance with those previously reported [40].

2,4-Dimethoxystyrene **677**

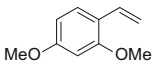

2,4-Dimethoxybenzaldhyde (1.66 g, 10 mmol) was added to potassium carbonate (2.2 g, 16 mmol) and methyltriphenylphosphonium bromide **335** (4.2 g, 12 mmol) in anhydrous tetrahydrofuran (10 mL), and heated at reflux for 16 h. The reaction mixture was cooled, filtered and concentrated in vacuo. The residue was purified by flash chromatography (5 % EtOAc/hexane) to give 2,4-dimethoxystyrene **677** as a colourless oil (1.19 g, 73 %).

^{1}H NMR (400 MHz, $CDCl_3$) 7.41 (d, *J* = 8.5 Hz, 1H, ArH), 6.97 (dd, *J* = 18.0, 11.0 Hz, 1H, CH), 6.49 (dd, *J* = 8.5, 2.5 Hz, 1H, ArH), 6.46 (d, *J* = 2.5 Hz, 1H, ArH), 5.64 (dd, *J* = 18.0, 1.5 Hz, 1H, CH), 5.16 (dd, *J* = 11.0, 1.5 Hz, 1H, CH), 3.84 (s, 3H, CH_3), 3.83 (s, 3H, CH_3). **^{13}C NMR** (100 MHz, $CDCl_3$) 160.6 (C), 157.8 (C), 131.2 (CH), 127.2 (CH), 119.9 (C), 112.3 (CH), 104.7 (CH), 98.4 (CH), 55.4 (CH_3), 55.3 (CH_3).

Data were in accordance with those previously reported [40].

2,5-Dimethoxystyrene **678**

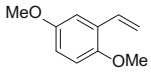

2,5-Dimethoxybenzaldhyde (831 mg, 5 mmol) was added to potassium carbonate (1.1 g, 8 mmol) and methyltriphenylphosphonium bromide **335** (2.1 g, 6 mmol) in anhydrous tetrahydrofuran (5 mL), and heated at reflux for 16 h. The reaction mixture was cooled, filtered and concentrated in vacuo. The residue was dissolved in hot *n*-pentane, cooled to 0 °C, filtered, and washed with cold *n*-pentane. The filtrate was dried ($MgSO_4$) and concentrated in vacuo to give 2,5-dimethoxystyrene **678** as a colourless oil (623 mg, 76 %).

^{1}H NMR (400 MHz, $CDCl_3$) 7.07-7.05 (m, 1H, ArH), 7.05 (dd, *J* = 17.5, 11.0 Hz, 1H, CH), 6.85-6.78 (m, 2H, ArH), 5.75 (dd, *J* = 17.5, 1.5 Hz, 1H, CH), 5.29 (dd, *J* = 11.0, 1.5 Hz, 1H, CH), 3.82 (s, 3H, CH_3), 3.81 (s, 3H, CH_3). **^{13}C NMR** (100 MHz, $CDCl_3$) 153.7 (C), 151.2 (C), 131.5 (CH), 127.6 (C), 114.9 (CH), 113.8 (CH), 112.2 (CH), 111.8 (CH), 56.2 (CH_3), 55.7 (CH_3). **IR** (neat) ν_{max} cm^{-1} 3085, 2997, 2941, 2906, 2833, 1625, 1580, 1492, 1463, 1426, 1418, 1282, 1217, 1179, 1161, 1119, 1058, 1038, 1024.

Data were in accordance with those previously reported [40].

2,6-Dimethoxystyrene **679**

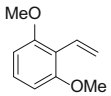

2,6-Dimethoxybenzaldhyde (1.66 g, 10 mmol) was added to potassium carbonate (2.2 g, 16 mmol) and methyltriphenylphosphonium bromide **335** (4.2 g, 12 mmol) in anhydrous tetrahydrofuran (10 mL), and heated at reflux for 16 h. The reaction mixture was cooled, filtered and concentrated in vacuo. The residue was purified by flash chromatography (5 % EtOAc/hexane) to give 2,6-dimethoxystyrene **679** as a colourless oil (1.18 g, 72 %).

^{1}H NMR (400 MHz, $CDCl_3$) 7.17 (t, *J* = 8.5 Hz, 1H, ArH), 6.99 (dd, *J* = 18.0, 12.0 Hz, 1H, CH), 6.58 (d, *J* = 8.5 Hz, 2H, ArH), 6.08 (dd, *J* = 18.0, 3.0 Hz, 1H, CH), 5.47 (dd, *J* = 12.0, 3.0 Hz, 1H, CH), 3.86 (s, 6H, CH_3). **^{13}C NMR** (100 MHz, $CDCl_3$) 158.6 (2 × C), 128.2 (CH), 127.3 (CH), 118.4 (CH), 114.9 (C), 103.9 (2 × CH), 55.7 (2 × CH_3).

Data were in accordance with those previously reported [41].

3-Benzyloxystyrene **680**

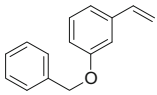

3-Benzyloxybenzaldhyde (1.06 g, 5 mmol) was added to potassium carbonate (1.1 g, 8 mmol) and methyltriphenylphosphonium bromide **335** (2.1 g, 6 mmol) in anhydrous tetrahydrofuran (5 mL), and heated at reflux for 16 h. The reaction mixture was cooled, filtered and concentrated in vacuo. The residue was dissolved in hot *n*-pentane, cooled to 0 °C, filtered, and washed with cold *n*-pentane. The filtrate was dried ($MgSO_4$) and concentrated in vacuo to give 3-benzyloxystyrene **680** as a colourless oil (934 mg, 89 %).

^{1}H NMR (400 MHz, $CDCl_3$) 7.49-7.45 (m, 2H, ArH), 7.44-7.39 (m, 2H, ArH), 7.38-7.32 (m, 2H, ArH), 7.30-7.24 (m, 1H, ArH), 7.09-7.03 (m, 2H, ArH), 6.93-6.89 (m, 1H, ArH), 6.71 (dd, *J* = 17.5, 11.0 Hz, 1H, CH), 5.76 (dd, *J* = 17.5, 1.0 Hz, 1H, CH), 5.27 (dd, *J* = 11.0, 1.0 Hz, 1H, CH), 5.10 (s, 2H, CH_2). **^{13}C NMR** (100 MHz, $CDCl_3$) 159.0 (C), 139.1 (C), 137.0 (C), 136.7 (CH), 129.5 (CH), 128.6 (2 × CH), 128.0 (CH), 127.5 (2 × CH), 119.2 (CH), 114.21 (CH), 114.17 (CH), 112.6 (CH), 70.0 (CH_2). **IR** (neat) ν_{max} cm^{-1} 3032, 2867, 1597, 1575, 1487, 1441, 1258, 1241, 1155, 1025. **HRMS** (ESI^+) calculated for $C_{15}H_{14}ONa^+$ 233.0937. Found 233.0942.

Data were in accordance with those previously reported [42].

4-Allyloxystyrene **681**

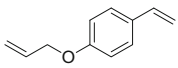

4-Allyloxybenzaldhyde (1.62 g, 10 mmol) was added to potassium carbonate (2.2 g, 16 mmol) and methyltriphenylphosphonium bromide **335** (4.2 g, 12 mmol) in anhydrous tetrahydrofuran (10 mL), and heated at reflux for 16 h. The reaction mixture was cooled, filtered and concentrated in vacuo. The residue was dissolved in hot *n*-pentane, cooled to 0 °C, filtered, and washed with cold *n*-pentane. The filtrate was dried ($MgSO_4$) and concentrated in vacuo to give 4-allyloxystyrene **681** as a colourless oil (951 mg, 59 %).

^{1}H NMR (400 MHz, $CDCl_3$) 7.38-7.33 (m, 2H, ArH), 6.92-6.86 (m, 2H, ArH), 6.68 (dd, *J* = 17.5, 11.0 Hz, 1H, CH), 6.07 (ddt, *J* = 17.5, 10.5, 5.5 Hz, 1H), 5.63 (dd, *J* = 17.5, 1.0 Hz, 1H, CH), 5.43 (app. dq, *J* = 17.5, 1.5 Hz, 1H, CH), 5.30 (app. dq, *J* = 10.5, 1.5 Hz, 1H, CH), 5.14 (dd, *J* = 11.0, 1.0 Hz, 1H, CH), 4.55 (app. dt, *J* = 5.5 Hz, 1.5 Hz, 2H, CH_2). **^{13}C NMR** (100 MHz, $CDCl_3$) 158.3 (C), 136.2 (CH), 133.2 (CH), 130.6 (C), 127.3 (2 × CH), 117.7 (CH), 114.7 (2 × CH),

111.6 (CH), 68.8 (CH_2). **IR** (neat) ν_{max} cm^{-1} 3084, 2864, 1691, 1628, 1605, 1576, 1508, 1456, 1423, 1410, 1300, 1290, 1240, 1225, 1175, 1115, 1018, 989, 923, 901, 831.

Data were in accordance with those previously reported [16].

2-(2-Methylphenyl)propanoic acid **α-682**

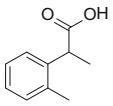

According to general procedure **E**, 2-methylstyrene (90 μL, 0.7 mmol), iron(II) chloride **279** (0.9 mg, 0.007 mmol), 2,6-bis-[1-(2,6-diisopropylphenylimino)ethyl] pyridine **273a** (3.4 mg, 0.007 mmol), ethylmagnesium bromide **280** (3 M in Et_2O, 0.3 mL, 0.9 mmol) and carbon dioxide were reacted in anhydrous tetrahydrofuran to give the crude reaction product, which was purified by flash silica chromatography (8:1 hexane:EtOAc) to give 2-(2-methylphenyl)propanoic acid **α-682** as a colourless amorphous solid (78 mg, 0.48 mmol, 68 %).

$\mathbf{R_f}$ = 0.22 (4:1 hexane:EtOAc). **^{1}H NMR** (500 MHz, $CDCl_3$) 7.32-7.29 (m, 1H, ArH), 7.23-7.16 (m, 3H, ArH), 4.00 (q, J = 7.0 Hz, 1H, CH), 2.39 (s, 3H, $ArCH_3$), 1.50 (d, J = 7.0 Hz, 3H, CH_3). **^{13}C NMR** (126 MHz, $CDCl_3$) 180.1 (C=O), 138.3 (C), 135.9 (C), 130.5 (CH), 127.2 (CH), 126.6 (CH), 126.5 (CH), 41.0 (CH), 19.6 (CH_3), 17.5 (CH_3). **GC-MS** [70-1] (M^+, relative abundance): 6.33 min (164, 93 %).

Data were in accordance with those previously reported [2].

2-(3-Methylphenyl)propanoic acid **α-683**

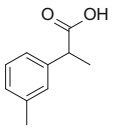

According to general procedure **E**, 3-methylstyrene (93 μL, 0.7 mmol), iron(II) chloride **279** (0.9 mg, 0.007 mmol), 2,6-bis-[1-(2,6-diisopropylphenylimino)ethyl] pyridine **273a** (3.4 mg, 0.007 mmol), ethylmagnesium bromide **280** (3 M in Et_2O, 0.3 mL, 0.9 mmol) and carbon dioxide were reacted in anhydrous tetrahydrofuran to give the crude reaction product, which was purified by acid-base work-up to give *2-(3-methylphenyl)propanoic acid* **α-683** as colourless needles (107 mg, 0.65 mmol, 93 %).

m.p. 62–63 °C (CH_2Cl_2). **^{1}H NMR** (400 MHz, $CDCl_3$) 11.03 (br. s, 1H, CO_2H), 7.26-7.21 (m, 1H, ArH), 7.16-7.08 (m, 3H, ArH), 3.72 (q, J = 7.0 Hz, 1H, CH), 2.36 (s, 3H, $ArCH_3$), 1.52 (d, J = 7.0 Hz, 3H, CH_3). **^{13}C NMR** (100 MHz, $CDCl_3$) 180.5 (C=O), 139.7 (C), 138.4 (C), 128.6 (CH), 128.3 (CH), 128.2 (CH),

124.6 (CH), 45.2 (CH), 21.4 (CH_3), 18.1 (CH_3). **IR** (neat) ν_{max} cm^{-1} 3023, 2980, 2935, 2722, 2619, 1695, 1454, 1321, 1244, 1221. **GC-MS** [70-1] (M^+, relative abundance): 6.28 min (164, 99 %). **HRMS** (ESI^-) calculated for $C_{10}H_{11}O_2^-$ 163.0765. Found 163.0766.

2-(4-Methylphenyl)propanoic acid **α-684**

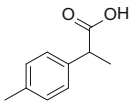

According to general procedure **E**, 4-methylstyrene (93 μL, 0.7 mmol), iron(II) chloride **279** (0.9 mg, 0.007 mmol), 2,6-bis-[1-(2,6-diisopropylphenylimino)ethyl] pyridine **273a** (3.4 mg, 0.007 mmol), ethylmagnesium bromide **280** (3 M in Et_2O, 0.3 mL, 0.9 mmol) and carbon dioxide were reacted in anhydrous tetrahydrofuran to give the crude reaction product, which was purified by acid-base work-up to give 2-(4-methylphenyl)propanoic acid **α-684** as a colourless amorphous solid (107 mg, 0.63 mmol, 90 %).

m.p. 34–35 °C (CH_2Cl_2). **^{1}H NMR** (300 MHz, $CDCl_3$) 11.27 (br. s, 1H, CO_2H), 7.27-7.20 (m, 2H, ArH), 7.20-7.13 (m, 2H, ArH), 3.72 (q, J = 7.0 Hz, 1H, CH), 2.34 (s, 3H, $ArCH_3$), 1.51 (d, J = 7.0 Hz, 3H, CH_3). **^{13}C NMR** (75 MHz, $CDCl_3$) 181.0 (C=O), 137.1 (C), 136.8 (C), 129.4 (2 × CH), 127.4 (2 × CH), 44.9 (CH), 21.0 (CH_3), 18.1 (CH_3). **IR** (neat) ν_{max} cm^{-1} 2983, 2940, 2920, 2735, 2631, 2546, 1695, 1513, 1418, 1231. **GC-MS** [70-1] (M^+, relative abundance): 6.35 min (164, 96 %).

Data were in accordance with those previously reported [2].

2-(4-*tert*-Butylphenyl)propanoic acid **α-685**

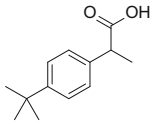

According to general procedure **E**, 4-*tert*-butylstyrene (128 μL, 0.7 mmol), iron(II) chloride **279** (0.9 mg, 0.007 mmol), 2,6-bis-[1-(2,6-diisopropylphenylimino)ethyl] pyridine **273a** (3.4 mg, 0.007 mmol), ethylmagnesium bromide **280** (3 M in Et_2O, 0.3 mL, 0.9 mmol) and carbon dioxide were reacted in anhydrous tetrahydrofuran to give the crude reaction product, which was purified by acid-base work-up to give 2-(4-*tert*-butylphenyl)propanoic acid **α-685** as colourless needles (112 mg, 0.54 mmol, 78 %).

m.p. 100–102 °C (CH_2Cl_2). **^{1}H NMR** (400 MHz, $CDCl_3$) 11.05 (br. s, 1H, CO_2H), 7.38-7.34 (m, 2H, ArH), 7.29-7.24 (m, 2H, ArH), 3.73 (q, J = 7.0 Hz, 1H, CH), 1.52 (d, J = 7.0 Hz, 3H, CH_3), 1.32 (s, 9H, $C(CH_3)_3$). **^{13}C NMR** (100 MHz,

$CDCl_3$) 180.6 (C=O), 150.2 (C), 136.6 (C), 127.2 (2 × CH), 125.6 (2 × CH), 44.8 (CH), 34.4 (C), 31.3 (3 × CH_3), 18.0 (CH_3). **IR** (neat) ν_{max} cm^{-1} 2965, 2905, 2870, 1693, 1509, 1458, 1413, 1285, 1262, 1229. **GC-MS** [70-1] (M^+, relative abundance): 7.33 min (206, 99 %).

Data were in accordance with those previously reported [43].

2-(4-iso-Butylphenyl)propanoic acid **α-686**

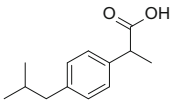

According to general procedure **E**, 4-iso-butylstyrene **66** (112 mg, 0.7 mmol), iron (II) chloride **279** (0.9 mg, 0.007 mmol), 2,6-bis-[1-(2,6-diisopropylphenylimino) ethyl]pyridine **273a** (3.4 mg, 0.007 mmol), ethylmagnesium bromide **280** (3 M in Et_2O, 0.3 mL, 0.9 mmol) and carbon dioxide were reacted in anhydrous tetrahydrofuran to give the crude reaction product, which was purified by acid-base work-up to give 2-(4-iso-butylphenyl)propanoic acid **α-686** as colourless needles (120 mg, 0.58 mmol, 83 %).

m.p. 76–77 °C (CH_2Cl_2). **^{1}H NMR** (500 MHz, $CDCl_3$) 11.74 (s, br, 1H, CO_2H), 7.26-7.22 (m, 2H, ArH), 7.14-7.10 (m, 2H, ArH), 3.73 (q, *J* = 7.0 Hz, 1H, CH), 2.47 (d, *J* = 7.0 Hz, 2H, CH_2), 1.87 (app. non., *J* = 7.0 Hz, 1H, CH), 1.52 (d, *J* = 7.0 Hz, 3H, CH_3), 0.92 (d, *J*= 6.6 Hz, 6H). **^{13}C NMR** (126 MHz, $CDCl_3$) 181.0 (C=O), 140.8 (C), 136.9 (C), 129.4 (2 × CH), 127.3 (2 × CH), 45.03 (CH_2), 44.96 (CH), 30.1 (CH), 22.4 (2 × CH_3), 18.1 (CH_3). **IR** (neat) ν_{max} cm^{-1} 3047, 2955, 2924, 2869, 2727, 1708, 1507, 1462, 1418, 1379, 1321, 1230. **GC-MS** [70-1] (M^+, relative abundance): 7.38 min (206, 97 %).

Data were in accordance with those previously reported [44].

2-(2,4-Dimethylphenyl)propanoic acid **α-687** and 3-(2,4-dimethylphenyl)propanoic acid **β-687**

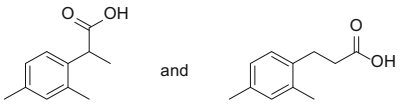

According to general procedure **E**, 2,4-dimethylstyrene (102 μL, 0.7 mmol), iron (II) chloride **279** (0.9 mg, 0.007 mmol), 2,6-bis-[1-(2,6-diisopropylphenylimino) ethyl]pyridine **173a** (3.4 mg, 0.007 mmol), ethylmagnesium bromide **280** (3 M in Et_2O, 0.3 mL, 0.9 mmol) and carbon dioxide were reacted in anhydrous tetrahydrofuran to give the crude reaction product, which was purified by acid-base work-up to give *2-(2,4-dimethylphenyl)propanoic acid* **α-687** and *3-(2,4-dimethylphenyl)propanoic acid* **β-687** as a colourless amorphous solid (56 mg, 0.32 mmol, 45 %, α:β 4:5). The isomers were separated by flash silica chromatography (0.01:8:1 AcOH:hexane:EtOAc).

When ethylmagnesium bromide **280** was replaced with cyclopentylmagnesium bromide **655** (0.45 mL, 2 M in Et_2O, 0.9 mmol), 2-(2,4-dimethylphenyl)propanoic acid **α-687** and 3-(2,4-dimethylphenyl)propanoic acid **β-687** were obtained as a colourless amorphous solid (92 mg, 0.52 mmol, 74 %, α:β 13:61).

2-(2,4-Dimethylphenyl)propanoic acid **α-687**: **m.p.** 106–108 °C (CH_2Cl_2). **^{1}H NMR** (400 MHz, $CDCl_3$) 7.21-7.17 (m, 1H, ArH), 7.05-6.99 (m, 2H, ArH), 3.96 (q, *J* = 7.0 Hz, 1H, CH), 3.35 (s, 3H, $ArCH_3$), 3.30 (s, 3H, $ArCH_3$), 1.49 (d, *J* = 7.0 Hz, 3H, CH_3). **^{13}C NMR** (100 MHz, $CDCl_3$) 180.5 (C=O), 136.8 (C), 135.7 (C), 135.4 (C), 131.3 (CH), 127.1 (CH), 126.5 (CH), 40.7 (CH), 20.9 (CH_3), 19.5 (CH_3), 17.6 (CH_3). **GC-MS** [70-1] (M^+, relative abundance): 6.75 min (178, 96 %). **HRMS** (ESI^-) calculated for $C_{11}H_{13}O_2^-$ 177.0921. Found 177.0927.

3-(2,4-Dimethylphenyl)propanoic acid **β-687**: **^{1}H NMR** (400 MHz, $CDCl_3$) 10.97 (br. s, 1H, CO_2H), 7.08-7.03 (m, 2H, ArH), 7.01-6.94 (m, 2H, ArH), 2.97-2.90 (m, 2H, CH_2), 2.67-2.60 (m, 2H, CH_2), 2.30 (s, 6H, CH_3). **^{13}C NMR** (125 MHz, $CDCl_3$) 178.4 (C=O), 136.0 (C), 135.8 (C), 135.2 (C), 131.2 (CH), 128.4 (CH), 126.8 (CH), 34.4 (CH_2), 27.6 (CH_2), 20.9 (CH_3), 19.1 (CH_3). **IR** (neat) ν_{max} cm^{-1} 2977, 2917, 2714, 2622, 1699, 1431, 1406, 1313, 1279, 1216. **GC-MS** [70-1] (M^+, relative abundance): 7.02 min (178, 96 %). **HRMS** (ESI^-) calculated for $C_{11}H_{13}O_2^-$ 177.0921. Found 177.0926.

2-(2,5-Dimethylphenyl)propanoic acid **α-688** and 3-(2,5-dimethylphenyl)propanoic acid **β-688**

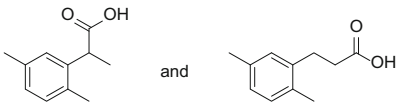

According to general procedure **E**, 2,5-dimethylstyrene (102 μL, 0.7 mmol), iron (II) chloride **279** (0.9 mg, 0.007 mmol), 2,6-bis-[1-(2,6-diisopropylphenylimino) ethyl]pyridine **273a** (3.4 mg, 0.007 mmol), ethylmagnesium bromide **280** (3 M in Et_2O, 0.3 mL, 0.9 mmol) and carbon dioxide were reacted in anhydrous tetrahydrofuran to give the crude reaction product, which was purified by acid-base work-up to give 2-(2,5-dimethylphenyl)propanoic acid **α-688** and *3-(2,5-dimethylphenyl)propanoic acid* **β-688** as a colourless amorphous solid (58 mg, 0.33 mmol, 47 %, α:β 27:20). The isomers were separated by flash silica chromatography (0.01:8:1 AcOH:hexane:EtOAc).

When ethylmagnesium bromide **280** was replaced with cyclopentylmagnesium bromide **655** (2 M in Et_2O, 0.45 mL, 0.9 mmol), 2-(2,5-dimethylphenyl)propanoic acid **α-688** and 3-(2,5-dimethylphenyl)propanoic acid **β-688** were obtained as a colourless amorphous solid (97 mg, 0.55 mmol, 78 %, α:β 14:64).

2-(2,5-Dimethylphenyl)propanoic acid **α-688**: **^{1}H NMR** (400 MHz, $CDCl_3$) 7.13-7.05 (m, 2H, ArH), 7.02-6.96 (m, 1H, ArH), 3.97 (q, *J* = 7.0 Hz, 1H, CH), 2.35 (s, 3H, CH_3), 2.32 (s, 3H, CH_3), 1.49 (d, *J* = 7.0 Hz, 3H, CH_3). **^{13}C NMR** (100 MHz, $CDCl_3$) 180.4 (C=O), 138.1 (C), 135.9 (C), 132.7 (C), 130.4 (CH),

127.9 (CH), 127.2 (CH), 41.0 (CH), 21.1 (CH_3), 19.1 (CH_3), 17.5 (CH_3). **GC-MS** [70-1] (M^+, relative abundance): 6.73 min (178, 99 %).

Data were in accordance with those previously reported [2].

3-(2,5-Dimethylphenyl)propanoic acid **β-688**: **^{1}H NMR** (400 MHz, $CDCl_3$) 7.09-7.03 (m, 1H, ArH), 7.01-6.93 (m, 2H, ArH), 2.97-2.90 (m, 2H, CH_2), 2.69-2.61 (m, 2H, CH_2), 2.31 (s, 3H, CH_3), 2.30 (s, 3H, CH_3). **^{13}C NMR** (100 MHz, $CDCl_3$) 178.9 (C=O), 138.1 (C), 135.6 (C), 132.7 (C), 130.3 (CH), 129.3 (CH), 127.2 (CH), 34.4 (CH_2), 28.0 (CH_2), 20.9 (CH_3), 18.7 (CH_3). **GC-MS** [70-1] (M^+, relative abundance): 7.01 min (178, 96 %). **HRMS** (ESI^-) calculated for $C_{11}H_{13}O_2^-$ 177.0921. Found 177.0927.

2-(2-Methoxyphenyl)propanoic acid **α-690**

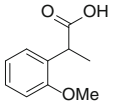

According to general procedure **E**, 2-vinylanisole **675** (94 mg, 0.7 mmol), iron(II) chloride **279** (0.9 mg, 0.007 mmol), 2,6-bis-[1-(2,6-diisopropylphenylimino)ethyl] pyridine **273a** (3.4 mg, 0.007 mmol), ethylmagnesium bromide **280** (3 M in Et_2O, 0.3 mL, 0.9 mmol) and carbon dioxide were reacted in anhydrous tetrahydrofuran to give the crude reaction product, which was purified by acid-base work-up to give 2-(2-methoxyphenyl)propanoic acid **α-690** as a colourless amorphous solid (117 mg, 0.65 mmol, 93 %).

m.p. 101–102 °C (CH_2Cl_2). **^{1}H NMR** (400 MHz, $CDCl_3$) 11.45 (br. s, 1H, CO_2H), 7.33-7.22 (m, 2H, ArH), 7.01-6.93 (m, 1H, ArH), 6.92-6.87 (m, 1H, ArH), 4.10 (q, J = 7.0 Hz, 1H, CH), 3.84 (s, 3H, OCH_3), 1.50 (d, J = 7.0 Hz, 3H, CH_3). **^{13}C NMR** (100 MHz, $CDCl_3$) 180.7 (C=O), 156.7 (C), 128.7 (C), 128.3 (CH), 128.0 (CH), 120.8 (CH), 110.7 (CH), 55.5 (OCH_3). 39.1 (CH), 16.8 (CH_3). **GC-MS** [70-1] (M^+, relative abundance): 6.75 min (180, 99 %).

Data were in accordance with those previously reported [2].

2-(3-Methoxyphenyl)propanoic acid **α-691**

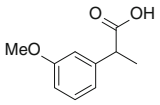

According to general procedure **E**, 3-vinylanisole **676** (94 mg, 0.7 mmol), iron(II) chloride **279** (0.9 mg, 0.007 mmol), 2,6-bis-[1-(2,6-diisopropylphenylimino)ethyl] pyridine **273a** (3.4 mg, 0.007 mmol), ethylmagnesium bromide **280** (3 M in Et_2O, 0.3 mL, 0.9 mmol) and carbon dioxide were reacted in anhydrous tetrahydrofuran to give the crude reaction product, which was purified by acid-base work-up to give 2-(3-methoxyphenyl)propanoic acid **α-691** as a yellow oil (115 mg, 0.64 mmol, 91 %).

m.p. 53–54 °C (CH_2Cl_2). **^{1}H NMR** (400 MHz, $CDCl_3$) 11.34 (br. s, 1H, CO_2H), 7.32-7.28 (m, 1H, ArH), 6.97-6.93 (m, 1H, ArH), 6.92-6.90 (m, 1H, ArH), 6.88-6.84 (m, 1H, ArH), 3.84 (s, 3H, OCH_3), 3.76 (q, J = 7.0 Hz, 1H, CH), 1.55 (d, J = 7.0 Hz, 3H, CH_3). **^{13}C NMR** (100 MHz, $CDCl_3$) 180.1 (C=O), 159.8 (C), 141.2 (C), 129.6 (CH), 119.9 (CH), 113.4 (CH), 112.7 (CH), 55.2 (OCH_3), 45.3 (CH), 18.1 (CH_3). **GC-MS** [70-1] (M^+, relative abundance): 6.97 min (180, 98 %).

Data were in accordance with those previously reported [45].

2-(4-Methoxyphenyl)propanoic acid **α-692**

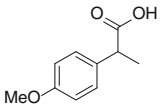

According to general procedure **E**, 4-vinylanisole (93 μL, 0.7 mmol), iron(II) chloride **279** (0.9 mg, 0.007 mmol), 2,6-bis-[1-(2,6-diisopropylphenylimino)ethyl] pyridine **273a** (3.4 mg, 0.007 mmol), ethylmagnesium bromide **280** (3 M in Et_2O, 0.3 mL, 0.9 mmol) and carbon dioxide were reacted in anhydrous tetrahydrofuran to give the crude reaction product, which was purified by acid-base work-up to give 2-(4-methoxyphenyl)propanoic acid **α-692** as a yellow amorphous solid (69 mg, 0.39 mmol, 55 %).

m.p. 53–54 °C (CH_2Cl_2). **^{1}H NMR** (300 MHz, $CDCl_3$) 10.17 (br. s, 1H, CO_2H), 7.29-7.22 (m, 2H, ArH), 6.91-6.83 (m, 2H, ArH), 3.80 (s, 3H, OCH_3), 3.70 (q, J = 7.0 Hz, 1H, CH), 1.50 (d, J = 7.0 Hz, 3H, CH_3). **^{13}C NMR** (75 MHz, $CDCl_3$) 180.7 (C=O), 158.9 (C), 131.8 (C), 128.6 (2 × CH), 114.1 (2 × CH), 55.3 (OCH_3), 44.4 (CH), 18.1 (CH_3). **IR** (neat) ν_{max} cm^{-1} 3035, 2836, 1704, 1512, 1302, 1248, 1180. **GC-MS** [70-1] (M^+, relative abundance): 7.03 min (180, 92 %).

Data were in accordance with those previously reported [2].

2-(2,4-Dimethoxyphenyl)propanoic acid **α-693**

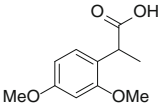

According to general procedure **E**, 2,4-dimethoxystyrene **677** (115 mg, 0.7 mmol), iron(II) chloride **279** (0.9 mg, 0.007 mmol), 2,6-bis-[1-(2,6-diisopropy lphenylimino)ethyl]pyridine **273a** (3.4 mg, 0.007 mmol), ethylmagnesium bromide **280** (3 M in Et_2O, 0.3 mL, 0.9 mmol) and carbon dioxide were reacted in anhydrous tetrahydrofuran to give the crude reaction product, which was purified by acid-base work-up to give 2-(2,4-dimethoxyphenyl)propanoic acid **α-693** as a colourless amorphous solid (125 mg, 0.60 mmol, 85 %).

m.p. 93–95 °C (CH_2Cl_2). **^{1}H NMR** (400 MHz, $CDCl_3$) 7.19-7.14 (m, 1H, ArH), 6.51-6.46 (m, 2H, ArH), 4.02 (q, J = 7.0 Hz, 1H, CH), 3.81 (s, 3H, OCH_3), 3.81 (s, 3H, OCH_3), 1.47 (d, J = 7.0 Hz, 3H, CH_3). **^{13}C NMR** (100 MHz, $CDCl_3$) 181.0 (C=O), 160.0 (C), 157.7 (C), 128.4 (CH), 121.2 (C), 104.3 (CH), 98.7 (CH), 55.5 (OCH_3), 55.3 (OCH_3), 38.4 (CH), 17.0 (CH_3).

Data were in accordance with those previously reported [2].

2-(2,5-Dimethoxyphenyl)propanoic acid **α-694**

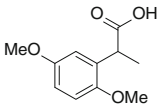

According to general procedure **E**, 2,5-dimethoxystyrene **678** (115 mg, 0.7 mmol), iron(II) chloride **279** (0.9 mg, 0.007 mmol), 2,6-bis-[1-(2,6-diisopropylpheny limino)ethyl]pyridine **273a** (3.4 mg, 0.007 mmol), ethylmagnesium bromide **280** (3 M in Et_2O, 0.3 mL, 0.9 mmol) and carbon dioxide were reacted in anhydrous tetrahydrofuran to give the crude reaction product, which was purified by acid-base work-up to give 2-(2,5-dimethoxyphenyl)propanoic acid **α-694** as a colourless amorphous solid (137 mg, 0.65 mmol, 93 %).

m.p. 102–104 °C (EtOAc/hexane). **^{1}H NMR** (400 MHz, $CDCl_3$) 11.46 (br. s, 1H, CO_2H), 6.86-6.81 (m, 2H, ArH), 6.80-6.76 (m, 1H, ArH), 4.07 (q, J = 7.0 Hz, 1H, CH), 3.80 (s, 3H, OCH_3), 3.78 (s, 3H, OCH_3), 1.48 (d, J = 7.0 Hz, 3H, CH_3). **^{13}C NMR** (126 MHz, $CDCl_3$) 180.3 (C=O), 153.7 (C), 150.9 (C), 129.8 (C), 114.6 (CH), 112.3 (CH), 111.9 (CH), 56.2 (OCH_3), 55.7 (OCH_3), 39.1 (CH), 16.8 (CH_3). **IR** (neat) ν_{max} cm^{-1} 2984, 2938, 2837, 2719, 2623, 1703, 1611, 1589, 1497, 1455, 1406, 1239, 1219, 1180, 1159, 1044, 1023. **GC-MS** [70-1] (M^+, relative abundance): 7.77 min (210, 99 %).

Data were in accordance with those previously reported [2].

2-(2,6-Dimethoxyphenyl)propanoic acid **α-695**

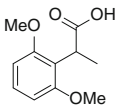

According to general procedure **E**, 2,6-dimethoxystyrene **679** (115 mg, 0.7 mmol), iron(II) chloride **279** (0.9 mg, 0.007 mmol), 2,6-bis-[1-(2,6-diisopropyl phenylimino)ethyl]pyridine **273a** (3.4 mg, 0.007 mmol), ethylmagnesium bromide **280** (3 M in Et_2O, 0.3 mL, 0.9 mmol) and carbon dioxide were reacted in anhydrous tetrahydrofuran to give the crude reaction product, which was purified by acid-base work-up to give *2-(2,6-dimethoxyphenyl)propanoic acid* **α-695** as a colourless amorphous solid (16 mg, 0.60 mmol, 11 %).

m.p. 136–138 °C. **^{1}H NMR** (400 MHz, $CDCl_3$) 7.20 (t, J = 8.5 Hz, 1H, ArH), 6.57 (d, J = 8.5 Hz, 2H, ArH), 4.29 (q, J = 7.0 Hz, 1H, CH), 3.82 (s, 6H, OCH_3), 1.38 (d, J = 7.0 Hz, 3H, CH_3). **^{13}C NMR** (100 MHz, $CDCl_3$) 181.1 (C=O), 157.5 (2 × C), 128.1 (CH), 118.2 (C), 104.2 (2 × CH), 55.7 (2 × OCH_3), 34.5 (CH), 15.2 (CH_3). **IR** (neat) ν_{max} cm^{-1} 2967, 2940, 2909, 1701, 1595, 1476, 1458, 1435, 1410, 1325, 1275, 1244, 1194, 1179, 1107, 1090, 1063, 1032, 941, 779, 754, 727, 698. **HRMS** (EI) calculated for $C_{11}H_{14}O_4$ 210.08866. Found 210.08865.

2-(3,4-Dimethoxyphenyl)propanoic acid **α-696**

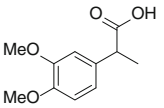

According to general procedure **E**, 3,4-dimethoxystyrene (104 μL, 0.7 mmol), iron (II) chloride **279** (0.9 mg, 0.007 mmol), 2,6-bis-[1-(2,6-diisopropylphenylimino) ethyl]pyridine **273a** (3.4 mg, 0.007 mmol), ethylmagnesium bromide **280** (3 M in Et_2O, 0.3 mL, 0.9 mmol) and carbon dioxide were reacted in anhydrous tetrahydrofuran to give the crude reaction product, which was purified by flash silica chromatography (7:1 hexane:EtOAc) to give *2-(3,4-dimethoxyphenyl)propanoic acid* **α-696** as a yellow amorphous solid (38 mg, 0.18 mmol, 26 %).

^{1}H NMR (500 MHz, $CDCl_3$) 10.94 (br s., 1H, CO_2H), 6.90-6.80 (m, 3H, ArH), 3.89 (s, 3H, OCH_3), 3.87 (s, 3H, OCH_3), 3.70 (q, J = 7.0 Hz, 1H, CH), 1.52 (d, J = 7.0 Hz, 3H, CH_3). **^{13}C NMR** (125 MHz, $CDCl_3$) 179.8 (C=O), 149.0 (C), 148.4 (C), 132.3 (C), 119.7 (CH), 111.2 (CH), 110.8 (CH), 55.9 (OCH_3), 55.9 (OCH_3), 44.8 (CH), 18.2 (CH_3). **GC-MS** [70-1] (M^+, relative abundance): 7.85 min (210, 92 %). **HRMS** (ESI^-) calculated for $C_{11}H_{13}O_4^-$ 209.0819. Found 209.0826.

2-(3-(Benzyloxy)phenyl)propanoic acid **α-697**

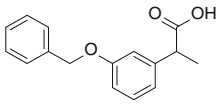

According to general procedure **E**, 3-(benzyloxy)styrene **380** (147 mg, 0.7 mmol), iron(II) chloride **279** (0.9 mg, 0.007 mmol), 2,6-bis-[1-(2,6-diisopropylpheny limino)ethyl]pyridine **273a** (3.4 mg, 0.007 mmol), ethylmagnesium bromide **280** (3 M in Et_2O, 0.3 mL, 0.9 mmol) and carbon dioxide were reacted in anhydrous tetrahydrofuran to give the crude reaction product, which was purified by acid-base work-up to give *2-(3-(benzyloxy)phenyl)propanoic acid* **α-697** a colourless amorphous solid (129 mg, 0.50 mmol, 72 %).

m.p. 121–123 °C (CH_2Cl_2). **^{1}H NMR** (400 MHz, $CDCl_3$) 10.29 (br. s, 1H, CO_2H), 7.46-7.42 (m, 2H, ArH), 7.41-7.37 (m, 2H, ArH), 7.35-7.31 (m, 1H, ArH), 7.28-7.24 (m, 1H, ArH), 6.99-6.97 (m, 1H, ArH), 6.95-6.92 (m, 1H, ArH), 6.91-6.88 (m, 1H, ArH), 5.06 (s, 2H, CH_2), 3.73 (q, J = 7.0 Hz, 1H, CH), 1.52 (d, J = 7.0 Hz, 3H, CH_3). **^{13}C NMR** (125 MHz, $CDCl_3$) 178.8 (C=O), 159.0 (C), 141.3 (C), 136.9 (C), 129.7 (CH), 128.6 (2 × CH), 128.0 (CH), 127.6 (2 × CH), 120.2 (CH), 114.4 (CH), 113.5 (CH), 70.0 (CH_2), 45.1 (CH), 18.1 (CH_3). **IR** (neat) ν_{max} cm^{-1} 3032, 2972, 2915, 2725, 2621, 2541, 1704, 1595, 1495, 1447, 1385, 1268, 1250, 1225, 1164, 1021. **HRMS** (ESI^-) calculated for $C_{16}H_{15}O_3^-$ 255.1027. Found 255.1031.

Methyl 2-(4-morpholinophenyl)propanoate **α-698**

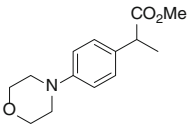

According to general procedure **E**, 4-morpholinostyrene (132 mg, 0.7 mmol), iron (II) chloride **279** (0.9 mg, 0.007 mmol), 2,6-bis-[1-(2,6-diisopropylpheny limino)ethyl]pyridine **273a** (3.4 mg, 0.007 mmol), ethylmagnesium bromide **280** (3 M in Et_2O, 0.3 mL, 0.9 mmol) and carbon dioxide were reacted in anhydrous tetrahydrofuran to give the crude reaction product. HCl (2 M in Et_2O, 0.45 mL, 0.9 mmol) was added and the solution was concentrated to dryness in vacuo. Oxalyl chloride (up to 5 mL) was added until the evolution of gas ceased, and the reaction was concentrated under a static vacuum. The residue was dissolved in anhydrous methanol (10 mL) and triethylamine (0.5 mL, 3.5 mmol) and stirred under a nitrogen atmosphere for 2 h. The reaction was concentrated in vacuo, dissolved in diethyl ether (20 mL) and washed with water. The aqueous phase was extracted with diethyl ether (2 × 20 mL), and the combined organic fractions were dried ($MgSO_4$), and concentrated in vacuo to give the crude product, which was purified by flash chromatography (10 % EtOAc/petroleum ether) to give *methyl 2-(4-morpholinophenyl)propanoate* **α-698** as a colourless amorphous solid (108 mg, 0.43 mmol, 62 %).

^{1}H NMR (400 MHz, $CDCl_3$) 7.24-7.19 (m, 2H, ArH), 6.90-6.85 (m, 2H, ArH), 3.88-3.83 (m, 4H, CH_2), 3.67 (q, J = 7.0 Hz, 1H, CH), 3.66 (s, 3H, OCH_3), 3.18-3.13 (m, 4H, CH_2), 1.48 (d, J = 7.0 Hz, 3H, CH_3). **^{13}C NMR** (126 MHz, $CDCl_3$) 175.3 (C=O), 150.3 (C), 131.9 (C), 128.2 (2 × CH), 115.8 (2 × CH), 66.9 (2 × CH_2), 51.9 (OCH_3), 49.3 (2 × CH_2), 44.5 (CH), 18.5 (CH_3). **IR** (neat) ν_{max} cm^{-1} 2965, 2859, 1732, 1676, 1611, 1514, 1450, 1375, 1366, 1333, 1302, 1233, 1209, 1196, 1163, 1121, 1067, 1032, 926, 858, 826, 806. **HRMS** (EI) calculated for $C_{14}H_{19}O_3N$ 249.13595. Found 249.13549.

2-(4-Fluorophenyl)propanoic acid **α-699**

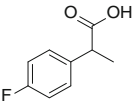

According to general procedure **E**, 4-fluorostyrene (83 μL, 0.7 mmol), iron(II) chloride **279** (0.9 mg, 0.007 mmol), 2,6-bis-[1-(2,6-diisopropylphenylimino)ethyl] pyridine **273a** (3.4 mg, 0.007 mmol), ethylmagnesium bromide **280** (3 M in Et_2O, 0.3 mL, 0.9 mmol) and carbon dioxide were reacted in anhydrous tetrahydrofuran to give the crude reaction product, which was purified by flash silica chromatography (8:1 hexanes:ethyl acetate) to give *2-(4-fluorophenyl)propanoic acid* **α-699** as a colourless oil (44 mg, 0.26 mmol, 37 %).

^{1}H NMR (500 MHz, $CDCl_3$) 7.32-7.27 (m, 2H, ArH), 7.05-6.99 (m, 2H, ArH), 3.74 (q, J = 7.0 Hz, 1H, CH), 1.51 (d, J = 7.0 Hz, 3H, CH_3). **^{13}C NMR** (125 MHz, $CDCl_3$) 180.1 (C=O), 162.1 (d, J = 246 Hz, CF), 135.4 (d, J = 3 Hz, C), 129.2 (d, J = 8 Hz, 2 × CH), 115.5 (d, J = 21 Hz, 2 × CH), 44.5 (CH), 18.2 (CH_3). **^{19}F NMR** (470 MHz, $CDCl_3$) −115.3. **GC-MS** [70-1] (M^+, relative abundance): 5.78 min (168, 97 %). **HRMS** (ESI^-) calculated for $C_9H_8FO_2^-$ 167.0514. Found 167.0520.

2-(2-Biphenyl)propanoic acid **α-700**

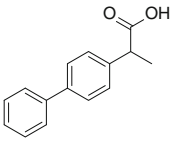

According to general procedure **E**, 4-vinylbiphenyl (126 mg, 0.7 mmol, added as a tetrahydrofuran solution (1 mL)), iron(II) chloride **279** (0.9 mg, 0.007 mmol), 2,6-bis-[1-(2,6-diisopropylphenylimino) ethyl]pyridine **273a** (3.4 mg, 0.007 mmol), ethylmagnesium bromide **280** (3 M in Et_2O, 0.3 mL, 0.9 mmol) and carbon dioxide were reacted in anhydrous tetrahydrofuran to give the crude reaction product, which was purified by acid-base work-up to give 2-(2-biphenyl)propanoic acid **α-700** as a yellow amorphous solid (63 mg, 0.28 mmol, 40 %).

m.p. 142–144 °C (CH_2Cl_2). **^{1}H NMR** (400 MHz, $CDCl_3$) 10.17 (br. s, 1H, CO_2H), 7.60-7.55 (m, 4H, ArH), 7.47-7.39 (m, 4H, ArH), 7.38-7.33 (m, 1H, ArH), 3.81 (q, J = 7.0 Hz, 1H, CH), 1.57 (d, J = 7.0 Hz, 3H, CH_3). **^{13}C NMR** (100 MHz, $CDCl_3$) 180.2 (C=O), 140.7 (C), 140.4(C), 138.8(C), 128.7 (2 × CH), 128.0 (2 × CH), 127.4 (2 × CH), 127.3 (CH), 127.1 (2 × CH), 45.0 (CH), 18.1 (CH_3). **IR** (neat) ν_{max} cm^{-1} 3032, 2982, 2919, 2849, 2622, 1693, 1486, 1409. **GC-MS** [70-1] (M^+, relative abundance): 9.04 min (226, 99%). **HRMS** (ESI^-) calculated for $C_{15}H_{13}O_{2\text{-}2}$25.0921. Found 225.0920.

Data were in accordance with those previously reported [46].

5-Phenylpentanoic acid **723**

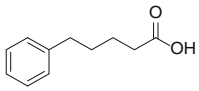

According to general procedure **E**, 4-phenylbutene **361** (105 μL, 0.7 mmol), iron(II) chloride **279** (0.9 mg, 0.007 mmol), 2,6-bis-[1-(2,6-diisopropylpheny limino)ethyl]pyridine **273a** (3.4 mg, 0.007 mmol), ethylmagnesium bromide **280** (3 M in Et_2O, 0.3 mL, 0.9 mmol) and carbon dioxide were reacted in anhydrous tetrahydrofuran to give the crude reaction product, which was purified by acid-base work-up to give 5-phenylpentanoic acid **723** as a colourless amorphous solid (35 mg, 0.20 mmol, 28 %).

m.p. 55–57 °C (CH_2Cl_2). **^{1}H NMR** (400 MHz, $CDCl_3$) 7.33-7.25 (m, 2H, ArH), 7.23-7.15 (m, 3H, ArH), 2.68-2.60 (m, 2H, $ArCH_2$), 2.41-2.34 (m, 2H, CH_2CO_2H), 1.64-1.71 (m, 4H, CH_2).

Data were in accordance with those previously reported [47].

2-(4-(3-Butenyl)phenyl)propanoic acid **α-724**, 2-(4-(2-butenyl)phenyl)propanoic acid **α-725** and 5-(4-vinylphenyl)pentanoic acid **726**

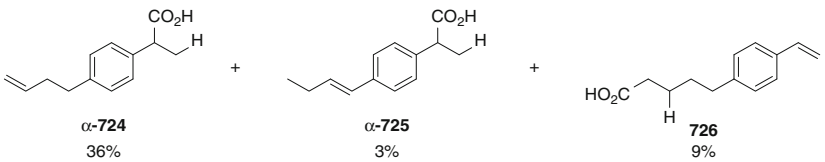

According to general procedure **E**, 4-(3-butenyl)-styrene **326** (111 mg, 0.7 mmol), iron(II) chloride **279** (0.9 mg, 0.007 mmol), 2,6-bis-[1-(2,6-diisopropylpheny limino)ethyl]pyridine **273a** (3.4 mg, 0.007 mmol), ethylmagnesium bromide **280** (3 M in Et_2O, 0.3 mL, 0.9 mmol) and carbon dioxide were reacted in anhydrous tetrahydrofuran to give the crude reaction product, which was purified by acid-base work-up to give a mixture of *2-(4-(3-butenyl)phenyl)propanoic acid* **α-724**, *2-(4-(2-butenyl)phenyl)propanoic acid* **α-725** and *5-(4-vinylphenyl)pentanoic acid* **726** as a colourless oil. Trimethoxybenzene (23.5 mg, 0.14 mmol) was added as an internal standard, and a yield for the reaction determined by ^{1}H NMR spectroscopy

2-(4-(3-butenyl)phenyl)propanoic acid **α-724**: **^{1}H NMR** (400 MHz, $CDCl_3$) 7.28-7.23 (m, 2H, ArH), 7.20-7.17 (m, 3H, ArH), 5.87 (ddt, J = 17.0, 10.5, 6.5 Hz, 1H, CH), 5.10-4.97 (m, 2H, CH), 3.73 (q, J = 7.0 Hz, 1H, CH), 2.74-2.67 (m, 2H, $ArCH_2$), 2.41-2.34 (m, 2H, CH_2), 1.52 (d, J = 7.0 Hz, 3H, CH_3).

2-(4-(2-butenyl)phenyl)propanoic acid **α-725**: only trace amount—most signals overlapping, significant vinyl signals observed: **^{1}H NMR** (400 MHz, $CDCl_3$) 6.37 (d, J = 16.0 Hz, 1H, CH), 6.26 (dt, J = 16.0, 6.5 Hz).

5-(4-Vinylphenyl)pentanoic acid **726**: 7.36-7.32 (m, 2H, ArH), 7.17-7.12 (m, 2H, ArH), 6.71 (dd, J = 17.5, 10.5 Hz, 1H, CH), 5.71 (dd, J = 10.5, 1.0 Hz, 1H, CH), 5.20 (dd, J = 10.5, 1.0 Hz, 1H, CH), 2.66-2.60 (m, 2H, $ArCH_2$), 2.33-2.39 (m, 2H, $C\boldsymbol{H_2}CO_2H$), 1.66-1.71 (m, 4H, CH_2).

4-Chlorophenyl trifluoromethanesulfonate **729**

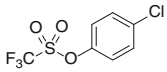

Prepared according to a literature procedure [48].

Trifluoromethanesulfonic anhydride (2.85 mL, 17 mmol) was added over 15 min to a stirred mixture of 4-chlorophenol (1.74 g, 13.5 mmol) and K_3PO_4 (8 g, 37.5 mmol) in toluene (22 mL) and water (25 mL) at 0 °C. The reaction was allowed to warm to room temperature over 1 h. The organic layer was separated and washed with water (2 × 20 mL), dried ($MgSO_4$), and concentrated in vacuo to give 4-chlorophenyl trifluoromethanesulfonate **729** as a pale yellow oil (3.39 g, 13 mmol, 96 %).

^{1}H NMR (400 MHz, $CDCl_3$) 7.47-7.41 (m, 2H, ArH), 7.27-7.21 (m, 2H, ArH). **^{13}C NMR** (101 MHz, $CDCl_3$) 147.9 (C), 134.3 (C), 130.4 (2 × CH), 122.7 (2 × CH), 118.7 (q, J = 321 Hz, CF_3). **^{19}F NMR** (376 MHz, $CDCl_3$) −72.7.

Data were in accordance with those previously reported [49].

4-Chloro-(2-methylpropyl)benzene **730**

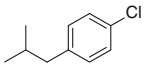

4-Chlorophenyl trifluoromethanesulfonate **729** (2.08 g, 8 mmol) was added to a solution of iron(III) acetylacetonate **133** (141 mg, 0.4 mmol) and *N*-methyl-2-pyrrolidinone **292** (0.77 mL, 8 mmol) in anhydrous tetrahydrofuran (15 mL) at room temperature. The reaction was cooled to 0 °C, and iso-butylmagnesium chloride (5.2 mL, 2 M in tetrahydrofuran, 10.4 mmol) was added over 30 min at 0 °C. The reaction was allowed to warm to room temperature over 30 min. Aqueous sulfate buffer solution (10 mL) was added and the aqueous phase was extracted with diethyl ether (3 × 30 mL). The combined organic phases were washed sequentially with water and brine, dried ($MgSO_4$), and concentrated in vacuo to give the crude reaction products, which were purified by flash silica chromatography (hexane) to give 4-chloro-(2-methylpropyl)-benzene **790** as a colourless oil (1.11 g, 6.58 mmol, 82 %).

Rf = 0.72 (hexane). **^{1}H NMR** (500 MHz, $CDCl_3$) 7.26-7.22 (m, 2H, ArH), 7.10-7.05 (m, 2H, ArH), 2.45 (d, J = 7.0 Hz, 2H, CH_2), 1.84 (app. non., J = 7.0 Hz, 1H, CH), 0.90 (d, J = 6.5 Hz, 6H, CH_3). **^{13}C NMR** (126 MHz, $CDCl_3$) 140.1 (C), 131.3 (C), 130.4 (2 × CH), 128.2 (2 × CH), 44.7 (CH_2), 30.2 (CH), 22.2 (2 × CH_3).

Data were in accordance with those previously reported [50].

Bis(1-phenylethyl)magnesium **733** and 1-phenylethylmagnesium bromide **734**

733 **734**

1:1 mixture of diastereoisomers

d_8-Tetrahydrofuran was distilled from sodium/benzophenone under reduced pressure.

Ethylmagnesium bromide **280** (0.5 mL, 1 M in THF, 0.5 mmol) was added to an oven-dried Schlenk flask under a nitrogen atmosphere. The solvent was removed under reduced pressure to give a colourless solid. d_8-Tetrahydrofuran (0.2 mL) was added under a nitrogen atmosphere, and then removed under reduced pressure. d_8-Tetrahydrofuran (1 mL) was added to fully dissolve the colourless solid. Styrene **53** (57 μL, 0.5 mmol), 2,6-bis-[1-(2,6-diisopropylphenylimino)ethyl]pyridine iron (II) chloride **743** (^{iPr}BIP) (2.5 mg, 0.004 mmol, 0.8 mol%) and d_8-tetrahydrofuran (1.5 mL) were added to an oven-dried Schlenk flask under a nitrogen atmosphere. Ethylmagnesium bromide **280** (0.5 mmol, 0.5 M in d_8-THF, 1 mL) was added and the reaction stirred for 2 h at room temperature. A 0.6 mL sample was removed and added to an oven-dried J. Young's NMR tube under a nitrogen atmosphere.

1,4-Dioxane·$MgBr_2$ precipitation: A sample of the above reaction mixture (1 mL, approx. 0.2 mmol) was removed and added to an oven-dried Schlenk flask under a nitrogen atmosphere. Anhydrous 1,4-dioxane (85 μL, 1 mmol) was added and stirred for 2 h, during which time a precipitate formed. The reaction was filtered through a Pasteur pipette plugged with a glass fibre paper into an oven-dried J. Young's NMR tube under a nitrogen atmosphere.

^{1}H, ^{13}C, COSY, HSQC and HMBC NMR spectra were recorded for characterisation of the organomagnesium reagents.

Bis(1-phenylethyl)magnesium **733** (1:1 mixture of diastereoisomers). **^{1}H NMR** (500 MHz, d_8-THF) 6.87-6.82 (m, 8H, Ar**H^e**), 6.79-6.76 (m, 8H, Ar**H^d**), 6.40-6.36 (m, 4H, Ar**H^f**), ~1.80-1.73 (obscured by d_8-THF signal, **CH^b**) 1.54 (d, J = 7.0 Hz, 6H, **H^a**), 1.53 (d, J = 7.0 Hz, 6H, **H^a**). **^{13}C NMR** (126 MHz, d_8-THF). 161.38 (2 × **C^c**), 161.35 (2 × **C^c**), 128.5 (8 × **CH^e**), 122.1 (8 × **CH^d**), 115.98 (2 × **CH^f**), 115.96 (2 × **CH^f**), 29.8 (2 × **CH^b**), 29.6 (2 × **CH^b**), 17.99 (2 × **CH$_3^a$**), 17.95 (2 × **CH$_3^a$**).

1-Phenylethylmagnesium bromide **734**. **^{1}H NMR** (500 MHz, d_8-THF) 6.89-6.84 (m, 2H, Ar**H^e**), 6.79-6.76 (m, 2H, Ar**H^d**), 6.40-6.36 (m, 1H, Ar**H^f**), ~1.75-1.68 (obscured by d_8-THF signal, **CH^b**) 1.52 (d, J = 7.0 Hz, 3H, **CH$_3^a$**). **^{13}C NMR**

(126 MHz, d_8-THF). 161.2 (**C**$^{\mathbf{c}}$), 128.3 (2 × **C**H$^{\mathbf{e}}$), 122.6 (2 × **C**H$^{\mathbf{d}}$), 116.5 (**C**H$^{\mathbf{f}}$), 30.1 (**C**H$^{\mathbf{b}}$), 17.6 (**C**H$_3^{\mathbf{a}}$).

^{1}H-^{1}H COSY NMR spectra of mixture of **733** and **734**

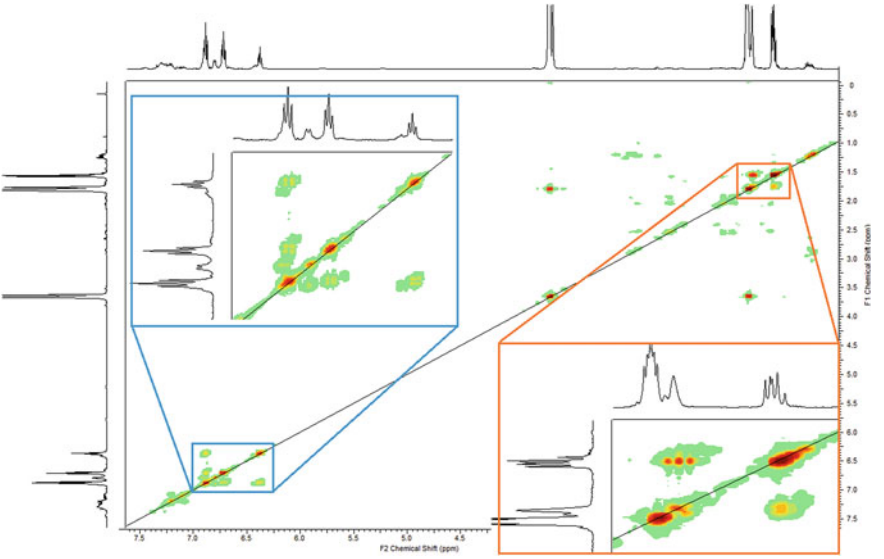

^{1}H-^{13}C HSQC NMR spectra of mixture of **733** and **734**

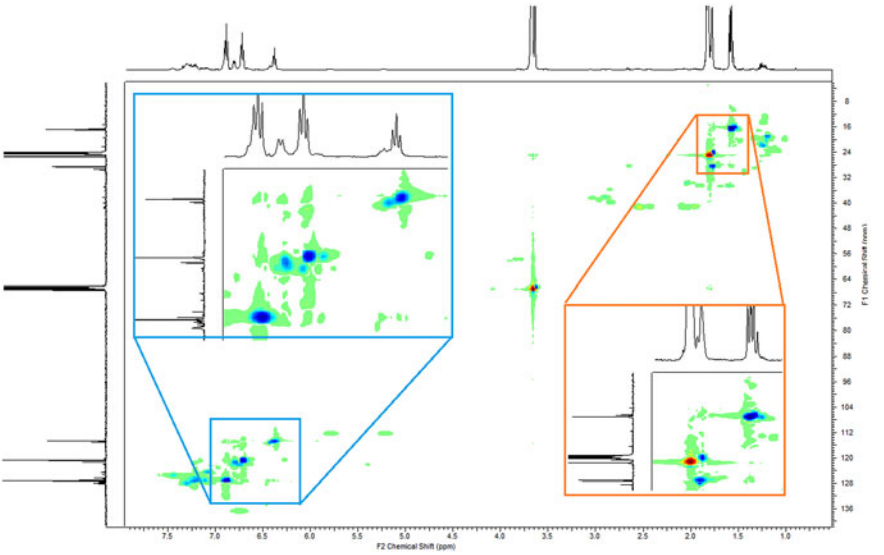

^{1}H-^{13}C HMBC NMR spectra of mixture of **733** and **734**

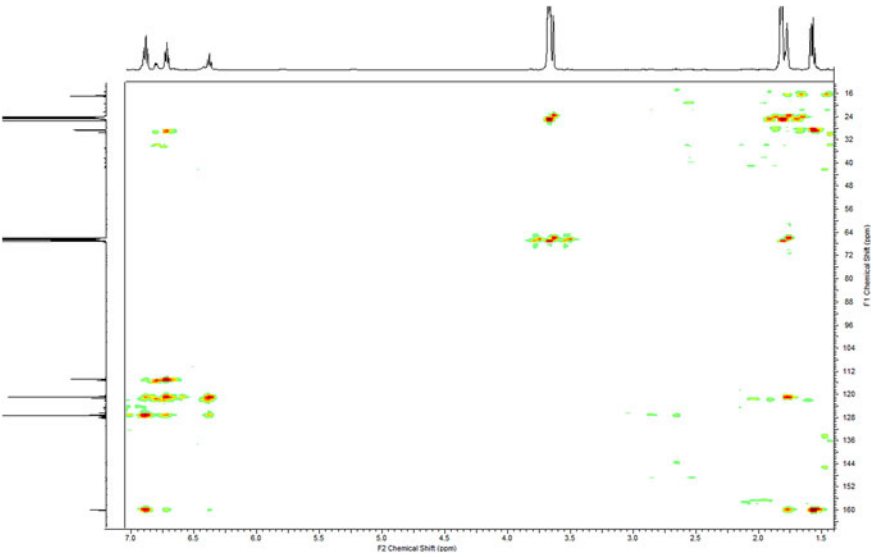

Variable Temperature NMR spectroscopy analysis

For determination of the effect of temperature on the position of the Schlenk equilibrium, ^{1}H and ^{13}C NMR spectra were recorded at 10 °C intervals from 5 to 55 °C. Insufficient baseline separation was observed in the proton spectra for quantitative analysis, so data from carbon spectra were used for estimation of K_{eq} at each temperature by integration of the corresponding peaks for 1-phenylethylmagnesium bromide **734** and bis(1-phenylethyl)magnesium **733**. Each signal corresponding to 1-phenylethylmagnesium bromide **734** was set to 1.00, and the integration value measured for bis(1-phenylethyl)magnesium **733** (both diastereoisomers) was halved (as signal represents twice as many carbons) to give an estimation of the ratio between the two species (except PhCH carbon, as only one of the two diastereoisomers was integrated, see below).

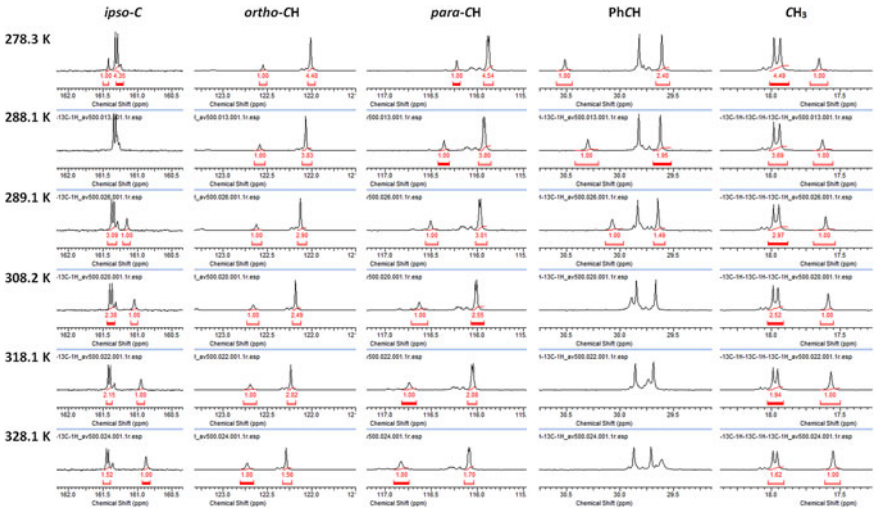

For the reaction:

$$MgBr_2\mathbf{732} + R_2Mg\mathbf{733} \rightleftharpoons 2 \times RMgBr\mathbf{734}$$

$$K_{eq} = [RMgBr\mathbf{734}]^2/[MgBr_2\mathbf{732}] \times [R_2Mg\mathbf{733}]$$

Assuming that $MgBr_2$ **732 =** R_2Mg **733**, gives: K_{eq} = [RMgBr **734**]^2/[R_2Mg **733**]^2

[RMgBr] **734** set as 1.00, therefore: K_{eq} = 1/[R_2Mg **733**]^2

From above raw data:

Temperature/K	**278.3**	**288.1**	**298.1**	**308.2**	**318.1**	**328.1**
733:734 ratio CH_3	2.245	1.845	1.485	1.26	0.97	0.81
733:734 ratio PhCH	2.40	1.95	1.49			
733:734 ratio *para-CH*	2.27	1.90	1.505	1.275	1.04	0.85
733:734 ratio *ortho-CH*	2.24	1.915	1.45	1.245	1.01	0.78
733:734 ratio *ipso-C*	2.175		1.545	1.19	1.075	0.76
Average **733:734** ratio	2.27	1.90	1.50	1.24	1.02	0.80
K_{eq}	0.19	0.28	0.44	0.65	0.96	1.56
ln(K_{eq})	−1.64	−1.28	−0.81	−0.43	−0.04	0.45
Stand. dev. of raw data	0.08	0.04	0.03	0.04	0.04	0.04
2SD of lnK (upper)	0.12	0.08	0.08	0.11	0.15	0.16
2SD of lnK (lower)	−0.18	−0.10	−0.11	−0.14	−0.21	−0.26

From van't hoff equation:
$\ln(K_{eq}) = -\Delta H/RT + \Delta S/R$
Plotting $\ln(K_{eq})$ against $10^3/T$ gives:

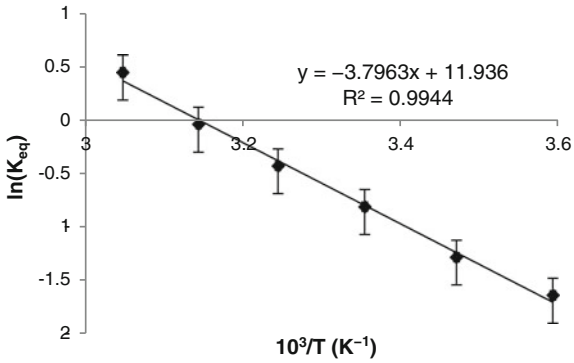

where the gradient = $-\Delta H/R$; and intercept = $\Delta S/R$.
Therefore,

$$\begin{aligned}\Delta H &= 3.7963 \times 10^3\,\mathrm{K}^{-1} \times 8.314\,\mathrm{J\,mol}^{-1}\,\mathrm{K}^{-1} \\ &= 31.56\,\mathrm{kJ\,mol}^{-1} \\ \Delta S &= 11.936 \times 10^{-3} \times 8.314\,\mathrm{J\,mol}^{-1}\,\mathrm{K}^{-1} \\ &= 0.0992\,\mathrm{kJ\,mol}^{-1}\,\mathrm{K}^{-1}\end{aligned}$$

Error estimated by plotting the two extreme values on the x-axis ± the error calculated from 2 standard deviations of the raw the data:

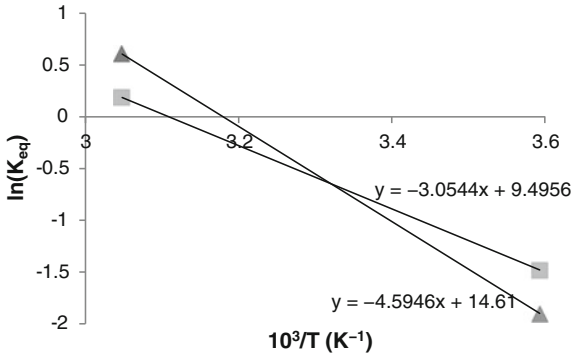

Therefore,

$$\Delta H_{max} = 4.5946 \times 8.314 = 38.20\,kJ\,mol^{-1} (6.64\ above\ average)$$
$$\Delta H_{min} = 3.0544 \times 8.314 = 25.39\,kJ\,mol^{-1} (6.17\ below\ average)$$
$$\Delta S_{max} = (14.61 \times 8.314)/1000 = 0.121\,kJ\,mol^{-1}\,K^{-1} (0.022\ above\ average)$$
$$\Delta S_{min} = (9.4956 \times 8.314)/1000 = 0.0789\,kJ\,mol^{-1}\,K^{-1} (0.020\ below\ average)$$

so, $\Delta H = 32 \pm 7$ kJ mol$^{-1;}$ and $\Delta S = 0.10 \pm 0.03$ kJ mol^{-1} K^{-1}.

2,6-Bis-[1-(2,6-diisopropylphenylimino)ethyl]pyridine iron(II) chloride **743** (^{iPr}BIPFeCl$_2$)

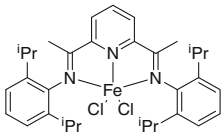

Prepared according to a literature procedure [4].

2,6-Bis-[1-(2,6-diisopropylphenylimino)ethyl]pyridine **273a** (1.01 g, 2.1 mmol) and iron(II) chloride **279** (265 mg, 2.1 mmol) were stirred in anhydrous tetrahydrofuran (40 mL) under a nitrogen atmosphere at room temperature for 6 h. The volume was reduced in vacuo to around 30 mL, and anhydrous diethyl ether (60 mL) was added and the resulting suspension stirred for 10 min. The reaction was filtered to give a blue solid, which was washed with diethyl ether (2 × 20 mL) and dried under high vacuum for 3 h. The complex was dissolved in anhydrous dichloromethane (30 mL) and filtered to remove unreacted iron(II) chloride. The solvent was removed in vacuo and the complex dried under high vacuum for 3 h at 120 °C, and a further 7 h at room temperature to give 2,6-bis-[1-(2,6-diisopropylphenylimino)ethyl]pyridine iron(II) chloride **743** (^{iPr}BIPFeCl$_2$) as a blue solid (1.18 g, 1.94 mmol, 92 %).

^{1}H NMR (500 MHz, CD_2Cl_2) 80.3 (3H), 14.8 (4H), −5.2 (12H), −6.1 (12H), −10.5 (2H), −21.9 (4H), −36.8 (6H).

Data were in accordance with those previously reported [4].

trans-1-Propenyl-2-vinylbenzene **(*E*)-752** and *cis*-1-propenyl-2-vinylbenzene **(*Z*)-752**

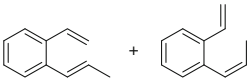

According to general procedure **E**, 2-allylstyrene **323** (101 mg, 0.7 mmol), iron(II) chloride **279** (0.9 mg, 0.007 mmol), 2,6-bis-[1-(2,6-diisopropylphenylimino)ethyl]

pyridine **273a** (3.4 mg, 0.007 mmol), ethylmagnesium bromide **280** (3 M in Et_2O, 0.3 mL, 0.9 mmol) and carbon dioxide were reacted in anhydrous tetrahydrofuran to give the crude reaction products, which were analysed by quantitative ^{1}H NMR spectroscopy, using 1,3,5-trimethoxystrene as an internal standard.

trans-1-Propenyl-2-vinylbenzene **(*E*)-752**: **^{1}H NMR** (500 MHz, $CDCl_3$) 7.56-7.11 (m, 4H, ArH), 7.02 (dd, *J* = 17.5, 11.0 Hz, 1H, CH), 6.67 (dq, *J* = 15.5, 1.5 Hz, 1H, CH), 6.08 (dq, *J* = 15.5, 6.5 Hz, 1H, CH), 5.61 (dd, *J* = 17.5, 1.5 Hz, 1H, CH), 5.30 (dd, *J* = 11.0, 1.5 Hz, 1H, CH), 1.91 (dd, *J* = 6.5, 1.5 Hz, 3H, CH_3).

Data were in accordance with those previously reported [51].

cis-1-Propenyl-2-vinylbenzene **(*Z*)-752**: **^{1}H NMR** (500 MHz, $CDCl_3$) 7.56-7.11 (m, 4H, ArH), 6.89 (dd, *J* = 17.5, 11.0 Hz, 1H, CH), 6.53 (dq, *J* = 11.5, 1.5 Hz, 1H, CH), 5.86 (dq, *J* = 11.5, 7.0 Hz, 1H, CH), 5.67 (dd, *J* = 17.5, 1.5 Hz, 1H, CH), 5.26 (dd, *J* = 11.0, 1.5 Hz, 1H, CH), 1.69 (dd, *J* = 7.0, 1.5 Hz, 3H, CH_3).

Data were in accordance with those previously reported [52].

Benzaldehyde-functionalised polystyrene resin **754**

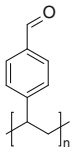

Prepared according to a literature procedure [53].

Merrifield's resin **753** (100–200 mesh, 2 mmol g^{-1}, 10 g, 20 mmol) and sodium hydrogen carbonate (9.5 g, 113 mmol) were added to dimethyl sulfoxide (120 mL) and heated at 160 °C for 6 h. The reaction was cooled and filtered. The resin was washed sequentially with dimethyl sulfoxide (2 × 30 mL), hot water (2 × 30 mL), THF:water (2:1, 2 × 30 mL), THF (2 × 30 mL), acetone (2 × 30 mL), ethanol (2 × 30 mL) and dichloromethane (2 × 30 mL). The benzaldehyde-functionalised polystyrene resin **754** was dried under high vacuum at 100 °C for 1 h, and then at 50 °C for 16 h.

HRMAS ^{1}H NMR (600 MHz, $CDCl_3$) 9.99 (br., 1H, CHO), 7.84-7.42 (br., 2H, ArH), 7.43-6.29 (br., 24H, ArH), (3.69, 0.16H), 2.44-1.06 (br., 11H). **IR** (neat) ν_{max} cm^{-1} 3024, 2922, 1699, 1603, 1493, 1452, 1211, 1167, 826, 758, 696.

Vinyl-functionalised polystyrene resin **756**

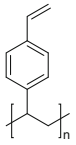

Prepared according to a literature procedure [54].

Phenyllithium **438** (2 mL, 1.8 M in Bu_2O, 3.6 mmol) was added to a suspension of methyltriphenylphosphonium bromide **335** (1.29 g, 3.6 mmol) in anhydrous tetrahydrofuran (70 mL) at room temperature under a nitrogen atmosphere, and the reaction stirred for 1 h. The resulting yellow solution was added to a suspension of benzaldehyde-functionalised polystyrene resin **754** (1 g, <2 mmol) in tetrahydrofuran (70 mL) over 30 min. The reaction was then heated at reflux for 6 h. The reaction was cooled, potassium *tert*-butoxide **755** (3.37 g, 30 mmol) was added, and the reaction heated at reflux for 14 h. The reaction was cooled, water (5 mL) was added and the reaction was filtered. The vinyl-functionalised polystyrene resin **756** was washed sequentially with THF (2 × 10 mL), water (2 × 10 mL), methanol (2 × 10 mL), dichloromethane (2 × 10 mL) and methanol (2 × 10 mL). The resin was dried under high vacuum at 50 °C for 10 h.

HRMAS ^{1}H NMR (600 MHz, $CDCl_3$) 7.53-6.30 (br., 32H, ArH), 5.79 (br., 1H, CH), 5.30 (br., 1H, CH), (3.71, 0.21H), 2.42-1.05 (br., 14H). **IR** (neat) ν_{max} cm^{-1} 3024, 2920, 2845, 1601, 1512, 1493, 1450, 1028, 988, 903, 837, 756, 696.

5,6,11,12-Tetrahydrodibenzo[a,e]cyclooctene **758**

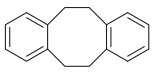

Prepared according to a literature procedure [55].

α,α′-Dibromo-*o*-xylene **757** was sublimed under vacuum prior to use to give a colourless crystalline solid. α,α′-Dibromo-*o*-xylene **757** (10.6 g, 40 mmol) in anhydrous tetrahydrofuran (16 mL) was added over 90 min to a suspension of granular lithium (700 mg, 100 mmol) in anhydrous tetrahydrofuran (25 mL). The reaction was heated for an additional 2 h at reflux. The reaction was cooled, filtered and concentrated in vacuo. Dichloromethane (70 mL) was added to the residue and stirred for 2 min. The suspension was filtered through a plug of silica, which washed subsequently washed with dichloromethane (2 × 70 mL). The filtrate was dried ($MgSO_4$) and concentrated in vacuo to give a pale yellow solid, which was purified by flash silica chromatography (pet. ether) to give 5,6,11,12-tetrahydrodibenzo[a,e]cyclooctene **758** as colourless plates (1.99 g, 9.55 mmol, 48 %).

$\mathbf{R_f}$ = 0.18 (pet. ether). **m.p.** 118–119 °C. **^{1}H NMR** (500 MHz, $CDCl_3$) 7.04-6.98 (m, 8H, ArH), 3.08 (s, 8H, CH_2). **^{13}C NMR** (126 MHz, $CDCl_3$) 140.6 (4 × C), 129.7 (4 × CH), 126.1 (4 × CH), 35.2 (4 × CH_2).

Data were in accordance with those previously reported [55].

5,11-Dibromo-5,6,11,12-tetrahydrodibenzo[a,e]cyclooctene **760**

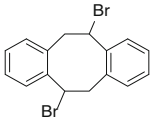

N-Bromosuccinimide **759** (2.30 g, 12.9 mmol) was added to a solution of 5,6,11,12-tetrahydrodibenzo[a,e]cyclooctene **760** (1.25 g, 6 mmol) in tetrachloromethane (13 mL) under a nitrogen atmosphere. The reaction was heated at reflux for 2 h. The hot reaction mixture was filtered through a sinter, which was washed with tetrachloromethane (10 mL). The solvent was removed in vacuo and the yellow residue washed on a sinter using water (2 × 20 mL), and dried under high vacuum. The crude product (2 g) was determined to be approximately 95 % pure by ^{1}H NMR spectroscopy, and was used without further purification.

^{1}H NMR (500 MHz, $CDCl_3$) 7.14 (td, *J* = 7.5, 1.5 Hz, 2H, ArH), 7.09 (dd, *J* = 7.5, 1.5 Hz, 2H, ArH), 7.05 (td, *J* = 7.5, 1.5 Hz, 2H, ArH), 6.99 (dd, *J* = 7.5, 1.5 Hz, 2H, ArH), 5.35 (dd, *J* = 11.0, 8.5 Hz, 2H, CHBr), 4.30 (dd, *J* = 14.0, 11.0 Hz, 2H, CH_2), 3.67 (dd, *J* = 14.0, 8.5 Hz, 2H, CH_2). **^{13}C NMR** (126 MHz, $CDCl_3$) 138.4 (2 × C), 136.4 (2 × C), 131.0 (2 × CH), 130.8 (2 × CH), 129.1 (2 × CH), 127.9 (2 × CH), 53.0 (2 × CHBr), 43.7 (2 × CH_2).

Data were in accordance with those previously reported [55].

Dibenzo[a,e]cyclooctene **761**

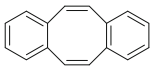

5,11-Dibromo-5,6,11,12-tetrahydrodibenzo[a,e]cyclooctene **760** (2 g, ~5.1 mmol) in anhydrous tetrahydrofuran (10 mL) was added over 13 min to a solution of potassium *tert*-butoxide **755** (2.45 g, 21.6 mmol) in anhydrous tetrahydrofuran (8 mL) at 0 °C, under a nitrogen atmosphere. The reaction was allowed to warm to room temperature and was stirred for an additional 2 h. Water (1 mL) was added and the mixture filtered through a silica plug (wetted with diethyl ether), and washed with diethyl ether (2 × 30 mL). The organic phase was dried ($MgSO_4$) and concentrated in vacuo to give a brown solid, which was purified by flash silica chromatography (pet. ether) to give dibenzo[a,e]cyclooctene **761** as colourless plates (701 mg, 3.43 mmol, 67 %).

R_f = 0.20 (pet. ether). **m.p.** 115–117 °C. **^{1}H NMR** (500 MHz, $CDCl_3$) 7.19-7.14 (m, 4H, ArH), 7.09-7.05 (m, 4H, ArH), 6.77 (s, 4H, CH). **^{13}C NMR** (126 MHz, $CDCl_3$) 137.1 (4 × C), 133.2 (4 × CH), 129.1 (4 × CH), 126.8 (4 × CH).

Data were in accordance with those previously reported [55].

Aldehyde-functionalised polystyrene resin **763**

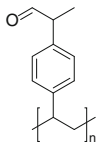

Ethylmagnesium bromide **280** (0.17 mL, 3 M in Et_2O, 0.5 mmol) was added to a suspension of vinyl-functionalised polystyrene resin **756** (100 mg, pot. 0.2 mmol), *tert*-butylstyrene **764** (37 μL, 0.2 mmol), iron(II) chloride **279** (1.3 mg, 0.01 mmol) and 2,6-bis-[1-(2,6-diisoprpylphenylimino)ethyl]pyridine **273a** (4.9 mg, 0.01 mmol) in anhydrous tetrahydrofuran (1 mL) at room temperature and under a nitrogen atmosphere. The reaction was stirred at room temperature for 2 h. *N*,*N*-dimethylformamide **744** (0.15 mL, 2 mmol) was added and the reaction stirred for 30 min. Aqueous sulphate buffer solution (10 mL) was added, followed by diethyl ether (20 mL). The reaction was filtered and the resulting resin washed with water (2 × 10 mL), THF (10 mL), and diethyl ether (2 × 10 mL). The organic phase of the filtrate was separated, and the aqueous phase extracted with diethyl ether (2 × 30 mL). The combined organic extracts were washed sequentially with water and brine, dried ($MgSO_4$) and concentrated in vacuo to give the crude reaction products (solution phase). Trimethoxybenzene (23.5 mg, 0.14 mmol) was added as an internal standard, and a yield for the (solution phase) reaction determined by ^{1}H NMR spectroscopy.

The resin was washed sequentially with THF (2 × 10 mL) and dichloromethane (2 × 10 mL) and dried under high vacuum at 50 °C for 10 h.

HRMAS ^{1}H NMR (600 MHz, $CDCl_3$) 9.69 (br., 1H, CHO), 7.48-6.24 (br., 39H, ArH), 3.65 (br., 1H, ArCH), 2.35-1.06 (br., 21H). **IR** (neat) ν_{max} cm^{-1} 3024, 2922, 2855, 1721, 1601, 1493, 1452, 1261, 1099, 1016, 908, 758, 731, 696.

3-(4-methoxyphenyl)propylmagnesium bromide **765**

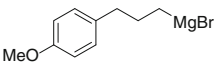

1-(3-Bromopropyl)-4-methoxybenzene (5.45 g, 23.8 mmol) was 'freeze-pump-thaw degassed' three times to remove any dissolved oxygen from the substrate. Magnesium turnings (750 mg, 30.9 mmol) were added to an oven-dried multi-necked round-bottomed flask with a reflux condenser attached, under a nitrogen atmosphere. Anhydrous diethyl ether (24 mL) was added, followed by approximately 10 % of the 'freeze-pump-thaw degassed' 1-(3-bromopropyl)-4-methoxybenzene (approx. 0.5 g, 0.4 mL, 2.2 mmol). The reaction was stirred at room temperature, however the reaction temperature did not increase, therefore a small crystal of iodine was added. Upon gently heating the reaction, the brown colouration of iodine disappeared and the reaction temperature began to increase. The remaining 1-(3-bromopropyl)-4-methoxybenzene was added over 30 min at a rate to maintain reflux. The solution was heated at 35 °C for a further 45 min, before being allowed to cool and settle. The prepared Grignard reagent, 3-(4-methoxyphenyl)propylmagnesium bromide **765**, was transferred by syringe to an oven-dried J. Young's sample flask. The concentration of 3-(4-methoxyphenyl) propylmagnesium bromide **765** was determined to be 0.7 M by titration using 2-hydroxybenzaldehyde phenylhydrazone.

Diethyltetramethyldisiloxane **776**

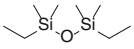

Tetramethyldivinyldisiloxane **775** (161 μL, 0.7 mmol) was added to a solution of iron(II) chloride **279** (0.9 mg, 0.007 mmol), 2,6-bis-[1-(2,6-diisoprpylphenylimino) ethyl]pyridine **273a** (3.4 mg, 0.007 mmol) and 1,3,5-trimethoxybenzene (23.5 mg, 0.14 mmol) in anhydrous tetrahydrofuran (5 mL) at room temperature and under a nitrogen atmosphere. Ethylmagnesium bromide **280** (0.3 mL, 3 M in Et_2O, 0.9 mmol) was added in one portion and the reaction was stirred for 15 min. Methanol was added, followed by aqueous sulphate buffer solution (10 mL). The aqueous phase was extracted with diethyl ether (3 × 20 mL), and the combined organic extracts were washed sequentially with water and brine, dried ($MgSO_4$) and concentrated in vacuo to give the crude reaction products. Based upon quantitative ^{1}H NMR spectroscopy, complete conversion of the starting material had occurred to give diethyltetramethyldisiloxane **776** in 83 % yield.

^{1}H NMR (500 MHz, $CDCl_3$) 0.92 (t, J = 8.0 Hz, 6H, $CH_2C\boldsymbol{H_3}$), 0.49 (q, J = 8.0 Hz, 4H, $SiCH_2$), 0.04 (s, 12H, $SiCH_3$).

Data were in accordance with those previously reported [56].

5.4 Procedures and Data for Tables and Figures

Oxidation state of iron catalyst (Hydrosilylation) (Table 2.9)

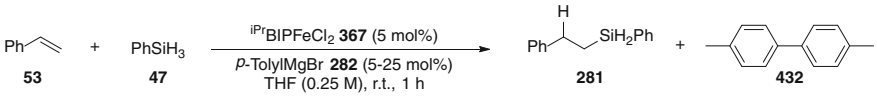

Styrene (80 μL, 0.7 mmol) (0.7 mmol) was added to a solution of 2,6-bis-[1-(2,6-diethylphenylimino)ethyl]pyridine iron(II) chloride **367** (^{Et}BIPFeCl$_2$) (19.3 mg, 0.035 mmol, 5 mol%), in anhydrous tetrahydrofuran (3 mL) at room temperature under an atmosphere of nitrogen. Tolylmagnesium bromide **282** (0.035–0.175 mL, 1 M in THF, 0.035–0.175 mmol) was added, followed by phenylsilane **47** (95 μL, 0.77 mmol) and the reaction was stirred at room temperature for 1 h. Aqueous sulfate buffer (10 mL) was added and the aqueous phase extracted with diethyl ether (3 × 20 mL). The combined organic extracts were washed with water and brine, dried ($MgSO_4$) and concentrated in vacuo. Trimethoxybenzene (23.5 mg, 0.14 mmol) was added as an internal standard, and a yield for each product was determined by ^{1}H NMR spectroscopy.

Known compounds were identified by ^{1}H NMR spectroscopy, and characterised by comparison with authentic samples of spectral data.

Oxidation state of iron catalyst (Hydroboration) (Table 3.8)

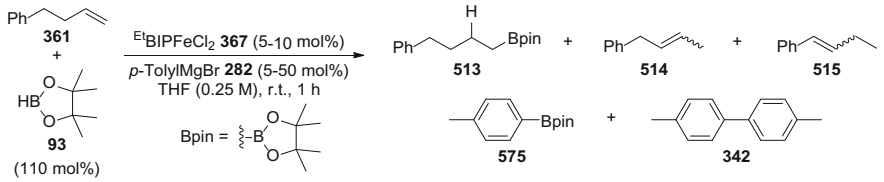

4-Phenylbutene (105 μL, 0.7 mmol) (0.7 mmol) was added to a solution of 2,6-bis-[1-(2,6-diethylphenylimino)ethyl]pyridine iron(II) chloride **367** (^{Et}BIPFeCl$_2$) (19.3–38.7 mg, 0.035–0.07 mmol, 5–10 mol%), in anhydrous tetrahydrofuran (3 mL) at room temperature under an atmosphere of nitrogen. Tolylmagnesium bromide **282** (0.035–0.35 mL, 1 M in THF, 0.035–0.35 mmol, 5–50 mol%) was added, followed by pinacol borane **93** (110 μL, 0.77 mmol) and the reaction was stirred at room temperature for 1 h. Aqueous sulfate buffer (10 mL) was added and the aqueous phase extracted with diethyl ether (3 × 20 mL). The combined organic extracts were washed with water and brine, dried ($MgSO_4$) and concentrated in vacuo. Trimethoxybenzene (23.5 mg, 0.14 mmol) was added as an internal standard, and a yield for each product was determined by ^{1}H NMR spectroscopy.

Known compounds were identified by ^{1}H NMR spectroscopy, and characterised by comparison with authentic samples of spectral data.

Hydromagnesiation of 2-methoxystyrene using different alkyl Grignard reagents (Table 4.6)

2-Methoxystyrene **675** (47 μL, 0.35 mmol) was added to a solution of 2,6-bis-[1-(2,6-diisopropylphenylimino)ethyl]pyridine iron(II) chloride **743** (^{iPr}BIPFeCl$_2$) (0.25 mL, 0.0014 M in THF, 0.00035 mmol, 0.1 mol%) and 1,3,5-trimethoxybenzene (11.8 mg, 0.07 mmol, 20 mol%) in anhydrous tetrahydrofuran (total volume 2 mL after addition of Grignard reagent). A Grignard reagent (0.52 mmol, 150 mol%) was added in one portion, and the reaction was stirred at room temperature (20–22 °C). Aliquots (<100 μL) were periodically removed and added to HPLC vials containing anhydrous *N*,*N*-dimethylformamide **744** (approx. 10 μL, 0.13 mmol). The samples were shaken for 30 min, after which aqueous sulfate buffer (approx. 0.3 mL) was added to each vial followed by diethyl ether (approx. 0.7 mL). The vial was shaken and the layers were allowed to settle. The diethyl ether layer was removed and added to a 7 mL glass vial, from which the diethyl ether was allowed to evaporate at room temperature (approx. 10–15 min) until the majority of the solvent had evaporated. The residue was dissolved in $CDCl_3$ and added to an NMR tube for analysis by ^{1}H NMR spectroscopy.

The percentage yield of each product was determined by quantitative ^{1}H NMR spectroscopy, using 1,3,5-trimethoxybenzene (20 mol%) as an internal standard. All products were identified by comparison to previously reported data: 2-(2-methoxyphenyl)-propanal **α-745** [57], 3-(2-methoxyphenyl)-propanal **β-745** [58].

Empty cells indicate that data was not collected.

Time	EtMgBr			DecMgBr		
	α-745	**β-745**	α:β ratio	**α-745**	**β-745**	α:β ratio
0.5	0.3			0.1		
1	7.1			3.2		
1.33	19.9					
1.5				6.8		
1.66	27.1					
2	32.6	0.4	82:1	10.1		
2.5	39	0.5	78:1	11.6		
3.5	46.9	0.5	94:1	15.7	0.5	31:1
5	54.6	0.6	91:1	19.2	0.5	38:1
6	59.8	0.7	85:1			
7				24.6	0.6	41:1
10	70	0.8	88:1	30.1	0.8	38:1
15	81.2	0.8	102:1			
20				42.3	1.1	38:1
30	92.9	1	93:1	47.8	1.1	43:1
60	98	1	98:1	60.3	1.3	46:1
90	98.9	1	99:1	69.3	1.3	53:1
120				74.1	1.3	57:1
150						
180	98.6	1	99:1	78.1	1.3	60:1
Time	3-(4-Methoxyphenyl) propylmagnesium bromide			^{i}BuMgBr (1 mol% ^{iPr}BIPFeCl$_2$)		
	α-745	**β-745**	α:β ratio	**α-745**	**β-745**	α:β ratio
0.5						
1	5.3					
1.33						
1.5	8.6					
1.66						
2	10.9	0.3	36:1			
2.5	12.9	0.3	43:1	0.7		
3.5	16.7	0.4	42:1			
5	20.5	0.45	46:1	1.9		
6						
7	24	0.45	53:1			
10	27.2	0.5	54:1	3.4		
15	34.3	0.6	57:1			
20	38.1	0.7	56:1			
30	45.9	0.9	51:1	7.5	0.5	15:1
60						
90	69.7	1	70:1	14.5	0.9	16:1

(continued)

(continued)

Time	3-(4-Methoxyphenyl) propylmagnesium bromide			^{i}BuMgBr (1 mol% ^{iPr}BIPFeCl$_2$)		
	α-745	**β-745**	α:β ratio	**α-745**	**β-745**	α:β ratio
120						
150						
180	75.1	0.92	82:1	23.4	1.1	21:1
Time	CyclopentylMgBr			^{i}PrMgBr		
	α-745	**β-745**	α:β ratio	**α-745**	**β-745**	α:β ratio
0.5	2.4					
1	4.8	0.5	10:1			
1.33						
1.5	6.6	0.6	11:1	1.8		
1.66						
2	8.8	0.8	11:1			
2.5	10.2	0.9	11:1	2.7		
3.5	12.2	1.1	11:1	3.7		
5	14.8	1.3	11:1	4.9		
6						
7	18.4	1.5	12:1	6.8	0.7	10:1
10	22.9	2	11:1	8.2	0.7	12:1
15						
20	32.9	2.6	13:1	13.6	1.2	11:1
30	39.8	3.2	12:1	19.5	1.2	16:1
60	57.2	4.8	12:1	32	2.1	15:1
90	70.2	4.9	14:1	42.8	2.4	18:1
120	78.3	5.4	15:1	52.6	2.5	21:1
150				58.4	2.8	21:1
180	84.7	5.3	16:1	62.1	2.8	22:1
Time	^{t}BuMgCl (1 mol% ^{iPr}BIPFeCl$_2$)			(2-Phenylethyl)magnesium bromide		
	α-745	**β-745**	α:β ratio	**α-745**	**β-745**	α:β ratio
0.5						
1						
1.33						
1.5				0.3		
1.66						
2				2.8	0.7	4:1
2.5				11.2	3.6	3:1
3.5				23.8	4.7	5:1
5				35.8	6.4	6:1
6						
7				41.1	6.9	6:1

(continued)

(continued)

Time	^{t}BuMgCl (1 mol% ^{iPr}BIPFeCl$_2$)			(2-Phenylethyl)magnesium bromide		
	α-745	**β-745**	α:β ratio	**α-745**	**β-745**	α:β ratio
10	0.9			46.2	9.8	5:1
15						
20				60.1	9.7	6:1
30	1.5			69.1	10.2	7:1
60				79	10.5	8:1
90	2.8			81.3	10.4	8:1
120				81.9	9.7	8:1
150						
180	4.3			82	8.3	10:1

Procedure and product analysis for the hydromagnesiation of 2-methoxystyrene using either d_5-EtMgBr or d_7-^{i}PrMgBr (Figs. 4.6 and 4.7)
2-Methoxystyrene **675** (94 μL, 0.7 mmol) was added to a solution of 2,6-bis-[1-(2,6-diisopropylphenylimino)ethyl]pyridine iron(II) chloride **743** (4.3 mg, 0.007 mmol, 1 mol%) and 1,3,5-trimethoxybenzene (23.5 mg, 0.14 mmol, 20 mol %) in anhydrous tetrahydrofuran (total volume 4 mL after addition of Grignard reagent). A deuterium-labelled Grignard reagent (1.05 mmol, 150 mol%) was added in one portion, and the reaction was stirred at room temperature (20–22 °C). Aliquots (2 sets, 100 μL each) were periodically removed and added to HPLC vials containing anhydrous *N*,*N*-dimethylformamide (approx. 10 μL, 0.13 mmol), and the samples shaken for 30 min.

Aqueous sulfate buffer (approx. 0.3 mL per vial) was added to one set of vials followed by diethyl ether (approx. 0.7 mL). The vial was shaken and the layers were allowed to settle. The diethyl ether layer was removed and added to a 7 mL glass vial, from which the diethyl ether was allowed to evaporate at room temperature (approx. 10–15 min) until the majority of the solvent had evaporated. The residue was dissolved in $CDCl_3$ and added to an NMR tube for analysis by ^{1}H and ^{13}C NMR spectroscopy.

The second (identical) set of sample vials were processed for analysis by ^{2}H NMR spectroscopy. Aqueous sulfate buffer (approx. 0.3 mL) was added to each vial followed by CH_2Cl_2 (approx. 0.7 mL). The vial was shaken and the layers were allowed to settle. The CH_2Cl_2 layer was removed and added to an NMR tube for analysis by ^{2}H NMR spectroscopy.

The percentage yield of each product was calculated using ^{13}C, ^{2}H and quantitative ^{1}H NMR spectroscopy, using 1,3,5-trimethoxybenzene (20 mol%) as an internal standard (see below for sample analysis). All products were identified by comparison to previously reported data: 2-(2-methoxyphenyl)-propanal **α-745** [57].

See below for data tables and example (d_5-EtMgBr, 5 min) of raw data analysis and method for calculating %yields.

Time	Products						Substrate/intermediate						
						% Yield total					%Total styrene deriv.	Total %D incorporated	Mass balance
d_5-EtMgBr													
0	0	0	0	0	0	0	100	0	0	0	100	0	100
0.5	5.3	29.6	5.3	0	0	40.2	36	15.6	1.2	0	52.8	58.2	93
1	7.1	36.3	7.8	0	0	51.2	26	15.6	2.2	0	43.8	71.9	95
2	8.5	45.7	11	0	0	65.2	14	12.4	4.2	0	30.6	88.5	95.8
3	8.5	47	15.3	3.4	0	74.2	8	9.6	4.2	0	21.8	105.8	96
5	8.3	49.8	19.9	4.2	0.4	82.2	4	6	3.6	0	13.6	115.8	95.8
7	9.1	49.5	22.7	6.3	1.1	87.6	1.5	3.6	3.5	0	8.6	125.5	96.2
15	9.1	50.3	25.6	11	1.8	96	0.5	0.4	1	0	1.9	138.7	97.9
d_7-^{i}PrMgBr													
0	0	0	0	0	0	0	100	0	0	0	100	0	100
1	11.3	4.3	0.6	0	0	16.2	64	13	0	0.6	77–77.6	19.1	93.2–93.8
2.5	19.4	10.7	2.7	0.6	0.9	33.4	35	18.4	3	2	56.4–58.4	45.2	89.8–91.8
5	26.3	17.6	5.5	1.3	1.6	50.7	19	15.6	6	2.6	40.6–43.2	64.3	91.3–93.9
10	31	23.5	9.6	3.1	2.6	67.2	7	10	8	2.6	25–27.6	83.2	92.2–94.8
20	32.7	29.3	14.5	4.6	4.3	81.1	2	4.8	4	2.1	10.8–12.9	91.3	91.9–94.0
60	33.6	31.3	17.9	5.7	6.9	88.5	0.5	0.4	3	1	3.9–4.9	98.5	92.4–93.4

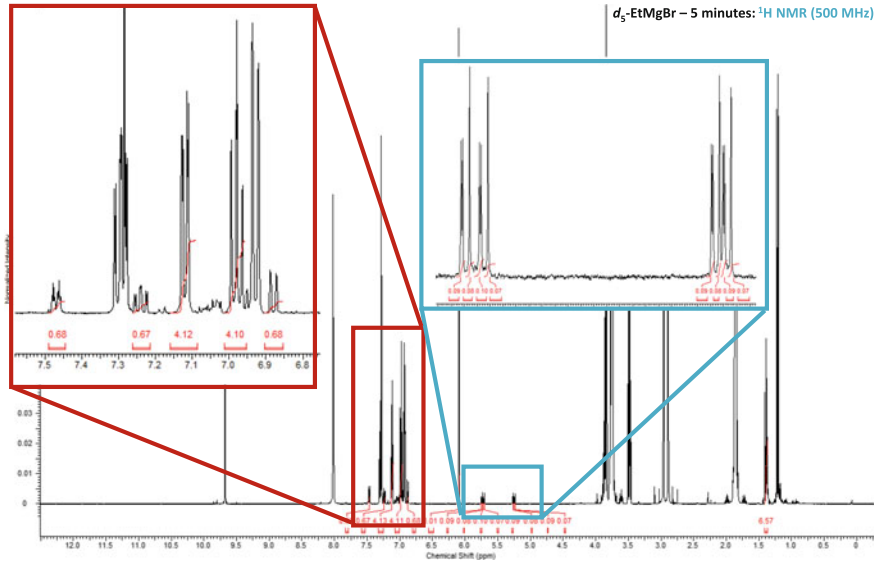
d_5-EtMgBr – 5 minutes: ^{1}H NMR (500 MHz)
0.68
0.67
4.12
4.10
0.68
6.57
Chemical Shift (ppm)

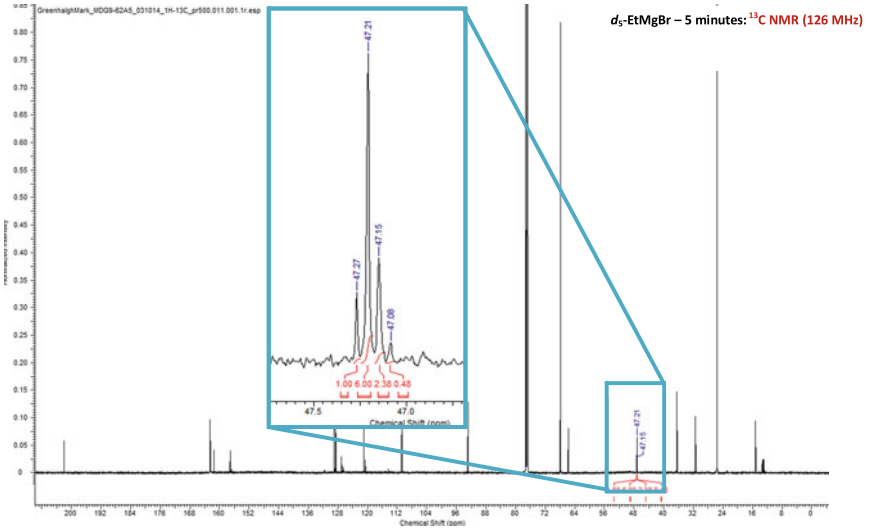
d_5-EtMgBr – 5 minutes: ^{13}C NMR (126 MHz)
47.21
47.15
47.27
47.09
1.00 6.00 2.38 0.48
Chemical Shift (ppm)

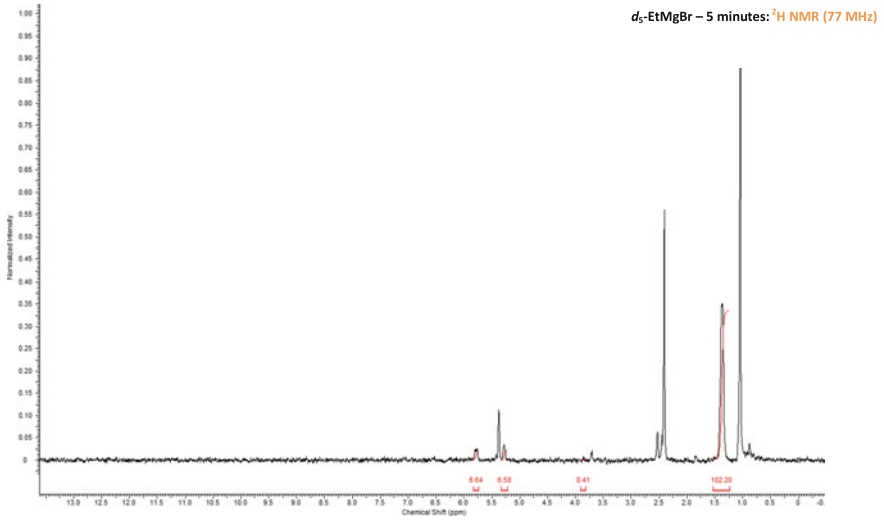

Data analysis example: d5-EtMgBr (5 minutes)

	Products						Substrate/Intermediate						
Time	CHO Ar^1 CH$_3$	CHO Ar^1 CH$_2$D	CHO Ar^1 CHD$_2$	CHO Ar^1 CD$_3$	OHC D Ar^1 Me	%Yield total	Ar^1	Ar^1 CHD	Ar^1 CD$_2$	D Ar^1	% Total Styrene deriv.	Total %D incorporated	Mass Balance
5	8.3	49.8	19.9	4.2	0.4	82.2	4	6	3.6	0	13.6	115.8	95.8

Colour coding in tables corresponds to where the calculated values are found in the text

^{1}H NMR spectra

Trimethoxybenzene (20 mol%) signal at 6.1 ppm integrated as 3H, therefore percentage of any product = (integration of signal/number of protons represented by signal) × 20

Yield of combined α-aryl aldehyde products based upon integration of aromatic peaks at 7.14-7.10 ppm (m, 1H) and 7.00-6.96 ppm (m, 1H). Integrate as 4.12H and 4.10H respectively, average therefore = 4.11, and gives a total yield of **82.2%** [(4.11/1) × 20].

Yield of Styrene products: Styrene proton signals (5.74 ppm, dd, J = 1.5, 17.5 Hz, 1H; 5.26, dd, J = 1.5, 11.0 Hz, 1H) integrate as 0.18–0.19 H, therefore yield of **3.6-3.8%** [(0.18–0.19/1) × 20]. *trans*-β-deuteriostyrene signal (5.72 ppm, d, J = 17.5 Hz, 1H) integrates as 0.15, therefore yield of **3%** [(0.15/1) × 20]. *cis*-β-deuteriostyrene signal (5.25 ppm, d, J = 11.0 Hz, 1H) integrates as 0.15, therefore yield of **3%** [(0.15/1) × 20]. Aromatic peaks for styrene at 7.49-7.45 ppm (m, 1H), 7.27-7.21 ppm (m, 1H) and 6.90-6.86 (m, 1H)

each integrate as 0.68, therefore yield of **13.6%** [(0.68/1) × 20]. Only 10 % styrene derivatives accounted for by protons signals in β-position, therefore presence of another styrene derivative (**3.6%**) with no protons in β-position indicated ($ArCH{=}CD_2$—see 2D NMR spectra analysis below for further support for this product)

^{13}C NMR spectra

Four signals between 47.3 and 47.1 ppm correspond to α-aryl carbon of 2-(2-methoxyphenyl)-propanal with 0, 1, 2 and 3 deuterium in β-position.

Compound				
Chemical shift of α-aryl carbon (ppm)	47.27	47.21	47.15	47.08
Ratio from ^{13}C NMR spectra	1	6.0	2.4	0.5
% Yield based upon 82.2% overall yield (from **^{1}H NMR spectra**)	**8.3%**	**49.8%**	**19.9%**	**4.2%**

Total %D incorporation in β-position = (8.3 × 0) + (49.8 × 1) + (19.9 × 2) + (4.2 × 3) = **102.2% D**

^{2}H NMR spectra

From **^{13}C NMR spectra** 102.2 % D incorporation in β-position of 2-(2-methoxyphenyl)-propanal. Signal for these compounds at 1.40-1.23 ppm in **^{2}H NMR spectra** therefore integrated as 102.2. Signals arising from deuterium in the β-position of styrene derivatives at 5.77-5.67 ppm and 5.26-5.18 ppm integrate as 6.6. Indicates 6.6 % deuterium in each position. Consistent with data obtained from **^{1}H NMR spectra** – **3%** of each *cis*- and *trans*-β-deuteriostyrene, and **3.6%** of a styrene derivative with two deuterium in the β-position ($ArCH{=}CD_2$). No signal at 7.05-6.95 indicates no styrene derivative with deuterium in the α-position. Small signal at 3.80 ppm assigned as 2-(2-methoxyphenyl)-propanal with deuterium in the α-position. Integration indicates **0.4%** of this product.

Calculation of total %D incorporation:
Sum of all deuterium-containing products (including styrene derivatives):

Comp							Total %D
% Yield	**49.8**	**19.9**	**4.2**	**0.4**	**6**	**3.6**	
% D	49.8	39.8	12.6	0.4	6	7.2	115.8

Calculation of mass balance:

Sum of all different products. The 2-(2-methoxyphenyl)-propanal derivative with deuterium in α-position however has already been accounted for in the total yield of 2-(2-methoxyphenyl)-propanal derivatives (and this will be a combination of those with 0–3 deuterium in the β-position) therefore this product is not counted in the mass balance calculation.

When using d_7-iPrMgBr, it could not be confirmed that the styrene derivative with deuterium incorporation in the α-position did not also have deuterium incorporation in the β-position and therefore, to account for the possibility of counting the same product twice, the mass balances for this reaction are given as a range.

Isomerisation of (2-phenylethyl)magnesium bromide (Fig. 4.8)

An alkene derivative (0–0.035 mmol, 0–10 mol%) was added to a solution of 2,6-bis-[1-(2,6-diisopropylphenylimino)ethyl]pyridine iron(II) chloride **743** (0.25 mL, 0.0014 M in THF, 0.00035 mmol, 0.1 mol%) and 1,3,5-trimethoxybenzene (11.8 mg, 0.07 mmol, 20 mol%) in anhydrous tetrahydrofuran (total volume 1.7 mL). (2-Phenylethyl)magnesium bromide **635** (0.3 mL, 1.15 M in Et_2O, 0.35 mmol, 100 mol%) was added in one portion, and the reaction was stirred at room temperature (20–22 °C). Aliquots (<100 μL) were periodically removed and added to HPLC vials containing anhydrous *N*,*N*-dimethylformamide **744** (10 μL, 0.13 mmol). The samples were shaken for 30 min, after which aqueous sulfate buffer (approx. 0.3 mL) was added to each vial followed by diethyl ether (approx. 0.7 mL). The vial was shaken and the layers were allowed to settle. The diethyl ether layer was removed and added to a 7 mL glass vial, from which the diethyl ether was allowed to evaporate at room temperature (approx. 10–15 min) until the majority of the solvent had evaporated. The residue was dissolved in $CDCl_3$ and added to an NMR tube for analysis by ^{1}H NMR spectroscopy.

The percentage yield of each product was determined by quantitative ^{1}H NMR spectroscopy, using 1,3,5-trimethoxybenzene (20 mol%) as an internal standard. All products were identified by comparison to previously reported data: 2-phenylpropanal **α-748** [59], 3-phenylpropanal **β-748** [59], nonanal [60].

Empty cells indicate that data was not collected.

Time	No added Alkene		Styrene (10 mol%)	
	α-748	**β-748**	**α-748**	**β-748**
0	0	95	0	95
1	0	93	0.4	95
5	0.2	94	2.2	93
10			3.6	91
20			5.9	90
45	0.4	95	9.5	86
90	0.5	94	14	84
120				
180	0.7	94	18.6	74

(continued)

(continued)

Time	No added Alkene		Styrene (10 mol%)	
	α-748	**β-748**	**α-748**	**β-748**
210				
300	1.1	92	23.3	67

Time	1-Octene (100 mol%)		
	α-748	**β-748**	1-Nonanal
0	0	91	0
1	0.3	92	0.5
5			
10	1	87	3.8
20	1.7	82	5.3
45	3.7	79	8.4
90	6.6	75	11.1
120			
180	10.1	68	14.2
210			
300	13.2	61	15.1

Time	α-Methylstyrene (10 mol%)		β-Methylstyrene (10 mol%)		Indene (10 mol %)		Cyclopropene (10 mol%)	
	α-748	**β-748**	**α-748**	**β-748**	**α-748**	**β-748**	**α-748**	**β-748**
0	0	87	0	94	0	94	0	102
1								
5								
10								
20								
45	0.2	84	0.35	93	0.2	94	0.3	103
90								
120	0.4	87	0.4	92				
180								
210					0.3	93	0.4	100
300	0.5	88	0.5	93	0.4	94	0.4	101

Hydromagnesiation using electronically-differentiated styrene derivatives (Fig. 4.9)

A styrene derivative (0.35 mmol) was added to a solution 2,6-bis-[1-(2,6-diisopropylphenylimino)ethyl]pyridine iron(II) chloride **743** (0.5 mL, 0.0014 M in d_8-THF, 0.0007 mmol, 0.2 mol%) and 1,3,5-trimethoxybenzene (11.8 mg, 0.07 mmol, 20 mol%) in anhydrous d_8-tetrahydrofuran (total volume 1.48 mL). Ethylmagnesium bromide **280** (0.52 mL, 1 M in d_8-THF, 0.52 mmol, 150 mol%) was added in one portion, and the reaction was stirred at room temperature (20–22 °C). Aliquots (<100 μL) were periodically removed and added to HPLC vials containing anhydrous methanol (approx. 10–15 μL, 0.25–0.37 mmol).

After all samples were taken, aqueous sulfate buffer (approx. 0.3 mL) was added to each vial followed by $CDCl_3$ (approx. 0.7 mL). The vial was shaken and the layers were allowed to settle. The $CDCl_3$ layer was removed and added to an NMR tube for analysis by ^1H NMR spectroscopy.

The percentage yield of each product was determined by quantitative ^1H NMR spectroscopy, using 1,3,5-trimethoxybenzene (20 mol%) as an internal standard. All products were identified by comparison to previously reported data: ethylbenzene [61], 1-ethyl-4-methoxybenzene [61], 1-ethyl-4-*tert*-butylbenzene [61], 1-ethyl-4-fluorobenzene [61], 1-ethyl-3-methoxybenzene [62], 1-ethyl-4-methylbenzene [63], 1-ethyl-2-methoxybenzene [64].

4-Methoxystyrene

Time	Yield (%)			
	1-ethyl-4-methoxybenzene	4-methoxystyrene	Unidentified products[a]	Mass balance
0	0	100	0	100
0.5	1.7	98	0	99.7
1	3.9	97	0	100.9
1.5	5.8	95	0	100.8
2.5	8.8	91	0	99.8
4	13.2	88	0	101.2
6	16.5	82.5	0	99
9	20.7	79	0	99.7
15	26.6	75	0	101.6
30	36.3	65	0	101.3
60	44.3	55	0	99.3
90	47.7	50	0	97.7
180	54.2	43.5	0	97.7
300	58	39.5	0	97.5

[a]Based upon difference between integration of aromatic region and those identified products listed

4-*tert*-Butylstyrene

Time	Yield (%)			
	1-ethyl-4-*tert*-butylbenzene	4-*tert*-butylstyrene	Unidentified products[a]	Mass balance
0	0	99	0	99
0.5	1.1	98	0	99.1
1	2.3	97	0	99.3
1.5	3.5	96	0	99.5
2.5	7	92	0	99

(continued)

(continued)

Time	Yield (%)			
	1-ethyl-4-*tert*-butylbenzene	4-*tert*-butylstyrene	Unidentified products[a]	Mass balance
4	12.3	87	0	99.3
6	19.2	80	0	99.2
9	29.2	70	0	99.2
15	43.5	55	0	98.5
30	65.3	32	0	97.3
60	76.2	21	1	98.2
90	82.9	14	2	98.9
180	88.3	9	4	101.3
300	89.1	6	5	100.1

[a]Based upon difference between integration of aromatic region and those identified products listed

4-Methylstyrene

Time	Yield (%)			
	1-ethyl-4-methylbenzene	4-methylstyrene	Unidentified products[a]	Mass balance
0	0.0	99	0	99.0
0.5	0.9	98	0	98.9
1	2.3	96	0	98.3
1.5	3.6	96	0	99.6
2.5	6.6	92	0	98.6
4	11.6	87.5	0	99.1
6	18.7	81.5	0	100.2
9	27.2	74	0	101.2
15	39.5	60.5	0	100.0
30	56.1	44	0	100.1
60	67.2	30	2	99.2
90	73.5	23	3	99.5
180	80.8	15.5	4	100.3
300	83	11.5	6	100.5

[a]Based upon difference between integration of aromatic region and those identified products listed

Styrene

Time	Yield (%)			
	Ethylbenzene	Styrene	Unidentified products[a]	Mass balance
0	0	99	0	99
0.5	0.5	99	0	99.5

(continued)

(continued)

Time	Yield (%)			
	Ethylbenzene	Styrene	Unidentified products[a]	Mass balance
1	1	98	0	99
1.5	1.3	98	0	99.3
2.5	2.2	97	0	99.2
4	3.8	94	0	97.8
6	5.9	93	0	98.9
9	9.5	90	0	99.5
15	17	81.5	0	98.5
30	36.4	59	3	98.4
60	62.2	30	6	98.2
90	77.3	8	10	95.3
180	81.9	4	12	97.9
300	82	2	8	92

[a]Based upon difference between integration of aromatic region and those identified products listed

4-Fluorostyrene

Time	Yield (%)				
	1-ethyl-4-fluorobenzene	4-fluorostyrene	Styrene[a]	Unidentified products[b]	Mass balance
0	0	98	0	0	98
0.5	0.2	98	0	0	98.2
1	0.4	97.5	0	0	97.9
1.5	0.7	98	0	0	98.7
2.5	1.2	97.5	0	0	98.7
4	1.6	96.5	0	0	98.1
6	2.5	95.5	0	0	98
9	3.3	96	0.5	0	99.8
15	5	94	1	0	100
30	8.7	89.5	2	0	100.2
60	9.1	86	2.5	2	99.6
90	9.4	80.5	3	8	99.9
180	10.8	70	4	10	94.8
300	11.8	56.5	4	19	91.3

[a]Assignment as styrene based upon GCMS analysis, see below
[b]Based upon difference between integration of aromatic region and those identified products listed

Example NMR spectra showing the formation of a second styrene derivative over time:

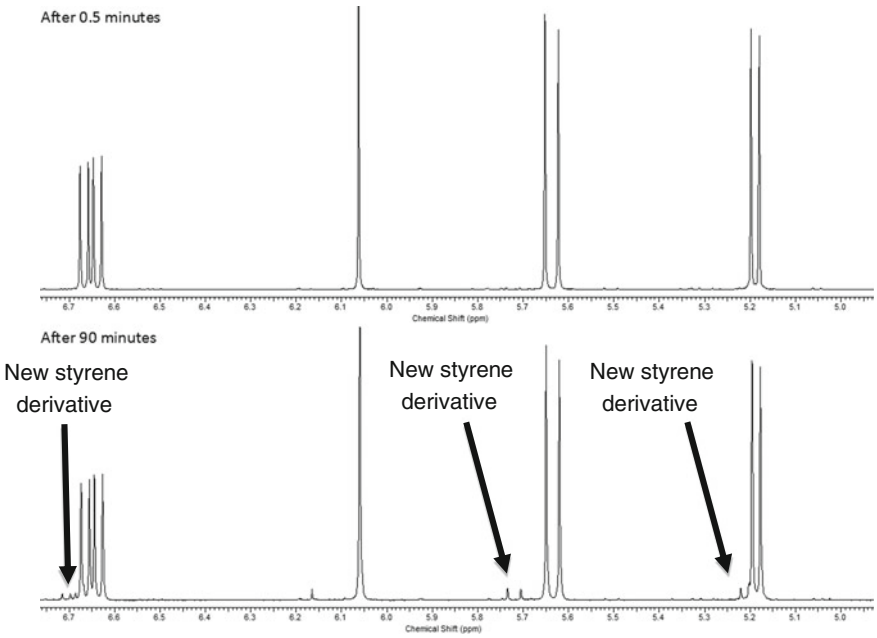

GCMS analysis identified the new styrene derivative to be styrene. A small amount of ethylbenzene was also present (presumably formed following hydromagnesiation of the in situ formed styrene):

GCMS method: Injector temperature 210 °C. Oven temperature 30 °C for 7 min, ramp at 5 °C min^{-1} to 275 °C, hold for 5 min.

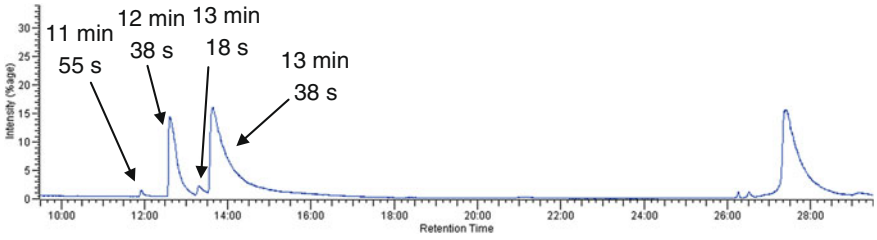

Retention time (M+, identity): 11 min 55 s (106, ethylbenzene); 12 min 38 s (124, 1-ethyl-4-fluorobenzene); 13 min 18 s (104, styrene); 13 min 38 s (122, 4-fluorostyrene).

11 min 55 s: ethylbenzene

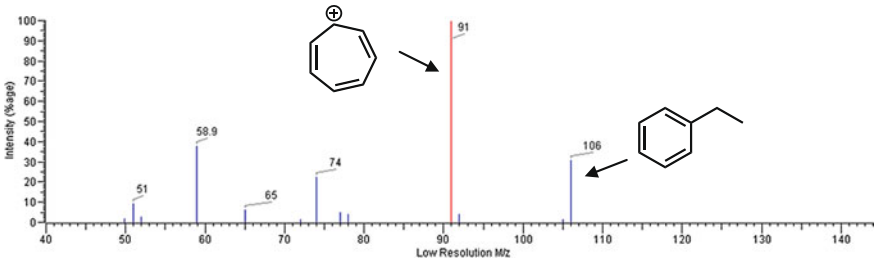

12 min 38 s: 1-ethyl-4-fluorobenzene

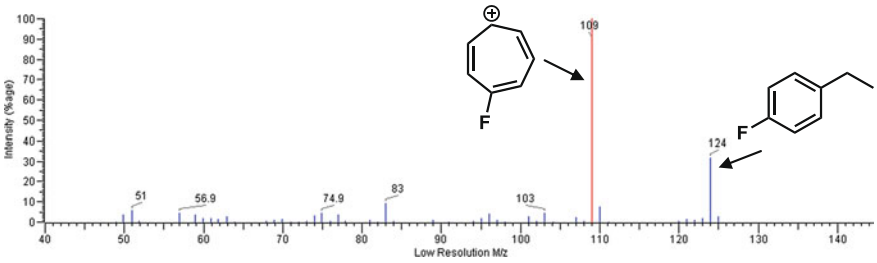

13 min 18 s: styrene

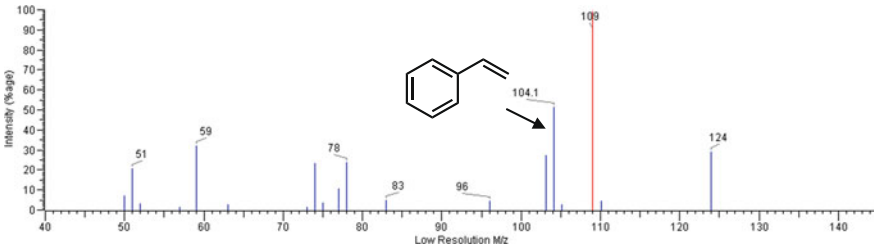

13 min 38 s: 4-fluorostyrene

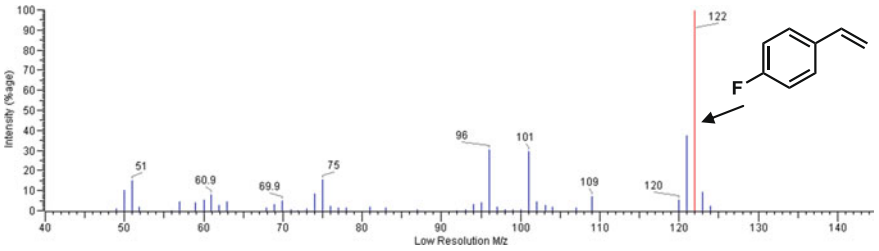

3-Methoxystyrene

Time	Yield (%)			
	1-ethyl-3-methoxybenzene	3-methoxystyrene	Unidentified products[a]	Mass balance
0	0	100	0	100
0.5	0.4	100	0	100.4
1	0.7	99	0	99.7
1.5	1.1	97	0	98.1
2.5	1.9	97	0	98.9
4	3.1	95	0	98.1
6	4.7	95	0	99.7
9	6.9	91	0	97.9
15	11.2	87	0	98.2
30	23.4	73	4	100.4
60	49.1	37	12	98.1
90	72.8	12	15	99.8
180	81.3	5	11	97.3
300	85	1	9	95

[a]Based upon difference between integration of aromatic region and those identified products listed

3-Trifluoromethylstyrene

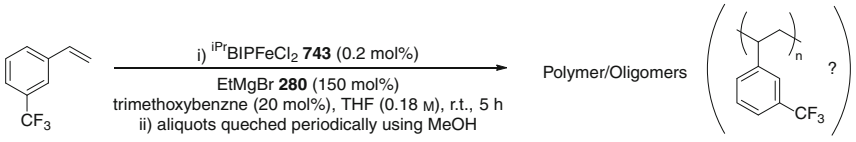

Time	Yield (%)			
	1-ethyl-3-trifluoromethylbenzene	3-trifluoromethylstyrene	Unidentified polymer/oligomers[a]	Mass balance
0	0	102	0	102
0.5	0	100	1	101
1	0	97	4	101
1.5	0	94	7	101
2.5	0	87	12	99
4	0	80	18	98
6	0	73	23	96
9	0	65	28	93
15	0	57	35	92
30	0	45	44	89
60	0	30	52	82
90	0	23	59	82
180	0	15	65	80
300	0	10	70	80

[a]Based upon integration of aromatic region

Electronic effects on substrate reactivity: Hammett Plots (Fig. 4.10)
Maximum initial rates for each substrate calculated using data given above.

Substituent	Max rate (%/min)	Log(k_R/k_H)	σ [65]	σ^+ [65]	$\sigma^\cdot$ [65–67]		
					Arnold	Jiang	Creary
4-F	0.70	−0.27	0.06	−0.07	−0.011	−0.02	−0.08
4-MeO	4.40	0.53	−0.27	−0.78	0.018	0.23	0.24
H	1.29	0.00	0	0	0	0	0
3-MeO	0.82	−0.20	0.12	0.047	−0.001	0.1	−0.02
4-Me	3.53	0.44	−0.17	−0.31	0.015	0.15	0.11
4-^{t}Bu	3.53	0.44	−0.2	−0.26	0.008	0.26	0.13

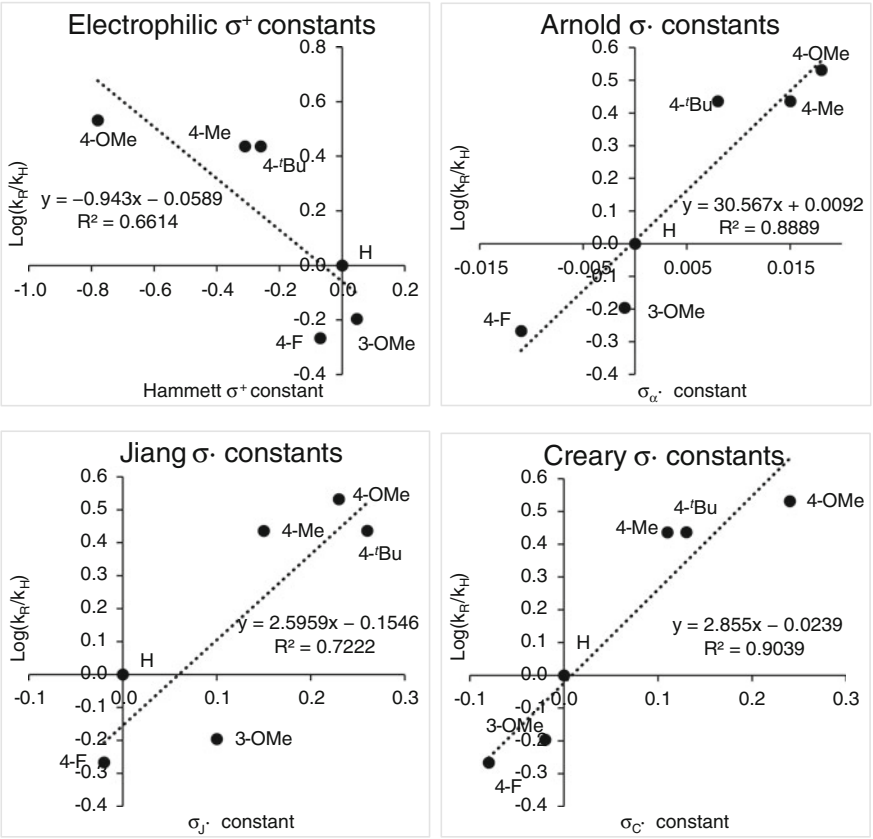

Rate Equation Kinetic Analysis (Figs. 4.11, 4.12 and 4.13)
Reactions were performed in a glovebox (20–22 °C) to facilitate easy aliquot sampling.

Standard solutions of 2,6-bis-[1-(2,6-diisopropylphenylimino)ethyl]pyridine iron (II) chloride **743** (0.0009 M in THF), 2-methoxystyrene **675** (0.8 M in THF) and trimethoxybenzene (0.16 M in THF) were used for all reactions. The standard solutions were stored in a glovebox in the dark at −35 °C between reactions, and were not stored for more than 3 weeks.

The concentration of 2,6-bis-[1-(2,6-diisopropylphenylimino)ethyl]pyridine iron (II) chloride **743**, 2-methoxystyrene **675** and ethylmagnesium bromide were varied, with the concentration of only one reagent changed in each experiment.

General procedure
2-Methoxystyrene **675** (0.1–1.1 mL, 0.8 M in THF, 0.08–0.88 mmol) was added to a solution 2,6-bis-[1-(2,6-diisopropylphenylimino)ethyl]pyridine iron(II) chloride **743** (0.25–0.75 mL, 0.00036 M in THF, 0.00009–0.00027 mmol) and

1,3,5-trimethoxybenzene (0.5 mL, 0.16 M in THF, 0.08 mmol) in anhydrous tetrahydrofuran (total volume after Grignard reagent 4 mL). Ethylmagnesium bromide **280** (0.1–0.8 mL, 1 M in THF, 0.1–0.8 mmol) was added in one portion, and the reaction was stirred at room temperature (20–22 °C). Aliquots (<100 μL) were periodically removed and added to HPLC vials containing anhydrous methanol (approx. 10–15 μL, 0.25–0.37 mmol). After all samples were taken, aqueous sulfate buffer (approx. 0.3 mL) was added to each vial followed by diethyl ether (approx. 0.7 mL). The vial was shaken and the layers were allowed to settle. The diethyl ether layer was removed and added to a 7 mL glass vial, from which the diethyl ether was allowed to evaporate at room temperature (approx. 10–15 min) until the majority of the solvent had evaporated. The residue was dissolved in $CDCl_3$ and added to an NMR tube for analysis by ^1H NMR spectroscopy.

The concentration of each product was determined by quantitative ^1H NMR spectroscopy, using 1,3,5-trimethoxybenzene as an internal standard.

In these experiments, no side-products were observed and the mass balance could be accounted for by a combination of product (1-ethyl-2-methoxybenzene **750** [64], and starting material (2-methoxystyrene **675**). For clarity only yields of product (1-ethyl-2-methoxybenzene **675**) are given in the tables below.

Reaction order with respect to 2,6-bis-[1-(2,6-diisopropylphenylimino)ethyl] pyridine iron(II) chloride **743** concentration (Fig. 4.11)

2-Methoxystyrene **675** (0.4 mmol, 0.1 M) and ethylmagnesium bromide **280** (0.4 mmol, 0.1 M) kept constant in all reactions. The concentration of 2,6-bis-[1-(2,6-diisopropylphenylimino)ethyl]pyridine iron(II) chloride **743** was varied in the range 0.0000225–0.0000675 M. The data for product formation given in the table below is the concentration of 1-ethyl-2-methoxybenzene **750** (M) formed in the reaction (0.1 M = 100 % yield)

Time	1-ethyl-2-methoxybenzene **750** (M)				
	0.0000225 M	0.0000315 M	0.000045 M	0.000054 M	0.0000675 M
0	0	0	0	0	0
0.333333	0.0001	0.0006	0.0013	0.0015	0.0017
0.666667	0.0009	0.002	0.0053	0.0056	0.0076
1	0.002	0.004	0.0104	0.0122	0.0158
1.333333	0.0034	0.0069	0.015	0.0182	0.0223
1.5	0.0042	0.0086	0.0175	0.0204	0.0247
1.666667	0.005	0.0102	0.0191	0.0225	0.0265
2	0.0068	0.0128	0.0217	0.026	0.0297
2.5	0.0093	0.0162	0.026	0.0297	0.0332
3	0.0119	0.0191	0.0289	0.0333	0.0374
4	0.0161	0.0243	0.0341	0.0388	0.0426
5	0.0205	0.0286	0.038	0.0428	0.0472
6	0.0241	0.0324	0.0421	0.0463	0.0511
8	0.0301	0.0379	0.0486	0.0526	0.0573

(continued)

(continued)

Time	1-ethyl-2-methoxybenzene **750** (M)				
	0.0000225 M	0.0000315 M	0.000045 M	0.000054 M	0.0000675 M
10	0.0348	0.0429	0.0531	0.0585	0.0635
12	0.0396	0.0472	0.0575	0.0634	0.068
15	0.0455	0.0538	0.0634	0.0702	0.0743
20	0.054	0.062	0.0709	0.0772	0.0802
30	0.0682	0.074	0.0812	0.0879	0.0881
45	0.0794	0.0842	0.0881	0.0929	0.0936
75	0.086	0.0893	0.091	0.0953	0.0954
180	0.0894	0.0926	0.0936	0.0962	0.0965

Initial ^{iPr}BIPFeCl$_2$ **743** concentration (mol dm^{-3})	Max rate of reaction (mol dm^{-3} min^{-1})
0.0000225	0.005
0.0000315	0.00875
0.000045	0.01467
0.000054	0.0175
0.0000675	0.024

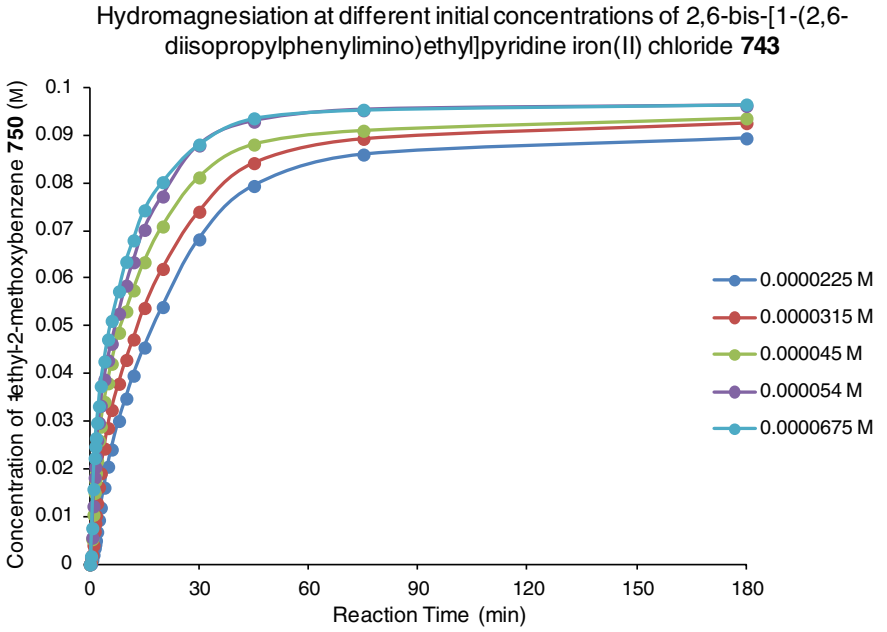

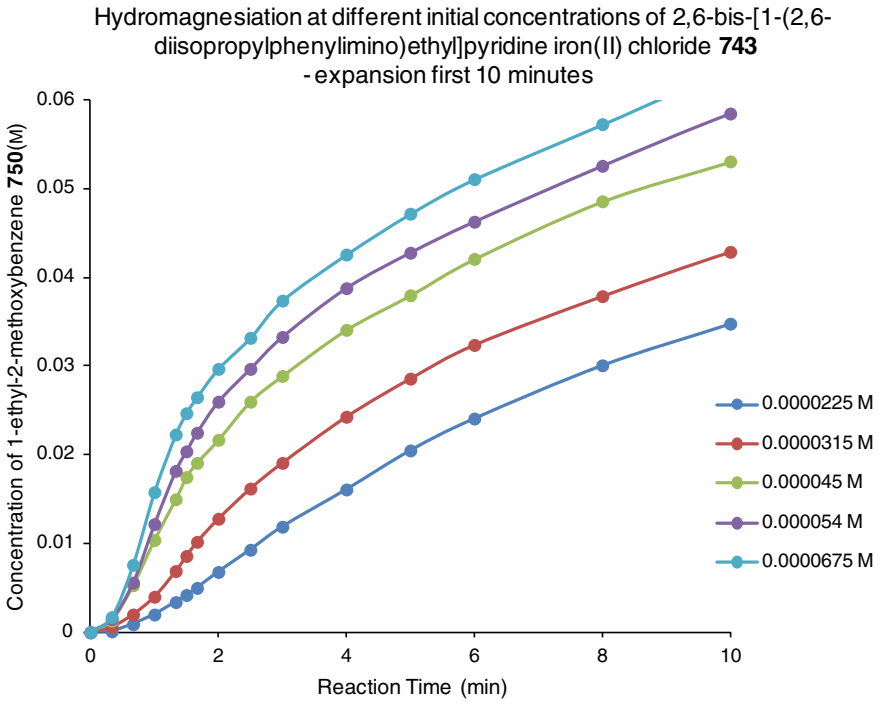

Reaction order with respect to 2-methoxystyrene **675** concentration (Fig. 4.12)

2,6-Bis-[1-(2,6-diisopropylphenylimino)ethyl]pyridine iron(II) chloride **743** (0.000126 mmol, 0.0000315 M) and ethylmagnesium bromide **280** (0.44 mmol, 0.11 M) were kept constant in all reactions. The concentration of 2-methoxystyrene **675** was varied in the range of 0.02–0.22 M. The data for product formation given in the table is the concentration of 1-ethyl-2-methoxybenzene (M) formed in the reaction.

Time	1-ethyl-2-methoxybenzene **750** (M)								
	0.02 M	0.04 M	0.06 M	0.08 M	0.1 M	0.12 M	0.14 M	0.18 M	0.22 M
0	0	0	0	0	0	0	0	0	0
0.333	0.0001	0.0003	0.0004	0.0005	0.0006	0.0005	0.0006	0.0005	0.0003
0.667	0.0002	0.0006	0.001	0.0013	0.002	0.0019	0.003	0.003	0.0015
1	0.0003	0.001	0.0021	0.0027	0.004	0.0038	0.0061	0.0062	0.0043
1.333	0.0006	0.0018	0.0038	0.0044	0.0069	0.0065	0.0094	0.0102	0.0077
1.667	0.0008	0.0028	0.0053	0.0063	0.0102	0.0096	0.0128	0.0144	0.0112
2	0.0011	0.0037	0.0071	0.0079	0.0128	0.0122	0.0166	0.0178	0.0146
2.5	0.0016	0.0056	0.01	0.0112	0.0162	0.0157	0.0206	0.0222	0.0186
3	0.0023	0.0072	0.0122	0.0142	0.0191	0.0189	0.0246	0.026	0.0228
4	0.0035	0.0101	0.0155	0.0186	0.0243	0.0247	0.0303	0.0323	0.029
5	0.0044	0.0123	0.019	0.0221	0.0286	0.0289	0.0356	0.0375	0.0347
6	0.0051	0.0141	0.0215	0.025	0.0324	0.0337	0.039	0.0434	0.0399
8	0.0068	0.0166	0.0255	0.0295	0.0379	0.0413	0.0484	0.0518	0.0489

(continued)

(continued)

Time	1-ethyl-2-methoxybenzene **750** (M)								
	0.02 M	0.04 M	0.06 M	0.08 M	0.1 M	0.12 M	0.14 M	0.18 M	0.22 M
10	0.008	0.0191	0.0281	0.0333	0.0429	0.0461	0.0547	0.0597	0.0572
12	0.0086	0.0203	0.0314	0.0364	0.0472	0.0524	0.0607	0.0663	0.0644
15	0.0096	0.0226	0.035	0.042	0.0538	0.0581	0.0689	0.0742	0.0725
20	0.0112	0.0248	0.0389	0.0485	0.062	0.0684	0.0802	0.087	0.0834
30	0.0118	0.0288	0.0456	0.0606	0.074	0.0829	0.0934	0.0968	0.1011
45	0.013	0.0309	0.0502	0.0683	0.0842	0.094	0.1	0.1017	0.1026
75	0.0133	0.0327	0.0538	0.0711	0.0893	0.0988	0.1028	0.1036	0.1029
180	0.0148	0.0348	0.0547	0.0755	0.0926	0.1015	0.1034	0.1034	0.1032

Initial 2-methoxystyrene **675** concentration (mol dm^{-3})	Max rate of reaction (mol dm^{-3} min^{-1})
0.02	0.0012
0.04	0.0033
0.06	0.0046
0.08	0.006
0.1	0.0086
0.12	0.0084
0.14	0.0105
0.18	0.011
0.22	0.01

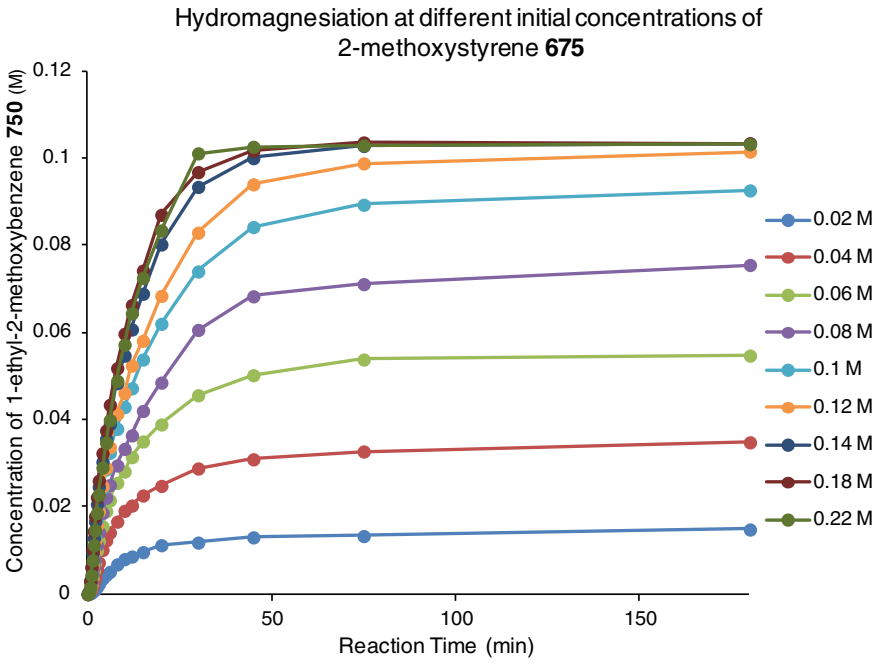

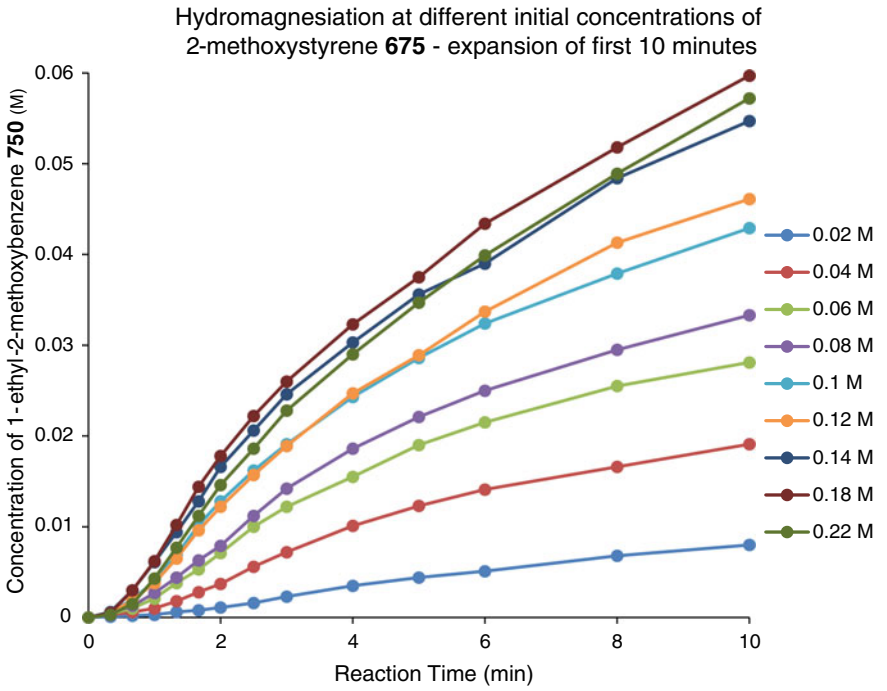

Reaction order with respect to ethylmagnesium bromide 280 concentration (Fig. 4.13).

2,6-Bis-[1-(2,6-diisopropylphenylimino)ethyl]pyridine iron(II) chloride **743** (0.000126 mmol, 0.0000315 M) and 2-methoxystyrene **675** (0.4 mmol, 0.1 M) were kept constant in all reactions. The concentration of ethylmagnesium bromide **280** was varied in the range of 0.0275-0.22 M. The data for product formation given in the table is the concentration of 1-ethyl-2-methoxybenzene (M) formed in the reaction.

Time	1-ethyl-2-methoxybenzene **750** (M)							
	0.0275 M	0.055 M	0.0625 M	0.083 M	0.11 M	0.1375 M	0.165 M	0.22 M
0	0	0	0	0	0	0	0	0
0.333	0.0002	0.0005	0.0005	0.0007	0.0012	0.001	0.0006	0.0002
0.667	0.0003	0.001	0.0018	0.0022	0.003	0.0028	0.0025	0.0011
1	0.0005	0.0018	0.003	0.0042	0.006	0.0058	0.0057	0.0033
1.333	0.0006	0.0026	0.0045	0.007	0.01	0.01	0.0102	0.0066
1.667	0.0009	0.0038	0.0068	0.0099	0.0136	0.0138	0.0144	0.0117
2	0.0014	0.0047	0.009	0.0129	0.0166	0.0167	0.017	0.0156
2.5	0.0024	0.0067	0.0121	0.017	0.0205	0.0208	0.0212	0.0201
3	0.0034	0.0088	0.0146	0.0201	0.0239	0.0242	0.0248	0.0237
4	0.0061	0.0126	0.0192	0.0252	0.0296	0.0294	0.0304	0.0292
5	0.0088	0.0165	0.0233	0.0298	0.0342	0.0342	0.0346	0.0339
6	0.0113	0.02	0.0268	0.0343	0.0393	0.0389	0.039	0.0385

(continued)

(continued)

Time	1-ethyl-2-methoxybenzene **750** (M)							
	0.0275 M	0.055 M	0.0625 M	0.083 M	0.11 M	0.1375 M	0.165 M	0.22 M
8	0.0157	0.0265	0.0338	0.0415	0.0462	0.0461	0.0459	0.0457
10	0.0187	0.0321	0.0402	0.0478	0.052	0.0516	0.0508	0.051
12	0.0209	0.0359	0.0446	0.0527	0.0563	0.056	0.0559	0.0548
15	0.023	0.0411	0.0502	0.0578	0.0628	0.0625	0.0623	0.0607
20	0.0242	0.0463	0.0546	0.066	0.0726	0.0723	0.0716	0.0679
30	0.026	0.0515	0.0594	0.0745	0.0844	0.0843	0.0839	0.0791
45	0.0267	0.0535	0.0615	0.0785	0.0904	0.0902	0.09	0.0867
75	0.0275	0.0544	0.0625	0.0819	0.0942	0.0944	0.0945	0.0906
180	0.0275	0.0546	0.0634	0.0823	0.0966	0.0969	0.0957	0.0938

Initial EtMgBr **280** concentration (mol dm^{-3})	Max rate of reaction (mol dm^{-3} min^{-1})
0.0275	0.00267
0.055	0.0048
0.0625	0.0067
0.083	0.0093
0.11	0.01167
0.1375	0.0122
0.165	0.013
0.22	0.0127

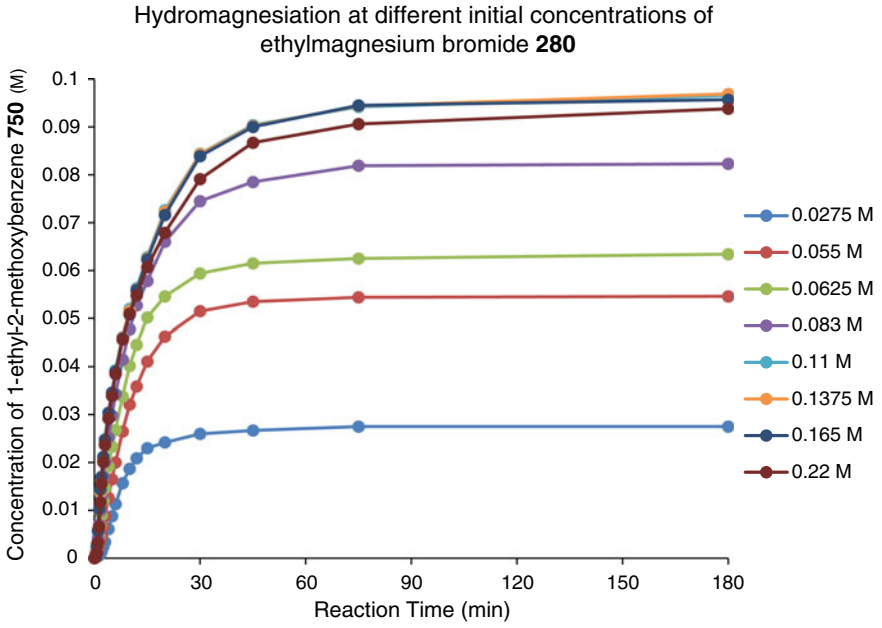

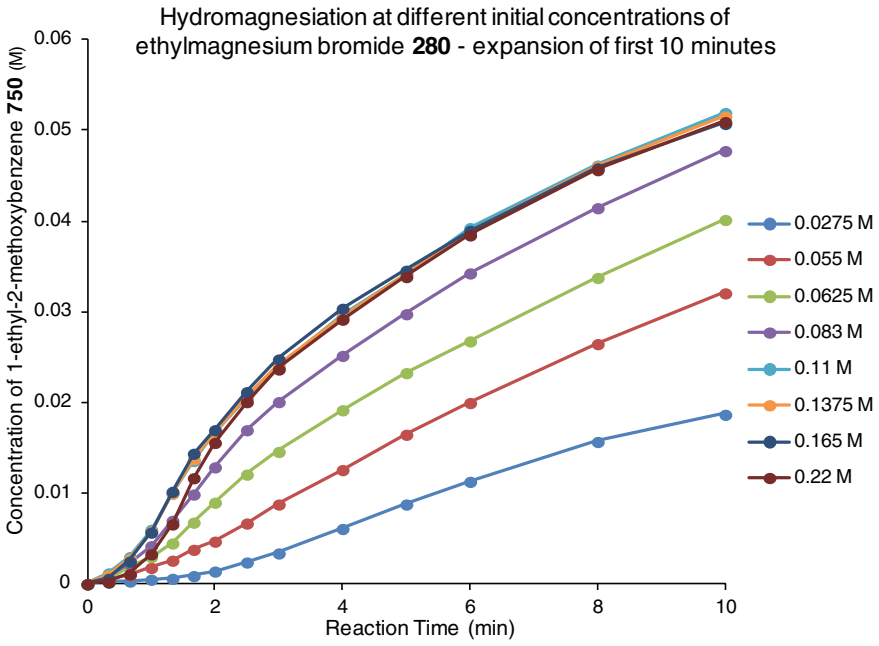

Hydromagnesiation at iron pre-catalyst concentration of 1.8×10^{-3} M (Fig. 4.14)

2-Methoxystyrene **675** (60 μL, 0.45 mmol) was added to a solution of iron pre-catalyst {either 2,6-bis-[1-(2,6-diisopropylphenylimino)ethyl]pyridine iron(II) chloride **743** (2.7 mg, 0.0045 mmol, 1 mol%); or iron(II) chloride **279** (1 mL, 0.045 M in THF, 0.0045 mmol, 1 mol%), TMEDA **136** (0-1.0 mL, 0.045 M in THF, 0–0.045 mmol, 0–10 mol%)]} and 1,3,5-trimethoxybenzene (15.1 mg, 0.09 mmol, 20 mol%) in anhydrous tetrahydrofuran (total volume 2.28 mL). Ethylmagnesium bromide **280** (0.22 mL, 3 M in Et_2O, 0.66 mmol, 150 mol%) was added in one portion, and the reaction was stirred at room temperature (20–22 °C). Aliquots (<100 μL) were periodically removed and added to HPLC vials containing anhydrous methanol (approx. 10–15 μL, 0.25–0.37 mmol). After all samples were taken, aqueous sulfate buffer (approx. 0.3 mL) was added to each vial followed by diethyl ether (approx. 0.7 mL). The vial was shaken and the layers were allowed to settle. The diethyl ether layer was removed and added to a 7 mL glass vial, from which the diethyl ether was allowed to evaporate at room temperature (approx. 10–15 min) until the majority of the solvent had evaporated. The residue was dissolved in $CDCl_3$ and added to an NMR tube for analysis by ^{1}H NMR spectroscopy.

The percentage yield of each product was determined by quantitative ^{1}H NMR spectroscopy, using 1,3,5-trimethoxybenzene (20 mol%) as an internal standard.

Empty cells indicate that data was not collected.

Time	^{iPr}BIPFeCl$_2$ **743**			$FeCl_2$ **279**		
	1-ethyl-2-methoxy benzene	2-methoxystyrene	Mass balance	1-ethyl-2-methoxy benzene	2-methoxystyrene	Mass balance
0	0.0	99.0	99.0	0.0	100.0	100.0
0.33	47.3	52.5	99.8	2.0	98.4	100.4
0.66	58.3	42.4	100.7	2.1	96.9	99.0
1	66.4	33.9	100.3	2.3	96.9	99.1
1.5	74.5	25.4	100.0	2.4	96.9	99.3
2	81.8	18.6	100.5	2.6	98.4	101.0
3	90.6	8.5	99.1	2.7	95.3	98.0
5	96.7	3.4	100.1	3.3	96.9	100.2
7	98.5	1.7	100.2	3.5	95.3	98.8
10	98.6	0.8	99.5	3.5	93.8	97.2
15	98.8	0.0	98.8	4.2	95.3	99.6
30				4.5	95.2	99.7
60	99.0	0.0	99.0	4.7	95.0	99.7
Time	$FeCl_2$ **279** + TMEDA **136** (0.5 mol%)			$FeCl_2$ **279** + TMEDA **136** (1 mol%)		
	1-ethyl-2-methoxy benzene	2-methoxystyrene	Mass balance	1-ethyl-2-methoxy benzene	2-methoxystyrene	Mass balance
0	0.0	100.0	100.0	0.0	100.0	100.0
0.33	5.0	95.0	100.0	9.3	90.2	99.4
0.66	11.1	86.7	97.8	19.3	78.7	98.0
1	13.1	85.0	98.1	24.3	73.8	98.1
1.5	14.6	83.3	97.9	26.7	68.9	95.6
2	16.3	83.3	99.6	28.9	68.9	97.7
3	17.1	80.0	97.1	31.4	65.6	97.0
5	19.4	81.7	101.1	34.9	62.3	97.2
7	21.0	78.3	99.3	37.0	59.0	96.0
10	22.7	76.7	99.4	41.1	55.7	96.9
15	25.0	73.3	98.3	46.0	52.5	98.5
30	29.1	68.3	97.5	56.1	41.0	97.1
60	35.7	60.0	95.7	71.7	21.3	93.0
Time	$FeCl_2$ **279** + TMEDA **136** (2 mol%)			$FeCl_2$ **279** + TMEDA **136** (5 mol%)		
	1-ethyl-2-methoxy benzene	2-methoxystyrene	Mass balance	1-ethyl-2-methoxy benzene	2-methoxystyrene	Mass balance
0	0.0	100.0	100.0	0.0	100.0	100.0
0.33	15.6	84.1	99.7	7.7	91.7	99.4
0.66	27.3	73.0	100.3	20.0	78.3	98.3
1	31.1	68.3	99.3	32.0	66.7	98.7
1.5	34.8	65.1	99.9	45.9	51.7	97.6
2	37.3	63.5	100.8	54.5	43.3	97.9
3	41.4	57.1	98.5	64.4	33.3	97.7
5	47.6	50.8	98.4	76.7	23.3	100.0
7	54.4	44.4	98.8	82.3	16.7	98.9

(continued)

(continued)

Time	$FeCl_2$ **279** + TMEDA **136** (2 mol%)			$FeCl_2$ **279** + TMEDA **136** (5 mol%)		
	1-ethyl-2-methoxy benzene	2-methoxystyrene	Mass balance	1-ethyl-2-methoxy benzene	2-methoxystyrene	Mass balance
10	62.7	36.5	99.2	87.6	11.7	99.2
15	75.0	25.4	100.4	93.8	5.0	98.8
30	95.2	4.8	99.9	98.3	1.7	100.0
60	98.2	1.6	99.8	97.9	1.2	99.1

Time	$FeCl_2$ **279** + TMEDA **136** (10 mol%)		
	1-ethyl-2-methoxybenzene	2-methoxystyrene	Mass balance
0	0.0	100.0	100.0
0.33	2.4	96.7	99.1
0.66	12.6	86.9	99.5
1	21.4	78.7	100.1
1.5	32.4	65.6	98.0
2	42.6	52.5	95.0
3	62.0	37.7	99.7
5	80.6	18.0	98.6
7	90.6	8.2	98.8
10	95.0	3.3	98.3
15	97.0	1.6	98.6
30	98.2	0.8	99.0
60	97.7	0.2	97.9

Hydromagnesiation at iron pre-catalyst concentration of 1.8×10^{-4} M (Fig. 4.15)

2-Methoxystyrene **675** (60 μL, 0.45 mmol) was added to a solution of iron pre-catalyst {either 2,6-bis-[1-(2,6-diisopropylphenylimino)ethyl]pyridine iron(II) chloride **743** (0.5 mL, 0.00135 M in THF, 0.000675 mmol, 0.15 mol%); or iron(II) chloride **279** (0.15 mL, 0.045 M in THF, 0.000675 mmol, 0.15 mol%), TMEDA **136** (0–15 μL, 0.045 M in THF, 0–0.000675 mmol, 0–0.15 mol%)} and 1,3,5-trimethoxybenzene (15.1 mg, 0.09 mmol, 20 mol%) in anhydrous tetrahydrofuran (total volume 3.53 mL). Ethylmagnesium bromide **280** (0.22 mL, 3 M in Et_2O, 0.66 mmol, 150 mol%) was added in one portion, and the reaction was stirred at room temperature (20–22 °C). Aliquots (<100 μL) were periodically removed and added to HPLC vials containing anhydrous methanol (10–15 μL, 0.25–0.37 mmol). After all samples were taken, aqueous sulfate buffer (0.3 mL) was added to each vial followed by diethyl ether (0.7 mL). The vials were shaken and the layers were allowed to settle. The diethyl ether layer was removed and added to a 7 mL glass vial, from which the diethyl ether was allowed to evaporate at room temperature (approx. 10–15 min) until the majority of the solvent had evaporated. The residue was dissolved in $CDCl_3$ and added to an NMR tube for analysis by ^1H NMR spectroscopy. The percentage yield of each product was determined by quantitative ^1H NMR spectroscopy, using 1,3,5-trimethoxybenzene (20 mol%) as an internal standard.

Time	^{iPr}BIPFeCl$_2$ **743**			FeCl$_2$ **279**		
	1-ethyl-2-methoxybenzene	2-methoxystyrene	Mass balance	1-ethyl-2-methoxybenzene	2-methoxystyrene	Mass balance
0	0.0	100.0	100.0	0.0	99.0	99.0
1	0.9	98.4	99.3	0.0	98.6	98.6
1.5	18.4	80.6	99.0	7.1	90.5	97.6
2	25.7	74.2	99.9	12.1	86.5	98.5
2.5	31.5	67.7	99.2	15.4	83.8	99.2
3	35.3	62.9	98.2	17.8	81.1	98.9
4	40.0	56.5	96.5	21.5	79.7	101.2
5	45.1	53.2	98.4	24.4	74.3	98.7
6	47.9	51.6	99.6	26.8	73.0	99.7
7	51.9	46.8	98.7	28.7	68.9	97.6
8	54.7	43.5	98.3	30.9	68.9	99.8
10	61.0	38.7	99.7	34.7	66.2	100.9
12	63.8	35.5	99.3	37.8	60.8	98.6
16	71.9	27.4	99.3	43.8	52.7	96.5
20	77.6	21.0	98.6	49.7	50.0	99.7
25	82.9	16.1	99.1	55.4	43.2	98.7
30	86.6	12.9	99.5	61.2	37.8	99.0
45	90.3	9.7	100.0	71.0	27.0	98.1
60	92.2	6.5	98.7	75.0	24.3	99.3
120	95.4	4.8	100.3	80.4	17.6	98.0

Time	FeCl$_2$ **279** + TMEDA **136** (0.15 mol%)		
	1-ethyl-2-methoxybenzene	2-methoxystyrene	Mass balance
0	0.0	100.0	100.0
1	0.9	98.4	99.3
1.5	18.4	80.6	99.0
2	25.7	74.2	99.9
2.5	31.5	67.7	99.2
3	35.3	62.9	98.2
4	40.0	56.5	96.5
5	45.1	53.2	98.4
6	47.9	51.6	99.6
7	51.9	46.8	98.7
8	54.7	43.5	98.3
10	61.0	38.7	99.7
12	63.8	35.5	99.3
16	71.9	27.4	99.3
20	77.6	21.0	98.6
25	82.9	16.1	99.1

(continued)

(continued)

Time	$FeCl_2$ **279** + TMEDA **136** (0.15 mol%)		
	1-ethyl-2-methoxybenzene	2-methoxystyrene	Mass balance
30	86.6	12.9	99.5
45	90.3	9.7	100.0
60	92.2	6.5	98.7
120	95.4	4.8	100.3

Hydromagnesiation of 2-methoxystyrene in the presence of DCT (Fig. 4.16)
2-Methoxystyrene **675** (94 μL, 0.7 mmol) was added to a solution of 2,6-bis-[1-(2,6-diisopropylphenylimino)ethyl]pyridine iron(II) chloride **743** (0.5 mL, 0.0014 M in THF, 0.0007 mmol, 0.1 mol%) and 1,3,5-trimethoxybenzene (23.5 mg, 0.14 mmol, 20 mol%) in anhydrous tetrahydrofuran (total volume 3.65 mL). Ethylmagnesium bromide **280** (0.35 mL, 3 M in Et_2O, 1.05 mmol, 150 mol%) was added in one portion, and the reaction was stirred at room temperature (20–22 °C). Aliquots (<100 μL) were periodically removed and added to HPLC vials containing anhydrous methanol (approx. 10–15 μL, 0.25–0.37 mmol). After all samples were taken, aqueous sulfate buffer (approx. 0.3 mL) was added to each vial followed by diethyl ether (approx. 0.7 mL). The vial was shaken and the layers were allowed to settle. The diethyl ether layer was removed and added to a 7 mL glass vial, from which the diethyl ether was allowed to evaporate at room temperature (approx. 10–15 min) until the majority of the solvent had evaporated. The residue was dissolved in $CDCl_3$ and added to an NMR tube for analysis by ^1H NMR spectroscopy.

The percentage yield of each product was determined by quantitative ^1H NMR spectroscopy, using 1,3,5-trimethoxybenzene (20 mol%) as an internal standard.

Reactions in the presence of DCT:

The above standard procedure was followed, with DCT **761** (0.05–0.2 mL, 0.007 M in THF, 0.05–0.2 mol%) added after 2 min.

Empty cells indicate that data was not collected.

Time	No DCT **761** added			DCT **761** (0.05 mol%) added at 2 min		
	1-ethyl-2-methoxybenzene	2-methoxystyrene	Mass balance	1-ethyl-2-methoxybenzene	2-methoxystyrene	Mass balance
0	0.0	98.0	98.0	0.0	99.0	99.0
0.5	8.0	91.0	99.0	7.9	91.0	98.9
1	17.9	81.0	98.9	19.2	81.0	100.2
1.5	23.0	76.0	99.0	23.8	75.0	98.8
2	26.5	72.0	98.5	27.3	72.0	99.3
2.5	29.3	69.0	98.3	29.1	70.0	99.1
3	32.1	67.0	99.1	31.2	67.0	98.2
3.5	34.2	64.0	98.2	31.8	66.0	97.8
4	35.9	63.0	98.9	33.1	66.0	99.1
4.5	37.5	61.0	98.5	33.7	66.0	99.7

(continued)

(continued)

Time	No DCT **761** added			DCT **761** (0.05 mol%) added at 2 min		
	1-ethyl-2-methoxybenzene	2-methoxystyrene	Mass balance	1-ethyl-2-methoxybenzene	2-methoxystyrene	Mass balance
5	39.6	59.0	98.6	34.5	65.0	99.5
6	42.3	57.0	99.3	35.9	64.0	99.9
7	44.9	54.0	98.9	36.6	63.0	99.6
8	47.8	51.0	98.8	38.3	61.0	99.3
9	49.8	49.0	98.8	38.5	60.0	98.5
11	54.4	45.0	99.4	40.3	58.0	98.3
13	57.9	41.0	98.9	41.7	56.0	97.7
15	61.9	37.0	98.9	42.9	55.0	97.9
17	65.0	33.0	98.0	44.1	54.0	98.1
19	67.4	31.0	98.4	45.6	53.0	98.6
Time	DCT **761** (0.1 mol%) added at 2 min			DCT **761** (0.2 mol%) added at 2 min		
	1-ethyl-2-methoxybenzene	2-methoxystyrene	Mass balance	1-ethyl-2-methoxybenzene	2-methoxystyrene	Mass balance
0	0	100	100	0	99	99
0.5	9.7	91	100.7	8.8	91	99.8
1	19.7	80	99.7	19.3	79	98.3
1.5	23.7	76	99.7	24.2	75	99.2
2	27.5	72	99.5	27	72	99
2.5	28.3	70	98.3	27.7	71	98.7
3	29	70	99	28.1	71	99.1
3.5	29.2	69	98.2	28.8	70	98.8
4	29.4	69	98.4	29	70	99
4.5	29.6	69	98.6	28.9	70	98.9
5	29.8	70	99.8	29.9	69	98.9
6	29.5	69	98.5	29.2	69	98.2
7	30.6	68	98.6	29.1	69	98.1
8	30.5	68	98.5	29.5	69	98.5
9	30.9	68	98.9	29.8	69	98.8
11				29.7	69	98.7
13				29.8	68	97.8
15				29.1	69	98.1
17				29.7	70	99.7
19	31.7	67	98.7	29.9	69	98.9

Hydromagnesiation procedure using 3-(4-methoxyphenyl)propylmagnesium bromide (Fig. 4.17)

2-Methoxystyrene **675** (35 μL, 0.26 mmol) was added to a solution of iron pre-catalyst {either: 2,6-bis-[1-(2,6-diisopropylphenylimino)ethyl]pyridine iron(II) chloride **743** (8.5–12.8 mg, 0.014–0.021 mmol, 5.4–8.1 mol%); or a combination of iron chloride **279** (1.8–2.7 mg, 0.014–0.021 mmol, 5.4–8.1 mol%) and *N*,*N*,*N*′,*N*′-tetramethylethylenediamine **136** (10–16 μL, 0.07–0.105 mmol, 27–41 mol%)}

and 1,3,5-trimethoxybenzene (23.5 mg, 0.14 mmol, 54 mol%) in anhydrous tetrahydrofuran (total volume 7.5 mL). 3-(4-Methoxyphenyl)propylmagnesium bromide **765** (0.5 mL, 0.7 M in Et_2O, 0.35 mmol, 135 mol%) was added in one portion, and the reaction was stirred at room temperature (20–22 °C). Aliquots (0.25 mL) were periodically removed and added to HPLC vials containing a solution of anhydrous *N*,*N*-dimethylformamide **744** in tetrahydrofuran (0.1 mL, 0.6 M in THF, 0.06 mmol). The samples were shaken for 30 min, followed by the addition of 2 drops of D_2O (to check for any unreacted Grignard reagent). Aqueous sulfate buffer (approx. 0.3 mL) was added to each vial followed by diethyl ether (approx. 0.7 mL). The vial was shaken and the layers were allowed to settle. The diethyl ether layer was removed and added to a 7 mL glass vial, from which the diethyl ether was allowed to evaporate at room temperature (approx. 10–15 min) until the majority of the solvent had evaporated. The residue was dissolved in $CDCl_3$ and added to an NMR tube for analysis by ^{1}H NMR spectroscopy.

The percentage yield of each product was determined by quantitative ^{1}H NMR spectroscopy, using 1,3,5-trimethoxybenzene (54 mol%) as an internal standard. All products were identified by comparison to previously reported data: 2-(2-methoxyphenyl)-propanal **α-745**, [57] 4-(4-methoxyphenyl)butanal **766** [68], 1-methoxy-4-propylbenzene **767** [69], 1,6-bis(4-methoxyphenyl)hexane **768** [70], 1-allyl-4-methoxybenzene **769** [71], (*E*)- and (*Z*)-1-methoxy-4-(prop-1-en-1-yl) benzene **(*E*)-** and **(*Z*)-770** [72].

Control reactions

In parallel to each reaction, 3 control reactions were conducted, which were set-up and run in an identical manner, except that no iron was added. In total, 4 aliquots were removed from each control reaction, which were quenched, extracted and analysed in the same way as described above. The quantity of each product was determined by quantitative ^{1}H NMR spectroscopy, using 1,3,5-trimethoxybenzene (54 mol%) as an internal standard.

In general, data from the control reactions identified the given products in the following ranges of %yield: 2-(2-methoxyphenyl)-propanal **α-745** (0 %); 1-methoxy-4-propylbenzene **767** [12–17 %—range of percentages related to quantity of TMEDA **136** added to control reaction (it is likely that a there was a low water content in TMEDA **136**)]; 1,6-bis(4-methoxyphenyl)hexane **768** (18–20 %), 4-(4-methoxyphenyl)butanal **766** (125–130 %), 1-allyl-4-methoxybenzene **769** (3–3.3 %), 1-methoxy-4-(prop-1-en-1-yl)benzene **770** (0 %).

Data for oxidation-state experiments

The data below has been modified from the raw data only by subtraction of the background quantity of each product expected based upon the respective control reactions. In no case was an increase in the concentration of 1,6-bis (4-methoxyphenyl)hexane observed under the reaction conditions (above the expected background concentration), and therefore no data has been given for this product in the following tables.

Each equivalent of 1-methoxy-4-propylbenzene **767** produced in the reduction of the iron pre-catalyst represents a two-electron reduction of iron, therefore:

$$\text{Average } \# \text{ electron reduction} = 2 \times \left(\frac{\%\ \text{Yield of 1-methoxy-4-propylbenzene } \mathbf{767}}{\text{mol}\%\ \text{of iron precatalyst used}} \right)$$

Time	% Yield of products				% 'starting reagents'		Average # electron reduction
	α-745	**767**	**769**	**770**	**675**	**766**	
Expt 1*—^{iPr}*BIPFeCl$_2$* ***743 *(5.4 mol%)*							
0.5	0.3	9.2	7.6	0.0	99.9	105.3	3.4
1	0.8	10.3	8.9	1.1	98.6	102.6	3.8
2	1.6	10.0	8.9	1.1	97.2	101.3	3.7
2.5	2.4	10.8	10.3	0.0	95.9	98.6	4.0
3	3.0	10.5	11.6	2.2	94.5	98.6	3.9
4	4.1	10.5	13.0	1.6	93.2	95.9	3.9
7	7.8	11.6	17.0	2.7	91.8	87.8	4.3
10	11.1	12.2	21.1	3.2	89.1	82.4	4.5
15	15.4	12.7	25.1	3.8	83.7	78.3	4.7
20	18.6	12.2	29.2	4.3	79.7	77.0	4.5
30	24.0	12.4	31.9	4.9	74.3	68.9	4.6
90	34.3	11.3	41.3	7.0	63.5	58.1	4.2
Expt 2*—^{iPr}*BIPFeCl$_2$* ***743 *(5.4 mol%)*							
0.5	0.3	8.6	8.9	0.5	98.6	101.3	3.2
1	1.1	8.1	10.3	1.6	98.6	99.9	3.0
2	1.9	11.9	13.0	1.6	99.9	97.2	4.4
2.5	3.0	9.7	13.0	2.2	95.9	97.2	3.6
3	3.5	10.3	14.3	2.7	95.9	94.5	3.8
4	5.1	10.5	15.7	2.7	94.5	94.5	3.9
7	8.6	10.8	18.4	2.7	91.8	90.5	4.0
10	11.1	11.3	21.1	3.2	89.1	87.8	4.2
15	14.9	13.0	25.1	3.8	81.0	77.0	4.8
20	18.4	11.6	29.2	3.8	79.7	75.6	4.3
30	23.5	12.2	33.2	4.3	75.6	67.5	4.5
90	32.1	12.4	41.3	6.5	64.8	52.7	4.6
Expt 3*—^{iPr}*BIPFeCl$_2$* ***743 *(5.4 mol%)*							
0.5	0.8	9.2	10.3	0.0	99.9	102.6	3.4
1	1.4	8.9	10.3	1.1	98.6	101.3	3.3
2	2.7	11.3	13.0	1.1	97.2	98.6	4.2
2.5	3.0	10.5	13.0	1.6	97.2	97.2	3.9
3	5.1	10.8	14.3	1.6	95.9	95.9	4.0
4	5.9	11.1	15.7	2.7	93.2	94.5	4.1

(continued)

(continued)

Time	% Yield of products				% 'starting reagents'		Average # electron reduction
	α-745	**767**	**769**	**770**	**675**	**766**	
7	9.2	12.2	19.7	3.2	91.8	91.8	4.5
10	11.6	12.7	22.4	3.8	90.5	87.8	4.7
15	14.3	11.9	23.8	3.2	86.4	83.7	4.4
20	17.0	12.2	26.5	3.8	83.7	79.7	4.5
30	20.0	13.5	29.2	3.2	79.7	75.6	5.0
90	25.1	11.6	34.6	4.3	75.6	64.8	4.3
Expt 4*—^{iPr}*BIPFeCl$_2$* ***743 *(8.1 mol%)*							
0.5	0.8	14.9	14.3	1.1	99.9	93.2	3.7
1	1.4	13.5	15.7	2.2	98.6	90.5	3.3
2	2.4	15.4	17.0	3.2	97.2	87.8	3.8
2.5	3.8	15.9	18.4	3.8	94.5	86.4	3.9
3	4.9	15.9	19.7	3.8	93.2	82.4	3.9
4	6.2	16.5	21.1	4.3	91.8	78.3	4.1
7	11.3	18.4	26.5	5.9	89.1	74.3	4.5
10	15.1	18.1	29.2	6.5	86.4	67.5	4.5
15	19.4	18.1	31.9	5.9	78.3	63.5	4.5
20	24.3	18.6	35.9	8.1	74.3	59.4	4.6
30	28.1	18.6	38.6	9.2	68.9	55.4	4.6
90	39.2	19.4	45.4	14.6	59.4	43.2	4.8
Expt 5*—^{iPr}*BIPFeCl$_2$* ***743 *(8.1 mol%)*							
0.5	0.3	14.6	10.3	1.1	101.3	98.6	3.6
1	1.4	15.7	13.0	2.2	97.2	93.2	3.9
2	2.4	15.4	15.7	2.7	94.5	89.1	3.8
2.5	3.2	17.3	17.0	3.2	95.9	86.4	4.3
3	4.6	16.7	18.4	3.8	91.8	85.1	4.1
4	5.7	16.5	21.1	4.1	91.8	83.7	4.1
7	11.1	17.0	25.1	5.4	86.4	75.6	4.2
10	14.9	17.3	29.2	5.9	83.7	72.9	4.3
15	19.4	17.3	33.2	7.0	78.3	67.5	4.3
20	22.4	20.0	35.9	8.1	74.3	60.8	4.9
30	26.7	19.4	40.0	9.2	70.2	55.4	4.8
90	34.0	19.2	44.0	11.3	56.7	43.2	4.7
Expt 6*—^{iPr}*BIPFeCl$_2$* ***743 *(8.1 mol%)*							
0.5	0.8	15.9	11.6	0.0	99.9	99.9	3.9
1	1.9	17.0	13.0	1.6	98.6	97.2	4.2
2	3.0	18.6	17.0	2.7	98.6	91.8	4.6
2.5	4.1	16.7	18.4	2.7	94.5	91.8	4.1
3	5.4	20.0	19.7	3.8	94.5	85.1	4.9

(continued)

(continued)

Time	% Yield of products				% 'starting reagents'		Average # electron reduction
	α-745	**767**	**769**	**770**	**675**	**766**	
4	6.8	17.3	21.1	3.8	90.5	86.4	4.3
7	12.7	17.3	26.5	5.9	85.1	79.7	4.3
10	16.5	18.9	30.5	7.0	83.7	74.3	4.7
15	21.1	18.6	34.6	7.6	78.3	70.2	4.6
20	24.0	18.6	37.3	8.6	75.6	64.8	4.6
30	28.4	18.1	41.3	8.6	70.2	60.8	4.5
90	39.2	17.3	44.0	13.0	54.0	48.6	4.3

Average number of electron reduction of ^{iPr}BIPFeCl$_2$

Time	^{iPr}BIPFeCl$_2$ (5.4 mol%)			^{iPr}BIPFeCl$_2$ (8.1 mol%)			Average # electron reduction	Standard deviation
	Expt 1	Expt 2	Expt 3	Expt 4	Expt 5	Expt 6		
0.5	3.4	3.2	3.4	3.7	3.6	3.9	3.5	0.26
1	3.8	3.0	3.3	3.3	3.9	4.2	3.6	0.44
2	3.7	4.4	4.2	3.8	3.8	4.6	4.1	0.37
2.5	4.0	3.6	3.9	3.9	4.3	4.1	4.0	0.22
3	3.9	3.8	4.0	3.9	4.1	4.9	4.1	0.41
4	3.9	3.9	4.1	4.1	4.1	4.3	4.1	0.13
7	4.3	4.0	4.5	4.5	4.2	4.3	4.3	0.19
10	4.5	4.2	4.7	4.5	4.3	4.7	4.5	0.20
15	4.7	4.8	4.4	4.5	4.3	4.6	4.5	0.19
20	4.5	4.3	4.5	4.6	4.9	4.6	4.6	0.20
30	4.6	4.5	5.0	4.6	4.8	4.5	4.7	0.20
90	4.2	4.6	4.3	4.8	4.7	4.3	4.5	0.25
							Av. St. Dev.	0.26

Time	% Yield of products				% 'starting reagents'		Average # electron reduction
	α-745	**767**	**769**	**770**	**675**	**766**	
***Expt 7—FeCl$_2$ 279** (5.4 mol%) + TMEDA **136** (27 mol%)*							
0.5	0.0	7.6	6.2	0.0	99.9	110.7	2.8
1	1.1	6.8	7.6	0.0	97.2	106.7	2.5
2	6.5	8.1	13.0	0.0	91.8	104.0	3.0
2.5	8.1	7.6	14.3	0.0	87.8	101.3	2.8
3	9.5	7.6	15.7	0.0	89.1	101.3	2.8
4	10.3	7.3	17.0	0.0	86.4	98.6	2.7

(continued)

(continued)

Time	% Yield of products				% 'starting reagents'		Average # electron reduction
	α-745	**767**	**769**	**770**	**675**	**766**	
7	12.2	7.6	18.4	0.0	83.7	98.6	2.8
10	13.0	8.1	18.4	1.1	83.7	97.2	3.0
15	13.2	7.6	18.4	1.6	82.4	94.5	2.8
20	14.6	7.8	19.7	1.6	82.4	90.5	2.9
30	16.5	7.8	21.1	1.6	83.7	93.2	2.9
90	18.9	8.4	23.8	2.2	81.0	89.1	3.1
***Expt 8**—$FeCl_2$ **279** (8.1 mol%) + TMEDA **136** (41 mol%)*							
0.5	0.0	11.9	8.9	0.0	99.9	108.0	2.9
1	0.8	11.6	10.3	0.0	99.9	105.3	2.9
2	5.1	13.8	13.0	0.0	94.5	99.9	3.4
2.5	6.2	10.8	15.7	0.0	93.2	97.2	2.7
3	8.4	11.6	17.0	0.0	90.5	97.2	2.9
4	9.5	12.7	18.4	0.5	89.1	94.5	3.1
7	11.1	11.6	19.7	1.1	87.8	91.8	2.9
10	12.2	12.7	21.1	1.4	86.4	90.5	3.1
15	13.9	12.4	22.4	2.7	86.4	90.5	3.1
20	15.1	13.0	23.8	2.2	83.7	89.1	3.2
30	16.7	13.0	25.1	2.7	82.4	86.4	3.2
90	23.2	12.7	30.5	3.8	72.9	67.5	3.1
***Expt 9**—$FeCl_2$ **279** (8.1 mol%) + TMEDA **136** (41 mol%)*							
0.5	0.0	11.6	8.9	0.0	99.9	93.2	2.9
1	0.8	10.8	8.9	0.0	98.6	90.5	2.7
2	2.4	11.6	10.3	0.0	98.6	87.8	2.9
2.5	4.3	11.9	13.0	0.0	95.9	86.4	2.9
3	6.2	10.3	15.7	0.5	93.2	82.4	2.5
4	8.4	12.7	17.0	0.8	91.8	78.3	3.1
7	9.5	13.0	19.7	1.1	90.5	74.3	3.2
10	10.8	13.2	19.7	1.9	90.5	67.5	3.3
15	12.4	12.2	21.1	2.7	85.1	63.5	3.0
20	14.0	13.0	21.1	1.6	86.4	59.4	3.2
30	15.9	13.2	22.4	2.2	85.1	55.4	3.3
90	18.9	13.0	26.5	3.2	81.0	43.2	3.2

Average number of electron reduction of $FeCl_2$ + TMEDA

Time	$FeCl_2$ **279** (5.4 mol %) + TMEDA **136** (27 mol%)	$FeCl_2$ **279** (8.1 mol %) + TMEDA **136** (41 mol%)		Average # electron reduction	Standard deviation
	Expt 7	Expt 8	Expt 9		
0.5	2.8	2.9	2.9	2.9	0.06
1	2.5	2.9	2.7	2.7	0.18
2	3.0	3.4	2.9	3.1	0.27
2.5	2.8	2.7	2.9	2.8	0.13
3	2.8	2.9	2.5	2.7	0.17
4	2.7	3.1	3.1	3.0	0.25
7	2.8	2.9	3.2	3.0	0.21
10	3.0	3.1	3.3	3.1	0.13
15	2.8	3.1	3.0	3.0	0.13
20	2.9	3.2	3.2	3.1	0.17
30	2.9	3.2	3.3	3.1	0.19
90	3.1	3.1	3.2	3.1	0.05
				Av. St. Dev.	0.17

References

1. Smith, C. R.; RajunBabu, T. V. *Tetrahedron*. **2010**, *66*, 1102
2. Shiina, I.; Nakata, K.; Ono, K.; Onda, Y.; Itagaki, M. *J. Am. Chem. Soc.* **2010**, *132*, 11629
3. Prince, P. D.; Bearpack, M. J.; McGrady G. S., Steed, J. W. *Dalton Trans.* **2008**, 271
4. Small, B. L.; Brookhart, M.; Bennett, A. M. A. *J. Am. Chem. Soc.* **1998**, *120*, 4049
5. Esteruelas, M. A.; López, A. M.; Méndez, L.; Oliván, M.; Oñate E. *Organometallics* **2003**, *22*, 395
6. Britovsek, G. J. P.; Bruce, M.; Gibson, V. C.; Kimberley, B. S.; Maddox, P. J.; Mastroianni, S.; McTavish, S. J.; Redshaw, C.; Solan, G. A.; Strömberg, S.; White, A. J. P.; Williams, D. J. *J. Am. Chem. Soc.* **1999**, *121*, 8728
7. Cristau, H.-J.; Ouali, A.; Spindler, J.-F.; Taillefer, M. *Chem. Eur. J.* **2005**, *11*, 2483
8. (a) DuBois, D. L.; Miedaner, A. *Inorg. Chem.* **1986**, *25*, 4642. (b) Bedford, R. B.; Carter, E.; Cogswell, P. M.; Gower, N. J.; Haddow, M. F.; Harvey, J. N.; Murphy, D. M.; Neeve, E. C.; Nunn, J. *Angew. Chem. Int. Ed.* **2013**, *52*, 1285
9. Ge, S.; Meetsma, A.; Hessen, B. *Organometallics* **2008**, *27*, 3131
10. Nielsen, L.; Skrydstrup, T. *J. Am. Chem. Soc.* **2008**, *130*, 13145
11. Green, M.; Spencer, J. L.; Stone, F. G. A.; Tsipis, C. A. *J. Chem. Soc., Dalton Trans.* **1977**, *16*, 1519
12. Marciniec, B.; Szubert, K.; Fiedorow, R.; Kownacki, I.; Potrebowski, M. J.; Dutiewicz, M.; Franczyk, A. *J. Mol. Catal. A: Chem.* **2009**, *310*, 9

13. (a) Nakazawa, H.; Itazaki, M.; Tanaka, K.; Itagaki, A.; Kojima. T. Wo. Patent 2010/016416 A1, February 11, 2010. (b) Stober, M. R.; Musolf, M. C.; Speier, J. J. *J. Org. Chem.* **1965**, *30*, 1651
14. Kumar, A.; Akula, H. K.; Lakshman, M. K. *Eur. J. Org. Chem.* **2010**, 2709
15. Chatterjee, T.; Dey, R.; Ranu, B. C. *New J. Chem.* **2011**, *35*, 1103
16. Paul, C. E.; Rajagopalan, A.; Lavandera, I.; Gotor-Fernández, V.; Kroutil, W.; Gotor, V. *Chem. Commun.* **2012**, *48*, 3303
17. Baker, K. V.; Brown, J. M.; Hughes, N.; Skarnulis, A. J.; Sexton, A. *J. Org. Chem.* **1991**, *56*, 698
18. Crisp, G. T.; Papadopoulous, S. *Aust. J. Chem.* **1989**, *42*, 279
19. Görl, C.; Alt, H. G. *J. Mol. Cat. A: Chem.* **2007**, *273*, 118
20. Molander, G. A.; Julius, M. *J. Org. Chem.* **1992**, *57*, 6347
21. Trifonov, A. A.; Spaniol, T. P.; Okuda, J. *Dalton Trans.* **2004**, 2245
22. Small, B. L. Methods for producing a hexadentate bimetallic complex. U.S. Patent 2006/0128958 A1, June 15, 2006
23. Szostal, M.; Spain, M.; Procter, D. J. *Chem. Eur. J.* **2014**, *20*, 4222
24. Belger, C.; Plietker, B. *Chem. Commun.* **2012**, *48*, 5419
25. Moseley, J. D.; Stauton, J.; *J. Heterocyclic Chem.* **2005**, *42*, 819
26. Ringstand, B.; Oltmanns, M.; Batt, J. A.; Jankowiak, A.; Denicola, R. P.; Kaszynski, P. *Belstein J. Org. Chem.* **2011**, *7*, 386
27. Chen, C.; Nagy, G.; Walker, A.; Maurer, K.; McShea, A.; Moeller, K. D. *J. Am. Chem. Soc.* **2006**, *128*, 16020
28. Zhao, B.; Lu, X. *Org. Lett.* **2006**, *8*, 5987
29. Molander G. A.; Sandrock, D. L. *J. Am. Chem. Soc.* **2008**, *130*, 15792
30. Ortiz-Marciales, M.; Tirado, L. M.; Colón, R.; Ufret, M. L.; Figueroa, R.; Lebrón, M.; DeJesús, M.; Martínez, J.; Malavé, T. *Synth. Commun.* **1998**, *28*, 4067
31. Forbes, M. D. E.; Ruberu, S. R.; Dukes, K. E. *J. Am. Chem. Soc.* **1994**, *116*, 7299
32. Rokade, B. V.; Prabhu, K. R. *J. Org. Chem.* **2012**, *77*, 5364
33. Datta, S.; Chang, C.-L.; Yeh, K.-L.; Liu, R.-S. *J. Am. Chem. Soc.* **2003**, *125*, 9294
34. Radeke H. Hanson, K.; Yalamanchili, P.; Hayes, M.; Zhang, Z.-Q.; Azure, M.; Yu, M.; Guaraldi, M.; Kagan, M.; Robinson, S.; Casebier, D. *J. Med. Chem.* **2007**, *50*, 4304
35. Zhang, L.; Peng, D.; Leng, X.; Huang, Z. *Angew. Chem. Int. Ed.* **2013**, *52*, 3676
36. Caballero, A.; Sabo-Etienne, S. *Organometallics*, **2007**, *26*, 1191
37. Kim H. R.; Yun, J. *Chem. Commun.* **2011**, *47*, 2943
38. Pereira, S.; Srebnik, M. *Organometallics* **1995**, *14*, 3127
39. Molander, G. A.; Brown, A. R. *J. Org. Chem.*, **2006**, *71*, 9681
40. Sun, B.; Hoshino, J.; Jermihov, K.; Marler, L.; Pezzuto, J. M.; Mesecar, A. D.; Cushman, M. *Bioorg. Med. Chem.* **2010**, *18*, 5352
41. Saá, J. M.; Martorell, G.; García-Raso, A. *J. Org. Chem.* **1992**, *57*, 678
42. Shen, R.; Chen, T.; Zhao, Y.; Qiu, R.; Zhou, Y.; Yin, S.; Wang, X.; Goto, M.; Han, L.-B. *J. Am. Chem. Soc.* **2011**, *133*, 17037
43. Konrad, T. M.; Fuentes, J. A.; Slawin, A. M. Z.; Clarke, M. L. *Angew. Chem., Int. Ed.* **2010**, *49*, 9197
44. Nugent, W. A.; McKinney, R. J. *J. Org. Chem.* **1985**, *50*, 5370
45. Kubler, W.; Petrov, O.; Winterfeldt, E. *Tetrahedron*, **1988**, *44*, 4371
46. Damodar, J.; Mohan, S. R. K.; Reddy, S. R. J. *Electrochemistry Communications.* **2001**, *3*, 762
47. Foubelo, F.; Lloret, F.; Yus, M. *Tetrahedron* **1992**, *48*, 9531
48. Frantz, D. E.; Weaver, D. G.; Carey, J. P.; Kress, M. H.; Dolling, U. H. *Org. Lett*. **2002**, *4*, 4717
49. Chung, C. W. Y.; Toy, P. H. *Tetrahedron* **2005**, *61*, 709
50. O'Connell, J. L.; Simpson, J. S.; Dumanski, P. G.; Simpson, G. W.; Easton, C. J. *Org. Biomol. Chem*. **2006**, *4*, 2716

51. Bräse, S.; Rümper, J.; Voigt, K.; Albecq, S.; Thurau, G.; Villard, R.; Waegell, B.; de Meijere, A. *Eur. J. Org. Chem.* **1998**, 671
52. Duguid, R. J.; Morrison, H. *J. Am. Chem. Soc.* **1991**, *113*, 1271
53. Frechet, J. M.; Schuerch, C. *J. Am. Chem. Soc.* **1971**, *93*, 492
54. Collman, J. P.; Kosydar, K. M.; Bressan, M.; Lamanna, W.; Garrett, T. *J. Am. Chem. Soc.* **1984**, *106*, 2569
55. Franck, G.; Brill, M.; Helmchen, G. *Org. Synth.* **2012**, *89*, 55
56. Park, S.; Bezier, D.; Brookhart, M. *J. Am. Chem. Soc.* **2012**, *134*, 11404
57. Fuchs, C. S.; Hollauf, M.; Meissner, M.; Simon, R. C.; Besset, T.; Reek, J. N. H.; Riethorst, W.; Zepeck, F.; Kroutil, W. *Adv. Synth. Catal.* **2014**, *356*, 2257
58. Chen, M.; Wang, J.; Chai, Z.; You, C.; Lei, A. *Adv. Synth. Catal.* **2012**, *354*, 341
59. Bézier, D.; Park, S.; Brookhart, M. *Org. Lett.* **2013**, *15*, 496
60. Straub, A. T.; Otto, M.; Usui, I.; Breit, B. *Adv. Synth. Catal.* **2013**, *355*, 2071
61. Carter, T. S.; Guiet, L.; Franck, D. J.; West, J.; Thomas, S. P. *Adv. Synth. Catal.* **2013**, *355*, 880
62. Tieze, L. F.; Vock, C. A.; Krimmelbein, I.; K.; Nacke, L. *Synthesis* **2009**, 2040
63. Sakai, N.; Nagasawa, K.; Ideka, R.; Nakaike, Y.; Konakahara, T. *Tetrahedron Lett.* **2011**, *52*, 3133
64. Wang, H.; Li, L.; Bai, X.-F.; Shang, J.-Y.; Yang, K.-F.; Xu, L.-W. *Adv. Synth. Catal.* **2013**, *355*, 341
65. McDaniel, D. H.; Brown, H. C. *J. Org. Chem.* **1958**, *23*, 420
66. Jiang, X.-K. *Acc. Chem. Res.* **1997**, *30*, 283
67. (a) Creary, X. *J. Org. Chem.* **1980**, *45*, 280. (b) Creary, X.; Mehrsheikh-Mohammadi, M. E.; McDonald, S. *J. Org. Chem.* **1987**, *52*, 3254
68. Jefferies, L. R.; Cook, S. P. *Org. Lett.* **2014**, *16*, 2026
69. Fan, X.; Cui, X.-M.; Guan, Y.-H.; Fu, L.-A.; Lv, H.; Guo, K.; Zhu, H.-B. *Eur. J. Org. Chem.* **2014**, 498
70. Horino, Y.; Takahashi, Y.; Koketsu, K.; Abe, H.; Tsuge, K. *Org. Lett.* **2014**, *16*, 3184
71. Ackermann, L.; Kapdi, A. R.; Schulzke, C. *Org. Lett.* **2010**, *12*, 2298
72. Chen, C.; Dugan, T. R.; Brennseeel, W. W.; Weix, D. J.; Holland, P. L. *J. Am. Chem. Soc.* **2014**, *136*, 945